

INTERNATIONAL COUNCIL FOR BUILDING RESEARCH STUDIES AND DOCUMENTATION

WORKING COMMISSION W18 - TIMBER STRUCTURES

CIB - W18

MEETING TWENTY - SIX

ATHENS, GEORGIA

USA

AUGUST 1993

Lehrstuhl für Ingenieurholzbau und Baukonstruktionen
Universität Karlsruhe
Germany
Compiled by Rainer Görlacher
1994

ISSN 0945-6996

CONTENTS

- 0 List of Participants
 - 1 Chairman's Introduction
 - 2 Cooperation with other Organisations
 - 3 Reports from Sub-Groups
 - 4 Connections Made Using Punched Metal Plate Fasteners
 - 5 Structural EUROCODES including EUROCODE 5
 - 6 Mechanical Timber Joints
 - 7 Serviceability Considerations in Structural Timber Design
 - 8 Open Forum
 - 9 Any other Business
 - 10 Venue and Programme for the Next Meeting
 - 11 Close
 - 12 List of CIB W18 Papers/Athens, USA 1993
 - 13 Current List of CIB W18 Papers
- CIB-W18 Papers 25-6-1 up to 25-102-2

0 List of Participants

**INTERNATIONAL COUNCIL FOR BUILDING RESEARCH STUDIES
AND DOCUMENTATION**

WORKING COMMISSION W18 - TIMBER STRUCTURES

MEETING TWENTY-SIX

ATHENS, USA, 23-27 AUGUST 1993

LIST OF PARTICIPANTS

CANADA

C Lum	Forintek Canada Corp., Vancouver
I Smith	University of New Brunswick
C K A Stieda	Forintek Canada Corp., Vancouver

DENMARK

A Egerup	Euro-Truss, Denmark
H J Larsen	Danish Building Research Institute, Hørshølm

FINLAND

J Kangas	Technical Research Centre of Finland, Espoo
A Kevarinmäki	Helsinki University of Technology, Espoo
T Poutanen	Tampere University of Technology

FRANCE

F Rouger	C.T.B.A Paris
----------	---------------

GERMANY

J Ehlbeck	University of Karlsruhe
R Görlacher	University of Karlsruhe

ITALY

A Ceccotti	University of Florence
------------	------------------------

NETHERLANDS

H J Blass Delft University of Technology

NORWAY

E Aasheim Norwegian Institute of Wood Technology, Oslo

SWEDEN

B Källsner Swedish Institute for Wood Technology Research, Stockholm
J König Swedish Institute for Wood Technology Research, Stockholm
A Mårtensson Lund University
S Thelandersson Lund University

SWITZERLAND

E Gehri Eidgenössische Technische Hochschule, Zürich
U Meierhofer EMPA, Dübendorf

UK

A R Abbott TRADA Technology Limited, High Wycombe
A R Fewell Building Research Establishment, Watford
C J Mettem TRADA Technology Limited, High Wycombe
J Park COFI, London

USA

P Chow University of Illinois, Urbana
J D Dolan Virginia Polytechnic Institute and State University, Blacksburg
E Elias American Plywood Association, Tacoma
R Falk US Forest Products Laboratory, Madison
D W Green US Forest Products Laboratory, Madison
R Gupta Oregon State University,
M R O'Halloran American Plywood Association, Tacoma
J Showalter National Forest and Paper Association, Washington DC
E G Stern Virginia Polytechnic Institute and State University, Blacksburg
T Williamson American Plywood Association, Tacoma

- 1. Chairman's Introduction**
- 2. Cooperation with other Organisations**
- 3. Reports from Sub-Groups**
- 4. Connections Made Using Punched Metal Plate Fasteners**
- 5. Structural EUROCODES including EUROCODE 5**
- 6. Mechanical Timber Joints**
- 7. Serviceability Considerations in Structural Timber Design**
- 8. Open Forum**
- 9. Any other Business**
- 10. Venue and Programme for the Next Meeting**
- 11. Close**

**INTERNATIONAL COUNCIL FOR BUILDING RESEARCH STUDIES
AND DOCUMENTATION**

WORKING COMMISSION W18 - TIMBER STRUCTURES

MEETING TWENTY-SIX

ATHENS, USA, 23-27 AUGUST 1993

MINUTES

1. CHAIRMAN'S INTRODUCTION

The Chairman, PROF BLASS, welcomed the delegates to the twenty- sixth meeting of CIB-W18 and said that in his introduction, he would like to make several special mentions. DR FIELD was present on behalf of the University of Georgia, in Athens, and would himself say a few introductory words, both about the further education facilities and about the conference arrangements. DR CECCOTTI would deal with links with RILEM; MR LARSEN would cover the CEN TC activities, and DR STIEDA would provide information on ISO TC165.

It was noted with deep regret that since the last meeting of CIB W18, Professor Möhler had died. He had been the head of the Chair for timber structures at the University of Karlsruhe before Jürgen Ehlbeck took over. The Chairman said that Professor Möhler had made a major contribution to timber engineering in the period approximately 1970-1985 and had been instrumental in much of the important work reported at CIB-W18. As a mark of respect, a brief period of silence was held.

The Chairman regretted to inform delegates that, despite good intentions expressed at the previous meeting, papers had been issued very late, due to their last minute submission to the Secretariat. He hoped that it would be possible to improve on this situation, and urged all to cooperate.

After thanking APA for making the preliminary arrangements and for hosting the meeting, the Chairman called upon DR FIELD to explain the facilities at the University, and to tell delegates about the large further education programme and the forestry courses.

After the Chairman had drawn delegates' attention to the final version of the agenda, its contents were agreed. He then said that before proceeding with the next topic, it was necessary to discuss a point concerning cooperation within CIB. Correspondence had been received by all coordinators of CIB Working Commissions and Task Groups concerning CIB policy and its relationships with industry. Copies of the relevant letters had been copied for information of the delegates to CIB-W18.

The Chairman said that it had been noted that the general bodies within CIB, such as the Programme Committee and the Central Secretariat, had recently become more active. The Secretariat had distributed a letter concerning the relationship of CIB with industry and previously, coordinators of working commissions and task groups had been asked to complete a questionnaire concerning the activities of their groups. The Programme Committee had analysed the result of this survey. The Chairman said he would inform delegates of the outcome. He felt it would be appropriate for delegates to express views about the function of W18 as a CIB Working Commission and the prospects of its activities being assessed by a Programme Committee.

The Chairman said that from his point of view, when he first undertook the role, he foresaw only rather limited contacts with other parts of the CIB organisation. The review of the CIB-W18 work programme had given rise to some complimentary comments by the Programme Committee, but it had recommended that the Working Commission should formulate a programme of work and have a series of more closely defined aims. For some of the Working Commissions, information exchange is stated as an important aspect of their aims. It was noted that there was an attempt on the part of the CIB Secretariat to try to press for formal membership of the organisation on the part of delegates at meetings such as CIB-W18.

MR LARSEN said that he would like to comment, as he had experience of the operation of CIB through having been a chairman of the Programme Committee. Considerable debate used to occur on the lines just reported, since there was a tendency for CIB itself to wish to be seen as fulfilling a necessary role and having the results of its work identifiable. In his view, CIB should strive to create the environment for exchange of knowledge arising from research. In the case of his organisation, for example, there was already a very strong need for links with industry, and this had strict financial implications.

Further discussions ensued in which several delegates commented on CIB-W18's useful role as an international specialist timber engineering research group. It was felt that if CIB put too much pressure on the group to conform to its principles and to contribute financially, then either several of the organisations who regularly participate might be forced to reconsider or, alternatively, the formation of an independent timber research group might be suggested. It was agreed to leave the matter of responding to the CIB Secretariat and Programming Committee to the Chairman, knowing that he understood these views of the delegates to CIB-W18.

2. COOPERATION WITH OTHER ORGANISATIONS

a) CIB-W18B

A brief report on the activities of the CIB-W18B group had been received by post from DR LEICESTER. It was stated that discussions had been held on the structural use of tropical hardwoods when the group had met during an international timber conference in Kuala Lumpur in September 1992. Other than this, activities had been limited due to difficulties in obtaining travel funding for participants from developing countries.

b) ISO TC165

DR STIEDA reported on a meeting of ISO/TC165 Timber Structures which had taken place in Prague on 29 and 30 March 1993. Fourteen participants had attended. It had been decided to recommend to ISO Central Secretariat that a lot of the recent work which had been taking place to develop CEN Standards for timber structures could be taken advantage of by ISO. Consequently, four prEN Standards concerning test methods for fasteners, two concerning physical and mechanical properties and one concerning general principles for static load testing had been requested for circulation and for ISO DIS voting. Using the ISO voting "fast track procedure", another three prEN drafts concerning test methods and grading had similarly been submitted.

Commenting on this, DR CECCOTTI said that, whilst it was flattering that ISO/TC165 found the CEN work so useful, it should be borne in mind that more active ISO participation in the timber field from other regions of the world would make it easier for potential European participants to justify the time and costs involved in attending its meetings.

c) RILEM

DR CECCOTTI gave a report on the activities of the RILEM Technical Committees on structural timber. Three TC's had recently completed their work and had published "state of the art" reports. These were TC109-TSA 'Behaviour of timber structures under seismic actions', whose report is shortly to be published in 'Materials & Structures' journal; TC111-CST 'Behaviour of timber and concrete composite load-bearing structures', producing a book to be published by Chapman and Hall; and TC112-TSC 'Creep in timber structures', with a report already published by LRBB, Bordeaux. There are three additional Technical Committees whose work is in progress or just starting. These are TC133-TF 'Fracture of timber', chaired by Prof A Ranta-Maunus, VTT, Finland, doing work on test methods and design principles relating to fracture mechanics; TC149 - HTS 'Diagnosis and repair of historical load-bearing timber structures' chaired by Dr W Rug, Recontie, Berlin; and TC155-TCW 'Test methods for creep measurements of wooden materials' chaired by Dr C Le Govic, CTBA, Paris.

d) CEN

The Chairman conveyed to the delegates the apology of MR SUNLEY for not being able to attend this meeting of CIB-W18. It was the first that he had missed for many years, and his absence was mutually regretted. However, despite not being able to attend in person, reports had been submitted on the recent activities and progress of several of the CEN/TC committees which are drafting European Standards. Other CEN reports were prepared and presented by MR LARSEN. The following is a very abbreviated summary, since the information is available to the majority elsewhere.

TC38 'Durability of wood and related materials'.

TC38 is generally making good progress in completing its main mandated programme. Quite a few of its drafts had to go to a second enquiry stage before consensus was reached. TC38 has a programme of 48 Standards, 34 of which have been published or approved for final voting.

TC112 'Wood based panel products'.

TC112 has a current active programme of 72 Standards, many of which are now reaching the final stages. Good progress is also being made in another difficult area, which is how to deal with characteristic values for established products. Because a large number of the Standards are either product Standards or support these, it has been agreed that, to assist production, the implementation of TC112 Standards in Member States can be delayed until a common date, which, in this instance, is 31 December 1994.

TC124 'Timber structures'.

The paper on this subject tabled by MR LARSEN reminded delegates of the procedure for drafting and eventual approval of European Standards. TC124 has also been making progress in processing a large programme of Standards. In total, 39 Standards are listed at various stages. Three Standards are awaiting final editorial work and approval by CEN and can be expected to be published soon. It is understood that there is a translation bottleneck within the CEN system. About half of the TC124 programme of work is at the final drafting stage or beyond.

TC175 'Round and sawn timber'

This TC operates through four working groups, dealing with definitions, sawn timber, user requirements and round timber. TC175 was formed some two years later than the other timber committees. Consequently, its programme of 75 Standards is less advanced. Useful progress is being made in some areas, although some historic problems concerning sawn softwood and roundwood grading still seem a long way from resolution.

TC250 'Structural Eurocodes'

The following situation with regard to CEN TC250/SC5 Eurocode 5 'Design of timber structures' was reported by MR LARSEN:
Eurocode 5, Part 1-1 (ENV 1995-1-1): General Rules and Rules for Buildings was adopted as a European Prestandard (ENV) in November 1992. It is expected to be published in the three official languages (English, French, German) by the end of 1993, and immediately after in the other West European languages, together with National Application Documents stating the national conditions for the use of Eurocodes.

Eurocode 5, Part 1-2 (ENV 1995-1-2): Structural Fire Design was adopted as an ENV in June 1993. It is expected to be published in the three official languages in February 1994.

Eurocode 5, Part 2, Bridges: Drafting is expected to start January 1994 in an *ad hoc* group chaired by Professor E Gehri, Switzerland.

e) IABSE

It was reported that Vol.3 No.2 of 'Structural Engineering International' (the journal of IABSE) had timber structures as a main theme, covering timber bridges, large structures and testing papers, totalling ten. Five of the articles happened to be by authors who are members of CIB-W18. In September 1994, an IABSE seminar will be held in Birmingham, England, dealing with long-span structures for places of large assembly. A report on IABSE conferences in 1992 and 1993 was tabled.

f) IUFRO S5.02

It was announced that IUFRO S5.02 plans to meet for two and a half days in Sydney, Australia, at around the same date as the next CIB meeting and other events. State-of-the-art papers are planned, including topics such as creep and timber joints. It was also noted that there will be a IUFRO World Conference in Finland in 1995 and that this will present another opportunity for S5.02 to gather. A special meeting on engineering aspects of wood-based panel products is being considered.

g) CIB-W85 Structural Serviceability

DR OHLSSON had sent apologies for being unable to attend this meeting of CIB-W18, but he had sent in a report on the recent activities of CIB-W85 Structural Serviceability. These had centred around a joint CIB/IABSE colloquium on the structural serviceability of buildings which had been held in Göteborg, Sweden, 8-11 June 1993. Aspects of structural serviceability which are related to the load-bearing structure of the building had been the main theme. A total of 90 abstracts had been submitted, from which 45 technical papers had been selected. The general impression of the event was that structural serviceability is rapidly becoming the most important design objective in many instances. The successful conference was attended by over 80 participants from 25 countries.

h) STEP - Structural Timber Education Programme

PROF BLASS made a brief presentation on the Structural Timber Education Programme (STEP), which is being supported by EC COMETT and other funding. Recognising that timber engineering education needs to be linked to codes, it had been decided to relate the STEP programme, which began in 1992, to the Eurocode for timber,

EC5. Fourteen countries were participating in the programme with 43 specialists writing material on about 100 topics. The means of funding was explained. Subject areas included basic elements, components and connections. Outputs are planned to consist of sets of formal lecture notes, and seminar presentations. At a later stage, it is considered slide sets and computer programmes might be desirable. The present stage of the programme ends in 1995.

In discussions of the STEP programme, DR DOLAN said that the ASCE were working on similar lines. He hoped that the initiatives could be complementary and welcomed information on how the European material could be obtained. DR SMITH and others made observations on time-tabling restrictions in the university courses. It was agreed that freedom of choice in teaching principles had to be recognised and that there could not be too much attempt to influence distinct syllabi of the universities of particular countries.

3. REPORTS FROM SUB-GROUPS

There was little or no activity or progress to report concerning the following sub-groups:

- a) Derivation of Characteristic Values For Panel Products
- b) Stability of Structures
- d) Reliability Based Design

It was considered unlikely that the existence of the groups would continue to be formally recognised.

There was a brief report from the following sub-group:

- c) Assessment of Punched Metal Plate Timber Fasteners.

Reports on previous meetings of the group in Åhus, Sweden, and in Kirov, Russia, had been distributed. PROF STERN said that the group had been considering whether, and how, to harmonise Standards on this subject on an international basis. The sub-group was planning to meet again during the 1993 annual meeting of W18 recorded in these minutes. Comparisons between various national test methods were a topic for the agenda. It was noted that six of the papers on the agenda for the main meeting were related to the subject.

4. CONNECTIONS MADE USING PUNCHED METAL PLATE FASTENERS

Paper 26-14-1 "Test of nail plates subjected to moment" by E Aasheim was presented by DR AASHEIM. It aimed to provide a background for a CEN test method for moment connections. There was a discussion after the presentation, of elastic versus plastic moment equation principles and about the applicability of the proposed

methods to a broader range of plate types. In answer to points made by MR PARKS, the author agreed that it was not yet clear how the test results would be related to equations that could actually be used in design to provide for the combined effects of axial forces and moments. Possible variations in wood-to-wood contact areas were also discussed. MR MEIERHOFER suggested, and the author agreed, that time-dependent effects on moment rotation characteristics were likely to be important and were not yet fully investigated.

Paper 26-14-3 "Rotational stiffness of nail plates in moment anchorage" by A Kevarinmäki and J Kangas was discussed next, since it related to Paper 26-14-1. This was presented by DR KANGAS. The aim of this work is to permit moment resisting nail plated joints to be designed more accurately. Shear and tensile test specimens were used in the evaluations. Angles both between the grain direction and the nail, and the grain direction and the force, were varied.

DR SMITH said that he had doubts over the theoretical basis behind the analysis, although not regarding the results of the tests themselves. PROF BLASS felt that there was a need for greater communication between the various researchers in this topic, so that both principles and test procedures could be in greater harmony. MR LARSEN questioned whether rotational stiffness is a system property or a material property. Some of the difficulties that were discussed related to the fact that the deformations of the teeth in the plates are not a linear function of the plate size or area.

Paper 26-14-2 "Moment anchorage capacity of nail plates" by A Kevarinmäki and J Kangas was presented and discussed next. This contained all the Finnish test results to date on this topic, and complemented a paper presented at Meeting 25, Åhus. DR SMITH and several other delegates offered a possible criticism to the support arrangement in certain of the tests, which led to a statically indeterminate arrangement. In answer to a question from PROF EHLBECK, it was confirmed that as a result of the tests and analyses presented in the above papers, there was now a proposal to change some of the EC5 draft design equations relating to truss plates.

Paper 26-14-4 "Solution of plastic moment anchorage stress in nail plates" by DR KEVARINMÄKI was presented by the author. In discussing this, MR LARSEN pointed out that although it might be a more accurate solution than others, it was not, as stated, precise because of the assumption that a full share of the plastic force is carried by all nails, irrespective of their distance from the centroid. He also mentioned that at meetings involving the trussed rafter industry, system owners have expressed a preference for simpler design methods such as those drafted in EC5. Even in EC3, steel code writers have been cautious in introducing plastic design assumptions. DR DOLAN pointed out, however, that in seismic regions, any form of steel connector used to join structural timber members is required to have plastic yield capabilities.

Paper 26-14-5 "Testing of metal plate connected wood-truss joints" by DR GUPTA was presented by the author. The aim was to test complete truss nodes, containing joints, in configurations similar to those occurring in practice. MR LARSEN commented that the approach adopted by the author was analogous to solving the problem of column behaviour through the testing of thousands of varieties of column configuration, with a great range of eccentricities, etc. He believed there was a need for a sounder theoretical basis to testing and a more logical approach. DR DOLAN

suggested that if the author were to make a greater number of deformation and moment rotation measurements on his assemblies, plus tests on plated joints comparable with those described in papers 26-14-1 to 3, then such work could more usefully provide validation to the theories.

Paper 26-14-6 "Simulated accidental events on a trussed rafter roofed building" by C J Mettem and J P Marcroft was presented by MR METTEM. In answer to a question from DR O'HALLORAN, it was explained that the work reported in this paper related to accidental events to low-rise structures, mainly of the type caused by vehicle impacts. There was a new proposal within the UK to extend the subject to cover timber frame above three storeys, and in this case, gas explosions were likely to be considered to be of greater importance. DR THELANDERSSON said that he believed that it had been noted in the *post mortem* surveys of Hurricane Andrew (USA) that poor workmanship had exacerbated much of the structural damage. As confirmed by the authors of the disproportionate collapse paper, this was also an important issue in this respect. Quality control on site was now an important topic in the British construction industry.

Paper 26-15-1 "Bracing requirements to prevent lateral buckling in trussed rafters" by C J Mettem and P J Moss was presented by MR METTEM. DR STIEDA raised the question of relating theory and experiments more closely, but the presenter explained that the tests were a relatively simple series, testing in the laboratory typical trussed rafters as delivered to site, rather than ideally fabricated ones. These components contained initial lack of straightness and butt jointed plated splices in the rafters, etc. The paper did include a description of an elastic three-dimensional analytical model, which had been provided by Dr Moss, and it gave proposals for bracing, based on classic stability theories. It was felt that the problems are related to the wide gulf between parameters which must be assumed when applying present theories on the one hand, and actual construction practice on the other. MR PARKS agreed with the value of the work. He pointed out that roofs are seldom sheathed in the UK and that in construction practice, even the need to anchor bracing down, via walls to foundations, is not always appreciated. Many problems had occurred with unbraced, or incorrectly braced roofs in the UK.

Presentation 26-15-3 "Hurricane Andrew - Structural performance of buildings in South Florida" was made by means of a video by DR O'HALLORAN and a team from APA. In answer to a question from DR EGERUP, it was explained that, although incorrect edge distances in fastenings of sheathing was sometimes a critical issue, more often it was simply the case that many of the fixings were omitted. The damage assessment reports pointed to the need for greater attention to achieving Building Code requirements on site. In answer to a question from DR GUPTA, it was confirmed that the "Hurricane Iniki" (Hawaii) damage assessment showed that hipped roofs performed significantly better than gable ended ones. DR DOLAN said that the Alaskan earthquake assessments performed in the 1960s had placed less emphasis on building construction inaccuracy and omissions. He felt that this earlier construction had probably been of better quality and also took the form of more resistant building plans and shapes.

5. STRUCTURAL EUROCODES INCLUDING EUROCODE 5

Paper 26-15-2 "Eurocode 8 - Part 1.3 - Chapter 5. Specific rules for timber buildings in seismic regions" by K Becker *et al* was presented by DR CECCOTTI. It was explained that in order to meet seismic requirements, timber structures may be designed either as dissipative or non-dissipative structures. If the dissipative design route is elected, then the designer must demonstrate that within the structure, and especially the connections, there is the capability of dissipating the energy from the actions of the earthquake. With elastic analysis, action reduction factors can be elected according to building type and characteristics, provided that certain minimum requirements are met. These relate to serviceability and ductility. The latter will be defined by means of European Standards. Only very well known types of joint will be permitted to be designed without testing. Detailing rules provide extra restrictions.

In answer to a question from DR DOLAN, the presenter said that both numerical analyses and test results were used to make decisions on action reduction factors for joints. DR SMITH raised the difficulty of the need to vary such factors for a particular fastener type, according to the grain angles involved in the joint configuration. The presenter agreed that this was a problem. However, in cases of doubt there was always the option of commissioning specific tests to prove the design. MR MEIERHOFER said that, since research was in progress on structural timber composites which included artificial fibres, ductile members able to resist significant seismic forces may soon be envisaged. This led to a discussion as to how "forward thinking" the EC8 draft should be. MR LARSEN commented that, in his experience, it had been preferable to develop a relatively simple draft and then to expand and adapt it as necessary. A further aspect of the topic which was discussed involved the performance-based principles included in the draft, and whether, in practice, these would be likely to admit the use of plasterboard as a contributor to shear walls in seismic design. DR DOLAN raised the subject of mixed constructions, in relation to seismic design. DR CECCOTTI said that there was an entire chapter in the EC8 draft on this subject, but it was not addressed in the Paper.

Paper 26-16-1 "Structural fire design according to Eurocode 5, Part 1.2" was presented by the author, DR KÖNIG. It was explained that Part 1.2 was considerably simpler than earlier draft versions. Partial factor principles followed EC5, Part 1, but took different values. A materials partial factor especially for fire design was written in the present draft as a "boxed" (nationally variable) factor. DR CECCOTTI doubted whether, in practice, there would be much scope amongst the various members of the EU to elect to have different values for this factor. DR THELANDERSSON said that it was evident that those involved in drafting fire codes often came from a theoretical background rather than being experienced designers. There was a great need to establish more uniform safety levels and to achieve further simplicity.

Paper 26-12-1 "Norwegian bending tests with glued laminated beams -Comparative calculations with the Karlsruhe calculation model" by E Aasheim *et al* was presented by DR GÖRLACHER. From a large series of tests on Norwegian glulam beams (described in the following paper) data on lamination strengths and finger joint properties were input to the Karlsruhe model. Generally, it had been shown that the model gives a good simulation of the strength of such beams. The work had led to proposals to adapt the model to simulate tension performance of glulams. In answer to

a request by DR SMITH, an explanation was given of some adjustments that were made between moduli of elasticity measured when machine grading the laminations and the ensuing moduli of the beams.

Paper 26-12-2 "Simulation analysis of Norwegian spruce glued laminated timber" by R Hernandez and R H Falk was presented by DR FALK. The aims of the work were to determine CEN Standard strength class assignments for Norwegian glulam and at the same time to collect data for both the European and the North American (PROLAM) glulam simulation models. Some special tests were performed to measure some extra properties for the PROLAM model. MR LARSEN expressed some reservations on the accuracy resulting from the PROLAM model, particularly when initial failures in laminations other than the outermost ones were suggested by the simulation.

Paper 26-12-3 "Investigation of laminating effects in glued-laminated timber" by F Colling and R H Falk was presented by DR FALK. The paper provided explanations for several laminating effects which are becoming recognised by European researchers but which are not yet universally acknowledged in North America. It separated laminating effects into several constituents such as the greater effect of eccentricities on the tensile strength of individual laminations; the reinforcing effect upon knots, and the dispersion effect. The paper was received without a great deal of comment or discussion.

Paper 26-12-4 "Comparison between EC5 design and CB71 design for French glulam" was presented by its author, DR ROUGER. Commenting upon the Paper, PROF EHLBECK pointed out that since the design calibrations all seem to have been reported with an assumption of 50% live loads and 50% dead loads, they may not be fully applicable to all of the economically important structural situations in which glulam will be designed with EC5.

6. MECHANICAL TIMBER JOINTS

Paper 26-7-1 "Proposed test method for dynamic properties of connections assembled with mechanical fasteners" was presented by the author, DR DOLAN. The test method described involves full reversal cyclic loading, with frequencies in the realms which are of importance in seismic design. The proposals were being circulated widely amongst timber researchers who are involved in seismic considerations, since it is felt that it would be highly desirable to achieve harmony in the testing and design of connections. DR CECCOTTI had several comments and questions. These concerned the frequencies of oscillations in real earthquakes, compared with the structural response of various sizes of construction, and also the ways of defining elastic-perfectly plastic load-displacement behaviour. The author said that there was a strong belief amongst North American earthquake experts who are involved in reinforced concrete structures, that seismic "pulse" loadings at peak levels lower than the absolute maxima were having a significant influence upon the subsequent behaviour of the assembly. He felt it was necessary also to assess this effect in timber connections. DR SMITH initiated some discussion of the response of timber connections when members at angles intermediate between zero and ninety degrees were involved, and also when there was "group action". It was agreed that there was a need for more

research on this topic. MR LARSEN was concerned over the complexities and cost of the test procedures inferred by the North American assumptions. He thought that for large displacements in real structures, full reversal loading at frequencies in the order of 1Hz would be difficult to control in the laboratory and should only be attempted if it was absolutely certain that full-sized structures or the relevant components behaved in this way in reality.

Paper 26-7-2 "Validatory tests and proposed design formulae for the load-carrying capacity of toothed plate connector joints" by C J Mettem, A V Page and G Davis was presented by MR METTEM. Referring to the proposed design equations, PROF BLASS pointed out that in his previous work, a minimum timber thickness was specified and he asked MR METTEM if this was taken into account. MR METTEM replied that this was not yet the case but that it was realised that it would be included when full design proposals compatible with EC5 were developed. MR LARSEN said that the formulae adopted in EC5 for dowels have a lower safety value and ignore friction and the toggle effect which occurs in bolted joints. He felt that the authors would be justified in making a similar decision in respect of connector joints. The reason for this was to keep the same equation formats for both bolts and dowels. PROF GEHRI noted that the values stated from these tests were for one set of connectors on a bolt and asked in the design context how many connectors would be permissible in a row. MR METTEM replied that this would be the subject of further ongoing work and that the group action effect would probably be considerable. MR LARSEN added that the paper showed three alternative expressions and that it would be interesting if all available test results of this type could be re-evaluated together, and the formulae applied to them. He noted that the results from the two laboratories appeared to correlate well. DR SMITH added that the methods presented seemed similar in general terms to the approach which was being adopted in the US.

Paper 26-7-3 "Definition of terms and multi-language terminology pertaining to metal connector plates" was presented by PROF STERN. Following the presentation of this Paper, there was considerable debate about the appropriateness of such a document and its intended purpose. It was noted that PROF STERN prepared this document with the help of experts, but that it did not have the general support of the meeting.

Paper 26-7-4 "Design of joints based on in V-shape glued-in rods" was presented by DR KANGAS. PROF BLASS asked the author how the connectors had been made. DR KANGAS replied that, in most cases, the plates were welded *in situ* to the rods which had previously been glued into the timber, the only exception being the rods in compression, which were welded before gluing. There appeared to be no problem with welding steel so close to timber. DR SMITH asked how shear connections were made using this technique. DR KANGAS replied that the holes for the rods were extended and the steel plate was fixed over the ends of the timber levellers. PROF GEHRI asked if the angle of the rods had any influence on the tension capacity of the joint. DR KANGAS replied that some splitting did appear at very steep angles but otherwise there was no appreciable effect.

Paper 26-7-5 "Timber-concrete-composite structural elements" was presented by the author, MR MEIERHOFER. It described work which is still in progress at EMPA. In order to ensure a fully composite action between timber and concrete, special shear connectors had been developed. These were applied at a variety of angles and

patterns, in order to obtain the optimum composite action. In full-sized bending tests, the influence of variable humidity conditions and load duration was being studied. The influence of climatic conditions seemed to be substantial, causing creep factors in the order of 2.2 to 3.3. In response to a question from MR ABBOTT as to the application of such forms of construction, the author said that in Switzerland timber-concrete composites were used in both residential and commercial construction. These methods could also have advantages compared with purely concrete constructions in seismic regions. PROF GEHRI added that timber-concrete composites are considered in some circumstances as a structural repair method.

7. SERVICEABILITY CONSIDERATIONS IN STRUCTURAL TIMBER DESIGN

Paper 26-9-1 "Long-term deformations of wood-based panels under natural climatic conditions - a comparative study" was presented by DR THELANDERSSON. In response to a question from PROF EHLBECK, the author confirmed that the creep factors in his work were based on definitions in Eurocode 5. PROF GEHRI asked if the loads applied for the initial deformation were representative of loads likely to be experienced in service. DR THELANDERSSON replied that attempts were made to set the levels according to design considerations. MR ABBOTT asked which material properties were used to calculate the initial deflections, to which the author replied that mean values of MOE from the Swedish Code were used. MR ABBOTT further asked whether the same relative performance between materials would have been achieved if the loads used were design loads based on ultimate limit states. DR THELANDERSSON replied that they would have been much higher. DR SMITH pointed out that the specimens were relatively small and that the high proportion of edges would greatly increase the moisture effects. DR THELANDERSSON replied that the researchers had been very careful to ensure that all edges were sealed prior to testing. DR SMITH said that with OSB, the size of the wafer is comparable to the depth of the specimen, and this could cause problems. PROF BLASS asked why it was not decided to measure initial deflections for all materials. DR THELANDERSSON replied that all were measured, but it was decided to present the results on a calculation basis.

8. OPEN FORUM

Paper 26-5-1 "Structural properties of French grown timber according to various grading methods" was presented by DR ROUGER. DR SMITH commented that the depth effect recorded was not surprising as it is dependent upon many factors, not just specimen geometry. Different sizes of depth effect would also be expected on different products. Referring to previous work by himself and DR BARRETT, MR FEWELL said that there is a lot of variability in depth factors which depend upon log type, grading method, sawing patterns, etc. In the work presented in the Paper, all material sizes were selected at random and therefore did not reflect commercial practice. With a commercial strength class system, only a single size factor is practicable. MR LARSEN questioned whether the rejects defined in the work were on the basis of low strength or low stiffness, and asked whether there was anything to link these together. He asked whether this information could be used to develop new

grading criteria. DR ROUGER said that the data are still being analysed and that he intends looking into this.

Paper 26-6-1 "Discussion and proposal of a general failure criterion for wood" by DR VAN DER PUT was presented by PROF BLASS. As the author was not present at the meeting, PROF BLASS asked that, if members had any particular questions or suggestions on this Paper, they should be referred directly to the author in writing.

9. ANY OTHER BUSINESS

There was none.

10. VENUE AND PROGRAMME FOR NEXT MEETING

PROF BLASS reported that the next meeting is scheduled for 7/8 July 1994 and will take place in Sydney, Australia. Only 1½ days have been allocated for the meeting, and therefore a maximum of 15 Papers will be considered. Priority topics already suggested are "Bridges" and "Serviceability".

It was also announced that in 1995, it is proposed that the meeting be held in Copenhagen from Tuesday, 18 April (starting at 1 p.m.) until Friday, 21 April. The meeting for 1996 has preliminarily been scheduled for the end of August or the beginning of September in Bordeaux, France.

It was mentioned that in 1994, a IUFRO meeting is to be held in Australia from 5 to 7 July. This will finish at lunch-time on the last day. Members should also note that the Pacific Timber Engineering Conference (PTEC 94) starts on 11 July. There is also a proposal for a meeting on full-scale testing of buildings in Australia in 1994 at about the same time as the Engineering Conference. It was hoped that DR LEICESTER will provide further details of this.

11. CLOSE

There being no further business, the Chairman declared the meeting closed.

**12. List of CIB-W18 Papers,
Athens, USA 1993**

12. LIST OF CIB-W18 PAPERS, Athens, USA 1993

- 26-5-1 Structural Properties of French Grown Timber According to Various Grading Methods - F Rouger, C De Lafond and A El Quadrani
- 26-6-1 Discussion and Proposal of a General Failure Criterion for Wood - T A C M van der Put
- 26-7-1 Proposed Test Method for Dynamic Properties of Connections Assembled with Mechanical Fasteners - J D Dolan
- 26-7-2 Validatory Tests and Proposed Design Formulae for the Load-Carrying Capacity of Toothed-Plate Connected Joints - C J Mettem, A V Page and G Davis
- 26-7-3 Definitions of Terms and Multi-Language Terminology Pertaining to Metal Connector Plates - E G Stern
- 26-7-4 Design of Joints Based on in V-Shape Glued-in Rods - J Kangas
- 26-7-5 Tests on Timber Concrete Composite Structural Elements (TCCs) - A U Meierhofer
- 26-9-1 Long Term Deformations in Wood Based Panels under Natural Climate Conditions. A Comparative Study - S Thelandersson, J Nordh, T Nordh and S Sandahl
- 26-12-1 Norwegian Bending Tests with Glued Laminated Beams-Comparative Calculations with the "Karlsruhe Calculation Model" - E Aasheim, K Solli, F Colling, R H Falk, J Ehlbeck and R Görlacher
- 26-12-2 Simulation Analysis of Norwegian Spruce Glued-Laminated Timber - R Hernandez and R H Falk
- 26-12-3 Investigation of Laminating Effects in Glued-Laminated Timber - F Colling and R H Falk
- 26-12-4 Comparing Design Results for Glulam Beams According to Eurocode 5 and to the French Working Stress Design Code (CB71) - F Rouger
- 26-14-1 Test of Nail Plates Subjected to Moment - E Aasheim
- 26-14-2 Moment Anchorage Capacity of Nail Plates - A Kevarinmäki and J Kangas

- 26-14-3 Rotational Stiffness of Nail Plates in Moment Anchorage -
A Kevarinmäki and J Kangas
- 26-14-4 Solution of Plastic Moment Anchorage Stress in Nail Plates -
A Kevarinmäki
- 26-14-5 Testing of Metal-Plate-Connected Wood-Truss Joints - R Gupta
- 26-14-6 Simulated Accidental Events on a Trussed Rafter Roofed Building -
C J Mettem and J P Marcroft
- 26-15-1 Bracing Requirements to Prevent Lateral Buckling in Trussed Rafters -
C J Mettem and P J Moss
- 26-15-2 Eurocode 8 - Part 1.3 - Chapter 5 - Specific Rules for Timber Buildings
in Seismic Regions - K Becker, A Ceccotti, H Charlier, E Katsaragakis,
H J Larsen and H Zeitter
- 26-15-3 Hurricane Andrew - Structural Performance of Buildings in South
Florida - M R O'Halloran, E L Keith, J D Rose and T P Cunningham
- 26-16-1 Structural Fire Design According to Eurocode 5, Part 1.2 - J König

13. Current List of CIB-W18(A) Papers

13. CURRENT LIST OF CIB-W18(A) PAPERS

Technical papers presented to CIB-W18(A) are identified by a code CIB-W18(A)/a-b-c, where:

- a denotes the meeting at which the paper was presented.
Meetings are classified in chronological order:

- 1 Princes Risborough, England; March 1973
- 2 Copenhagen, Denmark; October 1973
- 3 Delft, Netherlands; June 1974
- 4 Paris, France; February 1975
- 5 Karlsruhe, Federal Republic of Germany; October 1975
- 6 Aalborg, Denmark; June 1976
- 7 Stockholm, Sweden; February/March 1977
- 8 Brussels, Belgium; October 1977
- 9 Perth, Scotland; June 1978
- 10 Vancouver, Canada; August 1978
- 11 Vienna, Austria; March 1979
- 12 Bordeaux, France; October 1979
- 13 Otaniemi, Finland; June 1980
- 14 Warsaw, Poland; May 1981
- 15 Karlsruhe, Federal Republic of Germany; June 1982
- 16 Lillehammer, Norway; May/June 1983
- 17 Rapperswil, Switzerland; May 1984
- 18 Beit Oren, Israel; June 1985
- 19 Florence, Italy; September 1986
- 20 Dublin, Ireland; September 1987
- 21 Parksville, Canada; September 1988
- 22 Berlin, German Democratic Republic; September 1989
- 23 Lisbon, Portugal; September 1990
- 24 Oxford, United Kingdom; September 1991
- 25 Åhus, Sweden; August 1992
- 26 Athens, USA; August 1993

b denotes the subject:

- 1 Limit State Design
- 2 Timber Columns
- 3 Symbols
- 4 Plywood
- 5 Stress Grading
- 6 Stresses for Solid Timber
- 7 Timber Joints and Fasteners
- 8 Load Sharing
- 9 Duration of Load
- 10 Timber Beams
- 11 Environmental Conditions
- 12 Laminated Members
- 13 Particle and Fibre Building Boards
- 14 Trussed Rafters
- 15 Structural Stability
- 16 Fire
- 17 Statistics and Data Analysis
- 18 Glued Joints
- 19 Fracture Mechanics
- 100 CIB Timber Code
- 101 Loading Codes
- 102 Structural Design Codes
- 103 International Standards Organisation
- 104 Joint Committee on Structural Safety
- 105 CIB Programme, Policy and Meetings
- 106 International Union of Forestry Research Organisations

c is simply a number given to the papers in the order in which they appear:

Example: CIB-W18/4-102-5 refers to paper 5 on subject 102 presented at the fourth meeting of W18.

Listed below, by subjects, are all papers that have to date been presented to W18. When appropriate some papers are listed under more than one subject heading.

LIMIT STATE DESIGN

- 1-1-1 Limit State Design - H J Larsen
- 1-1-2 The Use of Partial Safety Factors in the New Norwegian Design Code for Timber Structures - O Brynildsen
- 1-1-3 Swedish Code Revision Concerning Timber Structures - B Noren
- 1-1-4 Working Stresses Report to British Standards Institution Committee BLC/17/2
- 6-1-1 On the Application of the Uncertainty Theoretical Methods for the Definition of the Fundamental Concepts of Structural Safety - K Skov and O Ditlevsen
- 11-1-1 Safety Design of Timber Structures - H J Larsen
- 18-1-1 Notes on the Development of a UK Limit States Design Code for Timber - A R Fewell and C B Pierce
- 18-1-2 Eurocode 5, Timber Structures - H J Larsen
- 19-1-1 Duration of Load Effects and Reliability Based Design (Single Member) - R O Foschi and Z C Yao
- 21-102-1 Research Activities Towards a New GDR Timber Design Code Based on Limit States Design - W Rug and M Badstube
- 22-1-1 Reliability-Theoretical Investigation into Timber Components Proposal for a Supplement of the Design Concept - M Badstube, W Rug and R Plessow
- 23-1-1 Some Remarks about the Safety of Timber Structures - J Kuipers
- 23-1-2 Reliability of Wood Structural Elements: A Probabilistic Method to Eurocode 5 Calibration - F Rouger, N Lheritier, P Racher and M Fogli

TIMBER COLUMNS

- 2-2-1 The Design of Solid Timber Columns - H J Larsen
- 3-2-1 The Design of Built-Up Timber Columns - H J Larsen
- 4-2-1 Tests with Centrally Loaded Timber Columns - H J Larsen and S S Pedersen
- 4-2-2 Lateral-Torsional Buckling of Eccentrically Loaded Timber Columns - B Johansson
- 5-9-1 Strength of a Wood Column in Combined Compression and Bending with Respect to Creep - B Källsner and B Norén
- 5-100-1 Design of Solid Timber Columns (First Draft) - H J Larsen
- 6-100-1 Comments on Document 5-100-1, Design of Solid Timber Columns - H J Larsen and E Theilgaard
- 6-2-1 Lattice Columns - H J Larsen
- 6-2-2 A Mathematical Basis for Design Aids for Timber Columns - H J Burgess
- 6-2-3 Comparison of Larsen and Perry Formulas for Solid Timber Columns - H J Burgess
- 7-2-1 Lateral Bracing of Timber Struts - J A Simon
- 8-15-1 Laterally Loaded Timber Columns: Tests and Theory - H J Larsen
- 17-2-1 Model for Timber Strength under Axial Load and Moment - T Poutanen
- 18-2-1 Column Design Methods for Timber Engineering - A H Buchanan, K C Johns, B Madsen
- 19-2-1 Creep Buckling Strength of Timber Beams and Columns - R H Leicester
- 19-12-2 Strength Model for Glulam Columns - H J Blaß

- 20-2-1 Lateral Buckling Theory for Rectangular Section Deep Beam-Columns
- H J Burgess
- 20-2-2 Design of Timber Columns - H J Blaß
- 21-2-1 Format for Buckling Strength - R H Leicester
- 21-2-2 Beam-Column Formulae for Design Codes - R H Leicester
- 21-15-1 Rectangular Section Deep Beam - Columns with Continuous Lateral
Restraint - H J Burgess
- 21-15-2 Buckling Modes and Permissible Axial Loads for Continuously Braced
Columns - H J Burgess
- 21-15-3 Simple Approaches for Column Bracing Calculations - H J Burgess
- 21-15-4 Calculations for Discrete Column Restraints - H J Burgess
- 22-2-1 Buckling and Reliability Checking of Timber Columns - S Huang,
P M Yu and J Y Hong
- 22-2-2 Proposal for the Design of Compressed Timber Members by Adopting
the Second-Order Stress Theory - P Kaiser

SYMBOLS

- 3-3-1 Symbols for Structural Timber Design - J Kuipers and B Norén
- 4-3-1 Symbols for Timber Structure Design - J Kuipers and B Norén
- 1 Symbols for Use in Structural Timber Design

PLYWOOD

- 2-4-1 The Presentation of Structural Design Data for Plywood - L G Booth
- 3-4-1 Standard Methods of Testing for the Determination of Mechanical Properties of Plywood - J Kuipers
- 3-4-2 Bending Strength and Stiffness of Multiple Species Plywood
- C K A Stieda
- 4-4-4 Standard Methods of Testing for the Determination of Mechanical Properties of Plywood - Council of Forest Industries, B.C.
- 5-4-1 The Determination of Design Stresses for Plywood in the Revision of CP 112 - L G Booth
- 5-4-2 Veneer Plywood for Construction - Quality Specifications
- ISO/TC 139. Plywood, Working Group 6
- 6-4-1 The Determination of the Mechanical Properties of Plywood Containing Defects - L G Booth
- 6-4-2 Comparison of the Size and Type of Specimen and Type of Test on Plywood Bending Strength and Stiffness - C R Wilson and P Eng
- 6-4-3 Buckling Strength of Plywood: Results of Tests and Recommendations for Calculations - J Kuipers and H Ploos van Amstel
- 7-4-1 Methods of Test for the Determination of Mechanical Properties of Plywood - L G Booth, J Kuipers, B Norén, C R Wilson
- 7-4-2 Comments Received on Paper 7-4-1
- 7-4-3 The Effect of Rate of Testing Speed on the Ultimate Tensile Stress of Plywood - C R Wilson and A V Parasin
- 7-4-4 Comparison of the Effect of Specimen Size on the Flexural Properties of Plywood Using the Pure Moment Test - C R Wilson and A V Parasin
- 8-4-1 Sampling Plywood and the Evaluation of Test Results - B Norén
- 9-4-1 Shear and Torsional Rigidity of Plywood - H J Larsen

- 9-4-2 The Evaluation of Test Data on the Strength Properties of Plywood
- L G Booth
- 9-4-3 The Sampling of Plywood and the Derivation of Strength Values
(Second Draft) - B Norén
- 9-4-4 On the Use of the CIB/RILEM Plywood Plate Twisting Test: a
progress report - L G Booth
- 10-4-1 Buckling Strength of Plywood - J Dekker, J Kuipers and
H Ploos van Amstel
- 11-4-1 Analysis of Plywood Stressed Skin Panels with Rigid or Semi-Rigid
Connections - I Smith
- 11-4-2 A Comparison of Plywood Modulus of Rigidity Determined by the
ASTM and RILEM CIB/3-TT Test Methods - C R Wilson and
A V Parasin
- 11-4-3 Sampling of Plywood for Testing Strength - B Norén
- 12-4-1 Procedures for Analysis of Plywood Test Data and Determination of
Characteristic Values Suitable for Code Presentation - C R Wilson
- 14-4-1 An Introduction to Performance Standards for Wood-base Panel
Products - D H Brown
- 14-4-2 Proposal for Presenting Data on the Properties of Structural Panels
- T Schmidt
- 16-4-1 Planar Shear Capacity of Plywood in Bending - C K A Stieda
- 17-4-1 Determination of Panel Shear Strength and Panel Shear Modulus of
Beech-Plywood in Structural Sizes - J Ehlbeck and F Colling
- 17-4-2 Ultimate Strength of Plywood Webs - R H Leicester and L Pham
- 20-4-1 Considerations of Reliability - Based Design for Structural Composite
Products - M R O'Halloran, J A Johnson, E G Elias and
T P Cunningham
- 21-4-1 Modelling for Prediction of Strength of Veneer Having Knots
- Y Hirashima

- 22-4-1 Scientific Research into Plywood and Plywood Building Constructions the Results and Findings of which are Incorporated into Construction Standard Specifications of the USSR - I M Guskov
- 22-4-2 Evaluation of Characteristic values for Wood-Based Sheet Materials - E G Elias
- 24-4-1 APA Structural-Use Design Values: An Update to Panel Design Capacities - A L Kuchar, E G Elias, B Yeh and M R O'Halloran

STRESS GRADING

- 1-5-1 Quality Specifications for Sawn Timber and Precision Timber - Norwegian Standard NS 3080
- 1-5-2 Specification for Timber Grades for Structural Use - British Standard BS 4978
- 4-5-1 Draft Proposal for an International Standard for Stress Grading Coniferous Sawn Softwood - ECE Timber Committee
- 16-5-1 Grading Errors in Practice - B Thunell
- 16-5-2 On the Effect of Measurement Errors when Grading Structural Timber - L Nordberg and B Thunell
- 19-5-1 Stress-Grading by ECE Standards of Italian-Grown Douglas-Fir Dimension Lumber from Young Thinnings - L Uzielli
- 19-5-2 Structural Softwood from Afforestation Regions in Western Norway - R Lackner
- 21-5-1 Non-Destructive Test by Frequency of Full Size Timber for Grading - T Nakai
- 22-5-1 Fundamental Vibration Frequency as a Parameter for Grading Sawn Timber - T Nakai, T Tanaka and H Nagao
- 24-5-1 Influence of Stress Grading System on Length Effect Factors for Lumber Loaded in Compression - A Campos and I Smith

- 26-5-1 Structural Properties of French Grown Timber According to Various Grading Methods - F Rouger, C De Lafond and A El Quadrani

STRESSES FOR SOLID TIMBER

- 4-6-1 Derivation of Grade Stresses for Timber in the UK - W T Curry
- 5-6-1 Standard Methods of Test for Determining some Physical and Mechanical Properties of Timber in Structural Sizes - W T Curry
- 5-6-2 The Description of Timber Strength Data - J R Tory
- 5-6-3 Stresses for EC1 and EC2 Stress Grades - J R Tory
- 6-6-1 Standard Methods of Test for the Determination of some Physical and Mechanical Properties of Timber in Structural Sizes (third draft) - W T Curry
- 7-6-1 Strength and Long-term Behaviour of Lumber and Glued Laminated Timber under Torsion Loads - K Möhler
- 9-6-1 Classification of Structural Timber - H J Larsen
- 9-6-2 Code Rules for Tension Perpendicular to Grain - H J Larsen
- 9-6-3 Tension at an Angle to the Grain - K Möhler
- 9-6-4 Consideration of Combined Stresses for Lumber and Glued Laminated Timber - K Möhler
- 11-6-1 Evaluation of Lumber Properties in the United States - W L Galligan and J H Haskell
- 11-6-2 Stresses Perpendicular to Grain - K Möhler
- 11-6-3 Consideration of Combined Stresses for Lumber and Glued Laminated Timber (addition to Paper CIB-W18/9-6-4) - K Möhler
- 12-6-1 Strength Classifications for Timber Engineering Codes - R H Leicester and W G Keating

- 12-6-2 Strength Classes for British Standard BS 5268 - J R Tory
- 13-6-1 Strength Classes for the CIB Code - J R Tory
- 13-6-2 Consideration of Size Effects and Longitudinal Shear Strength for Uncracked Beams - R O Foschi and J D Barrett
- 13-6-3 Consideration of Shear Strength on End-Cracked Beams - J D Barrett and R O Foschi
- 15-6-1 Characteristic Strength Values for the ECE Standard for Timber - J G Sunley
- 16-6-1 Size Factors for Timber Bending and Tension Stresses - A R Fewell
- 16-6-2 Strength Classes for International Codes - A R Fewell and J G Sunley
- 17-6-1 The Determination of Grade Stresses from Characteristic Stresses for BS 5268: Part 2 - A R Fewell
- 17-6-2 The Determination of Softwood Strength Properties for Grades, Strength Classes and Laminated Timber for BS 5268: Part 2 - A R Fewell
- 18-6-1 Comment on Papers: 18-6-2 and 18-6-3 - R H Leicester
- 18-6-2 Configuration Factors for the Bending Strength of Timber - R H Leicester
- 18-6-3 Notes on Sampling Factors for Characteristic Values - R H Leicester
- 18-6-4 Size Effects in Timber Explained by a Modified Weakest Link Theory - B Madsen and A H Buchanan
- 18-6-5 Placement and Selection of Growth Defects in Test Specimens - H Riberholt
- 18-6-6 Partial Safety-Coefficients for the Load-Carrying Capacity of Timber Structures - B Norén and J-O Nylander
- 19-6-1 Effect of Age and/or Load on Timber Strength - J Kuipers
- 19-6-2 Confidence in Estimates of Characteristic Values - R H Leicester

- 19-6-3 Fracture Toughness of Wood - Mode I - K Wright and M Fonselius
- 19-6-4 Fracture Toughness of Pine - Mode II - K Wright
- 19-6-5 Drying Stresses in Round Timber - A Ranta-Maunus
- 19-6-6 A Dynamic Method for Determining Elastic Properties of Wood
- R Görlacher
- 20-6-1 A Comparative Investigation of the Engineering Properties of
"Whitewoods" Imported to Israel from Various Origins - U Korin
- 20-6-2 Effects of Yield Class, Tree Section, Forest and Size on Strength of
Home Grown Sitka Spruce - V Picardo
- 20-6-3 Determination of Shear Strength and Strength Perpendicular to Grain
- H J Larsen
- 21-6-1 Draft Australian Standard: Methods for Evaluation of Strength and
Stiffness of Graded Timber - R H Leicester
- 21-6-2 The Determination of Characteristic Strength Values for Stress
Grades of Structural Timber. Part 1 - A R Fewell and P Glos
- 21-6-3 Shear Strength in Bending of Timber -U Korin
- 22-6-1 Size Effects and Property Relationships for Canadian 2-inch Dimension
Lumber - J D Barrett and H Griffin
- 22-6-2 Moisture Content Adjustements for In-Grade Data - J D Barrett and
W Lau
- 22-6-3 A Discussion of Lumber Property Relationships in Eurocode 5
- D W Green and D E Kretschmann
- 22-6-4 Effect of Wood Preservatives on the Strength Properties of Wood
- F Ronai
- 23-6-1 Timber in Compression Perpendicular to Grain - U Korin
- 24-6-1 Discussion of the Failure Criterion for Combined Bending and
Compression - T A C M van der Put

- 24-6-3 Effect of Within Member Variability on Bending Strength of Structural Timber - I Czmocho, S Thelandersson and H J Larsen
- 24-6-4 Protection of Structural Timber Against Fungal Attack Requirements and Testing - K Jaworska, M Rylko and W Nozynski
- 24-6-5 Derivation of the Characteristic Bending Strength of Solid Timber According to CEN-Document prEN 384 - A J M Leijten
- 25-6-1 Moment Configuration Factors for Simple Beams- T D G Canisius
- 25-6-3 Bearing Capacity of Timber - U Korin
- 25-6-4 On Design Criteria for Tension Perpendicular to Grain - H Petersson
- 25-6-5 Size Effects in Visually Graded Softwood Structural Lumber - J D Barrett, F Lam and W Lau
- 26-6-1 Discussion and Proposal of a General Failure Criterion for Wood - T A C M van der Put

TIMBER JOINTS AND FASTENERS

- 1-7-1 Mechanical Fasteners and Fastenings in Timber Structures - E G Stern
- 4-7-1 Proposal for a Basic Test Method for the Evaluation of Structural Timber Joints with Mechanical Fasteners and Connectors
- RILEM 3TT Committee
- 4-7-2 Test Methods for Wood Fasteners - K Möhler
- 5-7-1 Influence of Loading Procedure on Strength and Slip-Behaviour in Testing Timber Joints - K Möhler
- 5-7-2 Recommendations for Testing Methods for Joints with Mechanical Fasteners and Connectors in Load-Bearing Timber Structures
- RILEM 3 TT Committee
- 5-7-3 CIB-Recommendations for the Evaluation of Results of Tests on Joints with Mechanical Fasteners and Connectors used in Load-Bearing Timber Structures - J Kuipers

- 6-7-1 Recommendations for Testing Methods for Joints with Mechanical Fasteners and Connectors in Load-Bearing Timber Structures (seventh draft) - RILEM 3 TT Committee
- 6-7-2 Proposal for Testing Integral Nail Plates as Timber Joints - K Möhler
- 6-7-3 Rules for Evaluation of Values of Strength and Deformation from Test Results - Mechanical Timber Joints - M Johansen, J Kuipers, B Norén
- 6-7-4 Comments to Rules for Testing Timber Joints and Derivation of Characteristic Values for Rigidity and Strength - B Norén
- 7-7-1 Testing of Integral Nail Plates as Timber Joints - K Möhler
- 7-7-2 Long Duration Tests on Timber Joints - J Kuipers
- 7-7-3 Tests with Mechanically Jointed Beams with a Varying Spacing of Fasteners - K Möhler
- 7-100-1 CIB-Timber Code Chapter 5.3 Mechanical Fasteners; CIB-Timber Standard 06 and 07 - H J Larsen
- 9-7-1 Design of Truss Plate Joints - F J Keenan
- 9-7-2 Staples - K Möhler
- 11-7-1 A Draft Proposal for International Standard: ISO Document ISO/TC 165N 38E
- 12-7-1 Load-Carrying Capacity and Deformation Characteristics of Nailed Joints - J Ehlbeck
- 12-7-2 Design of Bolted Joints - H J Larsen
- 12-7-3 Design of Joints with Nail Plates - B Norén
- 13-7-1 Polish Standard BN-80/7159-04: Parts 00-01-02-03-04-05. "Structures from Wood and Wood-based Materials. Methods of Test and Strength Criteria for Joints with Mechanical Fasteners"
- 13-7-2 Investigation of the Effect of Number of Nails in a Joint on its Load Carrying Ability - W Nozynski

- 13-7-3 International Acceptance of Manufacture, Marking and Control of Finger-jointed Structural Timber - B Norén
- 13-7-4 Design of Joints with Nail Plates - Calculation of Slip - B Norén
- 13-7-5 Design of Joints with Nail Plates - The Heel Joint - B Källsner
- 13-7-6 Nail Deflection Data for Design - H J Burgess
- 13-7-7 Test on Bolted Joints - P Vermeijden
- 13-7-8 Comments to paper CIB-W18/12-7-3 "Design of Joints with Nail Plates" - B Norén
- 13-7-9 Strength of Finger Joints - H J Larsen
- 13-100-4 CIB Structural Timber Design Code. Proposal for Section 6.1.5 Nail Plates - N I Bovim
- 14-7-1 Design of Joints with Nail Plates (second edition) - B Norén
- 14-7-2 Method of Testing Nails in Wood (second draft, August 1980) - B Norén
- 14-7-3 Load-Slip Relationship of Nailed Joints - J Ehlbeck and H J Larsen
- 14-7-4 Wood Failure in Joints with Nail Plates - B Norén
- 14-7-5 The Effect of Support Eccentricity on the Design of W- and WW-Trussed with Nail Plate Connectors - B Källsner
- 14-7-6 Derivation of the Allowable Load in Case of Nail Plate Joints Perpendicular to Grain - K Möhler
- 14-7-7 Comments on CIB-W18/14-7-1 - T A C M van der Put
- 15-7-1 Final Recommendation TT-1A: Testing Methods for Joints with Mechanical Fasteners in Load-Bearing Timber Structures. Annex A Punched Metal Plate Fasteners - Joint Committee RILEM/CIB-3TT
- 16-7-1 Load Carrying Capacity of Dowels - E Gehri
- 16-7-2 Bolted Timber Joints: A Literature Survey - N Harding

- 16-7-3 Bolted Timber Joints: Practical Aspects of Construction and Design; a Survey - N Harding
- 16-7-4 Bolted Timber Joints: Draft Experimental Work Plan - Building Research Association of New Zealand
- 17-7-1 Mechanical Properties of Nails and their Influence on Mechanical Properties of Nailed Timber Joints Subjected to Lateral Loads - I Smith, L R J Whale, C Anderson and L Held
- 17-7-2 Notes on the Effective Number of Dowels and Nails in Timber Joints - G Steck
- 18-7-1 Model Specification for Driven Fasteners for Assembly of Pallets and Related Structures - E G Stern and W B Wallin
- 18-7-2 The Influence of the Orientation of Mechanical Joints on their Mechanical Properties - I Smith and L R J Whale
- 18-7-3 Influence of Number of Rows of Fasteners or Connectors upon the Ultimate Capacity of Axially Loaded Timber Joints - I Smith and G Steck
- 18-7-4 A Detailed Testing Method for Nailplate Joints - J Kangas
- 18-7-5 Principles for Design Values of Nailplates in Finland - J Kangas
- 18-7-6 The Strength of Nailplates - N I Bovim and E Aasheim
- 19-7-1 Behaviour of Nailed and Bolted Joints under Short-Term Lateral Load - Conclusions from Some Recent Research - L R J Whale, I Smith and B O Hilson
- 19-7-2 Glued Bolts in Glulam - H Riberholt
- 19-7-3 Effectiveness of Multiple Fastener Joints According to National Codes and Eurocode 5 (Draft) - G Steck
- 19-7-4 The Prediction of the Long-Term Load Carrying Capacity of Joints in Wood Structures - Y M Ivanov and Y Y Slavic
- 19-7-5 Slip in Joints under Long-Term Loading - T Feldborg and M Johansen

- 19-7-6 The Derivation of Design Clauses for Nailed and Bolted Joints in Eurocode 5 - L R J Whale and I Smith
- 19-7-7 Design of Joints with Nail Plates - Principles - B Norén
- 19-7-8 Shear Tests for Nail Plates - B Norén
- 19-7-9 Advances in Technology of Joints for Laminated Timber - Analyses of the Structural Behaviour - M Piazza and G Turrini
- 19-15-1 Connections Deformability in Timber Structures: A Theoretical Evaluation of its Influence on Seismic Effects - A Ceccotti and A Vignoli
- 20-7-1 Design of Nailed and Bolted Joints-Proposals for the Revision of Existing Formulae in Draft Eurocode 5 and the CIB Code - L R J Whale, I Smith and H J Larsen
- 20-7-2 Slip in Joints under Long Term Loading - T Feldborg and M Johansen
- 20-7-3 Ultimate Properties of Bolted Joints in Glued-Laminated Timber - M Yasumura, T Murota and H Sakai
- 20-7-4 Modelling the Load-Deformation Behaviour of Connections with Pin-Type Fasteners under Combined Moment, Thrust and Shear Forces - I Smith
- 21-7-1 Nails under Long-Term Withdrawal Loading - T Feldborg and M Johansen
- 21-7-2 Glued Bolts in Glulam-Proposals for CIB Code - H Riberholt
- 21-7-3 Nail Plate Joint Behaviour under Shear Loading - T Poutanen
- 21-7-4 Design of Joints with Laterally Loaded Dowels. Proposals for Improving the Design Rules in the CIB Code and the Draft Eurocode 5 - J Ehlbeck and H Werner
- 21-7-5 Axially Loaded Nails: Proposals for a Supplement to the CIB Code - J Ehlbeck and W Siebert
- 22-7-1 End Grain Connections with Laterally Loaded Steel Bolts A draft proposal for design rules in the CIB Code - J Ehlbeck and M Gerold

- 22-7-2 Determination of Perpendicular-to-Grain Tensile Stresses in Joints with Dowel-Type Fasteners - A draft proposal for design rules - J Ehlbeck, R Görlacher and H Werner
- 22-7-3 Design of Double-Shear Joints with Non-Metallic Dowels A proposal for a supplement of the design concept - J Ehlbeck and O Eberhart
- 22-7-4 The Effect of Load on Strength of Timber Joints at high Working Load Level - A J M Leijten
- 22-7-5 Plasticity Requirements for Portal Frame Corners - R Gunnewijk and A J M Leijten
- 22-7-6 Background Information on Design of Glulam Rivet Connections in CSA/CAN3-086.1-M89 - A proposal for a supplement of the design concept - E Karacabeyli and D P Janssens
- 22-7-7 Mechanical Properties of Joints in Glued-Laminated Beams under Reversed Cyclic Loading - M Yasumura
- 22-7-8 Strength of Glued Lap Timber Joints - P Glos and H Horstmann
- 22-7-9 Toothed Rings Type Bistyp 075 at the Joints of Fir Wood - J Kerste
- 22-7-10 Calculation of Joints and Fastenings as Compared with the International State - K Zimmer and K Lissner
- 22-7-11 Joints on Glued-in Steel Bars Present Relatively New and Progressive Solution in Terms of Timber Structure Design - G N Zubarev, F A Boitemirov and V M Golovina
- 22-7-12 The Development of Design Codes for Timber Structures made of Compositive Bars with Plate Joints based on Cylindrical Nails - Y V Piskunov
- 22-7-13 Designing of Glued Wood Structures Joints on Glued-in Bars - S B Turkovsky
- 23-7-1 Proposal for a Design Code for Nail Plates - E Aasheim and K H Solli
- 23-7-2 Load Distribution in Nailed Joints - H J Blass

- 24-7-1 Theoretical and Experimental Tension and Shear Capacity of Nail Plate Connections - B Källsner and J Kangas
- 24-7-2 Testing Method and Determination of Basic Working Loads for Timber Joints with Mechanical Fasteners - Y Hirashima and F Kamiya
- 24-7-3 Anchorage Capacity of Nail Plate - J Kangas
- 25-7-2 Softwood and Hardwood Embedding Strength for Dowel type Fasteners - J Ehlbeck and H Werner
- 25-7-4 A Guide for Application of Quality Indexes for Driven Fasteners Used in Connections in Wood Structures - E G Stern
- 25-7-5 35 Years of Experience with Certain Types of Connectors and Connector Plates Used for the Assembly of Wood Structures and their Components- E G Stern
- 25-7-6 Characteristic Strength of Split-ring and Shear-plate Connections - H J Blass, J Ehlbeck and M Schlager
- 25-7-7 Characteristic Strength of Tooth-plate Connector Joints - H J Blass, J Ehlbeck and M Schlager
- 25-7-8 Extending Yield Theory to Screw Connections - T E McLain
- 25-7-9 Determination of k_{def} for Nailed Joints - J W G van de Kuilen
- 25-7-10 Characteristic Strength of UK Timber Connectors - A V Page and C J Mettem
- 25-7-11 Multiple-fastener Dowel-type Joints, a Selected Review of Research and Codes - C J Mettem and A V Page
- 25-7-12 Load Distributions in Multiple-fastener Bolted Joints in European Whitewood Glulam, with Steel Side Plates - C J Mettem and A V Page
- 26-7-1 Proposed Test Method for Dynamic Properties of Connections Assembled with Mechanical Fasteners - J D Dolan
- 26-7-2 Validatory Tests and Proposed Design Formulae for the Load-Carrying Capacity of Toothed-Plate Connected Joints - C J Mettem, A V Page and G Davis

- 26-7-3 Definitions of Terms and Multi-Language Terminology Pertaining to Metal Connector Plates - E G Stern
- 26-7-4 Design of Joints Based on in V-Shape Glued-in Rods - J Kangas
- 26-7-5 Tests on Timber Concrete Composite Structural Elements (TCCs) - A U Meierhofer

LOAD SHARING

- 3-8-1 Load Sharing - An Investigation on the State of Research and Development of Design Criteria - E Levin
- 4-8-1 A Review of Load-Sharing in Theory and Practice - E Levin
- 4-8-2 Load Sharing - B Norén
- 19-8-1 Predicting the Natural Frequencies of Light-Weight Wooden Floors - I Smith and Y H Chui
- 20-8-1 Proposed Code Requirements for Vibrational Serviceability of Timber Floors - Y H Chui and I Smith
- 21-8-1 An Addendum to Paper 20-8-1 - Proposed Code Requirements for Vibrational Serviceability of Timber Floors - Y H Chui and I Smith
- 21-8-2 Floor Vibrational Serviceability and the CIB Model Code - S Ohlsson
- 22-8-1 Reliability Analysis of Viscoelastic Floors - F Rouger, J D Barrett and R O Foschi
- 24-8-1 On the Possibility of Applying Neutral Vibrational Serviceability Criteria to Joisted Wood Floors - I Smith and Y H Chui
- 25-8-1 Analysis of Glulam Semi-rigid Portal Frames under Long-term Load - K Komatsu and N Kawamoto

DURATION OF LOAD

- 3-9-1 Definitions of Long Term Loading for the Code of Practice - B Norén
- 4-9-1 Long Term Loading of Trussed Rafters with Different Connection Systems - T Feldborg and M Johansen
- 5-9-1 Strength of a Wood Column in Combined Compression and Bending with Respect to Creep - B Källsner and B Norén
- 6-9-1 Long Term Loading for the Code of Practice (Part 2) - B Norén
- 6-9-2 Long Term Loading - K Möhler
- 6-9-3 Deflection of Trussed Rafters under Alternating Loading during a Year - T Feldborg and M Johansen
- 7-6-1 Strength and Long Term Behaviour of Lumber and Glued-Laminated Timber under Torsion Loads - K Möhler
- 7-9-1 Code Rules Concerning Strength and Loading Time - H J Larsen and E Theilgaard
- 17-9-1 On the Long-Term Carrying Capacity of Wood Structures - Y M Ivanov and Y Y Slavic
- 18-9-1 Prediction of Creep Deformations of Joints - J Kuipers
- 19-9-1 Another Look at Three Duration of Load Models - R O Foschi and Z C Yao
- 19-9-2 Duration of Load Effects for Spruce Timber with Special Reference to Moisture Influence - A Status Report - P Hoffmeyer
- 19-9-3 A Model of Deformation and Damage Processes Based on the Reaction Kinetics of Bond Exchange - T A C M van der Put
- 19-9-4 Non-Linear Creep Superposition - U Korin
- 19-9-5 Determination of Creep Data for the Component Parts of Stressed-Skin Panels - R Kliger

- 19-9-6 Creep an Lifetime of Timber Loaded in Tension and Compression
- P Glos
- 19-1-1 Duration of Load Effects and Reliability Based Design (Single
Member) - R O Foschi and Z C Yao
- 19-6-1 Effect of Age and/or Load on Timber Strength - J Kuipers
- 19-7-4 The Prediction of the Long-Term Load Carrying Capacity of Joints in
Wood Structures - Y M Ivanov and Y Y Slavic
- 19-7-5 Slip in Joints under Long-Term Loading - T Feldborg and M Johansen
- 20-7-2 Slip in Joints under Long-Term Loading - T Feldborg and M Johansen
- 22-9-1 Long-Term Tests with Glued Laminated Timber Girders - M Badstube,
W Rug and W Schöne
- 22-9-2 Strength of One-Layer solid and Lengthways Glued Elements of Wood
Structures and its Alteration from Sustained Load - L M Kovaltchuk,
I N Boitemirova and G B Uspenskaya
- 24-9-1 Long Term Bending Creep of Wood - T Toratti
- 24-9-2 Collection of Creep Data of Timber - A Ranta-Maunus
- 24-9-3 Deformation Modification Factors for Calculating Built-up Wood-
Based Structures - I R Kliger
- 25-9-2 DVM Analysis of Wood. Lifetime, Residual Strength and Quality -
L F Nielsen
- 26-9-1 Long Term Deformations in Wood Based Panels under Natural
Climate Conditions. A Comparative Study - S Thelandersson, J Nordh,
T Nordh and S Sandahl

TIMBER BEAMS

- 4-10-1 The Design of Simple Beams - H J Burgess
- 4-10-2 Calculation of Timber Beams Subjected to Bending and Normal Force
- H J Larsen
- 5-10-1 The Design of Timber Beams - H J Larsen
- 9-10-1 The Distribution of Shear Stresses in Timber Beams - F J Keenan
- 9-10-2 Beams Notched at the Ends - K Möhler
- 11-10-1 Tapered Timber Beams - H Riberholt
- 13-6-2 Consideration of Size Effects in Longitudinal Shear Strength for
Uncracked Beams - R O Foschi and J D Barrett
- 13-6-3 Consideration of Shear Strength on End-Cracked Beams - J D Barrett
and R O Foschi
- 18-10-1 Submission to the CIB-W18 Committee on the Design of Ply Web
Beams by Consideration of the Type of Stress in the Flanges - J A Baird
- 18-10-2 Longitudinal Shear Design of Glued Laminated Beams - R O Foschi
- 19-10-1 Possible Code Approaches to Lateral Buckling in Beams - H J Burgess
- 19-2-1 Creep Buckling Strength of Timber Beams and Columns
- R H Leicester
- 20-2-1 Lateral Buckling Theory for Rectangular Section Deep Beam-Columns
- H J Burgess
- 20-10-1 Draft Clause for CIB Code for Beams with Initial Imperfections
- H J Burgess
- 20-10-2 Space Joists in Irish Timber - W J Robinson
- 20-10-3 Composite Structure of Timber Joists and Concrete Slab
- T Poutanen
- 21-10-1 A Study of Strength of Notched Beams - P J Gustafsson

- 22-10-1 Design of Endnotched Beams - H J Larsen and P J Gustafsson
- 22-10-2 Dimensions of Wooden Flexural Members under Constant Loads
- A Pozgai
- 22-10-3 Thin-Walled Wood-Based Flanges in Composite Beams - J König
- 22-10-4 The Calculation of Wooden Bars with flexible Joints in Accordance
with the Polish Standart Code and Strict Theoretical Methods
- Z Mielczarek
- 23-10-1 Tension Perpendicular to the Grain at Notches and Joints
- T A C M van der Put
- 23-10-2 Dimensioning of Beams with Cracks, Notches and Holes. An
Application of Fracture Mechanics - K Riipola
- 23-10-3 Size Factors for the Bending and Tension Strength of Structural Timber
- J D Barret and A R Fewell
- 23-12-1 Bending Strength of Glulam Beams, a Design Proposal - J Ehlbeck and
F Colling
- 23-12-3 Glulam Beams, Bending Strength in Relation to the Bending Strength
of the Finger Joints - H Riberholt
- 24-10-1 Shear Strength of Continuous Beams - R H Leicester and F G Young
- 25-10-1 The Strength of Norwegian Glued Laminated Beams - K Solli,
E Aasheim and R H Falk
- 25-10-2 The Influence of the Elastic Modulus on the Simulated Bending
Strength of Hyperstatic Timber Beams - T D G Canisius

ENVIRONMENTAL CONDITIONS

- 5-11-1 Climate Grading for the Code of Practice - B Norén
- 6-11-1 Climate Grading (2) - B Norén
- 9-11-1 Climate Classes for Timber Design - F J Keenan

- 19-11-1 Experimental Analysis on Ancient Downgraded Timber Structures
- B Leggeri and L Paolini
- 19-6-5 Drying Stresses in Round Timber - A Ranta-Maunus
- 22-11-1 Corrosion and Adaptation Factors for Chemically Aggressive Media
with Timber Structures - K Erler

LAMINATED MEMBERS

- 6-12-1 Directives for the Fabrication of Load-Bearing Structures of Glued
Timber - A van der Velden and J Kuipers
- 8-12-1 Testing of Big Glulam Timber Beams - H Kolb and P Frech
- 8-12-2 Instruction for the Reinforcement of Apertures in Glulam Beams
- H Kolb and P Frech
- 8-12-3 Glulam Standard Part 1: Glued Timber Structures; Requirements for
Timber (Second Draft)
- 9-12-1 Experiments to Provide for Elevated Forces at the Supports of Wooden
Beams with Particular Regard to Shearing Stresses and Long-Term
Loadings - F Wassipaul and R Lackner
- 9-12-2 Two Laminated Timber Arch Railway Bridges Built in Perth in 1849
- L G Booth
- 9-6-4 Consideration of Combined Stresses for Lumber and Glued Laminated
Timber - K Möhler
- 11-6-3 Consideration of Combined Stresses for Lumber and Glued Laminated
Timber (addition to Paper CIB-W18/9-6-4) - K Möhler
- 12-12-1 Glulam Standard Part 2: Glued Timber Structures; Rating (3rd draft)
- 12-12-2 Glulam Standard Part 3: Glued Timber Structures; Performance (3 rd
draft)
- 13-12-1 Glulam Standard Part 3: Glued Timber Structures; Performance (4th
draft)

- 14-12-1 Proposals for CEI-Bois/CIB-W18 Glulam Standards - H J Larsen
- 14-12-2 Guidelines for the Manufacturing of Glued Load-Bearing Timber Structures - Stevin Laboratory
- 14-12-3 Double Tapered Curved Glulam Beams - H Riberholt
- 14-12-4 Comment on CIB-W18/14-12-3 - E Gehri
- 18-12-1 Report on European Glulam Control and Production Standard - H Riberholt
- 18-10-2 Longitudinal Shear Design of Glued Laminated Beams - R O Foschi
- 19-12-1 Strength of Glued Laminated Timber - J Ehlbeck and F Colling
- 19-12-2 Strength Model for Glulam Columns - H J Blaß
- 19-12-3 Influence of Volume and Stress Distribution on the Shear Strength and Tensile Strength Perpendicular to Grain - F Colling
- 19-12-4 Time-Dependent Behaviour of Glued-Laminated Beams - F Zaupa
- 21-12-1 Modulus of Rupture of Glulam Beam Composed of Arbitrary Laminae - K Komatsu and N Kawamoto
- 21-12-2 An Appraisal of the Young's Modulus Values Specified for Glulam in Eurocode 5 - L R J Whale, B O Hilson and P D Rodd
- 21-12-3 The Strength of Glued Laminated Timber (Glulam): Influence of Lamination Qualities and Strength of Finger Joints - J Ehlbeck and F Colling
- 21-12-4 Comparison of a Shear Strength Design Method in Eurocode 5 and a More Traditional One - H Riberholt
- 22-12-1 The Dependence of the Bending Strength on the Glued Laminated Timber Girder Depth - M Badstube, W Rug and W Schöne
- 22-12-2 Acid Deterioration of Glulam Beams in Buildings from the Early Half of the 1960s - Preliminary summary of the research project; Overhead pictures - B A Hedlund

- 22-12-3 Experimental Investigation of normal Stress Distribution in Glue Laminated Wooden Arches - Z Mielczarek and W Chanaj
- 22-12-4 Ultimate Strength of Wooden Beams with Tension Reinforcement as a Function of Random Material Properties - R Candowicz and T Dziuba
- 23-12-1 Bending Strength of Glulam Beams, a Design Proposal - J Ehlbeck and F Colling
- 23-12-2 Probability Based Design Method for Glued Laminated Timber - M F Stone
- 23-12-3 Glulam Beams, Bending Strength in Relation to the Bending Strength of the Finger Joints - H Riberholt
- 23-12-4 Glued Laminated Timber - Strength Classes and Determination of Characteristic Properties - H Riberholt, J Ehlbeck and A Fewell
- 24-12-1 Contribution to the Determination of the Bending Strength of Glulam Beams - F Colling, J Ehlbeck and R Görlacher
- 24-12-2 Influence of Perpendicular-to-Grain Stressed Volume on the Load-Carrying Capacity of Curved and Tapered Glulam Beams - J Ehlbeck and J Kürth
- 25-12-1 Determination of Characteristic Bending Values of Glued Laminated Timber. EN-Approach and Reality - E Gehri
- 26-12-1 Norwegian Bending Tests with Glued Laminated Beams-Comparative Calculations with the "Karlsruhe Calculation Model" - E Aasheim, K Solli, F Colling, R H Falk, J Ehlbeck and R Görlacher
- 26-12-2 Simulation Analysis of Norwegian Spruce Glued-Laminated Timber - R Hernandez and R H Falk
- 26-12-3 Investigation of Laminating Effects in Glued-Laminated Timber - F Colling and R H Falk
- 26-12-4 Comparing Design Results for Glulam Beams According to Eurocode 5 and to the French Working Stress Design Code (CB71) - F Rouger

PARTICLE AND FIBRE BUILDING BOARDS

- 7-13-1 Fibre Building Boards for CIB Timber Code (First Draft)
- O Brynildsen
- 9-13-1 Determination of the Bearing Strength and the Load-Deformation
Characteristics of Particleboard - K Möhler, T Budianto and J Ehlbeck
- 9-13-2 The Structural Use of Tempered Hardboard - W W L Chan
- 11-13-1 Tests on Laminated Beams from Hardboard under Short- and
Longterm Load - W Nozynski
- 11-13-2 Determination of Deformation of Special Densified Hardboard under
Long-term Load and Varying Temperature and Humidity Conditions -
W Halfar
- 11-13-3 Determination of Deformation of Hardboard under Long-term Load in
Changing Climate - W Halfar
- 14-4-1 An Introduction to Performance Standards for Wood-Base Panel
Products - D H Brown
- 14-4-2 Proposal for Presenting Data on the Properties of Structural Panels
- T Schmidt
- 16-13-1 Effect of Test Piece Size on Panel Bending Properties - P W Post
- 20-4-1 Considerations of Reliability - Based Design for Structural Composite
Products - M R O'Halloran, J A Johnson, E G Elias and
T P Cunningham
- 20-13-1 Classification Systems for Structural Wood-Based Sheet Materials
- V C Kearley and A R Abbott
- 21-13-1 Design Values for Nailed Chipboard - Timber Joints - A R Abbott
- 25-13-1 Bending Strength and Stiffness of Izopanel Plates - Z Mielczarek

TRUSSED RAFTERS

- 4-9-1 Long-term Loading of Trussed Rafters with Different Connection Systems - T Feldborg and M Johansen
- 6-9-3 Deflection of Trussed Rafters under Alternating Loading During a Year - T Feldborg and M Johansen
- 7-2-1 Lateral Bracing of Timber Struts - J A Simon
- 9-14-1 Timber Trusses - Code Related Problems - T F Williams
- 9-7-1 Design of Truss Plate Joints - F J Keenan
- 10-14-1 Design of Roof Bracing - The State of the Art in South Africa - P A V Bryant and J A Simon
- 11-14-1 Design of Metal Plate Connected Wood Trusses - A R Egerup
- 12-14-1 A Simple Design Method for Standard Trusses - A R Egerup
- 13-14-1 Truss Design Method for CIB Timber Code - A R Egerup
- 13-14-2 Trussed Rafters, Static Models - H Riberholt
- 13-14-3 Comparison of 3 Truss Models Designed by Different Assumptions for Slip and E-Modulus - K Möhler
- 14-14-1 Wood Trussed Rafter Design - T Feldborg and M Johansen
- 14-14-2 Truss-Plate Modelling in the Analysis of Trusses - R O Foschi
- 14-14-3 Cantilevered Timber Trusses - A R Egerup
- 14-7-5 The Effect of Support Eccentricity on the Design of W- and WW-Trusses with Nail Plate Connectors - B Källsner
- 15-14-1 Guidelines for Static Models of Trussed Rafters - H Riberholt
- 15-14-2 The Influence of Various Factors on the Accuracy of the Structural Analysis of Timber Roof Trusses - F R P Pienaar

- 15-14-3 Bracing Calculations for Trussed Rafter Roofs - H J Burgess
- 15-14-4 The Design of Continuous Members in Timber Trussed Rafters with Punched Metal Connector Plates - P O Reece
- 15-14-5 A Rafter Design Method Matching U.K. Test Results for Trussed Rafters - H J Burgess
- 16-14-1 Full-Scale Tests on Timber Fink Trusses Made from Irish Grown Sitka Spruce - V Picardo
- 17-14-1 Data from Full Scale Tests on Prefabricated Trussed Rafters - V Picardo
- 17-14-2 Simplified Static Analysis and Dimensioning of Trussed Rafters - H Riberholt
- 17-14-3 Simplified Calculation Method for W-Trusses - B Källsner
- 18-14-1 Simplified Calculation Method for W-Trusses (Part 2) - B Källsner
- 18-14-2 Model for Trussed Rafter Design - T Poutanen
- 19-14-1 Annex on Simplified Design of W-Trusses - H J Larsen
- 19-14-2 Simplified Static Analysis and Dimensioning of Trussed Rafters - Part 2 - H Riberholt
- 19-14-3 Joint Eccentricity in Trussed Rafters - T Poutanen
- 20-14-1 Some Notes about Testing Nail Plates Subjected to Moment Load - T Poutanen
- 20-14-2 Moment Distribution in Trussed Rafters - T Poutanen
- 20-14-3 Practical Design Methods for Trussed Rafters - A R Egerup
- 22-14-1 Guidelines for Design of Timber Trussed Rafters - H Riberholt
- 23-14-1 Analyses of Timber Trussed Rafters of the W-Type - H Riberholt
- 23-14-2 Proposal for Eurocode 5 Text on Timber Trussed Rafters - H Riberholt

- 24-14-1 Capacity of Support Areas Reinforced with Nail Plates in Trussed Rafters - A Kevarinmäki
- 25-14-1 Moment Anchorage Capacity of Nail Plates in Shear Tests - A Kevarinmaki and J. Kangas
- 25-14-2 Design Values of Anchorage Strength of Nail Plate Joints by 2-curve Method and Interpolation - J Kangas and A Kevarinmaki
- 26-14-1 Test of Nail Plates Subjected to Moment - E Aasheim
- 26-14-2 Moment Anchorage Capacity of Nail Plates - A Kevarinmäki and J Kangas
- 26-14-3 Rotational Stiffness of Nail Plates in Moment Anchorage - A Kevarinmäki and J Kangas
- 26-14-4 Solution of Plastic Moment Anchorage Stress in Nail Plates - A Kevarinmäki
- 26-14-5 Testing of Metal-Plate-Connected Wood-Truss Joints - R Gupta
- 26-14-6 Simulated Accidental Events on a Trussed Rafter Roofed Building - C J Mettem and J P Marcroft

STRUCTURAL STABILITY

- 8-15-1 Laterally Loaded Timber Columns: Tests and Theory - H J Larsen
- 13-15-1 Timber and Wood-Based Products Structures. Panels for Roof Coverings. Methods of Testing and Strength Assessment Criteria. Polish Standard BN-78/7159-03
- 16-15-1 Determination of Bracing Structures for Compression Members and Beams - H Brüninghoff
- 17-15-1 Proposal for Chapter 7.4 Bracing - H Brüninghoff
- 17-15-2 Seismic Design of Small Wood Framed Houses - K F Hansen

- 18-15-1 Full-Scale Structures in Glued Laminated Timber, Dynamic Tests: Theoretical and Experimental Studies - A Ceccotti and A Vignoli
- 18-15-2 Stabilizing Bracings - H Brüninghoff
- 19-15-1 Connections Deformability in Timber Structures: a Theoretical Evaluation of its Influence on Seismic Effects - A Ceccotti and A Vignoli
- 19-15-2 The Bracing of Trussed Beams - M H Kessel and J Natterer
- 19-15-3 Racking Resistance of Wooden Frame Walls with Various Openings - M Yasumura
- 19-15-4 Some Experiences of Restoration of Timber Structures for Country Buildings - G Cardinale and P Spinelli
- 19-15-5 Non-Destructive Vibration Tests on Existing Wooden Dwellings - Y Hirashima
- 20-15-1 Behaviour Factor of Timber Structures in Seismic Zones. - A Ceccotti and A Vignoli
- 21-15-1 Rectangular Section Deep Beam - Columns with Continuous Lateral Restraint - H J Burgess
- 21-15-2 Buckling Modes and Permissible Axial Loads for Continuously Braced Columns - H J Burgess
- 21-15-3 Simple Approaches for Column Bracing Calculations - H J Burgess
- 21-15-4 Calculations for Discrete Column Restraints - H J Burgess
- 21-15-5 Behaviour Factor of Timber Structures in Seismic Zones (Part Two) - A Ceccotti and A Vignoli
- 22-15-1 Suggested Changes in Code Bracing Recommendations for Beams and Columns - H J Burgess
- 22-15-2 Research and Development of Timber Frame Structures for Agriculture in Poland - S Kus and J Kerste

- 22-15-3 Ensuring of Three-Dimensional Stiffness of Buildings with Wood Structures - A K Shenghelia
- 22-15-5 Seismic Behavior of Arched Frames in Timber Construction - M Yasumura
- 22-15-6 The Robustness of Timber Structures - C J Mettem and J P Marcroft
- 22-15-7 Influence of Geometrical and Structural Imperfections on the Limit Load of Wood Columns - P Dutko
- 23-15-1 Calculation of a Wind Girder Loaded also by Discretely Spaced Braces for Roof Members - H J Burgess
- 23-15-2 Stability Design and Code Rules for Straight Timber Beams - T A C M van der Put
- 23-15-3 A Brief Description of Formula of Beam-Columns in China Code - S Y Huang
- 23-15-4 Seismic Behavior of Braced Frames in Timber Construction - M Yasumara
- 23-15-5 On a Better Evaluation of the Seismic Behavior Factor of Low-Dissipative Timber Structures - A Ceccotti and A Vignoli
- 23-15-6 Disproportionate Collapse of Timber Structures - C J Mettem and J P Marcroft
- 23-15-7 Performance of Timber Frame Structures During the Loma Prieta California Earthquake - M R O'Halloran and E G Elias
- 24-15-2 Discussion About the Description of Timber Beam-Column Formula - S Y Huang
- 24-15-3 Seismic Behavior of Wood-Framed Shear Walls - M Yasumura
- 25-15-1 Structural Assessment of Timber Framed Building Systems - U Korin
- 25-15-3 Mechanical Properties of Wood-framed Shear Walls Subjected to Reversed Cyclic Lateral Loading - M Yasumura

- 26-15-1 Bracing Requirements to Prevent Lateral Buckling in Trussed Rafters - C J Mettem and P J Moss
- 26-15-2 Eurocode 8 - Part 1.3 - Chapter 5 - Specific Rules for Timber Buildings in Seismic Regions - K Becker, A Ceccotti, H Charlier, E Katsaragakis, H J Larsen and H Zeitter
- 26-15-3 Hurricane Andrew - Structural Performance of Buildings in South Florida - M R O'Halloran, E L Keith, J D Rose and T P Cunningham

FIRE

- 12-16-1 British Standard BS 5268 the Structural Use of Timber: Part 4 Fire Resistance of Timber Structures
- 13-100-2 CIB Structural Timber Design Code. Chapter 9. Performance in Fire
- 19-16-1 Simulation of Fire in Tests of Axially Loaded Wood Wall Studs - J König
- 24-16-1 Modelling the Effective Cross Section of Timber Frame Members Exposed to Fire - J König
- 25-16-1 The Effect of Density on Charring and Loss of Bending Strength in Fire - J König
- 25-16-2 Tests on Glued-Laminated Beams in Bending Exposed to Natural Fires - F Bolonius Olesen and J König
- 26-16-1 Structural Fire Design According to Eurocode 5, Part 1.2 - J König

STATISTICS AND DATA ANALYSIS

- 13-17-1 On Testing Whether a Prescribed Exclusion Limit is Attained - W G Warren
- 16-17-1 Notes on Sampling and Strength Prediction of Stress Graded Structural Timber - P Glos

- 16-17-2 Sampling to Predict by Testing the Capacity of Joints, Components and Structures - B Norén
- 16-17-3 Discussion of Sampling and Analysis Procedures - P W Post
- 17-17-1 Sampling of Wood for Joint Tests on the Basis of Density - I Smith, L R J Whale
- 17-17-2 Sampling Strategy for Physical and Mechanical Properties of Irish Grown Sitka Spruce - V Picardo
- 18-17-1 Sampling of Timber in Structural Sizes - P Glos
- 18-6-3 Notes on Sampling Factors for Characteristic Values - R H Leicester
- 19-17-1 Load Factors for Proof and Prototype Testing - R H Leicester
- 19-6-2 Confidence in Estimates of Characteristic Values - R H Leicester
- 21-6-1 Draft Australian Standard: Methods for Evaluation of Strength and Stiffness of Graded Timber - R H Leicester
- 21-6-2 The Determination of Characteristic Strength Values for Stress Grades of Structural Timber. Part 1 - A R Fewell and P Glos
- 22-17-1 Comment on the Strength Classes in Eurocode 5 by an Analysis of a Stochastic Model of Grading - A proposal for a supplement of the design concept - M Kiesel
- 24-17-1 Use of Small Samples for In-Service Strength Measurement - R H Leicester and F G Young
- 24-17-2 Equivalence of Characteristic Values - R H Leicester and F G Young
- 24-17-3 Effect of Sampling Size on Accuracy of Characteristic Values of Machine Grades - Y H Chui, R Turner and I Smith
- 24-17-4 Harmonisation of LSD Codes - R H Leicester
- 25-17-2 A Body for Confirming the Declaration of Characteristic Values - J Sunley

- 25-17-3 Moisture Content Adjustment Procedures for Engineering Standards -
D W Green and J W Evans

FRACTURE MECHANICS

- 21-10-1 A Study of Strength of Notched Beams - P J Gustafsson
- 22-10-1 Design of Endnotched Beams - H J Larsen and P J Gustafsson
- 23-10-1 Tension Perpendicular to the Grain at Notches and Joints
- T A C M van der Put
- 23-10-2 Dimensioning of Beams with Cracks, Notches and Holes. An
Application of Fracture Mechanics - K Riipola
- 23-19-1 Determination of the Fracture Energie of Wood for Tension
Perpendicular to the Grain - W Rug, M Badstube and W Schöne
- 23-19-2 The Fracture Energy of Wood in Tension Perpendicular to the Grain.
Results from a Joint Testing Project - H J Larsen and P J Gustafsson
- 23-19-3 Application of Fracture Mechanics to Timber Structures
- A Ranta-Maunus
- 24-19-1 The Fracture Energy of Wood in Tension Perpendicular to the Grain -
H J Larsen and P J Gustafsson

GLUED JOINTS

- 20-18-1 Wood Materials under Combined Mechanical and Hygral Loading
- A Martensson and S Thelandersson
- 20-18-2 Analysis of Generalized Volkersen - Joints in Terms of Linear Fracture
Mechanics - P J Gustafsson
- 20-18-3 The Complete Stress-Slip Curve of Wood-Adhesives in Pure Shear
- H Wernersson and P J Gustafsson

22-18-1 Perspective Adhesives and Protective Coatings for Wood Structures
- A S Freidin

CIB TIMBER CODE

- 2-100-1 A Framework for the Production of an International Code of Practice
for the Structural Use of Timber - W T Curry
- 5-100-1 Design of Solid Timber Columns (First Draft) - H J Larsen
- 5-100-2 A Draft Outline of a Code for Timber Structures - L G Booth
- 6-100-1 Comments on Document 5-100-1; Design of Solid Timber Columns
- H J Larsen and E Theilgaard
- 6-100-2 CIB Timber Code: CIB Timber Standards - H J Larsen and
E Theilgaard
- 7-100-1 CIB Timber Code Chapter 5.3 Mechanical Fasteners; CIB Timber
Standard 06 and 07 - H J Larsen
- 8-100-1 CIB Timber Code - List of Contents (Second Draft) - H J Larsen
- 9-100-1 The CIB Timber Code (Second Draft)
- 11-100-1 CIB Structural Timber Design Code (Third Draft)
- 11-100-2 Comments Received on the CIB Code
a U Saarelainen
b Y M Ivanov
c R H Leicester
d W Nozynski
e W R A Meyer
f P Beckmann; R Marsh
g W R A Meyer
h W R A Meyer
- 11-100-3 CIB Structural Timber Design Code; Chapter 3 - H J Larsen
- 12-100-1 Comment on the CIB Code - Sous-Commission Glulam

- 12-100-2 Comment on the CIB Code - R H Leicester
- 12-100-3 CIB Structural Timber Design Code (Fourth Draft)
- 13-100-1 Agreed Changes to CIB Structural Timber Design Code
- 13-100-2 CIB Structural Timber Design Code. Chapter 9: Performance in Fire
- 13-100-3a Comments on CIB Structural Timber Design Code
- 13-100-3b Comments on CIB Structural Timber Design Code - W R A Meyer
- 13-100-3c Comments on CIB Structural Timber Design Code - British Standards Institution
- 13-100-4 CIB Structural Timber Design Code. Proposal for Section 6.1.5 Nail Plates - N I Bovim
- 14-103-2 Comments on the CIB Structural Timber Design Code - R H Leicester
- 15-103-1 Resolutions of TC 165-meeting in Athens 1981-10-12/13
- 21-100-1 CIB Structural Timber Design Code. Proposed Changes of Sections on Lateral Instability, Columns and Nails - H J Larsen
- 22-100-1 Proposal for Including an Updated Design Method for Bearing Stresses in CIB W18 - Structural Timber Design Code - B Madsen
- 22-100-2 Proposal for Including Size Effects in CIB W18A Timber Design Code - B Madsen
- 22-100-3 CIB Structural Timber Design Code - Proposed Changes of Section on Thin-Flanged Beams - J König
- 22-100-4 Modification Factor for "Aggressive Media" - a Proposal for a Supplement to the CIB Model Code - K Erler and W Rug
- 22-100-5 Timber Design Code in Czechoslovakia and Comparison with CIB Model Code - P Dutko and B Kozelouh

LOADING CODES

- 4-101-1 Loading Regulations - Nordic Committee for Building Regulations
- 4-101-2 Comments on the Loading Regulations - Nordic Committee for Building Regulations

STRUCTURAL DESIGN CODES

- 1-102-1 Survey of Status of Building Codes, Specifications etc., in USA
- E G Stern
- 1-102-2 Australian Codes for Use of Timber in Structures - R H Leicester
- 1-102-3 Contemporary Concepts for Structural Timber Codes - R H Leicester
- 1-102-4 Revision of CP 112 - First Draft, July 1972
- British Standards Institution
- 4-102-1 Comparison of Codes and Safety Requirements for Timber Structures
in EEC Countries - Timber Research and Development Association
- 4-102-2 Nordic Proposals for Safety Code for Structures and Loading Code for
Design of Structures - O A Brynildsen
- 4-102-3 Proposal for Safety Codes for Load-Carrying Structures
- Nordic Committee for Building Regulations
- 4-102-4 Comments to Proposal for Safety Codes for Load-Carrying Structures -
Nordic Committee for Building Regulations
- 4-102-5 Extract from Norwegian Standard NS 3470 "Timber Structures"
- 4-102-6 Draft for Revision of CP 112 "The Structural Use of Timber"
- W T Curry
- 8-102-1 Polish Standard PN-73/B-03150: Timber Structures; Statistical
Calculations and Designing
- 8-102-2 The Russian Timber Code: Summary of Contents

- 9-102-1 Svensk Byggnorm 1975 (2nd Edition); Chapter 27: Timber Construction
- 11-102-1 Eurocodes - H J Larsen
- 13-102-1 Program of Standardisation Work Involving Timber Structures and Wood-Based Products in Poland
- 17-102-1 Safety Principles - H J Larsen and H Riberholt
- 17-102-2 Partial Coefficients Limit States Design Codes for Structural Timberwork - I Smith
- 18-102-1 Antiseismic Rules for Timber Structures: an Italian Proposal - G Augusti and A Ceccotti
- 18-1-2 Eurocode 5, Timber Structures - H J Larsen
- 19-102-1 Eurocode 5 - Requirements to Timber - Drafting Panel Eurocode 5
- 19-102-2 Eurocode 5 and CIB Structural Timber Design Code - H J Larsen
- 19-102-3 Comments on the Format of Eurocode 5 - A R Fewell
- 19-102-4 New Developments of Limit States Design for the New GDR Timber Design Code - W Rug and M Badstube
- 19-7-3 Effectiveness of Multiple Fastener Joints According to National Codes and Eurocode 5 (Draft) - G Steck
- 19-7-6 The Derivation of Design Clauses for Nailed and Bolted Joints in Eurocode 5 - L R J Whale and I Smith
- 19-14-1 Annex on Simplified Design of W-Trusses - H J Larsen
- 20-102-1 Development of a GDR Limit States Design Code for Timber Structures - W Rug and M Badstube
- 21-102-1 Research Activities Towards a New GDR Timber Design Code Based on Limit States Design - W Rug and M Badstube
- 22-102-1 New GDR Timber Design Code, State and Development - W Rug, M Badstube and W Kofent

- 22-102-2 Timber Strength Parameters for the New USSR Design Code and its Comparison with International Code - Y Y Slavik, N D Denesh and E B Ryumina
- 22-102-3 Norwegian Timber Design Code - Extract from a New Version - E Aasheim and K H Solli
- 23-7-1 Proposal for a Design Code for Nail Plates - E Aasheim and K H Solli
- 24-102-2 Timber Footbridges: A Comparison Between Static and Dynamic Design Criteria - A Ceccotti and N de Robertis
- 25-102-1 Latest Development of Eurocode 5 - H J Larsen
- 25-102-1A Annex to Paper CIB-W18/25-102-1. Eurocode 5 - Design of Notched Beams - H J Larsen, H Riberholt and P J Gustafsson
- 25-102-2 Control of Deflections in Timber Structures with Reference to Eurocode 5 - A Martensson and S Thelandersson

INTERNATIONAL STANDARDS ORGANISATION

- 3-103-1 Method for the Preparation of Standards Concerning the Safety of Structures (ISO/DIS 3250) - International Standards Organisation ISO/TC98
- 4-103-1 A Proposal for Undertaking the Preparation of an International Standard on Timber Structures - International Standards Organisation
- 5-103-1 Comments on the Report of the Consultation with Member Bodies Concerning ISO/TC/P129 - Timber Structures - Dansk Ingeniorforening
- 7-103-1 ISO Technical Committees and Membership of ISO/TC 165
- 8-103-1 Draft Resolutions of ISO/TC 165
- 12-103-1 ISO/TC 165 Ottawa, September 1979
- 13-103-1 Report from ISO/TC 165 - A Sorensen

- 14-103-1 Comments on ISO/TC 165 N52 "Timber Structures; Solid Timber in Structural Sizes; Determination of Some Physical and Mechanical Properties"
- 14-103-2 Comments on the CIB Structural Timber Design Code - R H Leicester
- 21-103-1 Concept of a Complete Set of Standards - R H Leicester

JOINT COMMITTEE ON STRUCTURAL SAFETY

- 3-104-1 International System on Unified Standard Codes of Practice for Structures - Comité Européen du Béton (CEB)
- 7-104-1 Volume 1: Common Unified Rules for Different Types of Construction and Material - CEB

CIB PROGRAMME, POLICY AND MEETINGS

- 1-105-1 A Note on International Organisations Active in the Field of Utilisation of Timber - P Sonnemans
- 5-105-1 The Work and Objectives of CIB-W18-Timber Structures - J G Sunley
- 10-105-1 The Work of CIB-W18 Timber Structures - J G Sunley
- 15-105-1 Terms of Reference for Timber - Framed Housing Sub-Group of CIB-W18
- 19-105-1 Tropical and Hardwood Timbers Structures - R H Leicester
- 21-105-1 First Conference of CIB-W18B, Tropical and Hardwood Timber Structures Singapore, 26 - 28 October 1987 - R H Leicester

INTERNATIONAL UNION OF FORESTRY RESEARCH ORGANISATIONS

- 7-106-1 Time and Moisture Effects - CIB W18/IUFRO 55.02-03 Working Party

INTERNATIONAL COUNCIL FOR BUILDING RESEARCH STUDIES AND DOCUMENTATION
WORKING COMMISSION W18 - TIMBER STRUCTURES

STRUCTURAL PROPERTIES OF FRENCH GROWN TIMBER
ACCORDING TO VARIOUS GRADING METHODS

by

F Rouger
C De Lafond
A El Quadrani
Centre Technique du Bois et de l'Ameublement
France

MEETING TWENTY - SIX

ATHENS, GEORGIA

USA

AUGUST 1993

Structural properties of French grown timber according to various grading methods

by

F. Rouger ¹, C. De Lafond ² and A. El Ouadrani ³

Abstract

Since 1983, CTBA has carried out a wide research program on strength properties of French grown species. This program, not only led to the establishment of a new visual grading system, but also gave a large amount of data to be analysed. One of the original ideas of this program is a forest based sampling. Trees are sampled in the producing regions according to the weight of each region. Boards are sampled in order to represent the variations of properties along the tree and through the cross-section. Knots measurements and physical properties are correlated to strength properties in order to evaluate the influence of silvicultural methods, but also to establish a new visual grading system. This program has been performed on five main species (Whitewood, Douglas Fir, Black Pine, Maritime Pine and Poplar). More than ten thousand boards were tested. This paper is aimed to summarize the basic properties of the resource, and to focuss on grading results. The world wide tendency of machine grading is also taken into account to analyze the data. The last part of the paper concerns depth effects, which have been already investigated by many authors.

Introduction

Since 1940, a huge amount of forest has been planted in France in order to increase the resource. New species as well as imported species have been implemented. Their properties were known only from small clear specimens. For this reason, CTBA decided in 1983 with the producers and with the end-users to study this material, with two objectives :

(1) Investigate the properties of the resource for structural and non structural uses and give advice on new silvicultural programs.

¹ Research Manager, Dept of Timber Engineering, CTBA, 10 av. de St Mandé, 75012 PARIS, FRANCE

² Research Engineer, Dept of Timber Engineering, CTBA, 10 av. de St Mandé, 75012 PARIS, FRANCE

³ Research Engineer, Dept of Timber Engineering, CTBA, 10 av. de St Mandé, 75012 PARIS, FRANCE

(2) Establish a grading system, based on full size tests, which could be used to revise the French Grading standard of 1946.

These studies have produced a large amount of data which is still being analysed. For each board, different measurements have been performed :

- location of the board within the tree,
- location of the tree within the forest,
- knots measurements (face knots, edge knots, KAR, volumes),
- rate of growth,
- density of the board,
- MOE, MOR in bending,
- MOR in tension,
- small clear specimens tests (tension perp., shear, tension parallel,...).

These measurements are entered in a database to carry out statistical analysis. The results of these analyses have been published in research reports available at CTBA, but not yet in technical meetings. This paper will only describe the grading results, in accordance with the CEN work on strength properties of structural timber.

Basic properties of the raw material

Results are reported in tables 1 to 5. In these tables, appears only the data which is used for establishing visual grades. The density, MOE and MOR have been adjusted according to *prEN 384* (depth effect for bending MOR, moisture content adjustments to 12% for density and for MOE). The test results are only reported for pieces that failed in the central third.

Whitewood (*Picea excelsa* & *Abies alba*)

This species is characterized by a low density ($\mu = 450 \text{ kg/m}^3$), combined with a low ring width ($\mu = 2.8 \text{ mm}$). MOE and MOR properties are average, as well as knots sizes.

Douglas Fir (*Pseudotsuga menziesii*)

This species is characterized by a large ring width ($\mu = 6.5 \text{ mm}$) which has no influence on mechanical properties. The MOE is rather high ($\mu = 12.2 \text{ GPa}$), compared with the MOR. Knots are larger and show a lower variability than for the other species.

Black Pine (*Pinus Nigra corsicana* & *Pinus Nigra Austriaca*)

This species is characterized by a high density ($\mu = 590 \text{ kg/m}^3$), combined with a low ring width ($\mu = 2.6 \text{ mm}$). As well as for whitewood, MOE and MOR are average, but show a higher variability (C.V. = 30% for MOE & C.V. = 45% for MOR).

Maritime Pine (*Pinus pinaster*)

This species is characterized by a high density ($\mu = 560 \text{ kg/m}^3$). The MOR is much more variable than for the other species (C.V. = 47%) and the MOE is slightly lower ($\mu = 10.7 \text{ GPa}$). Ring width and knots sizes are average.

Poplar (*Populus*)

This species is characterized by a large ring width ($\mu = 7.5 \text{ mm}$) and by small knots (knots sizes = 25%). The density, the MOE and the MOR are comparable to whitewood.

Visual grading

Visual grading is based on knots sizes (as proportions of the cross section dimensions). For the CF30 grade, an additional criteria is necessary :

Species	Density limitation	Ring width limitation
Whitewood	$\geq 460 \text{ kg/m}^3$	$\leq 3 \text{ mm}$
Douglas Fir	$\geq 460 \text{ kg/m}^3$	n.a.
Black Pine	$\geq 510 \text{ kg/m}^3$	$\leq 3 \text{ mm}$
Poplar	$\geq 405 \text{ kg/m}^3$	n.a.

The grading results are reported in tables 6 to 10. The values have been derived according to *prEN 384*. More detailed information is provided in document *TC124/WG2/AHxx*, especially concerning sampling methods and modification factors. The following information is part of the work carried out by the Ad'Hoc Group of CEN 124/WG2 on establishing characteristic values for European visual grades.

Whitewood (*Picea excelsa & Abies alba*)

For this species, 29% of the specimens have been rejected. The yield of CF30 is low (10%), compared with CF22 (49%). A proposal for assignment to European strength classes of *prEN 338* is given below :

CF18 --> C22

CF22 --> C24

CF30 --> C30

MOE and density profiles are close to *prEN 338* (see table 11), except for CF30 in which a density limitation has been applied.

Douglas Fir (*Pseudotsuga menziesii*)

For this species, 58% of the specimens have been rejected, which is much too high. This can be explained by knot sizes and ring width which are very large. The other yields are comparable. A proposal for assignment to European strength classes of prEN 338 is given below :

CF18 --> C22 CF22 --> C22 CF30 --> C27

The MOE and density profiles could be increased by 20%, but, as explained further, this can be explained by the grading method rather than by the material profiles.

Black Pine (*Pinus Nigra corsicana* & *Pinus Nigra Austriaca*)

For this species, 40% of the specimens have been rejected, which is high. The yield for CF30 is large enough, due to Corsican Pine which has good mechanical properties. A proposal for assignment to European strength classes of prEN 338 is given below :

CF18 --> C18 CF22 --> C18 CF30 --> C27

The MOE and density profiles could be increased by 20%, due to the same reasons than Douglas Fir.

Maritime Pine (*Pinus pinaster*)

In the case of this species, visual grading is not very efficient : only CF18 can be produced, with a yield of only 54%. The assignment to a C18 strength class allows an increase of 20% for the MOE and 50% for the density.

Poplar (*Populus*)

For this species, 27% of the specimens have been rejected, which is reasonable. The yield for CF30 is good (38%), mainly due to the *Robusta* clone. A proposal for assignment to European strength classes of prEN 338 is given below :

CF18 --> C22 CF30 --> C30

The MOE and density profiles are in agreement with prEN 338.

Optimal grading.

The results described above show yields which are rather low, especially for high grades, and profiles which are quite different from prEN 338. This lead us to closely examine the grading method, and try to predict what could be the optimum grading of the resource. As explained in prEN 338, a sample enters a strength class if three conditions are fulfilled :

- characteristic MOR > target value,
- characteristic density > target value,
- mean MOE > target value.

This method has been applied to the database, for the strength classes C18, C22 and C30.

Principle of the method

Question : From an initial population of size N , which sample can enter a class C_{xx} ?

(1) Density or MOR requirement ($f(X_k) = 0.05$).

In the initial population, let us assume that N_1 pieces have a lower value than the target value, i.e. :

$$f (X_k) = f_0 = \frac{N_1}{N} \quad (1)$$

To get the requirement, we need to take off the N_0 lower pieces, i.e. :

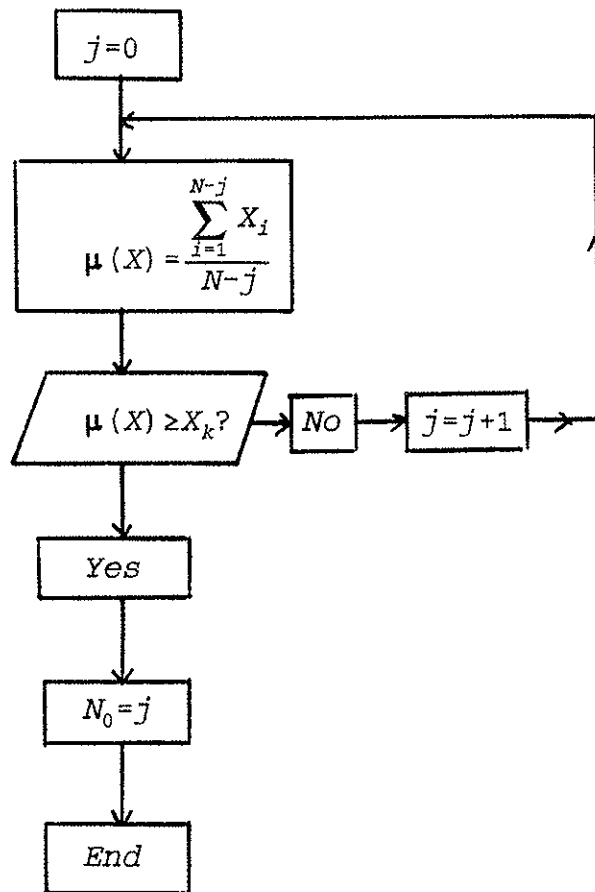
$$f (X_k) = \frac{N_1 - N_0}{N - N_0} = 0.05 \quad (2)$$

By combining equations (1) and (2), we get :

$$N_0 = 1.0526 (f_0 - 0.05) N \quad (3)$$

(2) MOE requirement ($\mu(X) = X_k$).

In this case, an iterative algorithm is necessary :

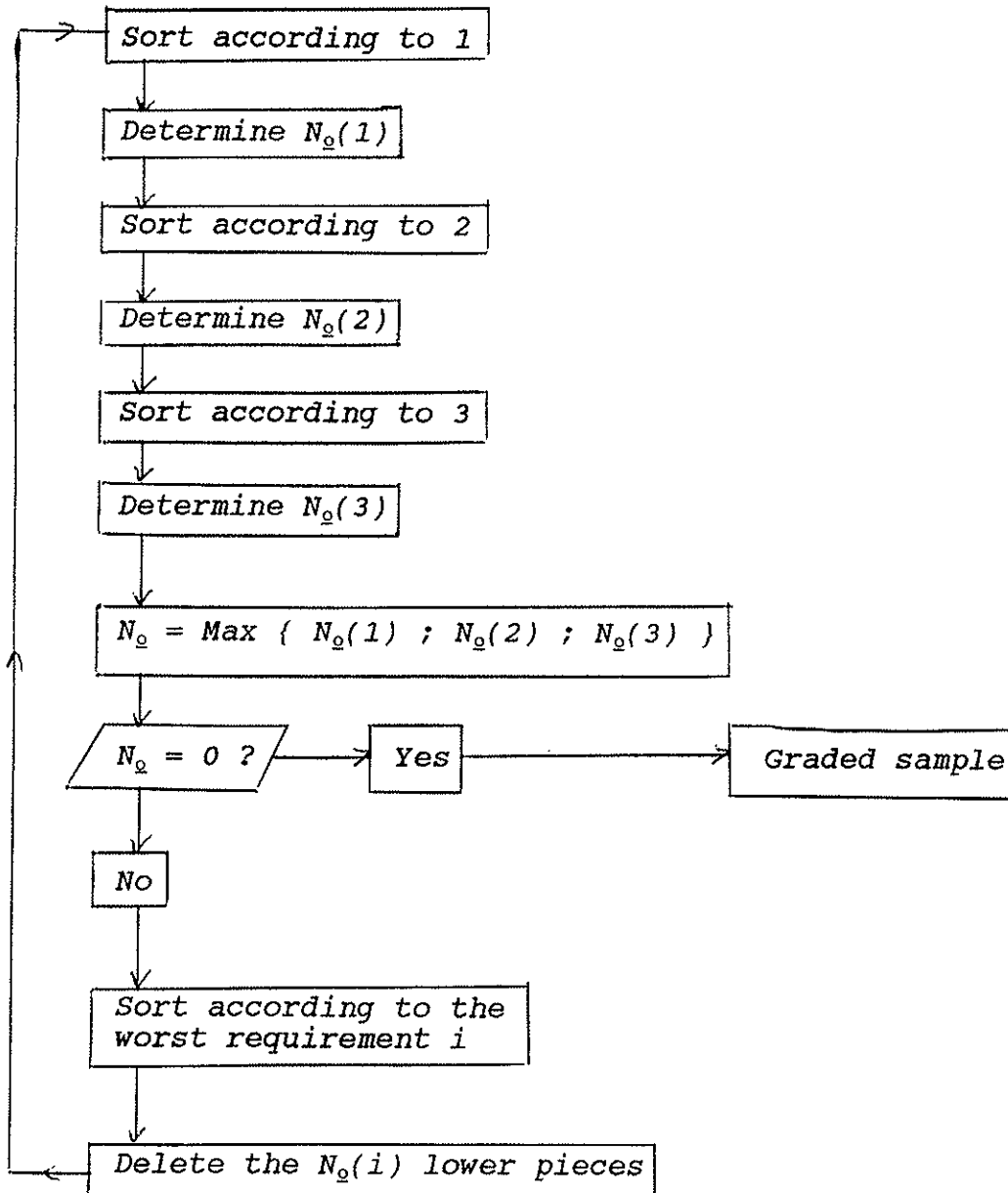


(3) All requirements together.

Let us assume that :

- MOR requirement --> 1
- density requirement --> 2
- MOE requirement --> 3

The algorithm is given below :



This method requires grading by descending order (i.e. C30 ; C22 ; C18).

Results

The results are reported in tables 12 to 16. They are spectacular. The amount of rejected pieces is always lower than 10%, except for Maritime Pine (18.5%). The yield for C30 ranges from 60% to 80%. These values show a great potential of the resource which is not optimized by a visual grading system. It can also be noticed that the most penalizing criteria are the MOE and the MOR. The density values are always larger than the requirements, which shows that the density profiles of prEN 338 could be increased. This is specially the case for Black Pine, Maritime Pine and to a lower extent for Douglas Fir. These profiles explain that the previous values of the visual grades were not due to the material behaviour but to the grading method. It should be reminded that this method could not be applied as a grading method (because the MOR values are known !!). However, it gives a way of determining what is the "natural strength class" of a sample. This leads us to simulate a machine grading method for three species, this being a first way to improve visual grading methods.

Machine grading.

Three species were so-called "machine graded", according to the MOE values of the specimens. The results are reported in tables 17 to 19. In the case of Whitewood, the machine grading method gives very good results, close to the optimum.

For Douglas Fir, the machine grading method reaches 50% of the optimum, but is much more efficient than the visual grading method :

- 47% of CF30 instead of 9%
- 20% of reject instead of 58%.

For Maritime Pine, the yield of rejected pieces is equivalent to the visual grading method. But with the machine grading, it is possible to get CF30 (25%) and CF22 (20%) which were not available when the visual grading method was applied.

This simulation shows that, using the MOE for predicting the MOR has a variable success among the species. Further research needs to be achieved to find other properties (local density,...) which can predict the strength of the material.

Size effects.

Many authors (Madsen 1992, Barrett 1992) have investigated the size effect, especially in bending. These authors seem to get contradictory results, depending on the test data. Barrett (1992) reported that for visually graded lumber, the depth effects could be masked by the "grading effect", in the case of grading rules in which the defect sizes vary with the size of the members. In order to investigate this theory on our database, we adjusted the depth factors for each grade. The conclusions are very surprising, and confirm the assumptions made by Barrett :

(1) For raw material, there is a slight depth effect ($k_n = 0.1$) for Whitewood and Douglas Fir. In the case of Maritime Pine, there is a negative depth effect ($k_n = -0.15$), which has been explained by the knots location in this species.

(2) For visually graded timber, this depth effect totally disappears for low grades and is strongly negative ($k_n = -0.4$) for high grade.

(3) For machine graded timber, the depth effect is obvious :

- $k_n = 0.2$ for Whitewood
- $k_n = 0.2$ to 0.6 for Douglas Fir
- $k_n = 0.35$ to 0.45 for Maritime Pine

These values clearly indicate that the size effect is strongly dependent on the grading method, and that it can completely disappear for visual grading. This could confirm that in previous studies where specimens were "ingrade tested", the size effect could be neglected. Among the worldwide available data, particular attention should be focussed on the grading method and on the sampling method .

Conclusion.

This paper focussed on the relationship between structural properties and grading methods. Three major ideas were discussed. Firstly, an optimal grading method was developed to get an estimate of the potential of the resource. Secondly, it was demonstrated that the MOE and density profiles were strongly dependent on the grading technique, and could not always be attributed to the material behaviour. Lastly, an investigation of the size effect exhibited a "grading effect" which was much larger than the material depth effect. This last point confirms some of the ideas developed previously and can be discussed. Of course, much research needs to be done to improve the grading methods and optimize the resource with respect to its structural properties. A program is initiated to develop stochastic finite element analysis of full size specimens and to try to understand the behaviour of such a composite material. This research should lead to accurate predictors of the strength which could be incorporated in grading methods. A worldwide cooperation is wished by the authors to work on this aspect.

References.

Barrett, J.D., and Lam, F. (1992). Size effects in visually graded softwood structural lumber. In: Proc. of the CIB W18 Meeting, Ahus, Sweden, Paper 25-6-5.

Madsen, B. (1992). Structural Behaviour of Timber. Timber Engineering Ltd., North Vancouver, B.C., Canada

Rouger, F. (1993). Volume and Stress Distribution Effects. STEP lecture B7.

Rouger, F. (1993). Characteristic values of French visually-graded timber. CEN 124/WG2/AHxx

Standards.

prEN 338 - 1991 - Structural Timber - Strength classes.

prEN 384 - 1991 - Structural Timber - Determination of characteristic values of mechanical properties and density.

Whitewood	Sample Size	Mean	Std Dev	C.V. (%)
MOR (MPa)	2400	45,4	14,7	32,38
MOE (GPa)	2400	11,3	2,3	20,35
Density (kg/m ³)	2400	450	38	8,44
Face knots (%)	2400	31	19,5	62,90
Edge knots (%)	2400	39	28,5	73,08
Ring width (mm)	2400	2,8	1,3	46,43

Table 1 : Basic properties for Whitewood

Douglas Fir	Sample Size	Mean	Std Dev	C.V. (%)
MOR (MPa)	1750	40,6	15,8	38,92
MOE (GPa)	1750	12,2	2,7	22,13
Density (kg/m ³)	1750	500	48,5	9,70
Face knots (%)	1750	48	20	41,67
Edge knots (%)	1750	50	26	52,00
Ring width (mm)	1750	6,5	1,9	29,23

Table 2 : Basic properties for Douglas Fir

Black Pine	Sample Size	Mean	Std Dev	C.V. (%)
MOR (MPa)	2630	46,8	20,8	44,44
MOE (GPa)	2630	11,6	3,5	30,17
Density (kg/m ³)	2630	590	72	12,20
Face knots (%)	2630	40	22	55,00
Edge knots (%)	2630	40	28	70,00
Ring width (mm)	2630	2,6	1,3	50,00

Table 3 : Basic properties for Black Pine

Maritime Pine	Sample Size	Mean	Std Dev	C.V. (%)
MOR (MPa)	1400	39,3	18,6	47,33
MOE (GPa)	1400	10,7	2,5	23,36
Density (kg/m ³)	1400	560	46	8,21
Face knots (%)	1290	42	23	54,76
Edge knots (%)	1290	42	31	73,81
Ring width (mm)	1400	3,7	1,3	35,14

Table 4 : Basic properties for Maritime Pine

Poplar	Sample Size	Mean	Std Dev	C.V. (%)
MOR (MPa)	770	45,9	14	30,50
MOE (GPa)	770	11,8	2,3	19,49
Density (kg/m ³)	770	440	49	11,14
Face knots (%)	770	25	23	92,00
Edge knots (%)	770	27	32	118,52
Ring width (mm)	770	7,5	2,1	28,00

Table 5 : Basic properties for Poplar

Whitewood	Char. MOR (MPa)	Mean MOE (GPa)	Char. density (kg/m ³)	Yield (%)
CF18	22,9	11,2	360	12
CF22	24,8	11,5	360	49
CF30	33,9	13,4	440	10

Table 6 : Visual grading for Whitewood

Douglas Fir	Char. MOR (MPa)	Mean MOE (GPa)	Char. density (kg/m ³)	Yield (%)
CF18	23,3	12,1	410	22
CF22	22,1	13,2	410	11
CF30	26,8	14,2	440	9

Table 7 : Visual grading for Douglas Fir

Black Pine	Char. MOR (MPa)	Mean MOE (GPa)	Char. density (kg/m ³)	Yield (%)
CF18	19,5	11,8	450	10
CF22	19,8	11,5	460	23
CF30	28,5	14,1	490	27

Table 8 : Visual grading for Black Pine

Maritime Pine	Char. MOR (MPa)	Mean MOE (GPa)	Char. density (kg/m ³)	Yield (%)
CF18	20	11,5	470	54

Table 9 : Visual grading for Maritime Pine

Poplar	Char. MOR (MPa)	Mean MOE (GPa)	Char. density (kg/m ³)	Yield (%)
CF18	23,4	11,3	340	35
CF30	31,7	12,9	400	38

Table 10 : Visual grading for Poplar

Strength Class	Char. MOR (MPa)	Mean MOE (GPa)	Char. density (kg/m ³)
C18	18	9	320
C22	22	10	340
C24	24	11	350
C27	27	12	370
C30	30	12	380

Table 11 : Strength profiles of prEN 338

Whitewood	Char. MOR (MPa)	Mean MOE (GPa)	Char. density (kg/m ³)	Yield (%)
C18	20,7	9	360	28
C22	22	10	370	1
C30	30,2	12	390	63

Table 12 : *Optimal grading for Whitewood*

Douglas Fir	Char. MOR (MPa)	Mean MOE (GPa)	Char. density (kg/m ³)	Yield (%)
C18	18,2	9,3	400	5
C22	22	10	410	13,5
C30	30	12,9	430	78

Table 13 : *Optimal grading for Douglas Fir*

Black Pine	Char. MOR (MPa)	Mean MOE (GPa)	Char. density (kg/m ³)	Yield (%)
C18	18,3	9	460	3
C22	22,1	10	470	7,5
C30	30	12,5	490	79

Table 14 : *Optimal grading for Black Pine*

Maritime Pine	Char. MOR (MPa)	Mean MOE (GPa)	Char. density (kg/m ³)	Yield (%)
C18	18,1	9	480	7,5
C22	22,1	10,2	490	13
C30	30,2	12	510	61

Table 15 : *Optimal grading for Maritime Pine*

Poplar	Char. MOR (MPa)	Mean MOE (GPa)	Char. density (kg/m ³)	Yield (%)
C18	18,3	9,1	330	5,5
C22	22,2	10	350	8,5
C30	30,5	12,4	380	83

Table 16 : Optimal grading for Poplar

Whitewood	Char. MOR (MPa)	Mean MOE (GPa)	Char. density (kg/m ³)	Yield (%)
CF18	22	9,3	370	37
CF30	31,2	12,3	390	54

Table 17 : Machine grading for Whitewood

Douglas Fir	Char. MOR (MPa)	Mean MOE (GPa)	Char. density (kg/m ³)	Yield (%)
CF18	19,8	10,2	420	8
CF22	23,6	11,2	430	24
CF30	30,9	14,5	460	47

Table 18 : Machine grading for Douglas Fir

Maritime Pine	Char. MOR (MPa)	Mean MOE (GPa)	Char. density (kg/m ³)	Yield (%)
CF18	18,6	10,2	500	22
CF22	23,2	11,7	510	19
CF30	31,4	14,1	530	24,5

Table 19 : Machine grading for Maritime Pine

Grade	Raw Material	Visual Grading	Machine Grading
CF18	0,1	0,01	0,23
CF22		-0,1	n.a.
CF30		-0,5	0,2

Table 20 : Depth factors for Whitewood

Grade	Raw Material	Visual Grading	Machine Grading
CF18	0,12	-0,01	0,6
CF22		0,01	0,5
CF30		-0,3	0,17

Table 21 : Depth factors for Douglas Fir

Grade	Raw Material	Visual Grading	Machine Grading
CF18	-0,15	-0,01	0,35
CF22		n.a.	0,34
CF30		n.a.	0,47

Table 22 : Depth factors for Maritime Pine

INTERNATIONAL COUNCIL FOR BUILDING RESEARCH STUDIES AND DOCUMENTATION

WORKING COMMISSION W18 - TIMBER STRUCTURES

DISCUSSION AND PROPOSAL OF A GENERAL FAILURE CRITERION FOR WOOD

by

T A C M van der Put
Delft University of Technology
The Netherlands

MEETING TWENTY - SIX

ATHENS, GEORGIA

USA

AUGUST 1993

ABSTRACT

Based on a polynomial expansion of the failure surface, a general failure criterion, satisfying equilibrium in all directions, was developed for wood long ago (IUFRO Boras 1982) and shown to apply for clear wood. For wood with (small) defects and (local) grain deviations, equivalent strengths can be defined in the main directions and a comparable equivalent failure criterion applies as was shown by K. Hemmer (PhD thesis 1985). It was shown at the last COST-508 meeting that the second order terms of the polynomial failure criterion represent the critical distortional energy of initial yield (or failure at initial yield when the test becomes unstable at this point). It will be shown that the third order terms represent special hardening effects (due to micro-crack arrest by strong layers), occurring after initial yield, determining ultimate failure in longitudinal direction in a stable test.

As known, the singularity approach of fracture mechanics predicts for the critical energy release rate: $G_C = G_{IC} + G_{IIc}$ for collinear crack propagation in grain direction. As p.e. mentioned in the RILEM State of the Art report on fracture mechanics of wood, this is against experimental evidence and in stead, the empirical Wu-equation is used for layered composites. It was shown at the COST 508-meeting at Bordeaux that this wrong prediction is due to this singularity method that, by the critical stress intensities, does not satisfy in all cases the failure criterion and, although this method is generally applied in fracture mechanics of materials, it therefore has to be rejected. It further was shown that the Wu-criterion can be derived from oriented (in grain direction) crack propagation of elliptic micro-cracks and is a necessary condition for the (right form of the) energy principle.

It now will be shown that this Wu- (or Mohr-) criterion is also determining the failure criterion of wood, showing the same oriented micro-cracking to be responsible for failure in general.

Based on this criterion, the existing criteria can be explained as the Hankinson, Norris, and Coulomb criterion. A derivation is given of an exact modified Hankinson criterion and of the general form of the higher order constants and how they can (safely) be determined from uni-axial tests in the main plane.

The exact criterion is as easy to apply as the invalid approximations, now used for the Codes.

INTRODUCTION

Failure criteria, like the Norris-, Hoffmann-, Tsai-Wu- criteria etc., can be seen as forms of a polynomial expansion of the real failure surface. This expansion of the failure surface in stress space into a polynomial, consisting of a linear combination of orthogonal polynomials, provides easily found constants (by the orthogonality property) when the expanded function is known, and the row can be extended, when necessary, without changing the already determined constants of the row. When choosing in advance a limited number of terms of the polynomial, up to some degree, the expansion procedure need not to be performed, because the result is in principle identical to a least square fit of the data to a polynomial of that chosen degree. This choice of the number of terms may depend on the wanted precision of the expansion and the practical use.

Based on this principle of a polynomial expansion of the failure surface, the failure criterion is general, satisfying equilibrium in all directions, and was for wood first developed in [1] and the most important aspects can be found in that publication. The in [1] given explanation of the existing criteria and the approximation of the coupling terms as F_{12} , are verified, p.e. in Madison [2], where it was shown that Cowins approximation [11] does not apply for wood.

A general approach for anisotropic, not orthotropic, behaviour of joints, (as punched out metal plates), and the simplification of the transformations by 2 angles as variables, is given in [3].

A confirmation of the results of [1] by means of coherent measurements (in the radial-longitudinal plane) and the generalization to an equivalent, quasi homogeneous. failure criterion for wood with small defects is given in [4], showing, as will be discussed here, a determining influence of crack propagation on the equivalent main strengths. There thus is no reason to maintain the used invalid approximations and to not apply this consistent criterion, also for the Codes, for all cases of combined stresses. Thus far only this criterion gives the possibility of a definition of the off-axis strength of anisotropic materials.

A GENERAL FAILURE CRITERION FOR WOOD

A yield-criterion gives the combinations of stresses whereby flow occurs in an elastic-plastic material like wood in compression. When partial flow (of some component) becomes noticeable, while most of the material remains elastic, initial yield occurs where below the material is regarded to be elastic. For more brittle tensile failures in polymers, there also is an initial yield boundary where above the gradual flow of components at peak stresses and micro-cracking may have a similar effect on stress redistribution as flow. It is discussed in [10] that these flow and failure boundaries may be regarded as equivalent elastic-plastic flow surfaces.

The flow- or failure criterion is a closed surface in the stress space (a more dimensional space with coordinates $\sigma_1, \sigma_2, \sigma_3, \sigma_4, \sigma_5, \sigma_6$).

A cut, (p.e. according to figure 1 through the plane of the co-ordinate axes $y = \sigma_1$ and $x = \sigma_2$), will show a closed curve and such a curve always can be described by a polynomial in x and y like:

$$ax + by + cx^2 + dy^2 + exy + fx^3 + gy^3 + hx^2y + ixy^2 + \dots = k \quad (1)$$



Figure - 1. General form of a failure-ellipsoid and definition of positive stresses.

whereby as much as terms can be accounted for, as is necessary for the wanted precision of the description. The surface will be convex because of the normality principle, (the requirement that "plastic" work done must be positive), and higher order terms, causing local peaks on the surface (and thus causing inflection points) are only possible by local hardening effects depending on the loading path and are outside the flow-criterion. These effects can be treated as given in [1] at:

"2.2. Hardenings rules" or by the approach of [10].

It can also be seen that the constants f and g are indeterminate and have to be taken zero because, for $y = 0$, eq.(1) becomes: $ax + cx^2 + fx^3 = k$, or in the real roots $x_0, -x_1, -x_2$:

$$(x - x_0) \cdot (x + x_1) \cdot (x + x_2) = 0. \quad (2)$$

Because there are only two points of intersection possible of a closed surface with a line, there are only two roots by the intersecting x -axis p.e. $x = x_0$ and $x = -x_1$ and the part $(x + x_2)$, being never zero within or on the surface and thus is indeterminate, has to be omitted. For a real convex surface f is necessarily zero.

The same applies for g , or: $g = 0$ following from the roots of y when $x = 0$.

The equation can systematically be written as stress-polynomial like:

$$F_1 \sigma_1 + F_{ij} \sigma_i \sigma_j + F_{ijk} \sigma_i \sigma_j \sigma_k + \dots = 1 \quad (i, j, k = 1, 2, 3, 4, 5, 6) \quad (3)$$

In [1] it is shown that clear wood can be regarded to be orthotropic in the main planes and the principal directions of the strengths are orthogonal (showing the common tensor transformations) and higher order terms normally (outer hardening) can be neglected so that eq.(3) becomes:

$$F_1 \sigma_1 + F_{ij} \sigma_i \sigma_j = 1 \quad (i, j, k = 1, 2, 3, 4, 5, 6) \quad (4)$$

In [10] it is shown that this equation represents the critical distortional energy of failure. For reasons of energetic reciprocity $F_{ij} = F_{ji}$ ($i \neq j$) and by orthotropic symmetry in the main planes (through the main axes along the grain, tangential and radial) there is no difference in positive and negative shear-strength and terms with uneven powers in σ_6 thus are zero or: $F_{16} = F_{26} = F_6 = 0$; and there is no interaction between normal- and shear-strengths or: $F_{ij} = 0$ ($i \neq j$; $i, j = 4, 5, 6$).

Thus eq.(4) becomes for a plane stress state in a main plane:

$$F_1 \sigma_1 + F_2 \sigma_2 + F_{11} \sigma_1^2 + 2F_{12} \sigma_1 \sigma_2 + F_{22} \sigma_2^2 + F_{66} \sigma_6^2 = 1 \quad (5)$$

For a thermodynamic allowable criterion (positive finite strain energy) the values F_{ij} must be positive and the failure surface has to be closed and cannot be open-ended and thus the interaction terms are constrained to:

$$F_{11} F_{22} > F_{12}^2. \quad (6)$$

For the uniaxial tensile strength $\sigma_1 = X$ ($\sigma_2 = \sigma_6 = 0$) eq.(5) becomes:

$$F_1 \sigma_1 + F_{11} \sigma_1^2 = 1 \quad \text{or:} \quad F_1 X + F_{11} X^2 = 1 \quad (7)$$

and for the compression strength $\sigma_1 = -X'$ this is:

$$F_1 X' - F_{11} X'^2 = 1 \quad (8)$$

and it follows from eq.(7) and (8) that F_1 en F_{11} are known:

$$F_1 = \frac{1}{X} - \frac{1}{X'}, \quad \text{and} \quad F_{11} = \frac{1}{XX'} \quad (9)$$

In the same way is for $\sigma_1 = \sigma_6 = 0$ in the direction perpendicular:

$$F_2 = \frac{1}{Y} - \frac{1}{Y'}, \quad \text{and} \quad F_{22} = \frac{1}{YY'} \quad (10)$$

Further it follows for $\sigma_1 = \sigma_2 = 0$ (pure shear), for the shear strength S , that:

$$F_{66} = 1/S^2 \quad (11)$$

$$\text{and is according to eq.(6):} \quad -1/\sqrt{XX'YY'} < F_{12} < +1/\sqrt{XX'YY'} \quad (12)$$

It can be shown (as discussed in [1]) that the restricted values of $2F_{12}$, based on assumed coupling according to the deviator stresses, as given by Norris [13], Hill or Hoffmann [14] as: $2F_{12} = -1/2XY$ or: $2F_{12} = -(1/X^2 + 1/Y^2 - 1/Z^2)$ are not general enough for orthotropic materials and don't apply for wood. There also is no coercive reason to restrict F_{12} according to p.e. Tsai and Hahn [15] as:

$$2F_{12} = -1/\sqrt{XX'YY'}, \quad \text{or according to Wu and Stachurski [16] as:} \quad 2F_{12} \approx -2/XX'$$

These values suggest that $2F_{12}$ is ~ 0.2 to 0.5 times the extreme value of eq.(12).

The properties of a real physical surface have to be independent on the orientation of the axes and therefore the tensor transformations apply for the stresses σ of eq.(5). These transformation are derivable from the equilibrium of the stresses on an element formed by the rotated plane and the original planes, or simply, by the circle of Mohr construction. For the uni-axial tensile stress then is:

$$\sigma_1 = \sigma_t \cos^2 \vartheta, \quad \sigma_2 = \sigma_t \sin^2 \vartheta, \quad \sigma_6 = \sigma_t \sin \vartheta \cos \vartheta.$$

Substitution in eq.(5) gives:

$$F_1 \sigma_t \cos^2 \vartheta + F_2 \sigma_t \sin^2 \vartheta + F_{11} \sigma_t^2 \cos^4 \vartheta + (2F_{12} + F_{66}) \sigma_t^2 \cos^2 \vartheta \sin^2 \vartheta + F_{22} \sigma_t^2 \sin^4 \vartheta = 1 \quad (13)$$

and substitution of the values of F :

$$\begin{aligned} & \sigma_t \cos^2 \vartheta \left(\frac{1}{X} - \frac{1}{X'} \right) + \sigma_t \sin^2 \vartheta \left(\frac{1}{Y} - \frac{1}{Y'} \right) + \frac{\sigma_t^2 \cos^4 \vartheta}{XX'} + 2F_{12} \sigma_t^2 \sin^2 \vartheta \cos^2 \vartheta + \frac{\sigma_t^2 \sin^4 \vartheta}{YY'} + \\ & + \frac{\sigma_t \sin^2 \vartheta \cos^2 \vartheta}{S^2} = 1 \end{aligned} \quad (14)$$

It can be seen that for $\vartheta = 0$ this gives the tensile- and compressional strength in p.e. the grain direction: $\sigma_t = X$ en $\sigma_t = -X'$, and for $\vartheta = 90^\circ$, the tensile and compressional strength perpendicular to the grain: $\sigma_t = Y$ and $\sigma_t = -Y'$, and that a definition is given of the tensile and compressional strength in every direction. These are the points of intersection of the rotated axes with the failure surface. Eq.(13) thus can be read in this strength component along the rotated x-axis: $\sigma_t = \sigma_1$ according to:

$$F_1' \sigma_1 + F_{11}' \sigma_1^2 = 1 \quad (15)$$

The same can be done for the other strengths giving the definition of the transformations of F_i and F_{ij} . The transformation of F_{ij} is also a tensor transformation (of the fourth rank) thus following from the rotation of the symmetry axes of the material. Transformation thus is possible in two manners. The stress-components can be transformed to the symmetry directions according to eq.(5). Or the symmetry axes can be rotated, leaving the stresses along the rotating axes unchanged. For this case the general polynomial expression eq.(16) applies:

$$F'_1 \sigma_1 + F'_2 \sigma_2 + F'_{11} \sigma_1^2 + 2F'_{12} \sigma_1 \sigma_2 + F'_{22} \sigma_2^2 + F'_{16} \sigma_1 \sigma_6 + F'_{26} \sigma_2 \sigma_6 + F'_{66} \sigma_6^2 = 1 \quad (16)$$

These transformations of F' are p.e. given in [1].

Transverse strengths

In [1] it is shown that for rotations of the 3-axis, when this axis is chosen along the grain, eq.(5) and (16) may precisely describe the peculiar behaviour of the compression- tension- and (rolling) shear-strength perpendicular to the grain and the off-axis strengths without the need of higher order terms.

When for compression the failure limit is taken to be the stress value after that the same, sufficient high, amount of flow strain has occurred, then the differences between radial- tangential- and off-axes strengths may disappear and one directional independent strength value remains (see fig. 2). For tension perpendicular to the grain, only in a rather small region (around 90° , see fig. 2) in the radial direction the strength is higher and because in practise, the applied direction is not precisely in that direction, there is some freedom, in timber, to choose the weakest plane for failure and the lower bound of the strength will apply being independent of the direction. This means that:

$$F_1 - F_2 = 0 \quad \text{and} \quad F_{11} - F_{22} = 0$$

and that also F_{12} is limited according to:

$$2F_{12} = F_{11} + F_{22} - F_{66}$$

Further then also is:

$$F'_6 = 0 \quad \text{and} \quad F'_{66} = F_{66} = 1/\tau_{\text{rol}}^2$$

From measurement it can be derived that F_{12} is small leading to:

$$F_{66} \approx F_{11} + F_{22} \quad \text{or} \quad \tau_{\text{rol}} \text{ is bounded by:}$$

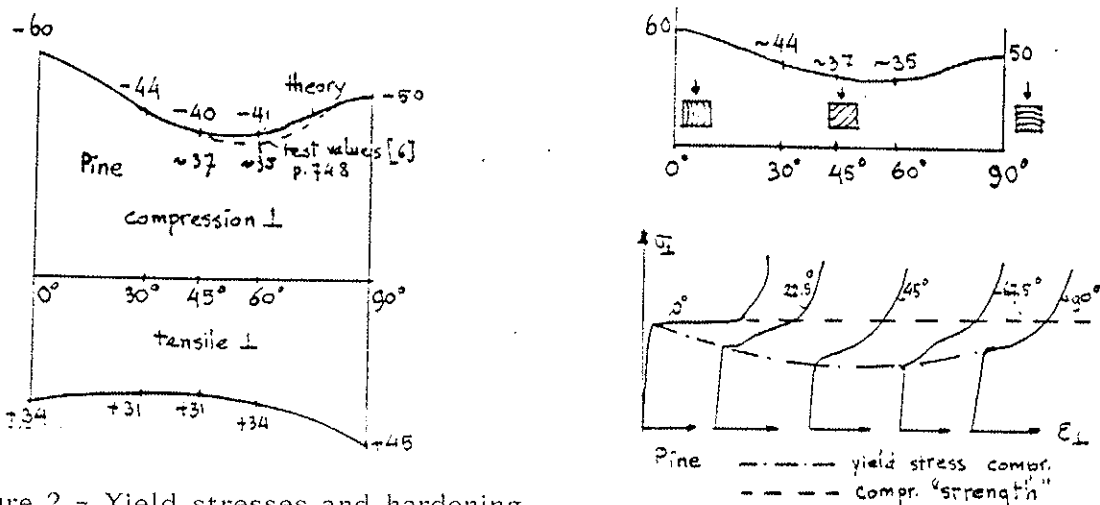


Figure 2 - Yield stresses and hardening

$$\tau_{\text{rol}} = \sqrt{XX'/2} = \sqrt{YY'/2}$$

and the behaviour can be regarded to be quasi isotropic in the transverse direction. The measurements further show for this rotation around the grain-axis that the "shear strengths" in grain direction in the radial- and the tangential plane, F_{44} and F_{55} , are uncoupled or $F_{45} = 0$, as is to be expected from symmetry considerations.

Longitudinal strengths

When now the 3-axis is chosen in the tangential or in the radial direction the same relations apply (with indices 1,2,6) as in the previous case. The equations for this case then give the strengths along and perpendicular to the grain and the shear-strength in the grain direction.

When the test remains stable above initial yield, a type of hardening may occur and third order terms are needed, according to eq.(3), to describe the behaviour. In [1] it was shown (by tests of [11] with σ_2 and σ_6 only), that the longitudinal shear strength in the radial plane increases with compression perpendicular to this plane according to the coupling term F_{266} (direction 2 is the radial direction; direction 1 is in the grain direction):

$$F_2 \sigma_2 + F_{22} \sigma_2^2 + F_{66} \sigma_6^2 + 3F_{266} \sigma_2 \sigma_6^2 = 1 \quad \text{or:} \quad \frac{\sigma_6}{S} = \sqrt{\frac{(1 - \sigma_2/Y) \cdot (1 + \sigma_2/Y')}{1 + c\sigma_2/Y'}} \quad (17)$$

with: $c = 3F_{266} Y' S^2 \approx 0.9$ (0,8 à 0,99).

It is seen from fig. 3, that $c < 1$ is necessary to have a closed surface and thus is determining for the upper bound of F_{266} .

When c approaches $c \approx 1$ (measurements of project A in fig. 3) eq.(17) becomes:

$$\left(\frac{\sigma_6}{S}\right)^2 + \frac{\sigma_2}{Y} \approx 1 \quad (17')$$

being the Mohr equation or the Wu-equation of fracture mechanics for mixed mode I - II failure (when expressed in stress intensity factors).

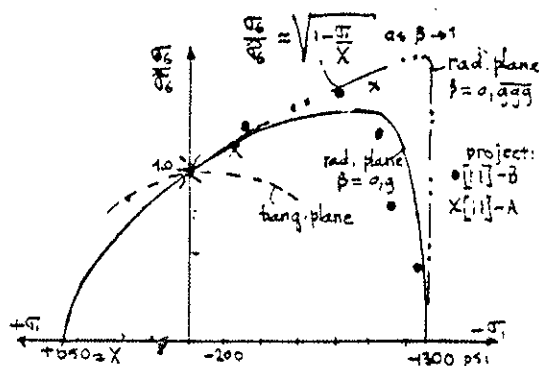


Figure 3 - Combined shear-tension and shear-compression strengths.

This equation (17') can fully be explained by collinear micro-crack propagation in grain direction [9]. As derived in [9], eq.(17') does not only apply for shear with tension but also for shear with compression σ_2 perpendicular to the flat crack.

For a high stress σ_2 the crack is closed at $\sigma_2 = \sigma_c$ and the crack tip notices only

the influence of $\sigma_2 = \sigma_c$ because for the higher part of σ_2 the load is directly transmitted through the closed crack and eq.(17') becomes:

$$\frac{\sigma_6}{S} = \frac{-\mu(\sigma_2 - \sigma_c)}{S} + \sqrt{1 - \frac{\sigma_c}{Y}} \quad \text{or:} \quad \sigma_6 = C + \mu|\sigma_2| \quad (17'')$$

where σ_2 and σ_c are negative, giving the Coulomb-equation with an increased shear capacity due to friction: $\mu\sigma_2$. This effect will be small for wood. For micro-cracks the crack closure stress σ_c will have about the value the tensile strength: $\sigma_c \approx -Y$. For maximal compression (at maximal shear), $\sigma_2 \approx -0.9Y'$, the shear strength will be maximal raised by a factor: $(1 + \mu(0.9Y' - Y)/S)$. Inserting measurements of [4] this factor is maximal: $(\sqrt{2} + 0.3(0.9 \cdot 5.6 - 3.7)/9.8)/\sqrt{2} = 1.03$ with respect to the failure without Coulomb friction. Because the possible parabolic fit by equation (17') the co-efficient of friction (above $\sigma_2 = \sigma_c \approx -Y$) is probably smaller than 0.3. It is thus seen that Coulomb friction is neglectable and does not increase the shear-strength by compression perpendicular. This increase is an equivalent hardening effect, caused by crack arrest by the strong layers, so that failure only is possible by longitudinal crack propagation according to the Wu-equation. At higher stresses σ_2 , compressional plasticity perpendicular to the grain (project A of [11]), or earlier instability of the test, (project B of [11] with oblique-grain compression tests) may become determining, showing a lower value c of eq.(17) than $c = 1$.

Because the slopes of the lines (at small σ_2) of project A and B of [11] are the same, there is no indication of an influence of the higher order terms: F_{112} , F_{122} , F_{12} and F_{166} of proj. B. Further the line of B is below the line of A and the c -value of B is lower, closer to the elliptic failure criterion. This strongly is an indication that hardening after initial yield (thus departure from the elliptic equation) of project B, the oblique-grain compression test, is much less than that of project A, and thus that the test is less stable. (Project C of [11] follows the elliptic failure criterion because of the influence of transverse failure due to rolling shear that is shown before to be elliptic).

The theory also explains why the parabolic Wu-equation of increased shear strength by transverse compression, did not occur in the tangential plane. If, there are large initial cracks in the tangential plane, (or trans-wall failures), the crack-closure-stress σ_c is small and when also μ is small: σ_6 is about constant in the compressional region (independent on the magnitude of the compression perpendicular) until there is influence of plasticity by compressional failure. This ultimate shear condition in the weak plane, independent of compression, is predicted by the singularity method and is the basis of the explanation of the Hankinson formula eq.(19), for $n = 2$, by this method [9]. As shown later $n = 2$ means that there are no higher order coupling terms (no higher than order 2). Because there thus is no influence of (the equivalent) F_{266} in the tangential plane (F_{355}), F_{266} of the radial plane diminishes quickly at axis-rotation (around the 1-axis), and this higher order effect is only a local effect, only noticeable when loading is in a plane rather close to the radial plane. This thus will hardly be noticeable in timber when failure is free to occur in the weakest plane. The high measured value of F_{266} (measured with $\sigma_1 = 0$) may indicate that for clear wood, F_{122} will be zero in the radial plane according to eq.(22). It also can be deduced from published Hankinson lines of clear wood that F_{122} and F_{266} can be zero in the tangential plane, (confirming the results of proj.

A and B of [11], mentioned above). For these Hankinson lines, $n \approx 2$ in eq.(19), showing all higher order terms to be zero. There is an indication that this is a general property of timber [11], because when shear failure is free to occur the plane of minimum resistance, as usually in large timber beams and glulam, it occurs in the tangential plane and $n = 2$, showing no higher order terms. On the other hand, this needs not to be a general property for all species and tests because it generally is mentioned by Kollmann that $n \approx 2.5$ for compression of clear wood showing that F_{112} and F_{122} will in general not be zero outside the radial plane. This may indicate some hardening by confined dilatation (depending on the test) as discussed in [10]. Because of the oriented crack-propagation, explaining eq.(17), $F_{166} \approx 0$ for clear wood because σ_1 is in the same direction as the flat crack and thus not influenced by that crack.

It was shown in [10] that eq.(5) represents the initial yield condition, being the extended critical distortional energy principle. Because at initial yield both, the elastic and yield conditions should be satisfied, the second order polynomial applies. For elastic behaviour, this follows from the Hankinson equations (with $n = 2$) that apply for the moduli of elasticity and because the modulus is proportional to the yield strengths, the Hankinson equations (18) apply for initial yield (being the second order polynomial). As mentioned in [10], for glulam in general, and for clear wood in tension, $n \approx 2$ and there are measurements, depending on the type of test, indicating that $n \approx 2$ is possible for compression of clear wood as well (by the "Shereisen" test) or that $n \approx 2$ in the neighbourhood of the tangential plane (following from oblique-grain compression tests), showing therefore no higher order terms and thus failure after initial yield. Thus the second order polynomial then also gives the failure condition. For this case, of no influence of higher order terms, eq.(13) or (14) applies, for the off-grain-axis tensile- and compressional- strengths and eq.(14) can be resolved into factors as follows:

$$\left(\frac{\sigma_t \cos^2 \vartheta}{X} + \frac{\sigma_t \sin^2 \vartheta}{Y} - 1 \right) \cdot \left(\frac{\sigma_t \cos^2 \vartheta}{X'} + \frac{\sigma_t \sin^2 \vartheta}{Y'} + 1 \right) = 0 \quad (18)$$

giving the product of the Hankinson equations for tension and for compression, (where X and X' are the strengths in grain direction). This is possible when:

$$2F_{12} + 1/S^2 \approx 1/X'Y + 1/XY'$$

In this equation, derived in [1], $(1/X'Y + 1/XY')$ is of the same order and thus about equal to $1/S^2$ and $2F_{12}$ is of lower order with respect to $1/S^2$. In [2] this equation of [1] was used as a measure for F_{12} , thus: $2F_{12} = 1/X'Y + 1/XY' - 1/S^2$ what is a difference of two higher order quantities and thus gives no information of the value of F_{12} that also can be neglected. In [17], wrongly the sum of: $1/S^2$ and $(1/X'Y + 1/XY')$ is taken to be equal to $2F_{12}$, being of higher order with respect to the real value of F_{12} and it is evident that this value did not satisfy eq.(12). Eq.(18) shows that the exponent n of the general Hankinson formula eq.(19):

$$\frac{\sigma_t \cos^n \vartheta}{X} + \frac{\sigma_t \sin^n \vartheta}{Y} = 1 \quad (19)$$

is $n = 2$ for tension. For compressional failure X and Y have to be replaced by resp. X' en Y' in eq.(19) and eq.(18) shows that $n = 2$ for compression as well when there are no higher order terms.

The equations for timber with defects are in principle derivable from the clear wood equations by analysing the stresses around knots, cracks etc. Descriptive, by the polynomial approach, it is also possible to regard the many possible complicated stress states leading to failure in timber with defects, when loaded in a direction as the strength by the mean stresses in that direction. In that case combined stresses determine the axial strengths. Where due to the grain- and stress deviations, the axial strength is determined by combined shear with tension perpendicular to the grain, stable crack propagation causing an increase of the effective shear-strength (according to the Wu-equation) may occur. Because always shear is involved in failure, also the higher order terms for (apparent pure) normal stresses show this parabolic increase of the effective strength, and the higher order terms are no longer neglectable.

For wood with small defects n can be as low as $n \approx 1.6$ in eq.(19) for tension showing higher order terms to be no longer neglectable for tension. This also has to be expected when knots and defects show a deviation of the grain-direction because the line of the strength has to shift according to that deviation. For compression about the same $n \approx 2.5$ can be expected because the strength depends on the mean grain-direction at yield. In [4] it is shown that F_{166} , F_{266} and F_{112} of the radial plane have influence, what is shown here to represent the equivalent hardening effect due to crack arrest. Eq.(18) thus needs to be extended to account for the smaller Hankinson value of $n < 2$ for tension and $n > 2$ for compression.

An equation of the fourth degree (eq.(21) in σ_t) can always be written as the product of two quadratic equations, eq.(20). For a real failure surface the roots will be real and because the measurements show that one of the quadratic equations is determining for compression and the other for tension and must be valid for zero values of C_t and/or C_d as well, this factorization leads as the only possible solution to be the product of the "Hankinson equations" for tension and compression:

$$\left(\frac{\sigma_t \cos^2 \vartheta}{X} + \frac{\sigma_t \sin^2 \vartheta}{Y} - 1 + \sigma_t^2 \sin^2 \vartheta \cos^2 \vartheta C_t \right) \cdot \left(\frac{\sigma_t \cos^2 \vartheta}{X'} + \frac{\sigma_t \sin^2 \vartheta}{Y'} + 1 + \sigma_t^2 \sin^2 \vartheta \cos^2 \vartheta C_d \right) = 0 \quad (20)$$

In general eq.(20) thus is (as can be seen by performing the multiplication):

$$F_1 \sigma_t \cos^2 \vartheta + F_2 \sigma_t \sin^2 \vartheta + F_{11} \sigma_t^2 \cos^4 \vartheta + (2F_{12} + F_{66}) \sigma_t^2 \cos^2 \vartheta \sin^2 \vartheta + F_{22} \sigma_t^2 \sin^4 \vartheta + 3(F_{112} + F_{166}) \sigma_t^3 \cos^4 \vartheta \sin^2 \vartheta + 3(F_{122} + F_{266}) \sigma_t^3 \sin^4 \vartheta \cos^2 \vartheta + 12F_{1266} \sigma_t^4 \cos^4 \vartheta \sin^4 \vartheta = 1 \quad (21)$$

giving the found, general valid, criterion of [4] where it appeared that F_{1122} and other possible higher order terms can be neglected except F_{1266} .

The values C_t and C_d can be found by fitting of the modified "Hankinson equations" (20) for uni-axial off-axis tension and compression giving the constants:

$$2F_{12} = 1/X'Y + 1/XY' - 1/S^2 + C_t - C_d; \quad 3(F_{112} + F_{166}) = C_t/X' + C_d/X; \\ 3(F_{122} + F_{266}) = C_t/Y' + C_d/Y \quad \text{and} \quad 12F_{1266} = C_t C_d - 12F_{1122} \approx C_t C_d. \quad (22)$$

Experimentally it is shown that a fit of the Hankinson eq.(19) always is possible. Thus different n values for tension and compression from $n = 2$ means that there are higher order terms and C_t and C_d are not zero as follows from eq.(22).

It was shown in [1] that F_{12} is small and can not be known with a high accuracy. Small errors in the strength values (X, X', Y, Y', S) may change F_{12} by more than

100 % or even change its sign [1] and the value thus is not important. The data of [4] of the principal stresses in longitudinal tension, being close to initial yield, show F_{12} to be zero at initial yield (when $C_t = C_d = 0$, thus F_{12} will be proportional to $C_d - C_t$). The possible estimate in [4], based on the third degree polynomial for all data, shows F_{12} to be negative and to be of lower order with respect to $1/S^2$, showing F_{12} here to be neglectable, and because also $C_d - C_t$ is of lower order, the equivalent shear-strength S follows from:

$$1/S^2 = 1/X'Y + 1/XY' + (1 - \alpha) \cdot (C_t - C_d) \approx 1/X'Y + 1/XY' \quad (23)$$

and consequently:

$$2F_{12} = \alpha(C_d - C_t) \quad (\approx 0), \quad (24)$$

where α is a constant found from fitting. Inserting the estimated values of the strengths of [4], based on all data, ($X = 55.5$; $X' = 43.1$; $Y = 3.7$; $Y' = 5.6$) and for $S = 9.4$ to 10.2 , then α has values between $\alpha = 0$ to $\alpha = 1$. A lower value of S as was measured for pure shear ($S = 9$), indicates a positive value of F_{12} and it is seen that F_{12} may easily switch between any (small) value (and thus can be neglected). For a practical criterion, a safe lower bound should be used that ignores the influence of numerous, still higher order terms, because it is not justified to use a complicated equation to account for only small influences. This also applies for F_{1266} wherefore a good estimate (including neglected highest order terms and thus need not to be bounded) will be eq.(22):

$$12F_{1266} = C_t C_d, \quad (\approx 0),$$

but will be shown to be neglectable.

As mentioned before, F_{166} is small or zero for clear wood. However, because of the grain- and stress deviations, F_{166} will not be zero for timber, because crack extension along the grain has components in longitudinal and transverse directions when there is a grain deviation and F_{166} and F_{266} are connected as components depending on the (local) structure. As crack extension component F_{166} will have a similar bound as given by eq.(17) for F_{266} as follows by replacing the index 2 by 1 and Y by X . Thus:

$$3F_{166} \leq 0.99/X'S^2.$$

Determining for wood however will not be this bound but the value of F_{166} , following from eq.(22), when F_{112} is known. F_{112} shows to be high by the form of the failure surface and an estimate of the bound of F_{112} has to be made. This form of the failure surface (for the principal stresses, where it is determined by F_{112}), shows a similar cut-off parabola as F_{266} , indicating a common cause with a value of F_{112} close to its upper bound, as found for F_{266} . A general method to determine this bound of F_{112} is given in [1] (for F_{266}). For the purpose here it is sufficient to satisfy eq.(29) of the following approximation.

The upper bound of F_{112} described above applies for $\sigma_6 = 0$. Because for nearly clear wood, the longitudinal crack extension theory predicts F_{166} and F_{122} to be small, the following equation applies:

$$\sigma_1 \left(\frac{1}{X} - \frac{1}{X'} \right) + \sigma_2 \left(\frac{1}{Y} - \frac{1}{Y'} \right) + \frac{\sigma_1^2}{XX'} + \frac{\sigma_2^2}{YY'} + 3F_{112} \sigma_2 \sigma_1^2 = 1 \quad (25)$$

This can be written:

$$\sigma_1 (X' - X) + \sigma_1^2 (1 + 3F_{112} \sigma_2 XX') = (1 - \sigma_2/Y) \cdot (1 + \sigma_2/Y') \cdot XX' \quad (26)$$

and, neglecting the first term, it can be seen that this equation reduces to a parabola when about: $3F_{112} \approx 1/XX'Y'$ (when the first term is small). The critical value of the bound of F_{112} (to just have a closed surface) will occur at high absolute values of σ_1 and σ_2 and can be expected to occur in the neighbourhood of $\sigma_1 \approx -X'$. For σ_1 approaching: $\sigma_1 \approx -X'$, the first term of eq.(26) is small with respect to the second term and because the compression strength perpendicular to the grain hardly is effected by the longitudinal stress, this maximal value can be inserted, as a good approximation, in this small term giving:

$$\sigma_1^2(1 + 3F_{112}\sigma_2XX' + (X' - X)/(-X')) = (1 - \sigma_2/Y) \cdot (1 + \sigma_2/Y') \cdot XX'$$

or:

$$\frac{\sigma_1}{X'} = \sqrt{\frac{(1 - \sigma_2/Y) \cdot (1 + \sigma_2/Y')}{1 + c\sigma_2/Y'}} \quad \text{where } c = 3F_{112}Y'X'^2 \quad (27)$$

It can be seen that when $c = 1$, the curve reduces to a parabola and the requirement to have a closed curve is $c < 1$. Thus: $3F_{112} < 1/(Y'X'^2)$. The same may apply at the tensile side giving the same equation (27), when X' is replaced by X , or:

$$\frac{\sigma_1}{X} = \sqrt{\frac{(1 - \sigma_2/Y) \cdot (1 + \sigma_2/Y')}{1 + c\sigma_2/Y'}} \quad \text{where } c = 3F_{112}Y'X^2 \quad (28)$$

The found parabolas are equivalent to the Wu-equation for shear with tension or compression. Because for wood with defects there always are deviations of the stress or of the grain for the regarded main directions, there always is shear present and when this shear, in the real material planes, is the cause of the failure then according to the maximal stress criterion (eq.(23) of [10]) σ_1/X of eq.(28) should be replaced by σ_6/S of the main plane. By this replacement eq.(28) is identical to eq.(17) and F_{122} is determined by F_{266} of the real material planes.

More general, when F_{12} and F_{122} are not neglectable, the bound: $c < 1$ becomes:

$$c \approx 3F_{112}X'^2Y' - 2F_{12}X'Y' + 3F_{122}Y'^2X' < 1 \quad \text{for compression} \quad (29)$$

where, besides $\sigma_1 \approx -X'$, also $\sigma_2 \approx -Y'$ is substituted in the contribution of the small term, as assumed determining point to just have a closed surface.

In the same way is, at the tensile side (replacing $-X'$ by X):

$$c \approx 3F_{112}X^2Y' + 2F_{12}XY' - 3F_{122}Y'^2X < 1 \quad \text{for tension} \quad (29')$$

To connect the longitudinal tension region, where F_{112} , F_{12} and F_{122} are about zero, (when this region is separately regarded), to the longitudinal compression region, where F_{112} dominates, it is necessary that for compression:

$$2F_{12} - 3F_{122}Y' \ll 3F_{112}X' \quad (30)$$

However for a precise fit still higher order terms (F_{1222} , F_{1112} , F_{1122}) are necessary. With the estimates of F_{266} and F_{112} to be close to their bounds for compression, and with zero normal coupling terms for tension, all constants of the general failure criterion eq.(21) are known, according to eq.(22), depending on C_d and C_t from uni-axial off-axis tension- and compression- tests.

Performing always the stress-transformation to the main planes, as done here, only simple transformation rules (circle of Mohr) have to be known for application.

Estimation of the polynomial constants by uni-axial tests

In fig. 4, a determination of C_d and C_t is given. In this figure of [4], the measurement $Y'/X' = 0.204$ is reduced to obtain a value of $Y'/X' = 0.13$ (at 90°) to be able to use the measured constants of the bi-axial tests. It is not mentioned how that possibly can be done but the drawn lines in the figure give the prediction of the uni-axial values based on the measured constants according to the general eq.(21) (given in [4] in the strength tensor form as given here by eq.(15)). For comparison the fits of the Hankinson equations are given here, following these drawn lines. For tension the equivalent Hankinson equation (20) becomes (by scratching the non zero term of the product):

$$\frac{\sigma_t \cos^2 \vartheta}{X} + \frac{\sigma_t \sin^2 \vartheta}{Y} + \sigma_t^2 \sin^2 \vartheta \cos^2 \vartheta C_t = 1 \quad (31)$$

and this equation fits the line for tension in fig. 4 when $C_t \approx 11.9/X^2$. The Hankinson equation (19) fits in this case for $n \approx 1.8$ and all 3 equations (21), (31) and (19) give the same result although for the Hankinson equations only the main tension- and compression strength have to be known and the influence of all other quantities are given by: n or C_t .

For compression, the same line as found in [4] was found in [1], (see fig. 11 of [1]), by the second order polynomial with the minimal possible value of F_{12} (according to eq.(12)), showing that except a negative F_{122} (as used in [4]) also a high negative F_{12} may cause the, strong peak at small angles. Because such a peak never is measured, the drawn line of [4] is only followed for the higher angles by the Hankinson equation. For the low angles, the line is drawn through the measured point at 15° , giving the expectable Hankinson value of $n = 2.4$ of eq.(19) and for eq.(32): $C_d \approx 4/X'^2$. Because of this low measured value, the predicted peak at 10°

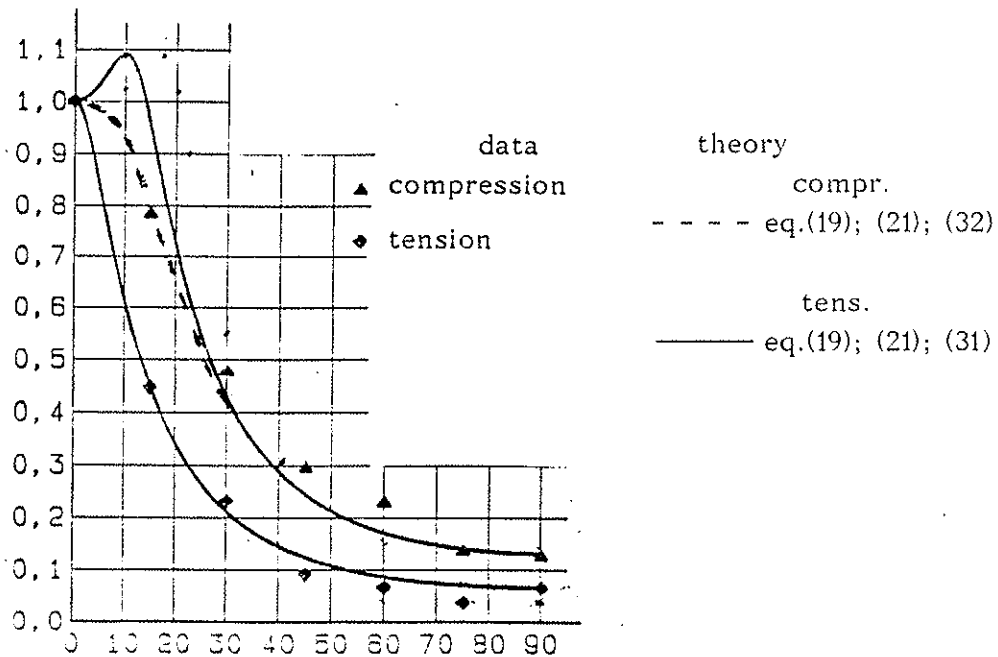


Figure 4 - Uni-axial tension- and compression strengths

is not probable (although theoretically possible, for a high shear strength, to occur at 18° in stead of 10° with C_d is $7.6/X^2$ in the Hankinson eq.(32)):

$$\frac{\sigma_t \cos^2 \vartheta}{X} + \frac{\sigma_t \sin^2 \vartheta}{Y} + \sigma_t^2 \sin^2 \vartheta \cos^2 \vartheta C_d = -1 \quad (32)$$

This shows that the fit of the polynomial constants, based on the best fit of the measurements of [4], is not well for the oblique grain test. The explanation of this deviation is probably the different state of hardening that can be more or less strong, depending on the stability of the type of test and is less in the Hankinson test. This, for instance, follows from the ratio of the compression strengths perpendicular to the grain and along the grain of 0.2 in the uni-axial tests and 0.1 in the bi-axial tests showing more hardening in the bi-axial test. Further the strong local peak is never measured in the common oblique grain test showing less stability than in the bi-axial test.

An analogous behaviour occurs in the oblique-grain test of clear wood where the tensile test shows $C_t = 0$ in eq.(20) and the compression test shows C_d to be not zero. A zero value of C_t indicates no higher order terms and thus C_d should be zero. However the tensile test will show unstable fracture at yield what need not to be so for the compression test that may show additional hardening.

Thus the criterion eq.(20) with only $C_t = 0$ may show two different hardening states. For the different hardening states in the two different types of tests, uni-axial and bi-axial, the lowest always possible value should be used for practise.

It thus has to be concluded that the strong hardening in the bi-axial test, will not occur in all circumstances and the hardening parameter F_{112} should be small or omitted for a safe lower bound criterion (according to the oblique grain test).

As generally found in [1] for spruce clear wood, a fit is possible for off-axis tension by a second order polynomial with $F_{12} = 0$. This also applies for wood with defects, as follows from a fit of the data of [4] by the second order polynomial (ellipse) for the principal stresses σ_1 and σ_2 (when $\sigma_6 = 0$), for longitudinal tension ($\sigma_1 > 0$; $F_{12} = 0$), see fig. 5. This means that F_{122} and F_{112} are zero (for $\sigma_1 > 0$) in the radial plane and because the Hankinson value for tension n is different from $n = 2$, there must be higher order terms for shear (F_{166}, F_{266}).

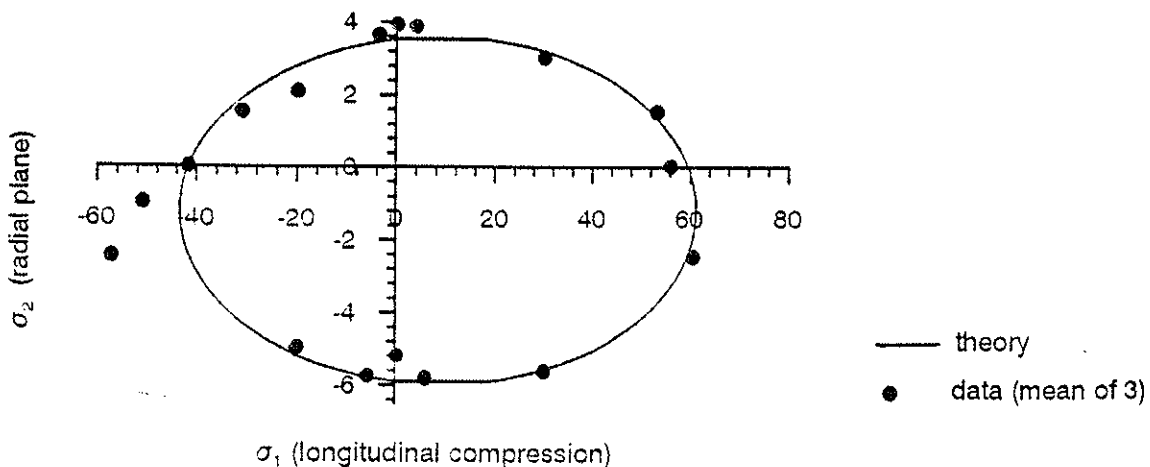


Figure 5 - First yield criterion eq.(5), with $F_{12} = 0$, for $\sigma_6 = 0$.

A first hypothesis thus is (by eq.(22)):

$3F_{266} = C_t/Y'$; $3F_{166} = C_t/X'$, (with $F_{112} = F_{122} = 0$) for tension and (by eq.(22)):

$3F_{122} = C_d/Y$ and $3F_{112} = C_d/X$, (with $F_{166} = F_{266} = 0$) for compression. This gives maximal values of F_{122} and F_{112} for the total fit.

The strength values according to this fit of [4] are (in N/mm²):

$X = 59.5$; $X' = 46.5$; $Y = 3.5$; $Y' = 5.9$; $S \approx 10$ and with: $C_t = 11.9/X^2$; $C_d = 4/X'^2$; $2F_{12} \approx C_d - C_t$, the predicted values are given in table 1 at column: hyp.1. It is seen that these values fit better than the best fit of the comparable eq.(62) of [4], given in the column indicated with [4]. However for $\sigma_6 = 0$, F_{122} must be negative for a precise fit when $\sigma_1 < 0$ and about zero when $\sigma_1 > 0$, showing that F_{122} has got the function to replace neglected still higher order terms, and a precise fit only can be expected to be possible with multiple higher order terms (with indices 1 and 2). As mentioned in [4], the values of σ_6 can be corrected by F_{1266} to be slightly lower when the sign of σ_1 and σ_2 is the same and to be slightly higher when the sign is opposite. This means that the first and third column value of column: hyp.1 (being 1.1 and 1.0) can be around 1.05. This shows that introduction of F_{1266} only gives a correction of a few percent and justifies the neglect of F_{1266} . The column values further are slightly too high when $\sigma_1 > 0$ and too low for $\sigma_1 < 0$, indicating that F_{166} is not precise. Neglecting the multiple higher order terms, the hypothesis has to be rejected, because F_{122} is too high, distorting the ellipse (at $\sigma_1 > 0$) too much for high negative values of σ_2 and causing the surface to be open at $\sigma_1 < 0$ and high negative σ_2 . It thus is probable that F_{122} is much smaller.

Without the higher order terms, F_{122} has to satisfy eq.(29) and the highest possible positive value of F_{122} becomes about 0.0001, being about 5 times smaller than according to first hypothesis. The fit now, with this small positive value of F_{122} , is about comparable with the best fit of [4] (that is based on a negative value of F_{122}), but now satisfies eq.(22) and will not show the compression peak in the Hankinson test (fig. 4). The fit is in total not better than a fit with changed constants and is also in total not better than assuming F_{12} , F_{122} and F_{112} to be zero for $\sigma_1 > 0$. This leads to the second hypothesis that the higher order terms for normal stresses are small at fracture (that thus is close to initial yield when $\sigma_1 > 0$) and can be neglected.

In table 1, column hyp.2, the fit is given for $F_{12} = F_{112} = F_{122} = 0$. Because the fit does not change much when data above the uni-axial compression strength: $X' = 41.7$ are neglected, the fit is based on this value and column hyp.2 gives the prediction of failure by the same hardening state as in to the oblique-grain test (where the strong compressional hardening does not occur). The constants are:

$$C_t = 11.9/X^2 = 11.9/59.5^2 = 0.00336; C_d = 4/X'^2 = 4/41.7^2 = 0.00230 \text{ and}$$

$$\text{by eq.(22): } 3F_{166} = C_t/X' + C_d/X = 0.00336/41.7 + 0.0023/59.5 = 0.000119 \text{ or:}$$

$$c_{166} = 0.000119 \cdot 9.7^2 \cdot 41.7 = 0.47$$

$$3F_{266} = C_t/Y' + C_d/Y = 0.00332/5.95 + 0.0023/3.5 = 0.00122 \text{ or:}$$

$$c_{266} = 0.00122 \cdot 9.7^2 \cdot 5.95 = 0.68$$

$$F_1 = \frac{1}{X} - \frac{1}{X'} = 1/59.5 - 1/41.7 = -0.0072; F_{11} = \frac{1}{XX'} = 1/59.5 \cdot 41.7 = 0.00040$$

$$F_2 = \frac{1}{Y} - \frac{1}{Y'} = 1/3.5 - 1/5.95 = 0.092; F_{22} = \frac{1}{YY'} = 1/3.5 \cdot 5.95 = 0.048 \text{ and:}$$

$$F_{66} = \frac{1}{S^2} = 1/9.7^2 = 0.0106; \quad F_{12} = F_{112} = F_{122} = 0.$$

The only strong deviation from the last supposition (of having small normal stress coupling terms) thus occurs in the torsion tube test for the principal compressional stresses ($\sigma_6 = 0; \sigma_1 < 0; \sigma_2 < 0$). The form of the curve is parabolic close to the Wu-equation, showing F_{112} to be high. However the fit is not precise because there appears to be also an other hardening effect, raising the longitudinal compression strength by lower and intermediate values of compression perpendicular σ_2 and F_{122} and F_{12} are also needed to describe this additional hardening effect.

For comparison the strength values of the best fit of all data of [4] are regarded: $X = 55.5; X' = 43.1; Y = 3.7; Y' = 5.6$. The shear strength S of 10 is too high as shown by table 1 and is taken to be 9.4, giving a mean factor of 1.0 in the table for this fit. This leads to the relation of S :

$$1/S^2 \approx 1.2(1/X'Y + 1/XY') = 1.2(1/(43.1 \cdot 3.7) + 1/(55.5 \cdot 5.6)) = 1.2(0.00627 + 0.00322) = 1.2 \cdot 0.00949 = 0.0113, \text{ giving the wanted } S \approx 9.4.$$

For the constants now is:

$$F_1 = \frac{1}{X} - \frac{1}{X'} = 1/55.5 - 1/43.1 = -0.0052; \quad F_{11} = \frac{1}{XX'} = 1/55.5 \cdot 43.1 = 0.00042;$$

$$F_2 = \frac{1}{Y} - \frac{1}{Y'} = 1/3.7 - 1/5.6 = 0.092; \quad F_{22} = \frac{1}{YY'} = 1/3.7 \cdot 5.6 = 0.048.$$

Further is:

$$C_t = 11.9/X = 11.9/55.5 = 0.00386 \text{ and } C_d = 4/X'^2 = 4/43.1^2 = 0.00215.$$

F_{12} is the only unknown and gives a reasonable fit with $\alpha \approx 1$ in eq.(24) or:

$$2F_{12}^2 \approx C_d - C_t = -0.0017.$$

This value satisfies eq.(30) and eq.(29) for compression, but not eq.(29') for tension, (showing the surface to be open for tension).

By the strong development of cracks, F_{266} and F_{112} will be high, giving:

$$3F_{266} = 0.9/S^2 Y' = 0.9/9.4^2 \cdot 5.6 = 0.00184$$

and according to eq.(22):

$$3F_{122} = C_t/Y' + C_d/Y - 3F_{266} = 0.00386/5.6 + 0.00215/3.7 - 0.00184 = -0.00057$$

$$3F_{112} = 0.9/5.6 \cdot 43.1^2 = 0.000086, \text{ (and consequently } 3F_{166} = 0.000042 \text{ with:}$$

$2F_{12}^2 \approx -0.0014$) gives the best fit for $\sigma_6 = 0$. However, for combined shear, given in table 1, column 3-compr., the values are comparable with those of column [4]

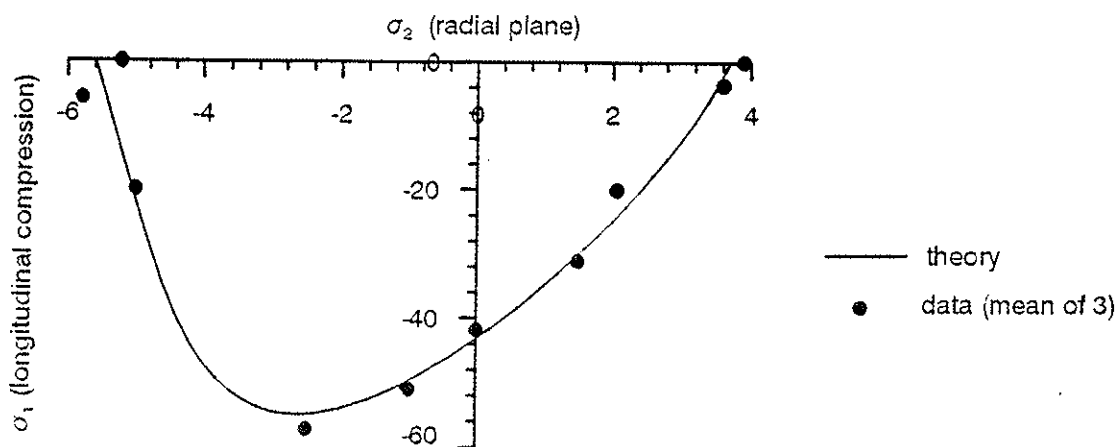


Figure 6 - Yield criterion for compression ($\sigma_1 < 0$) for $\sigma_6 = 0$.

and not well enough for practise. A better fit for the shear strengths is obtained by a slightly reduced factor 0.8 in stead of 0.9 for F_{112} (thus a diminished crack development similar to the oblique-grain test proj. B of fig. 3) giving:

$$3F_{112} = 0.8/5.6 \cdot 43.1 = 0.000077,$$

$$3F_{166} = C_t/X' + C_d/X - 3F_{112} = 0.000128 - 0.000077 = 0.000051$$

giving the c-values: $c_{166} = .000051 \cdot 9.4^2 \cdot 43.1 = 0.2$, and: $c_{266} = 0.9$ (starting point).

The combined shear strengths are given in table 1, column 4 (compressional fit), and it is seen that the fit is still less well than according to the 2 foregoing columns due to the negative value of F_{122} as mentioned before.

Further for $\sigma_6 = 0$, the "fit" is given in fig. 6 for compression while for longitudinal tension ($\sigma_1 > 0$) combined with high compression σ_2 perpendicular to the grain, the surface is open and still higher order terms are needed for a closed surface.

Table 1. Shear strength σ_6 for combined normal stresses

σ_1	σ_2	σ_6 test	factor: $\sigma_{6,theory}/\sigma_{6,test}$				
			[4]	hyp.1	hyp.2 tens.	3 compr.	4 compr.
30	1.5	5.8	1.07	1.10	1.03	0.9	1.02
30	0	8.5	0.88	0.97	0.91	0.77	0.92
30	- 2.5	7.9	0.99	1.00	1.10	0.91	1.29
7.3	0	9.2	1.04	1.07	1.03	0.96	1.01
0	2.9	3.7	1.38 !	1.25	1.13	1.39 !	1.19
0	1.5	8.5	0.96	0.95	0.89	0.93	0.86
0	0	9.0	1.11	1.11	1.08	1.04	1.04
0	- 2.5	10.9	0.96	0.98	1.05	0.86	1.07
0	- 5.4	6.8	0.53 !	0.82	1.12	0.45 !	1.12
- 7.7	0	9.6	1.05	1.04	1.01	1.03	0.96
- 20	1.5	7.7	0.84	0.89	0.83	0.93	0.68
- 20	0	9.6	0.99	0.98	0.96	1.10	0.88
- 30	- 2.5	11.3	1.04	0.98	0.90	1.16	0.94
mean factor			.99	1.01	1.0	0.96	1.0

To avoid many higher order terms separate criteria have to be used for longitudinal compression and tension. For compression ($\sigma_1 < 0$) eq.(21) becomes:

$$F_1\sigma_1 + F_2\sigma_2 + F_{11}\sigma_1^2 + F_{22}\sigma_2^2 + 2F_{12}\sigma_1\sigma_2 + F_{66}\sigma_6^2 + 3F_{112}\sigma_1^2\sigma_2 + 3F_{122}\sigma_1\sigma_2^2 + 3F_{166}\sigma_1\sigma_6^2 + 3F_{266}\sigma_2\sigma_6^2 = 1 \quad (33)$$

Because the C_t , C_d and n-values of the Hankinson equations are sufficiently close to the published extreme values of n, the here calculated c-values can be used in general and inserting F-values in eq.(33). this equation becomes:

$$\frac{\sigma_6^2}{S^2} \cdot \left(1 + 0.9 \cdot \frac{\sigma_2}{Y'} + 0.2 \cdot \frac{\sigma_1}{X'}\right) = \left(1 - \frac{\sigma_1}{X'}\right) \cdot \left(1 + \frac{\sigma_1}{X'}\right) + \left(1 - \frac{\sigma_2}{Y'}\right) \cdot \left(1 + \frac{\sigma_2}{Y'}\right) +$$

$$- \left(1 + 0.8 \cdot \frac{\sigma_2 \cdot \sigma_1^2}{Y' \cdot X'^2} - 0.77 \cdot \frac{\sigma_1 \cdot \sigma_2^2}{X' \cdot Y'^2} - 0.41 \cdot \frac{\sigma_1 \cdot \sigma_2}{X' \cdot Y'}\right) \quad (34)$$

For tension ($\sigma_1 \geq 0$) eq.(21) becomes (in the radial plane):

$$\frac{\sigma_6^2}{S^2} \cdot \left(1 + 0.68 \cdot \frac{\sigma_2}{Y'} + 0.47 \cdot \frac{\sigma_1}{X'}\right) = \left(1 - \frac{\sigma_1}{X'}\right) \cdot \left(1 + \frac{\sigma_1}{X'}\right) + \left(1 - \frac{\sigma_2}{Y'}\right) \cdot \left(1 + \frac{\sigma_2}{Y'}\right) - 1 \quad (35)$$

Because the compressional hardening according to eq.(34) only occurs for low values of σ_6 , only in the torsional tube test, eq.(35) more generally represents the failure criterion for both tension and compression for the more common loading case as occurs in the oblique-grain test. Neglecting the higher compression strengths far above the uni-axial compression strengths, at $\sigma_6 = 0$, the overall fit is very well and much better than the proposed fit of [4].

For the tangential plane there is a strong indication that the higher order terms are zero (causing $n = 2$ for timber and glulam). When this is the case, eq.(35) only applies locally near the radial plane and the mostly determining criterion becomes:

$$\frac{\sigma_6^2}{S^2} - \left(1 - \frac{\sigma_1}{X'}\right) \cdot \left(1 + \frac{\sigma_1}{X'}\right) - \left(1 - \frac{\sigma_2}{Y'}\right) \cdot \left(1 + \frac{\sigma_2}{Y'}\right) = -1$$

or worked out, identical to eq.(5) with $F_{12} = 0$:

$$\frac{\sigma_6^2}{S^2} + \frac{\sigma_1}{X'} - \frac{\sigma_1}{X'} + \frac{\sigma_1^2}{XX'} + \frac{\sigma_2}{Y'} - \frac{\sigma_2}{Y'} + \frac{\sigma_2^2}{YY'} = 1 \quad (36)$$

It therefore is necessary to use eq.(36) for the Codes in all cases, for timber and clear wood to replace the equivalent, now commonly used, not valid Norris-equations.

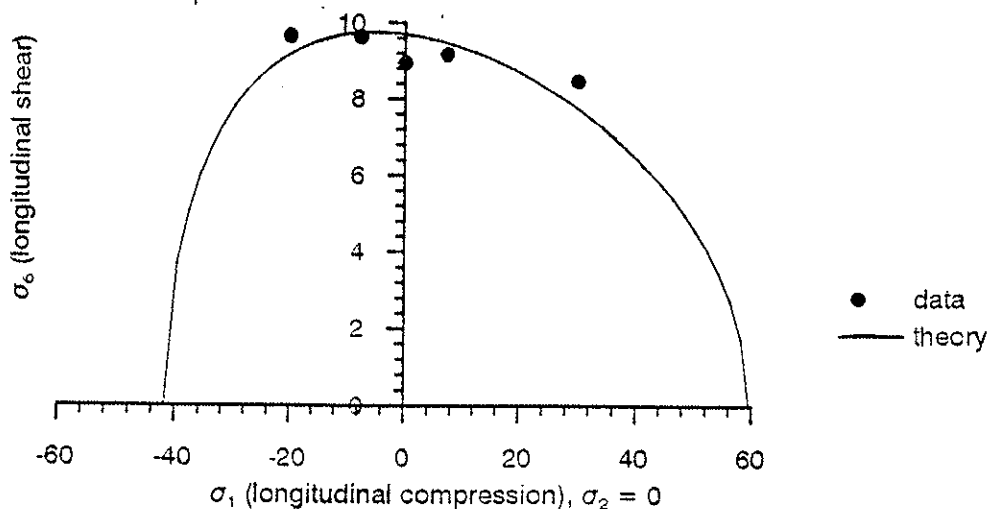


Figure 7 - Combined longitudinal shear with normal stress in grain direction.

For general applications and analysis of test result, the constants can be based on the measured C_d and C_t values or on the Hankinson equations (20) or (19) for the uni-axial stress case when n different from $n = 2$.

For $\sigma_2 = 0$, determining F_{166} , a plot is given in fig. 7.

For $\sigma_1 = 0$, giving F_{266} , a plot is given in fig. 8.

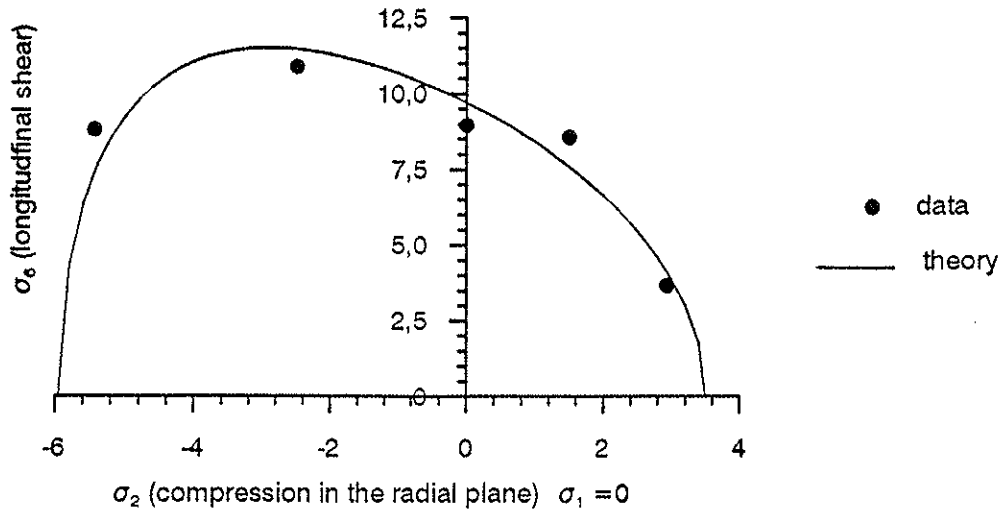


Figure 8 - Longitudinal shear strength ($\sigma_1 = 0$) depending on the normal stress σ_2 .

Application for tapered beams

These type of beams are designed according to the theory of orthotropic elasticity and for failure the Norris criterion is used (see eq.(26) of [10]). As shown in [10] this criterion may represent initial yield because, for the determining uni-axial stress state along the boundary, this equation is identical to the Hankinson equation with $n = 2$. Tests of [5] suggest, for not too small angles α , elastic behaviour up to failure because tension perpendicular is determining. However, for clear wood, for α below 5° to 10° , the elastic values do not apply because of plastic flow in compression (as follows from the much higher value of f_m with respect to f_c) and the used Norris-criterion based on f_m [8] is not right and the theory should be adapted for this case. Further also for higher values of α above about 15° , the slope may act as a notch and theory should be adapted to account for this, by fracture mechanics determined, strength.

As a scheme, in the elastic range, the beam is regarded as a wedge loaded at the top, wherefore the stress distribution is known [6], [7], what applies at a sufficient distance from the support. Based on this theory, the curve fitting, using one fictive shear strength for longitudinal tension as well as compression, ($f_{c,0} = 44$; $f_{c,90} = 4.0$; $f_v = 5$ MPa, for compression and $f_{t,0} = 44$; $f_{t,90} = 0.6$; $f_v = 5$ MPa, for tension), did not show a good fit. Following [8], by using a value of $f_v = 3.6$ for tension, the fit is good and in accordance with the derived value of the fictive shear-strength of: $f_v = \sqrt{XY/2} = \sqrt{44 \cdot 0.6/2} = 3.6$. If the given values in [7] and [8] of the uni-axial strengths ($f_{c,0}$, $f_{c,90}$, $f_{t,0}$, $f_{t,90}$) are representative, the best fits for glulam (in the whole range of α), and for clear wood (above $\alpha = 10^\circ$) are obtained with lower fictive shear strengths of about $f_v = \sqrt{XY/3}$ for tension and higher values of f_v than $f_v = \sqrt{XY/2}$ for compression, showing that higher order terms have an influence and

the Norris-equations (being equivalent to the Hankinson equations for $n = 2$) have to be replaced by the Hankinson equations (19) with n different from $n = 2$ (or the exact eq.(20) should be used). This has to be proposed for the future Codes.

CONCLUSION

- All following conclusions apply for the normally used softwoods.
- The tensor polynomial failure criterion can be regarded as an polynomial expansion of the real failure criterion. As a consequence, when a least square fitting procedure is used in stead of the expansion procedure, a, in principle, complete polynomial up to the chosen degree is necessary (whereby terms of this compound polynomial may vanish by general symmetry conditions). Further this fit by a limited number of terms need not to show the precise right values of the expanded components and need not to pass all mean values of the measurements precisely and also p.e. the normality rule and convexity requirement need not to apply exactly.
- In transverse direction a second order polynomial (eq.(36)) is sufficient to describe the strength. When for compression (perpendicular to the grain) the strength is defined as the value after flow and some strain hardening, a lower bound of the overall strength can be chosen that will be directional independent and the behaviour can be regarded to be quasi isotropic in the transverse direction.
- There is a strong indication that for initial yield, or when the tangential plane is determining (as follows from direct measurements and the oblique-grain test), also for the longitudinal strengths a second order polynomial (with $F_{12} = 0$) is sufficient as yield criterion. When the test becomes unstable early, at initial crack extension, as for instance in the oblique-grain tension test or for compression in the "Sher-eisen" test (probably also in the radial plane), there are no higher order terms. Higher order terms thus are due to hardening effects (real hardening or equivalent hardening by crack arrest) depending on the type of test that may provide stable or unstable crack propagation after initial yield.
- It is shown that, when the Hankinson parameter $n = 2$ in eq.(19) for tension and compression, all higher order terms are zero. It is probable that this is a general property for timber [11], because when shear failure is free to occur the plane of minimum resistance, as usually in large timber beams and in glulam, it occurs in the tangential plane, showing no higher order terms.
- For clear wood (and wood with small defects), in a stable test, the longitudinal shear strength in the radial plane increases parabolical with compression perpendicular to this plane depending on the coupling term F_{266} giving the Mohr equation or the Wu- equation, that can be explained by collinear micro-crack propagation in grain direction [9]. This increase is an equivalent hardening effect, due to crack arrest by the strong layers, causing failure only to be possible by longitudinal crack propagation. It is shown that the increase of the shear strength is not due to Coulomb friction, being small for wood.
- Because of the oriented crack-propagation, explaining the Wu-equation, $F_{166} \approx 0$ for clear wood because σ_1 is in the same direction as the flat crack and thus not influenced by that crack. Except for small clear specimens at compression, (providing a high shear strength by the volume effect), there also is no indication of an influence of the normal coupling terms F_{12} , F_{122} and F_{112} (due to hardening by

confined dilatation).

- For wood with (small) defects and local stress and grain deviations, an equivalent polynomial failure criterion is possible, showing therefore an influence of higher order terms. At least an fourth order polynomial is necessary for a reasonable description. A precise description by a third order polynomial is possible when 2 different criteria are regarded, one for longitudinal tension and for longitudinal compression (similar to the 2 Hankinson equations).

- The general form of the criterion for the uni-axial off-axis strength for wood with defects, is at least determined by a the fourth degree equation (eq.(21) in σ_t) and can always be factorized as a product of two quadratic equations, eq.(20). This leads to extended Hankinson equations, eq.(20), for higher order terms, when n of eq.(19) is different from $n = 2$.

- Because of grain- and stress deviations, F_{166} will not be zero for timber, as for clear wood, because crack extension along the grain has components in longitudinal and transverse directions when there is a grain deviation and F_{166} and F_{266} are connected as components depending on the (local) structure. As crack extension component F_{166} will show a similar cut-off parabola as F_{266} , indicating the common cause.

- For the same reason, the uni-axial tensile strength in the main direction is determined by the shear strength of the oblique material planes and F_{112} represents F_{266} of the real material planes, showing the same Wu-parabola. Similar to F_{166} , F_{122} may act as component in transverse direction of F_{112} .

- For wood with defects, when the principal strengths in the main planes ($\sigma_6 = 0$) are determining, F_{112} , F_{12} and F_{122} are zero, for longitudinal tension (due to early instability of the test). For combined shear failure (equivalent hardening), there are, for this case, small positive values of F_{112} and F_{122} . It is however shown that for a practical criterion these terms can be neglected and only F_{166} and F_{266} remain for longitudinal tension.

For longitudinal compression at $\sigma_6 = 0$, equivalent hardening by crack arrest, (high F_{112}) as well as hardening by confined dilatation (showing a negative F_{122} and F_{12}) may occur. This last type of hardening probably only occurs in the torsion tube test, because the negative F_{122} and F_{12} predict a compression peak (see fig.4) that does not occur in the oblique grain test. For structural elements, this effect thus has to be neglected and the lower bound criterion with only F_{166} and F_{266} (and zero F_{12} , F_{122} and F_{112}) applies also for compression in the radial plane as follows from the good fit.

- Because in the tangential plane, the higher order terms can be zero, the quadratic polynomial eq.(36):

$$\frac{\sigma_6^2}{S^2} + \frac{\sigma_1}{X} - \frac{\sigma_1}{X'} + \frac{\sigma_1^2}{XX'} + \frac{\sigma_2^2}{YY'} + \frac{\sigma_2}{Y} - \frac{\sigma_2}{Y'} = 1$$

should be used as lower bound for the Codes in all cases, for timber and clear wood, and because the equation represents initial yield as well it will apply for the lower 5th percentile of the strength.

- For large sized timber and glulam, where shear failure (or longitudinal tensile failure) may pass radial as well as in tangential directions in the same failure plane, the following (eq.(35)) will apply:

$$\frac{\sigma_6^2}{S^2} \left(1 + c_{266} \cdot \frac{\sigma_2}{Y'} + c_{166} \cdot \frac{\sigma_1}{X'} \right) = \left(1 - \frac{\sigma_1}{X} \right) \cdot \left(1 + \frac{\sigma_1}{X'} \right) + \left(1 - \frac{\sigma_2}{Y} \right) \cdot \left(1 + \frac{\sigma_2}{Y'} \right) - 1 \quad (52)$$

where c_{166} and c_{266} follows from oblique-grain tests according to eq.(22) based on the measured C_d and C_t values: $F_{166} = C_t/X' + C_d/X$; $F_{266} = C_t/Y' + C_d/Y$.

- For general applications and analysis of test results, eq.(52) can be used or for the uni-axial loading case, the Hankinson equations (20) or (19).

- The Norris equations are not generally valid and only apply for uni-axial loading, identical to the Hankinson equation with $n = 2$, when the right (mostly) fictive shear-strength is used. These equations thus should not be used any more.

- Therefore, for tapered beams and for all other cases with determining off-axis uni-axial strength, the general Hankinson equations for tension and compression (with n different from $n = 2$, depending on the measurements) should be used or the exact equations (31) and (32) (or of course eq.(52)).

REFERENCES

- [1] van der Put, T.A.C.M., A general failure criterion for wood, Proc. IUFRO meeting Boras, 1982 (or: Stevinreport 4-82-5 HA-14, Feb. '82).
- [2] Liu, J.Y. Evaluation of the tensor polynomial strength of wood, J. of Compos. Mater. Vol. 18, May 1984
- [3] van der Put, T.A.C.M., Discussion of the design of nailplate connections, Proceed. Pacific timber eng. conf., Auckland, New Zealand, I.P.E.N.Z. MAY 1984.
- [4] Hemmer, K., Versagensarten des Holzes der Weisstanne unter mehrsichtige Beanspruchung, Dissertation, Karlsruhe 1985.
- [5] Möhler K. and Hemmer K., IUFRO timber engineering meeting, augustus 1978.
- [6] Lekhnitskii, S.G., Anisotropic plates, Gordon and Breach Science Publ., 1968.
- [7] Ribberholt H., Tapered timber beams, CIB-W18/11-10-1, meeting Vienna, 1979.
- [8] Möhler K., Consideration of combined stresses for lumber and glued laminated timber CIB-W18/9-6-4, 1978 en CIB-W18/11-6-3, 1979.
- [9] van der Put, T.A.C.M., Explanation of the mixed mode interaction equation, Proceed. of the Cost 508 workshop on fracture mechanics, Bordeaux 1992.
- [10] van der Put, T.A.C.M., Post yielding behaviour of wood, Proc. of the Cost 508 workshop on yield and failure of wood, Limerick 1993.
- [11] Keenan, F.J. and Jaeger, T.A., Effect of transverse stress on shear strength and failure mechanism of Douglas-fir, Proc. first int. conf. on Wood fracture, Banff, Alberta, Canada, 1978.
- [12] Cowin, S.C., On the strength anisotropy of bone and wood, J. Applied Mechanics, ASME Transactions, vol. 46, no 4, 1979.
- [13] Norris, C.B., The elastic theory of wood failure, ASME Trans., vol.61, 3, 1939.
- [14] Hoffmann, O., J. Composite Materials, p. 200, 1967.
- [15] Tsai S.W., and Hahn H.T., Introduction to composite materials, Westport, CT: Technometric Publ. Co., Inc., 1980.
- [16] Wu R.Y., Stachurski Z., Evaluation of the normal stress interaction parameter in the polynomial strength theory for anisotropic mater. J. Comp. Mater. 1984.
- [17] Leichti R.J., Tang R.C., Predictin the load capacity of wood composite I-beams using the tensor polynomial strength theory. Wood Sci. and Technol. 23, 1989.

INTERNATIONAL COUNCIL FOR BUILDING RESEARCH STUDIES AND DOCUMENTATION
WORKING COMMISSION W18 - TIMBER STRUCTURES

PROPOSED TEST METHOD FOR DYNAMIC PROPERTIES OF CONNECTIONS
ASSEMBLED WITH MECHANICAL FASTENERS

by

J D Dolan
Virginia Polytechnic Institute and State University
USA

MEETING TWENTY - SIX

ATHENS, GEORGIA

USA

AUGUST 1993

PROPOSED TEST METHOD FOR DYNAMIC PROPERTIES OF CONNECTIONS ASSEMBLED WITH MECHANICAL FASTENERS¹

by

J.D. Dolan, Assistant Professor of Wood Engineering, Brooks Forest Products Laboratory, Virginia Polytechnic Institute and State University, 1650 Ramble Road, Blacksburg, Virginia, 24061-0503 United States of America

INTRODUCTION

Mechanically connected wood and wood-based materials, which act in shear, are the main source of energy dissipation and ductility when wood buildings respond to earthquakes and wind-gust loading. The damping and dynamic stiffness characteristics of such connections are often needed in structural design, but the current standard test methods for mechanical fasteners are usually limited to static monotonic loadings. Because testing conditions, such as a type, rate, and magnitude of loading affect dynamic properties, data from static testing cannot be extrapolated to dynamic loading. Special dynamic and pseudodynamic tests have been used for some time but have not been established in standards. The presented test method is for connections under pseudodynamic loading and incorporates procedures included in the **Sequential Phased Displacement Procedure** proposed by Porter (1987) and work completed by Polensek². This test method is also similar to one proposed by Reyer and Oji (1991). The use of this test method is recommended to generate comparable data and to eliminate variables in specimen assembly and testing methodology, and in data evaluation, which introduce variations in test data. These data reflect conditions similar to those expected in the service of buildings subjected to earthquakes and severe winds.

Mechanical connections provide the ductility and the medium for energy dissipation in many wood structures under seismic and wind loading. Factors that affect the ductility and energy dissipation include the physical and mechanical properties of the wood and wood-based material; the size, shape, and surface condition of the fastener; the speed and magnitude of the applied load; any physical changes between time of connection assembly and time of load application; orientation of wood fibers with respect to applied load; and the method of data evaluation.

A standard testing procedure allows the effects of fastener types and sizes, wood material properties, assembly techniques, and conditioning between assembly and loading time to be

¹ Paper prepared for presentation at the 26th Meeting of CIB W18 in Athens, Georgia, United States of America, August 23 to 27, 1993

² Parts of this standard are taken from a draft proposal written by A. Polensek (1988), that was never submitted to the ASTM committee.

evaluated. Since differences in methods of testing and data evaluation can have considerable influence on results, it is important that a standard procedure be specified and adhered to so that test results from different tests can be compared.

The test method is designed to evaluate the dynamic lateral response of a typical mechanical connection used in wood construction, by subjecting it to full reversal cyclic loading. The procedure determines the performance of single-fastener connections, and provides comparative data for various materials. This test method can also be used for evaluating any type and size of fastenings either in wood or other building materials, such as plywood, hardboard, steel, concrete, masonry, or combinations of materials. Furthermore, where required for specific purposes, the method can be used for evaluating the lateral resistance of various sizes of nails, staples, screws, bolts, or other fasteners different from those specified, and connections employing two or more fasteners.

Equivalent energy yield strength, hysteretic and equivalent viscous damping, dynamic stiffness, ductility, and capacity of the mechanical connections can be evaluated with this test procedure. The method is also designed for evaluating hysteresis loops of shear load versus slip from experimental traces for use in numerical modeling of connections.

PROCEDURE

Equipment

Any suitable testing machine, which is capable of operation in a two-directional, fully reversed, load-cycling mode with both a rate of motion and cycling load magnitude controlled up to 1% accuracy can be used for this test. However, the hydraulic actuator must be computer controlled in order to follow the phased displacement wave form used in the test.

Gripping devices capable of attaching one end of the specimen to the moving head of the testing machine in such a way as to ensure that the true axial loads and full reversing loading can be applied are required. Furthermore, the grips must hold the specimen so that the line of action of the loads is co-planer with the contact surface of the connection as shown in Figure 1.

A test fixture capable of holding the stationary side of the specimen so as to prevent movement in either the compression or tension directions of the testing machine must be manufactured. The fixture also prevents the specimen from moving perpendicular to the plane of the contact surface of the connection. The purpose of the fixture is to prevent the load on the connection from changing from shear to a combination of shear and axial loading on the fastener. Rollers are used to minimize any friction between the restraining fixture and the test specimen. Figures 2a - e show such a test fixture. The ends of the test specimen are secured with clamps, pins, bolts, or a combination of clamps and pins to prevent slipping. Figure 2a shows the empty fixture. Figure 2b shows a grip for the end of the specimen to be attached to the actuator.

Figures 2c - e show the placement of the specimen in the test fixture and attachment of the linear variable displacement transducers used to measure the slip of the connection.

At least two linear variable displacement transducers (LVDT) with a resolution of 0.025 mm (0.001 in.) or other suitable device for measuring deformation between the connection members under load must be used to record the connection slip. Figures 2c to e show a test specimen with the LVDTs attached. The load and deflection measurements for both of the LVDTs shall be recorded by a computer with an analog to digital converter at a minimum rate of 100 readings per cycle (100 Hz) to ensure that the hysteresis curves can be accurately represented for analysis. The readings from the two LVDTs are averaged to obtain the slip of the connection at the location of the fastener.

Specimen Description

Test specimens consist of two prisms of the materials to be tested, connected with one mechanical fastener installed at a right angle to the contact surface. Members shall be selected, and the fasteners positioned in them, in such a way that the results are not affected by natural or manufactured characteristics in the base material such as knots in wood. For wood connections, this frequently necessitates selecting members which are essentially clear and straight grained. Tests shall be made on connections loaded (a) parallel and (b) perpendicular to the base material's principal property directions. Figure 3 shows a few typical specimen configurations. The orientation of the stationary side of the connection or the side that is moved during the test can be changed to provide for the different configurations of load-to-material direction as required.

The width, length, and thickness of the connected members are selected with regard to the required edge and end distances and the net cross section remaining after the connectors are placed. The thickness of the specimen members should be representative of that anticipated in service. However, in some cases, the influences of member dimensions are the parameters being studied, and the dimensions will vary. Otherwise, the size of the specimens will usually depend of the size and type of fastener.

Holes drilled for bolts to be tested shall be between 0.8 and 1.6 mm (1/32 and 1/16 in.) larger than the fastener diameter and the holes shall be carefully bored perpendicular to the surface, so that the surface of the hole is smooth and uniform to assure good bearing of the fastener. Accurate centering of holes is required where a specification calls for two or more fasteners in a single connection.

For bolts, heavy round washers conforming to Federal Specification FF-W-92 for Washers, Metal, Flat (Plain), and hereafter referred to as standard washers, shall be placed between the member surface and the bolt head and nut. Abutting faces of the connection shall be brought into normally installed contact. For wood and other materials that exhibit creep that results in connections becoming loose over time, the nut shall then be backed off and retightened

to "finger tightness."

Except for special tests evaluating the effect of moisture content of the connected material on the strength of the connection, the tests shall be performed with specimens assembled with dry material (12% moisture content in the case of wood). When the material properties are affected by moisture content or temperature, the specimens shall be stored prior to testing in a room having a controlled temperature of $20^{\circ} \pm 3^{\circ}\text{C}$ ($68^{\circ} \pm 6^{\circ}\text{F}$) and controlled relative humidity of $65\% \pm 3\%$ for a period sufficiently long to bring them to approximately equilibrium. For most wood species, exposure to these conditions will result in a moisture content of approximately 12%. For special tests involving very dry or wet material, or different temperature conditions than stated above, care shall be taken to maintain the desired moisture content or temperature prior to and during testing.

Except for special circumstances that require delayed testing such as for driven fasteners, testing shall be performed within 1 hour after assembly. Specimens with driven fasteners shall be conditioned at the relative humidity and temperature conditions discussed above for a minimum of 14 days, to allow the material surrounding the fastener to relax.

Selection of representative test material on an objective and unbiased basis is mandatory, and proper sampling techniques should be used to prevent bias. This principle applies to the selection of the fasteners as well as to the base materials to be used. Materials tested for the purpose of obtaining reliable general averages and variations applying broadly to the materials need to be selected at random by a technique that permits correct physical properties that may influence test results to be determined. Sampling required for more limited experiments, such as for defining relationships or examining causes and effects, can accordingly be more limited, but shall be appropriate to the objectives of the testing program and use unbiased procedures.

Under all circumstances, tests shall be sufficiently extensive to provide reliable results. Where analysis by statistical procedures is contemplated, experience and advance estimates shall be used to establish the scope of testing and type of sampling needed to achieve the expected reliability. However, a minimum of 10 replications shall be required for each variable investigated. A larger number of observations may be desirable under some conditions. The precision required and, thus the manner of sampling and the number of tests, depends upon the specific objectives. General experience indicates that the coefficient of variation from tests of fasteners ranges from 15 to 30%. When such is the case, precision of 5 to 10%, with 95% confidence (an often accepted general measure of reliability) cannot be achieved without making a large number of tests.

Loading Function

The method used in this proposed standard is a slight modification of the "Sequential Phased Displacement" (SPD) procedure used by the Joint Technical Coordinating Committee on Masonry Research (TCCMAR) for the United States-Japan Coordinated Earthquake Research

Program. This procedure is used by TCCMAR to serve as a uniform basis for comparing components not subjected to real-time earthquake loading during testing. The procedure entails reversed-cyclic displacements of progressively increasing magnitude until a first major event (FME) occurs. The loading is then followed by a stabilization and degradation cycles before progressing to the next higher increment of displacements. This process is repeated until failure.

Failure is often defined as a catastrophic failure when the specimen is physically unable to carry any load. However, for some connections, failure will have to be defined by the investigator depending on the objectives of the test. A maximum displacement is one definition that is applicable to many test objectives.

The SPD procedure, described by Porter (1987), has been modified from a quasi-static displacement rate to a pseudodynamic displacement rate to account for the fact that the response of wood connections is dependent on the load rate. Therefore, the cyclic frequency of 1.0 Hz is used so that the connection response will approximate the frequency range expected during an earthquake or high-wind event. The displacement is a fully reversing, triangular, sinusoidal ramp function which is cycled between varying displacement amplitudes. Characteristic points on the experimental load-slip traces provide the data for calculating the dynamic properties of the connections.

The loading procedure involves ordinary reversed cyclic displacements for three cycles at each incremental level at low elastic behavior of displacement levels. At least three increments (more can be required in certain cases) of three cycles each shall be performed prior to the first yield or other inelastic behavior. Selection of the displacement levels prior to the first yield of non-linear behavior is dependent upon the type of connection being tested. The initial displacement shall be approximately 0.25 of the anticipated yield displacement, followed by approximately 0.50 and 0.75 of the yield displacement. A schematic of this procedure is shown in Figure 4.

Once yielding occurs, a sequential phased displacement (SPD) loading procedure is employed. The displacements of each set of cycles builds upon the preceding set of cycles. In each incremental set of cycles after yielding, four decay cycles are added. These decay cycles begin at the particular incremental displacement, and decay at a rate of 0.25 times the maximum displacement of the set of cycles. These decay cycles are followed by three cycles at the maximum displacement magnitude of the previous set of cycles, as is shown in Figure 4. Following the three cycles at the previous maximum displacement, the specimen is cycled one cycle at the next increment of displacement. Thus, the procedure includes phases of displacement history consisting of an initial displacement increment, followed by four decay cycles, followed by three or more cycles at the initial displacement for each phase or set of cycles. Table 1 provides a step by step example of the procedure. Figure 5 shows one set of cycles that constitutes a phase in the displacement pattern.

The three cycles following the decaying cycles are used to determine a stabilized

hysteretic curve. A degradation of no more than 5% in load shall be present between the second and third cycles. If a larger degradation exists, the test shall be repeated with a higher number of cycles at this stage of the cycle set, in order to determine the level where the hysteresis stabilizes. This stabilized hysteresis curve is used to calculate the stabilized energy dissipation of the connection.

The SPD procedure more accurately represents an earthquake or wind excitation pattern than does the usual monotonic or simple reversed cyclic loading patterns used for many tests. The rationale behind this approach centers on two main concepts: Degrading of the displacements, to define the lower points within a given hysteretic curve and finding a stabilized hysteretic curve. Using the degrading cycles allows the lower bound within a given hysteretic curve to be identified.

VARIABLES OF INTEREST

The capacity of the connection is determined as the maximum load recorded during the entire test and the corresponding displacement is referred to as the maximum displacement. The capacity of the connection shall be limited by the deformation under load if required by the specifier, and the maximum displacement does not necessarily refer to the maximum slip of the connection experienced during the test.

When using reversed-cyclic loading and, for systems not exhibiting an ideal perfectly elastic-plastic behavior, the yield load and ductility ratio do not mean the usual point of first non-linearity and capacity to deflect a given amount past yield. Therefore, an equivalent elastoplastic system is defined for this procedure. Figure 6 shows the ideal elastoplastic system and the load-deflection curve which is derived from the envelope of the stabilized hysteresis curves for a connection. The lines for the elastic and plastic regions are drawn such that the indicated areas are equal, i.e., the equivalent system represents the same energy as the test specimen envelope curve. In other words, areas A_1 and A_1' are equal as well as areas A_2 and A_2' .

The yield strength is then defined as P_y as shown in Figure 6, and the ductility ratio is then defined as the ratio of the maximum displacement and the yield displacement. Therefore, the ductility ratio, D , is

$$D = \frac{\Delta_{max}}{\Delta_{yield}}$$

The ductility ratio is not a totally reliable index of performance under cyclic loading. The ductility defined for this procedure is based on the stabilized hysteresis curves of displacement history; however, it does not reflect the decrease in stiffness or load capacity that occurs with an increasing number of cycles past the stabilized SPD phase.

The hysteretic energy dissipation capacity of the connection at a given deflection level is calculated by integrating the area enclosed by the stabilized hysteresis curve at the same displacement. The integration can be accomplished by using a simple Simpson's rule algorithm or another equivalent method.

The cyclic or dynamic stiffness, k_c , is useful in defining the behavioral changes that occur during cyclic loading. This is especially true for comparing parametric changes in systems. The cyclic stiffness is determined by calculating the slope of a line extending between the maximum positive and negative load-displacement values of the stabilized hysteresis loop at each displacement phase of the test. The cyclic stiffness is illustrated in Figure 7. The stiffness degradation is a very important behavioral characteristic to be defined for each type of connection, because the connection stiffness directly affects the behavior of the structural components of which it is a part.

The equivalent viscous damping, ζ , is often used for comparing the damping characteristics and for numerical modeling of the dynamic response of structures. The equivalent viscous damping of a connection tested using the proposed procedure is calculated using the stabilized hysteresis. The areas required to determine the equivalent viscous damping are shown in Figure 8. The hysteretic energy is the area enclosed inside the hysteresis loop, and is determined in the manner presented above. The potential energy of the connection is the area enclosed by the triangles ABC and CDE. The equivalent viscous damping, ζ , is then calculated using the equation

$$\zeta = \frac{\text{HYSTERETIC ENERGY}}{2\pi \text{ POTENTIAL ENERGY}}$$

Supplementary tests can be performed using this procedure to investigate such topics as: the effect of bearing area, and length to diameter (L/d) relationship between connections, the effect of angle of load to principal material property directions, the minimum edge and end distances and the effect of their variations, the minimum thicknesses of the material that can be used with each connecting device and the effect of their variations, the optimum spacing between multiple fasteners both parallel and perpendicular to the principal material property directions and the effects of their variations, the effect of moisture content of material, and the effects of any other factors which affect the performance of the connection.

CONCLUSIONS

A new test procedure that has been proposed as a standard test method has been presented. The method is a modification of the Sequential Phased Displacement procedure used by the Joint Technical Coordinating Committee on Masonry Research (TCCMAR) for the United

States-Japan Coordinated Earthquake Research Program. The procedure allows the equivalent energy yield strength, hysteretic and equivalent viscous damping, dynamic stiffness, ductility, and capacity of the mechanical connections to be evaluated based on the stabilized hysteresis. The hysteresis loops of shear load versus slip from experimental traces can be determined for use in numerical modeling connections.

ACKNOWLEDGEMENTS

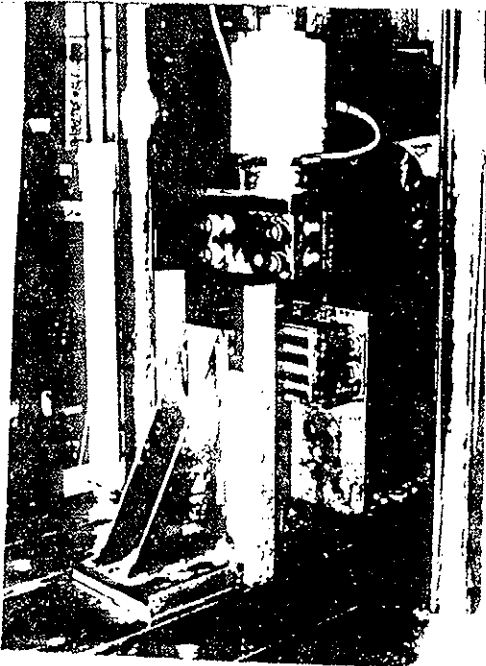
The author would like to acknowledge the support received from the American Forest and Paper Association for this work through research project number 230-11-110A-023-822663-1.

REFERENCES

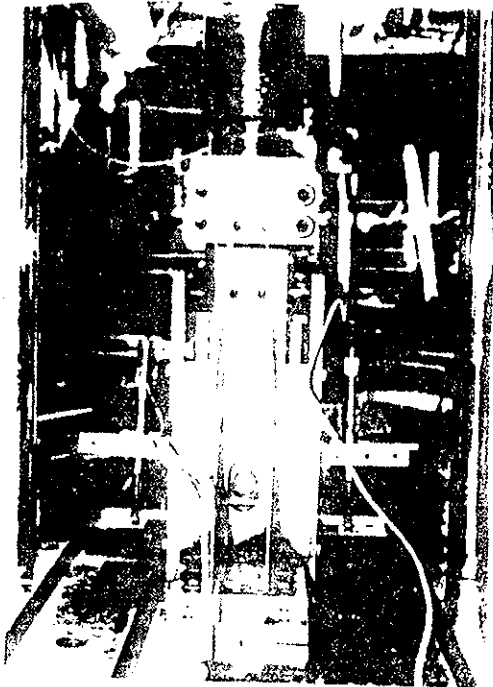
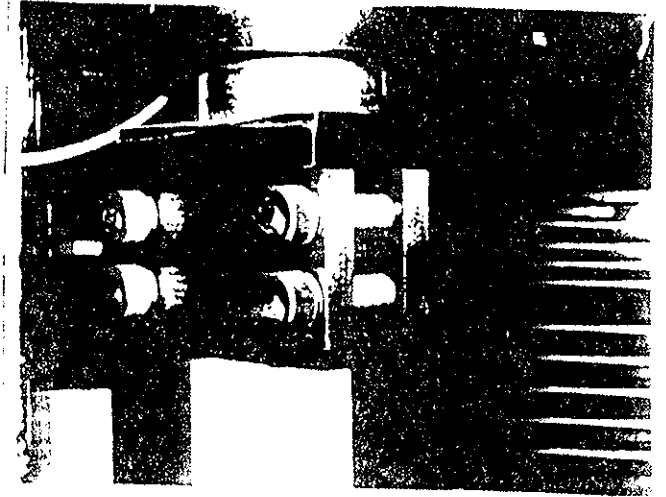
- Federal Specification FF-W-92 for Washers, Metal, Flat (Plain), ANSI B18.6.1 American National Standard for Slotted and Recessed Head Wood Screws.
- Porter, M.L., 1987. "Sequential Phased Displacement (SPD) Procedure for TCCMAR Testing" Proceedings of the Third Meeting of the Joint Technical Coordinating Committee on Masonry Research, U.S.-Japan Coordinated Earthquake Research Program, Tomamu, Japan.
- Reyer, E. and A.O. Oji, 1991. "Timber Structures - Joints made with Mechanical Fasteners - A Proposed Test Procedure", Presentation at the Meeting of the RILEM TC 109 TSA Meeting in Watford, England.

Table 1. Procedure for SPD loading (shown schematically in Figure 4)

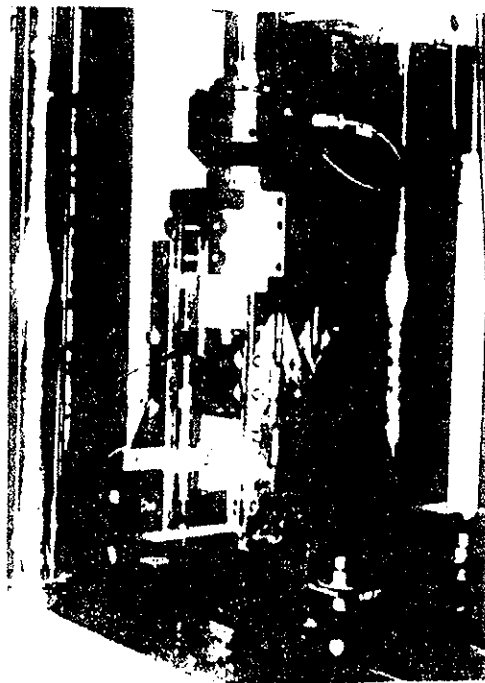
Cycle Number	Description
1-3	Apply 3 full-reversing cycles of displacement at approximately 25% of anticipated yield displacement.
4-6	Apply 3 full-reversing cycles of displacement at approximately 50% of anticipated yield displacement.
7-9	Apply 3 full-reversing cycles of displacement at approximately 75% of anticipated yield displacement.
10	Apply displacement to yield displacement. This displacement will increase with each successive set of cycles by the yield displacement.
11	Apply displacement to 75% of cycle 10.
12	Apply displacement to 50% of cycle 10.
13	Apply displacement to 25% of cycle 10.
14-16	Apply 3 full-reversing cycles of displacement at displacement of cycle 10.
	The set of cycles 10 to 16 is repeated with the displacement of cycle 10 increasing by the yield displacement for each successive set until the connection fails for ductile connections. The increment of increased displacement shall be 25% of the yield displacement for brittle connections.



(a)



(c)



(d)



Figure 2. Views of test fixture assembly for lateral cyclic test of connection is shear.

TO UNIVERSAL JOINT, LOAD CELL,
AND TEST FRAME

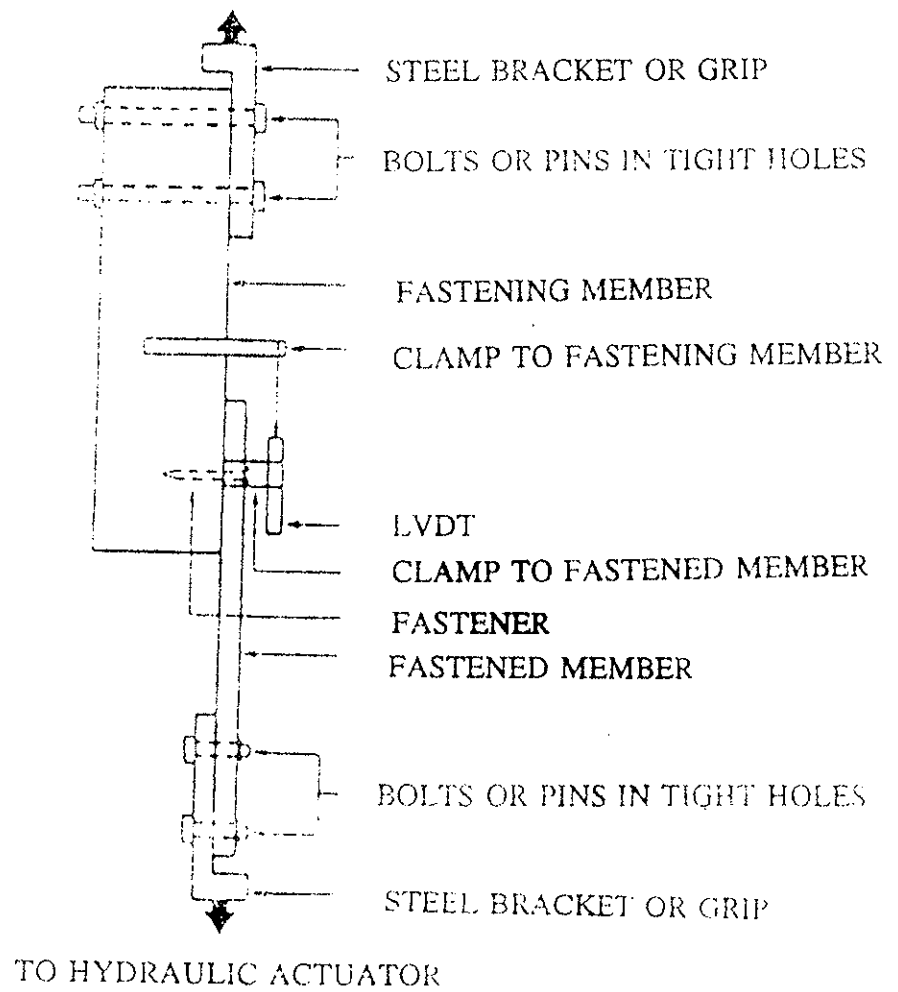


Figure 1. Test configuration of specimens subjected to cyclic loading.

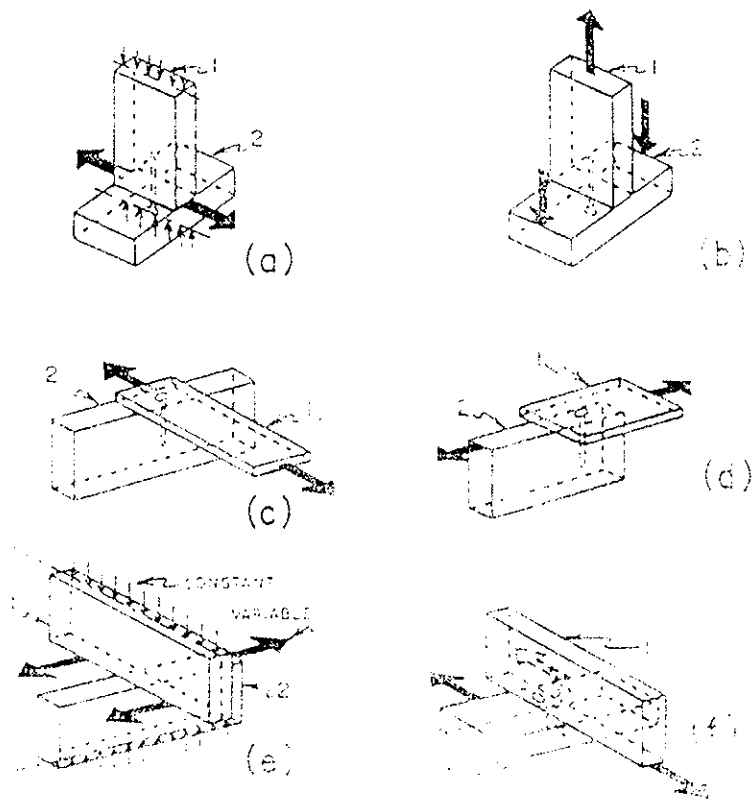


Figure 3. Typical configurations of connections.

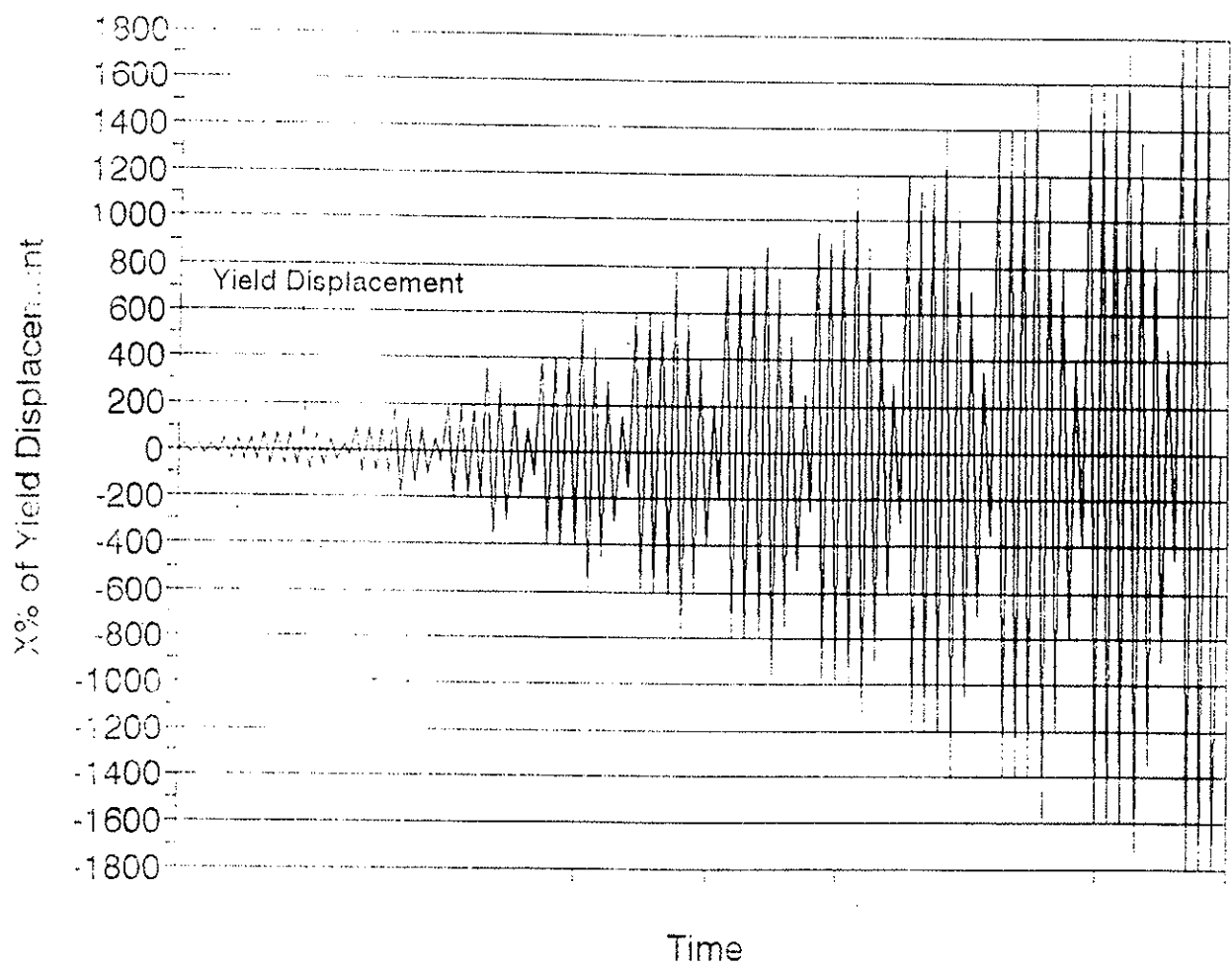


Figure 4. Displacement pattern for SPD loading.

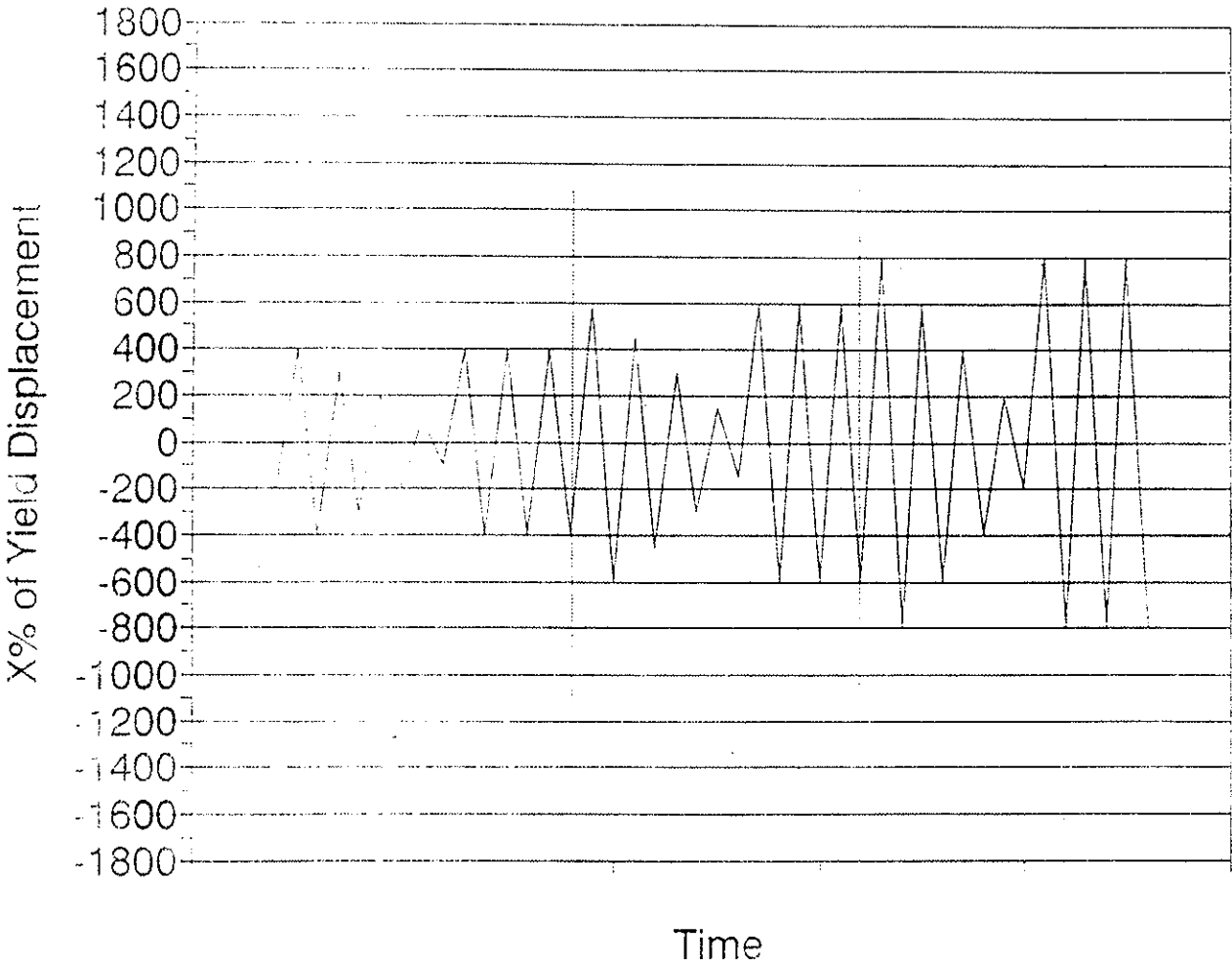


Figure 5. Cycle set for one phase of the loading pattern.

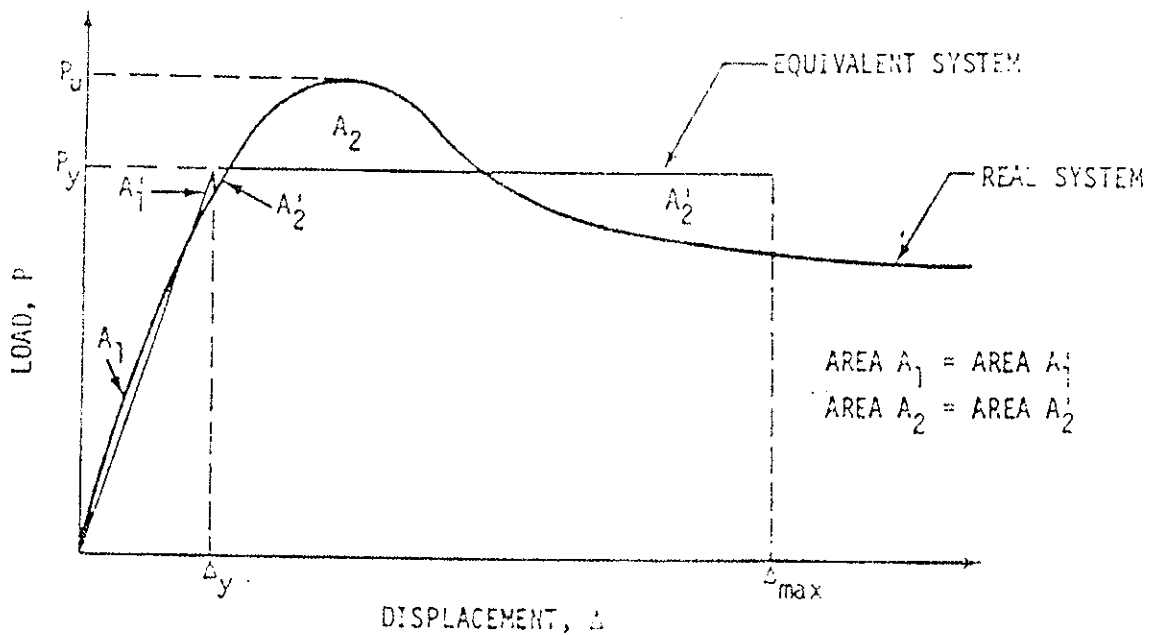


Figure 6. Equivalent energy elastic-perfectly plastic system.

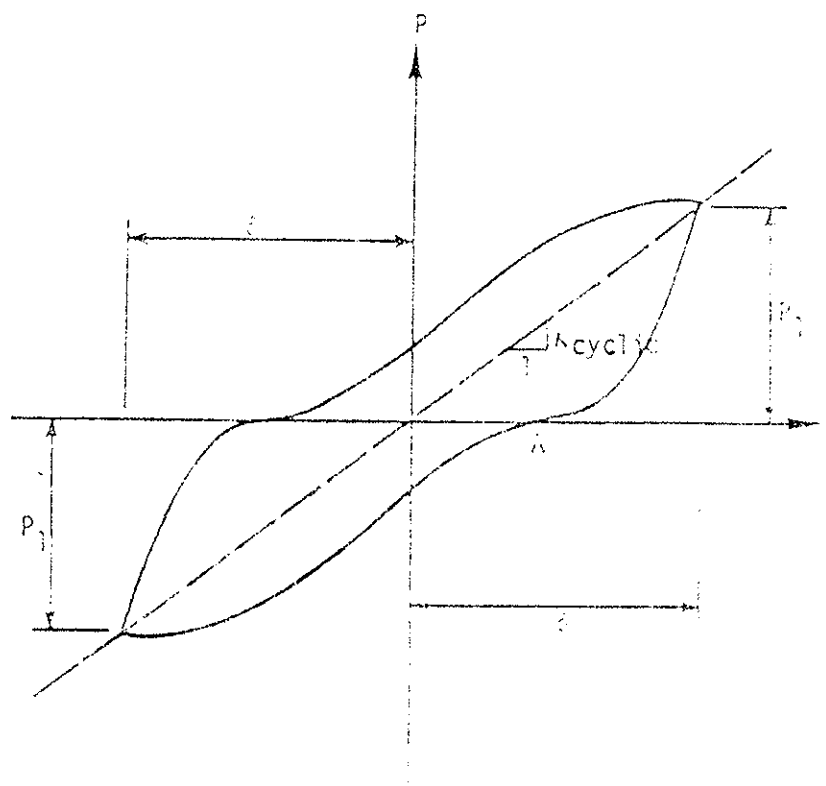


Figure 7. Calculation of average cyclic stiffness, k_c , from force-deflection hysteresis.

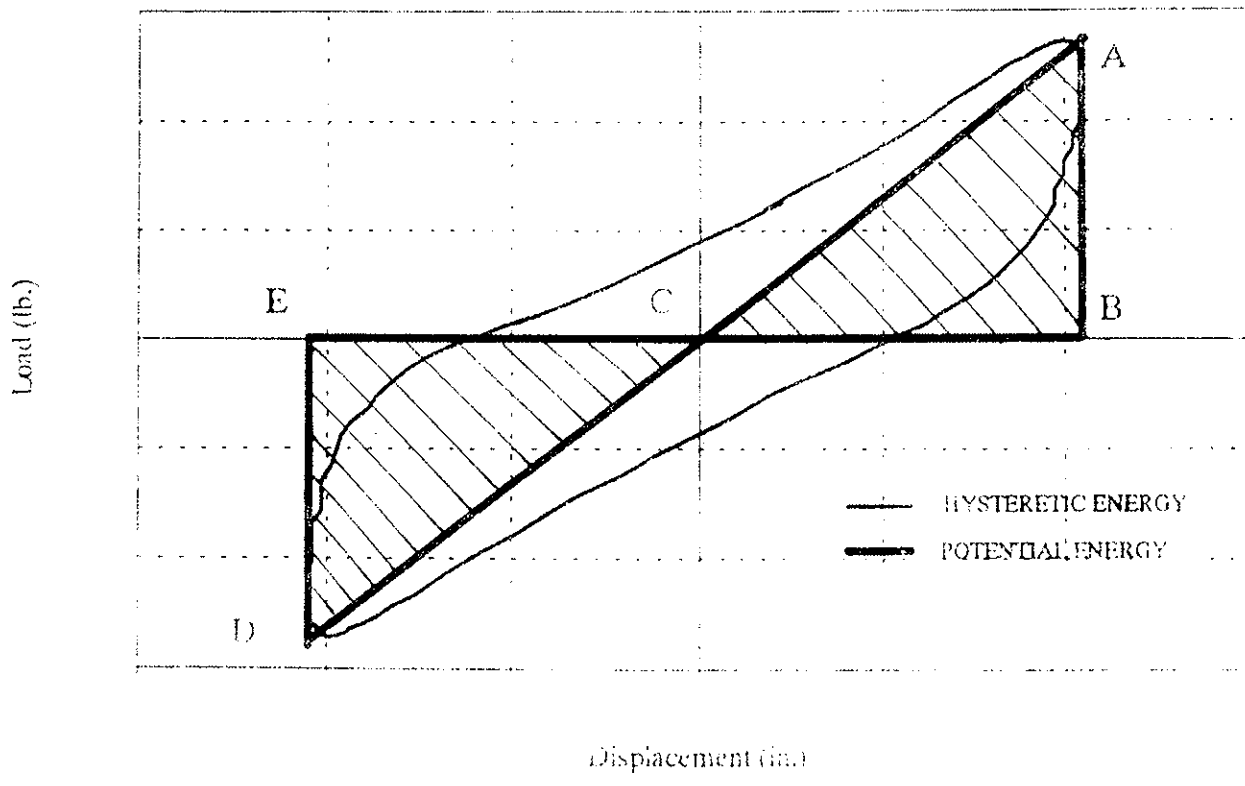


Figure 8. Hysteretic / potential energy relationship for a nail connection.

INTERNATIONAL COUNCIL FOR BUILDING RESEARCH STUDIES AND DOCUMENTATION
WORKING COMMISSION W18 - TIMBER STRUCTURES

VALIDATORY TESTS AND PROPOSED DESIGN FORMULAE FOR THE
LOAD-CARRYING CAPACITY OF TOOTHED-PLATE CONNECTED JOINTS

by

C J Mettem
A V Page
G Davis
TRADA Technology Limited
United Kingdom

MEETING TWENTY - SIX

ATHENS, GEORGIA

USA

AUGUST 1993

VALIDATORY TESTS AND PROPOSED DESIGN FORMULAE FOR THE LOAD-CARRYING CAPACITY OF TOOTHED-PLATE CONNECTED JOINTS

C.J. Mettem, A.V. Page and G. Davis
TRADA Technology Limited, United Kingdom

INTRODUCTION

An earlier paper [1] reviewed the basis of design data for ring connectors, plate connectors and toothed-plate connectors in the permissible stress design code, BS 5268. It then developed formulae for calculating the characteristic load-carrying capacities of timber-to-timber joints made with these connectors. These formulae, which were intended for use with EC5, produced values which were related to the permissible long-term loads given in BS 5268, but they were not related directly to experimentally measured ultimate loads.

This paper describes experimental work which was undertaken on timber joints made with toothed-plate connectors. The purpose was to provide some additional validatory tests to give a better basis to evaluate various formulae which have been proposed for calculating their load-carrying capacity. It is important that such formulae should be as simple as possible, and should predict with acceptable accuracy the measured load-carrying capacities of real joints, with safety levels similar to those associated with similar formulae for nails, bolts and other dowel-type fasteners. For the load-carrying capacity of any dowel-type joint, an accuracy of $\pm 10\%$ has previously been considered acceptable [2].

In the first stage of this research, an investigation was made of bolted joints, which were assembled in a similar configuration, and using similar bolts, to those used later for the connectors. The results of these bolt tests were compared with the now well-established EC5 formulae. There was a significant difference between the experimental load-carrying capacity and that predicted by theory, which is explained in the paper.

The second stage of the programme consisted of tests on a range of three-member, double shear joint specimens containing toothed plate connectors. The effects on load-carrying capacity of connector size, member thickness, timber species and density are being evaluated from these tests, and these factors are considered in this paper.

The measured values of the load-carrying capacities of the toothed-plate joints, and values previously reported from tests carried out in 1952 and 1961 [3] [4] were then compared with values produced by three formulae. The first was a formula proposed by Blass and Schlager [5], the second a development of this formula based on work previously reported by the authors, and the third was a new, simplified formula.

On average all three formulae predicted ultimate loads within 3% of the test values. However, only the second and third formulae correctly assessed the effects on joint strength of timber density and member thickness.

TESTS

Test programme

Since some design formulae which have been proposed involve separating the contribution of the bolt, it was decided to measure the strength of plain bolted joints made from timber of comparable density, and with bolts of the same two diameters that were used for the connected joints. As mentioned in the Introduction, it was discovered that the ultimate loads on these bolted joints considerably exceeded the values predicted by the formulae in EC5, so two further sets of tests were conducted using bolts without nuts and washers, one with members of European redwood, the other with Southern pine in order to include a timber of higher density. Some of the bolts themselves were tested to determine their ultimate tensile strength. Table 1 summarises the bolted joint test programme. The timber species and bolts are described more fully on pages 3 and 4.

Table 1 Test programme, bolted joints

Thickness of members: $t_a = 25$ mm, $t_b = 50$ mm

Series	Bolt	Nut and washer	d_b mm	d_w mm	t_w mm	Loading mode	N° of specimens
a	yes	yes	10	38	3	C	15
b	yes	yes	12	50	5	C	15
c	yes	no	12	-	-	C	5
d(SP)	yes	no	12	-	-	C	5

The key to this Table is given beneath Table 2.

Table 2 summarises the test programme on the toothed-plate connected joints. The aim of this programme was to measure the effects on joint strength of the mode of loading, the density of the timber, the size of the connector, and the thickness of the members. All the specimens were loaded parallel to the grain. They were all assembled with a bolt, nut, washers and two double-sided toothed plates. The washer sizes were based on the recommendations of BS 5268 : Part 2. As in the case of the plain bolted joints, one set of tests on Southern pine was included.

Table 2 Test programme, connected joints

Series	d_c mm	d_b mm	d_w mm	t_a mm	t_i mm	t_b mm	Loading mode	N° of specimens
A	63	12	50	5	25	50	T	10
C	63	12	50	5	25	50	C	15
E(SP)	63	12	50	5	25	50	C	10
F1	38	10	38	3	25	50	C	15
F2	50	12	38	3	25	50	C	15
F3	75	12	60	5	25	50	C	15
H1	63	12	50	5	16	32	C	15
H2	63	12	50	5	50	100	C	15

Key: d_b diameter of bolt
 d_c diameter of toothed plate
 d_w diameter of washer
 t_a thickness of each outer member
 t_i thickness of inner member
 t_b thickness of washer
C compression parallel to the grain
T tension parallel to the grain
SP Southern Pine

All dimensions are nominal, actual dimensions reported below and used in all calculations.

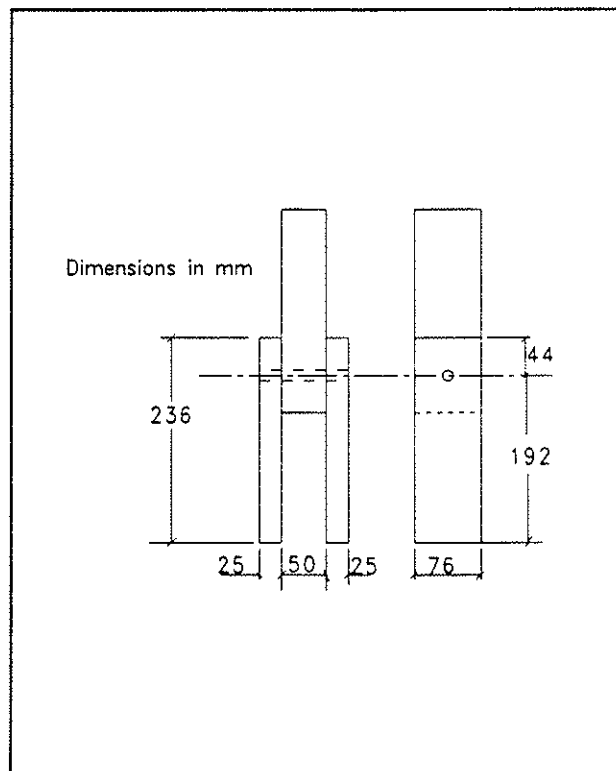
Test specimens

All the specimens consisted of three-member timber-to-timber joints, in which the central member was twice as thick as the two outer members. Figure 1 shows the dimensions of a typical test specimen, which was loaded in compression parallel to the grain. The edge distances and the unloaded end distance conformed to the standard distances specified for toothed-plate connectors in BS 5268 : Part 2. The loaded end distance, however, exceeded the standard distance specified in the Code. It was determined by some preliminary tests, not reported in this paper, which were conducted on specimens with four different lengths. These tests were undertaken to ensure that the end distance selected was sufficiently long to eliminate excessive effects of friction at the base of the specimen, and any bending or uneven load distribution produced by interaction between the specimen and the loading heads. In the tension tests, Series A, longer specimens were used to accommodate the grips of a tensile testing machine. The individual members in these specimens were 580 mm long, instead of 236 mm.

The thicknesses of the members were selected from the middle of the range of member thicknesses for which values are tabulated in BS 5268 : Part 2, except in the case of Series H1 and H2, where the minimum and maximum thicknesses tabulated in the Code were chosen in order to investigate the effect of member thickness on joint strength.

A set of five, ten or fifteen similar specimens was tested in each series.

Figure 1 Typical test specimen, connected joint, compression parallel to the grain



Materials

The timber was European redwood (*Pinus sylvestris*) in every case except Series d (bolts) and Series E (connectors), when Southern pine (*Pinus palustris*, *Pinus elliotti*, *Pinus echinata*, *Pinus taeda*) was used. All of the timber was conditioned before and after machining in an atmosphere of 20°C and 65% relative humidity. The individual specimens were made up from members with matched densities with a similar statistical distribution to that of the timber supplied, so that the densities of both the inner and outer members of each specimen increased in order through each set.

The connectors were round double-sided toothed plates, designated as Type C6 in prEN 912. In most tests, 63 mm diameter plates were used, in order to compare the effects of varying other parameters. However, in series F, plates of 38 mm, 50 mm and 75 mm diameter were tested to investigate the relationship between connector diameter and joint strength. In the 50 mm and 63 mm diameter plates, the thickness of the metal and the height of the teeth were found to be slightly below the minimum dimensions specified in the Standard, although these were connectors of a brand which is widely available commercially.

The bolts were black metric hexagon head bolts, manufactured from 4.6 Grade steel to BS 4190, with nuts made from Grade 4 steel. Six samples of each type of bolt were tested to determine their actual tensile strength. The metric washers were of the sizes and thicknesses specified in BS 5268 : Part 2 for toothed plate joints, and they were made from Grade 4 steel.

Bolt tightness

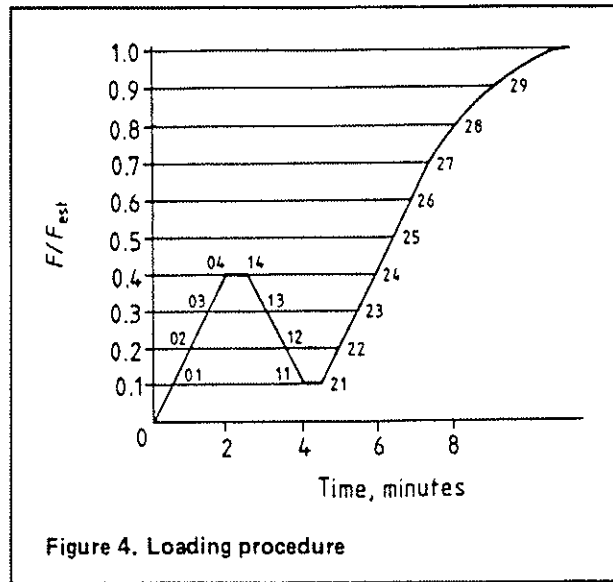
The EC5 formulae for laterally-loaded bolted joints predict the loads at which either the bolt yields in bending or the timber members fail by embedment, but they do not allow for any enhancement of the load-carrying capacity which may be produced by the effect which occurs when the bolt heads, nuts and washers tighten upon the timber as the bolt yields. For this reason, test specimens used for validity testing usually have a gap incorporated (sometimes with a soft spring included) between these constraints and the surfaces of the timber, in order to eliminate any such contribution to the strength [6]. The ultimate load thus measured or calculated will be less than the ultimate load in a real joint, but it has been argued that this is the proper value for designers to use, since, in practice, initially tight bolts may become loose, as a consequence of the timber drying and shrinking.

Connected joints, however, will not function properly with very loose nuts and bolts. The bearing area of a connector is reduced, if there is a gap between the members, and this gap can only be prevented by keeping the nuts and bolts at least finger-tight. Furthermore, with toothed-plate connectors, it is possible for the teeth to withdraw to some extent, if the members are not held together by a tightened nut, bolt and washers. Also, the importance of keeping nuts and bolts tight in real structures is emphasized by BS 5268 : Part 2, which states that the permissible loads are valid only if nuts and bolts are kept tight. It was concluded that these investigations of proposed design formulae and the associated tests should be based on tests conducted with the nuts finger-tight immediately prior to test. A further advantage was that this was the procedure adopted for the original tests on British toothed plates [3]. There were, however, two test series (series c and d) with bolts only which were tested with no nuts or washers to show the difference that tightness of the bolt and washers made on the joint.

Loading regime

The specimens were loaded parallel to the grain in accordance with BS 6948 : 1989, as shown in Figure 2. In this figure, F/F_{est} is the ratio of the applied load to the estimated ultimate load. The total time to failure for each test was between ten and fifteen minutes.

Figure 2 Loading regime



RESULTS

Bolt strength tests

The results of the tensile tests on the bolts themselves are shown in Table 3.

Table 3 Bolt strength test results

Size	Supplier	F_{mean} N/mm ²	Standard Deviation	F_{uk} N/mm ²
M10 x 120	Armstrong	494.1	27.19	439.3
M12 x 130	Armstrong	446.3	28.68	388.5
M12 x 260	GFD	368.4	5.44	357.4

Values of F_{uk} for the six specimens of each type were calculated as

$$F_{uk} = F_{mean} - (2.015 \times SD)$$

Plain bolted joint tests

The overall results for each of the four sets of plain bolted joint tests are given in Table 4. The dimensions given are the actual mean measurements of the test specimens in each Series at the time of testing. The densities were calculated from the dimensions and mass of the individual joint members just prior to joint assembly.

Table 4 Plain bolted joint test results

Series	Bolt		Outer member		Inner member		Load per shear plane		
	d_b mm	f_u N/mm ²	t_o mm	ρ_a kg/m ³	t_i mm	ρ_b kg/m ³	F_u kN	SD	$F_{u,k}$ kN
a	9.9	494	25.0	485.3	49.9	550.3	10.16	1.09	8.24
b	11.8	446	25.0	462.3	49.9	542.1	10.83	1.35	8.47
c	11.8	446	25.0	456.3	49.9	521.8	7.94	0.15	7.62
d	11.8	446	25.2	725.6	49.7	729.8	10.80	0.87	8.95

For Series a and b, 15 specimens each were tested, and $F_{u,k}$ was calculated as $F_{u,k} = F_{u,mean} - (1.761 \times SD)$. For Series c and d, 5 specimens each were tested, and $F_{u,k}$ was calculated as $F_{u,k} = F_{u,mean} - (2.132 \times SD)$.

Bolts with nuts

These specimens were three-member joints, each with a single bolt, finger-tight nut and washers, having the dimensions shown in Table 1.

In Figures 3 and 4, the ultimate load per shear plane for each specimen is plotted against the effective density of the joint. This was calculated according to EC5 : Part 1 : Clause 4.2a as $\sqrt{\rho_A \rho_B}$, where ρ_A is the density of the two outer members and ρ_B is the density of the inner member. In effect, this line gives a mean test value for any given density.

Another line in Figures 3 and 4 shows the load-carrying capacity per shear plane of each specimen calculated from the formulae given in EC5. For these calculations, the value used for the tensile strength of the bolts was the appropriate value of $F_{u,mean}$ taken from Table 2, since this was the most probable strength of the bolt used in any given test specimen. The densities of the members were the actual measured densities of the outer and inner members for each specimen. k_{mod} and γ_M were set at 1.0.

A third line shows a "secant yield load" which was derived from the load / deflection graph for each specimen in a manner analogous to the secant yield stress used in metallurgy. The derivation of the secant yield load is illustrated in Figure 5. This shows the load/deflection curve for the first M10 bolt test, corresponding to a timber density of 452 kg/m³. The gradient F/Δ at the steepest point of the curve, where initial slip ended but before failure occurred, was reduced by a factor of 0.7 to produce a second line which intersected the experimental curve at the secant yield load.

Figure 3

Ultimate load per shear plane of 3-member bolted joints made with a single M10 x 120 mm bolt, nut and washers (Series a) in European redwood, loaded in compression parallel to the grain.

$t_{a,mean} = 25.0 \text{ mm}$ $t_{b,mean} = 49.9 \text{ mm}$

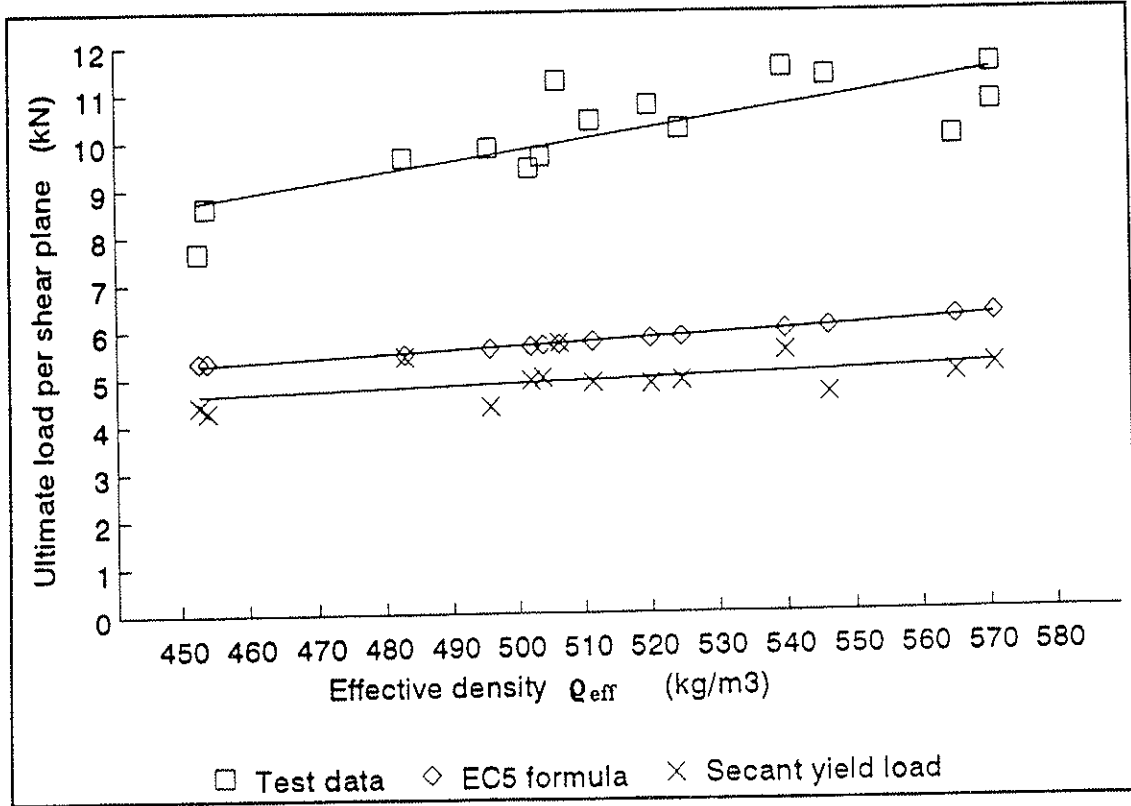


Figure 4 Ultimate load per shear plane of 3-member bolted joints made with a single M12 x 130 mm bolt, nut and washers (Series b) in European redwood, loaded in compression parallel to the grain
 $t_{a,mean} = 25.0 \text{ mm}$ $t_{b,mean} = 49.9 \text{ mm}$

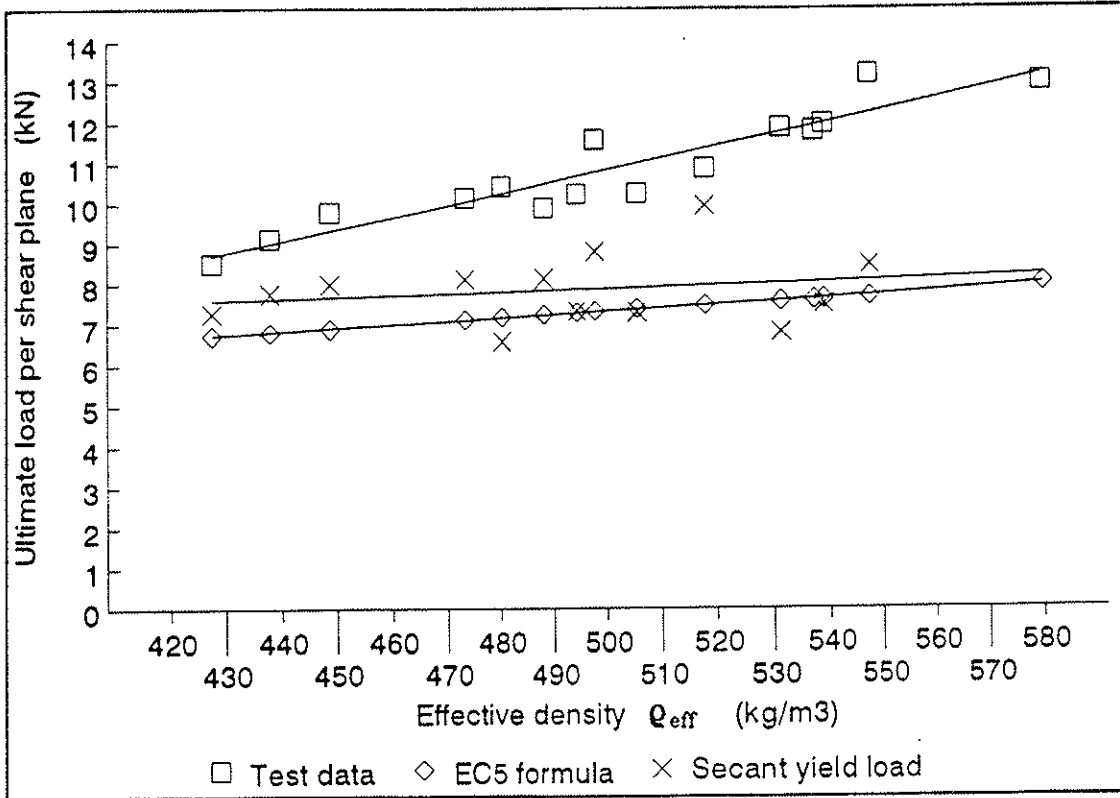
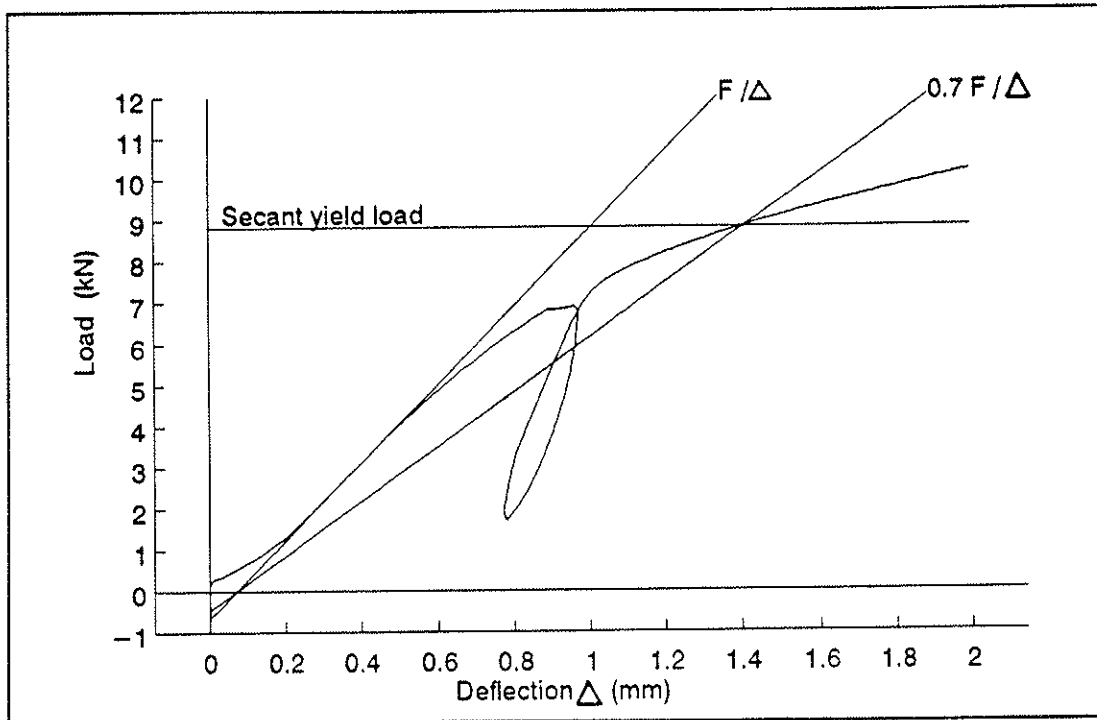


Figure 5 Derivation of secant yield load



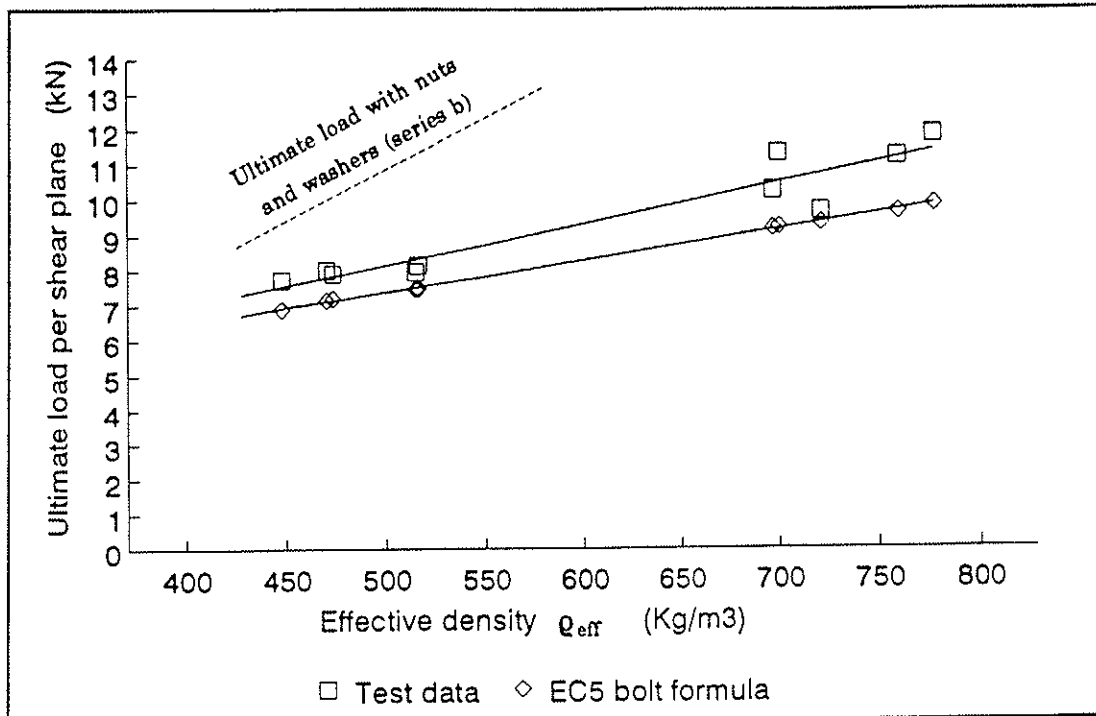
Bolts without nuts

As mentioned above, two further sets of plain bolted joint tests were conducted, using bolts with no nuts or washers (Series c and d). Figure 6 shows the ultimate load per shear plane achieved by all ten of these specimens. The specimens in Series c were made of European redwood and those in Series d of Southern pine. All the specimens were joined with an M12 bolt without a nut or washers. The corresponding ultimate loads plotted and calculated from the formulae in EC5, using similar procedures to those described for Figures 3 and 4, are also shown.

Figure 6

Ultimate load per shear plane of three-member bolted joints made with a single M12 x 130 mm bolt, and no nut or washers (Series c and d) in European redwood and Southern pine loaded in compression parallel to the grain

$$t_{a,mean} = 25.1 \quad t_{b,mean} = 49.8$$



Connected joints

The mean test results for each set of toothed plate joints are shown in Table 6. The dimensions given are the actual mean measurements of the test specimens at the time of testing, with the exception of the toothed plate dimensions where the nominal dimensions are given.

Table 6 Connected joint test results

Series	Toothed plate		Bolt		Outer member		Inner member		Effective density	Load per shear plane		
	$d_{c,dom}$ mm	h_c mm	d_b mm	f_u N/mm ²	t_a mm	ρ_a kg/m ³	t_b mm	ρ_b kg/m ³		$Q_{eff,k}$ kg/m ³	$F_{u,mean}$ kN	S.D.
A	63	8.3	11.8	446	25.1	534	50.0	504	415	16.08	1.24	13.81
C	63	8.3	11.8	446	25.2	494	50.0	498	405	14.65	1.08	12.75
E	63	8.3	11.8	446	25.2	715	49.9	733	661	23.55	1.54	20.73
F1	37	6.0	9.9	494	25.0	499	49.9	547	446	12.42	1.16	10.38
F2	50	6.8	11.8	446	25.2	522	49.9	548	465	11.72	0.92	10.11
F3	75	10.2	11.8	446	25.0	477	49.6	556	447	18.72	1.31	16.46
H1	63	8.3	11.8	446 *	15.9	452	32.1	468	416	12.18	0.70	10.96
H2	63	8.3	11.8	368	50.0	558	99.8	489	440	21.68	1.79	18.54

* value for M12 x 100 bolt assumed equal to measured value for M12 x 130 bolt.

In Table 6, values of $F_{u,k}$ were calculated as $F_{u,k} = F_{mean} - (1.833 \times S.D.)$ for Series A and E (10 specimens each), and $F_{u,k} = F_{mean} - (1.761 \times S.D.)$ for the other Series (15 specimens each).

ANALYSIS

Bolt strength tests

BS 4190 : 1967 requires a minimum tensile strength of 392 N/mm² for Grade 4.6 bolts. The M10 bolt was 16 % stronger than this, whereas the longer of the two M12 bolts was 8 % weaker. The values actually measured were used to calculate the predicted strengths of the bolted joints using the formulae in EC5.

Plain bolted joint tests

Figures 3 and 4 show that the actual ultimate loads per shear plane corresponding to various densities were from 30 % to 85 % higher than those predicted by EC5. However, the ultimate loads on joints made without a nut and washers were only 10 % to 16 % higher, as shown in Figure 6.

The differences may be explained as follows. For joints in which the initial mode of failure is the bending of the bolt, friction generated between the bolt and the timber can permit further load to be added after the bolt has started to bend. When a nut and washers are added, an additional "string effect" in the bent bolt is produced as the nut and washers are pulled into the timber, clamping the members together. This effect would occur even in joints which had become slightly loose through drying and shrinkage, since a bolt bent at an angle of 10° to horizontal in each half of the specimens tested would effectively shorten by 3 mm. The formulae given in EC5, however, do not allow for friction or for the clamping effect of a nut and washers, so the ultimate loads which they predict are lower than the actual ultimate loads.

It follows that the differences between the measured and predicted loads shown in Figures 3 and 4 are due to friction and clamping, while the differences shown in Figure 6 are due just to friction. Also, it follows that, in joints where the initial mode of failure was timber embedment, there should be no difference between the actual and predicted ultimate loads. This second conclusion was demonstrated to be true by projecting back the

lines corresponding to the measured and predicted ultimate loads in Figures 3 and 4 to the points at which they met. For both figures, the EC5 formulae showed that at the densities corresponding to the points of intersection, embedment failure and bolt failure occurred at similar loads.

In Figures 3 and 4, the secant yield loads derived from the load / deflection graphs were similar to the ultimate loads predicted by the EC5 formulae.

For series a and b, characteristic values of the ultimate loads $F_{u,k}$ were 8.24 kN and 8.47 kN per shear plane respectively, and the characteristic densities were 445 kg/m³ and 423 kg/m³ respectively. For these two characteristic densities, the EC5 formulae predict values of 5.22 kN and 6.80 kN respectively for $F_{u,k}$. These represent reductions of 0.63 and 0.80 on the experimental values of $F_{u,k}$, or a mean reduction of 0.715.

Three principal conclusions were drawn from these tests on bolted joints.

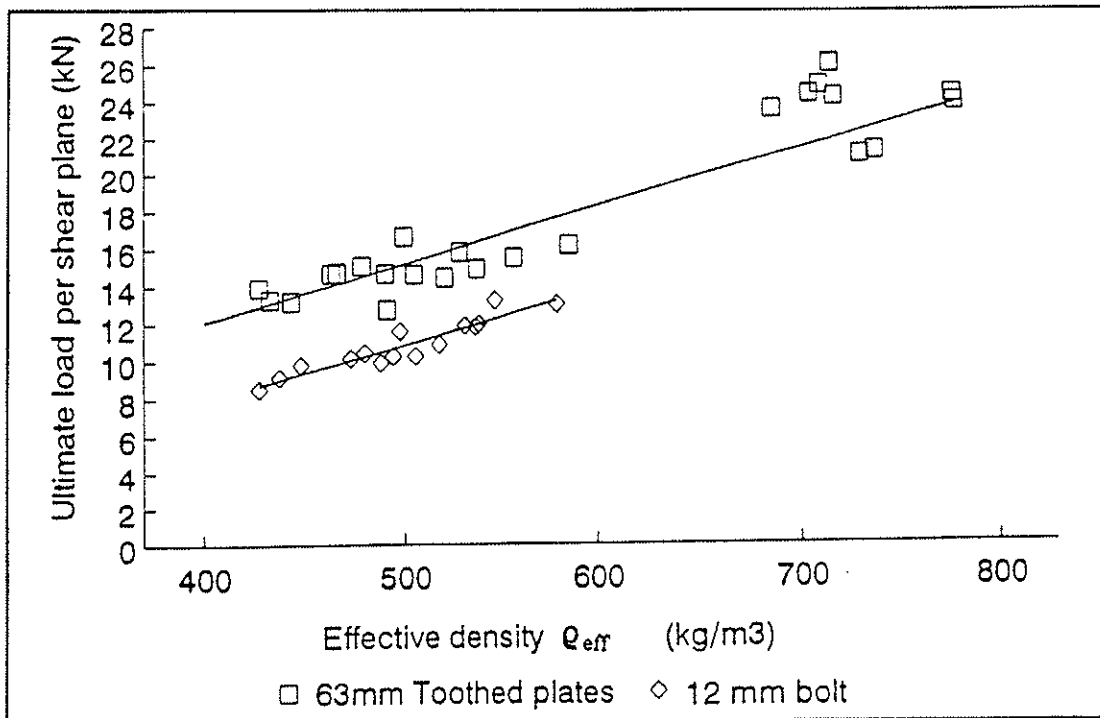
1. For three-member timber joints, made with a single bolt, nut and washers and loaded in compression parallel to the grain, the EC5 formulae give good predictions of the yield loads at which the initial failure occurs, but they do not predict accurately the ultimate loads for such joints.
2. The characteristic ultimate load-carrying capacities of the real bolted joints tested with nuts and washers were approximately 50% higher than the values predicted by the EC5 formulae. However, the load-carrying capacities of joints tested without nuts and washers were on average only 13% higher than the values predicted. The difference in the first case was ascribed to the "string effect" produced by the bolt-head, nut and washers, plus friction between the members produced by the consequent clamping effect, and friction between the bolt and the timber members inside the joint. The difference in the second case was ascribed to internal friction between the bolt and the timber members.
3. Formulae for connected joints based directly on the measured values of ultimate load will provide lower safety levels than the present EC5 formulae for 3-member bolted joints, since the latter formulae do not allow for the contribution of the bolt-head, nut, washer or friction.

Connected joints

In Table 6 the ultimate load for specimens loaded in compression (Series C) is slightly less than that for similar specimens loaded in tension (Series A). It was concluded that loading in compression is a valid test method for joints made with toothed plate connectors, provided that adequate end distance are ensured.

In Figures 7 to 10, the influence on joint strength of density, connector diameter and member thickness are considered in turn.

Figure 7 Ultimate load per shear plane for individual three-member toothed plate joints made with a single M12 x 130 mm bolt and two 63 mm toothed plates, nut and washers in European redwood and Southern pine (Series C and E), compared with ultimate load for 12 mm plain bolted joints in European redwood (Series b), loaded in compression parallel to the grain.



In Figures 7 and 8, the effective density of each specimen were calculated as $\sqrt{\rho_A \rho_B}$, as in Figures 3 and 4.

The difference between the two ultimate load lines shown in Figure 7 may be interpreted as the contribution to the load-carrying capacity provided by one 63 mm diameter double-sided toothed plate. It can be seen that this additional contribution changes very little with density. This suggests that failure occurred in the teeth of the toothed plate rather than in the timber in which they were embedded.

Figure 8 Ultimate load per shear plane for individual three-member toothed plate joints made with a single M12 x 130 mm bolt, nut, washers and two 63 mm diameter toothed plates in European redwood and Southern pine (Series C and E), loaded in compression parallel to the grain.

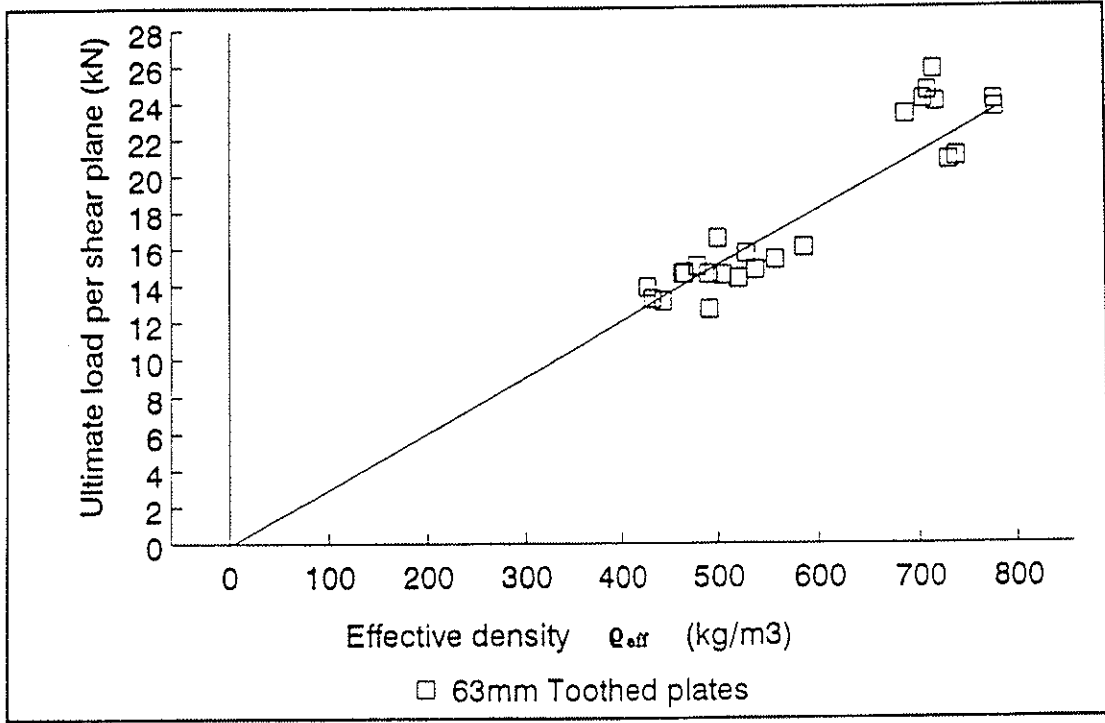


Figure 8 shows the ultimate load per shear plane for the individual "standard" specimens tested in Series C and E, plotted against effective density as in Figure 7, but extrapolated backwards to a density of zero. The result illustrates that the overall load-carrying capacity of a "standard" 63 mm toothed plate connected joint is directly proportional to the density of the timber.

Figure 9 Ultimate load per shear plane of three-member toothed plate joints made with toothed plates of four different sizes in European redwood (Series F1, F2, C and F3), loaded in compression parallel to the grain

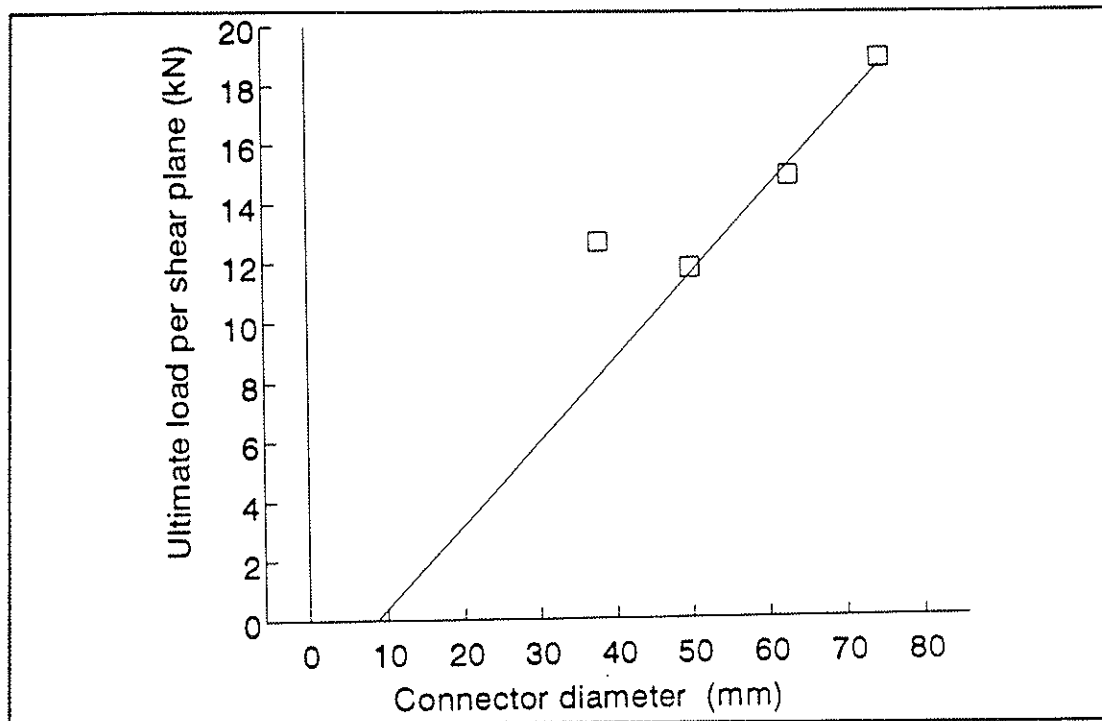


Figure 9 shows the mean ultimate loads per shear plane for each of the test series F1, F2, C and F3, corresponding to connector diameters of 38 mm, 51 mm, 63 mm and 75 mm respectively. Each of the four values was obtained from the regression line of load v. density for all 15 specimens in the set, reading the load at a density of 500 kg/m³. In this way the mean ultimate loads for the four connector diameters can be compared at the same density. It can be seen that the overall load-carrying capacity of the toothed plate joints tested is approximately proportional to the nominal diameter of the connectors.

In the figure, the regression line excludes the value for the joints made with the 38 mm connectors. It is believed that the relatively high ultimate loads for these joints are due to frictional effects, which are explained in Appendix A.

Figure 10 Ultimate load per shear plane of three-member toothed plate joints made with three different thicknesses of member in European redwood (Series H1, C and H2), loaded in compression parallel to the grain.

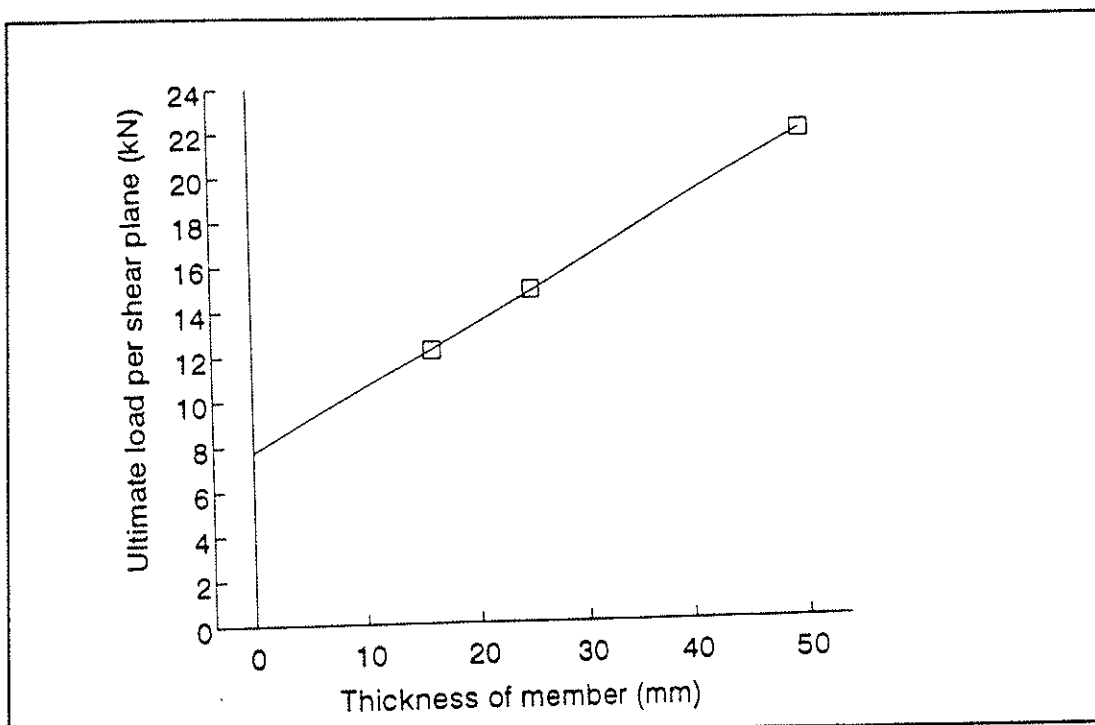


Figure 10 shows the ultimate loads per shear plane corresponding to a density of 500 kg/m³ for each of the test series H1, C and H2, as explained after Figure 9. These tests used specimens having outer member thicknesses of 16, 25 and 50 mm respectively, with the inner members twice as thick as the outer members. The line indicates an increase of joint strength right across the thickness range. However, further tests would be required to confirm the relationship between member thickness and joint strength, since the bolts used in each test series were found to have different strengths (see Table 6).

Five principal conclusions were drawn from the tests on connected joints.

1. In the 63 mm connector plates failure appeared to have occurred in the metal teeth rather than in the timber in which they embedded.
2. The overall load-carrying capacity of a standard toothed plate joint specimen was proportional to the density of the timber.
3. The overall load-carrying capacity of the specimens tested was approximately proportional to the diameter of the toothed plate connectors.
4. In joints made with 10 mm bolts the clamping effect of the bent bolt appeared to increase the load-carrying capacity by approximately 50%.
5. There was a linear relationship between the overall strength of the joints and the thickness of the members, right across the thickness range.

FORMULAE

Proposed formulae

A formula for calculating the load-carrying capacity of a joint made with Bulldog toothed plate connectors has been proposed by Blass and Schlager. It is

$$R_{j,k} = 18(d_{c,nom})^{1.5} + R_{b,k} \quad \text{N} \quad (1)$$

where $R_{j,k}$ = the characteristic load-carrying capacity of one double-sided connector and its bolt in N

$d_{c,nom}$ = the nominal diameter of the connector in mm

$R_{b,k}$ = the characteristic load-carrying capacity of the bolted part of the joint (one shear plane) calculated from the formulae in EC5 in N

Two alternative formulae are proposed here, based on the results of these tests. The tests were carried out on samples which contained double shear planes, since double shear joints are more common where toothed plate joints are used. The formulae, however, calculate the load per shear plane. Formula A is a development of the Blass/Schlager formula:-

$$R_{j,k} = 0.0014 (t_{min})^{0.5} (Q_{eff,k})^{1.25} (d_{c,nom})^{1.5} + R_{b,k} \quad \text{N} \quad (2)$$

where $Q_{eff,k}$ = $\sqrt{Q_A Q_B}$ in kg/m^3

Q_A and Q_B = characteristic densities of the members on each side of the toothed plate.

t_{min} = minimum of t_A and t_B in mm

In 2-member joints t_A and t_B are the thicknesses of the two members.

In 3-member joints t_A is the thickness of the outer member and t_B is half the thickness of the inner member.

Formula B is an entirely empirical one, which has the advantage that it obviates the need to go through the EC5 bolt design formula to calculate the assumed contribution of the bolt. It is:-

$$R_{j,k} = 0.0077 \gamma_{eff,k} d_{c,nom} [t_{min} + 40] \quad \text{N} \quad (3)$$

Evaluation

The reliability of the three proposed formulae is assessed in Table 7, where comparison indices R_j/F_u are given.

In Table 7 $F_{u,k}$ is the characteristic load-carrying capacity per shear plane for each test series taken from Table 6 and multiplied by a factor of $500/Q_{eff,k}$ (or $750/Q_{eff,k}$ in the case of Series E) to provide a common comparison basis. This procedure is based on the earlier finding that the overall load-carrying capacities of individual specimens were proportional to their densities.

$R_{b,k}$ is the contribution of the bolt calculated from the formulae for 3-member joints given in EC5. A timber density of 500 kg/m^3 was used (or 750 kg/m^3 in the case of Series E), and k_{mod} and γ_M were set at 1.0. As in Tables 3 and 4, the actual strength of the bolt types was used.

Table 7 Evaluation of design formulae: 1993 tests

Series	Purpose	$F_{u,k}$	$R_{b,k}$	Formula (1) Blass/Schlager		Formula (2) TRADA A		Formula (3) TRADA B	
				$R_{j,k}$	$R_{j,k}/F_{u,k}$	$R_{j,k}$	$R_{j,k}/F_{u,k}$	$R_{j,k}$	$R_{j,k}/F_{u,k}$
				kN	kN	kN	kN	kN	kN
A	Tensile loading	16.61	7.42	16.42	0.99	15.70	0.95	15.77	0.95
C	Standard reference	15.73	7.42	16.42	1.04	15.70	1.00	15.77	1.00
E	Denser species	23.50	9.58	18.58	0.79	23.32	0.99	23.66	1.01
F1	38 mm plate	11.65	5.74	9.96	0.85	9.62	0.83	9.51	0.82
F2	51 mm plate	10.87	7.42	13.98	1.29	13.45	1.24	12.76	1.17
C	63 mm plate	15.73	7.42	16.42	1.04	15.70	1.00	15.77	1.00
F3	75 mm plate	18.40	7.42	19.11	1.04	18.17	0.99	18.77	1.02
H1	Thin members	13.17	6.83	15.82	1.20	13.45	1.02	13.58	1.03
C	Standard members	15.73	7.42	16.42	1.04	15.70	1.00	15.77	1.00
H2	Thick members	21.06	9.12	18.12	0.86	20.82	0.99	21.83	1.04
Maximum				1.29		1.24		1.17	
Minimum				0.79		0.83		0.82	
Range				0.50		0.41		0.35	
Mean of eight values				1.01		1.00		1.00	

All three formulae give results which are on average equal, or almost equal, to the experimentally-determined values of $F_{u,k}$.

Formula (1) does not provide sufficient allowance for the influence of timber density (Series C and E) or member thickness (Series H1, C and H2). It handles reasonably well the anomalous results for the tests on connector diameter (Series F1, F2, C and F3 - see Figure 9).

Formulae (2) and (3) allow well for the influence of timber density and member thickness, and handle reasonably well the influence of connector diameter. All three formulae give too high a result for the 51 mm connector.

From the designer's point of view, Formula (3) is the easiest of the three to use. However, it relates only to joints made with 4.6 grade bolts of the diameters tested in 1993, i.e. 10 mm for 38 mm connectors and 12 mm for larger sizes. In the UK this is not a problem, because these are the only sizes that are recommended with toothed plate connectors made in the UK, but this would be a disadvantage in countries where different diameters of bolt may be used.

In comparing the results from the formulae with experimental results, actual values of bolt strength and timber density were used, and γ_M was set at unity. In use, additional safety factors would be introduced to the R_b term by using characteristic values of material properties and values of γ_M of 1.1 or 1.3 as appropriate. It has been stated in this paper that for both the bolt and the toothed plate connector the initial mode of failure occurs in the metal rather than the wood. For all these reasons it is argued that for design purposes the first term in Formula (2) and the whole of Formula (3) should be divided by a factor of $\gamma_M = 1.1$ to obtain a design value. It is not obvious how changes in the load duration and service class will affect the performance of a toothed-plate joint, but for safety's sake it seems sensible to use k_{mod} in conjunction with the afore-mentioned γ_M until better information is available. The modified formulae are shown as (2a) and (3a) on page 21.

Whether similar factors should also be applied to the first term of Formula (1) depends on how it was calibrated.

Additional confirmation from earlier tests

In 1952 Brock [3] conducted various tests on both round and square toothed plate connectors. The results of the tests on round "Bulldog" connectors using the standard loaded end distances and washer diameters given in BS 5268 : Part 2 are shown in Table 8. Only mean values of the density and the failure load for each test series were recorded, so the mean densities have been used in the three formulae to obtain an approximate comparison. The mean failure loads were halved in order to convert them to loads per shear plane. To calculate R_b a standard value of 392 N/mm² was assumed for the strength of the bolts, since Brock did not measure the strength of the bolts, and k_{mod} and γ_M were set at 1.0.

In the 1952 report it was stated that the washers used for the tests on the 51 mm and 75 mm connectors were too thin and too small to develop pressure across the joint, and the loaded end distances for the tension tests were too short for the joint to develop its full strength. In the 63 mm connector tests, standard washer thicknesses (5 mm) and loaded end distances (95 mm) were used, but only two specimens were tested for each mode of loading. The results from these 1952 tests can therefore give an indication only of the reliability of the three formulae, and, for the reasons given, only the 63 mm connector results will be used for comparison purposes.

For the 63 mm diameter connectors Formula (1) gives excellent results, with comparison indices of 1.00 and 0.96 for loading in compression and tension respectively. Formulae (2) and (3) give somewhat lower results with indices ranging from 0.84 to 0.94.

Table 8 Evaluation of design formulae : 1952 tests on "Bulldog" connectors

Loading mode	d _c mm	d _b mm	SG	Q kg/m ³	t _A mm	t _B mm	F _{max} lb force	F _u per shear plane kN	R _b kN	Comparison indices (R _b /F _u) for the three formulae		
										(1)	(2)	(3)
Compression	51	12.7	0.45	513	19.0	34.9	5510	12.25	7.83	1.17	1.04	0.94
	63	12.7	0.43	490	22.2	44.4	7510	16.70	7.75	1.00	0.94	0.89
	75	12.7	0.41	467	22.2	47.6	7340	16.32	7.54	1.18	1.03	1.03
Tension	51	12.7	0.45	513	19.0	34.9	3560	7.92	7.83	1.82	1.61	1.46
	63	12.7	0.43	490	22.2	44.4	7880	17.53	7.75	0.96	0.88	0.84
	75	12.7	0.41	467	22.2	47.6	6930	15.41	7.54	1.25	1.09	1.09

Table 9 Evaluation of design formulae : 1961 tests on "Bulldog" connectors

Loading mode	d _c mm	d _b mm	Q lbs/ft ³	Q kg/m ³	t _A mm	t _B mm	F _{max} lb. force	F _u per shear plane kN	R _b kN	Comparison indices (R _b /F _u) for the three formulae		
										(1)	(2)	(3)
Compression	51	12.7	32.6	522	22.2	47.6	6870	15.28	8.03	0.95	0.92	0.83
	63	12.7	30.0	481	22.2	47.6	8170	18.17	7.67	0.92	0.83	0.80
	75	12.7	31.3	501	22.2	47.6	8400	18.68	7.84	1.05	0.96	0.96
Tension	51	12.7	32.9	527	22.2	47.6	6650	14.79	8.07	0.99	0.96	0.87
	63	12.7	34.1	546	22.2	47.6	7650	17.01	8.24	1.01	1.00	0.97
	75	12.7	34.5	553	22.2	47.6	8160	18.15	8.30	1.10	1.09	1.09

A further series of tests on toothed plates manufactured by MacAndrews and Forbes Ltd. was conducted by Lee and Lord in 1961 [4]. These plates were double-sided round toothed plates, similar to the other plates tested in 1993. However, there were three significant differences:

- (i) All the washers were 3.25 mm thick, whereas the washer thicknesses for the 50 mm, 63 mm and 75 mm connectors tested in 1993 were 3 mm, 5 mm and 5 mm thick respectively;
- (ii) the nuts were tightened with a spanner, instead of being only finger-tight;
- (iii) as shown in Table 9, the thicknesses of the members were different.

In Lee's and Lord's paper standard deviations were given for the ultimate loads, but not for the densities of the specimens, so the comparison shown in Table 9 between the results from the tests and the formulae is based on mean values, as in Table 8. Each set of results records the mean values for a set of 10 similar specimens.

On the basis of these tests, Formula (1) gives the most consistent and accurate results, but it must be noted that all the specimens tested had densities of around 500 kg/m³ and were made with thin members of similar thickness; and, as previously noted, the formula as it stands does not adequately allow for variations in these parameters.

All three formulae over-compensated for connector diameter according to these test results.

Safety levels

As previously mentioned, the safety levels provided by the EC5 formulae for 3-member bolted joints generally exceed the levels provided by the proposed formulae for toothed plate joints. It is desirable to maintain similar safety levels in all types of joint, but in this case it seems that the EC5 bolt formulae need to be changed. If, however, it was decided to adjust the proposed toothed plate formulae so that they provided safety levels similar to those provided by the current EC5 formulae for 3-member bolted joints, then a global reduction factor of 0.70 would have to be applied to them.

CONCLUSIONS

For real bolted joints made with nuts and washers, the bolt design formulae given in EC5 give good predictions of the yield loads but not of the absolute ultimate loads. The predicted loads appear to be about 70% of the experimental values. It may be considered that design formulae for joints made with toothed plate connectors should in a similar way predict load-carrying capacities which are less than the ultimate load-carrying capacity.

The results from a wide range of tests conducted in 1952, 1961 and 1993 on three-member timber-to-timber toothed plate joints were compared with the results predicted by three proposed formulae. The formulae proposed were:-

$$R_{j,k} = 18 (d_{c,nom})^{1.5} + R_{b,k} \quad N \quad (1)$$

$$R_{j,k} = 0.0014(t_{min})^{0.5}(Q_{eff,k})^{1.25}(d_{c,nom})^{1.5} + R_{b,k} \quad N \quad (2)$$

$$R_{j,k} = 0.0077Q_{eff,k}d_{c,nom}(t_{min} + 40) \quad N \quad (3)$$

For design purposes it is proposed that formulae (2) and (3) should be written:-

$$R_{j,d} = 0.00127(t_{min})^{0.5}(Q_{eff,k})^{1.25}(d_{c,nom})^{1.5}k_{mod} + R_{b,d} \quad (2a)$$

$$R_{j,d} = 0.007Q_{eff,k}d_{c,nom}(t_{min} + 40) k_{mod} \quad (3a)$$

Formulae (3) and (3a) are valid only for the bolt sizes specified in BS 5268 : Part 2, i.e. M10 for 38 mm diameter connectors and M12 for larger connectors.

Key:

$R_{j,k}$	=	characteristic load-carrying capacity of one double-sided round toothed plate and bolt loaded parallel to the grain, in Newtons
$R_{j,d}$	=	design load-carrying capacity of same, in Newtons
$R_{b,k}$	=	characteristic load-carrying capacity of the bolt, per shear plane, calculated from EC5, in Newtons
$R_{b,d}$	=	design load-carrying capacity of same, in Newtons
$d_{c,nom}$	=	nominal diameter of toothed plate, in mm
t_{min}	=	minimum of outer member thickness and half the inner member thickness, in mm, for 3-member joints; or minimum member thickness in mm, for 2-member joints: the value entered should not exceed 50 mm
$Q_{eff,k}$	=	characteristic effective density of the joint
	=	$\sqrt{Q_{A,k}Q_{B,k}}$ in kg/m ³

The reliability of the formulae was measured by means of a comparison index, $R_{j,k} / F_{j,k}$, $F_{j,k}$ being the characteristic ultimate test load per shear plane. Where characteristic tests loads were not available, the comparison index was calculated as $R_{j,mean} / F_{j,mean}$. The results of the comparison exercise are summarized in Table 10.

Table 10 Summary of comparison indices for proposed design formulae, from Tables 7-9*

Formula	Maximum	Minimum	Standard deviation	Mean comparison index for 16 different joint types
(1)	1.29	0.79	0.12	1.00
(2)	1.24	0.83	0.10	0.97
(3)	1.17	0.80	0.12	0.96

* Only values for the 63 mm connectors given in Table 8 were included.

Formula (1) gave good predictions for joint specimens in timber having a density of around 500 kg/m³ and with outer members around 25 mm thick, but it did not allow adequately for the effect of varying these parameters.

Formulae (2) and (3) gave good predictions across all parameters, with mean comparison indices of exactly 1.00 when measured against the 1993 tests. The lower values shown in Table 10 are caused mainly by the high test values obtained in the 1961 tests, possibly due to the fact that in those tests the nuts were tightened with a spanner, thereby increasing the frictional resistance between the members.

For designers, formula (3) is the easiest to use, and it would be the preferred option in the United Kingdom. However, it is applicable only to joints made with the bolt sizes specified in BS 5268 : Part 2. If other bolt sizes are used with similar toothed plates in other countries, then formula (2) is recommended.

REFERENCES

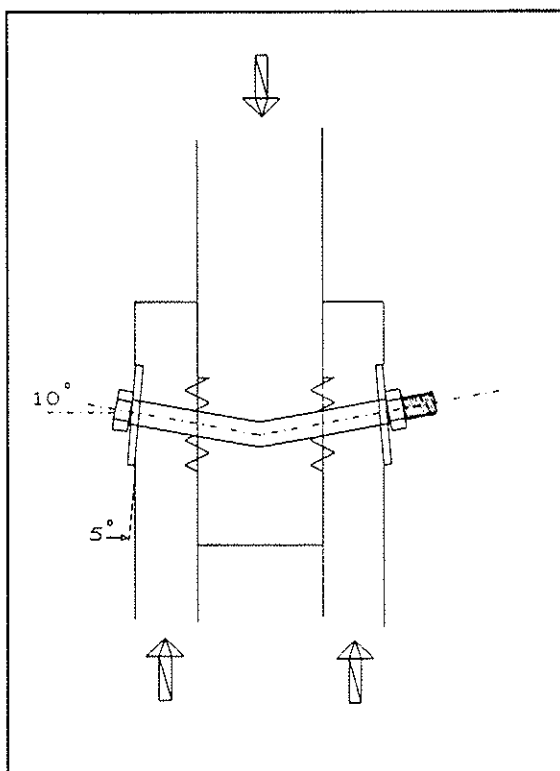
- [1] PAGE, A.V., DAVIS, G. and METTEM, C.J. Design rules for UK timber connectors. CEN/TC 124/WG4 February 1993
- [2] WHALE, L.R.J., SMITH, I. and LARSEN, H.J. Design of nailed and bolted joints - proposals for the revision of existing formulae in draft Eurocode 5 and the CIB code. CIB-W18A/20-7-1, Dublin, 1987
- [3] BROCK, G.R. The strength of toothed-plate connector joints. DSIR Forest Products Research Laboratory. Princes Risborough, 1952
- [4] LEE, I.D.G. and LORD, A.D. Loading tests on "Bulldog" timber connectors. Report no. E/TR/21, Timber Development Association Ltd., 1961
- [5] BLASS, H.J. and SCHLAGER, M. Trial calculations for determination of the load-carrying capacity of joints with Bulldog connectors. CEN/TC 124/WG4 N23, April 1993
- [6] WHALE, L.R.J. and SMITH, I. Mechanical timber joints. TRADA Research Report 18/86. Hughenden Valley, TRADA, 1986

Appendix A

The effect of friction on the load-carrying capacity of a joint made with bolts.

Final failure of all the joints tested occurred with splitting of the inner member from the centre of the bolt hole along the grain in both directions. At failure the deflected angles of the M10 bolts in the outer members were 10° , and the corresponding angles of the M12 bolts in the standard C series tests were 2.5° . The washers were embedded at an inclination of approximately half these angles, as shown in Figure A.

Figure A M10 bolt and washer at joint failure



At failure the ultimate load applied to the inner member is resisted by three actions on the member:

- (i) the load-carrying capacity of the teeth in the toothed plate connectors (assuming for the reason given previously that failure occurred in the teeth rather than the timber in which they were embedded) - this is a function of the size and material strength of the connector;
- (ii) the embedment strength of the inner member - this is a function of the density, geometry and species of the timber;
- iii) the frictional resistance generated between the inner and outer members - this is a function of the lateral strain in the timber caused by the effective shortening of the bolt as it bends, of the elasticity of the timber and of the coefficients of friction between the timber and the steel of the toothed plates, and between the timber/timber surfaces where these come into contact.

The ultimate load which the outer members can carry is similar to the above, but with an additional component provided by the inclined embedment of the washers. This explains why failure always occurred in the inner member rather than one or both outer members.

With nuts that are finger-tight before any load is applied to the joint, any bending of the bolt will effectively shorten the bolt and therefore compress the timber. A 10° angle of inclination in each side member will produce a contraction of 3.06 mm in the overall joint thickness, or a strain of 0.0306. A 25° angle will produce a strain of 0.0019. Taking $E_{90} = 625 \text{ N/mm}^2$ for European redwood and assuming that the calculated strains are applied to two-thirds of the nett area of the washers in order to allow for some bending, it is possible to calculate the total load applied by the bolt perpendicular to the plane of the joint. Using this value and a measured value of $\mu = 0.35$ for timber/steel and timber/timber contact, the contribution of friction to the load-carrying capacity of the joint types may be calculated.

For the joints made with 38 mm diameter connectors, M10 bolts and 38 mm diameter washers, the frictional contribution is 4.71 kN. For the joints made with 63 mm connectors, M12 bolts and 50 mm washers, the contribution is 0.51 kN, i.e. 4.2 kN less.

Therefore, although components (i) and (ii) of the load-carrying capacities of the 38 mm connector joints must be lower than the corresponding components in the 63 mm connector joints, component (iii) in the 38 mm connector joints is estimated to be 4.2 kN higher. This difference can be observed in Figure 9, in which the mean ultimate load per shear plane for the 38 mm connectors is 4.4 kN above the regression line for the other three connector sizes.

INTERNATIONAL COUNCIL FOR BUILDING RESEARCH STUDIES AND DOCUMENTATION
WORKING COMMISSION W18 - TIMBER STRUCTURES

DEFINITIONS OF TERMS AND MULTI-LANGUAGE TERMINOLOGY
PERTAINING TO METAL CONNECTOR PLATES

by

E G Stern
Virginia Polytechnic Institute and State University
USA

MEETING TWENTY - SIX

ATHENS, GEORGIA

USA

AUGUST 1993

**DEFINITIONS OF TERMS AND MULTI-LANGUAGE TERMINOLOGY
PERTAINING TO METAL CONNECTOR PLATES**

by

E. George Stern

Earle B. Norris Research Professor Emeritus of Wood Construction
Virginia Polytechnic Institute and State University
Blacksburg, VA 24063-0361 USA

ABSTRACT

The definitions of terms and multi-language terminology pertaining to metal connector plates provide meanings and explanations of 48 technical terms which are in common use by both the technical expert, such as the plate fabricator and user, and the non-expert architect, engineer, specification writer, building code official, and others who deal with metal connector plates in one way or another. The definitions are in English and the terminology is in English, French, Russian, German, Danish, Swedish, Finnish, Estonian, Latvian, Lithuanian, Polish, Hungarian, Portuguese, Japanese, Korean, and Thai. Terminology in additional languages is solicited.

Presented at 26th Meeting of Working Commission W18A on "Timber Structures" of International Council for Building Research Studies and Documentation in Athens, GA, USA, August 23 to 27, 1993.

DEFINITIONS OF TERMS AND MULTI-LANGUAGE TERMINOLOGY PERTAINING TO METAL CONNECTOR PLATES

INTRODUCTION

The definitions of terms and multi-language terminology pertaining to metal connector plates provide meanings and explanations of 48 technical terms which are in common use by both the technical expert, such as the plate fabricator and user, and the non-expert architect, engineer, specification writer, building code official, and others who deal with metal connector plates in one way or another. The definitions are in English and the terminology is in English, French, Russian, German, Danish, Estonian, Latvian, Lithuanian, Swedish, Finnish, Polish, Hungarian, Portuguese, Japanese, Korean, and Thai. Terminology in additional languages is solicited.

This terminology does not cover terms relating to the mechanical properties of the materials used for fabricating metal connector plates as well as their use.

The terms are listed in alphabetic sequence. Compound terms appear in the natural spoken order. Where the definitions are adopted verbatim from other sources, they are identified and fully referenced.

The use of brand and trade names in this document serves to restrict the findings to the particular product and does not constitute any endorsement of this product. Since the author has no control over the use of the information presented, he cannot accept responsibility for such happenings which result from its use.

Presented at 26th Meeting of Working Commission W18A on Timber Structures of International Council for Building Research Studies and Documentation in Athens, GA, USA, August 22 to 27, 1993.

RELATED REFERENCES

1. International Standards Organization, Geneva, Switzerland (ISO):
 - 1.1 ISO 6891 (1983) Timber Structures - Joints made with mechanical fasteners - General principles for the determination of strength and deformation characteristics.
 - 1.2 ISO 8969 (1990) Timber Structures - Testing of unilateral punched metal plate fasteners and joints.
 - 1.3 ISO/TC165 N118 (1987) Timber Structures - Testing of punched metal plate fasteners.
2. European Union of Agreement, Paris, France (UEAtc):
 - 2.1 M.O.A.T. No. 16 (1979) Rule for the assessment of punched metal plate timber fasteners.
3. International Union for Testing and Research Laboratories for Materials and Structures, Paris, France (RILEM):
 - 3.1 RILEM/CIB 3TT (1981) Testing methods for joints with mechanical fasteners in load-bearing timber structures, Annex A: Punched metal plate fasteners.
4. American Society for Testing and Materials, Philadelphia, PA, USA (ASTM):
 - 4.1 ASTM A446 (1976, 1981) and A446M (1980) Standard specification for steel sheet, zinc-coated (galvanized) by the hot-dip process, structural (physical) quality.
 - 4.2 ASTM A525 (1981) Standard specification for general requirements for steel sheet, zinc-coated (galvanized) by the hot-dip process.
 - 4.3 ASTM D1761 (1977) Standard methods of testing mechanical fasteners in wood.
 - 4.4 ASTM E8 (1981) Standard methods of tension testing of metallic materials.
 - 4.5 ASTM E489 (1981, 1987) Standard test method for tensile strength properties of metal connector plates.

- 4.6 ASTM E767 (1985, 1990) Standard test method for shear strength properties of metal connector plates.
 - 4.7 ASTM E631 (1989) Standard terminology of building constructions.
 - 4.8 ASTM F547 (1977, 1984) Standard definitions of terms relating to nails for use with wood and wood-base materials.
 - 4.9 ASTM F592 (1978, 1984) Standard definitions of terms relating to collated and cohered fasteners and their application tools.
 - 4.10 ASTM F680 (1980, 1987) Standard methods of testing nails.
 - 4.11 ASTM (1986) Compilation of ASTM standard definitions.
5. International Truss Plate Association, Rowlands Castle, Hampshire, England (ITPA):
- 5.1 ITPA SFB G12 - UDC 0691-11 (1990) Technical Handbook.

DEFINITIONS

1. Angle of placement of metal connector plate - Angle of inclination of lengthwise axis of metal connector plate parallel to longitudinal axis of coiled metal strip, that is, main direction of metal connector plate, to direction of test-load application to wood member of connection; with zero-degree angle defined as that of lengthwise plate axis being parallel to load direction; and angle greater than zero is defined as that of lengthwise plate axis being rotated clockwise away from the loading axis.
2. Butted wood member - Wood member with its squared end placed adjoining the squared end or side of another wood member; with both abutting members of same thickness and in a single plane.
3. Connection, n. - Structural junction of two or more wood members, components, or assemblies, designed to be connected with mechanical fasteners, adhesives, welds, or a combination of them, to transmit safely structural forces. Colloquially, the term joint is used in place of the term connection.
4. Connector, n. - Abbreviation for metal connector plate.
5. Connector hole - Opening in metal connector plate, resulting from punching integral tooth from, or nail hole in, connector plate during its fabrication. Also called slot when opening is not round.
6. Control plate - See solid metal-coupon control specimen.
7. Control specimen - See solid metal-coupon control specimen.
8. Fastener, n. - Integral tooth of connector plate and/or separate nail used to fasten connector plate to wood member.
9. Finished metal connector plate - Chemically or metallic-surfaced, or galvanized steel connector plate with or without prepunched plate or nail holes.
10. Gross cross-sectional connector plate area - Cross-sectional area of metal connector plate determined by multiplying gross thickness of plate by gross dimension of plate perpendicular to direction of load application. 4.5
11. Integral tooth of metal connector plate - Plate projection punched from metal connector plate at right angle to its surface, which remains attached to plate, and serves as fastening element.

12. Lateral resistance of metal connector plate - Resistance to slip and/or pulling from wood, in direction of applied external shear force, of integral teeth and/or separate nails fastening connector plate to wood members. See shear strength of metal connector plate.
13. Length of metal connector plate - Dimension of metal connector plate parallel to longitudinal axis of coiled metal strip from which plate was sheared during its fabrication. 4.5
14. Lumber, n. - See wood
15. Metal connector plate - Finished (coated, galvanized) steel or bare stainless-steel connector plate with or without integral multiple plate projections or nail holes, or a combination of both, with projections partially sheared from solid plate during its fabrication and projecting from the plate in a single direction or both directions perpendicular to the plate surface area; plate of specified thickness (gage), usually including the following as well as intermediate thicknesses, to which appropriate tolerances apply:

Mm	In.	Washburn & Moen Steel Gage	ASTM Standard A525 (Table 17) for Galvanized Sheet Steel, In.
0.9	0.035	20	0.0396
1.0	0.041	19	0.0456
1.2	0.047	18	0.0516
1.4	0.054	17	0.0575
1.6	0.063	16	0.0635
1.8	0.072	15	0.0710
2.0	0.080	14	0.0785

Metal connector plates are manufactured from coiled strips of structural quality sheet metal; produced in various lengths and widths; and designed to connect wood members so as to transmit forces from one wood member (or section) to another one or more wood members (or section). Other common terms include plate, metal plate, metal-plate connectors, nail plate, truss plate, but preferably termed metal connector plate.

16. Metal connector plate with integral teeth - Metal connector plate with integral multiple plate projections partially sheared from solid plate during its fabrication and projecting from the plate in a single direction or in both directions perpendicular to the plate surface area (see metal connector plate).
17. Mill certification - Producing mill certificate or proof of conformance with specified minimum allowable stresses for heat number of metal coil(s) from which metal

connector plates were fabricated.

18. Nail, n. - Straight, slender fastener, usually pointed and headed; designed to be driven through connector plate or plates with or without nail holes; serving as separate supplementary or primary fastener. 4.8
19. Nail hole - Round perforation in metal connector plate through which a nail can be driven to fasten plate to wood members (or section) and to transmit shear loads; providing predetermined location for appropriately locating nails to be driven (see plate, hole). 4.5
20. Nail-on plate - Solid or prepunched (or predrilled) metal connector plate of specified thickness (gage); manufactured to various sizes, that is, lengths and widths; designed to be fastened with nails (or staples) to wood members and to transmit forces from one wood member (or section) to another one or more wood members (or section).
21. Overpressed metal connector plate - Metal connector plate with teeth, fully penetrating wood member, with tooth side of plate pressed more than one-quarter of plate thickness below surface of wood member; in contrast to underpressed metal connector plate, the surface of which is not in contact with the surface of the wood members.
22. Peeling resistance of metal connector plate with integral teeth - Resistance to consecutive withdrawal of adjacent teeth of metal connector plate from wood member during eccentric shear load application.
23. Plate, n. - Abbreviation for metal connector plate.
24. Plate hole - Opening in metal connector plate, resulting from punching integral plate projection(s) from, or nail hole in, connector plate during its fabrication (see nail hole).
25. Perforated metal connector plate - Metal connector plate with prepunched or predrilled plate or nail holes. Also called punched metal connector plate.
26. Predrilled hole - Hole drilled through metal connector plate during its fabrication.
27. Prepunched hole - Hole punched through metal connector plate during its fabrication.
28. Shear strength of metal connector plate - Resistance to shear force by net plate cross-section, expressed as force per unit of length of full cross-section of connector plate, when used in connections composed of pairs of plates.
29. Shear transfer plate - Metal connector plate with integral teeth projecting from plate in both directions perpendicular to plate surfaces; designed to be placed between adjacent wood members and to connect and to transmit forces from one wood member to

30. Solid metal connector plate - Metal connector plate without any prepunched or predrilled plate or nail holes.
31. Solid metal-coupon control specimen - Solid metal connector plate sample of same material as metal connector plate under scrutiny; of dimensions meeting the requirements of ASTM Standard E8 (or other applicable standard or specification); without nail and plate holes or integral plate projections. 4.5
32. Strength, n. - Resistance to external force or load or generation of internal strain, expressed in terms of units of force, N, newtons (lbf, pounds force). Discussion: Strength is the resistance to tensile, compressive, or shear forces, or a combination of these; as compared to stress that is expressed in terms of units of force per unit area.
33. Stress, n. - Internal force developed by application of external force or load or generation of internal strain expressed in terms of unit of force per unit of area, MPa, megapascals (lbf/in.², psi, pounds force per square inch). When the forces are parallel to the plane on which it acts, the stress is called shear stress; when the forces are normal to the plane on which it acts, the stress is called normal stress; when the normal stress is directed toward the plane on which it acts, it is called compressive stress; when the normal stress is directed away from the plane on which it acts, it is called tensile stress. Sometimes referred to as unit stress, internal force, engineering stress, or total stress.
34. Stress ratio - Ratio of ultimate tensile stress of metal connector plate along its longitudinal axis to ultimate tensile stress of matched solid metal-coupon control specimen. Also called effectiveness ratio and efficiency ratio.
35. Structural quality sheet coil - Coiled sheet metal used for production of metal connector plates meeting minimum specified grade properties, including the elongation for a 50-mm (2.0-in.) gage length to be at least 16 pct for specified "Grade C" steel with minimum 275-MPa (40-ksi) yield point and minimum 380-MPa (55-ksi) ultimate tensile stress, according to ASTM Standard A446. Other applicable standards or specifications may govern, to meet the requirements of local jurisdictions.
36. Tensile strength of metal connector plate - Resistance to tensile force by net plate cross-section normal to the direction of load application, expressed as force per unit of width of full cross-section of connector plate, when used in pairs of plates.
37. Test piece - Member of test specimen.
38. Test specimen - Sample connection to be tested to determine a particular plate strength characteristic; fabricated by connecting two butted wood members with two parallel metal connector plates placed symmetrically on opposite sides along the butted ends.

39. Timber, n. - See wood.
40. Tooth, n. - Integral projection of metal connector plate formed in direction perpendicular to plate surface(s) during punching process. Also called prong, barb, plug, and nail; yet, preferably called tooth. 4.5
41. Truss plate - See metal connector plate. 4.5
42. Typical metal connector plate - Metal connector plate representative of single shipment of plate to be tested; with plate manufacturing procedure simulating actual production conditions anticipated during plate fabrication as well as during member and component assembly.
43. Ultimate strength - Maximum resistance to external force, load, or generation of internal strain of a material, member, connection, component, or assembly at which failure occurs; expressed in terms of units of force, N, newtons (lbf, pounds force); as compared to ultimate stress that is expressed in units of force per unit of area. Often referred to as maximum load, ultimate load, maximum strength, or nominal strength; and incorrectly (although commonly) referred to as ultimate stress.
44. Unilaterally punched metal connector plate - Metal connector plate with integral teeth projecting from plate in single direction perpendicular to plate surface area.
45. Von Mises yield theory - Stated ratio between shear and tension stress for an isotropic, solid material. Theoretical yielding in shear is assumed to occur at a stress equal to 0.577 of the yield stress in tension.
46. Width of metal connector plate - Dimension of metal connector plate perpendicular to longitudinal axis of coiled metal strip from which plate was sheared during its fabrication. 4.5
47. Wood, n. - In the English-speaking Commonwealth countries, timber; in the English-speaking non-commonwealth countries, lumber, a sawn piece of wood smaller than 100 mm (4.0 in.) in its least dimension, as well as wood and wood-base products, such as manufactured and glue-laminated wood members, plywood, particleboard, flakeboard, and other wood panels.
48. Yield stress - Limit to internal force developed by application of external force or load or generation of internal strain to a material, member, connection, component, or assembly beyond which a marked increase in the rate of deformation occurs without an appreciable increase in load; expressed in terms of units of force per unit of area, MPA, megapascals (lbf/in.², psi, pounds force per square inch). When the initial rate of force is non-linear, an agreed-on convention shall apply. Sometimes incorrectly referred to as yield strength and as ultimate strength.

ENGLISH

FRENCH

1. Angle of placement of metal connector plate 1. Angle d'orientation de la plaque d'assemblage
2. Butted wood member 2. Pièce aboutée
3. Connection 3. Assemblage
4. Connector 4. Connecteur, plaque d'assemblage
5. Connector hole 5. Perforation dans la plaque
6. Control plate 6. Plaque de contrôle, plaque de comparaison
7. Control specimen 7. Échantillon de contrôle
Échantillon de comparaison
8. Fastener 8. Agrafe, attache
9. Finished metal connector plate 9. Connecteur en métal traité en surface
10. Gross cross-sectional connector plate area 10. Section droite brute du connecteur
11. Integral tooth of metal connector plate 11. Dent en partie découpée dans la plaque
12. Lateral resistance of metal connector plate 12. Résistance du connecteur au glissement
13. Length of metal connector plate 13. Longueur de la plaque d'assemblage
14. Lumber 14. Bois, bois d'oeuvre, sciage
15. Metal connector plate 15. Plaque métallique d'assemblage
16. Metal connector plate with integral teeth 16. Plaque dentée
17. Mill certification 17. Certificat (de qualité) de fabrication
18. Nail 18. Clou, pointe
19. Nail hole 19. Perforation pour clou
20. Nail-on plate 20. Plaque à clouer
21. Overpressed metal connector plate 21. Plaque assemblée par pression
22. Peeling resistance of metal connector plate with integral teeth 22. |
23. Plate 23. Plaque
24. Plate hole 24. Perforation dans la plaque

RUSSIAN

1. Угол размещения металлической зубчатой коннекторной пластины
2. Деревянный элемент, стыкуемый в торце
3. Соединение
4. Коннектор или соединительный элемент
5. Коннекторное отверстие (гнездо)
6. Контрольная пластина
7. Контрольный образец
8. Крепежный (соединительный) элемент
9. Обработанная металлическая зубчатая пластина
10. Поперечное сечение соединительной пластины брутто
11. Зубец металлической зубчатой пластины
12. Сопротивление металлической зубчатой пластины сдвигу
13. Длина металлической зубчатой пластины
14. Лесоматериал (древесина)
15. Металлическая зубчатая (коннекторная) пластина, м.з.п.
16. Металлическая коннекторная пластина с выштампованными зубьями
17. Заводской сертификат
18. Гвоздь
19. Отверстие под гвоздь
20. Гвоздевая пластина
21. Запрессованная металлическая зубчатая пластина
22. Сопротивление металлической зубчатой пластины выдергиванию
23. Пластина
24. Отверстие в пластине

GERMAN

1. Einbauwinkel zwischen Kraft- und Laengerichtung der Nagelplatte
2. Stumpf gestossener Holzstab
3. Verbindung
4. Verbindungsmittel
5. Ausstanzoffnung
6. Vergleichsplatte
7. Vergleichsmuster
8. Verbindungsmittel
9. Fertig bearbeitete Nagelplatte
10. Bruttoquerschnitt der Nagelplatte
11. Integraler Nagel der Nagelplatte
12. Verschiebungsfestigkeit der Nagelplatte
13. Laenge der Nagelplatte
14. Bauholz
15. Nagelplatte
16. Nagelplatte mit integrierten Naegeln
17. Werkzeugeignis fuer Stahlguete
18. Nagel
19. Nagelloch
20. Lochplatte (Verbindungsplatte)
21. Uebergesserte Nagelplatte
22. Auszugswiderstand der Nagelplatte
23. Platte
24. Plattenloch

ENGLISH	FRENCH	RUSSIAN	GERMAN
25. <u>Perforated metal connector plate</u>	25. Connecteur métallique perforé	25. Перфорированная металлическая зубчатая пластина	25. Gebohrte Nagelplatte
26. <u>Predrilled hole</u>	26. Trou percé, trou foré	26. Рассверленное отверстие	26. Vorgebohrtes Loch
27. <u>Prepunched hole</u>	27. Trou découpé à l'emporte-pièce	27. Пробитое отверстие	27. Vorgestanztes Loch
28. <u>Shear strength of metal connector plate</u>	28. Résistance de la plaque au cisaillement	28. Несущая способность металлической зубчатой пластины при сдвиге	28. Scherfestigkeit der Nagelplatte
29. <u>Shear transfer plate</u>	29. Plaque pour transmettre le cisaillement	29. Пластина для передачи усилий сдвига	29. Scherkraft Übertragungsplatte (Zweiseitige Nagelplatte)
30. <u>Solid metal connector plate</u>	30. Plaque métallique non perforée	30. Сплошная металлическая соединительная пластина	30. Undurchlochte Verbindungsplatte
31. <u>Solid metal-coupon control specimen</u>	31. Échantillon de contrôle non perforé	31. Сплошной металлический контрольный образец	31. Undurchlochter Kontrollprüfkoerper
32. <u>Strength</u>	32. Résistance	32. Несущая способность	32. Festigkeit
33. <u>Stress</u>	33. Contrainte	33. Напряжение	33. Spannung
34. <u>Stress ratio</u>	34. Rapport de contrainte	34. Показатель относительной прочности	34. Spannungsverhaeltnis
35. <u>Structural quality sheet coil</u>	35. Voile de qualité charpente	35. Конструкционного качества металлический листовый рулон	35. Stahlblech Rolle
36. <u>Tensile strength of metal connector plate</u>	36. Résistance du connecteur à la traction	36. Несущая способность металлической зубчатой пластины при растяжении	36. Zugfestigkeit der Nagelplatte
37. <u>Test piece</u>	37. Pièce d'essai	37. Элемент испытательного образца	37. Probestueck
38. <u>Test specimen</u>	38. Échantillon d'essai	38. Испытательный (тестовый) образец	38. Prüfkoerper
39. <u>Timber</u>	39. Bois d'oeuvre	39. Древесина (лесоматериал)	39. Holz (Bauholz)
40. <u>Tooth</u>	40. Dent	40. Зуб	40. Plattennagel
41. <u>Truss plate</u>	41. Plaque (d'assemblage) de ferme	41. "Фермовая" пластина	41. Nagelplatte
42. <u>Typical metal connector plate</u>	42. Connecteur métallique type (ou représentatif)	42. Репрезентативная металлическая зубчатая пластина	42. Typische Nagelplatte
43. <u>Ultimate strength</u>	43. Résistance maximale, résistance à la rupture	43. Предельная несущая способность	43. Bruchfestigkeit
44. <u>Unilaterally punched metal connector plate</u>	44. Plaque dentée d'un côté	44. Штампованная металлическая зубчатая пластина с односторонним расположением зубцов	44. Einseitige Nagelplatte
45. <u>Von Mises yield theory</u>	45. Théorie du fluage de von Mises	45. Теория пластичности Мизеса	45. Von Mises Spannungstheorie
46. <u>Width of metal connector plate</u>	46. Largeur de la plaque d'assemblage	46. Ширина металлической зубчатой пластины	46. Breite der Nagelplatte
47. <u>Wood</u>	47. Bois	47. Лес (древесина)	47. Holz
48. <u>Yield stress</u>	48. Contrainte à la limite d'élasticité	48. Пластические напряжения	48. Fließspannung

ENGLISH

DANISH

SWEDISH

FINNISH

- | | | | |
|--|---|---|--|
| 1. <u>Angle of placement of metal connector plate</u> | 1. Vinkel mellem kraftretning og pladens hovedretning | 1. Vinkel mellan kraftriktning och plåtens huvudriktning | 1. naulalevyn suunnakulma |
| 2. <u>Butted wood member</u> | 2. Stumpet stød | 2. Stumskarvat virke | 2. jatkospuusauva |
| 3. <u>Connection</u> | 3. Forbindelsesmiddel | 3. Foerband | 3. liitos |
| 4. <u>Connector</u> | 4. Forbindelsesmiddel | 4. Forbindelsesmiddel | 4. liitin |
| 5. <u>Connector hole</u> | 5. Forbindelsens hul | 5. Plåthål, Spikplåthål, Spikningsplåthål | 5. liitimen reikä |
| 6. <u>Control plate</u> | 6. Kontrolplade | 6. Kontrolplade | 6. metallilevynälyte |
| 7. <u>Control specimen</u> | 7. Kontrolprøve | 7. Kontrol | 7. näytekappale |
| 8. <u>Fastener</u> | 8. Forbindelsesmiddel | 8. Foerbindare, Faestdon | 8. liitospiikki |
| 9. <u>Finished metal connector plate</u> | 9. Udstandset forbindelsesmiddel | 9. Ytbehandlad spikplåt (spikningsplåt) | 9. pintakäsitelty metallilevynliitin |
| 10. <u>Gross cross-sectional connector plate area</u> | 10. Pladens tværnsnitsareal | 10. Plåtens (Spikplåtens, Spikningsplåtens) bruttotværsnitsareal | 10. liitimen kokonaispoikkileikkäkausala |
| 11. <u>Integral tooth of metal connector plate</u> | 11. Pladens tand | 11. Spikplåttand | 11. naulalevyn piikki |
| 12. <u>Lateral resistance of metal connector plate</u> | 12. Pladens forankringsstyrke | 12. Plåtens (Spikplåtens, Spikningsplåtens) forankringshållfasthet | 12. naulalevyn tartuntalujuus |
| 13. <u>Length of metal connector plate</u> | 13. Pladens længde | 13. Plåtlængd, Spikplåtens længd, Spikningsplåtens længd | 13. naulalevyn pituus |
| 14. <u>Lumber</u> | 14. Konstruktionstræ | 14. Irke, Træ | 14. sahatavara |
| 15. <u>Metal connector plate</u> | 15. Metal forbindelsesmiddel | 15. Spikningsplåt | 15. metalliliitinlevy |
| 16. <u>Metal connector plate with integral teeth</u> | 16. Metal connector plate with integral teeth | 16. Spikplåt | 16. naulalevy |
| 17. <u>Mill certification</u> | 17. Værkscertifikat | 17. Charge intyg | 17. ainestodistus |
| 18. <u>Nail</u> | 18. Søm | 18. Spik | 18. naula |
| 19. <u>Nail hole</u> | 19. Sømhul | 19. Spikhål | 19. naulan reika |
| 20. <u>Nail-on plate</u> | 20. Sømplade | 20. Spikningsplåt | 20: naulauslevy |
| 21. <u>Overpressed metal connector plate</u> | 21. Profileret sømplade | 21. Profileret sømplade | 21. ylipuristettu naulalevy |
| 22. <u>Peeling resistance of metal connector plate with integral teeth</u> | 22. Peeling resistance of metal connector plate with integral teeth | 22. Peeling resistance of metal connector plate with integral teeth | 22. naulalevyn piikkien irtoamislujuus |
| 23. <u>Plate</u> | 23. Plade | 23. Plade | 23. levy |
| 24. <u>Plate hole</u> | 24. Pladehul | 24. Pladehul | 24. levyn reikä |

ENGLISH

DANISH

SWEDISH

FINNISH

25. <u>Perforated metal connector plate</u>	25. Perforeret metalplade	25. Perforerett liitin
26. <u>Pre-drilled hole</u>	26. Forboret hul	26. esiporattu reika
27. <u>Prepunched hole</u>	27. Udstandset hul	27. esilavistetty reikä
28. <u>Shear strength of metal connector plate</u>	28. Pladens forskydningsstyrke	28. naulalevyn leikkauslujuus
29. <u>Shear transfer plate</u>	29. Forskydningskraftoverførsel	29.
30. <u>Solid metal connector plate</u>	30. Massiv metalforbindelsesmiddel	30. rei'ittämätön metalliliitin
31. <u>Solid metal coupon control specimen</u>	31. Massiv metalkontrolllegeme	31. metallinäytteen vetosauva
32. <u>Strength</u>	32. Styrke	32. lujuus
33. <u>Stress</u>	33. Spaending	33. jännitys
34. <u>Stress ratio</u>	34. Spaendingforhold	34. jännityssuhde
35. <u>Structural quality sheet coil</u>	35. Tynpladekonstruktions stålrulle	35. rakenneteräskela
36. <u>Tensile strength of metal connector plate</u>	36. Pladens trækstyrke	36. liitinlevyn vetlujuus
37. <u>Test piece</u>	37. Prøve	37.
38. <u>Test specimen</u>	38. Prøvelegeme	38. koekappale
39. <u>Timber</u>	39. Trae	39. sahatavara
40. <u>Tooth</u>	40. Tand	40. hammas
41. <u>Truss plate</u>	41. Spaerfagsplade	41. naulalevy
42. <u>Typical metal connector plate</u>	42. Typisk forbindelsesplade	42. naulalevynäyte
43. <u>Ultimate strength</u>	43. Brudstyrke	43. murtolujuus
44. <u>Unilaterally punched metal connector plate</u>	44. Ensidigt udstandset tandplade	44. toispuolisesti lävistetty naulalevy
45. <u>Von Mises yield theory</u>	45. Von Mises plasticitetsteori	45. Von Misesin myötöteoria
46. <u>Width of metal connector plate</u>	46. Pladebredde	46. naulalevyn leveys
47. <u>Wood</u>	47. Trae	47. sahatavara
48. <u>Yield stress</u>	48. Flydespaending	48. myötöjännitys

ESTONIAN

1. Metallist ühendusplaadi asendusnurk
2. Jätkatud puitelement
3. Ühendus
4. Ühenduselement
5. Auk ogaplaadis
6. Kontrollogaplaat, võrdlusogaplaat
7. Kontrolliplaat, võrdlusiplaat
8. Ühenduselement
9. Töödeldud ühendusplaat
10. Ogaplaadi põiklõike kogupindala
11. Ogaplaadi oga
12. Ogaplaadi kandevõime nihkele
13. Ogaplaadi pikkus
14. Puit
15. Metallist ühendusplaat
16. Ogaplaat
17. Tehase sertifikaat
18. Nael
19. Naela auk
20. Metallist ühendusplaat naelaaukudega
21. Liiga sissepressitud ogaplaat
22. Ogaplaadi kandevõime ogade väljatõmbele
23. Plaat
24. Auk ühendusplaadis

LATVIAN

1. Zobainās metāla plāksnes novietojuma lenķis
2. Būvkokss, kas pagarināts ar piedur-savienojumu jeb taisnu saduru
3. Savienojums
4. Savienotājs
5. Savienotājcaurums (atvere)
6. Kontrolplāksne
7. Kontrolparaugs
8. Savienotājelements
9. Apstrādāta zobainā metāla plāksne
10. Savienotājplāksnes bruto skērsgrī- ezuma laukums
11. Metāla savienotājplāksnes zobs (štancētais)
12. Zobainās metāla plāksnes pretes-tība bīdei
13. Zobainās metāla plāksnes garums
14. Kokmateriāls
15. Zobainā metāla plāksne
16. Zobainā metāla plāksne ar štancē-tiem zobiem
17. Rūpnīcas sertifikāts
18. Nagla
19. Naglas caurums
20. Naglota plāksne
21. Iepresēta zobainā metāla plāksne
22. Zobainās metāla plāksnes (ar štan-cētiem zobiem) pretestība izaršanai
23. Plāksne, plātne
24. Caurums (atvere) plāksnē

LITHUANIAN

1. Dygiuotosios metalinės plokštelės įrengimo kampas
2. Medinio elemento sudūrimas galais
3. Sandūra
4. Jungiantis elementas
5. Lizdas jungiančiam elementui
6. Kontrolinė plokštelė
7. Kontrolinis bandinys
8. Tvirtinimo elementas
9. Paruošta dygiuotoji metalinė plokštelė
10. Jungiančiosios plokštelės skerspjūvis bruto
11. Dygiuotosios metalinės plokštelės dyglys
12. Dygiuotosios metalinės plokš-telės stiprumas šlyčiai
13. Dygiuotosios metalinės plokš-telės ilgis
14. Miško medžiaga
15. Dygiuotoji metalinė plokštelė
16. Dygiuotoji metalinė plokštelė su štampuotais dygliais
17. Gamyklinis sertifikatas
18. Vinis
19. Kiaurymė viniui
20. Vinimis dygiuota plokštelė
21. Įpresuota dygiuotoji metalinė plokštelė
22. Dygiuotosios metalinės plokš-telės ištraukimo stiprumas
23. Plokštelė
24. Kiaurymė plokštelėje

ENGLISH

ESTONIAN

25. Perforated metal connector plate
26. Predrilled hole
27. Prepunched hole
28. Shear strength of metal connector plate
29. Shear transfer plate
30. Solid metal connector plate
31. Solid metal connector plate with shear strength
32. Strength
33. Stress
34. Stress ratio
35. Structural quality sheet cup
36. Tensile strength of metal connector plate
37. Test piece
38. Test specimen
39. Timber
40. Tooth
41. Truss plate
42. Typical metal connector plate
43. Ultimate strength
44. Unilaterally punched metal connector plate
45. Von Mises yield theory
46. Width of metal connector plate
47. Wood
48. Yield stress

LATVIAN

25. Perforēta zobainā metāla plāksne
26. Izurbts caurums
27. Izsists caurums
28. Zobainās metāla plāksnes nestspēja bīdē
29. Plāksne bīdes spēku pārnesšanai
30. Vienlaidu metāla savienotājpāksne (bez perforācijas caurumiem)
31. Vienlaidu (monofits) metāla plāksnes kontrolparaugs
32. Nestspēja
33. Spriegums
34. Relatīvās stiprības rādītājs
35. Konstruktīvā metāla sloksnes rullis
36. Zobainās metāla plāksnes nestspēja stiepē
37. Izmēģināšanas (pārbaudes) parauga elements
38. Izmēģināšanas (pārbaudes) paraugs
39. Kokmateriāls
40. Zobs
41. Kopnes plāksne (kopnes mezgla savienotājpāksne)
42. Tipveida zobainā metāla plāksne
43. Nestspējas robežlielums
44. Zobainā metāla plāksne ar vienaspusējiem štancētiem zobiem
45. Mīzesa plastiskuma teorija
46. Zobainās metāla plāksnes platums
47. Kokmateriāls
48. Plūstamības robeža

LITHUANIAN

25. Perforuota dygiuotoji metalinė plokštelė
26. Išgręžta kiaurymė
27. Išpresuota kiaurymė
28. Dygiuotosios metalinės plokštelės laikymo galia šlyčiai
29. Plokštelė perimanti šlyties jėgas
30. Vientisa metalinė jungiančioji plokštelė
31. Vientisas metalinis kontrolinis bandinys
32. Laikymo galia
33. Įtempimas
34. Santykinio stiprumo rodiklis
35. Konstrukcinis ruloninis metalas
36. Dygiuotosios metalinės plokštelės laikymo galia tempiant
37. Bandinio elementas
38. Tiriamasis bandinys
39. Statybinė miško medžiaga
40. Dyglis
41. Santvarinė plokštelė
42. Tipinė dygiuotoji metalinė plokštelė
43. Ribinė laikymo galia
44. Vienpusė dygiuotoji metalinė plokštelė
45. Von Mises plastingumo teorija
46. Dygiuotosios metalinės plokštelės plotis
47. Mediena
48. Plastiški įtempimai

HUNGARIAN

1. A csatlakoztató lemez elhelyezési szöge
2. Tompán illesztett elem
3. Csatlakozás (fakötés)
4. Csatlakoztató elem
5. Nyílás a csatlakoztató elemén
6. Csatlakoztató lemez
7. Kontrol próbatest
8. Rögzítő elem
9. Felületkezelt fém csatlakoztató lemez
10. A csatlakoztató lemez keresztmetszete
11. A szeglemez saját fogazata
12. A csatlakoztató lemez ellenállása síkbeli terhelés esetén
13. A csatlakoztató lemez hossza
14. Fürészárú (deszka, palló)
15. Fém csatlakoztató lemez
16. Szeglemez
17. Gyártási tanúsítvány
18. Szeg
19. Szeg lyuk
20. Felszegezhető csatlakoztató lemez
21. Túlréselt csatlakoztató lemez
22. Szeglemez "hamozási" ellenállása
23. Lemez
24. Lyuk a lemezen

POLISH

1. kat usytuowanie metalowej płytki złączeniowej
 2. dołożone/łączone na styk/elementy drewniane
 3. złącze
 4. łącznik, środek złączeniowy
 5. otwór łącznika
 6. płytka kontrolna
 7. próbka/element/kontrolna
 8. środek złączeniowy
 9. powlekana metalowa płytka złączeniowa
 10. powierzcchnia brutto przekroju poprzecznego płytki
 11. zęb metalowej płytki złączeniowej
 12. nośność złączeniowej płytki metalowej
 13. długość metalowej płytki złączeniowej
 14. tarcica, dłużyca, element drewniany
 15. metalowa płytka złączeniowa
 16. metalowa płytka kolczaste
 17. atest/certyfikat/producta
 18. gwóźdź
 19. otwór na gwóźdź
 20. płytka otworowa
 21. wciskana metalowa płytka złączeniowa
 22. nośność metalowej płytki złączeniowej na wyciąganie
 23. płytka, płytka
 24. otwór w płycie, płytce
1. Angle of placement of metal connector plate
 2. Buted wood member
 3. Connection
 4. Connector
 5. Connector hole
 6. Control plate
 7. Control specimen
 8. Fastener
 9. Finished metal connector plate
 10. Gross cross-sectional connector plate area
 11. Integral tooth of metal connector plate
 12. Lateral resistance of metal connector plate
 13. Length of metal connector plate
 14. Lumber
 15. Metal connector plate
 16. Metal connector plate with integral teeth
 17. Mill certification
 18. Nail
 19. Nail hole
 20. Nail-on plate
 21. Overpressed metal connector plate
 22. Peeling resistance of metal connector plate with integral teeth
 23. Plate
 24. Plate hole

ENGLISH

- | | | |
|---|---|--|
| 25. <u>Perforated metal connector plate</u> | 25. perforowana metalowa płytką złączeniowa | 25. Perforált fém csatlakoztató lemez |
| 26. <u>Predrilled hole</u> | 26. otwór nawiercony | 26. Előfúrt lyuk |
| 27. <u>Prepunched hole</u> | 27. otwór przebity | 27. Előütött lyuk |
| 28. <u>Shear strength of metal connector plate</u> | 28. nośność metalowej płytki złączeniowej na ścinanie | 28. Csatlakoztató lemez nyírószilárdsága |
| 29. <u>Shear transfer plate</u> | 29. dwustronna płytką kolczasta | 29. Nyíróerőt átadó csatlakoztató lemez |
| 30. <u>Solid metal connector plate</u> | 30. pełna metalowa płytką złączeniowa | 30. Tömör fém csatlakoztató lemez |
| 31. <u>Solid metal-cylinder control specimen</u> | 31. próbka kontrolna metalowej pełnej płytki złączeniowej | 31. Tömör fém kontrol próbatest |
| 32. <u>Strength</u> | 32. nośność | 32. Szilárdság |
| 33. <u>Stress</u> | 33. naprężenie | 33. Feszültség |
| 34. <u>Stress ratio</u> | 34. naprężenie efektywna, współczynnik nośności | 34. Feszültség hányados |
| 35. <u>Structural quality sheet coil</u> | 35. jakość konstrukcyjnej blachy rolowej / ruonowej / | 35. Hengerelt szerkezeti acéllemez |
| 36. <u>Tensile strength of metal connector plate</u> | 36. nośność metalowej płytki złączeniowej na rozciąganie | 36. Csatlakoztató lemez húzószilárdsága |
| 37. <u>Test piece</u> | 37. element do badań | 37. Próbatest alkatrész |
| 38. <u>Test specimen</u> | 38. próbka badawcza | 38. Próbatest |
| 39. <u>Timber</u> | 39. drewno | 39. Fűszelít gerenda |
| 40. <u>Tooth</u> | 40. ząb, kolec | 40. Fog |
| 41. <u>Truss plate</u> | 41. płytką kolczasta | 41. Szeglemez |
| 42. <u>Typical metal connector plate</u> | 42. typowa metalowa płytką złączeniowa | 42. Tipikus fém csatlakoztató lemez |
| 43. <u>Ultimate strength</u> | 43. nośność graniczna | 43. Maximális szilárdság |
| 44. <u>Unilaterally punched metal connector plate</u> | 44. jednostronna metalowa płytką kolczasta | 44. Egyoldalón fogazott szeglemez |
| 45. <u>Von Mises yield theory</u> | 45. teoria wytrzymała Hubera-Misesa | 45. Von Mises elmélet |
| 46. <u>Width of metal connector plate</u> | 46. szerokość metalowej płytki złączeniowej | 46. A csatlakoztató lemez szélessége |
| 47. <u>Wood</u> | 47. drzewo, drewno | 47. Fa (fűszáru) |
| 48. <u>Yield stress</u> | 48. naprężenie na granicy proporcjonalności | 48. Folyási határfeszültség |

ENGLISH

1. Angle of placement of metal connector plate
2. Butted wood member
3. Connection
4. Connector
5. Connector hole
6. Control plate
7. Control specimen
8. Fastener
9. Finished metal connector plate
10. Gross cross-sectional connector plate area
11. Integral tooth of metal connector plate
12. Lateral resistance of metal connector plate
13. Length of metal connector plate
14. Lumber
15. Metal connector plate
16. Metal connector plate with integral teeth
17. Mill certification
18. Nail
19. Nail hole
20. Nail-on plate
21. Overpressed metal connector plate
22. Peeling resistance of metal connector plate with integral teeth
23. Plate
24. Plate hole

SPANISH

1. Angulo de colocación del conector placa metálica
2. Pieza de madera unida a tope
3. Conexión Unión
4. Empalme
5. Agujero de Empalme
6. Placa de Control
7. Muestra de Control
8. Elemento de Fijación
9. Placa metálica con acabado superficial
10. Area gruesa de sección transversal de la placa metálica de empalme
11. Placa metálica de empalme con dientes estampados
12. Resistencia lateral de la placa metálica de empalme
13. Longitud de la placa metálica de empalme
14. Madera serrada Tabla
15. Placa metálica de empalme
16. Placa metálica de empalme con dientes estampados
17. Certificado de laminación
18. Clavo
19. Agujero de Clavo
20. Placa fijada con clavo
21. Placa metálica fijada por presión
22. Resistencia al desprendimiento de la placa metálica de empalme con dientes estampados
23. Placa
24. Agujero de Placa

PORTUGUESE

1. Angulo de colocação da placa metálica
2. Peça unida de topo
3. Ligação
4. Conector, placa metálica
5. Perfuração no conector
6. Placa de controle
7. Testemunha, amostra de controle
8. Conector, elemento de fixação
9. Placa metálica com acabamento superficial
10. Area bruta da seção transversal da placa metálica
11. Placa dentada com dentes estampados
12. Resistência lateral de placa metálica
13. Comprimento da placa metálica
14. Madeira serrada
15. Placa conectora metálica
16. Placa conectora metálica com dentes estampados
17. Certificação de fábrica
18. Pregos
19. Furo de prego
20. Placa fixada com pregos
21. Placa metálica colocada por pressão
22. Resistência ao arrancamento da placa dentada por fendilhamento (clivagem)
23. Placa
24. Furo da placa

ENGLISH

SPANISH

25. <u>Perforated metal connector plate</u>	25. Placa metálica de empalme perforada
26. <u>Predrilled hole</u>	26. Agujero pre-taladrado
27. <u>Prepunched hole</u>	27. Agujero pre-punzonado
28. <u>Shear strength of metal connector plate</u>	28. Resistencia al cizallamiento de la placa metálica de empalme
29. <u>Shear transfer plate</u>	29. Placa de transmisión del cizallamiento
30. <u>Solid metal connector plate</u>	30. Placa de empalme metálica lisa
31. <u>Solid metal-coupon control specimen</u>	31. Muestra de control de chapa lisa
32. <u>Strength</u>	32. Resistencia
33. <u>Stress</u>	33. Relación de tensión
34. <u>Stress ratio</u>	34. Tensión
35. <u>Structural quality sheet coil</u>	35. Bobina de chapa de calidad estructural
36. <u>Tensile strength of metal connector plate</u>	36. Resistencia a la tracción de la placa metálica de empalme
37. <u>Test piece</u>	37. Pieza de ensayo
38. <u>Test specimen</u>	38. Muestra de ensayo
39. <u>Timber</u>	39. Madero
40. <u>Tooth</u>	40. Diente
41. <u>Truss plate</u>	41. Placa de refuerzo
42. <u>Typical metal connector plate</u>	42. Placa de empalme típica
43. <u>Ultimate strength</u>	43. Resistencia límite
44. <u>Unilaterally punched metal connector plate</u>	44. Placa metálica de empalme estampada en un solo lado
45. <u>Von Mises yield theory</u>	45. Teoría del límite elástico de Von Mises
46. <u>Width of metal connector plate</u>	46. Anchura de la placa metálica de empalme
47. <u>Wood</u>	47. Madera
48. <u>Yield stress</u>	48. Límite elástico

PORTUGUESE

25. Placa conectora metálica perfurada	25. Placa conectora metálica perfurada
26. Pré-furação com broca	26. Pré-furação com broca
27. Pré-furação por punção	27. Pré-furação por punção
28. Resistência ao cizalhamento da placa conectora metálica	28. Resistência ao cizalhamento da placa conectora metálica
29. Placa de transferência de cizalhamento	29. Placa de transferência de cizalhamento
30. Placa conectora metálica não perfurada	30. Placa conectora metálica não perfurada
31. Amostra de controle de chapa não perfurada	31. Amostra de controle de chapa não perfurada
32. Resistência	32. Resistência
33. Tensão	33. Tensão
34. Taxa de tensão	34. Taxa de tensão
35. Bobina de chapa de qualidade estrutural	35. Bobina de chapa de qualidade estrutural
36. Resistência à tração de placa conectora metálica	36. Resistência à tração de placa conectora metálica
37. Peça para ensaio	37. Peça para ensaio
38. Corpo de prova	38. Corpo de prova
39. Madeira, madeiramento	39. Madeira, madeiramento
40. Dente	40. Dente
41. Placa para treliça	41. Placa para treliça
42. Placa conectora metálica típica	42. Placa conectora metálica típica
43. Resistência limite	43. Resistência limite
44. Placa metálica estampada de um só lado	44. Placa metálica estampada de um só lado
45. Teoria de escoamento de Von Mises	45. Teoria de escoamento de Von Mises
46. Largura de placa conectora metálica	46. Largura de placa conectora metálica
47. Madeira	47. Madeira
48. Tensão de escoamento	48. Tensão de escoamento

ENGLISH

JAPANESE

KOREAN

THAI

1. Angle of placement of metal connector plate
2. Butted wood member
3. Connection
4. Connector
5. Connector hole
6. Control plate
7. Control specimen
8. Fisher
9. Finished metal connector plate
10. Gross cross-sectional connector plate area
11. Integral tooth of metal connector plate
12. Lateral resistance of metal connector plate
13. Length of metal connector plate
14. Lumber
15. Metal connector plate
16. Metal connector plate with integral teeth
17. Mill certification
18. Nail
19. Nail hole
20. Nail-on plate
21. Overpressed metal connector plate
22. Peeling resistance of metal connector plate with integral teeth
23. Plate
24. Plate hole

1. 接合員軸角度
Setsugōgaku jikukakado
2. バットジョイントした木材
Batto jointoshita mokuzai
3. 接合
Setsugō
4. 接合材
Konekutā
5. 接合材の穴
Konekutā no ana
6. 原板
Genban
7. コントロール試験片
Kontorōru shikenhen
8. 接合具
Setsugōgu
9. 表面処理したメタルコネクタプレート
Hyomenhorishita metaru konekutā purēto
10. コネクタプレートの見掛けの断面積
Konekutā purēto no mikakeno danmenseki
11. メタルコネクタプレートの幅
Metaru konekutā purēto no ha
12. メタルコネクタプレート接合のせん断耐力
Metaru konekutā purēto setsugō no sendan tairyoku
13. メタルコネクタプレートの長さ
Metaru konekutā purēto no nagasa
14. 製材
Seizai
15. メタルコネクタプレート、板釘
Metaru konekutā purēto, Itakuji
16. 歯付きメタルコネクタプレート
Hatsuki metaru konekutā purēto
17. 工場の保証書
Kōjō no hōshōsho
18. 釘
Kugi
19. 釘穴
Kugiana
20. Nail-onプレート
Nai-on purēto
21. 圧入したメタルコネクタプレート
Atsunuyishita metaru konekutā purēto
22. 剥離抵抗のあるメタルコネクタプレート
Atsunuyishita metaru konekutā purēto
23. プレート
Purēto
24. プレートの穴
Purēto no ana

1. 판형 금속 연결재의 측각도
2. 통나무 부재
3. 맞춤 목재의 접합
4. 접합부품, 접속기구
5. 연결재의 구멍
6. 원판
7. 콘트롤 시험편
8. 침쇠
9. 표면처리된 판형 금속 연결재
10. 판형 연결재의 전단면적
11. 판형 금속 연결재의 완전한 맞물림
12. 판형 금속 연결재의 전단 내력
13. 판형 금속 연결재의 길이
14. 제재목
15. 판형 금속 연결재
16. 완전 맞춤림 판형 금속 연결재
17. 제품 보증서
18. 못
19. 못 구멍
20. 구멍물린 판형 금속 연결재
21. 압입한 판형 금속 연결재
22. 완전 맞춤림 판형 금속 연결재의 마찰저항
23. 판형 금속 연결재
24. 판형 금속 연결재의 구멍

1. มุมยึดของแผ่นโลหะยึด
2. ไม้ท่อน
3. การยึด
4. อุปกรณ์ยึด
5. ช่องในอุปกรณ์ยึด
6. แผ่นสำหรับเปรียบเทียบ
7. ตัวอย่างสำหรับเปรียบเทียบ
8. เหล็กของแผ่นโลหะยึด
9. แผ่นโลหะยึดชนิดที่เคลือบผิว
10. พื้นที่หน้าตัดของแผ่นโลหะยึด
11. ขั้นของแผ่นโลหะยึด
12. แรงต้านทางข้างของแผ่นโลหะยึด
13. ความยาวของแผ่นโลหะยึด
14. ไม้แปรรูป
15. แผ่นโลหะยึด
16. แผ่นโลหะยึดที่พร้อมใช้
17. การรับประกันของโรงงาน
18. ตะปู
19. รูตะปู
20. แผ่นยึดด้วยตะปู
21. แผ่นโลหะยึดที่กดทับกัน
22. แรงต้านทานการลากของแผ่นโลหะยึด
23. แผ่น
24. ช่องในแผ่น

ENGLISH

JAPANESE

25. Perforated metal connector plate	25. 穴あきメタリックプレート Anaaki metaru konekutā purēto
26. Predrilled hole	26. 先穴 Sakiana
27. Prepunched hole	27. 打ち抜き穴 Uchinukiana
28. Shear strength of metal connector plate	28. メタリックプレートのせん断強さ Metaru konekutā purēto no sendantsuyosa
29. Shear transfer plate	29. せん断プレート Sendan purēto
30. Solid metal connector plate	30. メタリックプレートの原板 Metaru konekutā purēto no genban
31. Solid metal-coupon control specimen	31. メタリックプレートの原板試験片 Metaru konekutā purēto no genbanshikenhen
32. Strength	32. 強度, 強さ, 耐力 Kyōdo, Tsuyosa, Tairyoku
33. Stress	33. 応力度 Ōryokudo
34. Stress ratio	34. 応力度比 Ōryokudohi
35. Structural quality sheet coil	35.
36. Tensile strength of metal connector plate	36. メタリックプレートの引張強さ Metaru konekutā purēto no hipparitsuyosa
37. Test piece	37. 試験片 Shikenhen
38. Test specimen	38. 試験体 Shikentai
39. Timber	39. 製材 Seizai
40. Tooth	40. 歯 Ha
41. Truss plate	41. トラスプレート Torasu purēto
42. Typical metal connector plate	42.
43. Ultimate strength	43. 終局耐力 Shūkyokutairyoku
44. Unilaterally punched metal connector plate	44.
45. Von Mises yield theory	45.
46. Width of metal connector plate	46. メタリックプレートの幅 Metaru konekutā purēto no haba
47. Wood	47. 木材 Mokuzai
48. Yield stress	48. 降伏応力 Kōfukuōryoku

KOREAN

THAI

25. 구멍플레이트용 판형 금속연결재	25. แผ่นโลหะมีรูเจาะช่องแล้ว
26. 드릴로 뚫린 구멍	26. รูเจาะหน้า
27. 펀치로 뚫린 구멍	27. รูตอกหน้า
28. 판형 금속연결재의 전단강도	28. ความแข็งแรงเฉือนของแผ่นโลหะมีรู
29. 전단 전달 판형 금속연결재	29. แผ่นถ่ายเทแรงเฉือน
30. 구멍이 뚫리지 않은 판형 금속연결재	30. แผ่นโลหะมีรูแบบตัน
31. 판형 금속연결재의 시험편	31. ตัวอย่างแผ่นโลหะสำหรับเปรียบเทียบเพื่อ
32. 강도	32. ความแข็งแรง
33. 강도비	33. ความดัน
34. 응력도	34. อัตราส่วนความดัน
35.	35. แผ่นเหล็กคุณภาพโครงสร้าง
36. 판형 금속연결재의 인장 강도	36. ความแข็งแรงดึงของแผ่นโลหะมีรู
37. 시험편	37. ชิ้นทดสอบ
38. 시험편	38. ตัวอย่างทดสอบ
39. 재목	39. ไม้
40. 맞물림	40. ฟัน
41. 트러스용 판형 금속연결재	41. แผ่นโครงถัก
42. 판형 금속연결재	42. แผ่นยึดแฉกธรรมดาคา
43. 극한 강도	43. ความแข็งแรงสูงสุด
44. 외줄로 구멍뚫린 판형 금속연결재	44. แผ่นโลหะมีรูที่พับขึ้นเพื่อตัดเดียวกัน
45. 본미즈 항복이론	45. ทฤษฎีการกลายของวอนมีสส์
46. 판형 금속 연결재의 폭	46. ความกว้างของแผ่นโลหะมีรู
47. 목재	47. ไม้
48. 항복응력	48. ความดันคลาก

INTERNATIONAL COUNCIL FOR BUILDING RESEARCH STUDIES AND DOCUMENTATION
WORKING COMMISSION W18 - TIMBER STRUCTURES

DESIGN OF JOINTS BASED ON IN V-SHAPE GLUED-IN RODS

by

J Kangas
Technical Research Centre of Finland (VTT)
Finland

MEETING TWENTY - SIX

ATHENS, GEORGIA

USA

AUGUST 1993

DESIGN OF JOINTS BASED ON IN V- SHAPE GLUED-IN RODS

ABSTRACT

In this study a method is presented how to design the capacity of moment resisting joints of glued laminated timber structures based on the properties of in V- shape glued-in rods. Design rules for anchorage capacity of the rods and capacity of timber in the joint area are given. Design rules are based on an experimental research, which is briefly introduced.

INTRODUCTION

The technology has originally been developed in TSNIISK in Moscow. It was introduced in CIB-W18 meeting 22 in Berlin in 1989 by Dr. Turkovsky. Research work began already in 1975. It has been almost unknown for the rest of the world mainly because the publications were in Russian.

The method is based on ribbed steel rods, which have been glued at skew angles into the glulam. The rods take effectively the forces in their direction up to the tensile capacity of the steel. When the rods have been welded on to steel plates, the forces can be carried forward in the same manner as known in steel structures.

This article presents some results of the experimental research carried out in Technical Research Centre of Finland (VTT) during the years 1991-3. The goal of this research was to deepen and to enlarge the basis for design rules and instructions for production. The report is under work and it will be published in the near future.

TEST SERIES

In the first phase joints consisting of one ribbed steel rod were tested in order to get knowledge about the anchorage strength of the glueline. The rods were glued into spacious holes drilled in the timber at the angles of 30°, 45°, 60° and 90° with the grain direction. The rods were then loaded in tension or in compression, see Figs. 1 and 2. Thickness of the rods was 20 mm.

Two types of both epoxy and polyurethane adhesives were used in the joints. All gave good strength values. The most promising was the new PU adhesive, which is not sensitive to moisture. Injecting the joints by a pilot glueing machine was very easy.

In later phases the steel rods were welded into a steel plate, by which the joint was loaded. In the second phase different V-anchor joints of two rods were loaded in centric tension or in shear in the direction of the beam, see Figs. 3 and 4. In failure the steel rods often broke off (their strength was over 600 MPa). Thickness of the rods was 20 mm or 16 mm.

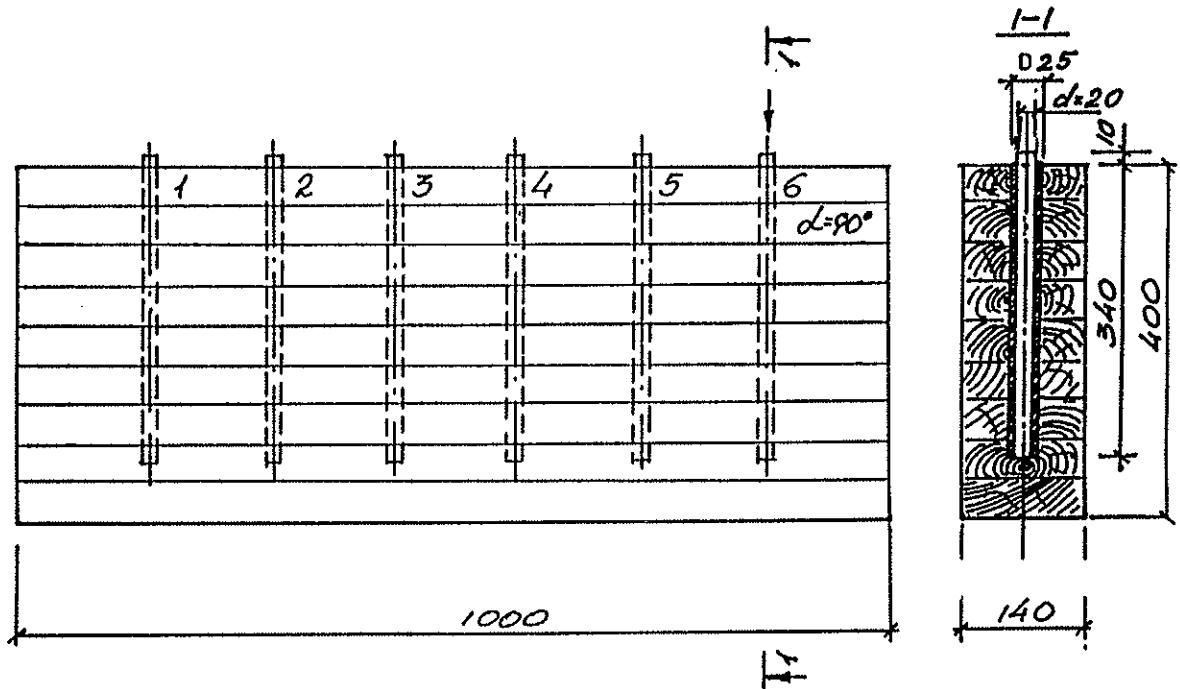


Fig. 1. Test specimen of compression test series $\alpha = 90^\circ$.

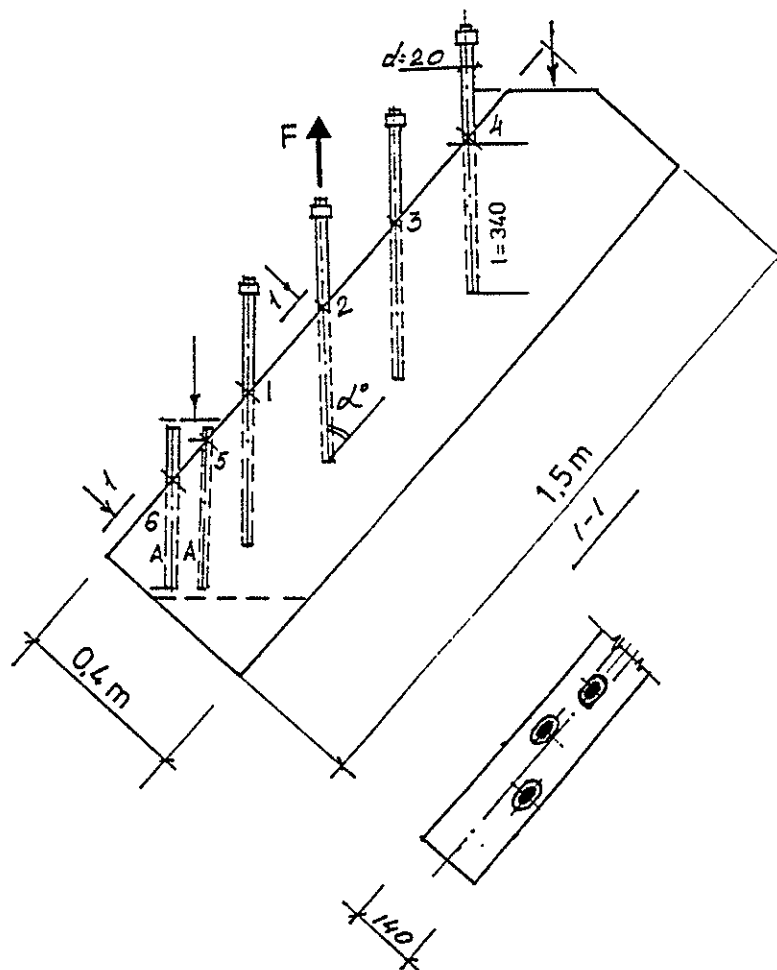


Fig. 2. Test specimen of tensile test series $\alpha = 45^\circ$.

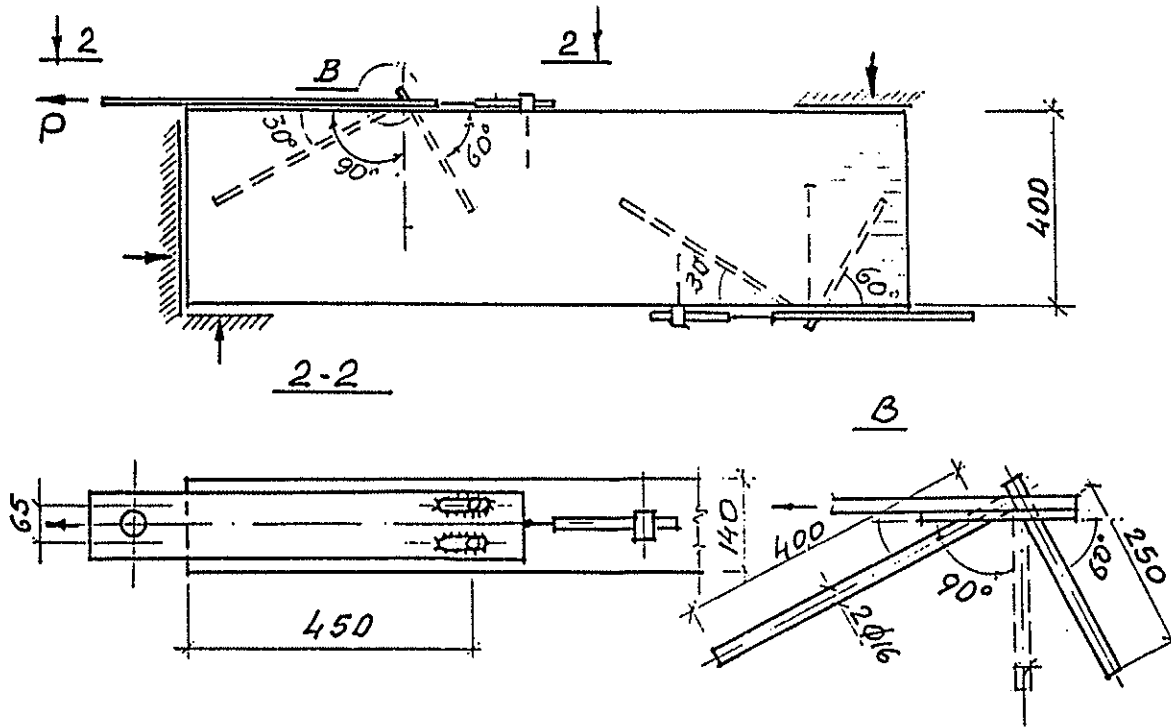


Fig. 5. Test specimen of small V-joints of four rods.

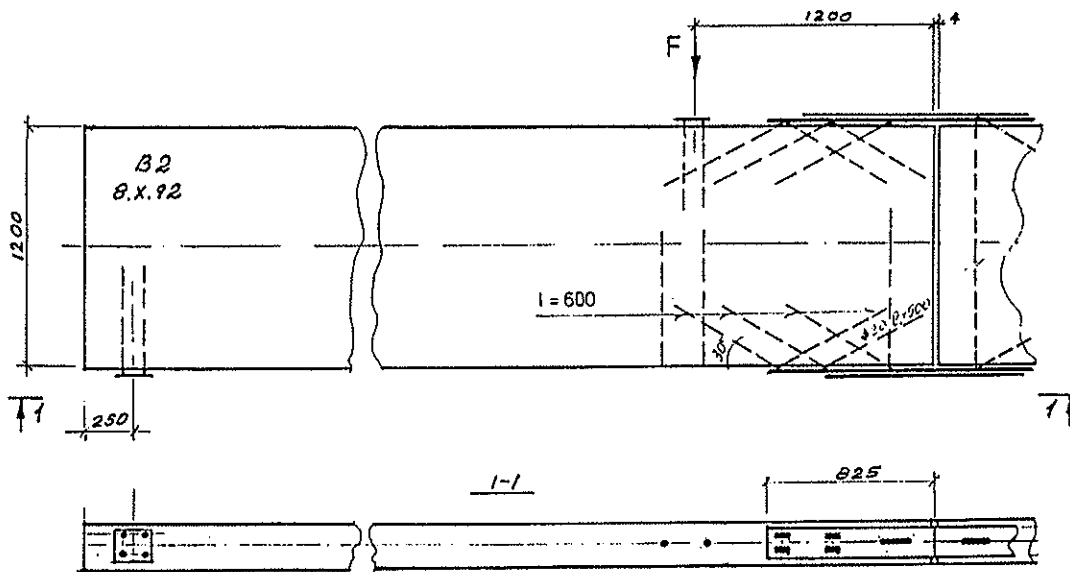


Fig. 6. Schema of the beam B₂.

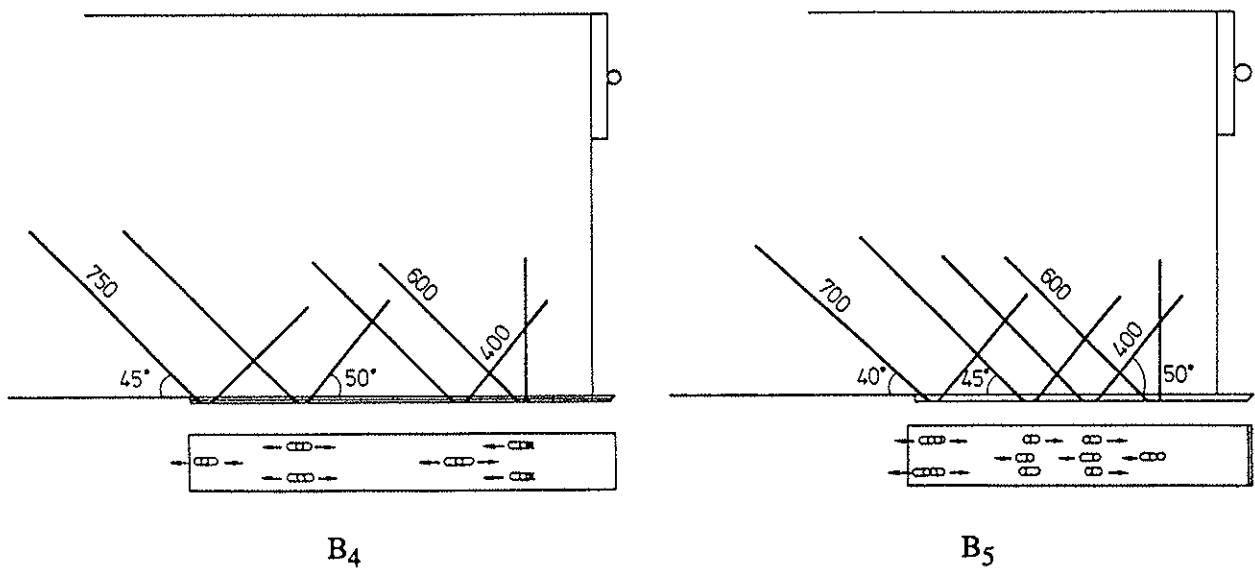


Fig. 7. Connections of beams B_4 and B_5 .

FAILURE MODES

Small joints

Based on the test results of one rod joints the glued lengths of the rods in small joints were chosen so that the anchorage and tensile capacities were close to each other. There were then two failure modes in all V-shaped joints. Some of the rods reached their tensile capacity and broke near the welded joint with the lug, which was used for the loading. Somewhat more often the rods were drawn out of the beam after losing the anchorage capacity. The joints are rigid and they have deformation capacity, see Fig. 8.

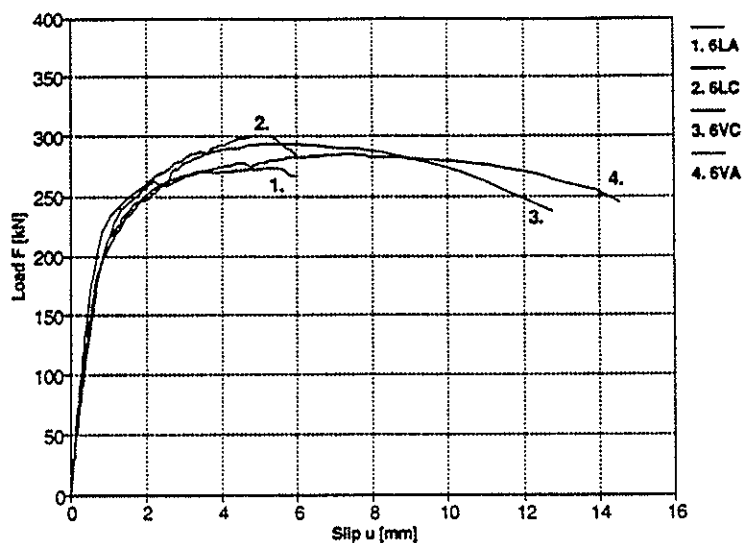


Fig. 8. Load- deformation curve of small V- joints.

Deep beams

In the last phase beams B₁ and B₂ broke in similar way in the tensile joint of the connection. A piece of timber broke off the beam. Size of it was the same which was hold by the anchoring rods.

In loading B₄ the timber member had a shear failure in the middle depth of the beam.

Beam B₅ broke in three stages. Welding of two tensile rods was not managed sufficiently well. They were torn one by one out of the steel plate after the maximum load $2F_{\max} = 2 \times 282$ kN. At each step the load F decreased by 30 kN. Finally two farthest tensile rods broke by the total load 440 kN.

Cracks of bending failure were afterwards found on other side of the connection at the foot of last rods. Beginning of that was not seen. Joint made by glued-in rods is obviously tough.

STRENGTH CHARACTERISTICS

Behaviour of V-joint

Relation of the load F and axial forces in rods S₁ and S₂ is illustrated in Fig. 9. Design is based on the capacity of the tensile rod. The compression rod is utilized in the proportion of equation (2). Based on the equilibrium of forces the relations derived are as follows:

$$F = S_1 \cos \gamma_1 + S_2 \cos \gamma_2 \quad (1)$$

$$S_1 \sin \gamma_1 + S_2 \sin \gamma_2 = 0, \quad (2)$$

where

$|\gamma| < 90^\circ$, when the rod is in tension

$|\gamma| > 90^\circ$, when the rod is in compression.

The capacity of symmetric V-anchor joint in tensile and shear test series is

$$F_{\max} = S_1 2 \cos \gamma_1 (+ R_D), \quad (3)$$

where

R_D is a dowel effect to be calculated separately .

In general case the capacity of V-anchor joint is

$$F_{\max} = S_1 \sin(\gamma_2 - \gamma_1) / \sin \gamma_2 (+ R_D). \quad (4)$$

In the case of many V-anchors the capacity of the joint is the arithmetical sum of their capacities. When there are different V-anchors in the same connection they are calculated separately and summed.

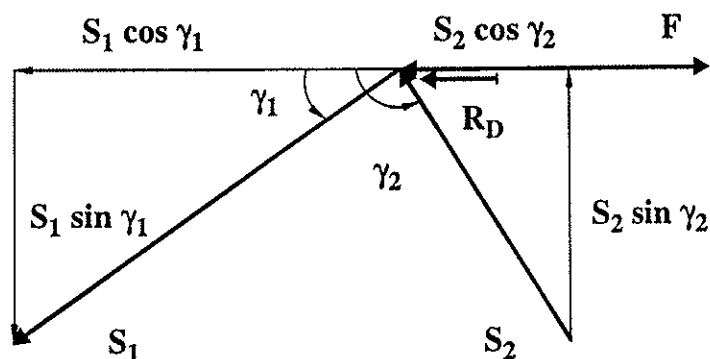


Fig. 9. Diagram about V- joint.

Dowel effect

When the rod in compression has steep angle or $\alpha_2 \geq 50^\circ$ ($\gamma_2 \leq 130^\circ$), it will also work as a dowel when the load is in grain direction. The load- carrying capacity of dowel in single shear steel-to-timber joints can be calculated in accordance with Eurocode No 5, from the formula

$$R = 1,5(2M_y f_h d)^{1/2}. \quad (5)$$

Its values in different combination of parameters of tested joints have been calculated as follows: The fastener yield moment is calculated from the formula $M_y = f_y W_p$, where $W_p = d^3/6$.

Embedding strength in timber can be taken as $f_h \approx 0,65f_c$, where f_c is strength in compression.

Small joints

The capacities of tested small joints have been analyzed according to the equations (3) and (4). The dowel effect has been taken into account when calculating the force of the rods in tensile failure. After that correction the calculated strength values of the rods were equal to the separately measured material strength.

Deep beams

As a result of the summing the V-anchors of the tensile connections the following normal forces N are obtained:

Beams B_1 and B_2 : $N = 7,8S_1 + 40 \text{ kN}$ (R_{dowel}),

Beams B_4 and B_5 : $N = 6,5S_1 + 50 \text{ kN}$,

Beam B_{5b} : $N = 4,5S_1 + 50 \text{ kN}$ (before final failure).

External bending moment in the connection of the deep beams is

$$M_{\text{ext}} = 4,55F \text{ kNm} + M_g,$$

where effect of gravity is $M_g = 23 \text{ kNm}$ for beams B_1 and B_2 . For beams B_4 and B_5 it is 19 kNm .

Internal bending moment in the connection of the symmetric beams B_1 and B_2 is

$$M_{\text{int}} = 1,20N \text{ kNm.}$$

Tensile force in the connection of beams B_1 and B_2 is then

$$N = 3,79F + 23 \text{ kN.}$$

Internal bending moment of beams B_4 and B_5 is

$$M_{\text{int}} = 1,02N \text{ kNm.}$$

Tensile force in the connection of beams B_4 and B_5 is then

$$N = 4,46F + 19 \text{ kN.}$$

Mean forces S_1 of the tensile rods by maximum load was calculated:

Beam B_1 : $S_1 = 134 \text{ kN}$,

Beam B_2 : $S_1 = 132 \text{ kN}$,

Beam B_4 : $S_1 = 193 \text{ kN}$ and

Beam B_5 : $S_1 = 189 \text{ kN}$.

Rods did not fail. Beams B_1 and B_2 broke in tension at the distance of farthest rods in the area where the rods were glued into. For the effective cross section calculated tensile strengths of timber were $f_t = 26,5$ and 26 N/mm^2 . They are a little higher than characteristic values of their density according to the draft EN TC 124. 207 January 1993.

In the loading of B_5 two rods were torn one by one out of the steel plate after it had reached the maximum load $F_{\text{max}} = 282 \text{ kN}$. At each step the load decreased by 30 kN . Finally two farthest tensile rods broke by the load $F_{\text{max}} = 220 \text{ kN}$. Developments of the failure can be seen in the Fig. 10, where the measured growth of the gap in tensile side of the connection is drawn. Calculated mean forces of the tensile rods were then $S_1 = 211 \text{ kN}$, which is also their tensile strength.

Bending stresses of beams B_4 and B_5 at maximum load were $\sigma_m = 31,6$ and $29,3 \text{ MPa}$, when whole cross section was used in calculation. Calculated bending stresses are at the same level as the tensile strength of beams B_1 and B_2 . Rods do not seem to reduce the bending capacity of V- joints.

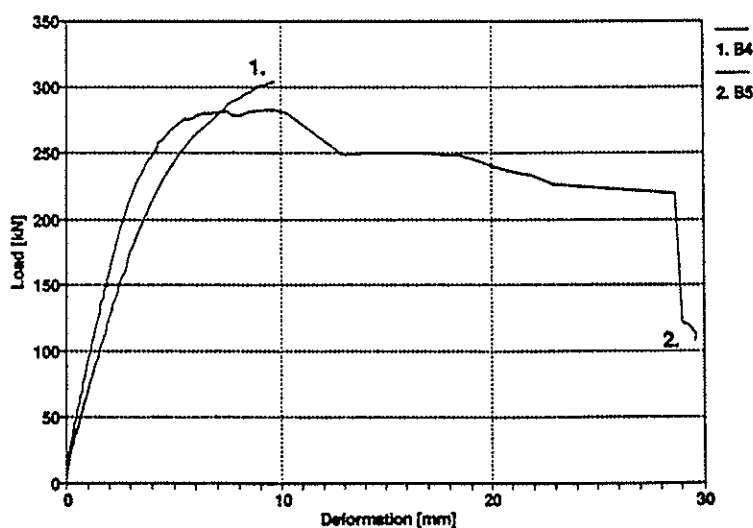


Fig. 10. Measured deformations in the tensile side of the gap in the connection of beams B₄ and B₅.

Strain gauge measurements

Strain gauges were glued on the steel plates of tensile side in the connections of beams B₄ and B₅. They gave information about the share of the load to the number of the rods, which were behind the measuring points. At the load $0,4F_{max}$ measured relative strains were:

Beam B₄:

Number of rods after gauge	10	6
Relative strain	1,0	0,65.

Beam B₅:

Number of rods after gauge	10	9	6,5	4
Relative strain	1,0	0,87	0,65	0,47.

Relative strains above prove with sufficient accuracy that the load is divided evenly to the rods.

TIMBER CAPACITY

Effective cross section of the beam in the connection is calculated by reducing the width b of the beam on the tensile side by the drilled portion:

$$b_{ef} = b - nD, \quad (6)$$

where n is the number of parallel drilled holes in the cross section. Generally only the farthest section needs to be checked, because the capacity of the rods in other sections can be taken into account. Bending capacity of the beam is calculated in that section.

The portion of cross section ($b_{ef}l\sin\alpha$), which is joined by rods, is designed by the normal force N in the joint, see Fig. 11.

$$b_{ef}l\sin\alpha f_t \geq N \quad (7)$$

When calculating the bending capacity of V- joints timber member can have the whole cross section without reduction on condition that the angle of rod is $\alpha \leq 45^\circ$.

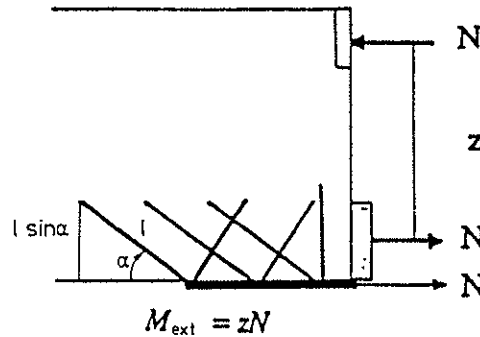


Fig. 11. Diagram about the design of connection of in V- shape glued-in rods.

ANCHORAGE CAPACITY

Mean anchorage strength f_a of the rods depends on the effective anchorage length l_{ef} . It can be given the formula:

$$f_{a,u} = 7(1 - 0,01l_{ef}/d) \text{ [MPa]}. \quad (8)$$

Design anchorage capacity $R_{a,d}$ of the rod is calculated on the outer surface of glued joint, when the diameter of the drilled hole is $D \leq 1,25d$:

$$R_{a,d} = \pi D l_{ef} f_{a,d}. \quad (9)$$

CAPACITY OF STEEL MEMBERS

In calculating the capacity of rods and other steel members the regulations of steel constructions are to be followed.

CONCLUSIONS

In this study a general method is presented how to design the capacity of moment resisting multirod joints of glued laminated timber structures. It is based on the design of separate joints of in V- shape glued-in rods. Design rules for anchorage capacity of the rods and capacity of timber in the joint area are given. Design rules are proved by the experimental research.

Because of glueing V- shaped joint is rigid. It has also deformation capacity like mechanical joints, which is lowering otherwise possible stress concentrations.

When calculating the bending capacity of V- joints timber member can have the whole cross section without reduction on condition that the angle of rod is $\alpha \leq 45^\circ$. Moment resisting connections of glued laminated timber can then be made without reducing its bending capacity.

Connections based on this method are relatively easy to fabricate. Because of glueing there must be strict regulations for quality control.

REFERENCES

[1] Turkovsky, S. B." Designing of glued wood structures joints on glued-in bars", CIB-W18/22-7-13, 1989.

[2] Kangas, J. Research on joints of glued laminated timber structures based on glued-in ribbed steel rods. To be published as a VTT publication, Technical Research Centre of Finland.

[3] EUROCODE 5, Design of timber structures, Part 1-1: General Rules and Rules for Buildings, 1992.

[4] EN TC 124. 207: Timber Structures - Glued Laminated Timber - Strength Classes and Determination of Characteristic Values, Draft dated January 1993.

INTERNATIONAL COUNCIL FOR BUILDING RESEARCH STUDIES AND DOCUMENTATION
WORKING COMMISSION W18 - TIMBER STRUCTURES

TESTS ON TIMBER CONCRETE COMPOSITE STRUCTURAL ELEMENTS (TCCS)

by

A U Meierhofer
EMPA Wood Department
Switzerland

MEETING TWENTY - SIX

ATHENS, GEORGIA

USA

AUGUST 1993

Tests on Timber Concrete Composite Structural Elements (TCCs)

A Summary

An extensive research and development work had been undertaken to achieve a ready-to-apply Timber Concrete Composite Structural Elements (TCCs)- system mainly to be used as medium span floors (for residential construction and office buildings). The various project works were basically performed by three partners forming an efficient team: SFS Stadler AG, Heerbrugg, developed a special high strength steel connector, the engineering office H. Wieland AG, Maienfeld, set up a computer program for an easy static analysis and proportioning of TCCs and added a lot of experience of building practical value to the project. Finally the Swiss Federal Laboratories for Materials Testing and Research (EMPA), especially the Wood Department, performed a vast testing program to optimized the mechanical behavior and the efficiency of such TCCs and to increase the knowledge of this type of construction to form a solid base for a design by the structural engineer.

The build up of the TCCs is extremely simple: a set of timber beams of adequate cross section is positioned on the top of the erected walls. The beams are covered up with boards of about 20mm thickness which act as the formwork for the concrete and may - if of appropriate quality - serve at the same time as a decorative lining of the ceiling. The boards are covered with two sheets of building plastic to make sure that no laitance leaches through the boards, soiling them. Afterwards, the connectors are placed by screwing them into the beams through the plastic sheets and the boards (some staples may be used to preassemble beams, boards and plastic together). Finally about 80mm of concrete (maximum size of aggregates 16mm) is cast on the top in two layers with some light nominal reinforcement in between.

It is obvious, that for the achievement of efficient composite action the connection, resp. the connectors, play a decisive role which is reflected by the focal points of the performed investigations.

Just as important as the efficiency of the connection, however, is its economy, which has a decisive influence on the acceptability of the building market. It seems, that the developed system has considerable advantages especially in this regard, due to the slender design of the connectors, which allows them to be placed within seconds with an ordinary drilling machine (without any predrilling) and reduces the installation costs - a major handicap of other systems - to a minimum.

Due to the slenderness of the connector, however, no sufficient stiffness of the connection could be reached with the initial vertical arrangement of the connectors even using a high number. This led to a new arrangement of the connectors under an angle of 45° and later - inspired by a trussconfiguration - to an arrangement using two angles of the connectors, $\pm 45^\circ$ and $45^\circ/90^\circ$, the latter of which was selected from a practical building viewpoint. The stiffness of the new arrangement is basically due to the fact, that the connectors are no longer loaded in bending but in tension and compression, i. e. axially. This signified, however, that the withdrawal strength and stiffness gained a considerable importance.

For this reason a number of a number of short-term and long-term *withdrawal tests* have been performed with concrete and with spruce timber (grain angle 90° and 45°). The short-term strength of the connectors showed to be in the region of 11kN. The 6-month long-term withdrawal tests were performed using load levels of 1kN, 2kN, 3kN and 4kN. The creep deformation of the latter did not stabilize within the test period which suggests a (serviceability) limit stage of about 3kN. The maximum creep factor (creep deformation/initial elastic deformation) observed after 6 months was 1.2.

Important results on the structural behavior of the connections have been obtained by various *shear tests*. The main test parameter was the arrangement of the connectors (see paragraph above). By optimizing the arrangement of the connectors, the short-term stiffness of the connection (per connector) could be increased from about 10kN/mm up to 150kN/mm.

The knowledge acquired with the shear test was finally implemented in two series of bending tests. The TCC bending test specimens had a length of 4m. Short-term tests have been performed to establish the load/deformation behavior as well as the ultimate load. The creep deformations were observed in long-term tests lasting over one year. The bending tests fully confirmed the results of the shear tests in respect to the primary importance of the arrangement of the connectors. The TCCs with the (optimal) crossed arrangement of the connector proved to be more than three times as stiff in the short-term tests as the ones with perpendicular arrangement.

The long-term bending test were conducted under relatively unfavorable conditions: outside under roof, i.e. the specimens were fully exposed to the natural temperature changes and drying and wetting cycles which proved to be a very dominating influence. Depending on the initial moisture content - some specimens had been installed having a relatively high moisture content (about 25%), the creep factor after one year varied between 2 and 4. In spite of these high factors the ratio between deflection and span was very acceptable for the optimized test alternatives.

By maintaining good workmanship in the shop and on the building site as well as considering the rules of good building practice (use of dry, quality timber, avoiding gaps between timber beams and formwork, shoring the timber during and after casting of the concrete etc.), strong, stiff and economical structures may be obtained as had been demonstrated by a great number of existing buildings.

A. U. Meierhofer, EMPA Wood Department. 93 8 24

INTERNATIONAL COUNCIL FOR BUILDING RESEARCH STUDIES AND DOCUMENTATION

WORKING COMMISSION W18 - TIMBER STRUCTURES

LONG TERM DEFORMATIONS IN WOOD BASED PANELS UNDER
NATURAL CLIMATE CONDITIONS. A COMPARATIVE STUDY

by

S Thelandersson

J Nordh

T Nordh

S Sandahl

Department of Structural Engineering, Lund University

Sweden

MEETING TWENTY - SIX

ATHENS, GEORGIA

USA

AUGUST 1993

Long term deformations in wood based panels under natural climate conditions. A comparative study.

Thelandersson S., Nordh J., Nordh T., Sandahl S.

Department of Structural Engineering, Lund University

Introduction

Most long term studies of the behaviour of wood based panel products has been performed under controlled moisture conditions, mainly with constant relative humidity. In practice, the relative humidity is always more or less variable. For this reason, the relative ranking in design codes of the materials with respect to creep factors and moisture sensitivity might not reflect the performance in practice in an adequate way. The objective of the investigation reported here was to study the relative performance of some wood based materials under rather humid and variable conditions. To this end, comparative long term tests were performed for a number of panel products exposed to the same natural conditions. The design codes considered in the analysis of results given in this paper are Eurocode 5 [1] and the Swedish building code "Nybyggnadsregler" (NR) [2].

Test methods and materials

Creep tests are performed in bending for six different board materials. Reference tests of small beams made of wood were also included in the investigation. The dimensions of the specimens and the test set up are shown in Fig. 1. The tested beams consist of two parallel strips with a depth of 45 mm separated from each other with rectangular distance elements of wood glued to the strips at the supports and at the loading points. The strips are placed vertically so that bending occurs with respect to an axis perpendicular to the plane of the panels. This loading mode is considered as representative for the case when the panel is used as component material (e.g. web) in light weight composite structural elements. The choice of cross section was mainly motivated by the requirement that moisture exchange shall take place through both faces of the panel strips. Moisture exchange at the edges of the strips was prevented by moisture tight tape attached along all edges.

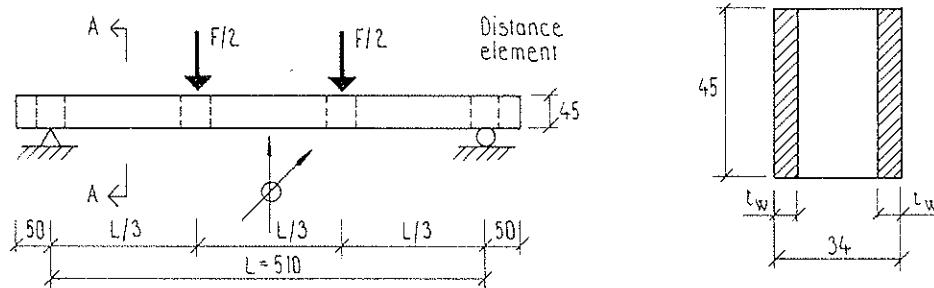


Fig. 1. Test arrangement and beam cross section.

Materials

The following seven materials were used in the tests:

- 1) Wood. Nearly defect free strips of wood with thickness 12 mm and depth 45 mm were sawn from structural timber with strength class K30. These specimens were included as reference material in the tests.
- 2) Plywood P30. Thickness = 10 mm, with 5 plies of equal thickness. Classified for structural use in service classes 1-3 according to the Swedish building code and EN 112.406 [3].
- 3) Fibre board (K40) with thickness 7.5 mm. Nominal density = 870 kg/m^3 . It has been manufactured in a wet process method with defibration in accordance with the original Mason process. The panel is of quality K 40 according to the Swedish Building Code, where it is classified for use in service class 1 and 2. The EN-classification for this panel is unclear at the moment, but the nearest existing classification is prEN 622-3 (HB).
- 4) Particle board V313 with thickness 10 mm. Nominal density = $700\text{-}720 \text{ kg/m}^3$. It is classified for structural use in service class 1 and 2 according to the Swedish Building Code. In EN 124.406 its preliminary classification is EN 312-5, "Load bearing boards for use in humid conditions."
- 5) Particle board V20 with thickness 10 mm. Nominal density = $650\text{-}700 \text{ kg/m}^3$. Not classified for structural use.
- 6) Medium density fibre board (MDF). Thickness = 8 mm. Nominal density = 750 kg/m^3 . Not classified for structural use in Sweden or in relation to Eurocode 5.
- 7) Oriented strand board (OSB). Thickness = 11 mm. Nominal density = 650 kg/m^3 . Intended for structural use.

Nominal densities given above are taken from product information provided by the manufacturers. No precise definition was given of the density measure used. The actual density of the tested panels will be determined after the tests have been terminated.

Short term bending strength

The short term bending strength was determined for all materials with the same test set up as that used in the long term tests, see Fig. 1. Six specimens were used for each material. The moisture content in the panels was measured in connection with the testing.

Creep tests

Long term tests with constant loading were performed with the test set up shown in Fig. 1. Three specimens were used for each material. The specimens were placed in a large steel container (length 6 m, width 2.5 m, height 2.5 m). The container is ventilated and was placed outdoors in the vicinity of the Civil Engineering laboratory at Lund University. The climate conditions inside the the container may be regarded as representative of the conditions in a non-heated space under a ventilated roof. Temperature and relative humidity is recorded

continuously during the test period, which is intended to last for two years. This report gives the results obtained for the first year of the test period.

The constant load applied during the creep tests was chosen to a predetermined fraction of the average ultimate load in bending determined from the short term tests. The load level was chosen as to be representative of the design load level in the serviceability limit state. Thus, the load was taken to 16 % of the ultimate short term load for wood and 13% for plywood. All the other panel materials were loaded to 11% of the ultimate short term load. The difference reflects the fact that the strength reduction for long term loading is smaller for wood and plywood than for the other materials. Thus the working load will usually be higher for these materials in relation to the short term strength.

The deflection of the beams was measured at the mid section. This was made with dial gauges placed on an aluminium frame, rigidly attached to a steel frame supporting the test beams, see Fig. 2. Each measurement was repeated three times to eliminate errors associated with inappropriate fitting at the support of the dial gauge. A reference frame of aluminium was used to compensate for thermal movements in the measuring rig and in the dial gauge. Readings were taken on the reference frame immediately before and immediately after each set of measurements on the test specimens. All results presented here have been adjusted based on the reference readings. Despite this there can still be an error due to the rather drastic variation in temperature during the test period from +40 C to - 10 C. This error was estimated to ± 0.03 mm, with the deflections being overestimated during cold periods and underestimated during warm periods.

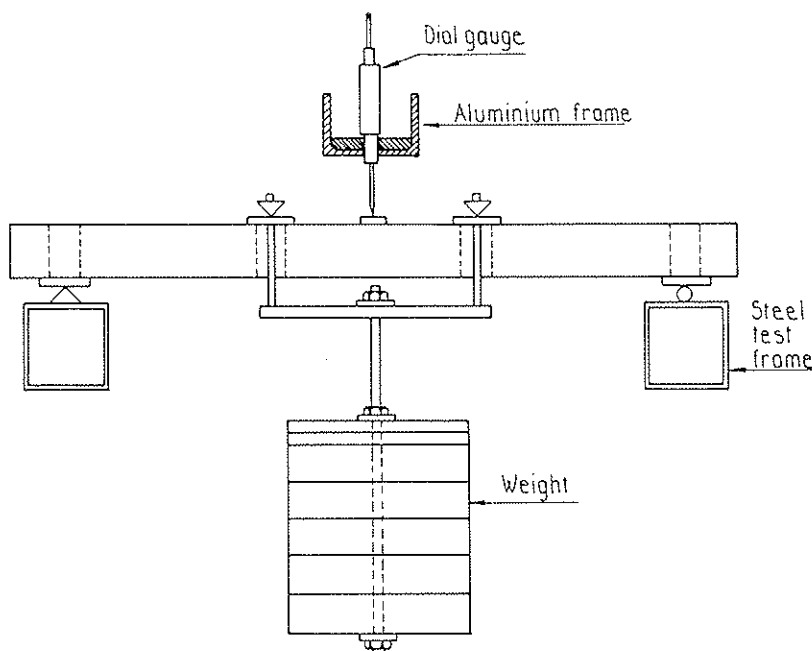


Fig. 2. Arrangement for deflection measurements.

Test results

Short term strength

The results from the short term tests are given in Table 1 for the different materials. Characteristic values in tension according to NR [2] and EN 124.406 are also given for some of the materials in the table. Note that the values from EN 124.406 are based on medium sized specimens, which means that they are not directly comparable in this case.

Material	Thickness mm	MC %	Bending strength Test Mpa	C.O.V. %	f_{tk} (MPa) NR [2]	f_{tk} (MPa) EN 124.406**
Wood	12	9.7	66.6	19	--	--
PLY P30	10	9.3	38.8*	20	15*	14.5*
FB K40	7.5	6.8	42.5	6	22	18
PB V313	10	7.4	13.8	10	10	9.4
PB V20	10	6.6	6.7	10	--	--
MDF	8	7.3	28.0	8	--	--
OSB	11	5.9	23.8	16	--	--

* Based on total thickness

** Preliminary classification

f_{tk} = characteristic tensile strength

Table 1. Average bending strength from 6 test specimens from each material.

There is a rather large variation in bending strength between the materials. The measured average strengths for plywood and fibre board are well above the characteristic values given in the Swedish Building code NR. For particle board type V313, the measured average strength is at a level which can be expected for this type of panel. The measured value for wood is of a magnitude that can be expected for clear wood without defects.

Results from long term tests

The test results reported here refer to a period of one year. The climatic conditions in the test container during this period are shown in Fig. 3. The figure shows weekly averages of daily maxima and minima in temperature as well as relative humidity. There is a considerable variation during each day. A typical daily variation during summer is shown in Fig. 4a. During winter the most common situation was fairly constant temperature around 0 °C and a high relative humidity with small variation during the day, see Fig. 4b. For sunny periods in the winter time, however, there is a significant rise in temperature around noon and a corresponding drop in relative humidity, see Fig. 4c.

The constant bending stresses applied during the long term tests are given in Table 2, together with the measured initial deflections (average from three specimens). The initial deflections are compared with calculated deflections for the test beams under the given loads. Shear deformations were considered in the calculations, which were based on mean values of elastic and shear moduli specified for the different materials as described in Table 2. The calculated

shear deflection was between 1 and 6% of the total deflection, with the highest percentage for plywood.

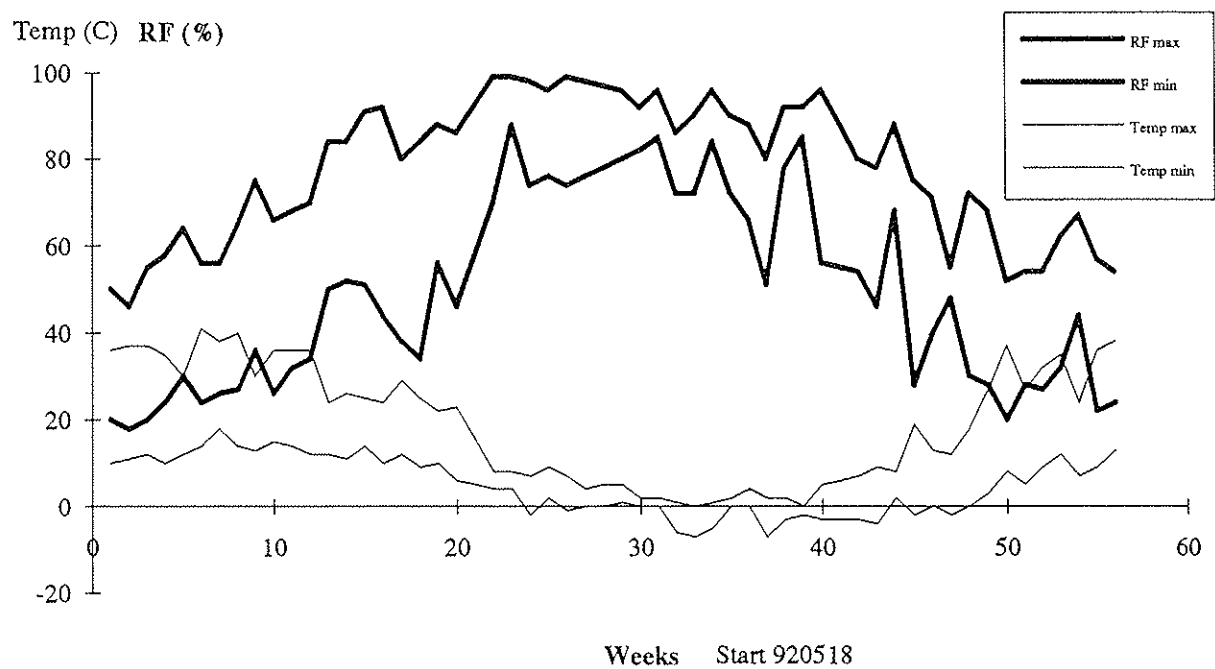


Fig. 3. Climate condition during the test period.

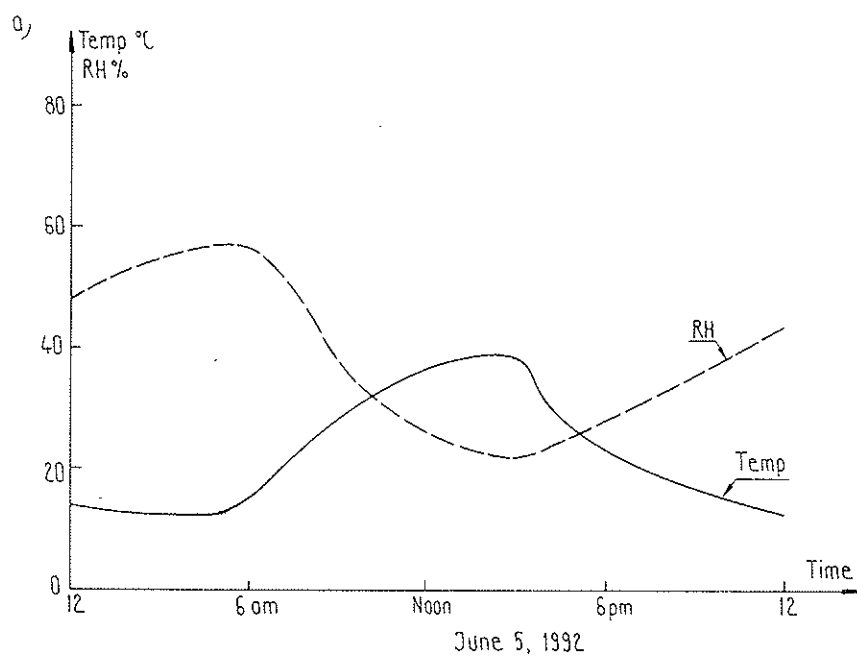


Fig. 4. Daily variations of temperature and relative humidity.
a) Typical summer day.

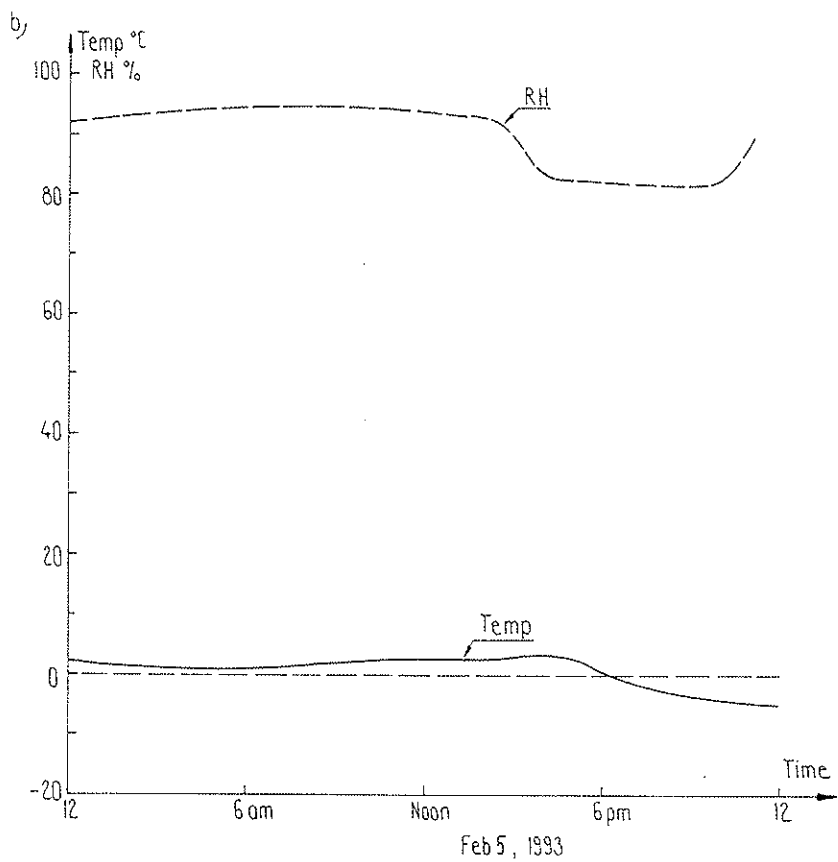


Fig. 4. b) Typical winter day.

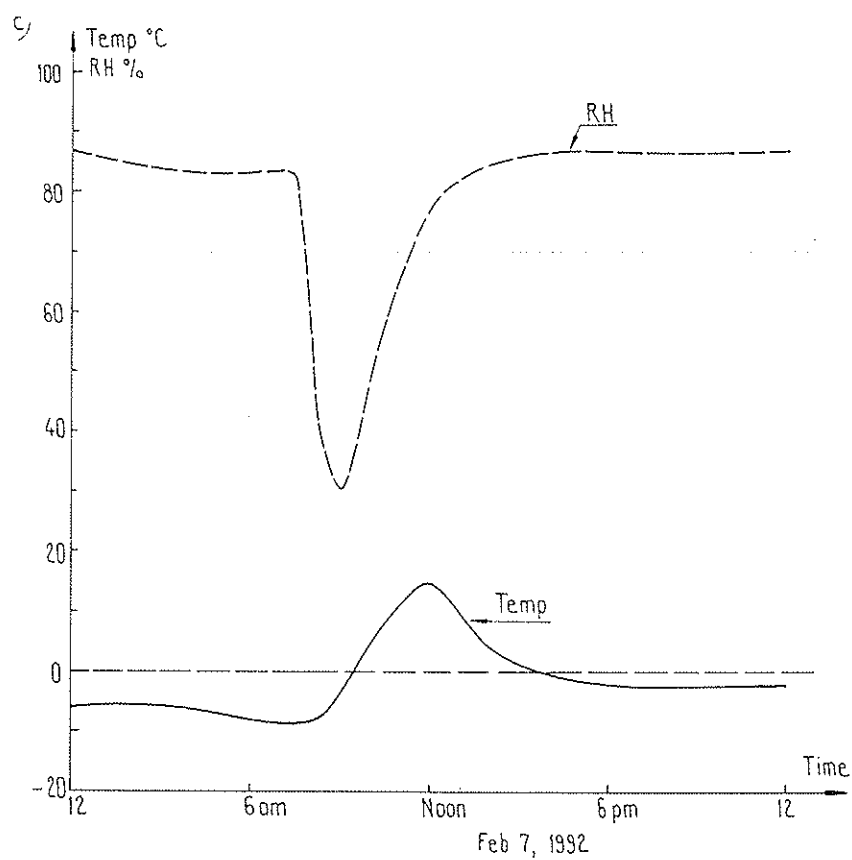


Fig. 4. Daily variations of temperature and relative humidity. c) Sunny winter day.

Material	Applied bending stress (Mpa)	Initial Test	deflection (mm) Calculated (y_0)	Stiffness parameters
Wood	10.4	1.25**	--	--
PLY P30	5.1***	0.88	0.93	NR [2]
FB K40	5.1	1.07	1.27	NR [2]
PB V313	1.5	0.70	0.74	NR [2]
PB V20	0.8	1.03	0.62*	Value given by the supplier
MDF	3.1	1.11	0.89*	Value given by the supplier
OSB	2.3	0.64	--	Not available

* Estimated from flatwise bending stiffness values. (PB V20: $E_{\text{tension}} = E_{\text{bending}} / 1.7$; MDF: $E_{\text{tension}} = E_{\text{bending}}$)

** Initial deflection for the applied load determined from the short term tests. Initial deflection not available from long-term tests due to experimental difficulties.

*** Based on total thickness

Table 2. Applied stress and initial deflection in long term bending tests

The calculated deflections are slightly higher than the measured ones for plywood, fibre board and particleboard V313, which all are classified in relation to the Swedish building code NR. For the non-classified materials PB V20 and MDF the measured initial deflections are larger than those calculated on the basis of material data supplied by the producer.

The creep deformations of all three specimens for each of the materials are shown in Fig. 5. The results are normalised with respect to the calculated initial deflection y_0 given in Table 2, except for wood and OSB where the measured average is used as reference. The reason for this is that the definition of initial deflection in the tests is somewhat arbitrary. The initial deflection calculated from established mean values gives a more general reference value for the relative deflection, and it is more logical to compare the relative deflection defined in this way with that predicted by creep coefficients given in design codes.

It is interesting to note that the deflection in wood increases during drying periods, but decreases during periods with increasing moisture. This is in accordance with the experience from laboratory tests [4]. For fibreboard, particleboard and MDF the rate of creep increases significantly during humid periods and slows down during dry periods. Plywood, which is the material with the lowest relative creep shows a behaviour resembling that of wood, but without the strong springback during winter. The behaviour of OSB could be characterised as a compromise between plywood and particleboard.

The maximum relative deflections recorded during the first year are compiled in Table 3.

Material	Calculated initial deflection, y_0 mm	Measured relative deflection y_{max}/y_0	NR[2] y_{max}/y_0 SC 2	NR [2] y_{max}/y_0 SC 3	Eurocode 5 y_{max}/y_0 SC 2	Eurocode 5 y_{max}/y_0 SC 3
WOOD	1.25**	2.73	2.5	3.33	1.8	3.0
PLY P30	0.93	2.12	2.0	3.33	2.0	3.5
FB K40	1.27	4.84	5.0	*	*	*
PB V313	0.74	3.95	5.0	*	4.0	*
PB V20	0.62	16.4	*	*	*	*
MDF	0.89	13.2	*	*	*	*
OSB	0.64**	4.73	***	***	***	***

* Not classified for structural use in this service class

** Mean value of measured initial deflections, see Table 2.

*** Intended for structural use but classification not available

SC = service class

Table 3. Relative deflections in one year creep tests under natural climate conditions.

It is evident from Table 3 that the creep occurring in the tests already after one year is of the same order of magnitude as that predicted by the creep factors in codes for the structurally classified materials. In some cases, it is also somewhat higher and a natural conclusion could be that the creep factors in both the Swedish code and Eurocode 5, which should represent the behaviour during 40-50 years, are too low. Clearly, the exposure in this investigation is a little more severe than service class 2 according to its definition. On the other hand applications of service class 2 in practice include e.g. non-heated spaces under roof, where the climatic conditions may be the same as in the ventilated container used in the present tests.

The creep factors for wood in the codes are valid for timber in structural sizes, which could be expected to be lower than for the small wood specimens tested here. Full scale timber is more insensitive to moisture fluctuations than clear wood in small sizes. According to the test results, long term deformation of plywood seems to be rather insensitive to effects of moisture variations compared to clear wood.

It can also be noted that particle board type V20 and MDF, which are not classified for structural use, are very sensitive to climatic exposure. Particle board V 313, which is classified for use in service class 2, exhibits creep after one year which is almost equal to that given by the creep factor specified in Eurocode 5 for service class 2. Fibre board K40 which is classified for use in service class 2 according to the Swedish Building code NR but not yet according to EN standard shows a behaviour which could justify a classification in service class 2. For OSB, the creep factor obtained in the test is of the same order of magnitude as those for fibreboard and the weather resistant particleboard V313. In the case of OSB the creep factor is related to the average of the measured values of initial deflection, since no reliable stiffness values are available for that particular board.

Summary and conclusions

The following main conclusions can be drawn from the investigation so far:

- 1) The relative ranking between the tested materials used in Eurocode 5 and in the Swedish building code is reasonably correct with regard to creep factors.
- 2) The creep factors specified in the codes seem to be somewhat underestimated for all structurally classified materials considered in the investigation.
- 3) The rate of creep deflection for materials with a high degree of processing such as hardboard, MDF and particleboard is markedly higher during wet periods than under dry periods.
- 5) For wood the rate of creep is largest during dry (or drying) periods. During wetting periods the wood beams exhibit a spring back i. e. the beams rise against the load.
- 4) Plywood and OSB exhibit similar behaviour as wood, but the rate of creep is less dependent on humidity changes.

The tests will continue for at least another one year period. This may give further experience, which could modify the above preliminary conclusions.

Acknowledgements

The investigation reported here was partly sponsored by Masonite AB, Rundvik, Sweden. Valuable comments on the report have been given by Carl Johan Johansson and Annika Mårtensson. We are also indebted to Per Olof Rosenquist, who performed much of the experimental work both during the preparatory stage and the measuring period. Thanks are also due to Ingbritt Larsson, who prepared the figures in the report, and to Clary Persson for help with editing of the text.

References

- [1] Eurocode 5. Design of timber structures. Part 1:1, prENV 1995-1-1, CEN 1992.
- [2] Nybyggnadsregler. BFS 1988:18, Allmänna Förlaget, Stockholm 1989.
- [3] EN 112.406. Wood-based panels. Characteristic values for established products. Second draft (March 1993).
- [4] Mårtensson, A. Mechanical behaviour of wood exposed to humidity variations. Dep. of Struct. Eng., Lund University. Report TVBK-1006, Lund 1992.

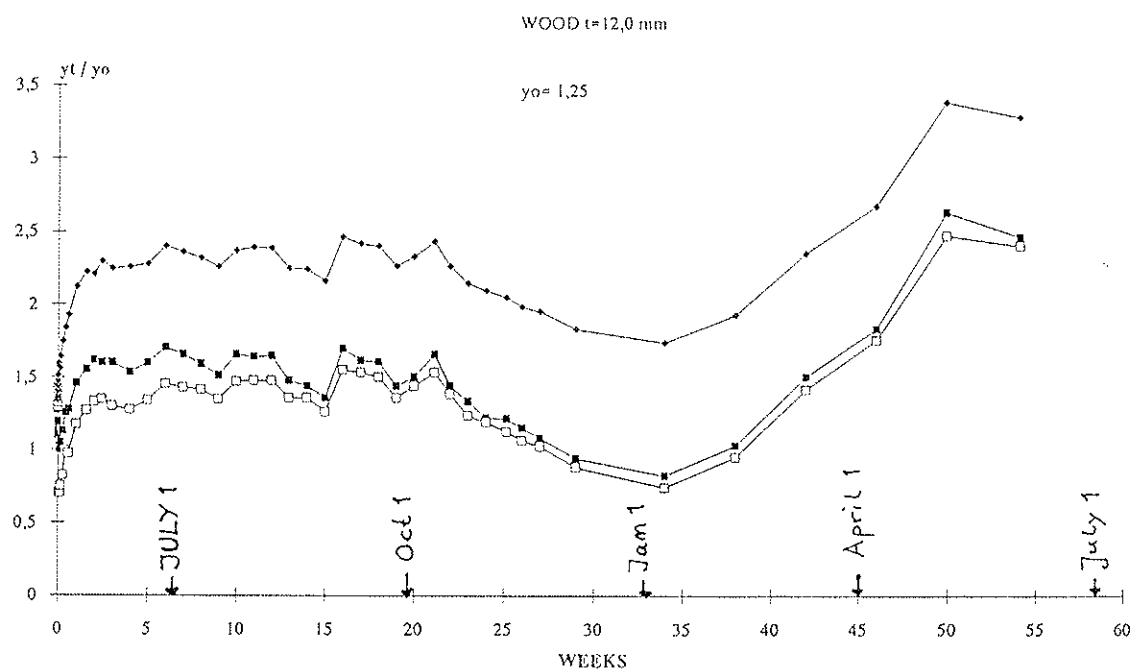


Fig. 5a: Wood.

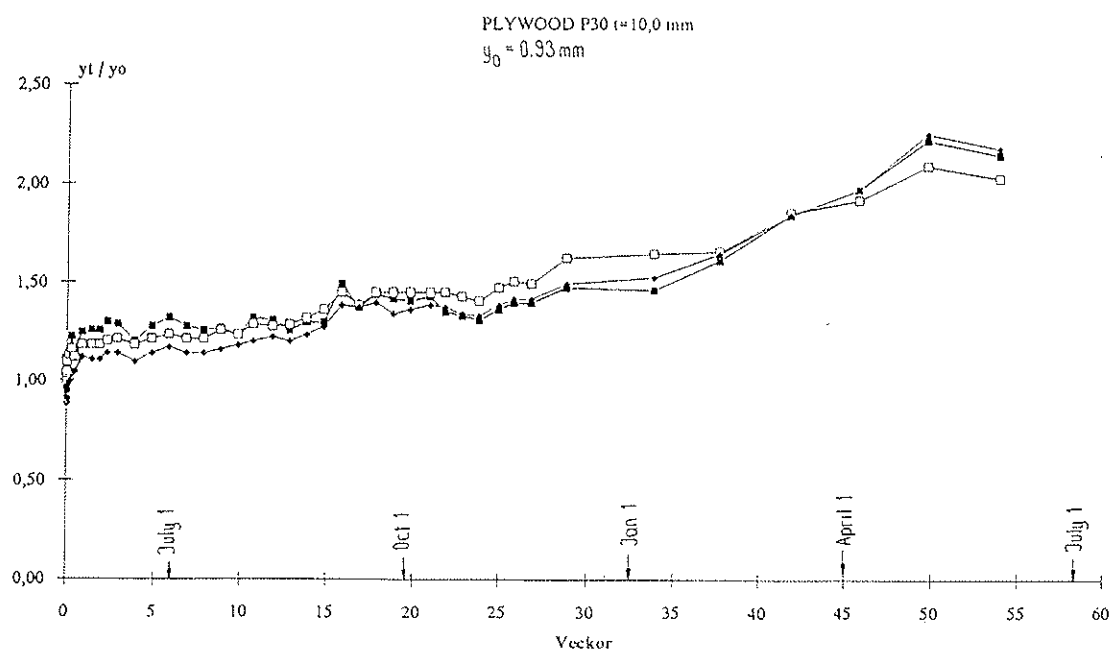


Fig. 5b: Plywood P 30.

Fig. 5. Relative deflection of the test beams during one year. Three specimens for each material.

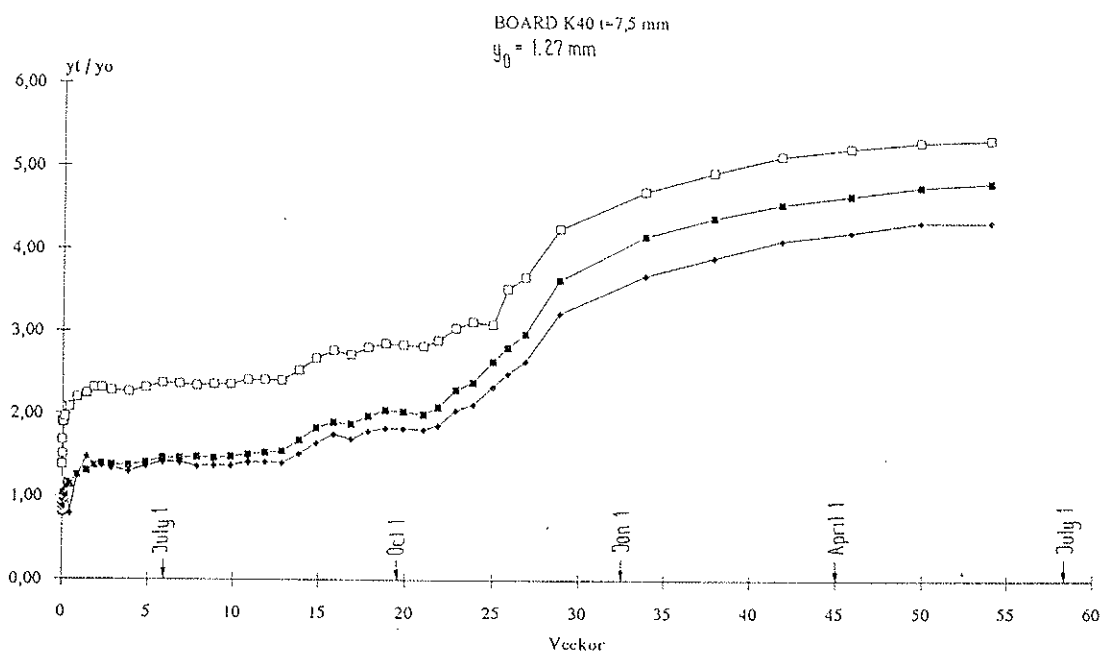


Fig. 5c: Fibre board K 40.

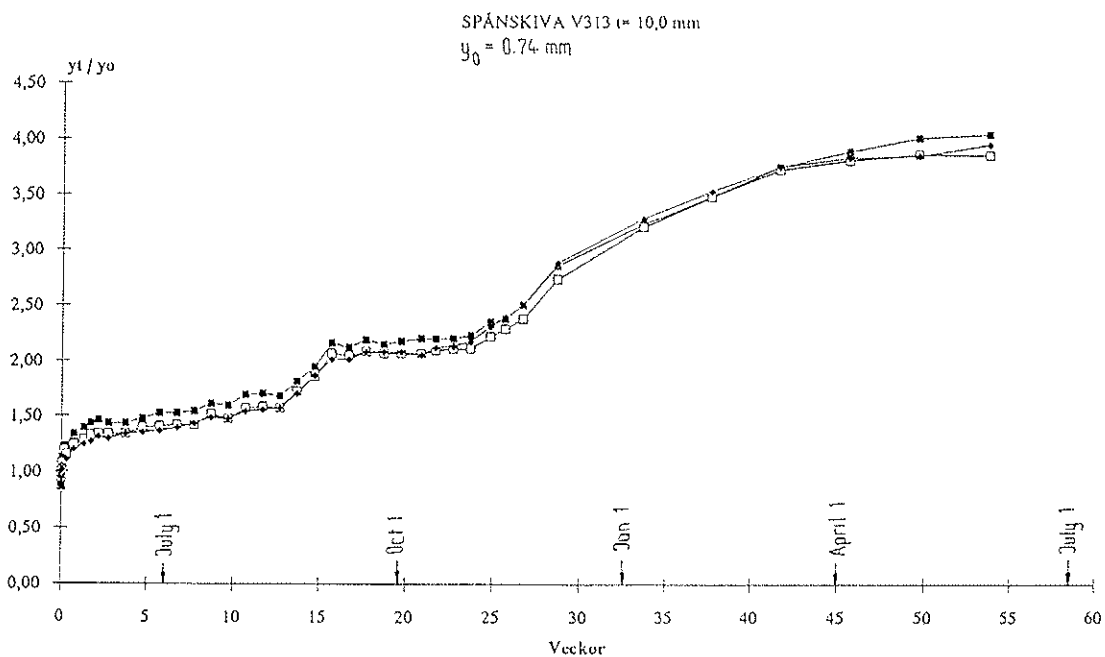


Fig. 5d: Particle board V 313.

Fig. 5. Relative deflection of the test beams during one year. Three specimens for each material.

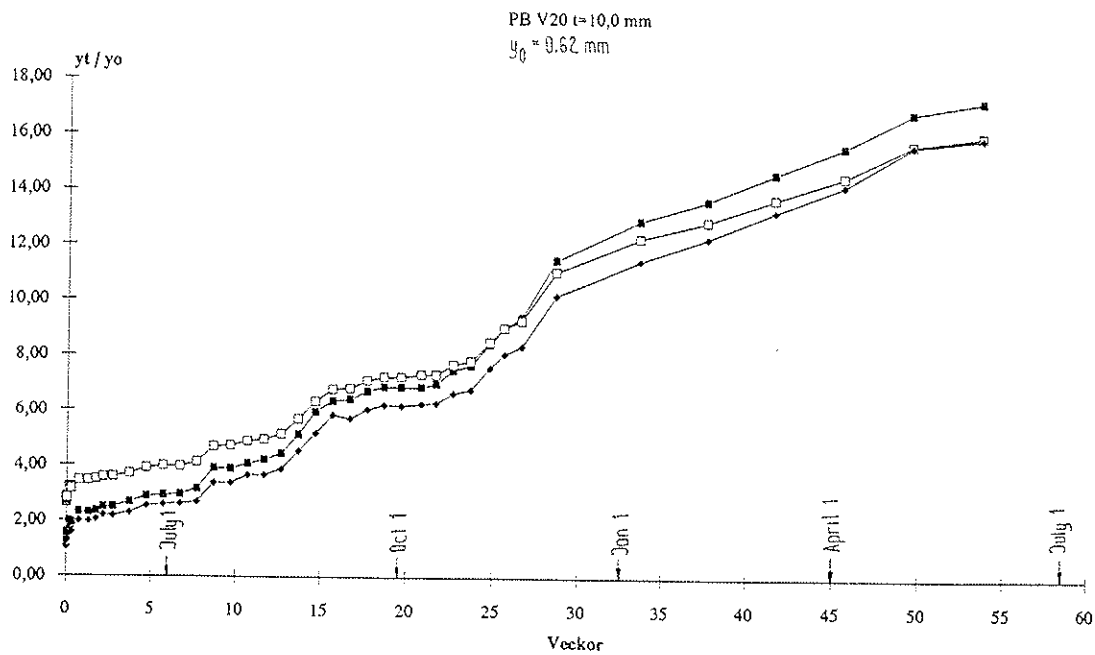


Fig. 5e: Particle board V 20.

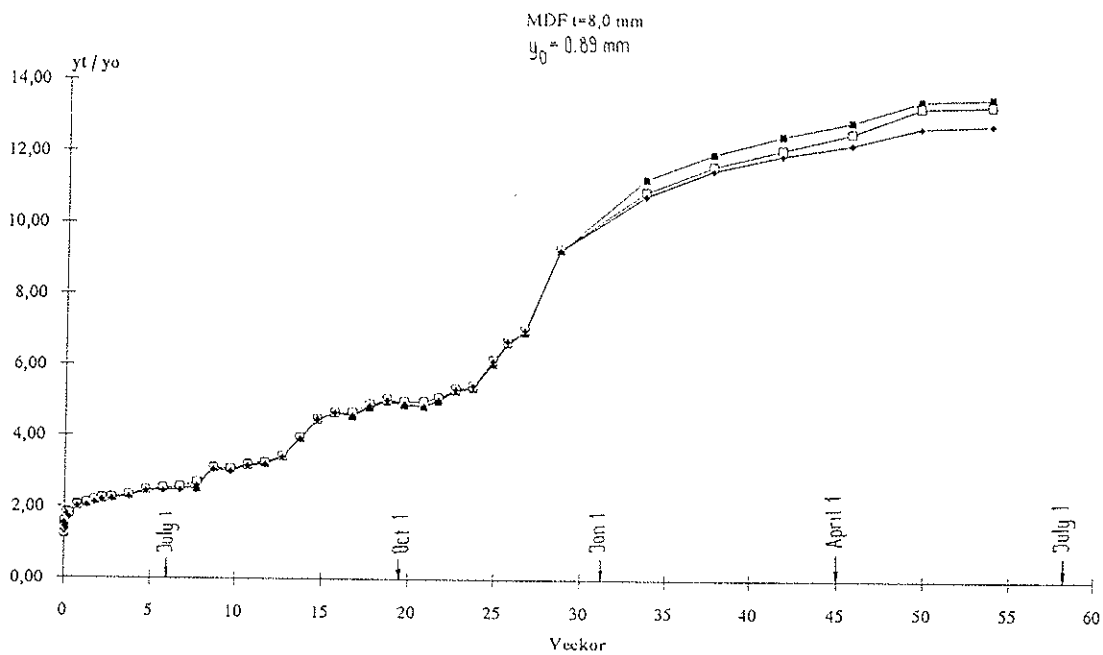


Fig. 5f: MDF.

Fig. 5. Relative deflection of the test beams during one year. Three specimens for each material.

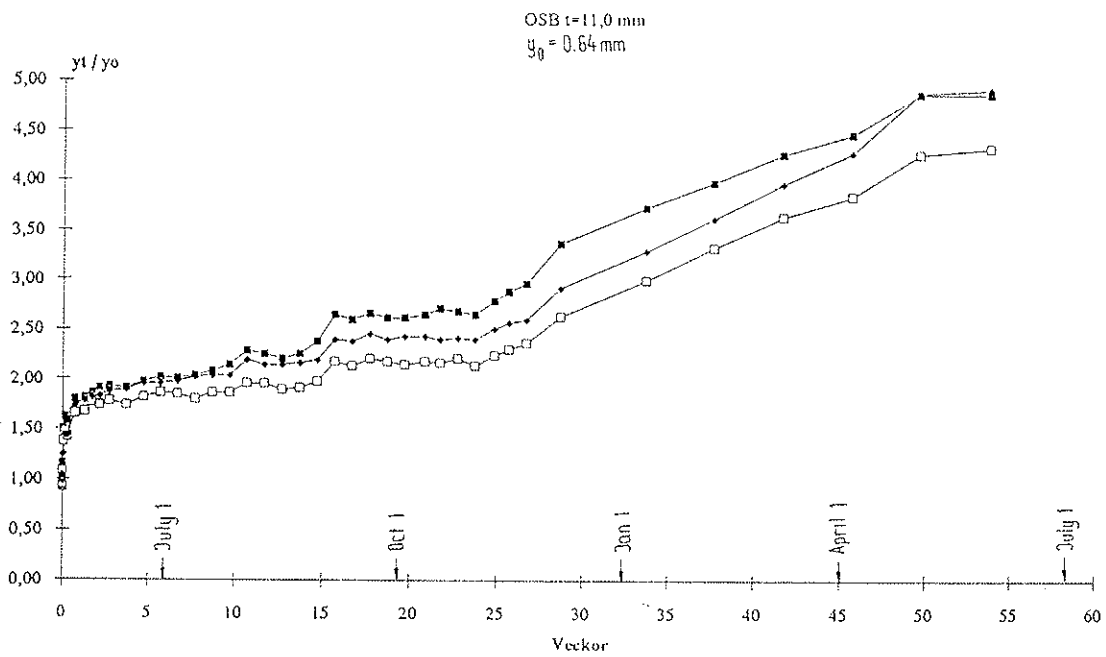


Fig. 5g: OSB.

Fig. 5. Relative deflection of the test beams during one year. Three specimens for each material.

INTERNATIONAL COUNCIL FOR BUILDING RESEARCH STUDIES AND DOCUMENTATION
WORKING COMMISSION W18 - TIMBER STRUCTURES

NORWEGIAN BENDING TESTS WITH GLUED LAMINATED BEAMS
-COMPARATIVE CALCULATIONS WITH THE "KARLSRUHE CALCULATION MODEL"

by

E Aasheim

K Solli

The Norwegian Institute of Wood Technology, Norway

F Colling

Entwicklungsgemeinschaft Holzbau, Munich, Germany

R H Falk

Forest Products Laboratory, Madison, USA

J Ehlbeck

R Görlacher

University of Karlsruhe, Germany

MEETING TWENTY - SIX

ATHENS, GEORGIA

USA

AUGUST 1993

Norwegian Bending Tests with Glued Laminated Beams

- Comparative Calculations with the "Karlsruhe calculation model"

E Aasheim, F Colling, J Ehlbeck, R H Falk, R Görlacher, K Solli

1 Introduction

In 1990 and 1991 extensive and systematic studies on the strength of glued laminated beams (glulam beams) have been carried out at the "Norwegian Institute of Wood Technology" in Oslo/Norway (Falk, Solli, Aasheim 1992). It was aimed to obtain given strength values by variation of the properties of the laminations (density and modulus of elasticity).

The investigations described in this paper were performed to estimate and to predict the bending strengths of these glulam test beams with the "Karlsruhe calculation model" (Colling, Ehlbeck, Görlacher). The calculations were based on the informations made available and described in section 2. The test results (bending strength and modulus of elasticity) obtained in Oslo were unknown before finalizing the calculations and publishing the results.

Altogether, three different combinations of different built-up have been studied. In all cases the beam depth was 300 mm with nine laminations of 33,3 mm nominal thickness. The three beam combinations are shown in **Fig. 1**. The test set-up is illustrated in **Fig. 2**.

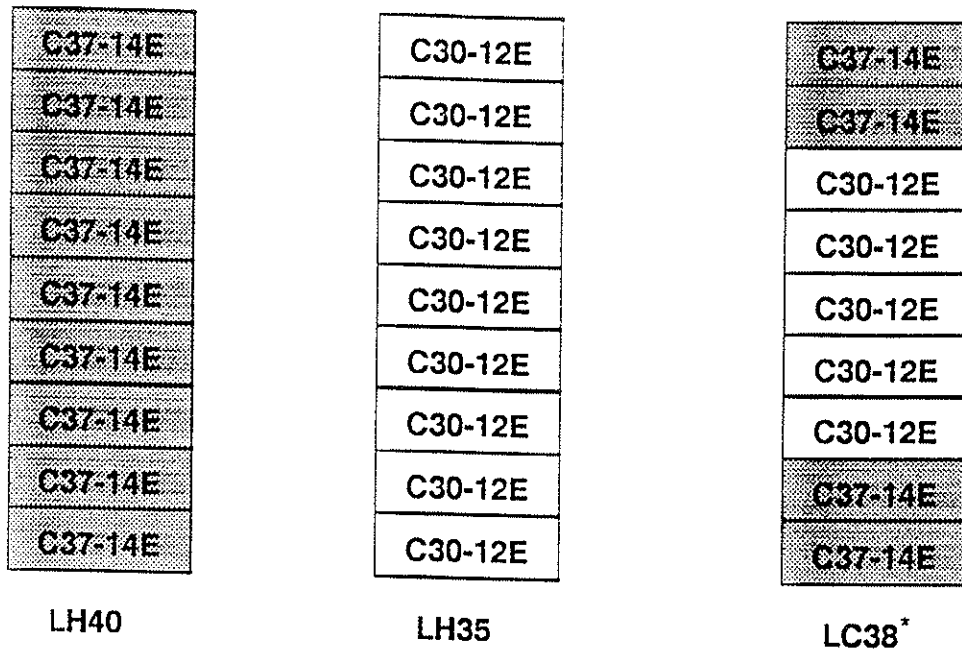


Fig 1: Beam combinations tested

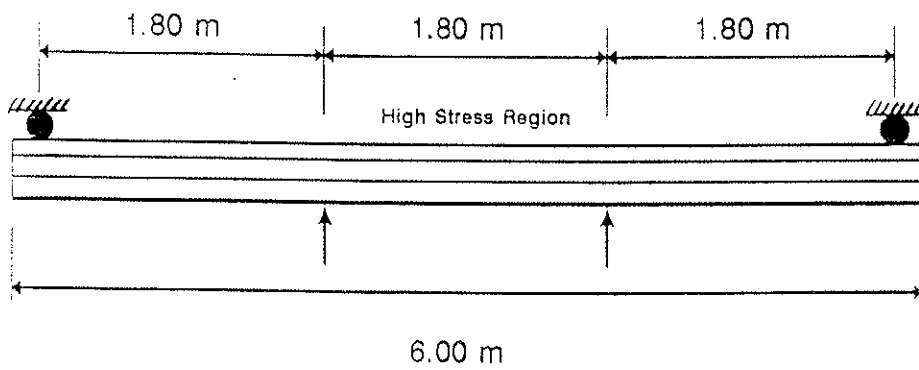


Fig 2: Beam test configuration

2 Input data for the calculation model

2.1 Knots

No information has been submitted about the knots and their distribution along the board length. Therefore it was assumed that the KAR-values (KAR = Knot Area Ratio) within the board sections (cells) correspond approximately to a minimum quality given by the S 10-grade of the German standard DIN 4074. Thus, it was fixed a value of max KAR = 0,55.

2.2 Density

The "Karlsruhe calculation model" is based on regression equations including the oven-dry density of board sections (called "cells") of 15 cm length, but not on the overall mean density of the board at a moisture content of 12 %.

In the simulation calculations performed a constant density along the whole length of each board was assumed, i.e. for simplification it was assumed that all cells of one board have the same density (equal to the overall mean density of the board).

For each board a value of DEN_{12} (density at 12 % m.c.) was randomly chosen from the given density distribution function of the appertaining strength class (Table 1). From this value the DEN_0 -value (oven-dry density) - which was needed for the simulation calculation - was calculated from the expression:

$$DEN_0 = \frac{DEN_{12}}{1 + m.c. - 0,00085 \cdot DEN_{12} \cdot m.c.} \quad \text{with m.c.} = 0,12 \quad (1)$$

2.3 Modulus of elasticity (MOE)

For determination of MOE of the laminations all laminations were machine-graded (Computermatic MK-IV) in that way that under flatwise bending the MOE-values were obtained in sections. MOE in this context is defined, however as the mean MOE of the board, calculated from the single values of the board sections (Table 1).

In the Karlsruhe calculation model the MOE-values in tension of each cell are calculated on the basis of regression equations; from these single values the mean MOE of the board in tension are calculated. This simulated MOE-value of each board is compared with a preconceived value; in case this value does not fit into a certain tolerance limit (± 5 %) the simulation calculation for this board shall be repeated. This presumes that the procedures to simulate as well as to preconceive the MOE-value

correspond to each other. This is, however, not the case with the test material under scrutiny.

Therefore, the machine stress graded bending- MOE had to be adopted to the tension- MOE-values on which the Karlsruhe model is based.

In Fig. 3 the MOE over mean density is shown. The data came from investigations in Karlsruhe with more than 1000 boards taken from several German glulam production plants. The MOE-values were obtained from a procedure based on measuring the longitudinal vibration time of the boards. Multiplying the Norwegian data of MOE - determined with a machine stress grader in Norway - with a factor of 1,27 results in a regression line practically identical with the regression line obtained with the Karlsruhe test procedure (see Fig. 3).

The difference between the MOE values of about 27 % can be explained by mainly two reasons:

- the machine graded MOE is significantly lower than the real (laboratory tests) MOE (10 - 15 %)
- the dynamic MOE determined by longitudinal vibrations (Karlsruhe model) is about 5 % (tension) to 10 % (bending) higher than the MOE determined by static tests

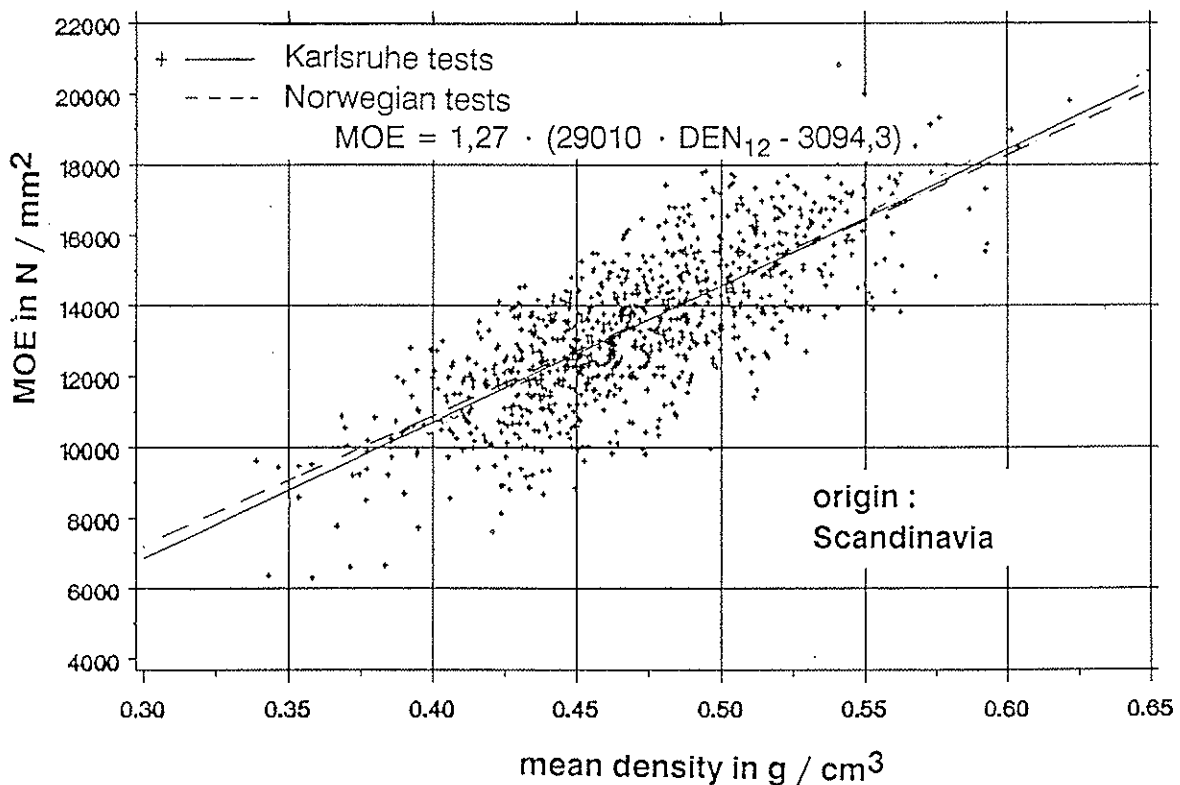


Fig 3: Regression between average density and MOE

For this reason, in the simulation calculations for the boards one value was chosen from the distribution function of the MOE of the appertaining strength class and multiplied by a factor of 1,27 before using it as a comparative value in the subsequent strength and stiffness calculations.

Table 1: Parameter estimates for established C30-12E and C37-14E lamination Grades

		Weibull Parameters			Lognormal Parameters		
		Shape	Scale	Loc.	Mean	S.D.	Loc.
C30-12E	Density				5,586	0,1358	208,9
	MOE _{mac}	7,141	8639,3	2316,5			
	f _{t,fi}	3,48	17,67	19,91			
C37-14E	Density				5,739	0,1308	208,86
	MOE _{mac}				8,871	0,2282	6077,9
	f _{t,fi}	4,631	24,37	15,37			
	Length	5,56	271,38	180,0			

2.4 Board length

The simulation of the board lengths happened by chance using the frequency distribution given in Table 1.

2.5 Finger-joint strength

For the simulation calculations the finger-joint tensile strength was simulated in two different manners:

- on the one hand to each finger-joint a tensile strength value was assigned by using the distribution given in Table 1,
- on the other hand the finger-joint tensile strength values were calculated by means of existing regression equations.

The reason for this was as follows:

The Norwegian tests to obtain the finger-joint tensile strength values were carried out by using a test set-up with the clamping device being hinge-mounted fastened to the cross-head of the testing machine. Thus, any lateral deformations due to structural imperfections of the boards were inevitably possible. These lateral deformations cause additional moments in the test piece and lead to a reduction of the tensile strength by way of simplified calculation.

The regression equations used in the "Karlsruhe calculation model" were found out, however, by using a test set-up which prevents any lateral deformation by means of a rigid clamping device. This test method simulates the situation in a glulam beam in which the single laminations are prevented to deform laterally by the adjacent lamellations rigidly glued.

Based on tests performed in Karlsruhe and Munich the finger-joint tensile strength can be calculated by using the following relationship:

$$\ln(f_{t, fj}) = 2,72 + 6,14 \cdot 10^{-5} \cdot MOE_{t, fj} \quad r = 0,58 \quad (2)$$

The variation of the residuum is taken into account for the simulation calculations by assuming a Gaussian distribution with a mean of zero and a standard deviation of 0,195.

This equation (2) was derived from 235 test results with finger-joint profiles of 20 mm length. Recent investigations in Germany have proved a 5 to 10 % strength increase for profiles of 15 mm length. Therefore, the strength values obtained from equ. (2) were multiplied by a factor of 1,07 assuming a 7 % strength increase.

A regression equation for determining the tensile MOE of finger-joints was derived as follows:

$$\ln(MOE_{t, fj}) = 8,407 + 2,63 \cdot 10^{-3} \cdot DEN_{0, min} \quad r = 0,64 \quad (3)$$

with $DEN_{0, min}$ in kg/m^3 as the smaller of the two oven-dry densities of the two pieces (boards) jointed by the finger-joint.

The variation of the residuum is taken into account by assuming a Gaussian distribution with a mean of zero and a standard deviation of 0,135.

In order to estimate the effect of these different ways of allocating the finger-joint tensile strength values on the simulation results, the calculations were carried out by using eqs. (2) and (3) as well as by randomly assigning the finger-joint tensile strength values from the distributions given in Table 1, respectively.

3 Simulation calculations

The following parameters were varied:

- *Beam layup*

As shown in Fig. 1 three different combinations were studied

- *Density, modulus of elasticity*

For each lamination class the appertaining boards were simulated by assuming the density and the modified MOE distribution according Table 1 and section 2.3

- *Finger-joint strength*

The tensile strength of the finger-joints was taken into account once on the basis of the distribution (DIS) of test results (table 1) and on the other hand by using the regression analysis (REG), see section 2.5.

In the Norwegian test programme in total 100 bending tests were carried out with each beam combination. Therefore, for each beam combination and variant a sample of 100 beams was simulated and the bending strength of each beam was predicted by the "Karlsruhe calculation model". In order to check in which range the test results may vary, for each of the 6 variants three series of 100 beams were simulated.

3.1 Simulation results

Strength values

An outline of the results is given in **Tables 2 to 4** with the 5-percentiles calculated assuming a Gaussian distribution. This was justified in all cases (Kolmogorov-test).

Comparison of the series DIS against REG

A comparison of the series belonging together, e.g. series DIS and REG, leads to the following tendencies:

- beams belonging to DIS-series demonstrate lower mean values as well as 5-percentiles of the bending strength,
- beams belonging to DIS-series give more finger-joint failures as those belonging to REG-series.

These findings can be explained with the differently assumed distributions of the finger-joint tensile strengths as described in section 2.5.

Table 2: Simulation results (LH 40)

simulations series	all beams			beams with finger-joint failure			beams with wood failure		
	m	v	x5	N	m	v	N	m	v
	N/mm ²	%	N/mm ²		N/mm ²	%		N/mm ²	%
DIS	47,8	17,9	33,7	68	45,7	18,3	32	52,2	14,1
	48,5	16,8	35,1	50	45,7	18,5	50	51,4	13,3
	46,7	19,3	31,9	57	43,5	17,7	43	50,9	17,7
REG	51,6	16,4	37,7	39	49,0	19,8	61	53,2	13,6
	52,4	16,2	38,4	35	50,4	18,7	65	53,5	14,6
	51,8	17,4	37,0	34	47,4	17,6	66	54,0	15,7

Table 3: Simulation results (LH 35)

simulations series	all beams			beams with finger-joint failure			beams with wood failure		
	m	v	x5	N	m	v	N	m	v
	N/mm ²	%	N/mm ²		N/mm ²	%		N/mm ²	%
DIS	40,4	15,1	30,4	54	39,4	15,8	46	41,6	14,0
	40,4	17,0	29,1	58	39,4	19,2	42	41,7	13,4
	41,5	15,4	31,0	45	39,8	18,0	55	43,0	12,5
REG	41,6	15,8	30,8	36	38,3	16,6	64	43,4	13,8
	43,0	15,8	31,8	33	40,9	16,3	67	44,0	15,2
	43,3	14,6	32,9	33	41,4	15,7	67	44,2	13,7

Table 4: Simulation results (LC 38)

simulations series	all beams			beams with finger-joint failure			beams with wood failure		
	m	v	x5	N	m	v	N	m	v
	N/mm ²	%	N/mm ²		N/mm ²	%		N/mm ²	%
DIS	44,8	18,4	31,2	60	41,6	17,9	40	49,7	13,9
	45,7	18,7	31,6	61	42,6	18,0	39	50,5	15,1
	47,4	20,0	31,8	65	44,8	20,8	35	52,2	15,2
REG	49,6	16,8	35,9	41	46,9	18,7	59	51,4	14,7
	50,5	16,7	36,6	36	49,3	18,8	64	51,1	15,5
	49,9	16,3	36,5	34	47,1	18,9	66	51,3	14,4

3.2 Comparison with the Norwegian bending tests

The strength values given in **Table 5** can be expected for the three beam combinations tested. These values are based on the simulation calculations of the series called REG, because in this case the narrow correlation between strength and MOE is taken into account for the boards (laminations) as well as for the finger-joints. Moreover, any imponderabilities in connection with the determination of the finger-joint tensile strength by means of the test device used are excluded.

The strength values of the Norwegian bending test are also given in Table 5. In all cases there is a very good agreement between the calculated and the tested values especially between the values of the 5-percentiles.

Table 5: Predicted and tested beam bending strengths

beam combination		mean value	5-percentile (non-parametric)
		N/mm ²	N/mm ²
LH 40	"Karlsruhe calculation model"	51,9	38,7
	Norwegian bending tests	52,5	39,4
	quotient	0,99	0,98
LH 35	"Karlsruhe calculation model"	42,6	32,7
	Norwegian bending tests	44,3	32,8
	quotient	0,96	1,00
LC 38	"Karlsruhe calculation model"	49,6	37,5
	Norwegian bending tests	47,7	37,9
	quotient	1,04	0,99

6 Summary

In 1990 and 1991 extensive and systematic studies on the strength of glued laminated beams have been carried out at the "Norwegian Institute of Wood Technology" in Oslo. For this purpose the mechanical properties of the laminations were determined and classified according to CEN draft standards of that time (C30-12E and C37-14E). Glued laminated test beams following different strength classes (LH 35, LH40 and LC38) were constructed and tested in strength and stiffness.

At the same time strength and stiffness values of these beams were calculated independently by means of the Karlsruhe calculation model. Informations about the properties of the laminations i.e. the statistical distribution of density and modulus of elasticity of the boards used for the three different combinations, about the finger-joints, and about the built-up of the beams were known from the Norwegian pre-tests. The results of the beam tests were kept secret until the predictive calculations were available.

The strength of all beam combinations (mean value and 5-percentile) were proved to be in very good agreement with the calculated values (within 4 % deviation). By this study it became once more evident that the Karlsruhe calculation model is suitable to predict the strength of glued laminated beams. It is on that account an appropriate aid for the evaluation of standards on strength classes for glulam based on the relevant properties assigned to the laminations and the finger-joints.

Literature

Colling, F.

Bending strength of glulam beams - a statistical model. IUFRO 1990, Saint John/ New Brunswick, Canada. 1990

Colling, F., Ehlbeck, J., Görlacher, R.

Norwegian bending tests with glued laminated beams - Comparative calculations with the "Karlsruhe calculation model". Versuchsanstalt für Stahl, Holz und Steine, Abteilung Ingenieurholzbau, Karlsruhe. 1993

Falk, R.H., Solli, K.H. and Aasheim, E.

The performance of glued laminated beams manufactured from machine stress graded norwegian spruce. The Norwegian Institute of Wood Technology, Oslo. 1992

Solli, K.H, Aasheim, E. and Falk, R.H.

The strength of norwegian glued laminated beams. CIB-W18/25-10-1 Åhus/Sweden, 1992

INTERNATIONAL COUNCIL FOR BUILDING RESEARCH STUDIES AND DOCUMENTATION
WORKING COMMISSION W18 - TIMBER STRUCTURES

SIMULATION ANALYSIS OF NORWEGIAN SPRUCE GLUED-LAMINATED TIMBER

by

R Hernandez
R H Falk
Forest Products Laboratory, Madison
USA

MEETING TWENTY - SIX

ATHENS, GEORGIA

USA

AUGUST 1993

Simulation Analysis of Norwegian Spruce Glued-Laminated Timber

by

Roland Hernandez and Robert H. Falk

Research Engineers
Engineered Wood Products and Structures

USDA Forest Service
Forest Products Laboratory¹
One Gifford Pinchot Drive
Madison, WI USA 53705-2398

ABSTRACT

A computer analysis model, referred to as PROLAM, was used to simulate the performance of glued-laminated (glulam) timber beams manufactured from Norwegian spruce lumber. Mechanical properties of tested lumber and finger joints were analyzed to determine the input properties required by the model, and Monte Carlo simulation procedures were used to compile and characterize bending strength and stiffness distributions of the glulam beams. Simulated glulam beam results compared reasonably well with actual results. Sensitivity analyses were also conducted to observe both the effects of redistribution of stresses within a glulam beam, and the influence of finger-joint tensile strength on glulam beam bending strength.

INTRODUCTION

Recently, a large-scale research program was conducted at the Norwegian Institute of Wood Technology to study the performance of glued-laminated (glulam) timber manufactured from Norwegian spruce lumber (Falk et al. 1992). The laminating grades of Norwegian spruce involved in this research program were the C37-14E and C30-12E grades specified in the EN TC 124.203 Standard (Comite European de Normalisation 1990a). The glulam layups studied were the homogeneous LH35 and

¹The Forest Products Laboratory is maintained in cooperation with the University of Wisconsin. This article was written and prepared by U.S. Government employees on official time, and it is therefore in the public domain and not subject to copyright.

LH40 as specified in the EN TC 124.207 Standard (Comite European de Normalisation 1990b) and a modified version of the LC38 combined layup. Extensive information was gathered on the laminating lumber and finger joints, which made it possible to analyze the glulam beams using procedures from both the European and American standards (Falk and Hernandez, In press). Information on strength, stiffness, density, and knot size for the lumber specimens was then used as input for advanced glulam simulation models such as those by Ehlbeck and Colling (1986), and by Hernandez et al. (1992). This paper deals with the simulation analysis of glulam beams manufactured from Norwegian spruce lumber using the Hernandez et al. model, referred to as PROLAM.

Preliminary work was conducted to analyze the mechanical properties of the Norwegian spruce laminating lumber. This work included analyzing lumber and end-joint properties to characterize statistical distributions of strength and stiffness, as well as to determine the correlations between strength and stiffness. The specific information on the laminating lumber was used as input for the PROLAM model to simulate the performance of the glulam beams.

OBJECTIVES

The overall objective of this study was to verify that the PROLAM model can predict the performance of glulam beams of European manufacture. Specific objectives of this paper were to

- (1) compare actual and simulated performance of glulam beams made from Norwegian spruce laminating stock, and
- (2) conduct sensitivity analyses to observe the effects of varying manufacturing parameters.

BACKGROUND

The PROLAM model uses distributions of mechanical properties of laminating stock and finger joints to determine the mechanical properties of full-size glulam beams. In addition, the model considers within-piece correlation between the tensile strength of the lamination ($f_{t, \text{lamm}}$) and the flatwise modulus of elasticity (MOE_{flat}). The sequence of events in the simulation of a single beam using PROLAM involves simulating the beam layup, assigning lamination and finger-joint properties, determining beam strength using a simple transformed section method, and determining beam stiffness using a complementary virtual work procedure. A detailed description of this simulation process is described in Hernandez et al. (1991). Prior to this study, modifications were made to the PROLAM model. One modification was simulating finger-joint tensile strength $f_{t, \text{fj}}$ from statistical distributions fitted to actual test data, rather than from a regression relationship between finger-joint stiffness and $f_{t, \text{fj}}$. A

second modification was the implementation of a method to consider the interaction of tensile and bending stresses in the laminations of shallow glulam beams.

PROCEDURES

In this study, a detailed analysis was conducted on the laminating lumber properties described by Falk et al. (1992). The following sections describe the characterization of input required by the PROLAM model.

Characterizing lumber and finger-joint properties

In PROLAM, lumber length is simulated by entering a range and mode of length and a triangular distribution function to generate the values. In Falk et al. (1992), a relative frequency histogram of laminating lumber length used in the manufacture of the Norwegian spruce glulam beams was reported. The required distribution parameters for PROLAM were approximated from this histogram. The range of lumber length was approximately 2.2 to 5.6 m (7.2 to 18.4 ft) and the mode value of lumber length was approximately 4.5 m (14.8 ft). These parameters were used in PROLAM to generate lumber length for both the C37-14E and C30-12E grades.

MOE_{flat} properties were characterized using results of static tests conducted to verify machine stress grader output MOE_{mac} . These static tests were conducted across a 91.4-cm (36-in.) span on the full-length lumber specimens using a simply supported, center-point loading configuration (same configuration as the machine stress grader). Also, the location of the static test along the board length was selected such that a maximum visual defect existed between the supports. Appendix A1 lists the statistical summaries of MOE_{flat} for both the C37-14E and C30-12E grades.

In addition to MOE_{flat} properties, PROLAM also requires a ratio between the MOE and modulus of rigidity to analyze beam stiffness. The ratios used for the C37-14E and C30-12E grades were determined from the EN TC 124.203 Standard, which specifies design levels for both "MOE Mean Parallel" and "Shear Modulus Mean". The determined MOE to shear modulus ratios for C37-14E and C30-12E are 17.5 and 16.0, respectively. No adjustments were made to the calculated MOE_{flat} properties to adjust to a shear-free value because the estimated adjustment would have been less than 3 percent.

As explained in Falk et al. (1992), groups of C37-14E and C30-12E lumber were sorted for subsequent ultimate tensile strength ($f_{t,lam}$) testing. This testing was conducted specifically for the requirements of the PROLAM model, that is, with a 61-cm (24-in.) span between the grips. Two tension specimens were cut from each board. The tensile strength values were from a matched group of lumber not reported in Falk et al. (1992). The reported tension tests were tested across a 1-m (39-in.) span and had a maximum visual defect located between the tension grips. The lumber tested for PROLAM input was not biased with respect to selection based on

visual defects. Appendix A2 shows the statistical summaries of the 61-cm (24-in.) $f_{t,lam}$ properties compared with the 1-m (39-in.) span $f_{t,lam}$ properties reported in Falk et al. The $f_{t,lam}$ values tested at 61 cm (24 in.) were 8 and 11 percent higher at the 50th percentile level than were the f_t results tested at a 1-m (39-in.) span for the C37-14E and C30-12E grades, respectively; at the 5th percentile level, this difference was 19 and 26 percent higher, respectively. The 5th percentile difference can probably be attributed to a combination of length effect in tension testing and also to the fact that the 1-m (39-in.) tests were conducted with a maximum visual defect within the test span.

In addition to solid lumber, Falk et al. (1992) also tested finger joints from the C37-14E and C30-12E grades that were manufactured during the same production run as the manufacture of the full-size glulam beams. The ultimate finger-joint tensile strength $f_{t,fj}$ was determined across a 30-cm (12-in.) span. This test span was chosen so that the majority of the failures occurred at the finger-joint location. Appendix A3 summarizes the $f_{t,fj}$ properties for both the C37-14E and C30-12E laminating grades.

Determining correlation between lumber properties

To simulate localized laminating properties with PROLAM, a model developed by Taylor and Bender (1991) was used that considers the lengthwise correlation of the segmented values of MOE_{flat} and of $f_{t,lam}$ along a piece of laminating lumber, as well as the correlation between these two properties. This lengthwise correlation of one property is referred to as serial correlation, and the correlation between properties is referred to as cross correlation. Also, the correlation between segments is referred to as lag correlation. For example, correlations between the four segments marked on the tested lumber specimens were related such that segment 1 and segment 2 had a lag-1 correlation, segment 1 and segment 3 had a lag-2 correlation, and segment 1 and segment 4 had a lag-3 correlation. To establish these correlations from actual lumber properties, MOE_{flat} and $f_{t,lam}$ data on adjacent 61-cm (24-in.) lumber segments are needed.

For this study, however, MOE_{flat} properties were not obtained on adjacent segments. Therefore, the serial correlation of MOE_{flat} was estimated from the MOE_{mac} properties. Estimates of the lag-1, lag-2, and lag-3 serial correlations of MOE_{mac} were determined on 1,460 specimens of C37-14E lumber and 1,483 specimens of C30-12E lumber.

Serial correlation for $f_{t,lam}$ was determined from the results of tested lumber. Because segments 1 and 4 were tested in tension, lag-3 serial correlation of $f_{t,lam}$ was determined from the test results. Lag-1 and lag-2 values were estimated. To determine the serial correlation for $f_{t,lam}$, 93 specimens were used for the C37-14E grade and 100 specimens were used for the C30-12E grade.

Cross correlation between MOE_{mac} and $f_{t,lam}$ was determined from the same test group used for determining serial correlation of $f_{t,lam}$. Appendix A4 shows the estimates of

the lag-0 through lag-3 serial and cross correlations of MOE_{mac} and $f_{t,lam}$ for the C37-14E and C30-12E laminating grades, as well as for both grades combined.

When all data were combined, the estimated serial and cross correlations for MOE_{mac} and $f_{t,lam}$ increased. A possible explanation for this increase is that when data were combined, a larger range of properties were being analyzed and trends in the within-piece correlations of MOE_{mac} and $f_{t,lam}$ were better detected.

Comparing actual and simulated glulam beam properties

The three combinations of glulam that were studied in Falk et al. (1992) were the homogeneous LH35 and LH40 layups and the combination LC38* layup (Fig. 1). The LC38 layup was modified to LC38* because C30-12E lumber grade was used in the core laminations instead of the specified C24-12E grade. The lumber properties previously discussed for the C37-14E and C30-12E grades were used as input in the PROLAM model, along with the dimensions, layup, and loading configuration of the actual glulam beams.

The glulam beam results were analyzed by comparing cumulative distribution functions (CDF) and/or statistical summaries of the actual and simulated bending strength and stiffness. Bending strength refers to modulus of rupture (MOR) and bending stiffness refers to MOE. Simulation results of 1,000 beams of each glulam beam combination were compiled to construct the CDFs. In addition, 10 independent batches of 104, 96, and 112 beams (actual sample sizes of each tested beam group) were simulated for the LH35, LC38*, and LH40 layups, respectively, to construct 90 percent confidence intervals (at 75 percent tolerance) on each property. Figures 2 through 4 compare TEST and SIMULATED glulam MOR for the LH35, LC38*, and LH40 layups, respectively. Table 1 lists the statistical summaries of the TEST and SIMULATED results for both glulam MOR and MOE.

Figures 2 through 4 indicate that both the TEST and SIMULATED glulam beam bending strengths have nearly equal MOR properties at the 5th percentile levels. Table 1 shows that TEST results were not bounded well by the confidence intervals constructed on the SIMULATED results for all properties and beam layups at the 50th percentile level. At the 5th percentile levels, TEST results were bounded (or nearly so) by the confidence intervals constructed on the SIMULATED results. The differences between TEST and SIMULATED glulam MOR results were 10, 5, and 11 percent at the 50th percentile and 2, 6, and 3 percent at the 5th percentile for the LH35, LC38*, and LH40 layups, respectively. It appears that glulam MOR at the lower percentiles was predicted to within 6-percent of the TEST results. However, results at the upper percentiles were within 11 percent. Also, differences between TEST and SIMULATED glulam MOE at both the 50th and 5th percentiles were within 4 percent for the LC38* and LH40 layups, and within 10 percent for the LH35 layup.

It is speculated that part of the rather large difference in TEST and SIMULATED MOE results of the LH35 layup compared with the other layups could be attributed to the possibility that the input MOE_{flat} properties for the C30-12E grade were somewhat low. For example, Appendix A1 shows an average MOE_{flat} value of 13.9 GPa (2.02×10^6 lb/in²) for the C37-14E grade; correspondingly, Table 1 shows a 50th percentile glulam MOE value of 14.1 GPa (2.05×10^6 lb/in²) for the LH40 layup. Because the C37-14E grade is less likely to have large stiffness-reducing knots, it is logical that only a 1.4-percent difference was observed between the MOE_{flat} properties of the C37-14E grade and the MOE properties of a homogeneous glulam beam made from the same grade. On the other hand, the average MOE_{flat} value for the C30-12E grade in Appendix A1 is 11.2 GPa (1.63×10^6 lb/in²) and Table 1 shows a 50th percentile glulam MOE value of 12.1 GPa (1.76×10^6 lb/in²) for the LH35 layup. The difference between MOE_{flat} and glulam beam MOE for the C30-12E grade was 7.4 percent. Because the lower quality C30-12E grade likely possesses larger stiffness-reducing knots, compounded with the fact that these maximum visual defects were purposely placed in the test span, it is suspected that the MOE_{flat} estimates for this grade are somewhat low.

In addition to influencing the SIMULATED glulam beam MOE, the MOE_{flat} properties of the lumber also influenced the SIMULATED beam MOR through the distribution of stresses in the transformed section analysis. For example, Table 1 shows that the lower 5th percentile of the TEST glulam MOR of the LC38* layup were not bounded by the confidence interval of the SIMULATED results. However, because the LC38* layup consists of C30-12E core laminations, it is possible that the lower MOE_{flat} properties in these core laminations caused a greater amount of stress to be distributed to the outer C37-14E laminations; this may have caused the simulated beams to reach failure criteria prematurely. This redistribution of stresses is the topic of the first sensitivity analysis in the next section.

Sensitivity analyses

Redistribution of stresses

The effect of redistribution of stresses from lower stiffness to higher stiffness laminations was studied in this sensitivity analysis. Simulations dealt with a homogeneous 9-lamination beam that had an MOE_{flat} distribution with an average of 13.8 GPa (2.00×10^6 lb/in²) and a coefficient of variation (COV) of 10 percent. Although this layup was not the same as that for the LH40 beams, the same size and loading configurations as those for the 9-lamination beams studied earlier were used. The input $f_{t,lam}$ distribution was determined using the $MOE/f_{t,lam}$ regression relationship established by Falk et al. (1992). To observe the effect of redistributed stresses on glulam beam bending strength, the MOE_{flat} of the single top and bottom laminations were kept constant and mean values of MOE_{flat} of the inner seven laminations were reduced by 5 percent for each subsequent simulation run (13.1 GPa, 12.4 GPa, etc.) to a value of 10.3 GPa (1.49×10^6 lb/in²). The COV of each MOE_{flat} distribution was held constant at 10 percent, and the $f_{t,lam}$ distribution was held constant at a level

corresponding to a 13.8-GPa MOE_{flat} distribution. Finger-joint tensile strength was excluded from this analysis. This scaling of the MOE_{flat} distribution while holding the $f_{t,lam}$ constant allowed us to directly observe the effect of redistributing stresses from lower to higher stiffness laminations on glulam beam strength. Scaling the MOE_{flat} and holding the $f_{t,lam}$ constant did not simulate the behavior of actual beams, because lower stiffness lumber generally would have lower tensile strengths. For this reason, a second simulation analysis was conducted where in addition to scaling the MOE_{flat} properties, the corresponding $f_{t,lam}$ properties were determined from the same MOE_{flat} - $f_{t,lam}$ regression relationship for each new level of MOE_{flat} . Thus, the first case scenario showed the effect of redistribution of stresses, solely caused by changing lamination stiffness. The second case scenario simulated the same phenomenon; however, decreasing $f_{t,lam}$ was considered.

Figure 5 illustrates the results of varying the MOE_{flat} values of the core laminations. In Figure 5, the difference between the MOE_{flat} values of the single outer lamination (OUTER) and the MOE_{flat} of the remaining core laminations (CORE) was varied from a 0-percent difference between OUTER and CORE to a 25-percent difference between OUTER and CORE. Figure 5 illustrates that even with a OUTER/CORE difference in MOE_{flat} as high as 25 percent, the 5th percentile of glulam MOR, referred to as MOR_{05} , dropped only 3.4 percent when compared to the homogeneous layout with the $f_{t,lam}$ held constant. However, when the $f_{t,lam}$ distribution was determined for each corresponding level of MOE_{flat} , the MOR_{05} results dropped by 15.3 percent when the OUTER/CORE MOE_{flat} difference was 25 percent.

This result implies that for nonhomogeneous glulam layouts, if the decrease in strength at the 5th-percentile level MOR_{05} was arbitrarily limited to 10 percent, then the OUTER/CORE MOE_{flat} difference should be no larger than 15 percent. This applies to beams with 10 percent higher quality material on the top and bottom laminations. These results also indicated that SIMULATED glulam MOE decreased by 5 percent when the core lamination MOE_{flat} values were decreased by 10 percent. When the MOE_{flat} value of the core was decreased by 25 percent, the glulam beam MOE decreased by 14 percent.

Finger-joint tensile strength

Another parameter studied was the influence of finger-joint tensile strength $f_{t, fj}$ on glulam beam performance. In PROLAM, an option is provided that allows the user to bypass the influence of $f_{t, fj}$ when determining the maximum moment carrying capacity of the glulam beams. Table 2 shows simulated results without the influence of finger joints (referred to as No FJ) for both the 50th and 5th percentiles of MOR, MOR_{50} and MOR_{05} , respectively. Also in Table 2, ratios between simulated results without finger joints and with finger joints were compared. At both percentile levels of MOR, bending strength values were within 4 percent for all three beam layouts when compared with the SIMULATED results of Table 1. In Falk et al. (1992), the ratio between ACTUAL mean glulam beam bending strength for all beams and those beams that failed only in the lamination was 0.99, 0.98, and 1.02 for the LH35, LC38*, and

LH40 layups, respectively. Thus, both the No FJ and SIMULATED results indicate that the tensile strength of the finger joints had little influence on the overall bending strength performance of the shallow glulam beams evaluated in this study. This observation, however, is not typical of all glulam beam tests.

CONCLUSION

In summary, the lumber and finger-joint data from Falk et al. (1992) were analyzed to develop input properties required by a glulam beam simulation model developed by Hernandez et al. (1991). When the input lamination property values were used to simulate glulam beam performance, SIMULATED results compared well with the TEST results.

Sensitivity analyses indicated that when the tensile strength of all the laminations were held constant and only the CORE laminations were reduced in stiffness, the decrease in bending strength was less than 4 percent. However, when the same stiffness configurations were modeled while considering the reduction in lamination tensile strength corresponding to the reduced stiffness of the core laminations, the reduction in glulam bending strength was approximately 15 percent. This implies that the difference between OUTER and CORE lamination stiffness be kept to a minimum of 15 percent to minimize the reduction in glulam bending strength to within 10 percent.

The second sensitivity analysis involved studying the influence of finger-joint tensile strength on the performance of the glulam beams in this study. Comparing simulated results without the influence of finger joints to simulated results with the influence of finger joints were only within 4 percent at both the 50th and 5th percentiles of glulam MOR. This suggested that for the glulam layups evaluated in this study, finger joints played a marginal role in the overall bending strength performance of the beams. This observation was supported by the actual results of the tested glulam combinations.

REFERENCES

Comite European de Normalisation. 1990a. Draft Standard EN TC 124.203, Structural Timber - Strength Classes.

Comite European de Normalisation. 1990b. Draft Standard EN TC 124.207, Glued-Laminated Timber - Strength Classes and Determination of Characteristic Properties.

Ehlbeck, J. and F. Colling. 1986. Strength of Glued Laminated Timber, CIB W18/19-12-1.

Falk, R.H. and R. Hernandez. In press. The Performance of Glued-Laminated Beams of European Manufacture.

Falk, R.H., K.H. Solli, and E. Aasheim. 1992. The Performance of Glued-Laminated Timber Beams Manufactured from Machine Stress Graded Norwegian Spruce, Report No. 77, Norwegian Institute of Wood Technology, Oslo.

Hernandez, R., D.A. Bender, B.A. Richburg, and K.S. Kline. 1992. Probabilistic Modeling of Glued-Laminated Timber Beams. *Wood and Fiber Science*, 24(3):294-306.

Taylor, S.E. and D.A. Bender. 1991. Stochastic Model for Localized Tensile Strength and Modulus of Elasticity in Lumber. *Wood and Fiber Science*, 23(4):501-519.

Table 1: TEST and SIMULATION results of glulam beam modulus of rupture (MOR) and modulus of elasticity (MOE)^a

Glulam layout	Sample size	MOR _{.60} ^b (MPa)	MOR _{.05} ^b (MPa)	MOE _{.60} ^b (GPa)	MOE _{.05} ^b (GPa)
TEST results					
LH35	104	44.5	33.2	12.1	11.0
LC38*	96	47.8	39.2	13.4	12.4
LH40	112	52.6	39.9	14.1	12.8
SIMULATED results					
LH35	1040	40.6 (39.4, 41.9)	32.4 (30.1, 34.6)	11.0 (10.9, 11.1)	10.3 (10.1, 10.4)
LC38*	960	45.5 (43.4, 47.6)	36.9 (34.7, 39.1)	13.1 (12.9, 13.2)	12.5 (12.3, 12.6)
LH40	1120	47.6 (46.4, 48.9)	38.6 (35.7, 41.5)	13.6 (13.4, 13.7)	12.9 (12.7, 13.1)
Ratio TEST/SIMULATED MOR					
LH35		1.10	1.02		
LC38*		1.05	1.06		
LH40		1.11	1.03		
Ratio TEST/SIMULATED MOE					
LH35				1.10	1.07
LC38*				1.02	0.99
LH40				1.04	0.99

^a Statistics are based on nonparametric estimates.

^b Values in parentheses are 90 percent confidence interval limits at 75 percent tolerance (lower, upper); 1 MPa = 145.0 lb/in², 1 GPa = 0.15x10⁶ lb/in².

Table 2: Simulated glulam beam properties without the influence of finger-joint tensile strength^a

Glulam layup	Sample size	MOR _{.60} ^b (MPa)	MOR _{.06} ^b (MPa)	Ratio No FJ/Simulated	
				MOR _{.60}	MOR _{.06}
No FJ^c					
LH35	1040	41.8 (40.6, 43.0)	33.3 (30.7, 35.8)	1.03	1.03
LC38*	960	47.5 (45.4, 49.7)	38.4 (35.9, 40.9)	1.04	1.04
LH40	1120	49.6 (48.3, 50.9)	39.8 (37.3, 42.3)	1.04	1.03

^a Statistics based on nonparametric estimates.

^b Values in parentheses are 90 percent confidence interval limits at 75 percent tolerance (lower, upper).

^c Simulated glulam beam results when finger joint tensile strength not considered in determination of ultimate moment carrying capacity of glulam beams.

Appendix A1: Statistical summary of lumber MOE_{flat}

Lumber grade	Sample size	Average MOE_{flat} (GPa ($\times 10^6$ lb/in ²))	COV (%)
C37-14E	204	13.9 (2.016)	14.8
C30-12E	221	11.2 (1.628)	11.9

PROLAM input distribution parameters for MOE_{flat} ($\times 10^6$ lb/in²)

Lumber grade	Distribution type	Location	Scale ^a	Shape ^a
C37-14E	LogNormal	0.6722	0.2848	0.1472
C30-12E	Weibull	0.4144	1.2935	7.4242

^a For the lognormal distribution, Scale is mean of $\ln(X)$ and Shape is standard deviation of $\ln(X)$.

Appendix A2: Statistical summary of $f_{t,lam}$ and f_t^a

Lumber grade	Sample size	Average (MPa ($\times 10^6$ lb/in ²))	COV (%)	5th percentile (MPa ($\times 10^6$ lb/in ²))
$f_{t,lam}$				
C37-14E	186	44.0 (6.380)	17.9	31.2 (4.530)
C30-12E	200	37.3 (5.410)	17.9	26.2 (3.800)
f_t^a				
C37-14E	199	40.9 (5.940)	22.0	26.2 (3.790)
C30-12E	215	33.7 (4.880)	21.8	20.8 (3.010)

^a f_t tested across a 1-m (39-in.) span from Falk et al. (1992), unadjusted for width.

PROLAM input distribution parameters for $f_{t,lam}$

Lumber grade	Distribution type	Location ($\times 10^3$ lb/in ²)	Scale ($\times 10^3$ lb/in ²)	Shape
C37-14E	Weibull	3.1058	3.6535	3.1441
C30-12E	Weibull	2.3033	3.4500	3.5602

Appendix A3: Statistical summary of $f_{t,ij}$

Lumber grade	Sample size	$f_{t,ij,mean}$ (MPa ($\times 10^3$ lb/in ²))	COV (%)	$f_{t,ij,.05}$ (MPa ($\times 10^3$ lb/in ²))
C37-14E	100	37.7 (5.470)	14.7	27.9 (4.050)
C30-12E	99	33.8 (4.910)	14.9	25.7 (3.720)

PROLAM input distribution parameters for $f_{t,ij}$

Lumber grade	Distribution type	Location ($\times 10^3$ lb/in ²)	Scale ($\times 10^3$ lb/in ²)	Shape
C37-14E	Weibull	1.6081	4.1806	5.5364
C30-12E	Weibull	2.8174	2.3338	3.1389

Appendix A4: Summary of estimated serial and cross correlations for MOE_{mac} and $f_{t,lam}$

C37-14E	Serial MOE_{mac}	Serial $f_{t,lam}$	Cross $MOE-f_{t,lam}$
lag-0	1.0000	1.0000	0.3340
lag-1	0.7096	0.6888	0.2370
lag-2	0.5632	0.4744	0.1881
lag-3	0.3572	0.3268	0.1193
C30-12E	Serial MOE_{mac}	Serial $f_{t,lam}$	Cross $MOE-f_{t,lam}$
lag-0	1.0000	1.0000	0.3685
lag-1	0.6679	0.5653	0.2461
lag-2	0.4270	0.3195	0.1573
lag-3	0.2980	0.1806	0.1098
C37-C30 Combined	Serial MOE_{mac}	Serial $f_{t,lam}$	Cross $MOE-f_{t,lam}$
lag-0	1.0000	1.0000	0.5372
lag-1	0.8720	0.6448	0.4684
lag-2	0.7604	0.4158	0.4085
lag-3	0.6631	0.2681	0.3562

9-laminations

90-mm (3.54-in.) width
 300-mm (11.81-in.) depth
 6-m (19.7-ft) length

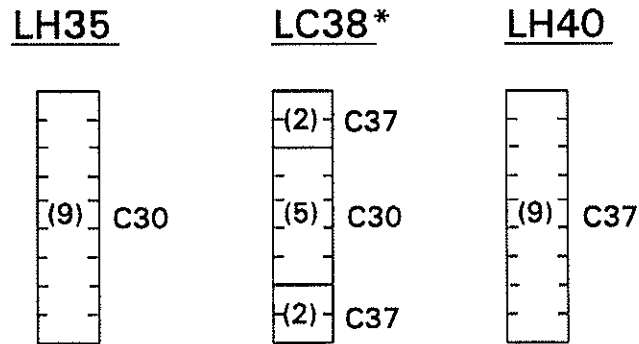


Figure 1: Norwegian spruce glulam layups showing placement of laminating lumber grades.

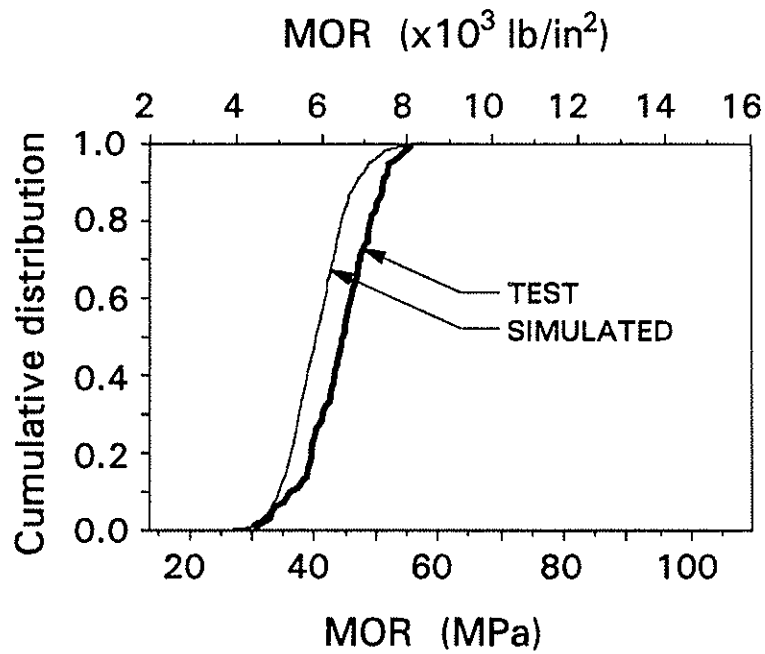


Figure 2: Empirical cumulative distribution functions of TEST and SIMULATED MOR for LH35 Norwegian spruce glulam beam layout.

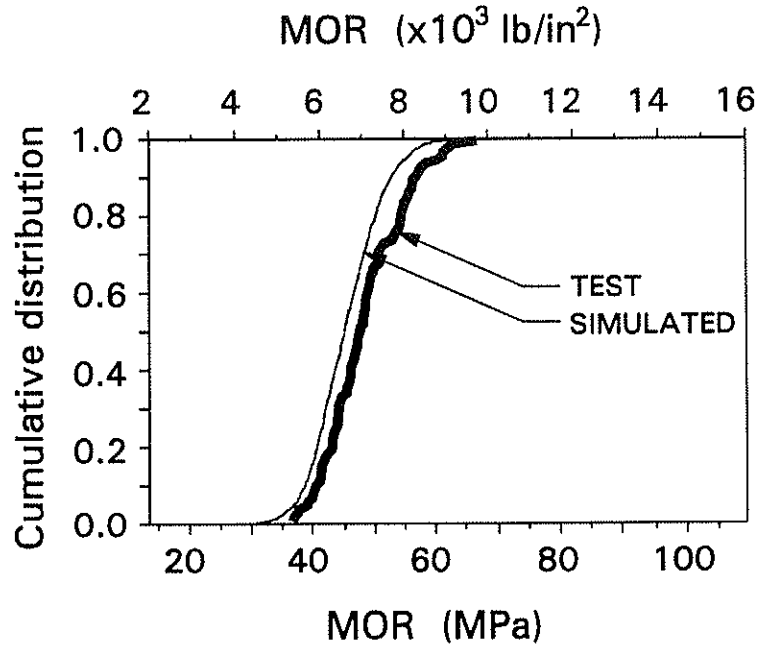


Figure 3: Empirical cumulative distribution functions of TEST and SIMULATED MOR for LC38* Norwegian spruce glulam beam layup.

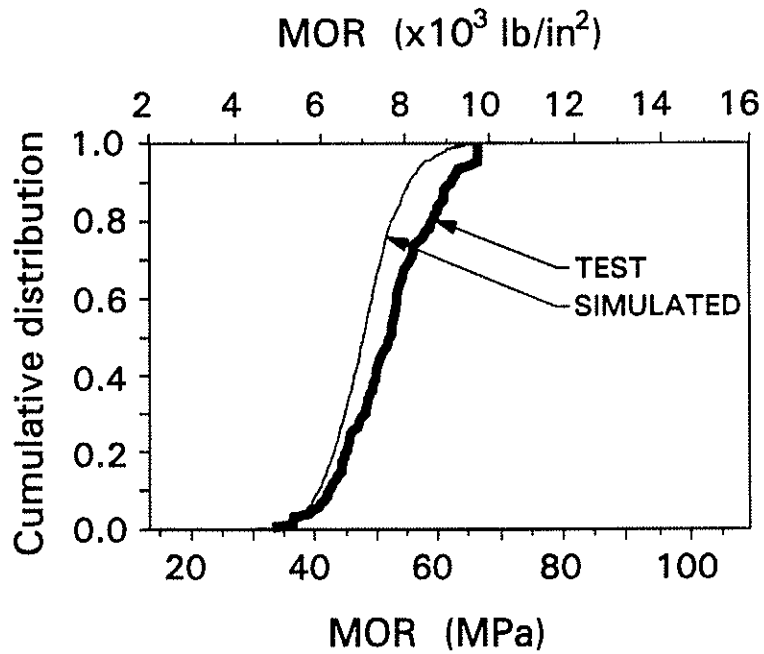


Figure 4: Empirical cumulative distribution functions of TEST and SIMULATED MOR for LH40 Norwegian spruce glulam beam layup.

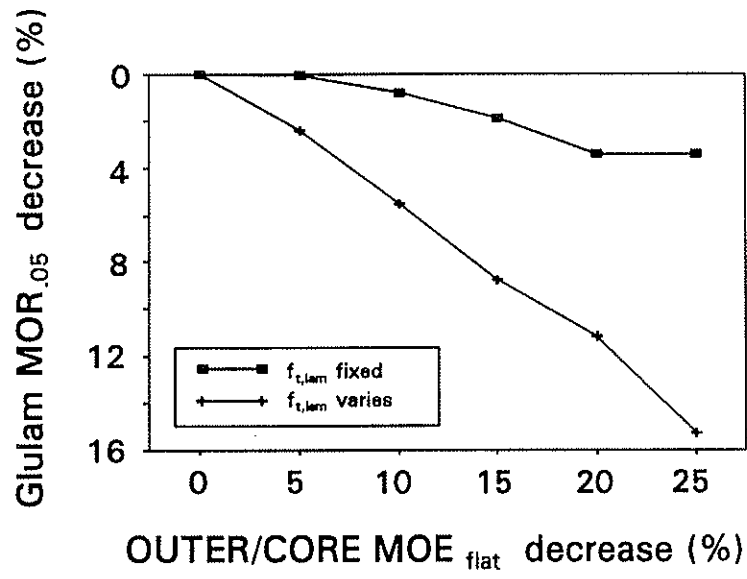


Figure 5: Graph showing change in glulam MOR_{0.05} as OUTER to CORE lamination MOE_{flat} changes.

INTERNATIONAL COUNCIL FOR BUILDING RESEARCH STUDIES AND DOCUMENTATION
WORKING COMMISSION W18 - TIMBER STRUCTURES

INVESTIGATION OF LAMINATING EFFECTS IN
GLUED-LAMINATED TIMBER

by

F Colling
Entwicklungsgemeinschaft Holzbau, Munich,
Germany
R H Falk
Forest Products Laboratory, Madison,
USA

MEETING TWENTY - SIX

ATHENS, GEORGIA

USA

AUGUST 1993

INVESTIGATION OF LAMINATING EFFECTS IN GLUED-LAMINATED TIMBER

François Colling¹ and Robert H. Falk²

Abstract

In this study, existing lamination and beam test results were analytically reviewed in an attempt to quantify the laminating effect for glued-laminated (glulam) timber. Laminating effect is defined as the increase in strength of lumber laminations when bonded in a glulam beam compared to their strength when tested by standard test procedures. In this study, fundamental concepts are presented to describe the laminating effect, estimates are made of the various physical factors that make up the effect, and a relationship is presented to quantify the magnitude of the effect.

Introduction

An important characteristic of glued-laminated (glulam) beams is that the bonding of laminations can result in beams with strengths higher than that of the individual lumber pieces from which the beams are constructed. This increase in strength is called the laminating effect and is of significant importance because quality control measures used to determine necessary lamination quality are dependent on the magnitude of this strength increase.

The objectives of this paper are to review the laminating effect and the physical characteristics which can be used to define it as well as to quantify the effect through an analysis of test data and analytical simulation.

Fundamental Concepts

The most fundamental definition of the laminating effect is a strength increase of a lamination as a result of being bonded into a glulam beam. A measure of this effect, the laminating factor λ , is typically computed by determining the ratio of the bending strength of a population of glulam beams to the tensile strength of a population of laminations:

$$\lambda = f_{b,glulam}/f_{t,lam} \quad (1)$$

¹ Dr.-Ing., Entwicklungsgemeinschaft Holzbau (German Society for Wood Research), Munich, Germany.

² Research Engineer, USDA Forest Service, Forest Products Laboratory, Madison, Wisconsin, USA.

where $f_{b,glulam}$ is the mean bending strength of a population of glulam beams, and $f_{t,lam}$ is the mean tensile strength of a population of laminations.

Characteristic strength values (typically lower 5th percentiles) are used to establish design values for glulam; thus, there is a need to determine a laminating effect at this characteristic strength level. When determining characteristic strength values from a population of test data, the laminating factor λ_k can be directly determined using the following equation:

$$\lambda_k = f_{b,glulam,k}/f_{t,lam,k} \quad (2)$$

where k refers to characteristic.

Lamination and beam test results have indicated that the apparent strength increase caused by the lamination effect is a summation of separate, though interrelated, physical effects. Some of these effects are a result of the testing procedure and others the effect of the bonding process. These effects will be discussed next.

Effect of Tension Test Procedure, k_{test}

The tension performance of single laminations as measured by standard test methods differs from the actual performance of the laminations in a beam. Existing test methods for tension testing (i.e., ISO 8375 (ISO 1985), ASTM D198 (ASTM 1992)) suggest a test configuration that provides no lateral restraint to the tension member (unhindered). Although this test configuration is quite applicable for the simulation of free tension members, such as web members in trusses, it does not necessarily represent a lamination in a glulam beam.

When a lamination is tested according to the standard methods, uncentered defects (such as edge knots) or areas of unsymmetrical density in a lamination can induce lateral bending stresses that combine with the applied tensile stresses, reducing the measured tensile strength of the lamination. If the laminations are bonded together in a glulam beam, no lateral bending stresses develop, because these defects are rigidly and laterally restrained. Thus, the tension lamination in a glulam beam has an apparent tensile strength higher than that indicated in a free tension test.

Reinforcement of Defects, k_{reinf}

When bonded in a glulam beam, defects (e.g., knots) and other low-stiffness areas are reinforced (on at least one side) by adjacent laminations. This reinforcement provides alternative paths for stresses to flow around the defect through adjacent higher stiffness areas of neighboring laminations. Thus, the laminating process reinforces defects in a lamination, redistributing stresses around the defect through the clear wood of adjacent laminations and effectively increasing the capacity of the cross section containing the defect.

Although knots are typically lower in stiffness than is the surrounding clear wood, finger joint stiffness has been shown to be strongly correlated to the average stiffness of the clear wood of the laminations joined (Burk and Bender 1989). Therefore, it is speculated that little stress redistribution takes place around finger joints.

Dispersion of Low-Strength Lumber, k_{disp}

Experimental test data indicate that the bending strength distribution for glulam beams has a higher mean value and a lower coefficient of variation (COV) than does the tensile strength distribution of the lamination lumber. This characteristic is partly explained by the effect of testing procedure and the reinforcement of defects explained previously. Additionally, there is an effect of dispersion of low-strength lumber that affects the beam. For example, if a population of laminations are tested in tension, the lower strength pieces will be represented in the calculation of the characteristic estimate of the population ($f_{t,lam,k}$). However, if the same population of tension specimens were fabricated into a glulam beam, the probability that the lowest strength pieces would end up in a location in the beam that initiates failure is lessened. An additional strengthening effect may be expected because of this dispersion of laminations.

On the other hand, the bending strength of glulam beams with larger dimensions is not only affected by the quality of the outer lamination but failure may also be initiated in the second or third lamination (from the tension side). In this case, the higher number of potential failure points can lead to a negative dispersion effect.

From a statistical point of view, the dependency of beam failure on the probability of a low-strength lamination occurring in a high-stressed zone includes a so-called size effect. That is, if laminations with a given strength distribution are used to produce several glulam beams with different sizes (lengths and depths), the lamination factors determined according to Equations (1) and (2) will differ for each beam size, because the bending strength of the glulam depends on the dimensions of the beams. Also, lamination tensile strength is affected by the tested lamination lengths and depths.

Quantification of Laminating Effect

On the basis of the previous discussions, the lamination factor of Equation (1) may be written as

$$\lambda = k_{test} \cdot k_{reinf} \cdot k_{disp} \quad (3)$$

where k_{test} , k_{reinf} , and k_{disp} correspond, respectively, to the effects discussed in the previous sections. These factors vary and depend on various parameters, such as the quality (or grade) of laminations and the beam layup. Even in the improbable case of identical

lamination quality, different test series lead to different results. Consider, for example, tests performed to determine k_{test} . Assume that lateral displacements occurring in a free tension test are measured and k_{test} is calculated (estimated) for each lamination. The factor k_{test} will be statistically distributed. This creates a problem in that the actual value of k_{test} corresponding to the lamination with a mean strength is not necessarily identical to the mean value of the k_{test} distribution. This problem suggests that the values for k_{test} , k_{reinf} , and k_{disp} in Equation (3) can only be mean estimates derived on the basis of mean strength values. On the basis of characteristic strength values, the following relationship is valid:

$$\lambda_k = k_{\text{test},5} \cdot k_{\text{reinf},5} \cdot k_{\text{disp},5} \quad (4)$$

The factors $k_{\text{test},5}$, $k_{\text{reinf},5}$, and $k_{\text{disp},5}$ do not correspond to a 5th percentile of each factor but to a mean estimate of the corresponding effects when the characteristic strengths (5th percentiles) are used as a basis for calculation.

In addition to the statistical difficulties discussed previously, other influences affect the quantification of $k_{\text{test},5}$, $k_{\text{reinf},5}$, and $k_{\text{disp},5}$. For example, k_{test} increases as the grade of lamination decreases, because increasing knot size presumably increases the magnitude of lateral displacement. The same is true for k_{reinf} , which should also increase with decreasing grade, because there is likely an increased redistribution of stresses as the number of low-stiffness zones increases. The factor k_{disp} varies with the grade of lamination, with the size and layup of the beam (homogeneous or combined grades), and with the relative population size of the lamination and beam tests.

Experimental and Simulated Data Analysis

In spite of the described interrelations, attempts were made in Europe to quantify the factors described previously (Ehlbeck and Colling 1986; Colling et al. 1991). These works led to a rough estimation of the lamination factor λ_k and represented the basis for glulam beam design criteria used in the European Community (Comite European de Normalisation 1993). Because the intention of this paper is to give better insight into the laminating effect, previous studies involving both the analysis and testing of beams and laminations have been evaluated in an attempt to quantify some of the laminating factors described previously. This reevaluation involved both European and North American research data. This distinction is made because different factors are used in Europe than in North America to adjust test data. A more complete description of the data analyzed is given in Colling and Falk (1993).

For example, the influence of specimen size (length and depth of laminations and glulam beams) is an important consideration in adjusting data. In Europe, current practice is to adjust lamination strength values and beam strength values by multiplying the determined strength values by the following factors, respectively:

and,

$$k_{h,lam} = (h/150)^{0.2} \quad (5)$$

$$k_{h,gl} = (h/600)^{0.2} \quad (6)$$

where $k_{h,lam}$ adjusts lamination depth (or width) to a reference 150 mm (6 in.) and $k_{h,gl}$ adjusts beam depth to a reference 600 mm (24 in.).

Equations (5) and (6) were used to adjust all data analyzed in this study to the reference sizes. No adjustment for lamination length was made (except as noted), because little length effect was expected for lamination lengths ranging from 1.0 to 2.5 m (3.3 to 8.2 ft), as long as the grade defect was placed between the grips of the tension machine.

Estimates of test data characteristic values were used where given in the studies evaluated. In the case of data where no characteristic estimates were given, estimates were made based upon statistical assessments of data variability.

Testing Procedure

Estimation of k_{test}

Foschi and Barrett (1980) developed a finite-element-based glulam strength prediction model in which the lateral restraint of laminations was taken into account. Our analysis indicated that the lateral displacement was statistically distributed, depending on the number, size, and location of knots. Calculating the values of k_{test} for the four lamination grades tested by Foschi and Barrett indicated a range of 1.04 to 1.14, with $k_{test} = 1.04$ for the highest lamination quality (grade A) and $k_{test} = 1.14$ for the lowest grade lamination (grade D). These values were calculated at a mean strength level. The effect of the testing procedure was assumed to be higher at the characteristic strength level.

By measuring lateral deflections occurring in free tension tests (with hinged end conditions), Larsen (1982) attempted to quantify the factor for testing procedure (k_{test}). The free length of test specimen was 2.1 m (7.1 ft) and deflections were measured over a length of 600 mm (24 in.). The measured deflections were quite small (usually < 0.5 mm (< 0.02 in.)) and were highly variable. As a result of small and variable deflections, k_{test} ranged from 1.1 to 2.0, with a trend of increasing k_{test} with decreasing grade.

Estimation of k_{test} and $k_{test,5}$

Based on the determined density and MOE-properties of the two lamination grades used by Falk et al. (1992), Görlacher (1992) calculated hindered tension strengths of laminations with the help of regression equations given in Ehlbeck et al. (1985) and Colling (1988, 1990a). These calculations indicate a value of $k_{test} = 1.2$ and $k_{test,5} = 1.3$.

Defect Reinforcement and Low-Strength Lumber Dispersion

A finite-element-based computer model was developed in Germany for the analysis of glulam beams (Ehlbeck et al. 1985, Colling 1988, 1990a). This model, referred to as the "Karlsruhe Model", utilizes statistical input on the properties of the laminations and finger joints of glulam beams (lumber density, MOE, and strength) to predict the strength and stiffness of beams of various layups. Input data for the laminations are based on tension and compression tests that do not allow lateral displacements of the specimens; that is, $k_{\text{test}} = 1.0$.

Because the simulation results of Colling (1990a) excluded the effect of testing procedure, a value for $k_{\text{test},5}$ was needed for our calculations to transform the hindered tensile strength values of the laminations into unrestrained, or free, tensile strength values. Based on the calculations of Görlacher (1992), a value $k_{\text{test},5} = 1.3$ was used.

Estimation of $k_{\text{rein},5} \cdot k_{\text{disp},5}$ by Simulation

Using the Karlsruhe Model, Colling (1990a) calculated the bending strength of 300-mm- (12-in.-) deep glulam beams. Various grades of laminations were accounted for through different knot area ratios (KAR), density, and MOE (54 combinations in total). In a complementary study, Colling et al. (1991) calculated the corresponding tensile strengths of the laminations (4.5 m (14.8 ft) long) for each glulam combination by using the Karlsruhe Model regression equations for the laterally restrained, or hindered, tensile strength.

For our analysis, the simulated tensile strength values were increased by 12% to adjust them to a length of 2 m (6.6 ft). This increase was based upon the simulation modeling performed by Görlacher (1990). Therefore, our results correspond to the hindered tensile strength of the laminations, i.e., the product of $k_{\text{test}} \cdot f_{t,\text{lam}}$, where $f_{t,\text{lam}}$ corresponds to the free tensile strength of the lamination determined from standard test methods. Thus, with the effect of testing procedure being eliminated, the lamination factors determined on the basis of these calculations were reduced to the effects of reinforcement k_{rein} and dispersion k_{disp} .

The simulations performed in our study indicate a close relationship between the characteristic glulam bending strength and characteristic lamination tensile strength.

Estimation of $k_{\text{rein}} \cdot k_{\text{disp}}$ and $k_{\text{rein},5} \cdot k_{\text{disp},5}$ by Simulation and Tests

Verification of the Karlsruhe Model on the basis of bending tests with glulam beams having a depth of 600 mm (24 in.) was performed by Colling (1990a). Six test series were performed with seven tests each (see also Colling (1990b) and Ehlbeck and Colling (1990)). The glulam bending strength values (both simulations and tests) include glulam beams with finger-joint failures. Because the Karlsruhe Model uses hindered lamination tension strength input, k_{test} could not be quantified in our calculations.

Our analysis showed a clear tendency of decreasing lamination factor with increasing

lamination quality. The product of $k_{\text{reinf}} \cdot k_{\text{disp}}$ varied between 0.90 and 1.22, and $k_{\text{reinf},5} \cdot k_{\text{disp},5}$ varied between 1.09 and 1.51. Again, the lamination effects were found to be more pronounced at the 5th percentile level than at the mean strength level.

Estimation of k_{reinf}

A stress distribution analysis of 600-mm (24-in.) glulam beams (20 laminations) performed by Colling (1990a) measured the effect of reinforcement k_{reinf} . In Colling (1990a), the MOE of laminations was varied as well as the MOE of the single finite element cells representing defects. If the MOE of a single cell in the outer or second tension lamination of the beam is varied while the MOE of the rest of the beam is held constant, k_{reinf} can be measured. The results of Colling (1990a) indicated that the stiffness zones were strengthened significantly by the laminations to which they were bonded. The magnitude of this reinforcement effect depended on the difference between the MOE of the cell and the MOE of the surrounding wood and varied between about 1.15 and 1.50 depending on the visual grade (knot size) of the lamination. If the low-stiffness zone occurred in the second lamination, reinforcement from laminations above and below were shown to add even more reinforcement.

Laminating Effect

Estimation of λ

Foschi and Barrett (1980) studied the bearing capacity of glulam beams (Douglas-fir) of different sizes and beam layups. Analysis of this test data indicated a clear tendency of decreasing λ with increasing quality of the laminations. Our results indicated laminating factors of approximately 1.1 for the higher grade laminations (grade B) and approximately 1.25 for lamination grade D.

Larsen (1982) performed bending tests on a total of 144 glulam beams (233 mm (9.2 in.) in depth) with 33 different beam layups represented. Comparing mean tensile strength values of the laminations with the mean bending strength values of the glulam beams, a lamination factor λ was calculated for each beam. As with the values of k_{rest} , the values of λ were found to increase with decreasing grade and ranged from 1.06 to 1.37.

Estimation of λ and λ_k

Recent testing by Falk et al. (1992) offered insight into the relationship between strength characteristics of the laminations and the resulting bending strength of glulam beams and provided estimates of λ and λ_k . For beams constructed of C37-14E tension laminations, $\lambda = 1.25$ and $\lambda_k = 1.45$. For beams constructed of C30-12E tension laminations, $\lambda = 1.30$ and $\lambda_k = 1.55$. This investigation, which was based upon several hundred lamination and

beam bending tests, confirmed a decreasing lamination effect with increasing lamination quality and a higher lamination factor at the 5th percentile level than at the mean strength level.

Tests by Gehri (1992) estimated λ and λ_k based on 35 tension tests of high-stiffness laminations and 8 bending tests of 500-mm- (19.7-in.-) deep glulam beams. The results indicated $\lambda = 1.12$ and $\lambda_k = 1.56$.

Considering the test results of Falk et al. (1992), Gehri (1992) proposed the following relationships for estimating the characteristic bending strength of 600-mm- (24-in.-) deep glulam beams on the basis of the characteristic tensile strength of the laminations:

$$f_{b,glulam,k} = 12 + f_{t,lam,k} \quad (7)$$

or using Equation (2):

$$\lambda_k = 1 + 12 / f_{t,lam,k} \quad (8)$$

Equation (7) has been adopted into the current draft of the European standard EN TC.124.207 (Comite European de Normalisation 1993). Equations (7) and (8) are valid only for strength values in MPa.

According to Equation (8), a lamination with a characteristic tensile strength of 18 MPa (2600 lb/in²) would be strengthened by about 67% ($\lambda_k = 1.67$) after being bonded into a glulam beam. Equation (8) is valid only for 600-mm (24-in.) glulam beams.

Results

Specific values of the factors of Equations (3) and (4) have been estimated based upon the described analysis of the experimental and simulated data.

Effect of Testing Procedure

Based on our analysis, the following ranges of values of k_{test} (at mean strength level) and $k_{test,5}$ (at the characteristic strength level) may be expected:

$$k_{test} = 1.1 \text{ to } 1.3$$

$$k_{test,5} = 1.2 \text{ to } 1.4$$

These factors are strongly dependent on lamination quality, especially on the size and location of knots.

Effect of Defect Reinforcement

The strengthening effect of zones with low stiffness are estimated to be in the following range of values for k_{reinf} and $k_{\text{reinf},5}$:

$$k_{\text{reinf}} = 1.0 \text{ to } 1.25$$

$$k_{\text{reinf},5} = 1.15 \text{ to } 1.50$$

These factors are strongly dependent on knot sizes.

Effect of Low-Strength Lumber Dispersion

As explained previously, the dispersion effect includes size effects, i.e., the influence of both lamination and glulam length and depth. Based primarily on the Karlsruhe Model and the results of simulations, the following range of dispersion effect is expected:

$$k_{\text{disp}} = 0.9 \text{ to } 1.0$$

$$k_{\text{disp},5} = 0.9 \text{ to } 1.0$$

A value below 1.0 may be explained by the mutual influence of neighboring laminations in larger glulam beams. Furthermore, if the length of the lamination test specimen is less (approximately 2 m (6.6 ft)) than the average length of the laminations in the beams (approximately 4 m (13.2 ft)), the reference tensile strength of the laminations is apparently too high, thus resulting in a negative dispersion effect.

Laminating Effect

To graphically illustrate the laminating effect, the results of our analysis are combined and plotted in Figure 1. All the presented results are test results, with the exception of the data from Colling et al. (1991), which are a mixture of test data and simulation results using the Karlsruhe Model. Figure 1 indicates that a strong linear relationship exists between the lamination tensile strength and the beam bending strength. Lamination effects tend to be greater when tensile strengths (or grade) is lower. The results shown in Figure 1 may be described by the following regression equation (in Mpa):

$$f_{b,glulam,k} = 6.9 + 1.141 \cdot f_{t,lam,k} \quad (9)$$

with a coefficient of correlation $r = 0.945$. Or by using Equation (2), the results shown in Figure 1 may be described by:

$$\lambda_k = 1.141 + 6.9 / f_{t,lam,k} \quad (10)$$

The relationship proposed by Gehri (1992) is also plotted in Figure 1. A comparison with test and simulation results showed that this relationship overestimates lamination effects, especially in the case of low-quality laminations.

The systematic reevaluation of the described data made it possible to roughly estimate the different effects of laminating discussed in this paper. The total lamination factor λ_k may be described by the following relationship (in MPa):

$$\lambda_k = 1.15 + 7 / f_{t,lam,k} \quad (11)$$

This relationship indicates a range of λ_k of 1.4 to 1.9 for lamination tensile strengths (5th percentiles) ranging from 10 to 30 Mpa (1450 to 4350 lb/in²), with the highest value of λ_k corresponding to the lowest strength value.

Concluding Remarks

Although the analysis of research data showed a great deal of variability in measures of laminating factors, the following qualitative tendencies were apparent:

- Lamination effects were more pronounced at the characteristic strength level than at the mean strength level. This may be explained by the higher coefficient of variation of the lamination tensile strength compared with glulam bending strength data.
- Lamination effects decreased with increasing quality and strength of the laminations. This may be explained by a lower reinforcement effect (caused by smaller knots) and less influence of testing procedure (caused by more homogeneous material properties in a higher grade).
- Factors that contribute to the lamination effect were interrelated, making it difficult to accurately quantify them separately.

References

- ASTM 1992: ASTM D198, Standard Method of Static Tests of Timbers in Structural Sizes, American Society for Testing and Materials, Philadelphia, PA.
- Burk, A.G.; Bender, D.A. 1989: Simulating Finger-Joint Performance Based on Localized Constituent Lumber Properties, *Forest Products Journal*, 39(3):45-50.
- Colling, F. 1988: Estimation of the effect of different grading criterions on the bending strength of glulam beams using the "Karlsruhe calculation model". IURFO 55.2, Turku, Finland.
- Colling, F. 1990a: Tragfähigkeit von Biegeträgern aus Brettschichtholz in Abhängigkeit von den festigkeitsrelevanten Einflußgrößen, Dissertation, Universität Karlsruhe, Germany.
- Colling, F. 1990b: Bending strength of glulam beams - a statistical model. IUFRO S5.2, St. John, Canada.
- Colling, F.; Ehlbeck, J.; Görlacher, R. 1991: Glued Laminated Timber: Contribution to the Determination of the Bending Strength of Glulam Beams, CIB-W18/24-12-1, Oxford, England.
- Colling, F.; R.H. Falk 1993: Laminating Effects for Glued-Laminated Timber, In Preparation for publication.
- Comite European de Normalisation. 1993: Draft Standard EN TC 124.207: Timber Structures Glued Laminated Timber Strength Classes and Determination of Characteristic Values, Draft Jan. 1993.
- Ehlbeck, J.; Colling, F. 1986: Strength of Glued Laminated Timber, CIB W18/19-12-1, Florence, Italy.
- Ehlbeck, J.; Colling, F. 1990: Bending strength of glulam beams - a design proposal. CIB-W18, Lisbon, Portugal.
- Ehlbeck, J.; Colling, F.; R. Görlacher, 1985: Einfluß keilgezinkter Lamellen auf die Biegefestigkeit von Brettschichtholzträgern. *Holz als Roh- und Werkstoff* 43: 333-337, 369-373, 439-442.
- Falk, R.H.; Solli, K.H.; Aasheim, E. 1992: The Performance of Glued Laminated Beams Manufactured From Machine Stress Graded Norwegian Spruce, Norwegian Institute of Wood Technology, Report No.77, September.

Foschi, R.O.; Barrett, J.D. 1980: Glued-Laminated Beam Strength: A Model, Journal of the Structural Division, ASCE, Vol. 106, No.ST8:1735-1754.

Gehri, E. 1992: Determination of characteristic bending values of glued laminated timber. CIB-W18, Åhus, Sweden.

Görlacher, R. 1990: Klassifizierung von Brettschichtholzlamellen durch Messung von Longitudinal-schwingungen. Dissertation, Universität Karlsruhe, Germany.

Görlacher, R. 1992: Unpublished Calculations, Universität Karlsruhe, Germany.

ISO 1985: ISO 8375, Solid Timber in Structural Sizes: Determination of Some Physical and Mechanical Properties, International Standards Organization.

Larsen, H.J. 1982: Strength of Glued Laminated Beams: Part 5, Report No. 8201, Institute of Building Technology and Structural Engineering, Aalborg University, Aalborg, Denmark.

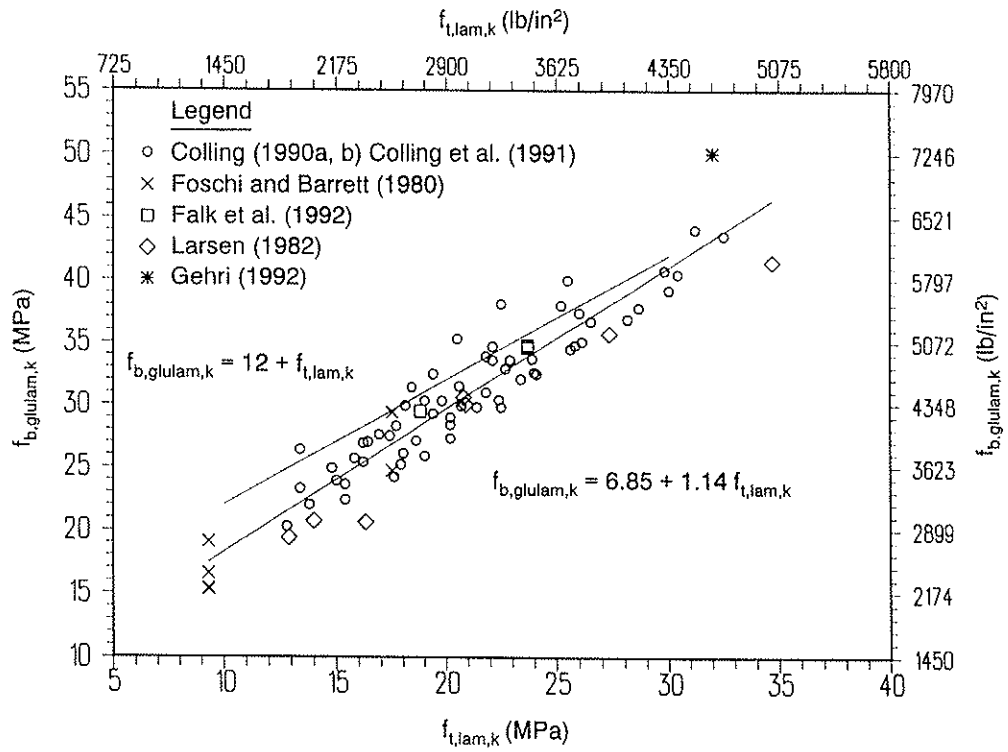


Figure 1
Lamination effect based on test data and simulations.

INTERNATIONAL COUNCIL FOR BUILDING RESEARCH STUDIES AND DOCUMENTATION

WORKING COMMISSION W18 - TIMBER STRUCTURES

COMPARING DESIGN RESULTS FOR GLULAM BEAMS

**ACCORDING TO EUROCODE 5 AND TO THE FRENCH WORKING STRESS DESIGN
CODE (CB71)**

by

F Rouger

Centre Technique du Bois et de l'Ameublement

France

MEETING TWENTY - SIX

ATHENS, GEORGIA

USA

AUGUST 1993

**Comparing design results for glulam beams
according to Eurocode 5 and to
the French working stress design code (CB 71)**

by

F. Rouger¹

Abstract

The publication of the EN TC124-207 standard draft about strength classes of glued-laminated timber gave rise to many questions from glued laminated timber design offices as from industrials. Those questions were especially about the characteristic values of the glued laminated timber issued from that of solid wood. However, we have to bear in mind that these characteristic strengths are used in the design methods via partial security coefficients defined as well as in the Eurocode 5 as in the CB 71 regulation. In order to have a significant idea of the changes due to the European regulation, it is necessary to compare practical cases of design. The aim of this paper is to explain Eurocode 5 options and to compare them to CB 71 regulation, and also to quantify the differences between those two regulations. An example of bending under self weight + snow load will be studied. The case of solid wood will also be investigated as a basis to that of glued-laminated timber.

Design of solid wood

Using Eurocode 5

It should be verified that :

$$R_d \geq S_d \quad (1)$$

that is to say :

$$\frac{\sigma_k \cdot k_{mod}}{\gamma_m} \geq \gamma_G G_k + \gamma_Q Q_k \quad (2)$$

where :

σ_k is the characteristic bending strength of the material
 γ_m is the partial security coefficient linked to the material
 k_{mod} is the modification factor taking into account the load duration and the service class
 γ_G is the partial security coefficient linked to self weight

¹ Research Manager, Dept of Timber Engineering, CTBA, 10, av. St Mandé, 75012 Paris, France

G_k is the characteristic value of self weight
 γ_Q is the partial security coefficient linked to snow load
 Q_k is the characteristic value of snow load

Simplified interpretation :

Let us assume that :

$$\gamma_G G_k + \gamma_Q Q_k = \gamma_X X_k \quad (3)$$

The following has to be verified :

$$\frac{\sigma_k \cdot k_{mod}}{\gamma_m} \geq \gamma_X X_k \quad (4)$$

$$\sigma_{design} = \frac{\sigma_k \cdot k_{mod}}{\gamma_m \gamma_X} = \frac{\sigma_k}{\gamma_{eq}} \geq X_k \quad (5)$$

Numerical application :

$$\gamma_X = \frac{\gamma_G + \gamma_Q}{2} = \frac{1.35 + 1.5}{2} = 1.43 \quad (6)$$

$$\gamma_m = 1.3 \quad (7)$$

$$k_{mod} = 0.9 \quad (8)$$

This implies that :

$$\gamma_{eq} = 2.06 \quad (9)$$

If we use a C30 strength class from prEN 338, we obtain :

$$\sigma_{design} = \frac{30}{2.06} = 14.56 \text{ MPa} \quad (10)$$

CB 71 Regulations - working stress design concepts

Four values describing the stresses are used in the CB 71 regulations (and the associated classifications standards) :

There are :

- | | |
|---|-----------------|
| - the allowable strength | σ_{adm} |
| - the conventional limit of elasticity | LEC |
| - the characteristic strength | σ_k |
| - the conventional strength at failure. | σ_{rupt} |

The first two values are used in design methods. The other two correspond to statistical estimates derived from tests. The characteristic strength corresponds to the lower 5% fractile. The conventional strength at failure is the mean value of the strength distribution. Each of these values can be deduced from each other through security coefficients.

	$\sigma_{adm} \times$	LEC \times	$\sigma_k \times$	$\sigma_{rupt} \times$
$\sigma_{adm} =$	1.0	0.57 (*)	0.44	0.36
LEC =	1.75 (*)	1.0	0.77	0.64
$\sigma_k =$	2.275	1.3	1.0	0.83
$\sigma_{rupt} =$	2.75	1.57	1.21	1.0

(*) for bending

Using CB 71 regulations - Normal actions

It should be verified that :

$$\sigma_{adm} \geq G + P_c \quad (11)$$

that is to say :

$$\frac{\sigma_k}{2.275} \geq G + P_c \quad (12)$$

where :

σ_{adm} is the allowable bending strength of the material
 σ_k is the characteristic bending strength of the material
 G is the characteristic value of the self weight
 P_c is the characteristic value of snow load
 (normal action)

Numerical application :

If we use a C30 strength class from prEN 338, we obtain :

$$\sigma_{design} = \frac{30}{2.275} = 13.2 \text{ MPa} \quad (13)$$

In such case the Eurocode 5 is more favourable of 10.3%

Using CB 71 regulations - extreme actions

It should be verified that :

$$LEC \geq 0.9 G + \gamma_{ce} P_{ce} \quad (14)$$

that is to say :

$$\frac{1.75 \sigma_k}{2.275} \geq 0.9 G + \gamma_{ce} P_{ce} \quad (15)$$

where :

LEC is the conventionnal limit of elasticity
 σ_k is the characteristic bending strength of the material
 γ_{ce} is the partial security coefficient linked to snow load
 G is the characteristic value of self weight
 P_{ce} is the characteristic value of snow load
 (extreme load)

Simplified interpretation :

Let us assume as in Eurocode 5 that :

$$0.9 G + \gamma_{ce} P_{ce} = \gamma_x X_k \quad (16)$$

It should then be verified that :

$$\frac{1.75 \sigma_k}{2.275} \geq \gamma_x X_k \quad (17)$$

that is to say :

$$\sigma_{design} = \frac{1.75 \sigma_k}{2.275 \gamma_x} \geq X_k \quad (18)$$

Numerical application :

$$P_{ce} = \frac{5}{3} P_c \quad (19)$$

$$\gamma_x = \frac{0.9 + \frac{5}{3} \gamma_{ce}}{2} = \frac{0.9 + 1.83}{2} = 1.37 \quad (20)$$

If we use a C30 strength class from prEN 338, we obtain :

$$\sigma_{design} = \frac{\sigma_k \cdot 1.75}{2.275 \cdot 1.37} = \frac{\sigma_k}{1.78} = 16.8 \text{ MPa} \quad (21)$$

In such case Eurocode 5 is less favourable of 15%

Design of glued-laminated timber

Using Eurocode 5

Two options are given in document CEN TC124.207 :

(1) *Using table B.1 of Annex B (appendix B)*

C30 \implies GL 28

When the equation n°5 is used, such result is obtained :

$$\sigma_{design} = 13.59 \text{ MPa} \quad (22)$$

(2) *Using formulae from table A.1 (appendix A)*

$$f_{m,g,k} = 12.0 + f_{t,0,1,k} \quad (23)$$

In the case of an homogeneous glulam made from C30, following results are obtained :

$$f_{m,g,k} = 30 \text{ MPa} \quad (24)$$

which corresponds to the creation of a GL30

When equation n°5 is used, it follows that :

$$\sigma_{design} = 14.56 \text{ MPa} \quad (25)$$

Using CB 71 - Normal actions

The allowable strength of the glued-laminated timber is that of the solid wood increased by 10%.

When equations n°12 (& n°13) are used, it follows that :

$$\sigma_{design} = 14.5 \text{ MPa} \quad (26)$$

Using CB 71 regulations - Extreme actions

When equation n°21 is used, it follows that :

$$\sigma_{design} = 18.5 \text{ MPa} \quad (27)$$

To sum it up, the design strength from the different options are as follows :

REGULATIONS	σ_{design} (MPa)
Eurocode 5 + 124.207 - GL 28	13.6
Eurocode 5 + 124.207 - GL 30	14.5
CB 71 - Normal actions	14.5
CB 71 - Extreme actions	18.5

Conclusion

In the case of solid wood, Eurocode 5 design results are between CB 71 normal actions and extreme actions design results, which is in agreement with soft calibration concepts. In the case of glulam, Eurocode 5 design results are always more penalizing than CB 71 design results. For this reason, the French glulam industry is concerned about its future and raised the question during the CEN 124 meetings. A possible answer could be to enable the use of Annex A as a normative Annex and to increase the values by 15%, which would place the glulam in the same position as solid wood. Of course, this would imply an increase of quality control in the industry. This option was already discussed in previous CEN and CIB meetings. It needs to be a compromise between a scientific reality and an economic reality...

References

CEN TC 124.207 - 1993 - Timber Structures - Glued Laminated Timber - Strength classes and determination of characteristic values.

prEN 338 - 1991 - Structural Timber - Strength Classes.

Eurocode 5 - 1993 - Design of Timber Structures.

CB 71 - Règles de calcul des structures en bois.

INTERNATIONAL COUNCIL FOR BUILDING RESEARCH STUDIES AND DOCUMENTATION

WORKING COMMISSION W18 - TIMBER STRUCTURES

TEST OF NAIL PLATES SUBJECTED TO MOMENT

by

E Aasheim

The Norwegian Institute of Wood Technology

Norway

MEETING TWENTY - SIX

ATHENS, GEORGIA

USA

AUGUST 1993

TEST OF NAIL PLATES SUBJECTED TO MOMENT

Erik Aasheim
Structural Engineer
The Norwegian Institute of Wood Technology

This paper describes tests of nail plate joints subjected to moment. The tests were performed at The Norwegian Institute of Wood Technology in the autumn of 1992. The aim was to establish a background for a proposal for new test specimen for moment resistance of nail plates in the coming CEN and ISO test standards.

INTRODUCTION

In the test standard ISO 8969 "Timber structures - Testing of unilateral punched metal plate fasteners and joints", no test specimen for determination of moment resistance is defined. In order to model trusses, frames and other systems in a realistic way, the modelling of the joints are essential. In this respect the rotational stiffness of the contact surface is fundamental.

During CEN/TC 124/WG 1-meetings this subject has been discussed. In the document EN TC 124.116 (June 92-version) "Timber structures - Test methods - Joints made of punched metal plate fasteners" a method is introduced. The test specimen is subjected to a combination of moment and shear force, and the method includes complicated calculations to find the rotational stiffness.

OBJECTIVES

The basic objective of this paper is to introduce a test specimen for a "direct" measurement of the rotational stiffness of the contact surface of the plate and the timber.

DESCRIPTION OF TEST SPECIMENS

The main idea was to test specimens where the contact surfaces are exposed to pure moment. Buckling failure in the plate could be a serious problem, and to avoid this a "stiffener" was introduced, as shown in figure 1.

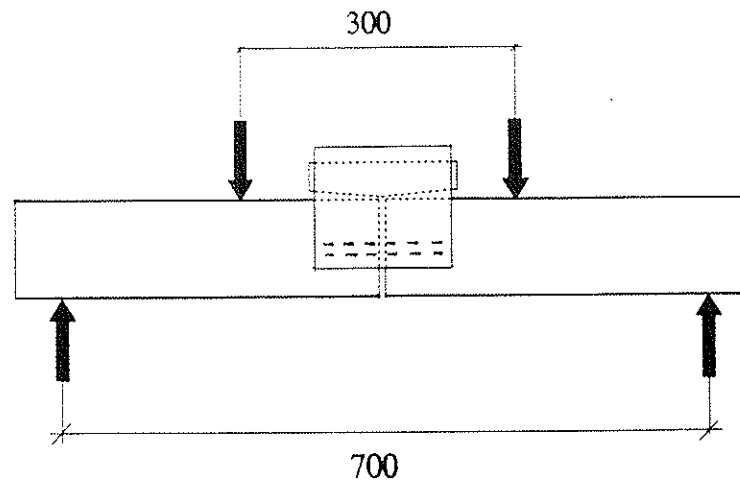


Figure 1

Pure moment test specimen with stiffener. Lengths in mm.

The stiffener is a piece of timber with the same thickness (34 mm) and the same grain direction as the two joined parts.

The cross section area of all the timber pieces is 34 x 95 mm, and the gap between the joined parts is 10 mm.

The nail plate type is Hydro Nail PTN with a thickness of 1.0 mm, teeth length 9 mm, teeth density 0.012 teeth/mm² and ultimate tensile strength 430 N/mm².

TEST PROCEDURE

The dimensions of the test pieces were chosen to fit the available testing equipment in our laboratory.

The rotations between timber and plate were measured with 4 Sangamo displacement transducers, one pair at each end of one of the nail plates, as shown in figure 2:

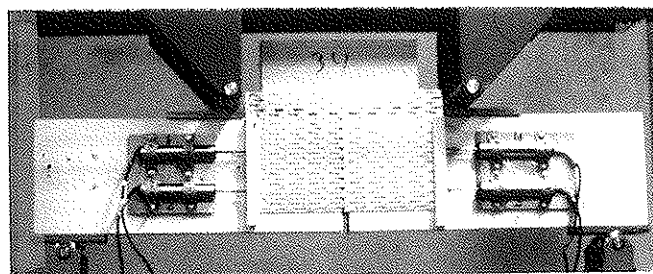


Figure 2

Rotation measurement setup.

One pair of transducers was fixed to a steel plate, which again was fixed to the timber. The deformations were measured to timber pieces glued to the edge of the nail plate.

The tests were performed with a constant load head movement speed of 0.1 mm/sek, which led to a testing duration of about 2 minutes.

5 series with 10 parallels in each series were tested, with different effective nail plate area and different timber density, as shown in table 1.

Table 1: Test series.

Series no.	Fig. no.	Density	Plate size	Eff. area
1	3	400	127x152	61x61
2	4	400	127x152	40x61
3	3	330	127x152	61x61
4	3	470	127x152	61x61
5	5	400	127x252	61x61

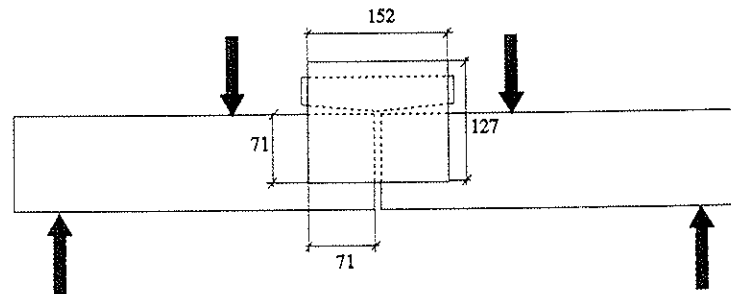


Figure 3
Test series 1,3 and 4.

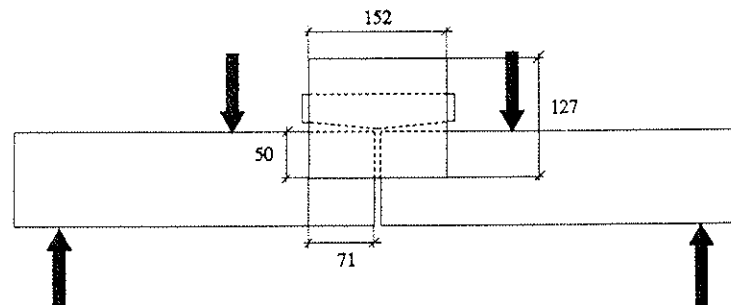


Figure 4
Test series 2.

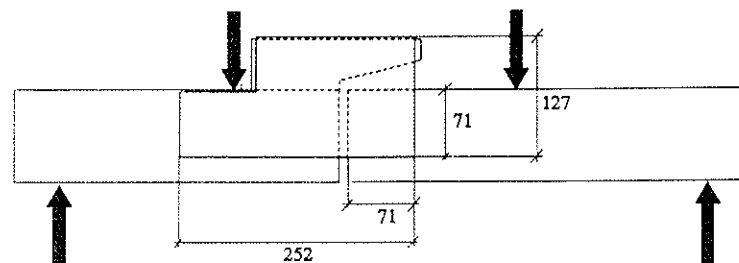


Figure 5
Test series 5.

TEST RESULTS

The moment/rotation relationship for the 10 test pieces of each of the 5 series was recorded. One curve was plotted for each test specimen, as a mean value from the two pairs of transducers. The results from series 1 are shown in figure 6.

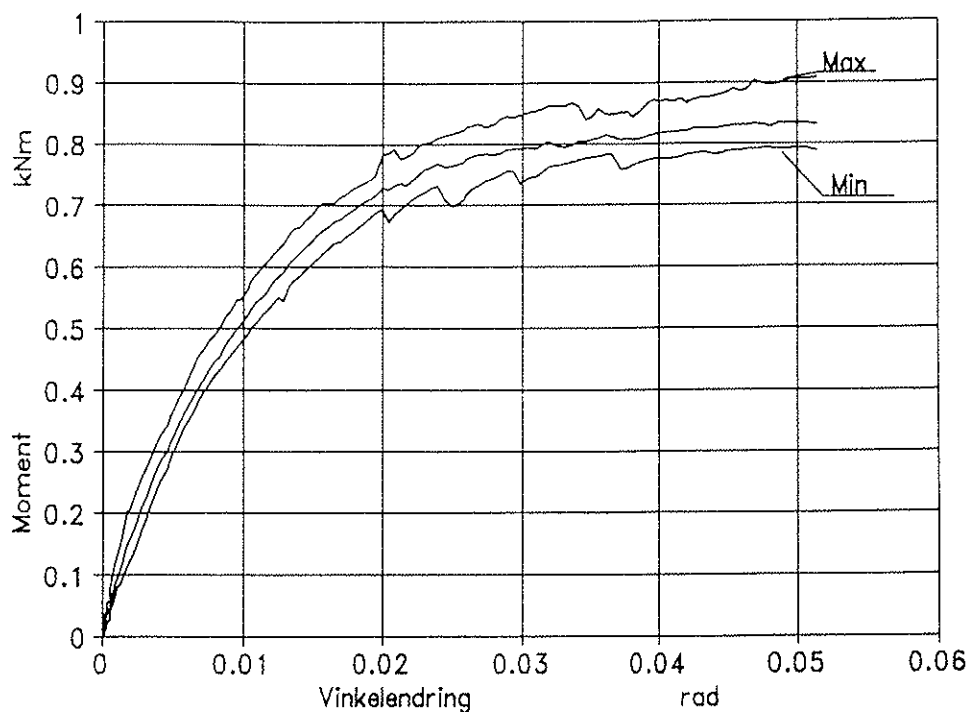


Figure 6
Moment/rotation-curves from test series 1.

In figure 6 the mean curve is shown in addition to the upper and the lower limits for the 10 specimens.

The mean curves may be expressed with the following equation:

$$M = k\varphi^{\frac{1}{1.55}}$$

The exponent is constant for all series, but k is different, as shown in table 2.

Table 2: k for all test series.

Series no.	k
1	9.8
2	5.5
3	8.3
4	11.4
5	11.5

Figure 7 shows how the graph of the results fit with $k=9.8$ in the equation for test series 1:

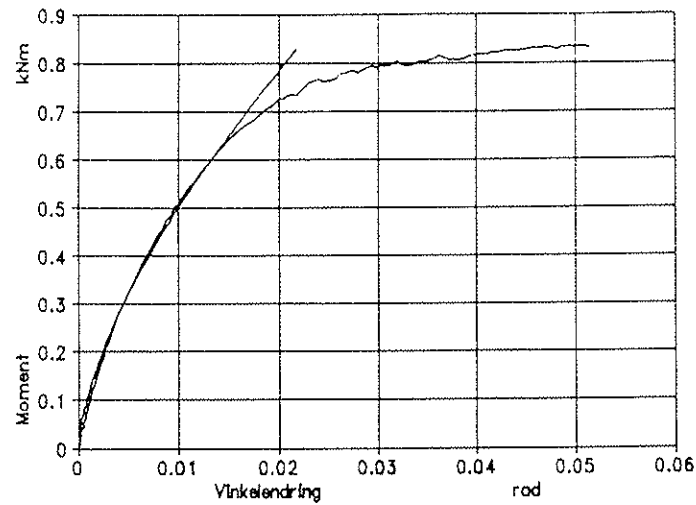


Figure 7

Mean curve for test series 1 compared to the equation.

DISCUSSION

To compare the test results presented in table 2, the values are corrected to the reference density and recalculated to stresses instead of moments. The result of this procedure is the following equation:

$$\tau = k_{\tau} \varphi^{\frac{1}{1.55}}$$

The k_{τ} -factors for the 5 series are then calculated with both elastic and plastic section modulus, and the results are shown in table 3.

Table 3:

Series no.	k_{τ} elastic	k_{τ} plastic
1	83.9	51.8
2	83.0	51.2
3	81.6	50.4
4	88.5	54.7
5	97.2	60.0

Note that series no. 5 is the unsymmetrical one shown in figure 5.

CONCLUSION

In general, the results of this study show that the proposed test specimen may be used to find the rotational stiffness of the contact surface. It can be seen from table 3 that the results are in the same order of magnitude for the different test series, and the results are much more reliable than those found by specimens subjected to a combination of shear force and moment.

CONCLUDING REMARKS

More research and experience is needed to use this rotational stiffness in practical design, but the introduction of a test piece in EN TC 124.116 similar to figure 1 in this paper is recommended. The gap between the joined parts should be reduced to 5 mm, and the plate size should be chosen to ensure that failure does not occur in the plate.

REFERENCES

1. Draft Standard EN TC 124.116 "Timber structures - Test methods - Joints made of punched metal plate fasteners", June 1992
2. International Organization for Standardization, ISO 8969 "Timber structures - Testing of unilateral punched metal plate fasteners and joints", 1990
3. International Organization for Standardization, ISO 6891 "Timber structures - Joints made with mechanical fasteners - General principles for the determination of strength and deformation characteristics", 1983
4. Kevarinmäki, A. and Kangas, J. "Moment anchorage capacity of nail plates in shear tests", CIB-W18/25-14-1, 1992
5. Aune, P. "Investigations on strength and stiffness of joints made with Hydro-Nail truss plates", Acta Polytechnica Scandinavica, Civil engineering and building construction series no 67, 1970
6. Edlund, G. "Rapport 40, Längdskurvning av träbalkar med spik-plåtsförband", Statens institut för bygnadsforskning, 1971
7. Perkins, R.H., Suddarth, S.K. and Dale, A.C. "Rotational resistance of three-membered nailed joints subjected to bending moment", Research Bulletin No. 753, Purdue University, 1962

INTERNATIONAL COUNCIL FOR BUILDING RESEARCH STUDIES AND DOCUMENTATION
WORKING COMMISSION W18 - TIMBER STRUCTURES

MOMENT ANCHORAGE CAPACITY OF NAIL PLATES

by

A Kevarinmäki
Helsinki University of Technology

J Kangas
Technical Research Centre of Finland (VTT)
Finland

MEETING TWENTY - SIX

ATHENS, GEORGIA

USA

AUGUST 1993

1. INTRODUCTION

The analysis of the nail plate joints anchorage moment capacity with 220 standard shear test results was presented in authors earlier CIB-W18 paper (KEVARINMÄKI & KANGAS, 1992). Now 72 new shear tests, where also the angle between grain and force (β) was a variable, have been carried out. New bending tests done in Norway (KYRKJEEIDE, AUNE & AASHEIM, 1992) have also been analyzed for comparison. The analysis of these test results, where the failure mode was anchorage failure, has been presented in this paper. The anchorage moment capacities of these specimens have been calculated according to Eurocode 5 (modified elastic method), with the simplified plastic design method (Norèns method) and with the accurate plastic theory solution.

2. SYMBOLS

A_{ef}	Effective nail plate area (the area of timber member covered by nail plate is reduced by 5 mm from its edges and by 10 mm from the end of the member in grain direction when it is loaded in tension) [mm ²]
F_A	Force acting on the plate at the centroid of effective area
F_{max}	Maximum applied load during a test [kN]
I_p	Polar moment of inertia of the effective area [mm ⁴]
V	Shear force [kN]
M	Bending moment [kNm]
M_A	Moment acting on the plate at centroid of the effective area
d	"Diagonal" length of the effective area [mm]
$f_{a,\alpha\beta,m}$	Mean value of the anchorage strength in the direction combination a and b
k_1, k_2, α_0	Constants in equations of the anchorage strength
n	Number of test pieces in different series
r_{max}	Distance from the centroid to the furthest point of the effective area [mm]
s	Standard deviation of sample
α	Angle between the force and the main direction of the nail plate [°]
β	Angle between the force and the grain direction [°]
γ	Angle between the main direction of the nail plate and the grain direction
$\rho_{o\omega}$	Density; mass at $\omega = 0$, volume at ω [kg/m ³]
τ_F	Anchorage stress from force F_A [N/mm ²]
$\tau_{M,el}$	Elastic anchorage stress from moment M_A [N/mm ²]
$\tau_{M,pl}$	Plastic anchorage stress from moment M_A [N/mm ²]
ω	Moisture content ratio [%]

Subscripts:

cal	Calculated value using the mean strength values
max	Mean value of the test series by the maximum values of test piece
Norèn	Simplified solution by Norèns method
red	Reduced mean value to the compression strength of 35 MPa
theor	Accurate solution by plastic theory

3. SHEAR TESTS

The shear tests reported in this paper have been carried out at the Technical Research Centre of Finland (VTT). The selection of the material and performance of tests are in agreement with the procedure described in CIB-W18 1985: paper 18-7-4. The test pieces and the load arrangements used in the shear tests are shown in Figure 3.1.

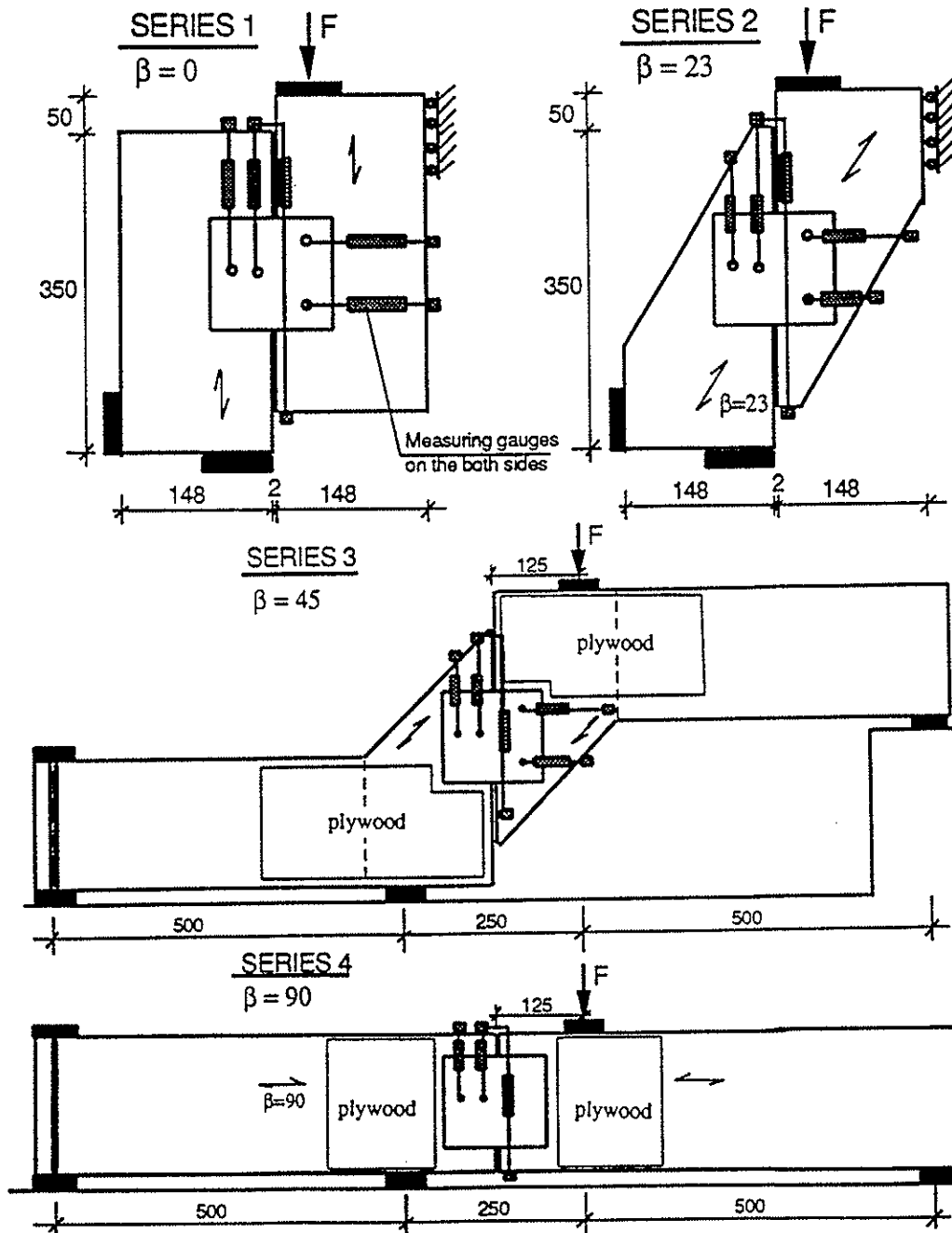


Figure 3.1 Shear test pieces and loading arrangements. Nail plate direction angle α was 0° , 45° and 90° in each series.

The standard shear tests are carried out in parallel to the grain ($b = 0^\circ$). Shear loading test series where also b-direction is a variable have been carried out with two different nail plates in the directions $b = 0^\circ, 23^\circ, 45^\circ$ and 90° . The angles a were $0^\circ, 45^\circ$ and 90° . Finnish nail plates used were W-nailplate ($96 \times 100 \text{ mm}^2$) and FIX-nailplate ($100 \times 100 \text{ mm}^2$). W-plate is 1.25 mm thick with three threaded nails punched from the same hole (Figure 3.2). FIX-plate is a 1.3 mm thick nail plate with 13 mm long threaded nails (Figure 3.3). Each test series contained three similar pieces. Summary of the variables of all 72 test pieces is shown in Table 3.1.

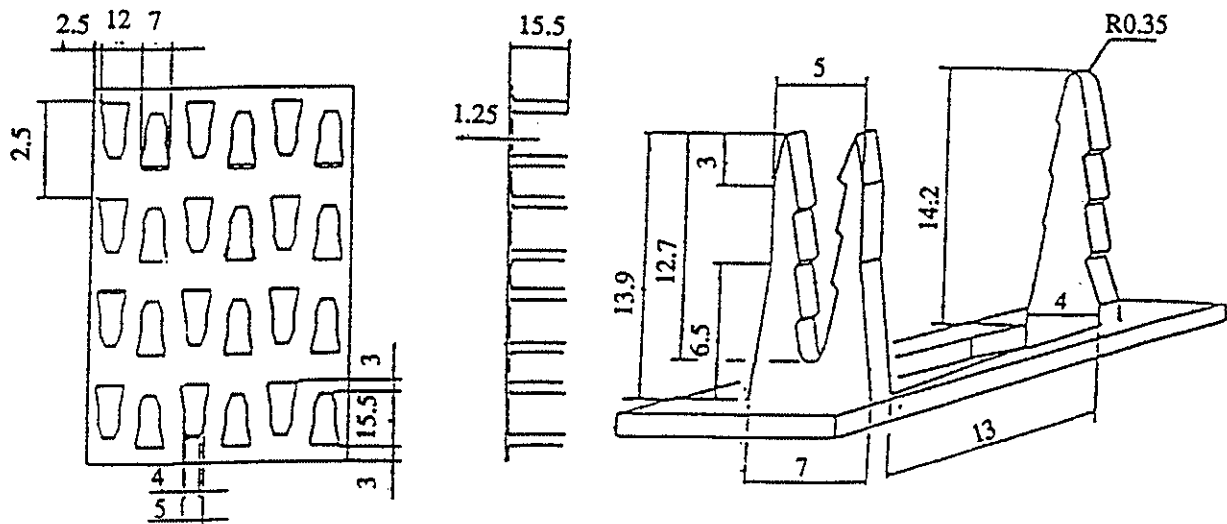


Figure 3.2 The geometry of W-nailplate

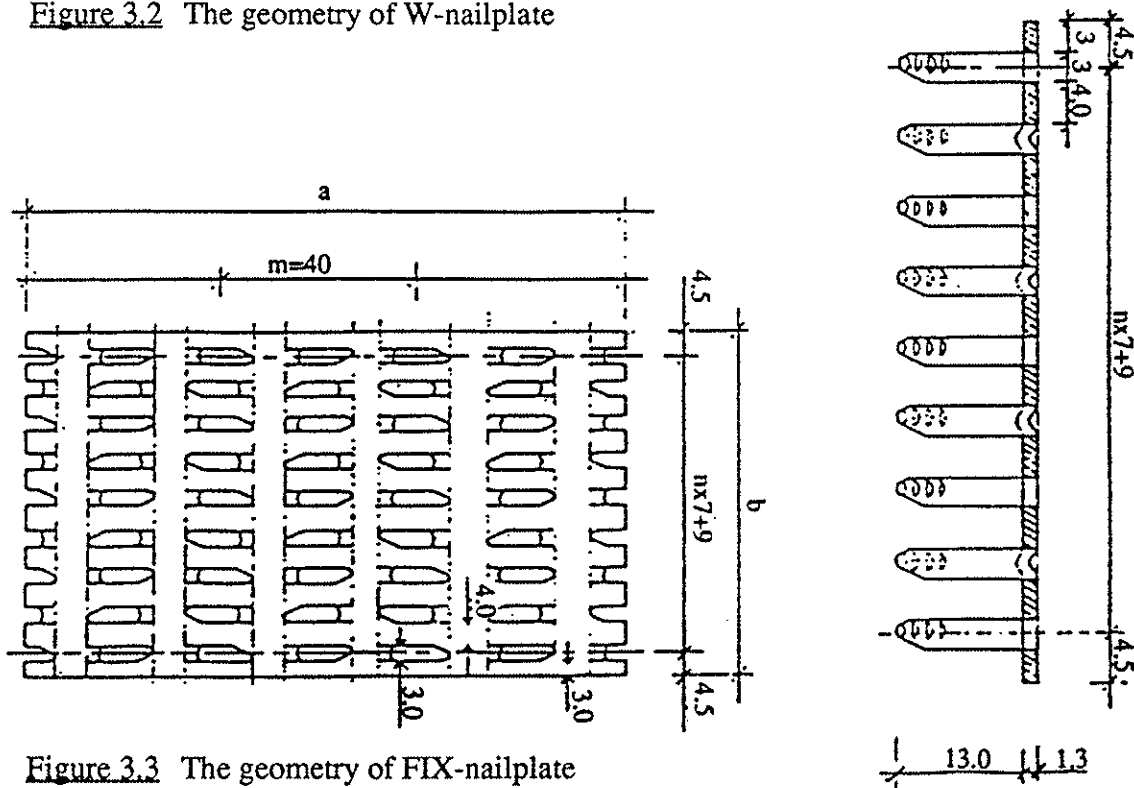


Figure 3.3 The geometry of FIX-nailplate

Table 3.1 Shear test series, direction angle variables, effective anchorage areas and properties of timber members.

Test pieces)	α	β	γ	A_{ef} [mm ²]	ρ_{ow} [kg/m ³]	ω [%]
W1A 4-6	0	0	0	4200	346	16.4
W1B 4-6	45	0	45	4004	346	16.4
W1C 4-6	90	0	90	4224	346	16.4
W2A 1-3	0	23	23	4200	353	15.0
W2B 1-3	45	23	67	4004	353	15.0
W2C 1-3	90	23	67	4224	353	15.0
W3A 1, 2	0	45	45	4200	348	15.0
W3B 1, 3	45	45	90	4004	355	15.0
W3C 2, 3	90	45	45	4224	357	15.0
W4A 1-3	0	90	90	4200	353	15.0
W4B 1-3	45	90	45	4004	353	15.0
W4C 1-3	90	90	0	4224	353	15.0
F1A 4-6	0	0	0	4400	346	16.4
F1B 4-6	45	0	45	4186	346	16.4
F1C 4-6	90	0	90	4400	346	16.4
F2A 1-3	0	23	23	4400	353	15.0
F2B 1-3	45	23	67	4186	353	15.0
F2C 1-3	90	23	67	4400	353	15.0
F3A 1-3	0	45	45	4400	353	15.0
F3B 1-3	45	45	90	4186	353	15.0
F3C 1-3	90	45	45	4400	353	15.0
F4A 1-3	0	90	90	4400	353	15.0
F4B 1-3	45	90	45	4186	353	15.0
F4C 1-3	90	90	0	4400	353	15.0

*) W = W-nailplate 96 x 100; F = FIX-nailplate 100 x 100

Timber material was finnish spruce (*Picea Abies*) of chosen mean densities $\rho_{ow} = 346$ kg/m³ (series $\beta = 0^\circ$) and $\rho_{ow} = 353$ kg/m³ (series $\beta \neq 0^\circ$). Cross section of the test pieces was 42 x 148 mm². The test pieces in the test series $\beta = 0^\circ$ were conditioned and tested separately from the others ($\beta \neq 0^\circ$), so the moisture contents were slightly different.

The loading procedure was in agreement with the ISO 8969 standards. The test pieces were loaded to failure by force controlled constant loading rate of 3 kN/min. The total loading time was about 10 minutes.

4. LOAD CARRYING CAPACITIES OF THE SHEAR TEST PIECES

4.1 Test series

The results of anchorage failure in shear tests are presented in Table 4.1. No contact appeared between the timber members before the maximal force was exceeded. The presented shear capacities (V_{red}) have been made comparable by reducing the mean values of the test series to the compression strength of 35 MPa (CIB-W18, PAPER 18-7-5):

$$V_{red} = \bar{V}_{max} \sqrt{35[\text{MPa}] / \bar{f}_{c, test}} \quad (4.1)$$

$$\bar{f}_{c, test} = 0.095 \bar{\rho}_{ow} (2 - \bar{\omega} / 15) \quad (4.2)$$

where ρ_{ow} is mean value of wood density of test series

$\bar{\omega}$ is mean value of moisture content of wood in the test series [%].

Table 4.1 The load carrying capacities of the shear test pieces.

Tests	α	β	γ	F_{max} [kN]	V_{max} [kN]	V_{red} [kN]	s [%]
W1A 4-6	0	0	0	22.40	22.40	24.27	2.41
W1B 4-6	45	0	45	21.84	21.84	23.67	7.58
W1C 4-6	90	0	90	19.94	19.94	21.60	4.61
W2A 1-3	0	23	23	22.89	22.89	23.38	3.14
W2B 1-3	45	23	67	19.65	19.65	20.07	0.82
W2C 1-3	90	23	67	21.09	21.09	21.54	2.54
W3A 1,2	0	45	45	25.79	20.63	21.23	1.48
W3B 1,3	45	45	90	22.69	18.15	18.49	2.09
W3C 2,3	90	45	45	26.19	20.95	21.28	3.70
W4A 1-3	0	90	90	22.25	17.80	18.18	1.31
W4B 1-3	45	90	45	24.36	19.49	19.91	3.49
W4C 1-3	90	90	0	26.11	20.89	21.34	4.40
F1A 4-6	0	0	0	19.16	19.16	20.76	2.67
F1B 4-6	45	0	45	16.63	16.63	18.02	3.01
F1C 4-6	90	0	90	18.15	18.15	19.67	4.36
F2A 1-3	0	23	23	20.60	20.60	21.04	3.50
F2B 1-3	45	23	67	19.52	19.52	19.94	2.45
F2C 1-3	90	23	67	20.68	20.68	21.12	3.94
F3A 1-3	0	45	45	23.95	19.16	19.57	6.90
F3B 1-3	45	45	90	23.36	18.69	19.09	6.60
F3C 1-3	90	45	45	23.46	18.77	19.17	9.04
F4A 1-3	0	90	90	21.98	17.58	17.95	4.03
F4B 1-3	45	90	45	21.31	17.05	17.42	3.32
F4C 1-3	90	90	0	22.90	18.32	18.71	5.05

The load carrying capacities of the shear test pieces have been calculated by the Eurocode 5 method and by the plastic theory. These maximum shear loads (V_{cal}) have been calculated by the mean anchorage strength values ($f_{a,\alpha\beta,m}$) from the design criteria's 4.6 (EUROCODE 5) and 4.7 (CIB-W18, PAPER 25-14-1).

$$\begin{cases} \tau_F \leq f_{a,\alpha\beta,m} \\ \tau_{M,el} = 2f_{a,9090,m} \\ \tau_F + \tau_{M,el} \leq 1.5f_{a,00,m} \end{cases} \quad (4.6)$$

$$\boxed{\left(\tau_F/f_{a,\alpha\beta,m}\right)^2 + \left(\tau_{M,pl}/f_{a,00,m}\right)^2 \leq 1} \quad (4.7)$$

The main mean anchorage strengths and the strength constants of the W-nailplate and the FIX-nailplate are shown in table 4.2. The dependence of the anchorage strength on the α - and β -directions has been taken into account according to the Eurocode 5 (D6.4). The mean anchorage strength values have been determined both by the earlier standard tension test results and by the additional tension test series of plate sizes 96 x 100 mm² (W) and 100 x 100 mm² (FIX) loaded in this study. The loading directions were (α,β) = (0°,0°); (0°,23°); (30°,0°); (30°,15°); (30°,30°); (30°,60°); (45°,23°) and (60°,23°) in the additional test series. The results of these tension test series have been reported in paper: CIB-W18 25-14-2.

Table 4.2 Mean anchorage strengths and strength constants used in analysis.

Plate	$f_{a,00,m}$ [N/mm ²]	$f_{a,9090,m}$ [N/mm ²]	k_1	k_2	α_0
W-plate	4.20	2.52	0.015	-0.035	40°
FIX-plate	3.50	2.45	-0.002	-	90°

4.3 Analysis of the results

The relations of the reduced shear test results and calculated capacities (V_{red}/V_{cal}) are shown in Table 4.3. The relation is close to value 1.0, if the agreement between theory and tests is good. In analysis of the shear tests by Eurocode 5 method the sum of stresses τ_F and τ_M was the critical factor in each case. The calculated plastic theoretical capacities are presented both by Norèns simplified method and by the accurate theoretical solution.

The tM design method given in ENV-Eurocode 5 seems to be conservative in cases where the loading direction was parallel to the grain ($\beta = 0^\circ$). The calculated mean capacities of test pieces were 25 % percent smaller by EC 5 method than by the accurate plastic theory. This result has been obtained also in the authors earlier CIB-W18 paper, where 220 standard shear tests results were analysed (CIB-W18 25-14-1). The method of EC 5 does not take into account the β -angle. There fore the calculated capacities may also be on the unsafe side, when β is close to 90° . The test results show very clearly that the grain direction has a significant effect on the joint capacities. According to the test results the capacity in loading direction $\beta = 90^\circ$ was $0.88 V_{max}$ of the test pieces loaded parallel to the grain ($\beta = 0^\circ$). In directions $\beta = 45^\circ$ and $\beta = 90^\circ$ the accurate plastic theory gave 6 % lower mean shear capacities of test pieces than the EC 5 method with the rectangle plate areas ($\alpha = 0^\circ$ and $\alpha = 90^\circ$). The variation range between the test results and the capacities calculated according to the EC 5 is rather high; from the relation 0.86 to 1.44, while the mean value was 1.13 and the standard deviation $s = 0.129$.

The plastic theoretical method gives more accurate results than the EC 5 method, because now both a and b angles are included. According to the Norèns simplification, calculated capacities are generally at the same level than the test results; the mean value of relations V_{red}/V_{cal} was 1.07 and the standard deviation was 0.080. In plate directions $\alpha = 45^\circ$ the Norèns method was somewhat conservative (12 %), but not so much than the EC 5 method (26 %). The difference between Norèns simplification and the accurate theoretical solution is biggest, when the effective plate areas are triangles.

The accurate plastic theoretical solution corresponded very well with the test results; the mean value of relations V_{red}/V_{cal} was 1.02. Some individual maximum test loads were slightly lower than the theoretical capacities, but these differences are explained by the normal variation of test results and by the used interpolated mean anchorage strengths ($f_{a,\alpha\beta,m}$). The standard deviation between this plastic theory and the tests results was 7.5 %.

Table 4.3 The shear test results and the comparison with the theories.

Shear tests 6-11.1992 VTT/RAT

Plate b x a	Directions		Test results				Eurocode 5		Plastic, Norens meth.		Plastic, theoretically		
	α	β	γ	τ_F	$\tau_{M,el}$	$\tau_{M,pl,Norens}$	$\tau_{M,pl,theor}$	Vcal	Vred/Vcal	Vcal	Vred/Vcal	Vcal	Vred/Vcal
W-plate 96x100	0	0	0	2.89	4.32	2.88	2.74	21.22	1.14	24.99	0.97	25.60	0.95
	45	0	45	2.96	6.08	3.79	2.97	16.49	1.44	21.39	1.11	24.80	0.95
	90	0	90	2.56	4.07	2.71	2.56	20.54	1.05	20.41	1.06	20.84	1.04
	0	23	23	2.78	4.16	2.77	2.64	21.22	1.10	22.78	1.03	23.23	1.01
	45	23	67	2.51	5.16	3.22	2.52	16.49	1.22	19.32	1.04	21.74	0.92
	90	23	67	2.55	4.06	2.70	2.56	20.54	1.05	19.25	1.12	19.58	1.10
	0	45	45	2.53	3.78	2.52	2.40	21.22	1.00	20.59	1.03	20.92	1.01
	45	45	90	2.31	4.76	2.96	2.31	16.49	1.12	17.75	1.04	19.59	0.94
	90	45	45	2.52	4.01	2.67	2.53	20.54	1.04	17.96	1.18	18.27	1.16
	0	90	90	2.17	3.23	2.15	2.05	21.22	0.86	18.17	1.00	18.40	0.99
	45	90	45	2.49	5.12	3.19	2.50	16.49	1.21	15.99	1.25	16.65	1.15
	90	90	0	2.53	4.02	2.68	2.53	20.54	1.04	17.96	1.19	18.27	1.17
FIX 100x100	0	0	0	2.36	3.63	2.42	2.30	18.21	1.14	21.51	0.97	22.05	0.94
	45	0	45	2.15	4.36	2.76	2.16	14.54	1.24	17.86	1.01	20.36	0.89
	90	0	90	2.24	3.44	2.29	2.17	18.21	1.08	20.94	0.94	21.49	0.92
	0	23	23	2.39	3.68	2.45	2.33	18.21	1.16	20.16	1.04	20.61	1.02
	45	23	67	2.38	4.82	3.05	2.38	14.54	1.37	16.74	1.19	18.81	1.06
	90	23	67	2.40	3.69	2.46	2.34	18.21	1.16	19.41	1.09	19.81	1.07
	0	45	45	2.22	3.42	2.28	2.16	18.21	1.07	18.89	1.04	19.26	1.02
	45	45	90	2.28	4.62	2.91	2.28	14.54	1.31	16.26	1.17	18.14	1.05
	90	45	45	2.17	3.35	2.23	2.12	18.21	1.05	17.52	1.09	17.84	1.07
	0	90	90	2.04	3.14	2.09	1.99	18.21	0.98	17.52	1.02	17.84	1.01
	45	90	45	2.08	4.21	2.66	2.08	14.54	1.20	15.28	1.14	16.81	1.04
	90	90	0	2.13	3.27	2.18	2.07	18.21	1.03	17.52	1.07	17.84	1.05
Mean value								18.21	1.13		1.07		1.02
Standard deviation s								18.21	6.129		0.080		0.077

5. MOMENT ANCHORAGE CAPACITY IN BENDING TESTS

KYRKJEEIDE, AUNE & AASHEIM (1992) have done a study for the moment anchorage capacity of nail plates. They have carried out 10 test series with 10 pieces in each series. The results of three bending test series (numbers 2, 7 and 8), where failure mode was the anchorage failure without timber contact, have been analyzed here.

The test pieces and the load arrangements are shown in Figures 5.1 and 5.2. The effective plate areas (shown in figures) and the shapes of nail plate surfaces were same in all these series, but the pieces of series number 7 had been made using higher density wood and the pieces of series number 8 were unsymmetrical. The nail plate was Hydro Nail PTN (Figure 5.3).

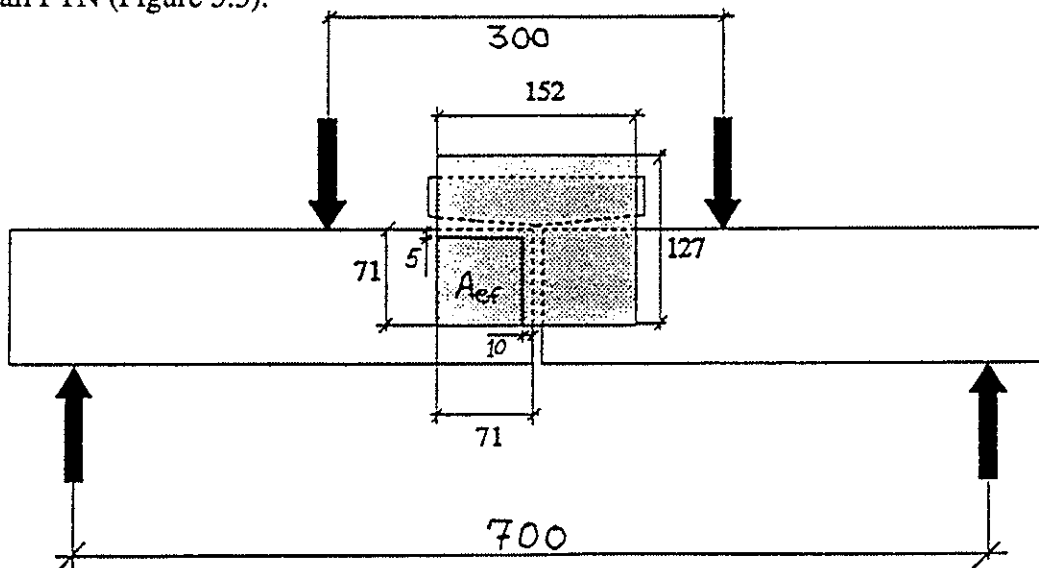


Figure 5.1 Test pieces and loading arrangements of series 2 and 7 (KYRKJEEIDE)

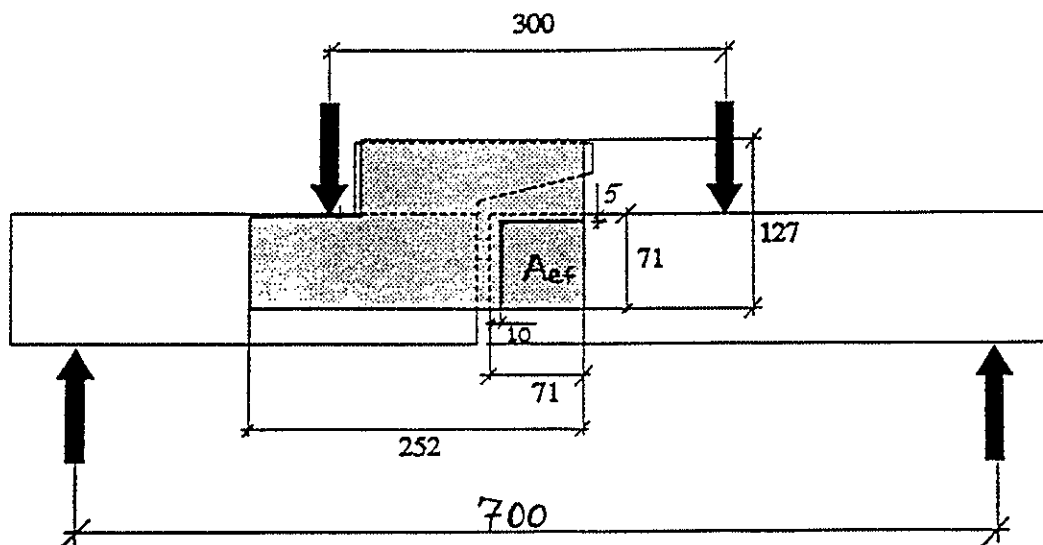


Figure 5.2 Test pieces and loading arrangements of series 8 (KYRKJEEIDE, 1992).

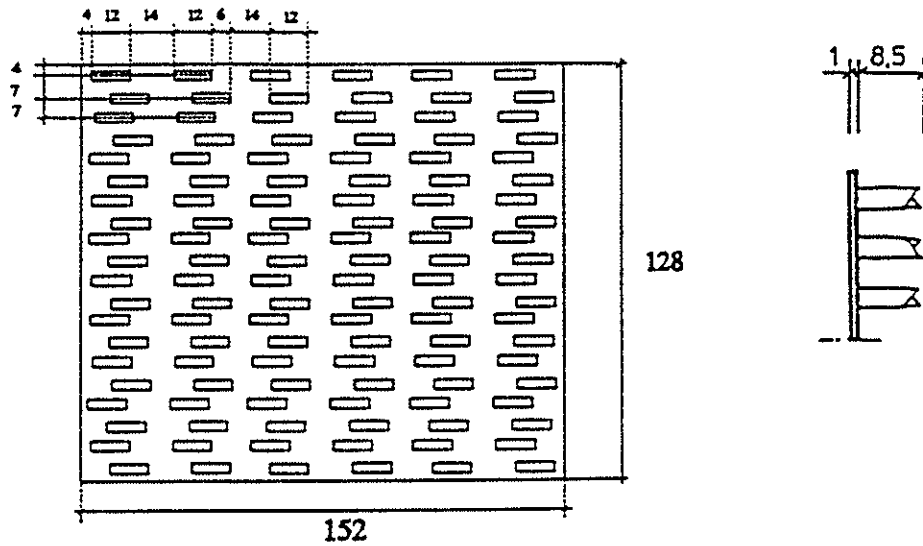


Figure 5.3 The geometry of the Hydro Nail PTN-nailplate.

The mean values of the bending test results are shown in Table 5.1. The reduced values (τ_{red}) have been made comparable by reducing the mean values of the test series to the compression strength 35 MPa by equations (4.1) and (4.2). The test specimens were loaded by pure bending i.e. force anchorage stress $\tau_F = 0$. The presented moment anchorage stresses τ_M have been calculated from the reduced mean bending moment capacities (M_{red}) by equation (4.4) of the elastic theory ($\tau_{M,el}$), by equation (4.5) of the simplified plastic theory ($\tau_{M,pl,Norén}$) and by the accurate plastic theory ($\tau_{M,pl,theor}$).

The calculated capacities of the test series are shown in Table 5.2. The calculations have been done using the mean anchorage strengths (reduced to density 360 kg/m³ and moisture content 15 %) with the Eurocode 5 method by equation (4.6) and with the plastic theory by equation (4.7). According to 10 tension tests carried out by KYRKJEEIDE, AUNE & AASHEIM (1992) the mean reduced anchorage strength $f_{a,00,m}$ of the Hydro Nail PTN -plate is 3.39 N/mm². As the anchorage strength $f_{a,9090,m}$ is used a value 2.37 N/mm², because the constant $c = 0.3$ for Hydro Nail PTN -plate (KYRKJEEIDE).

Table 5.1 Bending test series 2, 7 and 8; and the test results.

Test series	n	A_{ef} [mm ²]	$\rho_{0\omega}$ [kg/m ³]	ω [%]	M_{max} [kNm]	M_{red} [kNm]	$\tau_{M,el}$ [MPa]	$\tau_{M,pl,Norén}$ [MPa]	$\tau_{M,pl,theor}$ [MPa]
2	10	4026	390	13.1	0.84	0.77	6.38	4.25	3.94
7	10	4026	468	12.9	0.97	0.81	6.72	4.48	4.16
8	10	4026	388	12.6	0.98	0.88	7.30	4.86	4.51

This comparison shows that all these theories are conservative in the pure bending case ($\tau_F = 0$). The test results were 1.44 times higher than the calculated capacities by Eurocode 5 method. The accurate plastic theory is in closest agreement with the test results, but also there the test results were 17 - 33 % higher than the calculated capacities using the mean anchorage strengths. **The moment anchorage strength is clearly higher than the maximum tension anchorage strength, although the τ_M - stress is determined by the plastic theory.**

Table 5.2 The comparison between the test results and the theories.

Test series	Test results	Eurocode 5		Plastic, Norens meth.		Plastic, theoretically	
	M_{red} [kNm]	M_{cal} [kNm]	M_{red}/M_{cal}	M_{cal} [kNm]	M_{red}/M_{cal}	M_{cal} [kNm]	M_{red}/M_{cal}
2	0.77	0.572	1.35	0.613	1.26	0.660	1.17
7	0.81	0.572	1.42	0.613	1.32	0.660	1.23
8	0.88	0.572	1.54	0.613	1.44	0.660	1.33

6. CONCLUSIONS

This analysis, with the new kinds of shear and bending test pieces, supports the authors earlier conclusion, that the plastic theoretical τ_M design corresponds better with the test results and would be a better method than on the elastic theory based method given in ENV-Eurocode 5. The capacities of the shear test pieces were almost identically same than the values calculated by the accurate plastic theory. The simplified method presented by Norèn is always on the safe side and it gives generally some percents additional safety. Same safety level is obtained also by the new simplified method, which does not have geometrical limitations, presented by KEVARINMÄKI in CIB-W18 26-14-4. In pure bending case also the plastic theory was 17 - 33 % conservative (while it was 35 - 54 % by the EC 5 method). According to the bending test results the moment anchorage strength τ_M is higher than the tension anchorage strength in the direction $\alpha = \beta = 0^\circ$ ($f_{a,00}$).

The design is easier and clearer by the simplified plastic theory than by the method of ENV-EC 5. The geometrical values of the elastic method (I_p and r_{max}) are more difficult to determine than the diagonal d needed for the plastic design. There are three design criteria's that must be checked in the anchorage design of EC 5. In plastic design method only one design criteria is required: $(\tau_F/f_{a,\alpha\beta,d})^2 + (\tau_M/f_{a,00,d})^2 \leq 1$. This equation also has a similar form than many other design formulas of Eurocode 5.

7. REFERENCES

CIB W18, Warsaw 1981. Paper 14-7-1: Norèn, B., Design of Joints with Nail Plates. 39 p.

CIB W18, Beit Oren 1985. Paper 18-7-4: Kangas, J., A Detailed Testing Method for Nail Plate Joints. 8 p.

CIB W18, Åhus 1992. Paper 25-14-1: Kevarinmäki, A. & Kangas, J., Moment Anchorage Capacity of Nail Plates in Shear Tests. 13 p.

CIB W18, Åhus 1992. Paper 25-14-2: Kangas, J. & Kevarinmäki, A., Design Values of Anchorage Strength of Nail Plate Joints by 2-curve Method and Interpolation. 10 p.

CIB W18, Athens 1993. Paper 26-14-4: Kevarinmäki, A., Solution of Plastic Moment Anchorage Stress in Nail Plates. 10 p.

EUROCODE No. 5 - Design of Timber Structures, Part 1-1: 1992, Annex D: The Design of Trusses with Punched Metal Plate Fasteners. 100 p.

Kyrkjeide, O., (Aune, P. & Aasheim, E.), Spikerplater med momentpåkjenning. Universitet i Trondheim, 1992. 85 p.

INTERNATIONAL COUNCIL FOR BUILDING RESEARCH STUDIES AND DOCUMENTATION
WORKING COMMISSION W18 - TIMBER STRUCTURES

ROTATIONAL STIFFNESS OF NAIL PLATES
IN MOMENT ANCHORAGE

by

A Kevarinmäki
Helsinki University of Technology

J Kangas
Technical Research Centre of Finland (VTT)
Finland

MEETING TWENTY - SIX

ATHENS, GEORGIA

USA

AUGUST 1993

1. INTRODUCTION

Application of moment resisting rigid or semi-rigid nail plate joints in timber structures is missing at present. Including rotational stiffness and moment capacity into nail plate joint design opens following possibilities:

- it will lead to material savings and more economical nail plate structures.
- it will give more accurate and safer design in ordinary structures compared to pin joint theory.
- it enables the design of new kinds of structures, which will increase the competitiveness of the timber structures.

This kind of exact theory and design method is missing at present. In Finland the method where the moment rigidity of nail plate joints has been included is already in use, but it has simplified assumptions of material properties, which are on the safe side. ENV-Eurocode 5 is very general and insufficient. Concerning these matters measuring and determination of the nail plate joints rotational stiffness is not presented in any standard. That is the main obstacle in utilization of the nail plate joint rotational stiffness. The aim of this study was to develop a proposal for standard tests of nail plates rotational stiffness and a method for the determination of the rotational spring stiffness moduli.

In this paper the rotational stiffness of shear and bending test results of 102 nail plate joints have been analysed. The deformations between timber and the nail plates in each shear test were measured by 10 gauges. The rotational spring stiffness moduli have been calculated from these measurements. Rotational stiffnesses have been determined also from the results of Norwegian bending tests. This study showed following:

- the effect of the testing type,
- the effect of direction angles α and β ,
- the dependence on the shape of effective nail plate areas and
- the effect of the measuring point locations to the calculated results of rotational stiffness.

Based on this research a proposal for the standard test of nail plates rotational stiffness and a method for the determination of the rotational spring stiffness modulus $K_{\varphi,ser}$ from the test results are given.

2. SYMBOLS

A_{ef}	Effective nail plate area (the area of timber member covered by nail plate is reduced by 5 mm from its edges and by 10 mm from the end of the member in grain direction when it is loaded in tension) [mm ²]
F_{max}	Maximum applied load during a test [kN]
$K_{F,\alpha\beta}$	Displacement modulus in the direction combination a and b [N/mm ²]
K_{φ}	Rotational spring stiffness modulus [Nmm ⁻² rad ⁻¹]
M	Bending moment [kNm]
V	Shear force [kN]
l	Distance [mm]
n	Number of test pieces in different series
α	Angle between the force and the main direction of the nail plate [°]
β	Angle between the force and the grain direction [°]
γ	Angle between the main direction of the nail plate and the grain direction [°]
δ	Deformation [mm]
θ	Rotation angle [rad]
τ_F	Anchorage stress from force acting on the centroid of effective area
τ_M	Anchorage stress from moment acting on the centroid of effective area

Subscripts:

el	τ_M stress is calculated by elastic theory
pl	τ_M stress is calculated by plastic theory
max	Mean value of the test series by the maximum values of test piece
red	Reduced mean value to the compression strength of 35 MPa

3. ROTATIONAL STIFFNESS IN SHEAR TESTS

3.1 Tests and measurements

The shear test pieces and the testing procedure have been presented by the authors in paper CIB-W18 26-14-2. The deformations of nail plates in anchorage of each shear test piece has been measured between the nail plate and timber member by four gauges from both sides of the test piece, see Figure 3.2. Also the total shear deformation in the joint line has been measured from both sides of the test pieces. These measured deformations are presented here as mean values of the both sides. An example of these measured mean deformations by 10 gauges is shown in Figure 3.1.

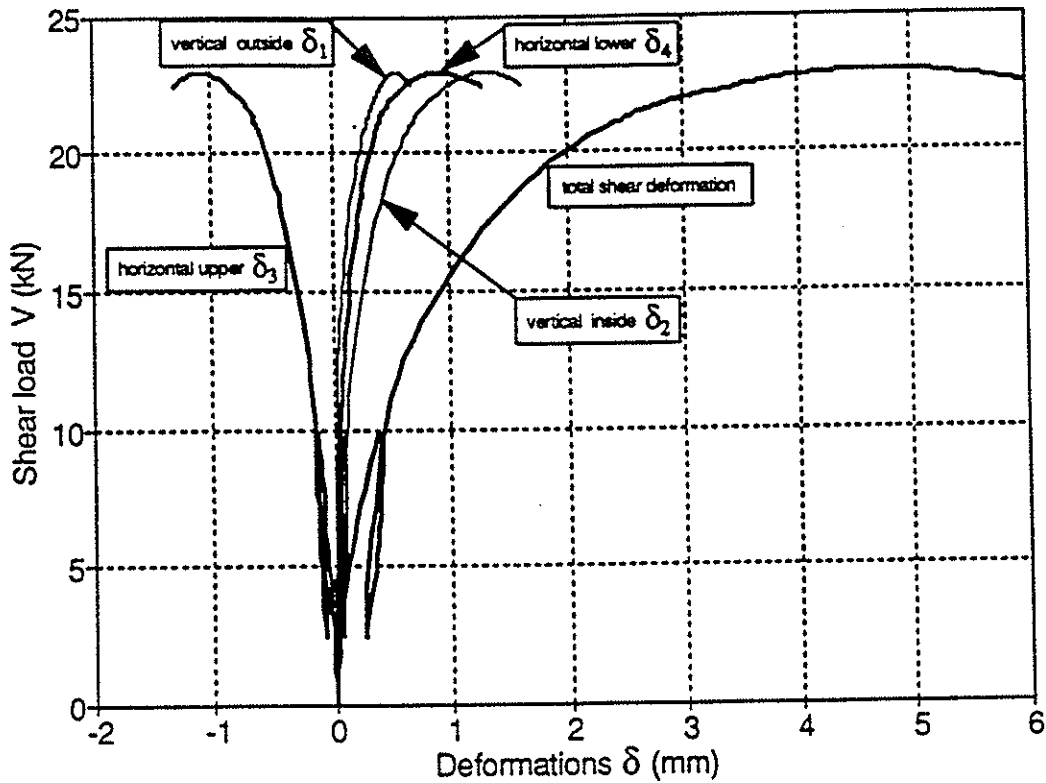


Figure 3.1 Measured mean deformations of test piece W1A4.

3.2 Calculation of the rotational spring stiffness modulus

The rotation angles (θ) in anchorage have been calculated from measured horizontal (h) and vertical (v) deformations by equations (3.1) and (3.2). An example of calculated τ_M versus θ dependences are shown in Figure 3.3.

$$\theta_v = (\delta_2 - \delta_1) / l_1 \quad [rad] \quad (3.1)$$

$$\theta_h = (\delta_4 - \delta_3) / l_2 \quad [rad] \quad (3.2)$$

where δ_1 , δ_2 , δ_3 and δ_4 are the measured deformations according to Figure 3.5

l_1 is the horizontal distance between vertical gauges (20 mm)

l_2 is the vertical distance between horizontal gauges (70, 75 or 80 mm).

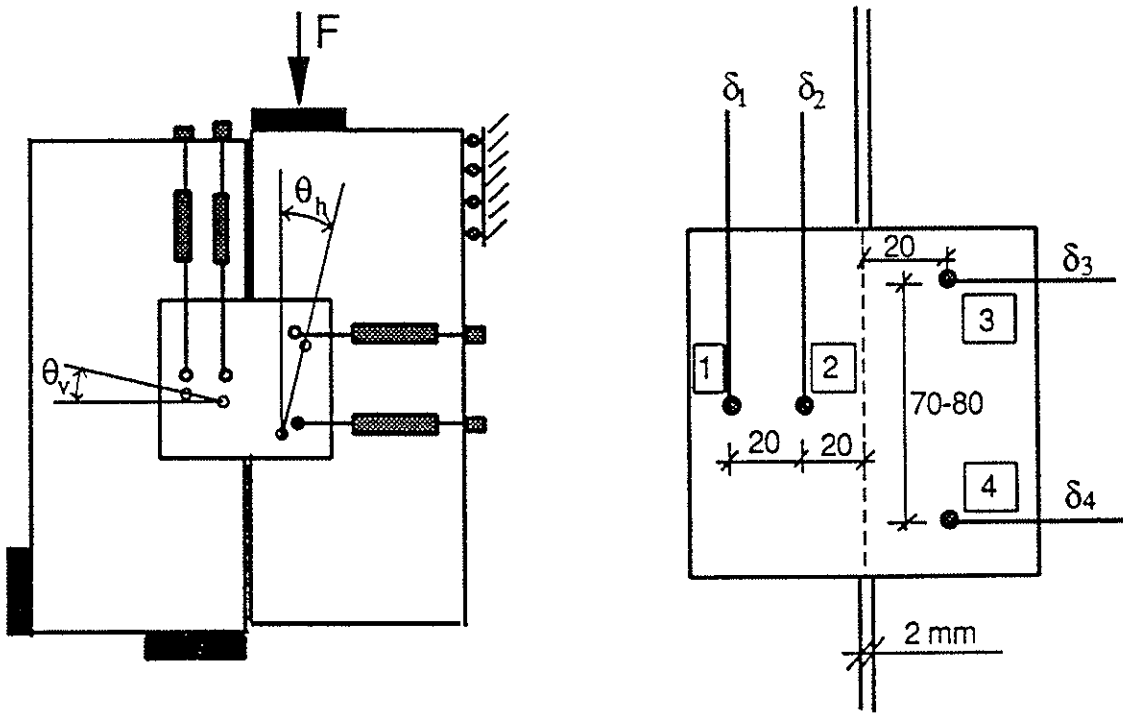


Figure 3.2 Locations and symbols of measuring points in nail plates.

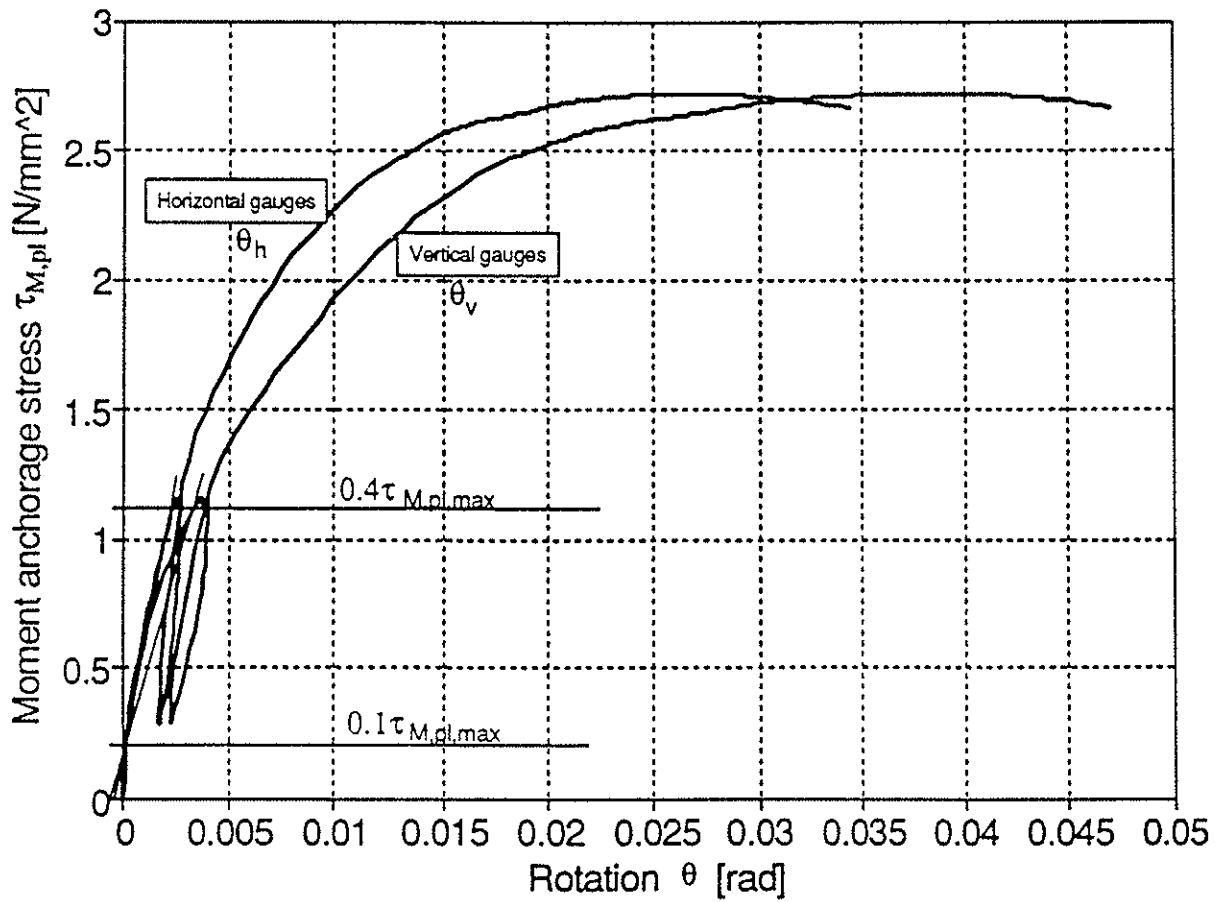


Figure 3.3 Measured τ_M versus θ -dependences in test piece W1A4.

The rotational spring stiffness moduli (K_φ) have been calculated by secant moduli from the changes of the rotation angles between moment anchorage stresses $0.1 \tau_{M,max}$ and $0.4 \tau_{M,max}$ ($\tau_{M,max}$ is the moment anchorage capacity in testing). This determination has been done with both, the horizontal and the vertical measurements, of the initial loading phase (Figure 3.3). The rotational spring stiffness modulus is

$$K_\varphi = 0.4 \tau_{M,max} / \theta_{i,mod} \quad (3.3)$$

where $\tau_{M,max}$ is elastic or plastic moment anchorage stress on the test load F_{max}
 $\theta_{i,mod} = 4/3 (\theta_{04} - \theta_{01})$
 θ_{04} is rotation angle by horizontal or vertical gauges with test load $0.4 F_{max}$
 θ_{01} is rotation angle by horizontal or vertical gauges with test load $0.1 F_{max}$

The rotational spring stiffness moduli have been calculated also from the measurements of the total shear deformations of the joint line. The measured total slip δ has been divided to the slip component δ_F caused by the force and to the slip component δ_M caused by the moment (Figure 3.4). The analysis has been done with the measured slips (δ) between loading points $0.1 F_{max}$ and $0.4 F_{max}$. The moment slip of joint line from rotation of nail plate has been calculated from

$$\delta_M = 1/2 (\delta_{i,mod} - 2\delta_F), \quad (3.4)$$

where $\delta_{i,mod} = 4/3 (\delta_{04} - \delta_{01})$
 δ_{04} is measured total shear slip of joint line at loading point $0.4 F_{max}$
 δ_{01} is measured total shear slip of joint line at loading point $0.1 F_{max}$

$$\delta_F = 0.4 V_{max} / (2A_{ef} K_{F,\alpha\beta}) \quad (3.5)$$

The mean value of the displacement modulus $K_{F,\alpha\beta}$ has been determined from the anchorage tension test results for the effective nail plate area:

$$K_{F,\alpha\beta} = 0.4 F_{max} / (A_{ef} \delta_{t,i,mod}), \quad (3.6)$$

where $\delta_{t,i,mod}$ is the modified total joint slip calculated from the measured slips of tension tests between the loading points $0.1 F_{max}$ and $0.4 F_{max}$.

The mean translational stiffness moduli of the tension test pieces loaded in this study are shown in table 3.1. Stiffness constants calculated from earlier standard anchorage test results of W- and FIX-plate have also been included from following loading directions: $(\alpha,\beta) = (45,0), (90,0), (0,45), (0,90)$ and $(90,90)$. Like strength values the $K_{F,\alpha\beta}$ values were reduced to the density and moisture content of the shear test pieces according to authors paper CIB-W18 26-xx-x.

Rotation angles $\theta_{i,mod}$ have been calculated from the total shear deformations of the shear test pieces. They have been determined using eccentricities e between joint line and the centre of gravity of the effective plate area:

$$\theta_{i,mod} = \delta_M / e \quad [rad] \quad (3.7)$$

The rotational spring stiffness moduli may be now solved by equation (3.3).

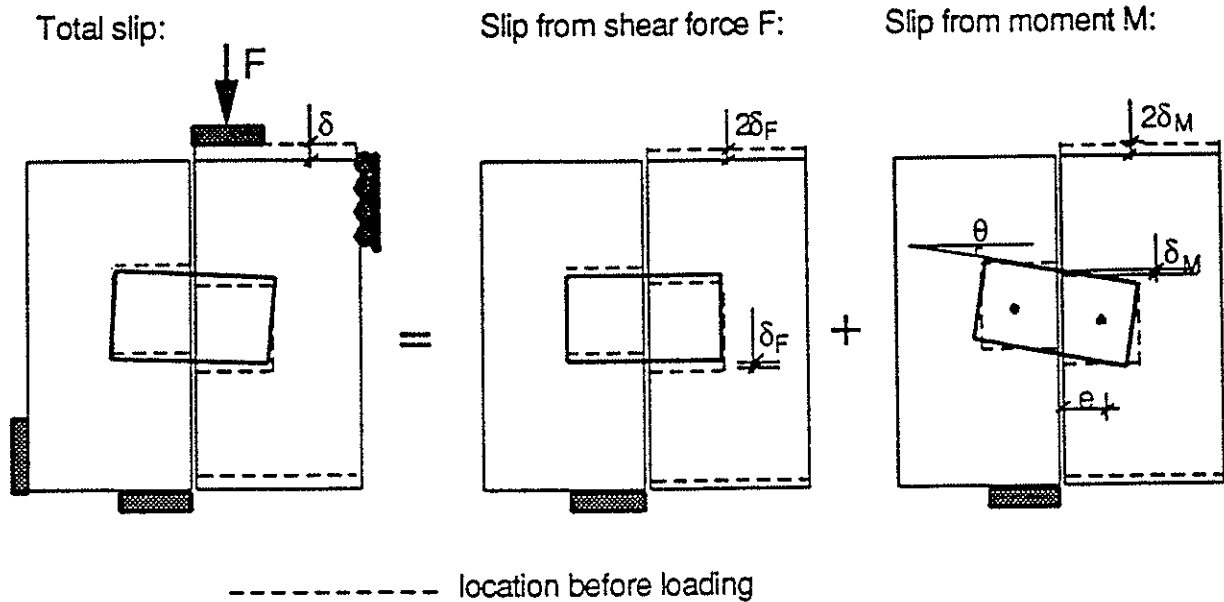


Figure 3.4 Dividing of measured total shear slip (δ) to force (δ_F) and moment slip (δ_M) components.

Table 3.1 Mean translational stiffness moduli $K_{F,\alpha\beta}$ of the tension test series.

Test pieces	n	α	β	γ	$0.4 F_{max}$ [kN]	$K_{F,\alpha\beta}$ [N/mm ²]	$K_{F,red}$ [N/mm ²]
W0A 1-6	6	0	0	0	11.81	8.27	8.92
W1,4 a)-j)	10	30	0	30	12.42	14.70	14.30
W2 a)-e)	5	30	15	15	11.28	20.28	19.59
W5A 1-6	6	0	23	23	11.18	13.79	14.88
W7B 1-6	6	45	23	23	9.01	12.61	13.60
W6B 1-6	6	45	23	67	9.69	16.66	17.97
W3 a)-e)	5	30	30	0	8.10	14.34	13.84
W6 f)-j)	5	60	30	90	7.63	17.78	17.44
W5 f)-j)	5	30	90	60	6.62	12.55	12.31
F0A 1-6	6	0	0	0	9.20	8.25	8.90
F5A 1-6	6	0	23	23	8.72	14.32	15.45
F7B 1-6	6	45	23	23	8.71	18.51	19.97
F6B 1-6	6	45	23	67	8.74	15.39	16.60

3.3 Rotational spring stiffness moduli of the shear test pieces

The calculated elastic $K_{\varphi,el}$ and plastic $K_{\varphi,pl}$ spring moduli are shown in tables 3.2 - 3.8. The $K_{\varphi,h}$ values have been solved from the horizontal measurements between the nail plate and timber member and the $K_{\varphi,v}$ values from the vertical measurements. Rotational stiffness moduli $K_{\varphi,el}$ calculated from the total shear slip are presented also graphically in Figure 3.5. The rotational moduli $K_{\varphi,el}$ have been determined with τ_M -stresses calculated by the elastic theory. In this case the rotational stiffness moduli are 1.5 times higher in plate direction $\alpha = 0^\circ$ and 90° and 1.6 times higher in direction $\alpha = 45^\circ$ than values calculated by the plastic theory ($\varphi_{pl} = \varphi_{el} \tau_{M,pl} / \tau_{M,el}$).

The test pieces loaded in parallel to the grain ($\beta = 0^\circ$) had the lowest K_φ values by the measurements of the vertical gauges (mean value 82 % from horizontal measurements). Rotational stiffness moduli K_φ calculated from the total shear slips were rather near to the mean value of the $K_{\varphi,h}$ and $K_{\varphi,v}$ stiffnesses. This means that no significant deformations occurred in the nail plates at the joint line. The lowest rotational stiffness in this grain direction was obtained in plate direction $\alpha = 90^\circ$.

Table 3.2 Rotational stiffness moduli with elastic $\tau_{M,el}$ in loading direction $\beta = 0^\circ$

Test pieces	α	$K_{F,red}$ N/mm ³	$0.4F_{max}$ kN	τ_F N/mm ²	$\tau_{M,el}$ N/mm ²	$K_{\varphi,h,el}$ Nmm ⁻² rad ⁻¹	$K_{\varphi,v,el}$ Nmm ⁻² rad ⁻¹	$\delta_{i,mod}$ mm	$K_{\varphi,el}$ Nmm ⁻² rad ⁻¹
W1A 4-6	0	8.23	8.96	1.067	1.595	774	425	0.396	621
W1B 4-6	45	13.54	8.74	1.093	2.244	806	647	0.296	899
W1C 4-6	90	8.16	7.98	0.945	1.502	586	611	0.375	587
F1A 4-6	0	8.21	7.66	0.871	1.340	437	334	0.404	392
F1B 4-6	45	12.97	6.65	0.794	1.609	572	534	0.282	564
F1C 4-6	90	6.70	7.26	0.827	1.358	333	314	0.466	347

Table 3.3 Rotational stiffness moduli with plastic $\tau_{M,pl}$ in loading direction $\beta = 0^\circ$

Test pieces	α	$K_{F,red}$ N/mm ³	$0.4F_{max}$ kN	τ_F N/mm ²	$\tau_{M,pl}$ N/mm ²	$K_{\varphi,h,pl}$ Nmm ⁻² rad ⁻¹	$K_{\varphi,v,pl}$ Nmm ⁻² rad ⁻¹	$\delta_{i,mod}$ mm	$K_{\varphi,pl}$ Nmm ⁻² rad ⁻¹
W1A 4-6	0	8.23	8.96	1.067	1.063	516	283	0.396	414
W1B 4-6	45	13.54	8.74	1.093	1.403	504	404	0.296	562
W1C 4-6	90	8.16	7.98	0.945	1.001	391	407	0.375	392
F1A 4-6	0	8.21	7.66	0.871	0.893	291	223	0.404	261
F1B 4-6	45	12.97	6.65	0.794	1.016	362	338	0.282	356
F1C 4-6	90	6.70	7.26	0.827	0.905	222	209	0.466	231

The rotational stiffness moduli $K_{\phi,h}$ were much higher than the $K_{\phi,v}$ values determined by the vertical gauges in shear tests loaded in $\beta = 23^\circ$ direction (mean value was 5.5-times higher). The stiffness moduli K_{ϕ} calculated from the total shear slip were about 15 % lower than $K_{\phi,v}$ values. Calculated K_{ϕ} moduli were generally almost same than in loading direction $\beta = 0^\circ$ (between mean values the difference is only 1 %).

Table 3.4 Rotational stiffness moduli with elastic $\tau_{M,el}$ in loading direction $\beta = 23^\circ$

Test pieces	α	$K_{F,red}$ N/mm ³	$0.4F_{max}$ kN	τ_F N/mm ²	$\tau_{M,el}$ N/mm ²	$K_{\phi,h,el}$ Nmm ⁻² rad ⁻¹	$K_{\phi,v,el}$ Nmm ⁻² rad ⁻¹	$\delta_{i,mod}$ mm	$K_{\phi,el}$ Nmm ⁻² rad ⁻¹
W2A 1-3	0	14.57	9.16	1.089	1.629	0.00202	807	0.309	551
W2B 1-3	45	17.60	7.86	0.983	2.021	0.00220	919	0.241	847
W2C 1-3	90	14.23	8.44	0.999	1.587	0.00192	828	0.283	623
F2A 1-3	0	15.13	8.24	0.936	1.441	0.00363	397	0.368	330
F2B 1-3	45	16.25	7.81	0.932	1.888	0.00356	531	0.293	593
F2C 1-3	90	15.02	8.27	0.940	1.445	0.00311	465	0.314	429

Table 3.5 Rotational stiffness moduli with plastic $\tau_{M,pl}$ in loading direction $\beta = 23^\circ$

Test pieces	α	$K_{F,red}$ N/mm ³	$0.4F_{max}$ kN	τ_F N/mm ²	$\tau_{M,pl}$ N/mm ²	$K_{\phi,h,pl}$ Nmm ⁻² rad ⁻¹	$K_{\phi,v,pl}$ Nmm ⁻² rad ⁻¹	$\delta_{i,mod}$ mm	$K_{\phi,pl}$ Nmm ⁻² rad ⁻¹
W2A 1-3	0	14.57	9.16	1.089	1.086	0.00202	538	0.309	367
W2B 1-3	45	17.60	7.86	0.983	1.263	0.00220	573	0.241	529
W2C 1-3	90	14.23	8.44	0.999	1.058	0.00192	552	0.283	415
F2A 1-3	0	15.13	8.24	0.936	0.961	0.00363	265	0.368	220
F2B 1-3	45	16.25	7.81	0.932	1.195	0.00356	336	0.293	375
F2C 1-3	90	15.02	8.27	0.940	0.963	0.00311	310	0.314	286

The lowest $K_{\phi,h}$ stiffness was obtained in $\beta = 45^\circ$ direction. On the other hand $K_{\phi,v}$ moduli had clearly higher values than in the loading direction $\beta = 0^\circ$ or 23° . The stiffness moduli K_{ϕ} ($\beta = 45^\circ$) were however about 10 % higher than those in grain directions ($\beta = 0^\circ$) calculated from the total slip.

No sensible values were obtained for the rotational stiffness $K_{\phi,v}$ when the test pieces had been loaded perpendicularly to the grain $\beta = 90^\circ$ (some values would be even below zero). The stiffness moduli K_{ϕ} calculated from the measured total slips were however at the same level than in other tests except for series W4B ($\alpha = 45^\circ$) where the rotational stiffness was highest of all results.

Table 3.6 Rotational stiffness moduli with elastic $\tau_{M,el}$ in loading direction $\beta = 45^\circ$

Test pieces	α	$K_{F,red}$ N/mm ³	$0.4F_{max}$ kN	τ_F N/mm ²	$\tau_{M,el}$ N/mm ²	$K_{\phi,h,el}$ Nmm ⁻² rad ⁻¹	$K_{\phi,v,el}$ Nmm ⁻² rad ⁻¹	$\delta_{i,mod}$ mm	$K_{\phi,el}$ Nmm ⁻² rad ⁻¹
W3A 1,2	0	15.65	8.25	0.983	1.469	570	1305	0.2337	734
W3B 1,3	45	16.80	7.26	0.909	1.865	819	1896	0.2136	961
W3C 2,3	90	15.50	8.38	0.991	1.578	419	3210	0.2607	665
F3A 1-3	0	16.57	7.66	0.869	1.339	351	839	0.2633	473
F3B 1-3	45	17.80	7.48	0.893	1.809	322	1209	0.2776	571
F3C 1-3	90	16.45	7.51	0.850	1.312	213	947	0.3275	328

Table 3.7 Rotational stiffness moduli with plastic $\tau_{M,pl}$ in loading direction $\beta = 45^\circ$

Test pieces	α	$K_{F,red}$ N/mm ³	$0.4F_{max}$ kN	τ_F N/mm ²	$\tau_{M,pl}$ N/mm ²	$K_{\phi,h,pl}$ Nmm ⁻² rad ⁻¹	$K_{\phi,v,pl}$ Nmm ⁻² rad ⁻¹	$\delta_{i,mod}$ mm	$K_{\phi,pl}$ Nmm ⁻² rad ⁻¹
W3A 1,2	0	15.65	8.25	0.983	0.979	380	870	0.2337	489
W3B 1,3	45	16.80	7.26	0.909	1.164	512	1185	0.2136	601
W3C 2,3	90	15.50	8.38	0.991	1.052	279	2140	0.2607	443
F3A 1-3	0	16.57	7.66	0.869	0.893	234	559	0.2633	315
F3B 1-3	45	17.80	7.48	0.893	1.144	204	765	0.2776	361
F3C 1-3	90	16.45	7.51	0.850	0.875	142	631	0.3275	219

Table 3.8 Rotational stiffness moduli from total slip in loading direction $\beta = 90^\circ$

Test pieces	α	$K_{F,red}$ N/mm ³	$0.4F_{max}$ kN	τ_F N/mm ²	$\tau_{M,el}$ N/mm ²	$\tau_{M,pl}$ N/mm ²	$\delta_{i,mod}$ mm	$K_{\phi,el}$ Nmm ⁻² rad ⁻¹	$K_{\phi,pl}$ Nmm ⁻² rad ⁻¹
W4A 1-3	0	8.56	7.12	0.850	1.263	0.842	0.2929	723	482
W4B 1-3	45	13.80	7.80	0.975	2.003	1.251	0.1824	2638	1648
W4C 1-3	90	8.03	8.36	0.991	1.574	1.049	0.4299	482	321
F4A 1-3	0	8.58	7.03	0.799	1.229	0.819	0.3960	328	219
F4B 1-3	45	13.55	6.82	0.814	1.648	1.041	0.2765	590	373
F4C 1-3	90	8.76	7.33	0.834	1.281	0.854	0.4625	264	176

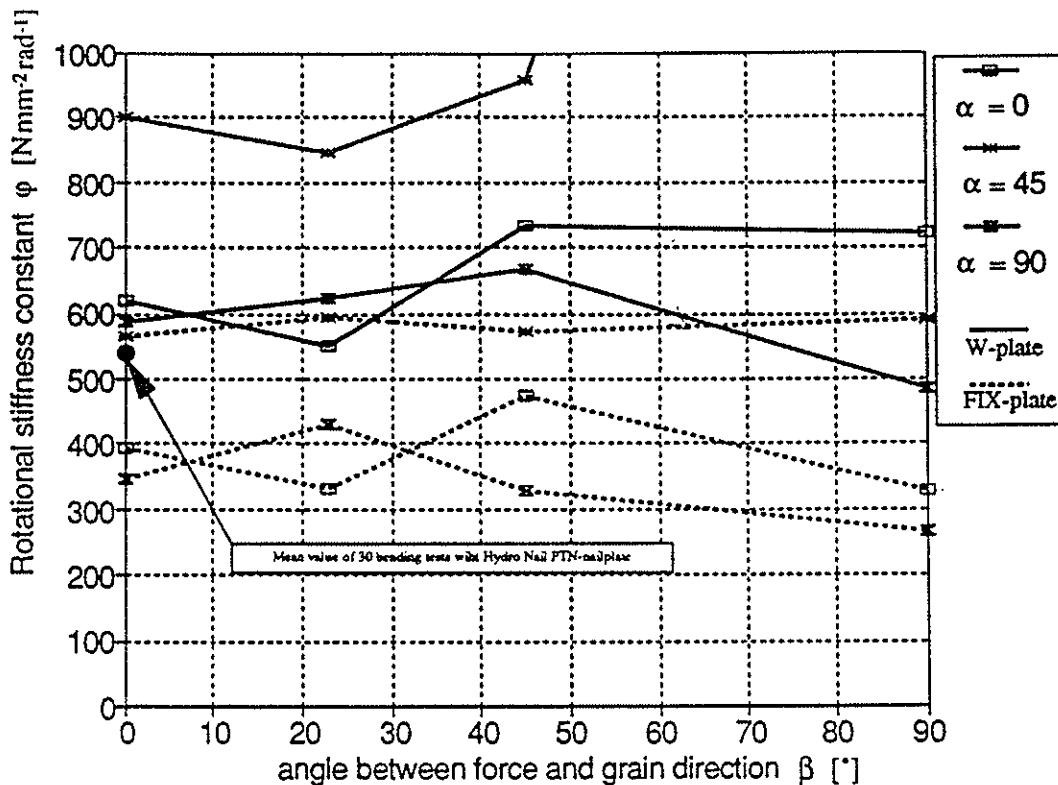


Figure 3.5 Rotational stiffness constants ϕ_{el} calculated from the total shear slip.

3.3 Conclusions from shear tests

Following conclusions may be drawn based on the analysis of shear test piece results:

- The rotational spring stiffness moduli may be calculated from the measured total shear slips of the joint line in all α and β directions. Measurements from the joint line ensures that the analysis is not distorted by local wood anisotropy.
- When loading direction is not parallel to the grain ($\beta \neq 0^\circ$) the measurements by the gauges between nail plate and timber member are not reliable for determination of rotational stiffness, because the deformations in wood perpendicular to grain may mix the result.
- The shape of the effective nail plate area has a significant effect on the measured rotational stiffness modulus. The highest values are obtained for the triangular plate shapes ($\alpha = 45^\circ$), because the τ_M stress is relatively high in the farthest corner of the triangle. The lowest rotation stiffness moduli are obtained when the effective anchorage area is square.
- The angle α itself has no significant effect on the rotational stiffness. Highest stiffness was obtained in direction $\alpha = 45^\circ$ (generally about 1.5-times higher value than in direction $\alpha = 0^\circ$) mainly because the shape of the plate area was triangular. In direction $\alpha = 90^\circ$ the rotational stiffness is generally only slightly lower than in direction $\alpha = 0^\circ$.
- The angle β has only small effect on the rotational stiffness; the lowest and almost similar values are obtained in directions $\beta = 0^\circ$ and $\beta = 90^\circ$.

4. ROTATIONAL STIFFNESS IN BENDING TESTS

The rotational stiffness in anchorage have been determined from bending test pieces of KYRKJEEIDE, AUNE & AASHEIM (1992). The test series presented in paper CIB-W18 26-xx-x have been analyzed here (three series with 10 test pieces in each). The location of measuring gauges is shown in Figure 4.1. The rotation angle with the moment has been calculated from measured deformations by KYRKJEEIDE. The rotation angle - moment dependences of test series 2 are shown in Figure 4.2.

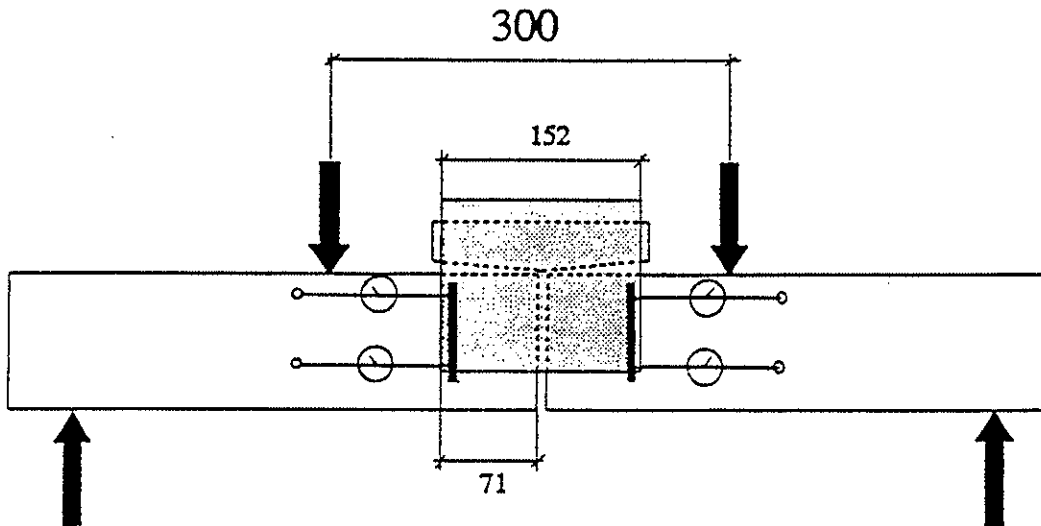


Figure 4.1 Locations of measuring gauges between nailplate and timber in bending tests

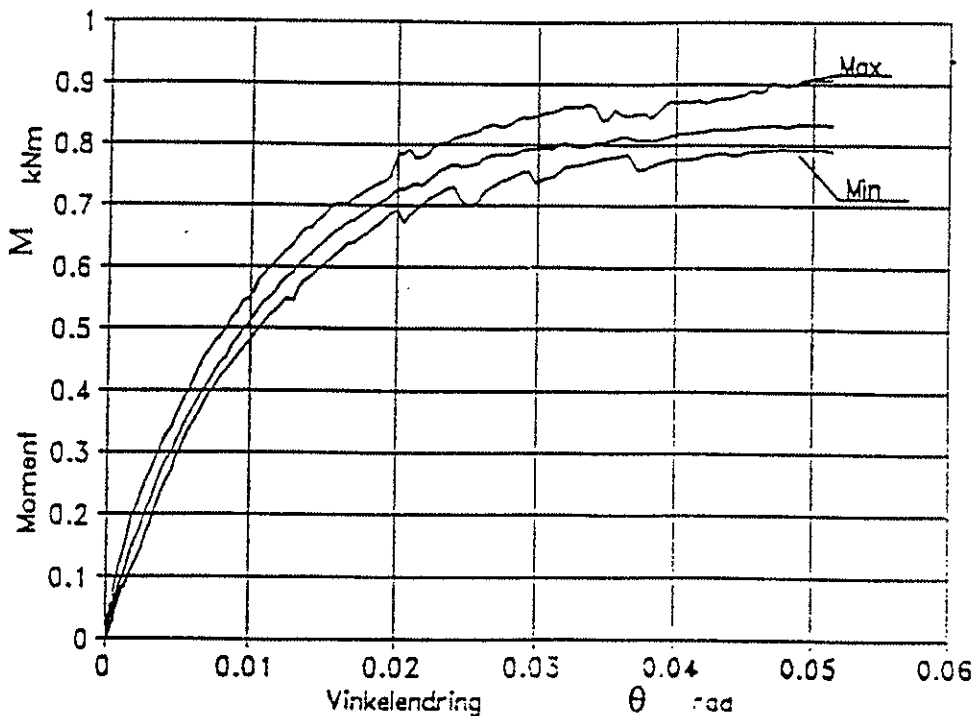


Figure 4.2 Rotation angle versus moment dependences of test series 2 (KYRKJEEIDE).

The rotational spring stiffness moduli (K_{φ}) have been solved according to equation (3.3) both by the elastic and plastic moment anchorage stress τ_M . The calculated rotational stiffness moduli are shown in Table 4.1.

Table 4.1 The rotational spring stiffness moduli of bending test series in anchorage.

Test series	$0.4 M_{\max}$ kNm	$0.4 \tau_{M,el,\max}$ N/mm ²	$\theta_{i,\text{mod}}$ rad	$K_{\varphi,el}$ N/(mm ² rad)	$K_{\varphi,pl}$ N/(mm ² rad)
2	0.336	2.78	0.00565	492	328
7	0.388	3.22	0.00584	551	367
8	0.392	3.25	0.00553	588	392

The values are at the same level as the results in the shear tests with FIX- and W-nailplates. As a conclusion: **the rotational stiffness in anchorage seems to be the same in both bending and shear tests.**

5. PROPOSALS FOR STANDARD TESTS OF ROTATIONAL STIFFNESS

5.1 Test pieces and testing procedure for determination of rotational stiffness

- The rotational stiffness for the actual type of nail plate shall be determined by shear test loading parallel to the grain ($\beta = 0^\circ$) in loading directions $\alpha = 0^\circ$ and $\alpha = 90^\circ$ (α is angle between the force and the main direction of nail plate). The obtained mean rotational stiffness of these test series will be given for the rotational spring stiffness modulus of the actual type of nail plate.
- Five (5) test pieces in both series shall be tested in accordance with CEN/TC 124.116 and EN 26891.
- The shape of nail plates (b x a): $\alpha = 0^\circ$: $b = 1.0-1.5 a$; $\alpha = 90^\circ$: $a = 1.0-1.5 b$.
- The size of the nail plate is chosen so that the failure mode will be anchorage.
- The total shear slips shall be measured continuously from both sides of the test piece (Figure 5.1).

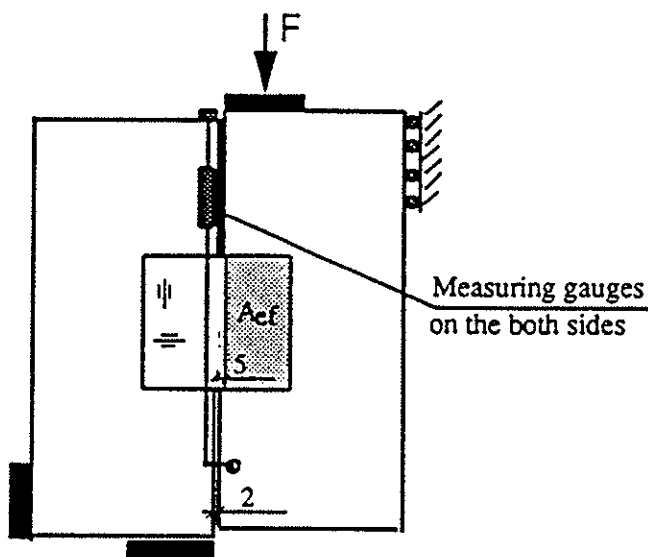
5.2 Reference tension test series for determination of translational stiffness moduli

- The tension tests series ($\beta = 0^\circ$) with five (5) test pieces in loading directions $\alpha = 0^\circ$ and $\alpha = 90^\circ$ shall be done in accordance with CEN/TC 124.116.
- Timber members shall be the same as in the corresponding shear tests.
- The deformations shall be measured continuously across the joint line from both edges of the test piece (Figure 5.1).

5.3 Processing of the measured test results

- The analysing points of each test: $0.1 F_{\max}$ and $0.4 F_{\max}$ (at initial loading phase)
=> calculation of the modified initial deformation $\delta_{i,\text{mod}}$
=> calculation of the "force" slip δ_F (with measured $K_{F,0}$ -stiffness of tension tests)
=> from difference ($\delta_{i,\text{mod}} - \delta_F$) the "rotation" slip δ_M
=> the rotation angle $\theta_{i,\text{mod}}$ by equation 3.7
=> the rotational spring stiffness modulus K_φ by equation 3.3
- Calculation of the mean values of the rotational stiffness moduli for both test series ($\alpha = 0^\circ$ and $\alpha = 90^\circ$).
- The obtained mean rotational stiffness of these test series is given for the rotational spring stiffness modulus $K_{\varphi,\text{ser}}$ of the actual type of nail plate.

Shear tests for rotational stiffness



Tension tests for $K_{F,0}$ and $K_{F,90}$

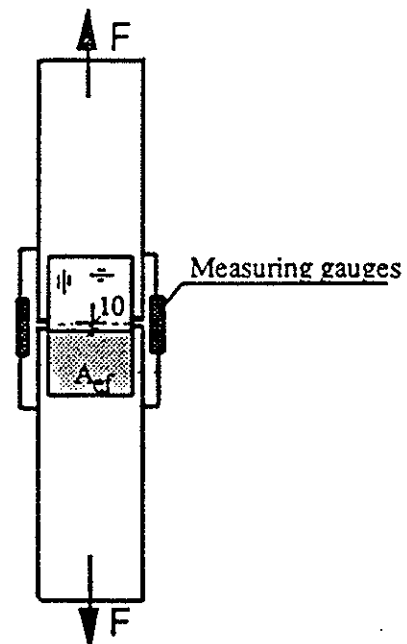


Figure 5.1 The test pieces and measuring arrangements of rotational and translational stiffness moduli.

5.4 Rotational spring stiffness moduli in design

The rotational spring stiffness modulus $K_{\varphi,ser}$ is calculated by the elastic moment anchorage stress $\tau_{M,el}$. If the plastic method is used in design the given rotational stiffness modulus is divided by factor 1.5.

The rotational spring stiffness moduli are used in design like the slip modulus in EUROCODE 5 (page 95): $K_{\varphi,u} = 2 K_{\varphi,ser}/3$; $K_{\varphi,u,fin} = K_{\varphi,u}/(1 + k_{def})$.

6. REFERENCES

CEN/TC 124.116, Timber structures - Test methods. Testing of joints made with punched metal plate fasteners. (Proposal for a draft of European Standards prEN 1075). 14 p.

CIB-W18, Warsaw 1981. Paper 14-7-1: Norèn, B., Design of Joints with Nail Plates. 39 p.

CIB-W18, Beit Oren 1985. Paper 18-7-4: Kangas, J., A Detailed Testing Method for Nail Plate Joints. 8 p.

CIB-W18, Åhus 1992. Paper 25-14-1: Kevarinmäki, A. & Kangas, J., Moment Anchorage Capacity of Nail Plates in Shear Tests. 13 p.

CIB-W18, Åhus 1992. Paper 25-14-2: Kangas, J. & Kevarinmäki, A., Design Values of Anchorage Strength of Nail Plate Joints by 2-curve Method and Interpolation. 10 p.

CIB-W18, Athens 1993. Paper 26-14-2: Kevarinmäki, A. & Kangas, J., Moment Anchorage Capacity of Nail Plates. 13 p.

CIB-W18, Athens 1993. Paper 26-14-4: Kevarinmäki, A., Solution of Plastic Moment Anchorage Stress in Nail Plates. 10 p.

EN 26891, Timber structures. Joints made with mechanical fasteners. General principles for the determination of strength and deformation characteristics.

EUROCODE No. 5 - Design of Timber Structures, Part 1-1: 1992, Annex D: The Design of Trusses with Punched Metal Plate Fasteners. 100 p.

Kyrkjeide, O., (Aune, P. & Aasheim, E.), Spikerplater med momentpåkjenning. Universitet i Trondheim, 1992. 85 p.

INTERNATIONAL COUNCIL FOR BUILDING RESEARCH STUDIES AND DOCUMENTATION

WORKING COMMISSION W18 - TIMBER STRUCTURES

**SOLUTION OF PLASTIC MOMENT ANCHORAGE STRESS
IN NAIL PLATES**

by

A Kevarinmäki
Helsinki University of Technology
Finland

MEETING TWENTY - SIX

ATHENS, GEORGIA

USA

AUGUST 1993

In Norèns simplification the "diagonal" length d is calculated from

$$d = 2 \sqrt{z_a^2 + z_b^2} \quad (2.3)$$

$$z_a = \frac{1 + c/a + (c/a)^2}{1 + c/a} \cdot a/3 \quad (2.4)$$

$$z_b = \frac{1 + 2c/a}{1 + c/a} \cdot b/3 \quad (2.5)$$

In case $c = 0$ (triangle) $d = 2/3 \sqrt{a^2 + b^2}$

In case $c = a$ (rectangle) $d = \sqrt{a^2 + b^2}$ i.e. d is the diagonal.

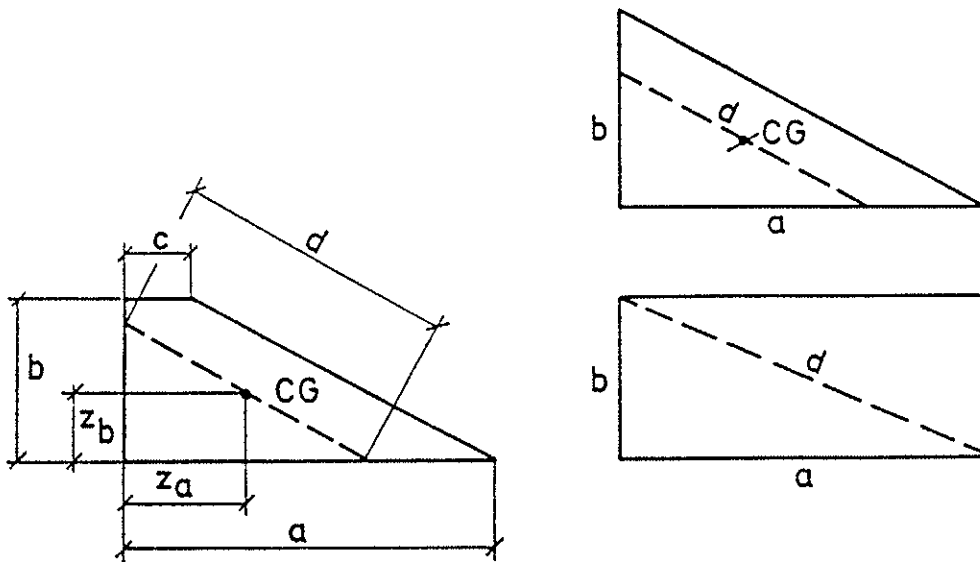


Figure 2.1 Diagonal d in trapezoid, triangle and rectangle shapes.

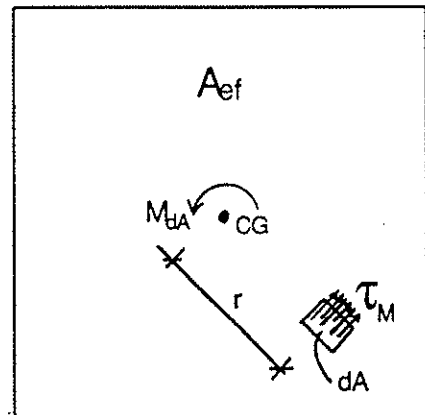
3. THEORETICAL BACKGROUND

The moment M_{dA} from stress τ_M in surface dA :

$$M_{dA} = \tau_M dA \cdot r \quad (3.1)$$

When stress τ_M is constant in the whole area A_{ef} :

$$M_A = \int_{A_{ef}} \tau_M r dA = \tau_M \int_{A_{ef}} r dA \quad (3.2)$$



where

$$\int r dA = W_p \quad (3.3)$$

When the torsional section modulus W_p is written to the form:

$$W_p = A_{ef} d/4 \quad (3.4)$$

the theoretical exact value for the symbol d is:

$$d = (4/A_{ef}) \int r dA \quad (3.5)$$

Symbol d is not theoretically the general geometric length of different surfaces. It is taken into use only for the simplification to be more illustrative. The exact value of d may be determined in most cases only by the numerical integration with a computer.

For the circle surface it is easy to calculate:

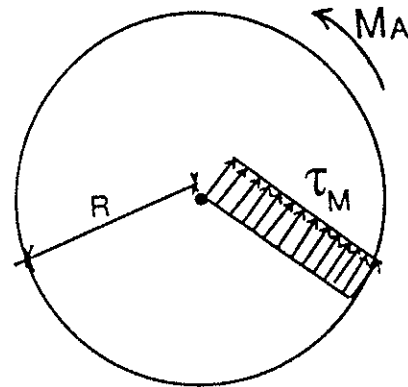
$$M_A = \int \tau_M r dA = 2 \pi R^3 \tau_M / 3 \quad (3.6)$$

With symbol d :

$$M_A = 1/4 \tau_M A d \quad (3.7)$$

From (3.6) & (3.7):

$$d = 8 R / 3 \quad (3.8)$$



4. COMPARISON OF NORÈNS METHOD AND ACCURATE PLASTIC THEORY

In Norèns method d is assumed to be the length of the "diagonal" of the effective area. Design is always on the safe side in the cases of rectangle, triangle or quadrilateral surfaces. The differences between the theoretical values of d (3.5) and this Norèns simplification are shown in Figure 4.1. The theoretical values are calculated by numerical integration. The theoretical and simplified W_p values of different surfaces are shown in the following examples.

Example 4.1 Square

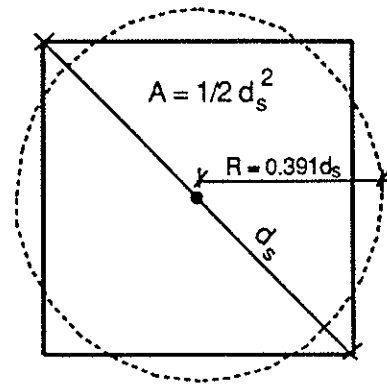
$$W_{p,\text{square,approx}} = A d_s / 4 = d_s^3 / 8$$

Circle which has the same W_p :

$$2 \pi R^3 / 3 = d_s^3 / 8 \Rightarrow R = 0.391 d_s$$

According to the equation (3.8): $R = 0.375 d$

\Rightarrow simplification by square is on the safe side.



Theoretically (by computer) the exact value with the square ($d = \text{diagonal}$):

$$W_{p,\text{theor}} = 0.135 d^3 \quad \Rightarrow \quad W_{p,\text{theor}} / W_{p,\text{approx}} = 1.08$$

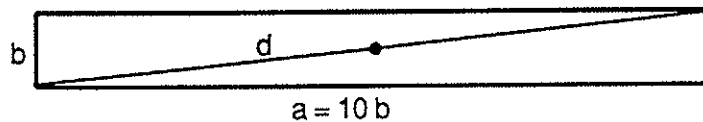
Norèns simplification by the square surfaces is 8 % on the safe side.

Example 4.2 Rectangle $a = 10 b$

$$W_{p,\text{approx}} = A d / 4 = 0.02512 a^3$$

$$W_{p,\text{theor}} = 0.02522 a^3$$

$$W_{p,t} / W_{p,a} = 1.004$$



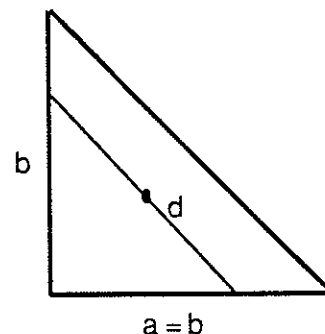
When $a \gg b \Rightarrow$ Norèns simplification is approaching the theoretically exact value of d .

Example 4.3 Triangle $a = b$

$$W_{p,\text{approx}} = A d / 4 = 0.1179 a^3$$

$$W_{p,\text{theor}} = 0.1513 a^3$$

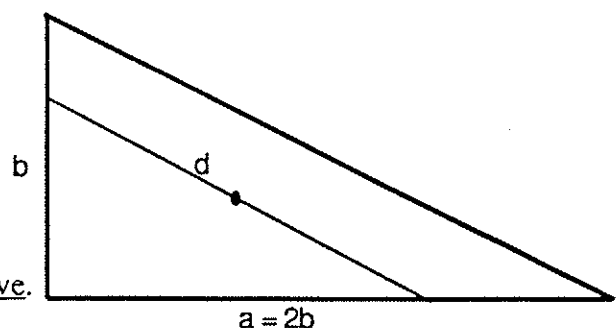
$$W_{p,t} / W_{p,a} = 1.28 \quad \Rightarrow \quad \underline{28 \% \text{ conservative.}}$$

Example 4.4 Triangle $a = 2b$

$$W_{p,\text{approx}} = A d / 4 = 0.0466 a^3$$

$$W_{p,\text{theor}} = 0.0584 a^3$$

$$W_{p,t} / W_{p,a} = 1.25 \quad \Rightarrow \quad \underline{25 \% \text{ conservative.}}$$

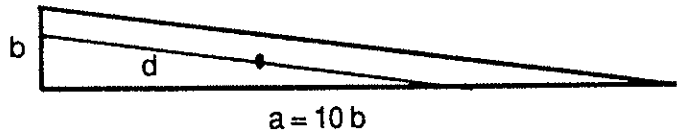


Example 4.5 Triangle $a = 10b$

$W_{p,approx} = A d/4 = 0.008375 a^3$

$W_{p,theor} = 0.009996 a^3$

$W_{p,t}/W_{p,a} = 1.19 \Rightarrow \underline{19 \% \text{ conservative.}}$



Example 4.6 Quadrilateral $a = b = 2c$

$W_{p,approx} = A d/4 = 0.2215 a^3$

$W_{p,theor} = 0.2584 a^3$

$W_{p,t}/W_{p,a} = 1.17 \Rightarrow \underline{17 \% \text{ conservative.}}$

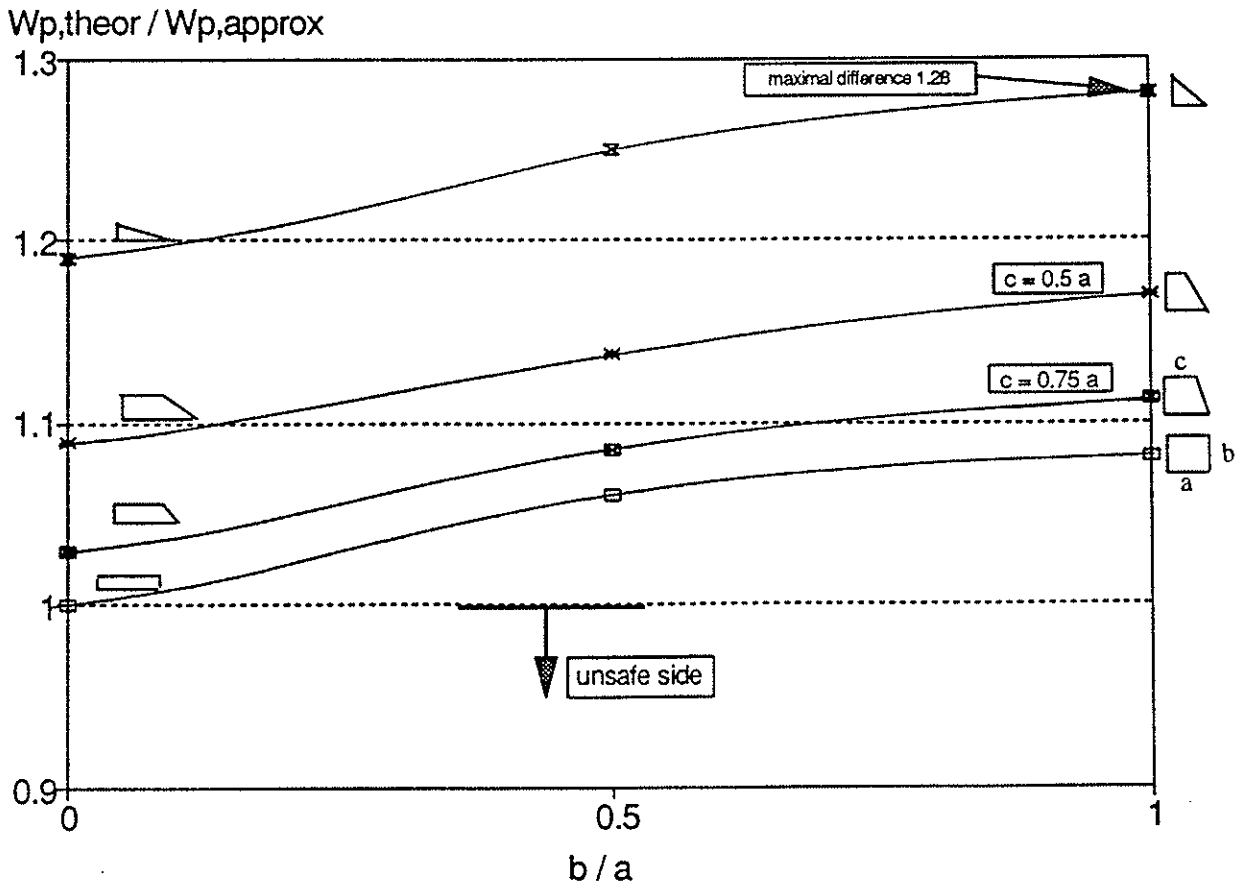
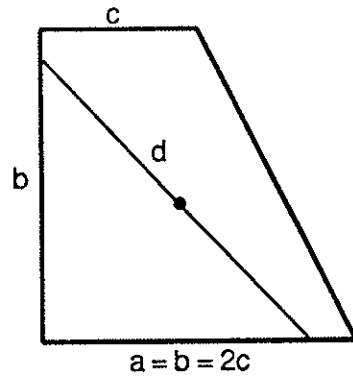


Figure 4.1 Summary of relations between accurate plastic theory and simplification by Norèn.

5. OTHER EFFECTIVE AREA SHAPES

The simplified calculation method of plastic W_p presented by B. Norèn is limited only to the rectangles, the right-angled triangles or the quadrilaterals where two angles are 90 degrees. Trussed rafters have usually many joints that have also other shapes of the effective nail plate area. Some of these cases are shown in Figure 5.1.

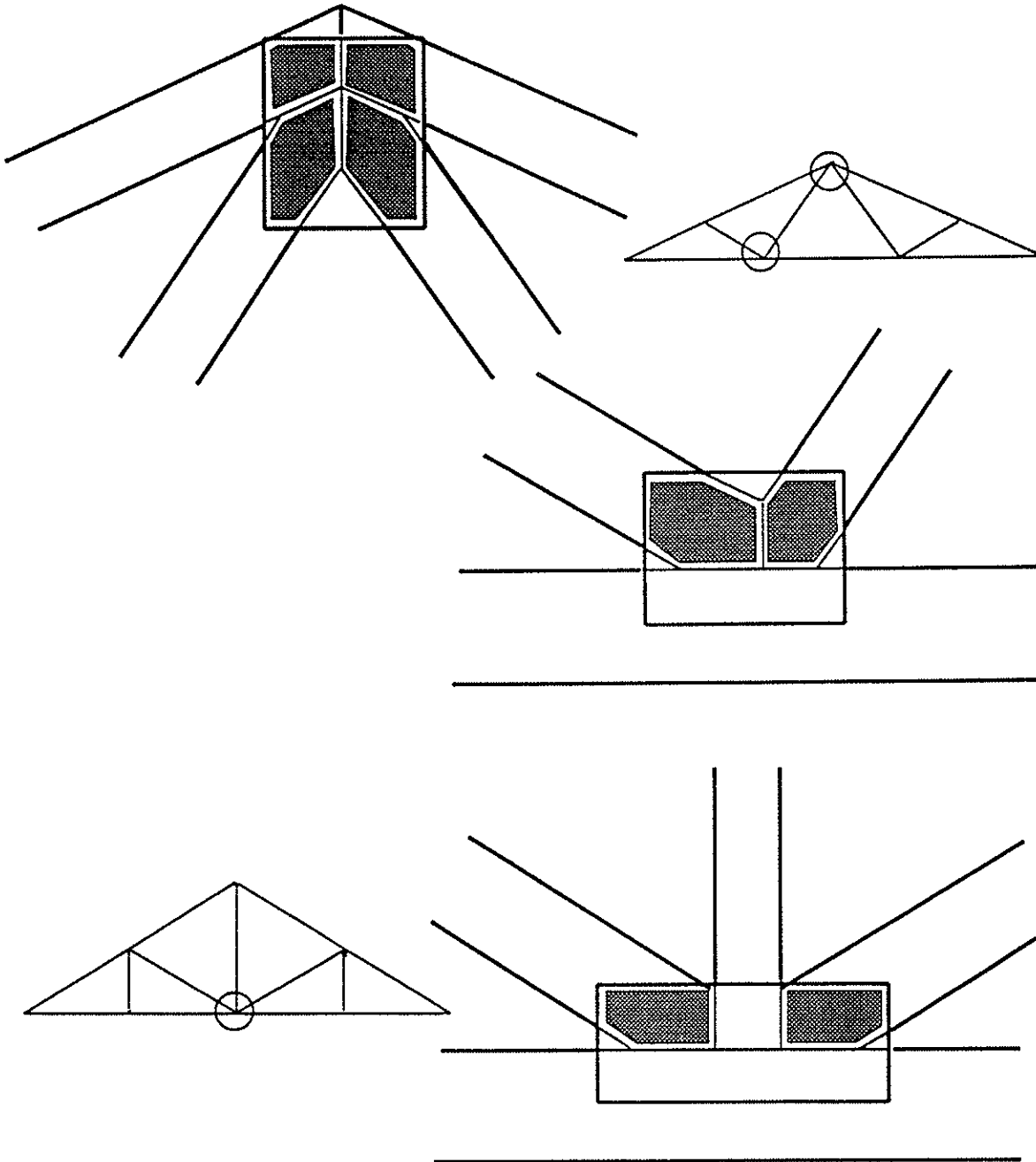


Figure 5.1 Shape examples of the effective area where the plastic W_p may not be solved by Norèn's simplification.

A proposal for calculating the length d for polygons and other shapes of the effective nail plate area:

The surface is replaced by the rectangle that has the same area. The height of the rectangle is same as the height of the original surface perpendicular to the longest side. Diagonal d is calculated for this fictional rectangle.

This is formulated:

$$d = \sqrt{(A_{ef}/h)^2 + h^2}, \quad (5.1)$$

where h is the maximum height of surface perpendicular to the longest side.

This solution is always on the safe side. The biggest difference from the theoretical value is obtained with very oblique parallelograms, where the lengths of all sides are same. The examples of different surfaces with the fictional rectangles are shown in Figure 5.2.

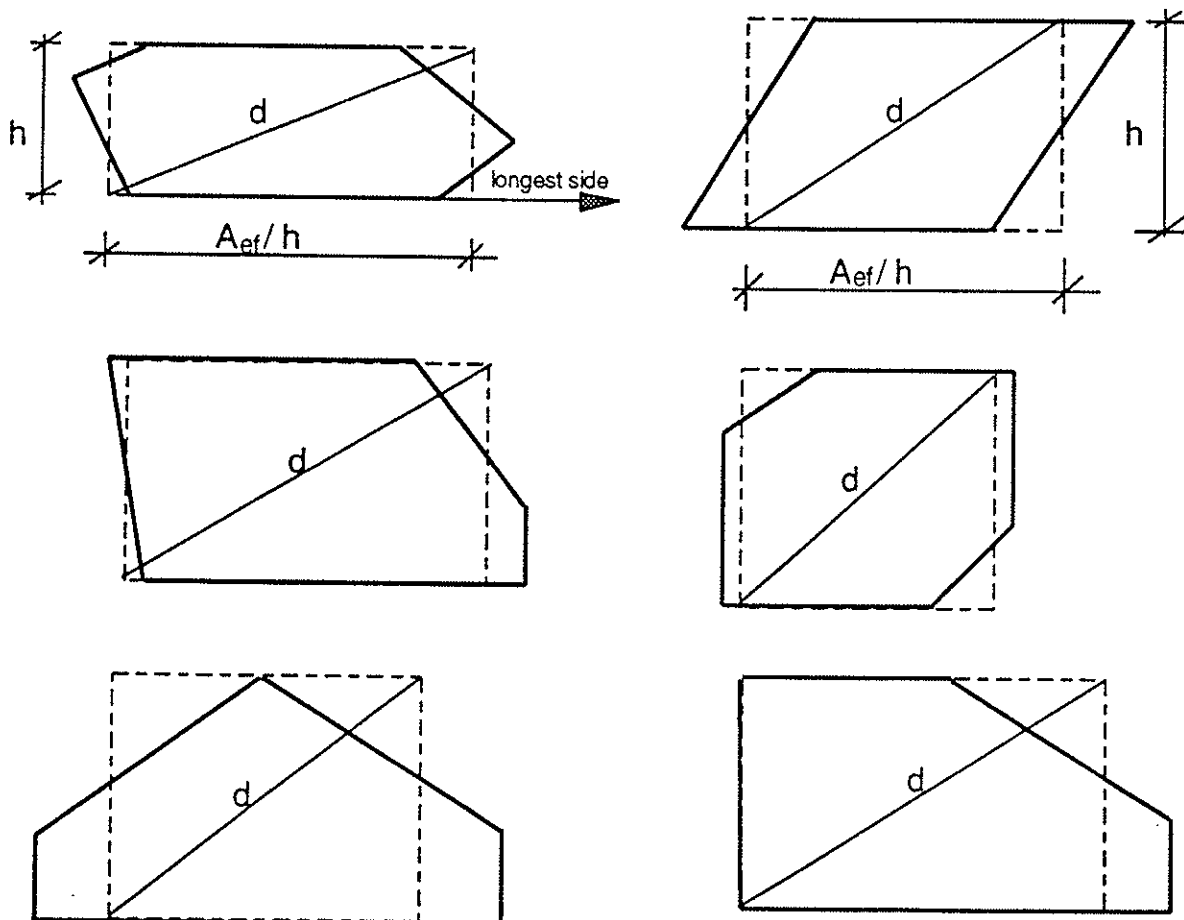


Figure 5.2 Examples of different surfaces with the fictional rectangles.

The simplification (5.1) may be used for all shapes of effective nail plate area. In the case of rectangle areas it gives exactly same result as Norèns method. With triangles and quadrilaterals this solution (5.1) is very close to the results of Norèns simplification (Examples 5.1 - 5.4). The height of the fictional rectangle is determined perpendicular to the longest side. The use of some other height may lead to unsafe result (Example 5.5). The use of the height perpendicular to the longest side is always on the safe side. The theoretical situation where the longest straight side is as short as possible is circle. This method is still about 5 % conservative compared with the circle surfaces (Example 5.6).

Example 5.1 Quadrilateral $a = b = 2c$

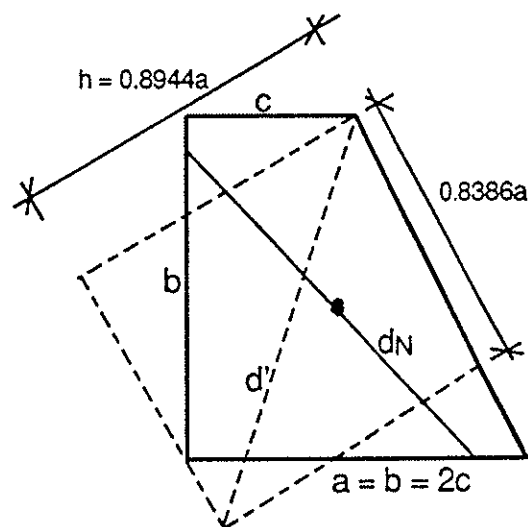
By Norèns method:

$$d_N = 1.181 a$$

By proposal method (5.1):

$$d' = 1.226 a$$

$$d_N/d' = 0.963$$



d' is 4 % bigger than the value of Norèns method $\Rightarrow W_p$ is bigger $\Rightarrow \tau_M$ is smaller \Rightarrow safety level is 4 % smaller. However, this solution is still 13 % conservative compared with the theoretical value.

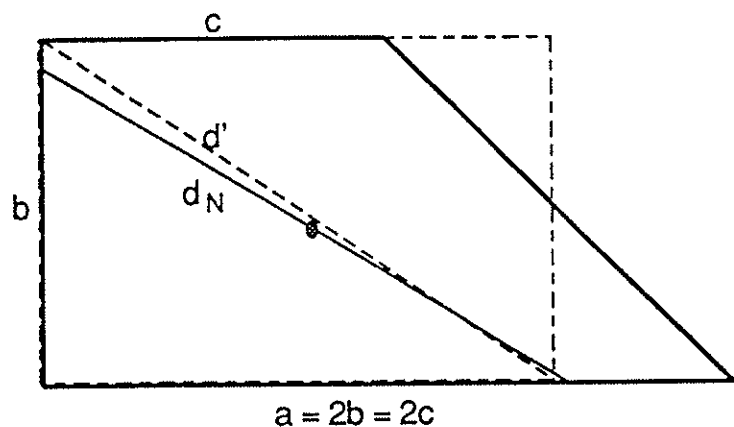
Example 5.2 Quadrilateral $a = 2b = 2c$

$$d_N = 0.8958 a$$

$$d' = 0.9014 a$$

$$d_N/d' = 0.994$$

\Rightarrow Difference is only 0.6 % !

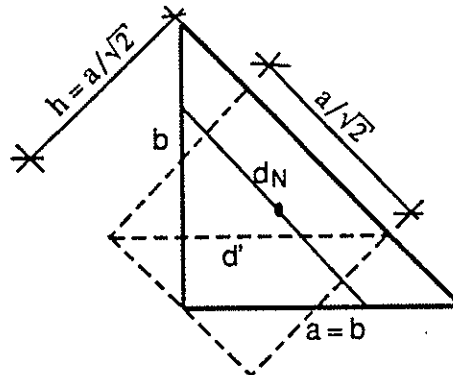


Example 5.3 Triangle $a = b$

$$d_N = 0.9428 a$$

$$d' = (1.0000) a$$

$$d_N/d' = 0.943$$



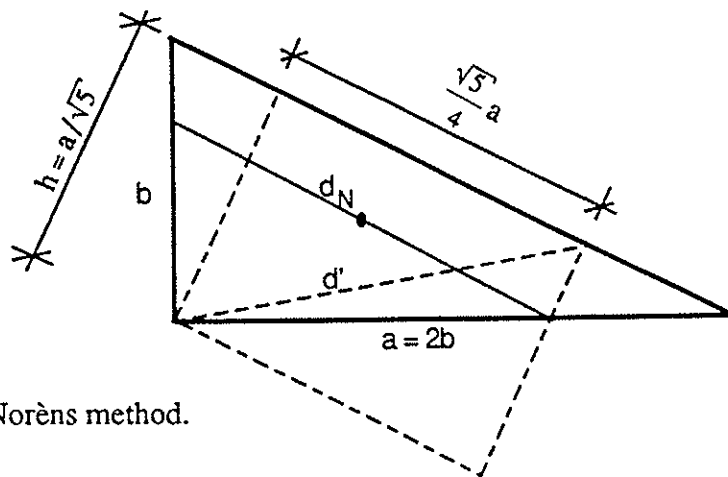
6 % smaller safety level than by Norèns method, but still 22 % conservative.

Example 5.4 Triangle $a = 2b$

$$d_N = 0.7454 a$$

$$d' = 0.7159 a$$

$$d_N/d' = 1.041$$



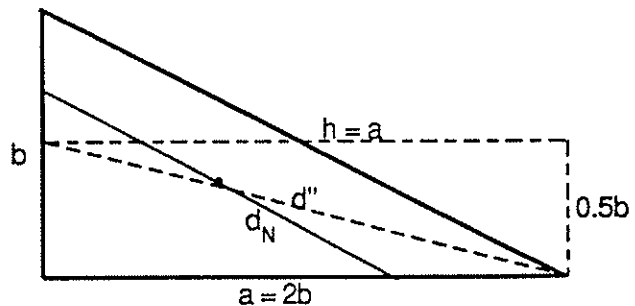
4 % more conservative than Norèns method.

Example 5.5 Triangle $a = 2b$, height h is chosen perpendicular to the shortest side.

$$d_N = 0.7454 a$$

$$d'' = 1.0308 a$$

$$\Rightarrow d'' = 1.38 d_N = 1.11 d_{\text{exact}}$$



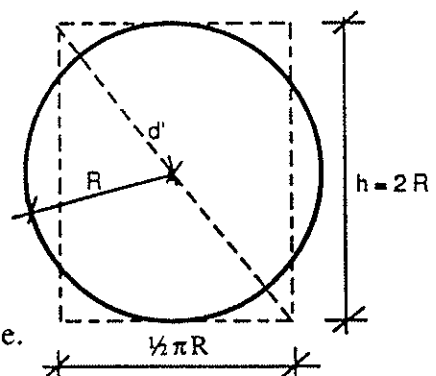
the d'' -value would be on an unsafe side. The height of the fictional rectangle (h) must be determined perpendicular to the longest side (as in Example 5.4), then the result always is on the safe side.

Example 5.6 Circle.

$$d_{\text{exact}} = 8/3 R$$

$$d' = \sqrt{(\pi R^2/2R)^2 + (2R)^2} = 2.543 R$$

$$d_{\text{exact}}/d' = 1.049 \Rightarrow \text{simplification is 5 \% on the safe side.}$$



6. CONCLUSIONS

The comparison between Norèns simplification and the accurate plastic theory shows that Norèns method is always on the safe side in determining the plastic τ_M anchorage stress of nail plate joint areas. With the rectangle shapes of the effective nail plate areas Norèns method is 0...8 % conservative. The biggest difference (28 %) from the theoretical solution occurs in the case of right-angled triangles where the sides are equal. Difference between the theoretically and approximately calculated $\tau_{M,pl}$ stresses seems to be relatively high in some cases. The effect to the design result however is quite small as the τ_M stress is only one part in the anchorage design criteria. Usually the τ_F stress has a bigger effect on the anchorage design.

Due to Norèns methods limitations, the new alternative approximate solution is presented. The nail plate surface may be replaced by the rectangle that has the same area and height perpendicular to the longest side as the original surface has. The plastic anchorage stress τ_M may then be calculated for this fictional rectangle. This method is at the same safety level as Norèns method and it is easy to use. The new method and its formulation suit very well together with the rules of the plastic τ_M anchorage design to be included in design codes.

7. REFERENCES

CIB-W18, Warsaw 1981. Paper 14-7-1: Norèn, B., Desing of Joints with Nail Plates. 39 p.

CIB-W18, Åhus 1992. Paper 25-14-1: Kevarinmäki, A. & Kangas, J., Moment Anchorage Capacity of Nail Plates in Shear Tests. 13 p.

EUROCODE No. 5 - Desing of Timber Structures, Part 1-1: 1992, Annex D: The Desing of Trusses with Punched Metal Plate Fasteners. 100 p.

INTERNATIONAL COUNCIL FOR BUILDING RESEARCH STUDIES AND DOCUMENTATION
WORKING COMMISSION W18 - TIMBER STRUCTURES

TESTING OF METAL-PLATE-CONNECTED WOOD-TRUSS JOINTS

by

R Gupta
Forest Research Laboratory
Oregon State University
USA

MEETING TWENTY - SIX

ATHENS, GEORGIA

USA

AUGUST 1993

TESTING OF METAL-PLATE-CONNECTED WOOD-TRUSS JOINTS

Rakesh Gupta, Assistant Professor
Department of Forest Products
Forest Research Laboratory
Oregon State University
Corvallis, OR-97331, USA

ABSTRACT

A testing apparatus with computerized data acquisition and control system was developed to test metal-plate-connected (MPC) wood-truss joints. The apparatus enabled testing of several different types of joints under various loading conditions without major modifications. The apparatus shows potential as an efficient testing procedure to assess joint behavior.

INTRODUCTION

The structural performance of MPC wood-truss joints has received extensive research attention in the last 20 years (Wolfe, 1990). However, most of the research has been focused on the performance of tensile joint and that too under axial loads only. Tensile joint under combined loads, and structural performance of other joints (e.g., heel and web joints) under realistic loads, have received little or no attention.

Testing of MPC joints has been a part of almost all the studies. Table 1 summarizes most of the available literature on testing of MPC joints. Almost all the work has been focused on tensile joints under uniaxial loads. Some recent work has been done on other joints (Gupta, 1990), and under combined loading conditions (Gupta, 1993 and Wolfe, 1990).

There are several standards (Table 2) that provide testing procedures for MPC joints to determine their structural characteristics. However, no standard exists for testing actual (different configurations) MPC wood-truss joints under simulated, in-service, loading (e.g., combined bending and tension) conditions. A standard is required to determine structural characteristics (strength, stiffness, failure modes, etc.) of actual MPC wood-truss joints which is directly relevant to truss design. Currently used specimens in different standards is not the most efficient for this purpose and that we should instead be testing actual truss joints (Quaile and Keenan 1979; Lau 1987).

A test apparatus that allows testing of different MPC joints and that simulates the in-service loading conditions on joints was developed and constructed. The testing apparatus enables testing

of several different types of joints under various loading conditions without major modifications. The development of this testing apparatus may also lead to the standardization of wood joint testing and design of new connections. The apparatus shows potential as an efficient testing procedure to assess joint behavior.

TESTING APPARATUS

The testing apparatus consists of a horizontal, rigid, steel frame (box section) bolted to the floor at several places to restrict its movement (Figure 1). The test frame is shaped as a half of a hexagon. This shape allows placement of numerous different configurations (e.g., heel and web joints at different angles) of actual MPC wood-truss joints for testing. The test frame, along with test specimens, supports reaction fixtures, links, restraints and hydraulic cylinders.

In-plane member forces were simulated by applying a force through hydraulic cylinders along the members. A system of calibrated force transducers measured the forces in the members that formed the joints. A electronically controlled hydraulic pressure control valve allowed close control of the pressure in the cylinder and, thereby, the forces exerted by the cylinders. Several displacement transducers monitored the displacement of the test specimens. Load-displacement information was collected and stored in a computer. The loading rate was chosen so that failure will occur in about 12 min. This is consistent with the ASTM D1761 recommendation that failure should occur between 55 and 20 min after loading (ASTM, 1988). Furthermore, this procedure provides a sufficient number of reading to determine the load-deflection curve.

DISCUSSION

Three types of joints were tested with the newly developed apparatus: heel, tensile and web joints. Tensile joints were under pure axial tension, pure bending and at four levels of combined tension and bending. The combined loads were applied as an eccentrically applied load with four different eccentricities: 13 mm, 25 mm, 38 mm and 51 mm. Heel joints were tested by applying a compressive force at the top chord. Web joints were tested by applying a compressive force to one of the web members and a tensile force to the other. The details of the joint testing are given in Gupta and Gebremedhin (1990). All joints were tested to failure, and their load-displacement characteristics and failure modes were recorded.

The average axial load capacity and average moment capacity for all six loading cases of tension joint are given in Table 3 along with failure modes. The axial capacity of the joint goes down (about 25%) as moment on the joint increases (Gupta 1993).

The relationship between applied load and joint displacement for tension splice, heel and web joints are shown in Figure 2. All test exhibited a nonlinear relationship between load and displacement. Figure 2 shows that the behavior of heel joint can be characterized as ductile. The behavior of web and tension joint can be characterized as brittle.

The system provided a method of loading that was consistent with in-service loadings. In this particular set of MPC joints, the characteristic failure traits were identified, e.g., the most common mode of failure for web joints was teeth withdrawal at the tension web member. Heel joints failed mainly by teeth withdrawal at the bottom chord. For other connection designs, the failure mode could be quite different.

SUMMARY

A testing apparatus to test actual MPC wood-truss joints is described. The apparatus and test procedure provide a method to properly evaluate (structural characteristics) in-service types of loadings and design alternatives. Further work is needed to standardize the test apparatus and procedures.

ACKNOWLEDGEMENT

The testing apparatus was fabricated at the Department of Agricultural and Biological Engineering, Cornell University, Ithaca, NY while the author pursued his Ph.D. under the supervision of Dr. K.G.Gebreghmedhin. The help of Doug Caveny for building the test apparatus, and of Marty Jorgensen in testing and instrumentation is appreciated. The help of Milan Vatovec, Graduate Research Assistant, Department of Forest Products, Oregon State University, Corvallis, OR in collecting literature is also appreciated.

BIBLIOGRAPHY

ASTM 1988. Standard Test Methods for Mechanical Fasteners in Wood. D 1761-88:297-308.

Beineke, L.A. and Suddarth, S.K. 1979. Modelling joints made with light-gage metal connector plates. Forest Products Journal, 29(8):39-45.

Canadian Standards Association 1980. CSA Standard S 347-M1980. Method of test for evaluation of truss plates used in lumber joints. pp 9-20.

Crovella, P.L. and Gebreghmedin, K.G. 1990. Analysis of light frame wood truss tension joint stiffness. Forest Prod. Journal, 40(4):41-47.

Gebremedhin, K.G, Jorgensen, M.C. and Woelfel, C.B. 1992. Load-slip characteristics of metal plate connected wood joints tested in tension and shear. *Wood and Fiber Science*, 24(2):118-132.

Gupta, R. 1993 Metal plate connected tension joints under different loading conditions. Submitted to wood and fiber science.

Gupta, R. 1990. Reliability analysis of semirigidly connected metal plate residential wood trusses. Ph.D. Dissertation, Cornell University.

Gupta, R. and Gebrehmedin, K.G. 1990. Destructive testing of metal-plate-connected wood truss joints. *Journal of Structural Engineering*, 116(7):1971-1982

Hayashi, T., Masuda, M. and Sasaki, H. 1979. Rotating bending fatigue properties of timber butt-joints with MPC. *Japanese Soc. of Material Sci. Japan*, 28(7):623-628

Hayashi, T. and Sasaki, H. 1982. Static Tensile Strength of Wood Butt Joints with Metal Plate Connectors. *Wood Research, Bulletin of the Wood Research Institute, Kyoto University*, March 1982, 68:22-36.

Heard, L.R., S.G. Winistorfer and O.A. Grossthanner 1988. Analysis of metal plate connected high capacity tension splices for wood trusses. *Proc. of the 1988 Int. Conf. on Timber Engineering*, 2:149-162.

International Standard (ISO 8969). Timber Structures - Testing of Unilateral punched Metal Plate Fasteners and Joints. Ref No. ISO 8969 : 1990 (E).

Kanaya, N. 1983. Mechanical properties of timber joints with metal plate connectors. *Journal of the Society of Material Science, Japan*. 32(359):86-92.

Kirk, L.S., McLain, T.E. and Woeste, F.E. 1989. Effect of gap size on performance of metal plated joints in compression. *Wood and Fiber Science*, 21(3):274-2288.

Lau, Peter W.C. 1987. Factors affecting the behaviour and modelling of toothed metal-plate joints. *Can. J. Civil Eng.* 14(2):183-195.

Maragechi, K. and Itani, R.Y. 1984. Influence of truss plate connectors on the analysis of light frame structures. *Wood and Fiber Sci.*, 16(3):306-322.

McAlister, R.H. and Faust, T.D. 1992. Load/deflection parameters for metal plate connectors in yellow poplar and sweetgum structural lumber. *Forest Products Journal*, 42(3):60-64.

McAlister, R.H. 1989. Interaction between truss plate design and type of truss framing. Forest Products Journal, 39(7/8):17-24.

McCarthy, M. and Wolfe, R.W. 1987. Assessment of truss plate performance model applied to southern pine truss joints. Forest Products Laboratory, Research Paper FPL-RP-483. Madison, WI.

Misra, R.D. and M.L. Esmay 1966. Stress distribution in the punched metal plate of a timber joint. Trans. ASAE 9(6):839-842,845.

Noguchi, M. 1980. Ultimate resisting moment of butt joints with plate connectors stressed in pure bending. Wood Science, 12(3):168-175.

Palka, L.C. 1985. Prediction of Short and Long Term Behavior of Truss-Plate Joints in Tension. Forintek Canada Corp. Special Publication No. SP-27. Vancouver, BC.

Quaile, A.T. and Keenan, F.J. 1979. Truss plate testing in Canada: test procedures and factors affecting strength properties. Metal Plate Wood Truss Conf., Forest Prod. Res. Soc., p 79-28, 2801, Marshall Court. Madison, WI, pp 105-112.

Reynolds, G.M. 1988. Analysis and testing of toothed metal plate wood truss connections. M.S. Thesis, Michigan Technological Univ.

RILEM/CIB 3TT 1981 Testing methods for joints with mechanical fasteners in load-bearing timber structures, Annex A: Punched metal plate fasteners.

Suddarth, S.K., Percival, D. H. and Q.B. Comus 1979. Variability in tension performance of metal plate connectors. Metal Plate Wood Truss Conf. Proceedings P-79-28, Forest Prod. Res. Soc., 2801 Marshall Ct., Madison, WI-53705.

Tokuda, M., Takeshita, M. and Sugiyama, H. 1979a. Creep behavior of metal plate connector joints subjected to tension force. J.Jap. Wood Res. Soc., 25(6):339-407.

Tokuda, M., Takeshita, M. and Sugiyama, H. 1979b. The behavior of metal plate connector joints subjected to repetitive tension force. J.Jap. Wood Res.Soc., 25(6):408-413.

TPI-85. Truss Plate Institute. Design Specification for Metal Plate Connected Wood Trusses, Madison, WI.

M.O.A.T. No. 16. UEAtc European Union of Agreement 1979. Rule for the Assessment of Punched Metal Plate Timber Fasteners.

Wolfe, R.W. 1990. Metal-plate connections loaded in combined bending and tension. Forest Prod Journal, 40(9):17-23.

Table 1. Available literature on testing MPC joints.

JOINT TYPE	TYPE OF LOADING	FAILURE	LUMBER SIZE	REFERENCE
Tension Joint	Uniaxial Tension	Tearing failure of the plates	2X4	Misra and Esmay 1966
Tension Joint	Tensile		2X4	Suddarth et al. 1979
Tension Joint	Tensile	Withdrawal of teeth and plate tension failure	40x90 mm	Hayashi and Sasaki 1982
Tension Joint	Combined bending and tension, Pure axial tension and pure bending		2x4	Wolfe 1990
Tension, heel, web joints	Simulated actual loading		2x4	Gupta 1990
Tension Joint	Axial compression		2x4	Kirk et al. 1989
Standard splice joints and Non standard joints	Tensile	Tooth withdrawal (95%)		McCarthy and Wolfe 1987
Four CSA Configurations	Tension		2x4	McAlister and Faust 1992
Four CSA Configurations	Tension		2x4	McAlister 1989
Tension and shear joints at different angles	Tension and shear		2x4	Gebremedhin et al. 1992
Heel joints Shear joint test	Not along members	Several different types of failures	138x235 mm 35x89 mm	Lau 1987
Splice joint	Ramp, tension, creep tests		2x4	Palica 1985
Tension joint	Axial tension		2x4	Crovella and Gebremedhin 1990
Tension joint	Pure bending		33.5 or 44.5x150 mm	Noguchi 1980
Tension joint	Axial tension		2x4	Beineke and Suddarth 1979
High capacity tension joints (blocked chord splices)	Tension		2x4, 2x6, 2x8	Heard et al. 1988
Tension joint and others	Dead tension load		34x88 mm	Tokuda et al. 1979A
Tension joints and others	Repetitive tension load	Tension fatigue, withdrawal	34x88 mm	Tokuda et al. 1979B
Tension joint	Cyclic reversed and non-reversed loading	Teeth Pullout, teeth shearing at the root	40x97 mm	Hayashi et al. 1980
Tension joint, shear joint	Tension	Shear		Kanaya 1983
4 configurations of shear ridge joints	Shear, Bending		2x6	Reynolds 1988
Tension joints	Axial tension, pure bending, shear test		2x4	Maraghechi and Itani 1984

Table 2. Standards used in testing MPC joints

Standard	Remarks
ASTM D1761	only tension joint, uniaxial tensile load
CSA S347-M1980	four load to grain configurations
ISO 8969	load-slip characteristics of contact surface of plate and timber: (a) load parallel to grain (four configurations), (b) load perpendicular to grain (two configurations).
MOAT No. 16	same as ISO 8969
RILEM/CIB 3TT	same as ISO 8969
TPI-85	tension test

Table 3. Average test results for metal plate connected tension splice joint tested under different loading conditions.

Loading Case	Number of tests	Average axial Load Capacity lbs (CV)	Average Moment Capacity lb-in (CV)	Failure mode
Axial tension	8	6305(10%)	0	Tooth Withdrawal/Wood Failure
Combined loading (axial tension & bending)				
e = 1/2"	6	5940(8%)	2970	Tooth Withdrawal/Wood Failure
e = 1"	6	5449(23%)	5449	Tooth Withdrawal/Wood Failure
e = 1-1/2"	6	5176(11%)	7764	Plate Tension Failure/Tooth Withdrawal
e = 2"	6	4711(13%)	9422	Plate Tension Failure/Tooth Withdrawal
Pure bending	8	0	10943(13%)	Plate Tension Failure/Tooth Withdrawal/Wood Failure

e: eccentricity

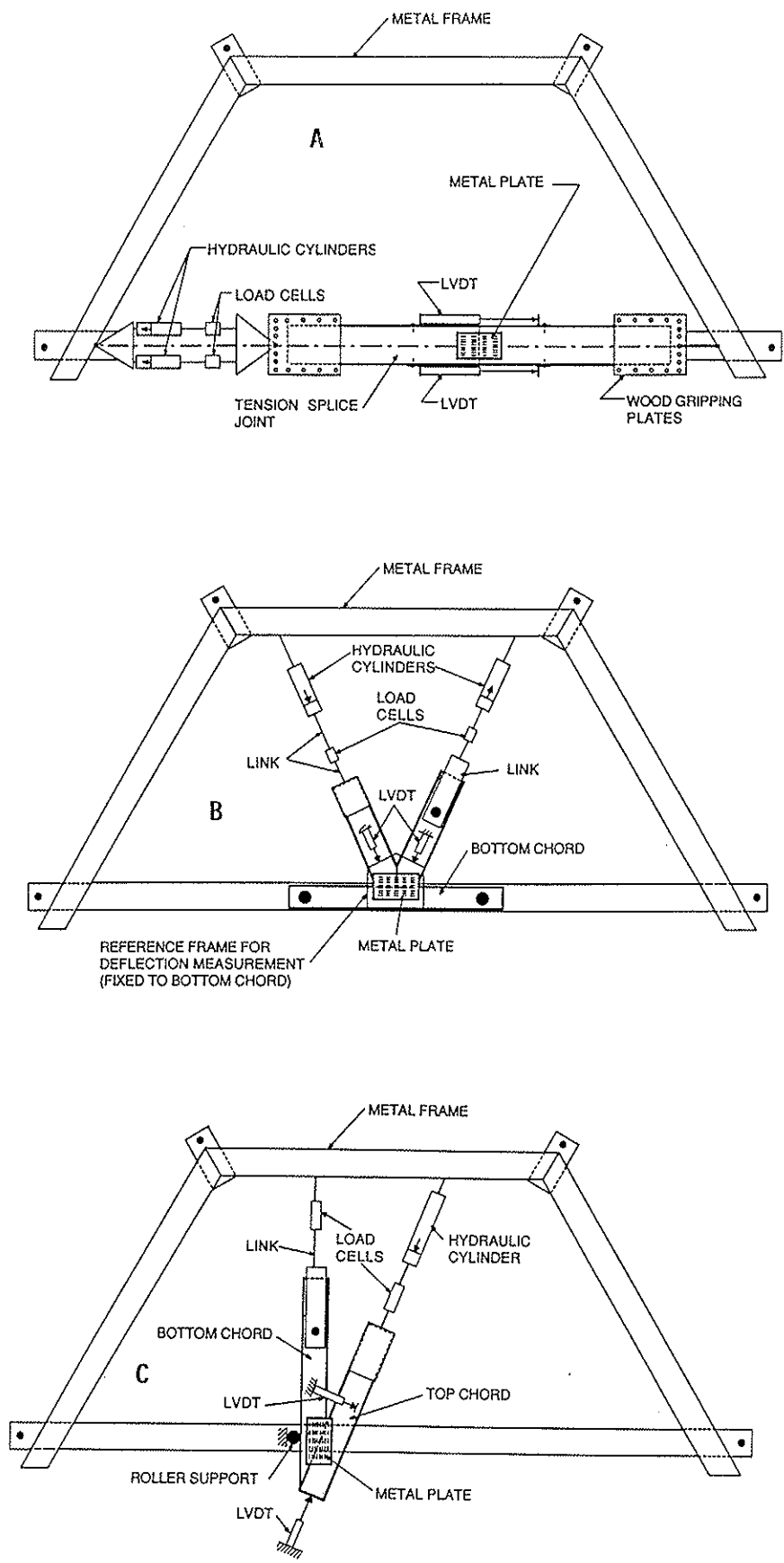


Figure 1. Test frame with three types of joints:
 (A) Tension Joint; (B) Web Joint; (C) Heel Joint

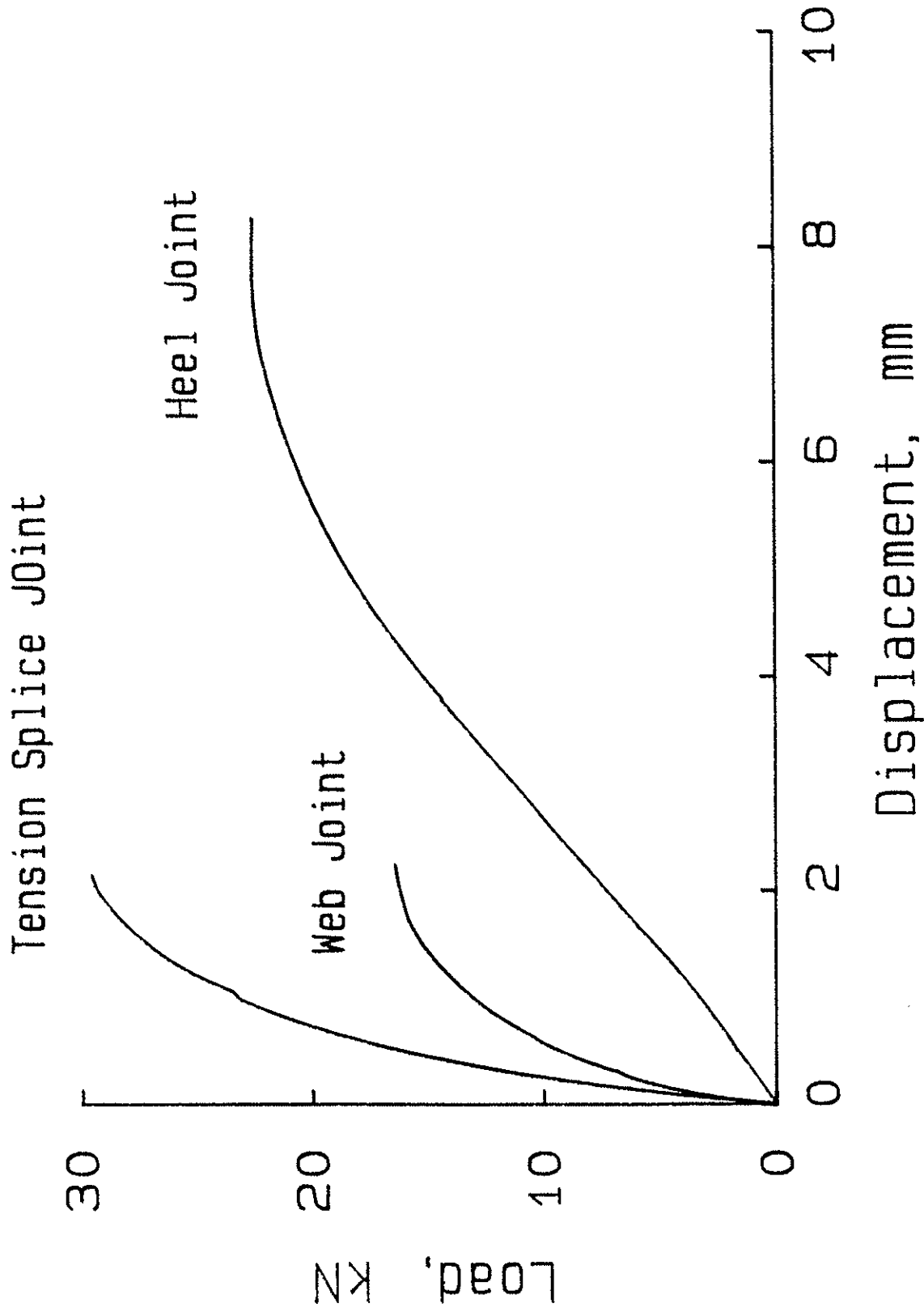


Figure 2. Load-displacement curves for three types of MPC joints.

INTERNATIONAL COUNCIL FOR BUILDING RESEARCH STUDIES AND DOCUMENTATION
WORKING COMMISSION W18 - TIMBER STRUCTURES

SIMULATED ACCIDENTAL EVENTS ON A
TRUSSED RAFTER ROOFED BUILDING

by

C J Mettem
J P Marcroft
TRADA Technology Limited
United Kingdom

MEETING TWENTY - SIX

ATHENS, GEORGIA

USA

AUGUST 1993

SIMULATED ACCIDENTAL EVENTS ON A TRUSSED RAFTER ROOFED BUILDING

C J Mettem and J P Marcroft
TRADA Technology Limited, United Kingdom

INTRODUCTION

As discussed in previous papers submitted by the authors to CIB W18 (1) (2), work has been in hand for several years to address the issues arising from the ideal that timber structures should be planned and designed in such a way that they are not unreasonably susceptible to the effects of accidents. In 1989, a preliminary paper was submitted (1), stating the problems in general terms, and suggesting that they are of concern to designers irrespective of whether timber or other materials are concerned, and also fundamentally irrespective of whether national or European-wide codes are to be followed. Potential disadvantages for timber were foreseen, if the fulfilment of such principles were to be deemed to be satisfied in certain ways. Naturally, this was of greatest concern to the authors with respect to the Approved Documents to the Building Regulations, which are published by the Department of the Environment in the UK, and which specifically issue guidance on "disproportionate collapse" in this context. However, it was realised that there were wider implications and that the subject is of more general interest.

A second CIB paper on the subject, presented in 1990, elaborated upon the way in which regulatory requirements were developing. It also described, with reference to a specific form of roof construction, ways in which the "disproportionate collapse" requirement might be interpreted in terms of the acceptable extent of damage, after an accident. The form of timber roof construction evaluated in this paper was parallel framed construction, where distinct principal beams, plus purlins and bracing existed. Two requirements were brought to the attention of the designer. Firstly, that of ensuring that in the event of a local failure of a primary frame, then the adjacent primary frames would not be dragged down. Secondly, the need to ensure that the undamaged areas on either side of the damaged zone would retain sufficient stability to remain standing.

Fortunately, and possibly in part as a consequence of this work, the more recent editions of the Building Regulations Approved Documents (3) have included revised guidance on the acceptable extent of collapse in the event of a local failure in a roof structure or its supports, for low rise public buildings. This guidance can be met with reasonable economy by well-designed versions of existing timber engineered types of building and detailing.

The ENV version of EC5 (4) has also adopted the principle of requiring design against the eventuality of collapse.

One of the fundamental requirements of the basis of design given in EC5 states:

- " A structure shall also be designed in such a way that it will not be damaged by events like explosions, impacts or consequences of human errors, to an extent disproportionate to the original cause."

However, in spite of the prominence of this principle, little or no detailed guidance is provided.

Whilst the work by TRADA Technology Limited in earlier years of the project focused upon the parallel framed structures mentioned above, it was evident that, for reasons of commercial economics, it would be important to include consideration of trussed rafter roofs. These occupy such a large proportion of the market for non-domestic roofs in the 9 to 15 metres range, that the project would have been incomplete if no account had been taken of them. It was felt necessary to address the assessment of the reaction of trussed rafter roofs to accidental events by experimental means rather than analytically, as explained below.

This paper describes a full-scale testing programme which simulated accidental events on a trussed rafter roofed building. The chosen configuration was a single-storey structure, 12 metres by 10 metres in plan, and containing no internal walls. Six "accidental events" were simulated on the building. The paper appraises the structural contributions made by various components of secondary construction, such as battens, bracing and the tiling layer. Finally, the paper addresses the question of whether the building met the requirements lying behind the principle stated in EC5, and also whether it was deemed satisfactory in the terms stated in the Building Regulations for England and Wales.

THE REQUIREMENT

In the UK Building Regulations, there are distinct requirements for designers to avoid the consequences of disproportionate collapse. For legal reasons, these apply in the precise form discussed here, only to England Wales. However, similar interpretations tend to be required elsewhere in the UK, where regulations are less prescriptive.

For those parts of a public building, shop or shopping mall having a roof with a clear span exceeding nine metres between supports, the regulations require that the building shall be constructed so that, in the event of failure of any part of the roof, including its supports, the building will not suffer collapse to an extent disproportionate to the cause. For a building of a type similar to that which was tested in the experiments described in this paper, this would mean that if a failure were to occur in the first instance within the part of the roof supported on timber framed wall panels, then any extension of the collapse to other parts of the roof supported on masonry walls, would be unacceptable.

RATIONALE FOR TESTING

It was decided to undertake testing upon trussed rafter roofs, which are frequently used for non-domestic public buildings of the type described above, rather than dealing with the problem analytically, for the following reasons:

1. Trussed rafter roofs of 9 to 15 metres span are being employed in significant quantities for public buildings, and this is a trend which is likely to continue. Hence, they are of great economic importance.
2. There are considerable difficulties in assessing the likely performance of a trussed rafter roof after a structural accident by analysis alone, since there are a number of indeterminate factors, several of which are described in a little more detail below.
3. Such types of trussed rafter roof cover a reasonably restricted span range, and contain a number of frequently repeated principles and details. Hence, it was reasonable to suppose that, by demonstrating the considerable robustness of certain forms of trussed rafter roof construction in a "typical" test structure, then it might be accepted that the findings would apply to such roofs within and throughout the normal non-domestic building range. It should be emphasised that this comment is restricted only to buildings of a low rise, to which the particular subdivision of the regulations concerned was also restricted.

Some of the analytical difficulties that were perceived are as follows:

1. Trussed rafter roof construction in Britain has evolved to include certain forms of diagonal bracing, and also "chevron" bracing, which forms a crude type of canted longitudinal trussed girder. Such types of bracing are not always continuous across and along an entire roof. Hence, in certain zones, the roof framework as a three-dimensional structure, is stiffer than in other zones, making for a difficult analysis.
2. Wall plates and other minor roof members such as tiling battens, contribute directly to the performance of the framework, in a way that is difficult to quantify, but that is greater in practice than in theory. Furthermore, they also provide the links for several important load paths, and thus cannot simply be omitted from analyses.

3. Even less quantifiable are the beneficial effects provided by roofing members such as felt held by battens and/or sarking (if any), and by the tiles themselves, which can lock together and resist horizontal actions in certain types of accidental situation (other than seismic events).
4. Tiling battens, which, as explained under 2 above, should be included in the analysis, can have a considerable variety of spanning and continuity arrangements, even in one particular roof.
5. Some of the bracing members, as well as being incomplete in certain zones of the roof, would have to be treated in an analysis as canted members of very slender cross section; a complex buckling design problem.

It was felt that a potentially beneficial effect of trussed rafter roof construction existed in the form of the continuity of the secondary longitudinal roof construction. Although the items comprising this continuity, such as tiling battens and bracing, mentioned above, would be difficult to assess purely by analysis, it was felt likely that they would lend considerable robustness to the roof when compared with, for example, simple single-span timber purlins between parallel frames, with discretely placed diagonal bracing. Hence, it was felt likely that there would be a successful outcome to a series of tests on a full-scale trussed rafter roof.

As mentioned above, this form of non-domestic trussed rafter roofed building tends to exhibit certain common characteristics, which were studied in order to ensure that a representative test structure could be planned with reasonable economy. Common features included the following:

1. Span range: Minimum span for Building Regulations disproportionate collapse requirements, nine metres. Spans above fifteen metres uncommon for the types of smaller public building concerned.
2. Pitch range: Pitches between 17° and 30° considered usual.
3. Spacing: A spacing between trussed rafters of 600mm almost invariably used in the UK.
4. Roof cladding: Interlocking tiles, usually of concrete, are common. These are supported on small battens, typically of 25mm by 38mm section.
5. Bracing: Diagonal, "chevron" and longitudinal bracing tends to be an extrapolation of domestic trussed rafter roof construction. In addition, horizontal "wind girders", fabricated by means of normal trussed rafter manufacturing equipment, tend to be added at eaves/ceiling tie level, when required in buildings of larger than domestic scale.

TEST OBJECTIVES

Two objectives were clearly identified for the planned series of tests which were intended to simulate events on a full-sized mock-up of a non-domestic trussed rafter roofed building. These objectives were as follows:

1. To simulate a series of accidents, representing the removal of a major portion of an external load-bearing wall of the building and, having done this, to examine the extent of the consequent roof collapse, judging whether it could be deemed to have collapsed to an extent disproportionate to the cause of the failure.
2. Assuming that total collapse would not occur during the early simulations, it was planned to evaluate the contribution to the overall robustness of the structure brought about by secondary elements of construction, such as bracing and roof claddings.

DESIGN OF TEST BUILDING

It was envisaged that it would be possible to design and build a full-sized mock-up test building in such a manner that about four or five alternative sets of details could be incorporated, with repeated simulated "accidental events". It was considered inadvisable to hope for a greater number of test replications than this, since damage would be likely to accumulate, particularly in the masonry parts of the structure. Clearly it would have been desirable to incorporate a greater variety of constructions, and the choice had to be made very selectively.

Common features of low rise non-domestic trussed rafter roofed buildings of the type considered were described above, in terms of span and pitch ranges, spacing, roof cladding and bracing types. Within this spectrum, the following choice was made.

Masonry support walls were used, consisting of a single leaf of 100mm thick concrete blockwork. In reality, cavity wall construction would be more common, but the single skin was chosen for economy, with a reduction in height compared with a double wall, to retain a comparable stiffness.

The building had plan dimensions of 12 metres length by 10 metres span. Its roof contained duo-pitch trussed rafters, running parallel from gable to gable, an extremely common arrangement. The building was of an "empty box" configuration, with no internal walls present to provide alternative load paths, following the occurrence of the "accidents". This arrangement was selected in order to create a worst case situation in a single-storey trussed rafter roofed building of this nature.

The trussed rafters were of fink configuration, with 25° pitch. Design followed the recommendations of BS 5268 : Part 3. They were fabricated from M75 timber and 20 gauge nailplates. They were located at the usual spacing of 600mm. The top chord cladding comprised interlocking tiles on felt and battens, which is the commonest cladding type used in conjunction with trussed rafters. The battens were a conventional size of 25mm by 38mm.

Galvanised steel holding-down straps were inserted in the support walls to resist the uplift of the roof under high wind loads. Again, this was an adverse situation, since in practice cavity or other more substantial wall constructions would be common. The gable walls were tied into the roof in the conventional manner, using timber blockings and packing, in conjunction with galvanised steel straps hooked around the external face of the gable wall. The wall plate was 50mm deep by 100mm wide. It was end-jointed using half-lap joints at typical locations. A 10mm wide gap down the full height of the wall was incorporated at mid-length of the 12-metre long wall.

A removable wall panel, discussed in more detail below, was incorporated in the length of one 12-metre long wall. This was constructed using conventional timber framing techniques, but with added stiffening rails, to resist the forces of sudden removal. Between the simulated accidents, the removable panel was structurally secured to the adjacent blockwork.

The design loads used to size the 10-metre span trussed rafters which were incorporated in the building are shown in Table 1. The following data were also used:

Wind:	Basic wind speed	40 m/s
	Ground roughness	2
	Building class	B

One third of the snow and of the full bottom chord imposed load were assumed to be present at the time of the simulated accidents.

A general impression of the design of the test building may be obtained by reference to Figures 1 and 2. Figure 1 shows the roof plan and end elevation. Figure 2 shows the plan on the wall plates, and details of the removable panel.

Table 1 Design loads of the 10-metre span trussed rafters

DESCRIPTION	LOADING
Top chord dead load	0.685 kN/m ² on slope
Snow load	0.600 kN/m ² on plan
Bottom chord dead	0.25 kN/m ²
Bottom chord imposed	0.25 kN/m ²

GENERAL METHODOLOGY

It was decided that the type of accident likely to lead to the removal of major lengths of supporting walls in a structure of this nature would be a vehicle impact. It would have been desirable, if possible within the scope, to cover accidents due to explosions, but this would have added magnitudes of time and expense to the project. It was never the intention of the project to embrace seismic considerations, a point of importance for some CIB members. It was recognised that possible variations on the vehicle impact included the length and location of the local load-bearing wall collapse. However, since it was required to vary several factors involving the roof construction, it was felt beyond the scope to change the aperture width and position.

The majority of the accidental events were simulated by rapidly pulling the 3.6 metre long stiffened timber frame wall panel out of the mid-length of one of the side walls of the building. The dimension of 3.6 metres was decided upon in comparison with the likely damage from a wide, or angled, lorry impact. In considering a suitable dimension for this removable length of wall, the definition of the term "disproportionate" was borne in mind.

The removal of the wall panel was achieved using a sideloader vehicle, pulling chains attached to steel hooks on the timber frame panel. Figure 3 shows this removable wall panel during the instant of displacement, in one of the tests. To prevent the timber framed wall panel from dragging directly upon the adjacent roof or wall construction during the simulated impact, fixings were omitted between the removable panel and its wall plate. Also, layers of polythene and small gaps were provided in certain positions, to achieve a clean pull out.

To represent a snow load of 0.2 kN/m² throughout the tests (one third of the normal design snow load), weight bags were attached to the tiling. In an area adjacent to the removable wall panel, the tiling was omitted to provide a clearer view of the behaviour of the secondary roof construction. In this area, heavier weight bags were placed to compensate for the absent tiles. Weight bags were also placed to simulate one third of the bottom chord design imposed loads.

Throughout the tests, two main types of measurement were made. Firstly, the total relative movements occurring during each simulation between the trussed rafters and the components of secondary construction were recorded at pre-selected locations. Prior to each simulation, thin indelible lines were marked on the components of secondary construction at the points where they overlapped the trussed rafters. Any movements of these lines from the sides of the trussed rafters following the simulation were recorded. Secondly, during each simulation, the deflections of the trussed rafters at seven locations were recorded on a single time axis. The timber framework to which the deflection transducers were fixed was self-supporting and entirely separate from the roof structure. The deflections measured by the transducers were recorded by an Advanced Data Acquisition Unit and were subsequently transferred to a computer disk.

Three video cameras were also used to record the behaviour of the structure throughout the simulations. One was aimed to view into the roof void, and was intended to record any progressive collapse beyond the supported area. Two further cameras were located on platforms above the building. These were trained on the particular areas of the roof which were likely to be directly affected.

CONSTRUCTION VARIABLES

As indicated above, it was intended to evaluate the contribution to the overall robustness of the structure brought about by a variety of elements of secondary construction in the roof. These were varied during four separate accidental event simulations, which are described in more detail immediately below. The structure proved to be so robust that it was relatively undamaged, even after four simulations. Advantage was taken of this, and a further series of simulated accidents were performed, closer to one of the gable walls. These additional simulations are described subsequently.

The first simulations assumed a construction with a suspended ceiling. On account of its probable negligible structural contribution, such a ceiling was actually omitted. Horizontal flat topped trussed rafters were inserted along each eaves, to act as wind girders to the side walls. At each gable, these wind girders were bolted to rolled steel angles, which in turn were bolted to the walls. They were also nailed to the underside of all of the trussed rafters. In addition to the wind girders, the stability bracing specified in BS 5268 : Part 3 was attached. The diagonal rafter bracing was of the cross type, rather than a diamond configuration. "Chevron" bracing was attached to the internal struts of the trusses, and longitudinal binders were also included.

The roof construction for Simulations 1 and 2 was broadly similar to one another. Immediately upon first testing, it was apparent that the wall plate above the void was making a significant contribution to the robustness. Since this might not be deemed to be a "fair test", it was decided to make a complete cross cut through this member, at the centre of the gap span. This was the main difference between Simulation 1 and Simulation 2.

For Simulation 3, the eaves wind girders were removed, and a 12.5mm thick plasterboard ceiling was fixed to the underside of the trussed rafters. The only other difference from the previous simulations was that the spanning capacity of the wall plate was completely immobilised by two additional saw-cuts through the wall plate close to each edge of the removable timber frame panel. These two changes, the fixing of a plasterboard ceiling and the immobilisation of the wall plate spanning capacity, also applied to all subsequent simulations.

The construction for Simulation 4 was approximately the same as that for Simulation 3, except that both lines of chevron bracing were also removed.

The principal construction variables in the main test series, as described above, are summarised in Table 2.

As mentioned above, no collapse of the roof occurred during the first four simulations, and the masonry construction was largely undamaged. Consequently it was decided to continue testing, incorporating additional construction variables. The first phase indicated that the interlocking tiles made a significant contribution to the longitudinal spanning capacity of the roof. It was recognised that other forms of roof covering, such as plain tiles, would be less capable of providing locking and frictional benefits. Consequently the structure was reorganised with tiles omitted from an area measuring 6.0 metres long by half-span (5.0 metres) wide. This reconstruction was referenced as Simulation 5.

The battens in the untiled area were all renewed, the top chord longitudinal bracings were also replaced, and the chevron bracings were reinserted. Some lightly damaged plasterboard panels were also renewed. Additional weight bags were placed over the untiled area to compensate for their mass.

A final series of simulations is described, involving a gap created near a gable wall, rather than at the centre of the longitudinal wall. These are all termed Simulation 6, with four subsidiary steps. These steps were taken in an ad hoc manner on a single day of testing, during which it was intended eventually to ensure that substantial areas of masonry were deliberately destroyed, in addition to the removable wall panel.

Table 2 Principal construction variables in the main series of simulations

SIMULATION NO.	CEILING TYPE	BRACING ARRANGEMENTS			WALL PLATE DETAILS
		Diagonal rafter bracing and longitudinal braces	"Chevron" bracing	Two horizontal wind girders	
1	Suspended ceiling assumed (none present)	Diagonal rafter bracing and longitudinal braces	"Chevron" bracing	Two horizontal wind girders	Continuous across gap
2	As above	As above	As above	As above	Cut at mid-gap
3	Plasterboard ceiling of 12.5mm thickness	As above	As above	No wind girders	Cut at three places in gap
4	As above	As above	No chevron bracing	No wind girders	As above

For Simulation 6, new blockwork was constructed in the gap formerly left for the removable panel. A new gap of 3.6 metres width was created, starting at a position in the side wall 775mm from the end gable blockwork, and extending away from the gable end. The wall plate above the gap was disabled by saw cuts. The remainder of the internal roof construction was as described for Simulation 5. The roof area above the new gap was tiled, as for Simulations 1-4.

RESULTS

The results of the simulations are described in this section of this paper in a very much abbreviated manner. A comprehensive description of the behaviour of the building under the accidental event simulations has been reported elsewhere (5) (6). The effects on the building's construction, the measurement of movement in the roof, the relative movements between the trussed rafter and the secondary components, and the transient movements, have all been recorded, tabulated and discussed.

The following are the salient features of the results.

Following Simulation 1, the building and the roof were inspected, and the recordings and marks reviewed, in order to assess any damage that had occurred in terms of the items mentioned above. No damage was observed to the trussed rafters themselves. Also, in general, there were no signs of distress in any of the elements of secondary construction, such as the various bracing members, tiling battens and horizontal wind girders. The wall plate over the gap caused by removing the wall panel was clearly bent to an extent likely to indicate overstressing, but it had not snapped. After this first simulation, the wall plate was deliberately severed, as described above. Small cracks appeared in the blockwork to either side of the gap, but these were insignificant from a structural viewpoint.

After Simulation 2, the structure appeared as illustrated in Figure 4. The vertical movements of the roof at this stage were only slightly larger than those following Simulation 1, despite the wall plate spanning capacity having been markedly reduced by a saw cut at mid-span. Some further hairline cracking occurred in the mortar joints at the top of the blockwork, to either side of the gap.

As a result of Simulation 3, the vertical movements of the roof were approximately twice those of Simulation 1. This was largely attributed to the ineffectiveness of the wall plate. At this stage also, the end joints of the chevron braces showed elongated nail holes, where there were attachments to trusses near to the area of damage.

For Simulation 4, both lines of chevron bracing were removed. This caused a further increase in the vertical roof movements following the "accident", with a maximum vertical drop of 237mm occurring at the mid-span of the wall plate. The final static position of the roof at this stage is shown in Figure 5. A number of the outer battens had failed in hogging, but again there was no total collapse of the roof. The roof hung in the bowed shape shown in Figure 5 for over half an hour.

Table 3 shows the vertical deflections of the wall plate at the centre of the gap after each of the four simulations described above. These deflections formed part of the basis for an approximate analysis which led to an estimate of the contributions of the various parts of the secondary construction. This is touched upon briefly in a following section of the paper, outlining the analysis.

Table 3 Vertical deflection of the wall plate at the centre of the gap, after each simulation.

SIMULATION NO.	DEFLECTION OF WALL PLATE AT CENTRE OF GAP (MM)
1	81
2	108
3	173
4	237

Simulation 5, in which no tiles were present along a 6.0 metre length of the roof where the mid-wall gap occurred, demonstrated the extreme resilience of a trussed rafter roof of this nature. The line of chevron bracing closer to the gap was clearly heavily stressed since most of the nailed end joints were pulled completely off the trusses. Nevertheless, the roof stood up in a stable, albeit deflected, manner with no serious transference of damage beyond the immediately affected area. Figure 6 illustrates the condition of the roof at this stage.

The final series of simulations, Simulation 6, Steps 1 to 4, involved removing first a 3.6 metre length of wall close to a gable, and then progressively removing more of the blockwork return to the gable, and finally the entire gable itself.

The results of Simulation 6, Step 1, in which the 3.6 metre panel was removed in a similar manner to Simulations 1-4, were, in general terms, no different to the earlier tests. There was no major distress in any part of the roof beyond the immediately affected area, and the "accidentally damaged" region merely drooped.

Following Steps 2 and 3 of Simulation 6, where areas of blockwork return to the gable end were rapidly snatched from beneath the truss, by means of chains attached to a vehicle, the roof structure was spanning a void of over 4.3 metres width. To one side, the roof was bearing directly onto the gable wall. At this stage, support was dependent almost entirely upon tiling battens and the steel restraint straps. Figure 7 shows the roof in this penultimate condition.

Collapse of the roof was finally provoked by Step 4 of Simulation 6, in which the entire gable wall on the test side of the ridge line was dragged from under the roof structure. Figure 8 shows the test building after the collapse. It is very important to note that no part of the roof supported on the blockwork to the left of the deliberately damaged area (as viewed in Figure 8) had fallen. The bracing and battens all failed in hogging, a short distance beyond the final supported truss. The total horizontal movement of the final truss which stood immediately to the left of the damaged area was only in the order of 40mm.

ANALYSIS

Approximate analyses were undertaken to determine the relative contributions of the various components of secondary construction, present during each simulation, to the overall collapse resistance of the roof. The assumptions, analysis method, and tabulated calculations are presented more fully elsewhere, and the following is a brief summary, leading to a presentation in a simple graphical form. Only Simulations 1-4 were dealt with analytically in this manner.

An analytical assumption was that, since complete roof collapse did not occur in any of the four simulations, their vertical and rotational equilibrium must have become regained in each of the situations depicted by Figures 4, 5 and 6. The rotational equilibrium was considered in a transverse plane of the roof, with a pivotal point at the bearing of the truss on the intact wall (that opposite the gap caused by the "accident"). It was recognised that each secondary longitudinal component must have made a contribution to upholding both the vertical and the rotational equilibrium. Their contribution to each type of static balance would have been unlikely to have been equal, but it was felt more meaningful to concentrate upon the rotational case.

The secondary components were listed and categorised as either:

- a) "behaviour largely known" (BLK) components, or
- b) "behaviour largely unknown" (BLU) components

Examples of the former included the top and bottom chord longitudinal bracings, the wind girder chords (where present) and the wall plates (where effective). Examples of the latter included the tiles and the chevron bracing. The contributions of the BLU components were estimated by means of a process of elimination, after approximate calculations concerning the BLK components. These calculations involved the stiffnesses (moments of inertia, moduli of elasticity); distances from the intact wall; mid-gap deflections (Table 3); vertical uniformly distributed loadings, and hence the resistant moments provided by the various elements. These were compared with the known total overturning moment of a unit length strip of roof, calculated from its total self-weight.

Figure 9 illustrates graphically the percentage contributions of the secondary components of the roof construction to the resistance against collapse, following the analysis summarised above.

Salient features of the analysis results were as follows. It was evident from Figure 9, Simulations 1 and 2, and also directly from Table 3, that the wall plate above the "damaged" area of wall was contributing considerably to the support action after the "accident". In Simulation 1, it was providing 32% of the total resistance against overturning of the residual roof structure. Of course, this might or might not occur in a real accidental event, dependent upon the angle and height at which the impact occurred. For this reason, the wall plate was disabled by deliberate cross cutting from Simulation 2 onwards. Nevertheless, it continued to play a significant role, as indicated in the subsequent diagrams in Figure 9. This is of interest to timber frame designers, since it provides a good justification for retaining such binding members in panelised construction, even though they are not included in most, or any, normal formal static design calculations.

From Simulation 2 onwards, the greatest single contribution from any particular element was obtained from the longitudinal top and bottom chord bracings. Again, these may be regarded by conventional designers as relatively insignificant members, whose purpose is largely overlooked or not understood. Their beneficial contribution depended upon their being fixed in such a manner that they would be capable of acting as continuous members across the unsupported zone of the roof.

Finally, it is very evident from the bar graphs of Figure 9 for Simulations 3 and 4, and from the photographs such as Figure 5 and Figure 7, that the tiles were able to act as an effective structural medium, either by themselves or, more probably, by forming some type of composite layer, together with the felt and battens. By the process of elimination described above, the flexural rigidity of the tile/batten layer was estimated. For illustrative purposes, to make timber designers aware of the order of magnitude of their potential, the effective EI of the tile/batten layer was found to be comparable with the stiffness that would have been provided had the roof been clad with a continuous layer of 20mm thick GS grade softwood boarding, laid parallel to the ridge.

CONCLUDING REMARKS

A full-scale testing programme was conducted upon a trussed rafter roofed building, to assess its response to simulated accidental events. The test building which was constructed represented a typical non-domestic trussed rafter roofed low rise structure, of moderate span, using masonry walls. It was roofed in a conventional manner, with trussed rafters of 10 metres span at 600mm centres. A number of variations of detail in the secondary roof construction were incorporated in the building, and for each of these, a simulated "structural accident" was replicated. Standard bracing, and in some cases additional bracing, was included.

In the case of public buildings of the type which the test structure was intended to represent, there is a distinct requirement in the Building Regulations (England and Wales) to construct in a manner such that, in the event of a failure of the roof or its supports, the building will not collapse to an extent disproportionate to the cause. Since there is also a general requirement by EC5 to design in such a manner as to avoid disproportionate damage, then the results of this project are of further and more universal relevance.

The type of accident envisaged in the simulations was the removal of a length of external load bearing masonry wall, through a vehicle impact.

As described above, the main series of tests involved the sudden removal of a 3.6 metre length of support wall, beneath the trussed rafter roof, with the ensuing gap appearing at the mid-length of a longitudinal external load bearing masonry wall. Four tests were carried out under these conditions, each with a progressively less robust degree of secondary and longitudinal construction incorporated in the roof detailing. However, under none of the construction detailing cases covered by these four simulations did any of the major parts of the roof structure collapse to the stage of reaching the ground. This was found to be the case both for the simulated suspended ceiling arrangements and for a plasterboard ceiling. Even with interrupted wall plates, simulating unconnected butt joints over the gap, and with parts of the obligatory roof bracing removed, the roof framework remained stable, albeit with large deflections.

The four secondary components found to contribute most substantially to the robustness of the roof in resisting collapse were as follows:

1. The wall plates: Clearly their contribution depended greatly upon the relative positions of the wall plate end joints and the removed length of support wall, but if the wall plates were to remain spanning the gap after the "accident", then they would seem to make a substantial contribution to the support of the affected length of roof.
2. The "chevron" bracing: It was found that the two lines of chevron bracing made a significant contribution to the longitudinal structural rigidity of the roof, despite their incomplete triangulation. Ultimately, their capacity was limited by the performance of their nailed end joints and, with better fixings, it would be possible to extend this bracing concept to obtain even greater resistance, if required.
3. The longitudinal bracings: The top and bottom chord longitudinal bracings, acting in conjunction with the other elements of the roof framework, also contributed in a surprising degree to the support of the damaged framework.
4. Other wind bracing components: The flat longitudinal wind girders, and the plasterboard ceiling, where present, also contributed in a more minor degree to the stiffness of the secondary construction.

By deduction, it was concluded that the "behaviour largely unknown" elements, particularly the tiles, felt and battens, were contributing significantly to the ability of the damaged structure to resist collapse. This is discussed further below.

The top chord roof cladding, consisting of interlocking tiles, was found to significantly increase the capacity of the timber secondary components to transfer loads from the unsupported zone of roof onto those trussed rafters still supported at both ends. This increase in resistance was between 20% and 60%, depending upon

which secondary timber components were present during the associated accidental event simulation. The longitudinal flexural rigidity of the tiles and underlying felt and battens was found to be broadly comparable to that of a diaphragm of continuous 20mm thick GS grade timber boarding laid parallel to the ridge.

Following the main series of four simulations with progressively less material incorporated in the secondary roof construction, the test building remained essentially intact and, with small repairs, further testing was possible.

Additional tests were conducted to assess:

1. The resistance to collapse of the roof, with another "accidental" gap created at mid-wall length, but with the structural contribution of the tiles removed completely (their weight being simulated).
2. The behaviour of the structure when a gap was created by the sudden removal of a length of support wall close to a gable end.
3. Finally, the resistance to collapse when portions of the gable masonry itself were removed.

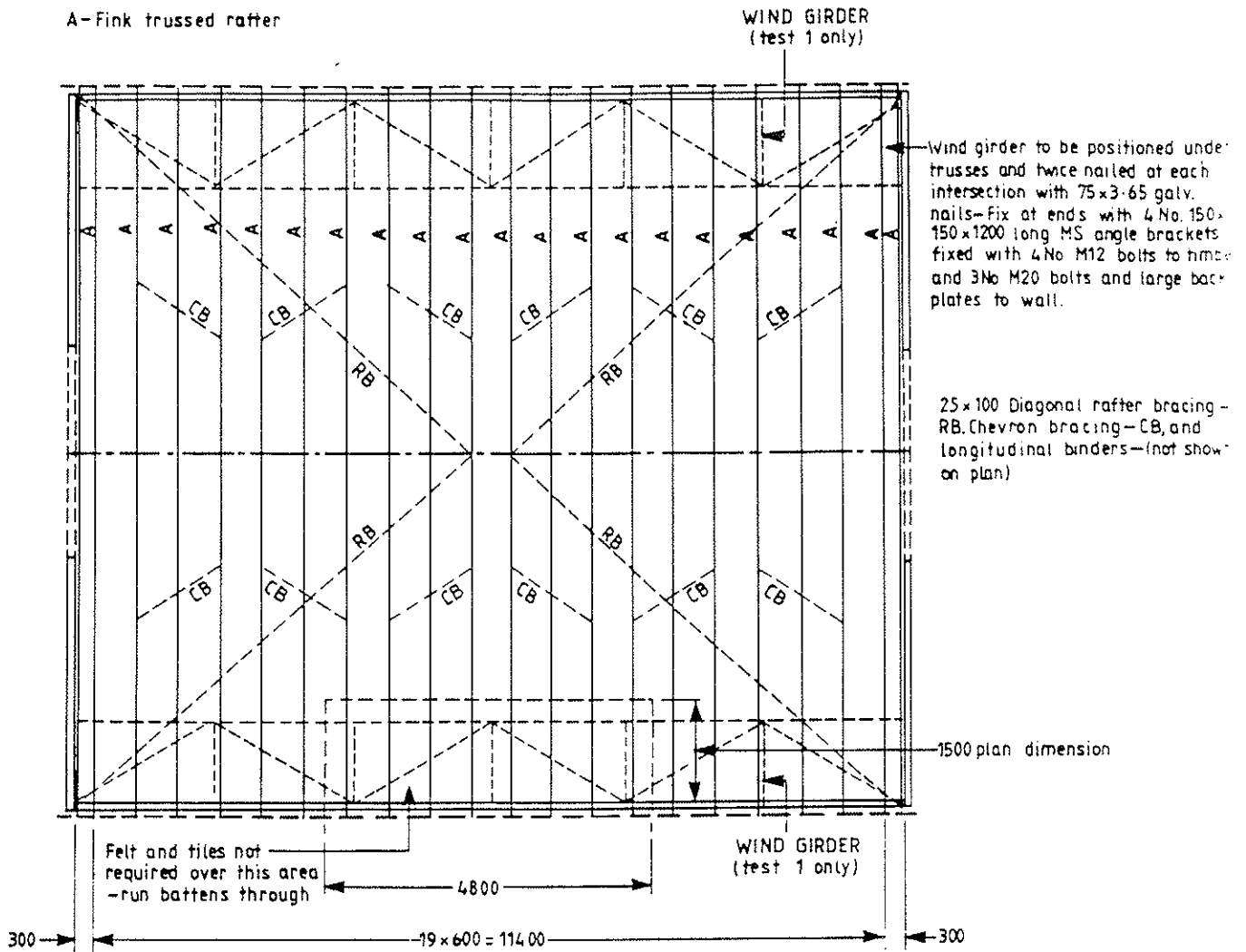
The roof did not collapse at all under the first condition described above. It was able to span a 3.6 metre void in the length of the support wall with structural resistance to collapse, provided in the longitudinal direction, only by means of tiling battens and longitudinal and chevron bracing.

The final phases of testing showed most dramatically the robustness of this trussed rafter roof construction in resisting such simulated accidents. The roof showed a capacity to span a void in the support wall, close to the gable end, of over 4.3 metres. When collapse of the roof was eventually provoked, by removal of the entire half of a masonry gable wall to the side where the truss heels stood, plus the remaining gap in the longitudinal wall, then no part of the roof beyond the unsupported areas collapsed to the ground, and the damage was still considered proportionate to the original cause of the failure. Horizontal deflections of the adjacent, undamaged roof were very small in terms of such a dramatic incident.

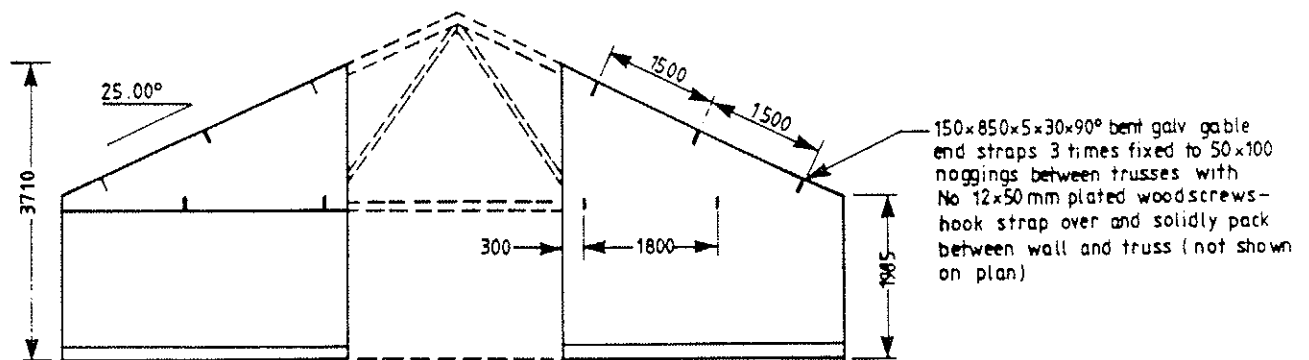
The general conclusions are therefore that braced trussed rafter roofs of this form have been demonstrated to be very robust in the face of accidental events of the nature likely to be caused by vehicle impacts and similar events. Large areas of roof support can apparently be removed without collapse occurring which is disproportionate to the cause of the foreseen structural damage. Such roofs are likely to satisfy the very specific requirements of the UK Building Regulations for avoidance of disproportionate collapse in low rise public buildings of 9-metre span or greater. The evidence of these tests is also of a more universal relevance, in view of the principle of EC5 that disproportionate damage should be avoided in design.

REFERENCES

- [1] Mettem, C.J. and Marcroft, J.P. The robustness of timber structures. CIB-W18A/22-15-6, Berlin, 1989.
- [2] Mettem, C.J. and Marcroft, J.P. Disproportionate collapse of timber structures. CIB-W18A/23-15-6, Lisbon, 1990.
- [3] Department of the Environment and The Welsh Office. The Building Regulations 1991, Approved Document A, HMSO (2nd Ed. 1992) London.
- [4] European Committee for Standardisation (CEN). ENV 1995-1-1:1993, Eurocode 5: Design of Timber Structures, Part 1: General rules and rules for buildings. Edited draft, 1993.
- [5] TRADA. Report for Disproportionate Collapse of Timber Structures - Full-scale testing programme simulating accidental events on a trussed rafter roofed building. Report No. PIF62/5, March 1992.
- [6] TRADA. Report for Disproportionate Collapse of Timber Structures - Extension to full-scale testing programme simulating accidental events on a trussed rafter roofed building. Report No. PIF 62/6, October 1992.



ROOF PLAN



ELEVATION ON ARROW C

Figure 1 Roof plan and end elevation of test structure

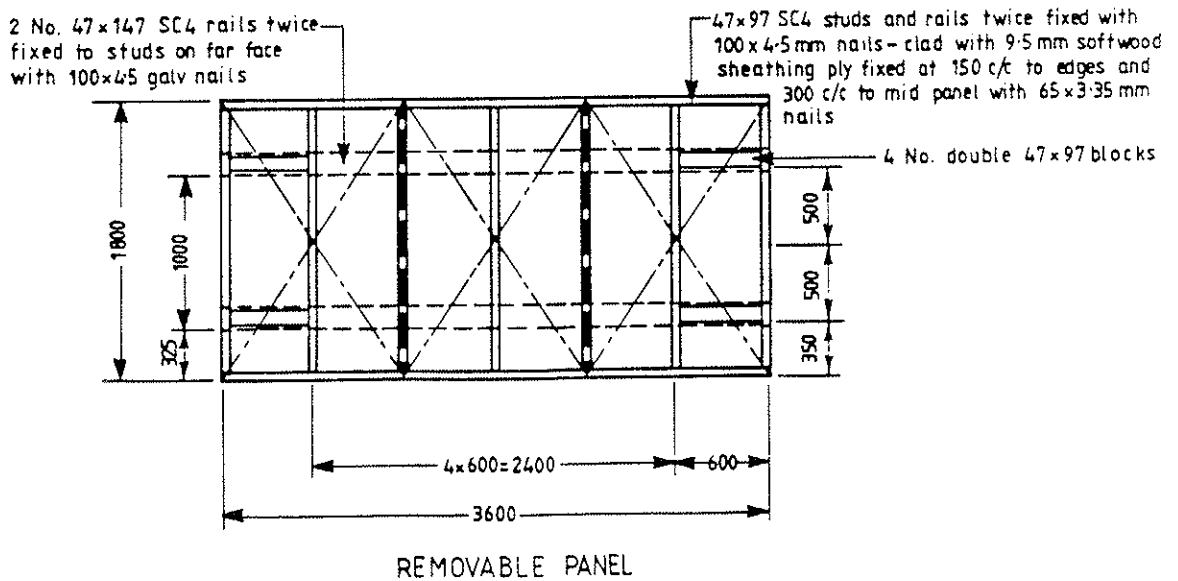
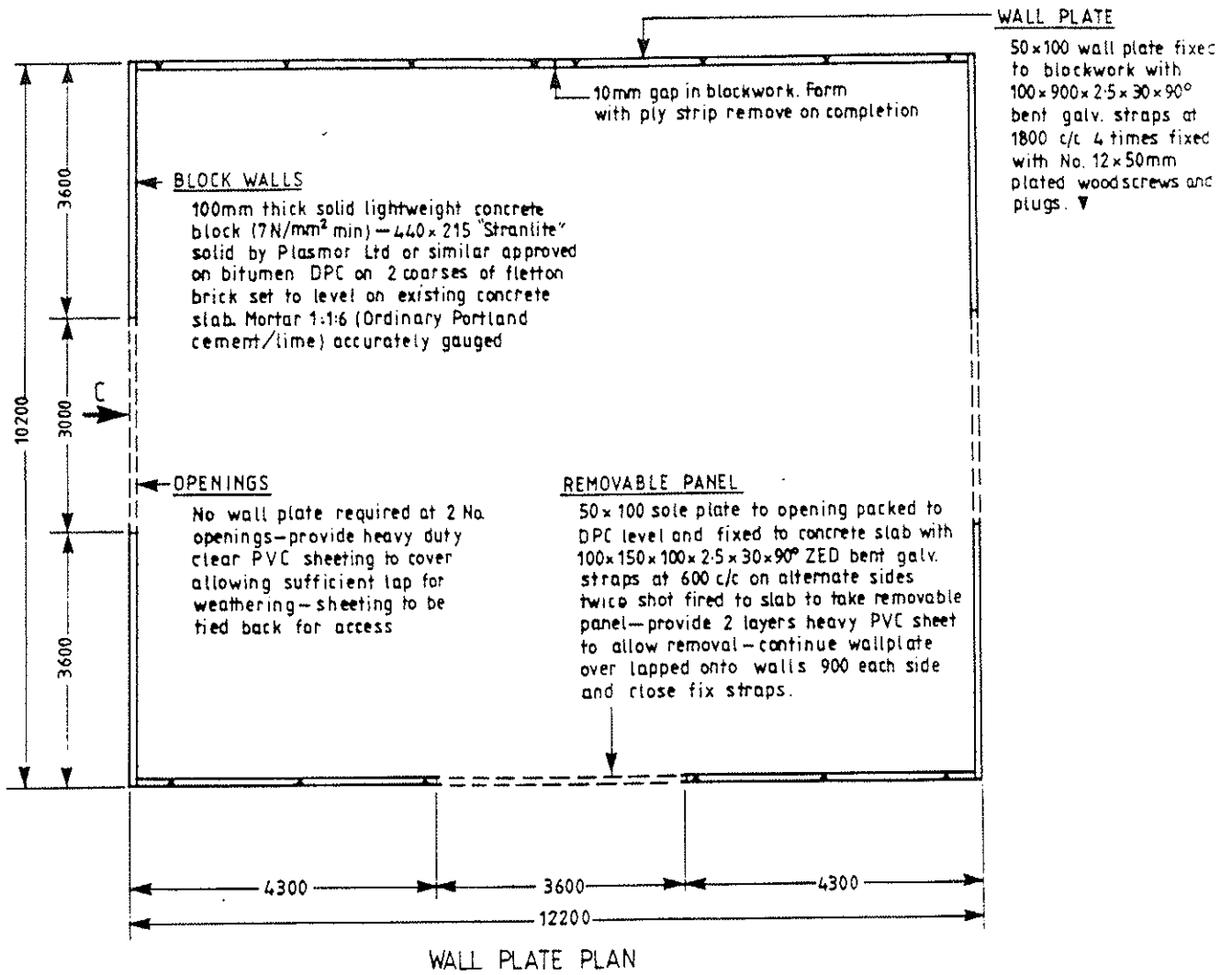


Figure 2

Plan on wall plates and details of the removable panel



Figure 3 Removable wall panel during the instant of displacement



Figure 4 Static position of roof after simulation 2



Figure 5 Static position of roof after simulation 4

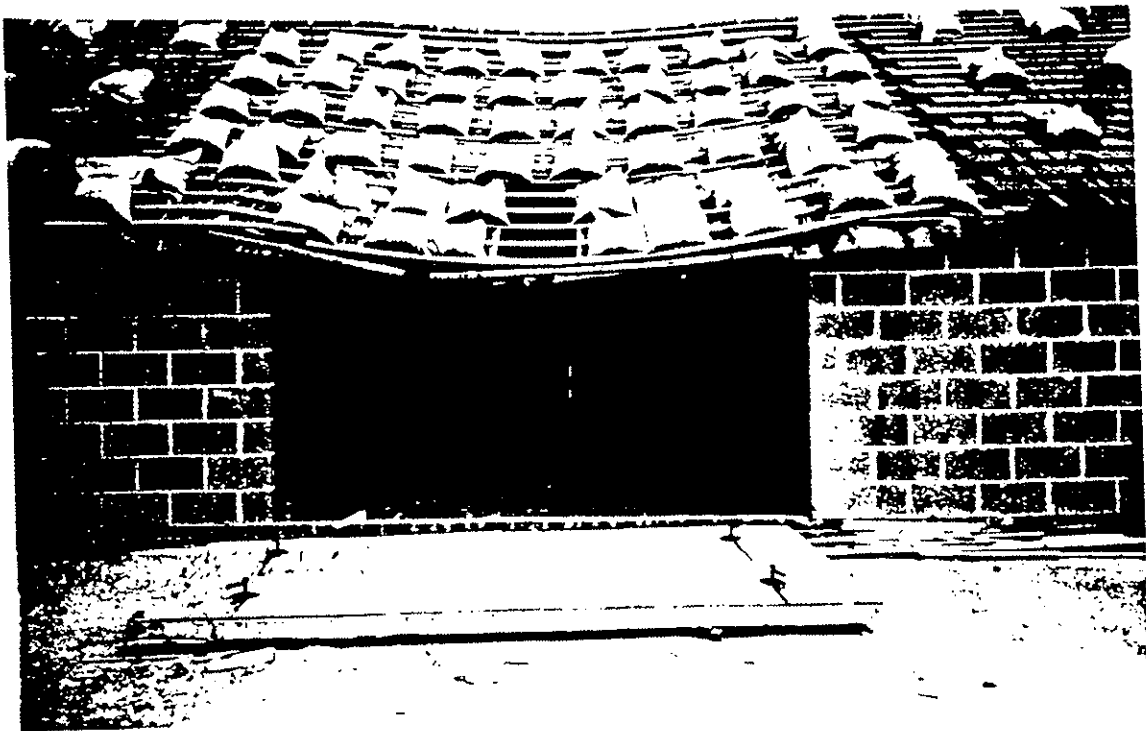


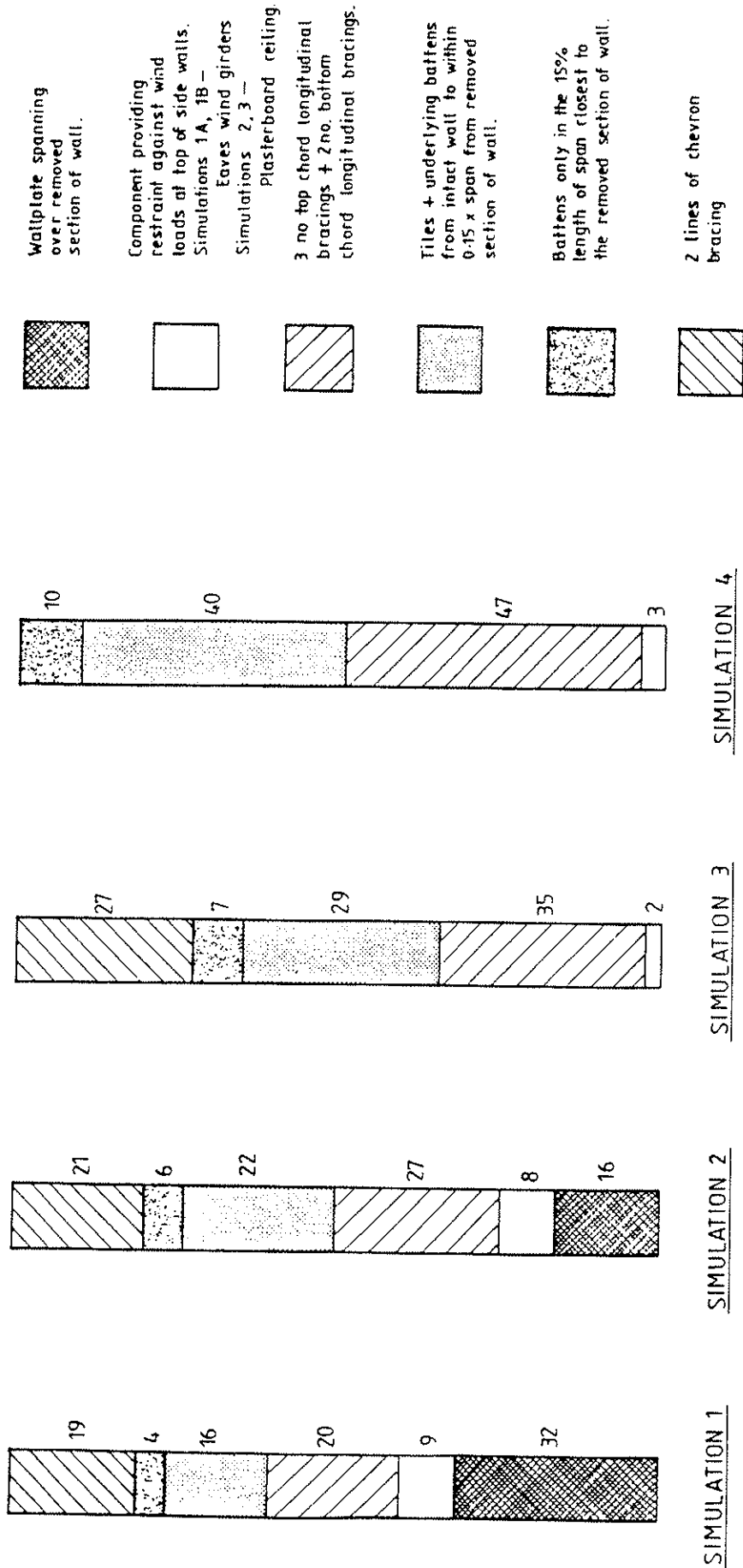
Figure 6 Static position of roof after simulation 5



Figure 7 Static position of roof after removal of corner masonry
(simulation 6, step 3)



Figure 8 Final collapse of roof, after simulated "accident" to gable end
(simulation 6, step 4)



NOTE
 The number beside the shading is the percentage contribution of the secondary component concerned.

Figure 9 Contributions (percent) of the secondary components of roof construction to the resistance against collapse

INTERNATIONAL COUNCIL FOR BUILDING RESEARCH STUDIES AND DOCUMENTATION

WORKING COMMISSION W18 - TIMBER STRUCTURES

BRACING REQUIREMENTS TO PREVENT
LATERAL BUCKLING IN TRUSSED RAFTERS

by

C J Mettem
TRADA Technology Limited
United Kingdom

P J Moss
University of Canterbury
New Zealand

MEETING TWENTY - SIX

ATHENS, GEORGIA

USA

AUGUST 1993

BRACING REQUIREMENTS TO PREVENT LATERAL BUCKLING IN TRUSSED RAFTERS

C.J. Mettem, TRADA Technology Limited, United Kingdom
P.J. Moss, University of Canterbury, New Zealand

INTRODUCTION

This paper describes a series of tests on trussed rafters, which were aimed at measuring their out-of-plane stiffness and hence determining directly the bracing stiffnesses and forces required to prevent their lateral buckling. The need for the work arose during a project on practical applications of bracing studies. This drew upon earlier research whose object had been to develop theories permitting calculations to be made in relation to topics such as the bracing of beams and columns, and the provision of discretely spaced braces for roof members [1]. A series of design guides is being developed relating to stability and bracing applications, and one of these is to deal with the design of bracing for newly constructed trussed rafter roofs, as opposed to remedial bracing. It was realized that little or no experimental determinations of the out-of-plane stiffness of trussed rafters, for the purpose of confirming parameters for their stability bracing, had ever been carried out. Consequently, these tests were planned. It was intended to compare the measured lateral stiffnesses of the trusses with theoretical predictions. It was recognized that it would have been preferable to carry out more extensive practical testing, including measurements on whole-roof frameworks as three dimensional assemblies. However, this was not possible within the present scope.

The tests described were of a non-standard type. Forces representing various normal vertical design load cases were applied at the node points of the trusses. The trusses were in fact tested in a horizontal arrangement, for convenience, but these normal 'vertical' loads are described as such throughout this paper. Small loads at right angles to the plane of each truss were also applied, whilst the trusses were subjected to the main vertical loadings. These secondary loads were used, in conjunction with precise lateral deflection measurements, to evaluate the out-of-plane stiffness for each truss configuration, load case and restraint arrangement.

TRUSS CONFIGURATIONS AND LOAD CASES

Four trussed rafters were tested. All were designed for a 9.6m span, to be spaced at 610mm centres. The components were of a normal 'Fink' (single W) configuration. Pitches varied, with one truss having a pitch of 15°, two pitched at 25° and one at 35°. The timber from which they were constructed was machine stress graded. The species was European whitewood, of M75 grade, and all members consisted of planed material of 35mm actual thickness. Table 1 summarises the truss configurations and the member sizes used within them.

Table 1 Truss configurations and member sizes

Span m	Pitch degrees	Member Sizes (M75 w.w.)		
		Top Chord mm	Bottom Chord mm	Webs mm
9.6	15	35 x 145	35 x 120	35 x 72
9.6	25	35 x 120	35 x 120	35 x 72
9.6	35	35 x 120	35 x 120	35 x 84

The trussed rafters were designed for normal vertical (in-plane) loadings in accordance with BS 5268 : Part 3. To this end, a trussed rafter system owner's software gave necessary information on member forces, moments and deflections at node points. The design loadings for the trusses are summarised in Table 2.

Table 2 Design loadings

Description	Abbreviation	Loading
Top chord self weight	TD	0.685 kN/m ² on slope
Snow load	SL, SR	0.75 kN/m ² on plan
Bottom chord self weight	BD	0.25 kN/m ²
Bottom chord imposed	BL	0.25 kN/m ²
Point load	ML	0.9 kN
Water tank	WT	0.45 kN/node

The design load cases which were considered were as follows:

Dead load:	TD + BD
Long term:	TD + BD + BL + WT
Medium term:	TD + BD + BL + WT + SR + SL
Short term:	TD + BD + BL + WT + SR + SL + 0.75ML

TEST METHOD

The trusses were tested in the horizontal plane for convenience of support and loading arrangements. The heels of each truss were supported horizontally and vertically at two reaction points, which were based on the laboratory strong floor. The apex and the panel points at the mid-length of each rafter and the third-points of each ceiling tie were supported in the lateral plane, off the strong floor. These supports were finely adjustable in height, so that the nodes could be precisely maintained at a horizontal level.

Forces representing the vertical loads were applied at the panel points by means of torque bolts. These bolts in turn were based on strong steel reaction frames anchored to the strong floor. Between the torque bolts and the loaded node positions of the truss chords, compression load cells were incorporated, to provide accurate measurement of the forces applied.

Loading procedure

A range of levels of vertical (in-plane) loadings were applied to each truss. These levels corresponded to five increments, ranging from Dead Load through Long Term Load, to full Medium Term Load. Three cycles of these in-plane loadings were performed, and the measurements obtained under each cycle were averaged. Whilst loaded in such a manner, it was found that the trusses would tend to buckle laterally. This was as intended, since they were unrestrained by any form of longitudinal or bracing construction, such as would be found in a real roof.

The lateral supports upon which the trusses were rested could be finely adjusted for height. Levels were used, to ensure that the trusses could be perfectly restored to their horizontal position. Out-of-plane deformations in the members were measured at the reaction points by means of dial gauges, and overall along their length by means of string lines, which were checked from levels off the horizontal testing floor. In-plane ('vertical') deflections at the nodes were also measured, using dial gauges.

'Lateral' loads (vertical, on the rig, since the trusses were tested horizontally) were applied at each node of the truss, according to the mode of buckling being investigated. A small hanger, pulley and cable system was used for this purpose. The counterbalancing weight that was required to reduce to zero each lateral support reaction, from a negative or positive value, was measured on the finely adjustable lateral supports. This counterbalancing weight represented the force required to prevent the trussed rafter from buckling laterally under the vertical (in-plane) loads. The counterbalancing weights that were found necessary to perform this operation were in the range 0 - 300 N.

TEST RESULTS

Table 3 shows the mean measured lateral stiffnesses at the apex of each truss. These are tabulated against the load level corresponding to the in-plane forces, which were determined according to the method of analysis described above. Each lateral stiffness measurement is an average of three loading cycles.

Since it did not appear that the stiffness varied systematically with the levels of vertical load which were applied, but fluctuated around an average value, grand means for the measured lateral stiffnesses at the apex of each truss are indicated at the foot of the table.

Table 4 shows in a similar way the measured lateral stiffnesses at the mid-rafter panel point, and the corresponding in-plane rafter forces determined from the analysis at this point. As with the values at the apex, there was no systematic relationship between lateral stiffness and in-plane force, and the grand means of lateral stiffness for each truss are indicated at the foot of the table.

Table 3 In-plane rafter forces and mean measured lateral stiffnesses at apex

Load level	In-plane rafter forces and lateral stiffnesses							
	Truss 1 (15°)		Truss 2 (25°)		Truss 3 (25°)		Truss 4 (35°)	
	Force	Stiffness	Force	Stiffness	Force	Stiffness	Force	Stiffness
	kN	N/mm	kN	N/mm	kN	N/mm	kN	N/mm
1	6.5	80	4.3	171	4.3	73	3.4	67
2	8.2	74	5.3	206	5.3	73	4.1	69
3	10.0	82	6.4	133	6.4	52	4.9	86
4	12.5	70	8.0	172	8.0	79	6.1	59
5	15.1	66	9.5	169	9.5	88	7.3	66
Grand means	-	74	-	170	-	73	-	69

Table 4 In-plane rafter forces and mean measured lateral stiffnesses at mid-rafter panel point

Load level	In-plane rafter forces and lateral stiffnesses							
	Truss 1 (15°)		Truss 2 (25°)		Truss 3 (25°)		Truss 4 (35°)	
	Force	Stiffness	Force	Stiffness	Force	Stiffness	Force	Stiffness
	kN	N/mm	kN	N/mm	kN	N/mm	kN	N/mm
1	7.4	75	4.9	58	4.9	57	3.9	107
2	9.1	49	6.0	84	6.0	62	4.6	120
3	10.8	78	7.0	56	7.0	53	5.4	109
4	13.8	69	8.9	51	8.9	83	6.9	125
5	16.9	75	10.8	53	10.8	57	8.3	151
Grand means	-	69	-	60	-	62	-	122

COMPARISON WITH COMPUTER ANALYSIS

As a basis for comparison with the tests, a series of linear elastic computer analyses were performed, in which the combined vertical and lateral loading arrangements were simulated. The software used for this purpose was MicroSTRAN 3D, Version 4, with the trusses modelled as three-dimensional frames, and with certain joints pinned. The three-dimensional analysis model which was used is illustrated in Figure 1.

The model was devised so that trusses were supported laterally, as in the tests, and were acted upon by the respective medium-term loads, which were applied at the rafter panel points and at the apex. At the same time, a 1kN out-of-plane disturbing force was applied to either the apex point or the mid-rafter panel point. It was possible to investigate a range of lateral support configurations and their ensuing stiffnesses, using the model. In order to describe the lateral support options which were included, reference should be made to Figure 2, in which the relevant rafter nodes in the analysis are numbered from 0 to 8.

The simulation cases which were run for combinations of out-of-plane support are described in Table 5 for the out-of-plane disturbing force at the apex, and in Table 6 for the out-of-plane disturbing force at the mid-rafter node. In these tables, the presence of an asterisk indicates that lateral support was provided at the node in question, otherwise support was absent. Out-of-plane support was in all cases provided at the two intermediate ceiling tie nodes, as indicated in Figure 1.

Table 5 Simulation cases for out-of-plane supports, with disturbing force at apex

Simulation case	Out-of-plane support at node number									
	0	1	2	3	4	5	6	7	8	
a	*	*	*	*		*	*	*	*	
b	*	*	*			*	*	*	*	
c	*	*	*			*		*	*	
d	*	*	*				*	*	*	
e	*		*				*	*	*	

* indicates support present

Table 6 Simulation cases for out-of-plane supports, with disturbing force at mid-rafter point

Simulation case	Out-of-plane support at node number									
	0	1	2	3	4	5	6	7	8	
a	*	*		*	*	*	*	*	*	
b	*	*			*	*	*	*	*	
c	*	*			*		*	*	*	
d	*				*	*	*	*	*	
e	*				*				*	

* indicates support present

The simulation cases indicated in Tables 5 and 6 generally fall in descending order of expected lateral stiffness, with decreasing degrees of lateral support to either side of the disturbing force, and with longer effective lateral buckling lengths in the relevant portion of rafter.

Table 7 indicates the lateral stiffnesses at the apex of each truss, predicted by means of the three-dimensional computer analysis, for the five simulated cases of lateral support which are indicated in Table 5. It can be seen that the stiffnesses descend with decreasing lateral support, as would be expected, and also that for each simulation case the stiffnesses decrease, with an increase in truss pitch. The latter phenomenon was not reflected in the test results.

Table 8 indicates the lateral stiffnesses at the mid-rafter position of each truss, predicted by the analysis, and presented in a similar manner to Table 7. The description of the simulations to which Table 8 refers are to be found in Table 6.

Table 7 Lateral stiffnesses at apex, predicted by 3D computer analysis, for five cases of lateral support

Simulation case	Truss 1 (15°)	Trusses 2 & 3 (25°)	Truss 4 (35°)
a	177	78	56
b	95	42	30
c	76	33	23
d	29	13	9
e	25	11	8

Table 8 Lateral stiffnesses at mid-rafter position, predicted by 3D computer analysis, for five cases of lateral support

Simulation case	Truss 1 (15°)	Trusses 2 & 3 (25°)	Truss 4 (35°)
a	454	219	159
b	182	86	60
c	182	85	60
d	48	26	18
e	46	25	18

COMPARISON WITH THEORY

To provide a comparison with bracing theory, the condition of 'full bracing' was considered, using assumptions based on the classic Winter (2) theory for full bracing with discrete restraints. Appendix A to this paper gives the basis for proposed design rules for imperfect timber members which have been developed on this basis and which contain equations for the required restraint stiffness and strength.

Referring to Figure 3, which happens to show four intermediate restraints, but which is intended to represent the general case, then the theory shows that each intermediate restraint should have a minimum spring stiffness, C_{req} , given by:

$$C_{req} = \alpha \pi^2 EI / a^3 \quad (1)$$

Note that for 'real' timber members with initial eccentricity and/or lack of straightness, as opposed to 'ideal' members,

$$\alpha = 4 (1 + \cos (\pi/m))$$

The other symbols are:

m = number of intervals between restraints

a = distance between restraints

EI = flexural rigidity of braced member

Burgess (3) has shown that in a trussed rafter roof in the span range covered by the trusses under test, and with typical tiling batten centres and diagonal bracing arrangements used in Britain, a brace will cross a truss at every third tiling batten position. The rows of directly braced battens are taken as intermediate restraints. For simplicity, the other rows of battens are discounted altogether, since they may act as 'mechanisms', although it is recognized that in practice they may contribute through friction. Furthermore, the points at which the bracing receives direct support from the trusses coincide approximately with half the distance between the top chord panel points of a normal fink truss, when a typical bracing angle is used. The top chords of the trusses are treated approximately as cranked beam-columns, with seven intermediate restraints, Figure 4.

Provided that the stiffness of each intermediate restraint exceeds the value C_{req} given by equation (1), then lateral buckling will only be possible between these restraints over effective length = a.

Calculations, for example, for the 35° tested truss were as follows:

Distance between restraints	a	=	1465 mm
Number of intervals	m	=	8
Top chord dimensions	b	=	35 mm
	h	=	120 mm
Flexural rigidity	I_{yy}	=	$\frac{hb^3}{12}$
		=	$428.7 \times 10^3 \text{ mm}^4$
	E_{min}	=	7000 N/mm^2

$$EI = 3.0 \times 10^9 \text{ Nmm}^2$$

For $m = 8$ and members with imperfections, $\alpha = 7.7$

$$\text{Hence } C_{req} = 7.7 \pi^2 \times 3.0 \times 10^9 / 1465^3$$

$$C_{req} = \underline{72.5 \text{ N/mm}}$$

Strength:

Each intermediate restraint, or theoretical brace, must be capable of withstanding an axial force F, in tension or compression, amounting to a maximum of 2% of the axial force in the main, or braced, member.

For the 35° tested trussed rafter, the maximum rafter force was 8.3 kN under Medium Term design load. In design, this might be multiplied by a load factor in the order of 1.5, in order to determine the bracing force according to the Winter theory. Alternatively, using the permissible stress approach of BS 5268, it might remain unmodified.

Taking an effective $P = 12.4 \text{ kN}$

$$F_{req} = 0.02 \times 12.4 \times 10^3 = \underline{248 \text{ N}}$$

In the top chord of a trussed rafter, a combination of compression and bending actually occurs. The lateral buckling tendency due to flexure alone will increase the required force and stiffness provided by the restraints. On the other hand, there are unmeasured beneficial effects, such as intermediate tiling battens and diaphragm action from roofing materials.

CONCLUDING REMARKS

The experimental work described above was carried out on typical examples of commercially available medium-span trussed rafters, of 35mm thickness and M75 grade, such as are sold in tens of thousands by normal stockists. These were not specially fabricated components, manufactured by laboratory staff. They incorporated 'initial lack of straightness' typical of such lightweight trusses. The trusses also contained punched metal plate fastener joints, whose rigidity was not complete in planwise bending, or in buckling about the minor axis. In the section of this paper dealing with the tests, it has been explained how the actual lateral stiffnesses at two important points on the rafters of the trusses were measured, whilst the components were subjected to a typical range of in-plane (vertical) design loadings.

The lateral buckling behaviour of the components under load was by no means as regular as is supposed in the normal theoretical treatments, such as those described by Burgess, where distinct 'second', 'third' and 'fourth' buckling modes, in discrete sinusoidal waves, can always be recognized. In order to restrain the components to behave in a manner even approaching these more ideal, theoretical conditions, a variety of sprung clamps and negative and positive restoring forces had to be applied on the test rig, through the cable-pulley system. Three of the trusses were re-tested inverted from their original positions, and the behaviour of the inverted component was not necessarily a mirror-image of the first arrangement.

As a basis for comparison, a series of linear elastic computer analyses were performed, in which the combined vertical and lateral loading arrangements were simulated. In general, these simulations indicated levels of lateral stiffness comparable to the test results, although in several instances they suggested that the tested components were in effect exhibiting one or two degrees of freedom from lateral restraint greater than was being aimed at through the test arrangement. Also, as mentioned above, the decreasing stiffnesses with increasing truss pitch, suggested by the computer model, were not reflected in the tests. This was likely to be due in part at least to some of the 'real' effects that were not modelled, including incomplete lateral stiffness of the truss plated joints, at the apex, and, for the taller trusses, at a rafter splice position.

A comparison with some simplified theoretical assumptions has been included, and this has shown that lateral stiffnesses can be predicted which again are of the same order of magnitude as both the test results and the three-dimensional model predictions. The result based on the classic Winter theory, together with Burgess' assumptions regarding restraint at every third batten position, should not be compared too closely with the computer model predictions, since it was not possible exactly to reconcile each of the assumptions. Nevertheless, it is reassuring that all three methods of assessing the lateral stiffness of trussed rafters under load yield results of a similar magnitude to one another.

The adaptation of the classical discrete bracing theory for 'real' timber members with imperfections, described in Appendix A, and used in the comparison with theory, contains several assumptions based on judgement of what is accepted in current design practice, and what codes permit, rather than being based soundly upon measurements. Throughout the project which has reviewed existing stability and bracing work in timber, there has been found to be a marked absence of experimental data, other than some very thorough beam-column tests by Larsen and Theilgaard (5) and some measurements of imperfections in timber columns by Ehlbeck and Blass (6). There is a need for better experimental backing for assumptions regarding 'real' beam columns in components such as trusses, based upon careful measurements of individual members, before going too far with whole-roof tests and with further extensions of theory.

At the same time, although the British trussed rafter code, BS 5268 : Part 3 gives guidance on ad hoc bracing for domestic-scale roofs, the designer is without advice on longer spans, which are increasingly important in the roofing of commercial and industrial properties. The tests described in this paper have highlighted the probable importance of several practical effects upon likely long-term bracing performance. These include initial lack of straightness of members and of the erected components as a whole, as well as the contributions of fastener slip and creep-buckling phenomena.

As a consequence of this, a research proposal has recently been made to undertake full-scale tests to investigate the response of braced roofs to their lateral design loads, and to include an assessment of the likely long-term effectiveness of the same bracing, for stability purposes.

REFERENCES

- (1) Burgess, H.J. Calculation of a wind girder loaded also by discretely spaced braces for roof members. CIB-W18A/23/15/1, Lisbon, 1990.
- (2) Winter, G. Lateral bracing of columns and beams. J. Struct. Div. ASCE, Vol. 84, No. ST2, March 1958.
- (3) Burgess, H.J. The stability and bracing of trussed rafter roofs. TRADA Research Report 5/85, High Wycombe, 1986.
- (4) Timoshenko, S.P. and Gere, J.M. Theory of elastic stability. 2nd Edition, McGraw Hill, New York, 1961.
- (5) Larsen, H.J. and Theilgaard, E. Laterally loaded timber columns. J. Struct. Div. ASCE, ST7, July 1979.
- (6) Ehlbeck, J. and Blass, H.J. Assumptions for imperfections of timber columns (in German). Holz als Roh- und Werkstoff 45, 231-235, 1987.

APPENDIX A

PROPOSED BASIS FOR DESIGN RULES FOR BRACING BY MEANS OF DISCRETE RESTRAINTS

Stiffness

Analysis (4) of the ideal case of an initially perfectly straight compression member provided with 1, 2, 3, etc., equally spaced, equally stiff, intermediate elastic restraints shows that the required restraint stiffness C_{id} for buckling to occur between restraints is given by:

$$C_{id} = \alpha \pi^2 EI / a^3 \quad (A.1)$$

with values of α for different numbers of restraints being as given in Table A.1.

Table A.1 Values of α for ideal case and various restraints

Number of restraints	m	α
1	2	2.00
2	3	3.00
3	4	3.41
4	5	3.63
many	-	4.00

Real compression members will not, however, be initially straight. Whilst analysis to include this effect is possible - leading to an amplification of the initial deflection as compressive loading increases - it is significantly more complex. Using a simplified treatment, Winter (2) has shown that at a load level approximately equal to that necessary to cause buckling between restraints and assuming similar shapes for the initial deflection δ_0 and for the additional deflection produced by the applied loading δ , the restraint stiffness C_{req} needed to so limit these additional deflections is:

$$C_{req} = C_{id} (\delta_0 / \delta + 1) \quad (A.2)$$

If the additional deflection is limited to the initial value, i.e. $\delta = \delta_0$, then the required restraint stiffness will be twice the theoretical value for a similar, initially straight member. The bracing stiffness rule of Eq. 1 is based on the analysis outlined above. Clearly, by adopting different values for δ and δ_0 , the value of α will vary. Several different suggestions for both quantities may be found in the technical literature. For convenience and noting that it corresponds to something near the "average" of these suggestions, it has been assumed that $\delta_0 = \delta = a/500$.

As an independent check on the Winter-type analysis, the particular case of a member provided with a single central restraint as shown in Figure 5 has been examined from first principles. Assuming a symmetrical mode of deformation, the additional deflection due to a load P may be expressed as:

$$\delta = (\phi \times \psi) \delta_0 \quad (A.3)$$

$$\begin{aligned}
\text{in which } \phi &= \frac{P/P_c}{1 - P/P_c} \\
\psi &= \left[\frac{4EI\omega^3}{4EI\omega^3 + 2C\tan(\omega L/2) - \omega CL} \right] \\
\omega^2 &= P/EI \\
C &= \text{restraint stiffness} \\
P_c &= \pi^2 EI/a^2
\end{aligned}$$

If P is taken as the value given by cl. 15.5 of BS 5268 for an effective length a, then Eq. A.3 may be evaluated to give values of bracing stiffness C needed to limit δ to a suitable multiple of δ_0 . This has been done for the range of values of $E/\sigma_{c,11}$ between 400 and 2000 covered by BS 5268 and for values of slenderness λ up to 120. The results show that the rule proposed as Eq. 1 will always be on the safe side.

Strength

The basis for the bracing strength requirement of 2% of main member force also originates from the Winter-type analysis. Clearly the force in a restraint will be equal to the product of its stiffness C and the additional deflection δ , i.e.

$$F = C_{req} \delta \quad (A.4)$$

Substituting for C_{req} from Eq. A.2 gives:

$$F = C_{rd} (\delta_0 + \delta) \quad (A.5)$$

and taking $\delta_0 = \delta = a/500$ gives:

$$F = (\alpha \pi^2 EI/a^3) (a/250) \quad (A.6)$$

$$= \frac{\alpha EI}{25a^2} \quad (A.7)$$

The Winter analysis assumes a main member compressive load equal to the buckling load of the perfect member, i.e. $P = \pi^2 EI/a^2$

$$\text{Therefore } F/P = \frac{\alpha}{250} \quad (A.8)$$

For the case of a single central restraint $\alpha = 2$ and

$$F/P = \frac{1}{125} \quad (A.9)$$

However, with more restraints present, larger values are required and 2% has been proposed as a safe, reasonable figure. Examination of the relevant technical literature suggests it to be a little on the conservative (high) side of the "average" of the proposals.

Independent verification of this suggestion has been obtained from the analysis that led to Eq. A.3. Clearly, the restraint force may be obtained as the product of pairs of values of δ and C satisfying Eq. A.3. In general terms, as restraint stiffness is increased, deflections decrease at a more rapid rate with the net effect that bracing force is reduced. Moreover, the original Winter analysis assumed main member loading equal to the buckling load, whereas limiting this to the BS 5268 values (which are significantly less than the elastic critical figures) considerably reduces the amplification effect (as measured by ϕ in Eq. A.3) and thus limits the additional deflection δ . Examination of these findings suggests that the 2% figure could in very many cases be reduced to 1% or even less. On the basis that meeting the 2% requirement will not normally prove difficult in practice, that failure of bracing would, of course, lead to failure of the braced member(s) and that the assumed value of δ_0 may sometimes be exceeded in practice, the conservative recommendation is judged to be reasonable.

Figure 1

Three-dimensional analysis model

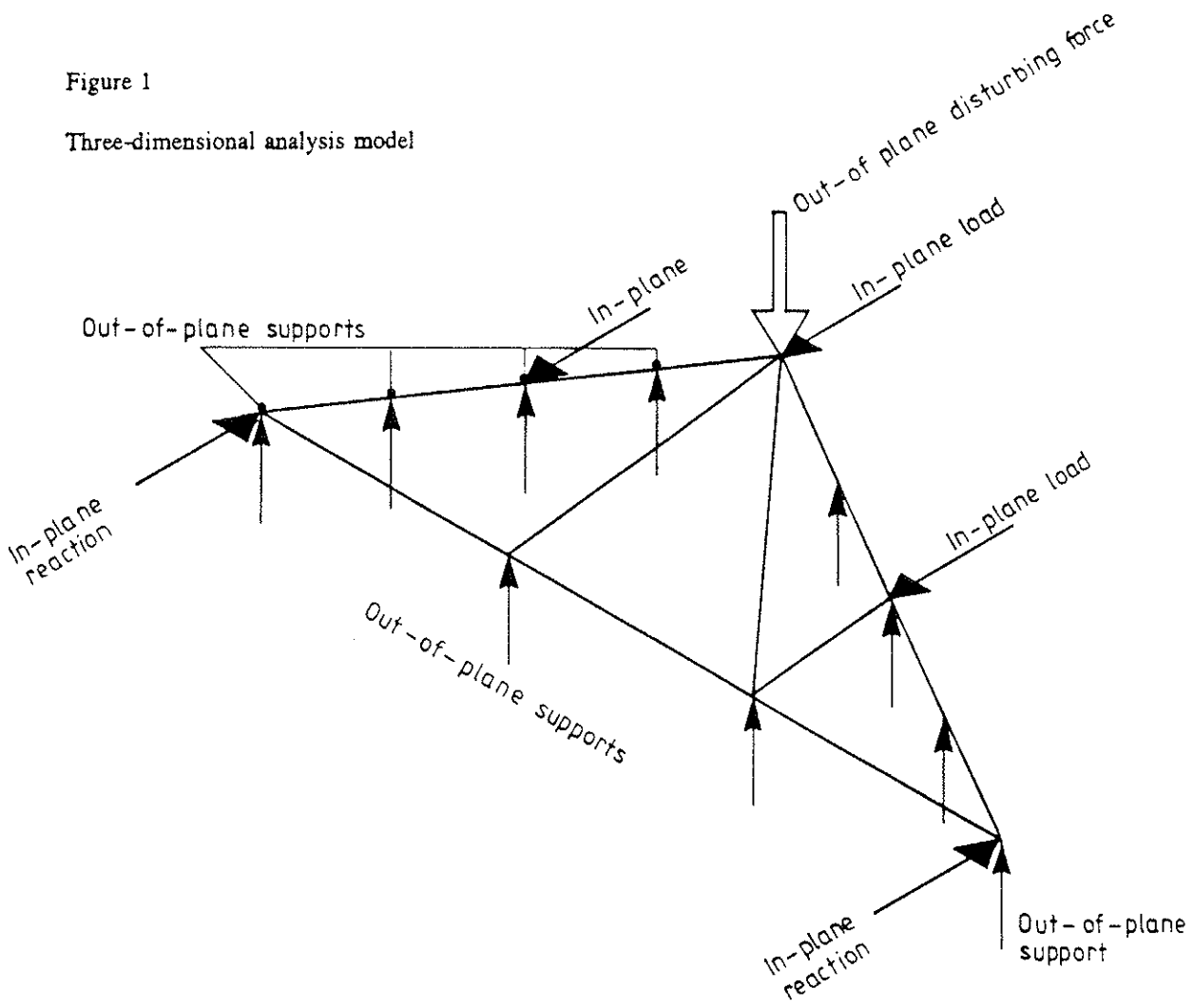


Figure 2

Rafter nodes at which lateral support could be present in the three-dimensional computer analysis

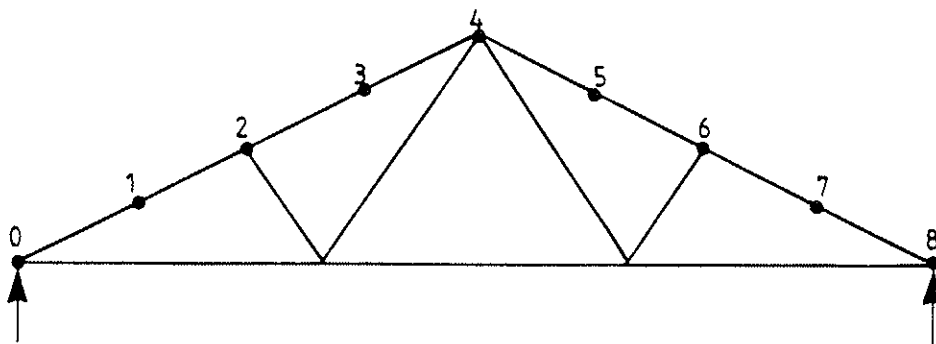


Figure 3

General case of full bracing with discrete restraints

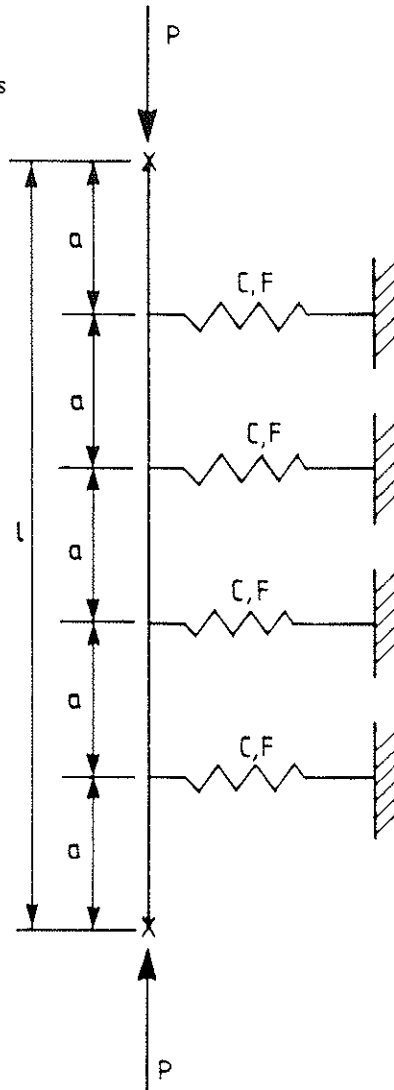


Figure 4

Top chords of a trussed rafter, treated approximately as a cranked beam-column, with discrete lateral restraints

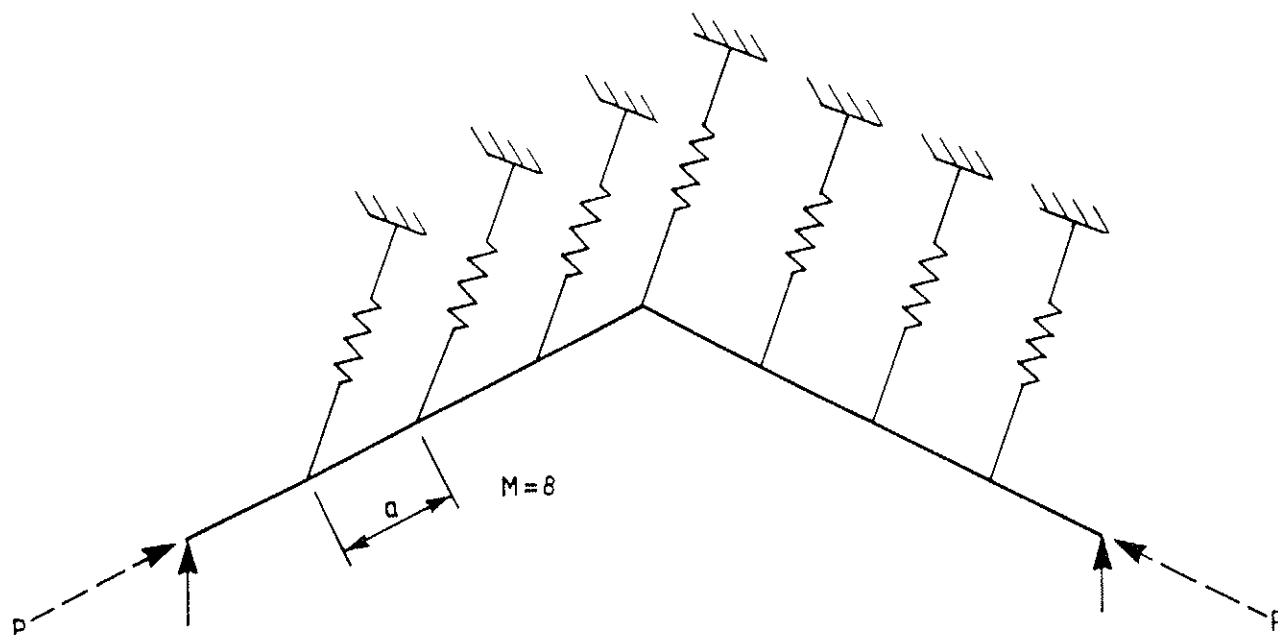
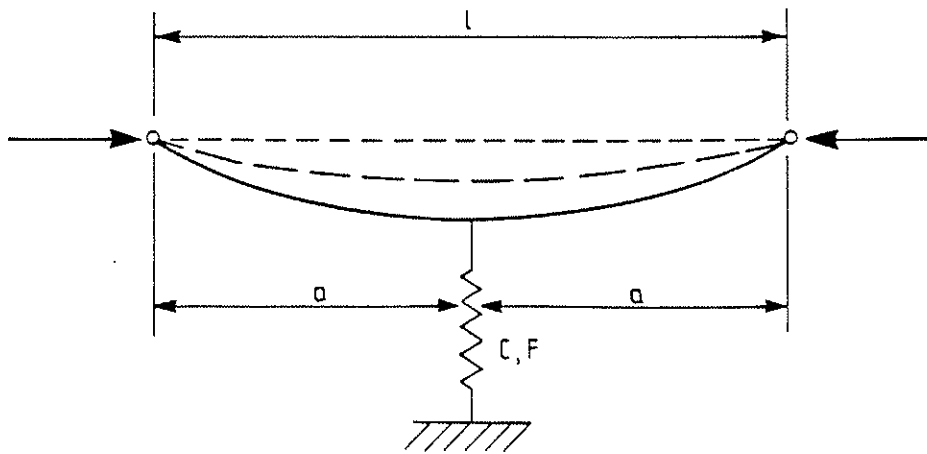


Figure 5

Initially bowed strut with single central restraint



INTERNATIONAL COUNCIL FOR BUILDING RESEARCH STUDIES AND DOCUMENTATION

WORKING COMMISSION W18 - TIMBER STRUCTURES

EUROCODE 8 - PART 1.3 - CHAPTER 5

SPECIFIC RULES FOR TIMBER BUILDINGS IN SEISMIC REGIONS

by

K Becker

Technical University of Darmstadt, Germany

A Ceccotti

University of Florence, Italy

H Charlier

Ministry of Economic Affairs, State of Baden-Wuerttemberg, Germany

E Katsaragakis

National Technical University of Athens, Greece

H J Larsen

Danish Building Research Institute, Horsholm, Denmark

H Zeitter

Technical University of Darmstadt, Germany

MEETING TWENTY - SIX

ATHENS, GEORGIA

USA

AUGUST 1993

INTRODUCTION

This paper presents the pertinent state of the drafting and redrafting work on the timber chapter in Eurocode 8 'Buildings in seismic regions'. The subpanel has been active since 1992 and elaborated this draft for the implementation of the ENV-version of Eurocode 8, which is projected for this autumn.

As there are still possibilities to complement necessary provisions in the code text or in the 'National Application Document' (NAD) every comment and criticism is very welcome during this CIB-meeting. The paper is aimed at opening of a discussion to provide substantial information.

On one hand it is very important to give guidance and rules for an adequate analysis, design and detailing for timber structures in seismic regions. The experience showed both during last earthquakes, an excellent behaviour as well as failures and more or less heavy damages on timber structures. The minority, the failures, originated from almost completely avoidable mistakes in modelling, design and mostly detailing. The development of a new code gave the possibility to elaborate the corresponding provisions with all the knowledge and experience of several seismic regions in the world.

On the other hand the use of timber for building purposes is to be strengthened face to face with other materials wherever possible. As the reasons for that engagement are well known, it is obvious to avoid huge masses of provisions, rules and prohibitions as for example the concrete part of Eurocode 8 takes almost the same size as the Eurocode 2. Designers, architects and engineers will stand away from timber, when they are exceptionally dealing with a seismic hazard and therefor confronted with too much confinements. For these reasons the code provisions should be short and precise. It is necessary and shall be possible to estimate realistically the stiffness and deformation properties with all timber-related scatter. To give the background information is the duty of conferences like this CIB-meeting and the Universities.

The formulation of several parts depend on the regulations in other parts of Eurocode 8 (e.g. the regularity-classes or the damping ratios), Eurocode 5 (e.g. design rules for nails) or other corresponding codes. As long as these codes are still in revision, redrafting or anyhow not in their final version some provisions may be changed.

The code requirements are mainly pointed on the attempt to provide sufficient ductile and hysteretic mechanisms in the structure. In opposite to other materials like concrete, steel and composite structures the ductility is mainly located in the connections, as the material itself shows in most cases a brittle behaviour.

The following pages will contain the code text. At text parts or pictures, which took more effort to formulate in the pertinent way, information and justification notes are given in boxes.

Part 1.3

BUILDINGS IN SEISMIC REGIONS

- SPECIFIC RULES FOR DIFFERENT MATERIALS AND ELEMENTS -

Chapter 5

SPECIFIC RULES FOR TIMBER BUILDINGS

CONTENTS:

5	SPECIFIC RULES FOR TIMBER BUILDINGS
5.1	DEFINITIONS AND SYMBOLS
5.2	GENERAL
5.3	PROPERTIES OF MATERIALS AND DISSIPATIVE ZONES
5.4	STRUCTURAL TYPES AND BEHAVIOUR FACTORS
5.5	STRUCTURAL ANALYSIS
5.6	DESIGN CRITERIA AND DETAILING RULES
5.6.1	DESIGN CRITERIA
5.6.2	DETAILING RULES FOR CONNECTIONS
5.6.3	DETAILING RULES FOR HORIZONTAL DIAPHRAGMS
5.7	SAFETY VERIFICATIONS AND LIMITATIONS
5.8	LIMITATION OF DAMAGE
5.9	CONTROL OF DESIGN AND CONSTRUCTION

5. SPECIFIC RULES FOR TIMBER BUILDINGS

5.1 DEFINITIONS AND SYMBOLS

P(1) The following definitions and symbols are used in this chapter with the following meanings:

Dissipative structures: Structures, which are able to dissipate energy by ductile hysteretic behaviour and friction.

Note according to 5.1. P(1):

Concerning the definition of dissipative structures it is a question of code philosophy, if the above text should be extended. In fact every structure somehow dissipates energy. Relating to the two concepts of design (see 5.2 P(2)) it has to be questioned whether the mechanisms of dissipation are sufficient to justify a consideration in analysis and the evaluation of substitutional forces. To obtain a precise interpretation of the code text the term 'dissipative structure' had to be mentioned in the list of definitions.

Dissipative zones: Determined parts of dissipative structures, where the dissipative properties are mainly located.

Static ductility: Ratio between the ultimate deformation and the deformation at the end of elastic behaviour evaluated in quasi-static, cyclic tests (see 5.4 P(4)).

Semi-rigid joints: Joints allowing significant loading deformation, the influence of which has to be considered in structural analysis according to Eurocode 5 (e.g. mechanical timber joints).

Note according to 5.1. P(1):

The definition of this term staggered between a simple hint to dowelled joints and the attempt to give a precise definition including several criteria. The pertinent suggestion suffers under the missing definition for 'significant loading deformation', as there are no limits given. The same problem occurs for the definition of 'Rigid joints'.

Rigid joints: Joints with insignificant loading deformation, which is negligible in structural analysis according to Eurocode 5 (e.g. glued solid timber joints).

Dowel-type joints: Joints with dowel-type mechanical fasteners (nails, staples, screws, dowels, bolts etc.) loaded perpendicular to their axis (activating embedding-resistance).

Note according to 5.1. P(1):

The intention was to introduce a general term for all connection techniques, which are based on the embedding resistance of the wood to transfer the load into the fastener and shear or respectively bending in the fastener.

Carpenter joints: Joints, where loads are transferred by means of pressure areas and without mechanical fasteners (e.g. skew notch, tenon, half joint)

Note according to 5.1.p(1):

Especially in regions with many traditional and old substance of timber buildings combined with a seismic risk the engineers need provisions, how to ensure the necessary safety in case of an earthquake. Therefore the traditional connections must be considered in the code text. On the other hand these manifold connections have different bearing mechanisms and are limited to specific regions.

d: diameter (respectively equivalent diameter) of dowel-type fastener.

Note according to 5.1.p(1):

As the diameter of the fastener in combination with the embedding-length is one of the most important parameters for the ductility of the connection, and in several places in Eurocode 5 or 8 the letter 'd' is used for other purposes, it had to be defined for this chapter. E.g. for staples it is additionally necessary to consider the fact, that the cross-section is not circular.

5.2 GENERAL

P(1) For the design of timber buildings Eurocode 5 applies. The following rules are additional to those given in Eurocode 5 with respect to seismic design.

Note according to 5.2 P(1):

Several structures are not covered in this chapter, because it is aimed just to 'buildings'. For example secondary rural structures, masts and bridges are either principally (without material specifications) ruled in other parts of Eurocode 8 or sufficiently considered in Eurocode 5. As far as in these parts specific timber related provisions are missing, reference to chapter 5 of part 1.3 is to be made.

P(2) Earthquake-resistant timber structures shall be designed according to one of the following concepts:

- a) Concept of non-dissipative structural behaviour
- b) Concept of dissipative structural behaviour

Note according to 5.2 P(2):

Independent from the real existing properties there are two different methods to design the structure. The method of analysing the dynamic behaviour of the structure is the same, but if the plastic and ductile properties shall be considered ('concept of dissipative structural behaviour'), several provisions for analysis, design and detailing have to be fulfilled.

- (3) When using concept a), the action effects - regardless of the structural type (see 5.4) - are calculated on the base of an elastic analysis without taking into account non-linear material-behaviour. When using the design response spectrum defined in Part 1.1, Clause 4.2.4 of Eurocode 8, the behaviour factor is taken as $q = 1$.
- (4) When using concept b), the capability of parts of the structure (dissipative zones) to resist earthquake actions by moving out of the elastic range, is taken into account. When using the design response spectrum defined in Part 1.1, Clause 4.2.4 of Eurocode 8, the behaviour factor is taken as $q > 1$. The value of q depends on the structural type (see 5.4).
- (5) Dissipative zones are mainly located in joints and connections with mechanical fasteners. The timber members themselves shall be regarded as non-dissipative.

Note according to 5.2 (5):

The wood members in a timber structure behave generally linear elastic during earthquakes and there is little energy dissipation in the timber, except maybe in zones with compression perpendicular to the grain.

Glued connections behave linear elastic until a mostly brittle failure, so they do not contribute to a dissipation in the structure. Well designed structures with mechanical fasteners show a significant ductility and dissipation even if there is a pronounced difference in the hysteretic behaviour to other materials.

Important to point out: 'shall' may be also used in application rules!

- P(6) The properties of dissipative zones shall be determined by tests either on single joints, on whole structures or on parts thereof according to EN XXX¹⁾. Provisions to avoid tests are given in 5.4 Clause (5).

Note according to 5.2 P(6):

As there are no requirements concerning the postelastic properties of timber structures in Eurocode 5 under cyclic loading, it has to be proved for the parts of the structure, which are intended to provide dissipation, that the necessary properties are existing.

The usual proceeding in the Eurocodes to refer to special standards containing the method for the determination of certain properties is not possible in that case, as there exists no related EN (or even a suggestion for a projected EN). For this reason the properties has to be described more precise in this chapter of Eurocode 8 (see also 5.4 P(4))

¹⁾ At this point of time no related EN exists. In the meantime it is referred to agreed international recommendations (e.g. RILEM - TC 109 TSA).

5.3 PROPERTIES OF MATERIALS AND DISSIPATIVE ZONES

P(1) Chapter 3, 6 and 7 of Eurocode 5 apply. According to the properties of steel parts chapter 3 of Eurocode 3 applies.

P(2) When using the concept of dissipative structural behaviour, in dissipative zones the following provisions apply:

Note according to 5.3 P(2) c:

On the first look one could think that these provisions could strongly harm the use of modern timber constructions. But it must be read carefully: These prohibitions are only valid for those parts of the structure, which are supposed to be dissipative. The use of improper materials and fasteners could significantly influence the properties, so the dissipation does not take place in the foreseen manner.

- a) Only materials and mechanical fasteners, which have an appropriate oligo-cyclic fatigue behaviour of the joint, are allowed.
- b) Large glued joints of the members are not allowed.

Note according to 5.3 P(2) b:

There is no reason to prohibit finger joints of glulam members or similar glued parts in the structure. But as mentioned above glued parts do not contribute to the energy dissipation, as they are considered as brittle. For this reason large glued joints shall be avoided in dissipative zones. When applied in knee-joints of frames the glueing can substantially harm the dynamic properties in comparison to a knee-joint with mechanical fasteners. Maybe a better formulation is >b) Large glued joints shall be considered as brittle <.

It is not possible to give limits for the term 'large' in this context. This concerns to the responsibility of the designer to apply adequate connections for the right purpose.

- c) Carpenter joints are only allowed with additional provisions - resulting from tests or given by the National Authorities - to provide dissipative mechanisms.

(3) A deemed-to-satisfy rule for P(2) a) is as follows: When tested to EN XXX (see footnote ¹⁾) joints shall be verified to have appropriate oligo-cyclic fatigue properties under large amplitudes to ensure a sufficient ductility according to their intended deformational mechanism and to justify the q-value assumed for analysis (see 5.4 P(4)).

Note according to 5.3 (3):

In the chapter dealing with the properties of materials and dissipative zones the fundamental requirement has to be ruled. On the other hand well known, appropriate behaving techniques should be applicable without the demand of testing in any case.

P(4) Sheathing-material for bracing-purposes of diaphragms (horizontal and vertical) shall meet the following conditions:

- a) density shall be at least 650 kg/m³ for particleboard-panels.
- b) plywood-sheathing shall be at least 9 mm thick.
- c) particleboard- and fibreboard-sheathing shall be at least 13 mm thick.

Note according to 5.3 P(4):

Experience in countries with a long term timber building tradition in seismic regions (e.g. California, New Zealand) showed, that for this purpose provisions additional to those of the usual timber design are necessary.

Strictly speaking the difference between one and more than one layers of sheathing has to be considered, but the lack of knowledge on that field does not justify according code provisions.

P(5) Steel-material for connections shall meet the following conditions:

- a) All connection-elements made of formed steel have to fulfil the requirements in Eurocode 3 and Part 1.3, Clause 3.2 of Eurocode 8.
- b) The ductility properties of the connection between the sheathing material and the timber framing in type C and D structures shall be shown in cyclic tests to fulfil the requirements in 5.4 P(4) considering the applied combination of sheathing-material and fastener.

5.4 **STRUCTURAL TYPES AND BEHAVIOUR FACTORS**

P(1) Timber buildings shall be referred to one of the following to four types A - D according to the ductile and hysteretic behaviour of their dissipative zones under seismic actions:

A	Non-dissipative structures	q = 1,0
B	Structures having low ability to dissipate energy	q = 1,5
C	Structures having medium ability to dissipate energy	q = 2,0
D	Structures having good ability to dissipate energy	q = 3,0

Note according to 5.4 P(1):

In difference to the version of May 1988 the number of structural types was increased from 3 to 4 types. The estimation of the q-values relating to the types was the central point of redrafting the old version (for all types q was stipulated to 1,0). The values for the types already include the damping properties according to the 5%-based response spectrum (see also the notes to figure 5.4.2)

(2) Examples for structural types and the corresponding behaviour factors q are given in figure 5.4.2.

- P(3) For structures having different, independent properties in the main directions in plan (e.g. halls with three-hinged arches (type A), trussed in the perpendicular direction by mechanically connected steel-trusses (type C), see figure 5.4.1) different q -values for both main directions of seismic action may be used.

Note according to 5.4 P(3):

The demand for a use of a spatial model (without a previous determination of the both 'main directions'), which is ruled in part 1.1 of Eurocode 8 according to the regularity classes, is independent from that, as the q -values are influencing the analysis on the action-side, so that there is no problem to consider the properties of the different directions by different q -values.

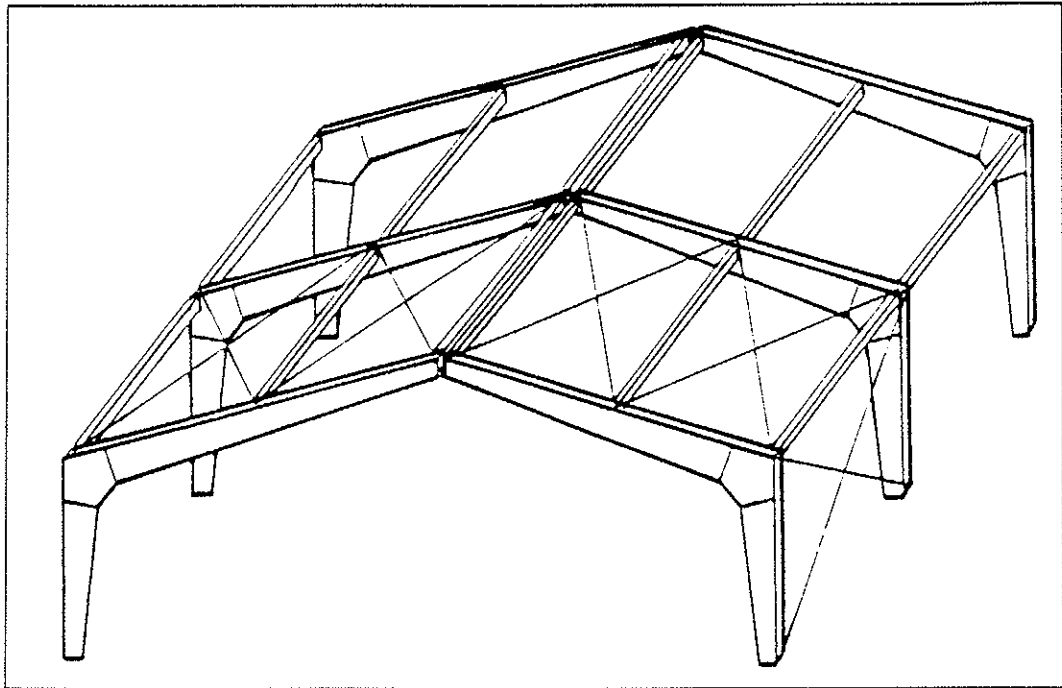


Figure 5.4.1 Example for a structure with different behaviour in the main directions

- P(4) In order to assure the accomplishment of the given q -values the dissipative zones shall be able to deform plastically for at least three fully reversed cycles at a static ductility ratio of 4 (for type B structures) and 6 (for type C and D structures) without impairment of their strength larger than 20 %.

Note according to 5.4 P(4):

In this clause the above mentioned related provisions concerning the testing of ductility properties are to be found. The described method to determinate the performance is just a simple proposal, but a more detailed evaluation would exceed the justifiable size of proofing provisions in the design code. For the time being the values '4' and '6' are so-called 'boxed values' to be stipulated by the National Authorities during the ENV-phase of the code. But as the National Authorities should only influence values concerning the safety level, these (research related) values should be fixed.

Further information concerning the ductility ratio contains [3].

(5) The provisions of P(4) and of 5.3 P(2) a) and P(5) b) may be regarded as satisfied for dissipative zones of all structural types if the following provisions are met:

- a) For doweled and nailed timber-to-timber and steel-to-timber joints, if the minimum thickness of the connected members is $8 \cdot d$ and if the dowel-diameter d does not exceed 12,0 mm.
- b) For the connection of sheathing to timber framing of diaphragms, if the sheathing material is wood-based and if the minimum thickness of the sheathing material is $4 \cdot d$ and if d does not exceed 3,0 mm.

Note according to 5.4 (5):

The earthquake experience in California and New Zealand and test results among others from European timber sheathed shearwalls [5] showed an excellent behaviour under cyclic loading, as long as the sheathing and its connection to the timber framing are fulfilling several provisions.

Concerning the provisions for the dowelled and nailed connection on the distinction in member-thickness between predrilled and not-predrilled nailing was renounced, as there is only a marginal difference between the adequate diameter limits for predrilled nailing and not-predrilled nailing according to Eurocode 5.

The estimation of the parameters (member-thickness, fastener-diameter, embedding-strength) to provide a ductile behaviour by a double curvature of the fastener can be found in [4]. Comments are welcome on that point.

P(6) Higher q -values may be used for specific structures, if they are demonstrated on the base of trial simulations and tests under a representative number of earthquakes.

P(7) If the building is not regular in elevation (see Part 1.2 Clause 2.2 of Eurocode 8) the listed q -values shall be reduced by 20 %, when using the concept of dissipative structural behaviour.

Note according to 5.4 P(7):

Irregularity in plan is already considered in part 1.2 in table 2.2.1. If the criteria given for the irregularity are fully valid for timber structures or if there is any addition necessary can be stipulated, when the final version of part 1.2 exists. Otherwise the experience during the ENV-phase will show, if the provision suited to timber buildings.

For masonry structures the spatial modelling can be omitted despite the demands in table 2.2.1 of part 1.2 (see chapter 6, clause 5.2.1 (1) of Eurocode 8, part 1.3). It should be examined, if a similar regulation is also efficient for timber structures. Furthermore the reduction of the q -value by 20 % requires reflection, if the reduction is too high or too low.

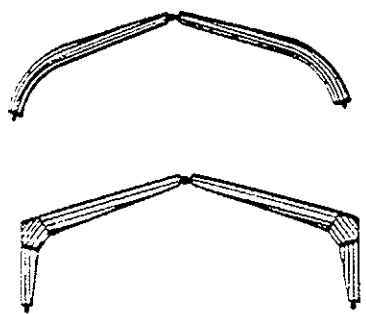
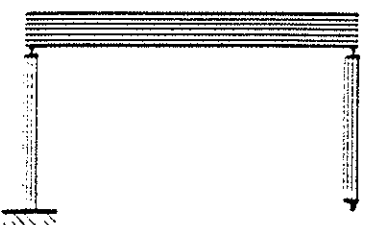
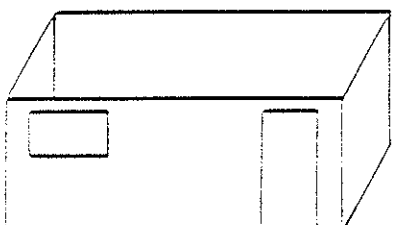
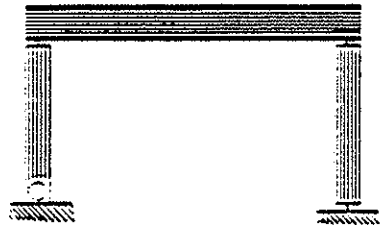
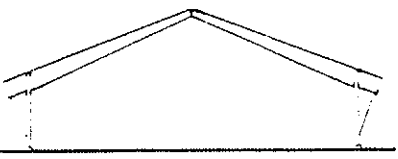
Type	Description	Examples	q
A	<p><u>Non-dissipative structures</u> having none or only a few joints with mechanical fasteners beyond the dissipative zones</p>	<ul style="list-style-type: none"> - Arches with hinged joints  <ul style="list-style-type: none"> - Cantilever structures with rigid connections at the base  <ul style="list-style-type: none"> - Buildings with wall-diaphragms without mechanical fasteners for interconnection as well as between sheathing and timber framing 	1,0
B	<p><u>Structures having low ability to energy-dissipation</u> due to the design of their load-carrying system and detailing</p>	<ul style="list-style-type: none"> - Structures with mechanically fixed-based columns  <ul style="list-style-type: none"> - Structures with few but effective dissipative zones 	1,5

Figure 5.4.2 Structural types and behaviour factors

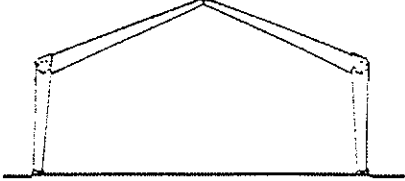
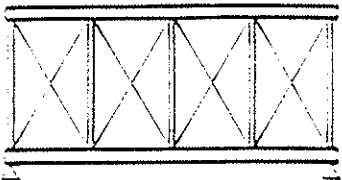
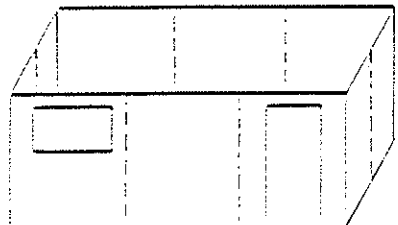
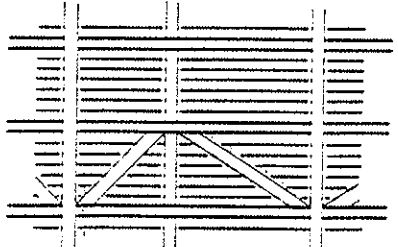
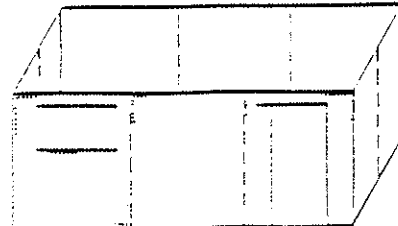
Type	Description	Examples	q
C	<p><u>Structures having medium ability to energy-dissipation</u> due to the design of their load-carrying system and detailing</p>	<ul style="list-style-type: none"> - Frames or beam-column structures with semirigid joints between all members. Connections with foundations may be semirigid as well as hinged (due to the load-carrying-system)  <ul style="list-style-type: none"> - Trussed frame structures with mechanical fasteners in the joints of the frame and/or the connections of the bracing elements  <ul style="list-style-type: none"> - Buildings with vertical diaphragms resisting the horizontal forces, where sheathing is glued to the framing. Diaphragms are interconnected by mechanical fasteners (horizontal diaphragms may be glued or nailed)  <ul style="list-style-type: none"> - Mixed structures consisting of timber framing (resisting the horizontal forces) and non-load-bearing infill 	2,0
D	<p><u>Structures having good ability to energy-dissipation</u> due to the design of their load-carrying system and detailing</p>	<ul style="list-style-type: none"> - Buildings with vertical diaphragms resisting the horizontal forces, where sheathing is fixed to the framing by mechanical fasteners as well as the interconnection of the wall-elements (horizontal diaphragms may be glued or nailed) 	3,0

Figure 5.4.2 ff Structural types and behaviour factors

Note according to fig. 5.4.2:

To enable an effective q-value of 3,5 initially the following footnote was foreseen: >The q-value for type D-structures may be increased, if the existence of sufficient friction mechanisms is provided. Under application of the rules given in chapter 5.6 this is to be valid. <.

Most of the timber structures show a damping ratio of generally more than 5 % in the elastic range; the equivalent viscous damping is even higher in the inelastic range. To correct the use of a 5%-based response spectrum there are two possibilities: Either to estimate the 'real' q-factors (according to the real damping ratios) and use the correction factor from the May 1988-version or to include the diverging damping ratio directly in a modified q-value.

The type D-structures are supposed to show the maximum of dissipation properties in timber buildings. A significant part of that is provided by friction mechanisms. As there is a (still running) discussion to implement the correction factor in Eurocode 8, if the friction is exceeding the 5%-value, which is the base of the response-spectrum, the proposed values (mainly for type C- and D-structures are not fixed yet.

The implementation of the masonry infilled timber structure gave also rise to the discussion concerning the q-values from clause 5.4 P(1), the classification of types and the examples in figure 5.4.1.

5.5 STRUCTURAL ANALYSIS

- P(1) Structures of type A shall and structures of type B, C and D may be designed according to 5.2 (3). Structures of type B, C and D may also be designed according to 5.2 (4), provided the corresponding requirements are fulfilled.
- P(2) Floors may be considered as rigid in plan for structural analysis, if the following conditions are met:
- a) The detailing rules for horizontal diaphragms given in 5.6.3 are applied.
 - b) The openings are limited, so that they do not significantly affect the overall in-plane rigidity of the floor.

Note according to 5.5 P(2):

Often the horizontal diaphragms are supposed to be rigid in plane without verification. But the knowledge of the realistic stiffness of the horizontal diaphragms is necessary for a control of deformation of the supporting elements. Initially the formulation was >...openings are limited in number and area, ...<. Limits and regarding application rules could be:

- *openings in corners should be avoided*
- *dimensions of an opening adjacent to a support should not exceed 20 % of that support*
- *edges and borders of openings as well as jump-in-corners should be stiffened by appropriate means*

But it seems to be impossible to give generally valid limitation-values. So the formulation aims at the responsibility of the designer to ensure the rigidity respectively the omission of a precise calculation of the in-plane-stiffness.

- P(3) In the dynamic analysis the slip in the joints of the structure shall be taken into account. An E_0 -modulus-value for instantaneous loading (10 % higher than the short term one) shall be used.

Note according to 5.5 P(3):

There are no E_0 -modulus values in Eurocode 5 foreseen for instantaneous loading. The value of 10 % increase is to be discussed.

5.6 DESIGN CRITERIA AND DETAILING RULES

5.6.1 DESIGN CRITERIA

- P(1) Structural systems with dissipative zones shall be designed so that these zones are located mainly in those parts of the structure, where yielding or local buckling or other phenomena due to hysteretical behaviour do not affect the overall stability of the structure.
- (2) In case of tension perpendicular to the grain additional provisions should be met to avoid splitting, as shown in figure 5.6.1 for instance:

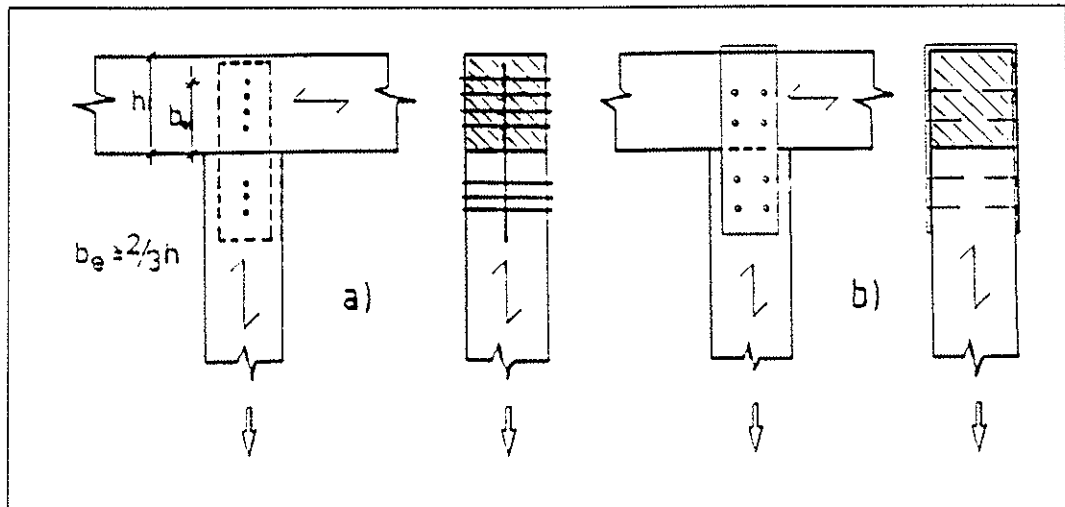


Figure 5.6.1 Examples for acceptable provisions in case of tension perpendicular to the grain: a) by a dowelled inner steel plate and b) by a cover plate

Note according to fig. 5.6.1:

The condition of $b_e \geq 2/3 h$ is a minimum requirement, which is necessary anyway, but not sufficient. The intention is to avoid stress conditions, which could lead to a brittle failure due to tension perpendicular to the grain.

5.6.2 DETAILING RULES FOR CONNECTIONS

Note according to chapter 5.6.2:

Initially a provision concerning proofing the performance and durability of the ductility properties of the connections by testing was included. The panel decided to rely on the sufficient rules in Eurocode 5.

- P(1) Compression members and their connections (e.g. carpenter-type joints), which may fail due to deformations caused by load reversals, shall be designed such that they are protected from separating and remain in their original position.

Note according to 5.6.2 P(1):

Some of the words of this clause are not lucky to describe the necessary provision.

- P(2) Bolts and dowels shall be tightened and tight fitting in the holes. Large bolts and dowels ($d > 16,0$ mm) shall only be used in secondary members except in combination with timber teeth connectors.

- (3) Smooth nails and staples should not be used without additional provision against withdrawal except in diaphragms for the connection of sheathing to the timber framing (see 5.4 (5) c)) and except in secondary members.

Note according to 5.6.2 (3):

In context with the NAD a list of fasteners for sheathing purposes should be elaborated, for which no further requirements exist.

5.6.3 DETAILING RULES FOR HORIZONTAL DIAPHRAGMS

- P(1) For horizontal diaphragms under seismic actions Clause 5.4.2 of Eurocode 5 applies with the following modifications:

- a) Clause 5.4.2 (2) and (6) of Eurocode 5 shall not be applied
- b) Differing from Clause 5.4.2 (5) of Eurocode 5 the distribution of the shear forces in the diaphragms shall be evaluated by taking into account the in-plan position of the horizontal load resisting elements.

- P(2) All sheathing edges not occurring on framing members shall be supported and connected to blocking (see fig. 5.6.3). Additionally blocking shall be provided in the horizontal diaphragm over every vertical load-resisting element (e.g. walls).

Note according to 5.6.3 P(2):

To ensure a load-transfer of the stiffening forces into the wall elements, blocking is to be provided. Perhaps this clause could be changed from a 'principle' to an 'application rule'.

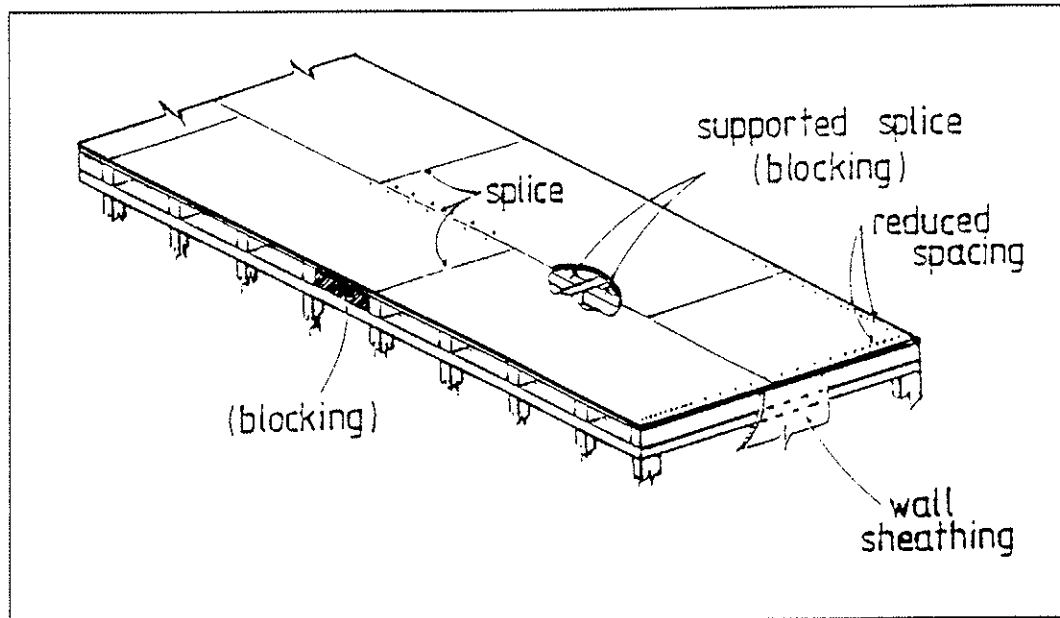


Figure 5.6.3 Supporting and nail-spacing in the edges of sheathing panels

- P(3) The continuity of beams and especially of headers shall be insured even in areas of diaphragm-disturbances.

Note according to 5.6.3 P(3):

This clause refers to the realistic estimation of the diaphragm-stiffness. Experience in California (and referring code requirements) showed, that a flange-extension, a so-called 'drag strut' with the relating nailing ensures a continuous load-carrying in the diaphragm. The application is necessary for:

- openings
- offsets in plan of the diaphragm
- vertical offsets in the diaphragm

- P(4) Slenderness of the beams shall be limited to $b/h < 4$.
- P(5) In seismic zones with a peak ground acceleration $a_g \geq 0,2 \cdot g$ the spacing of the fasteners shall be reduced by the factor 1,3 in areas of discontinuance (see figure 5.6.3), under consideration of the minimum spacings given in Eurocode 5.

Note according to 5.6.3 P(5):

In context with the overall stiffness-estimation of horizontal diaphragms this clause is to be discussed.

- P(6) If floors shall be considered as rigid in plan for structural analysis, there shall be no change of span-direction of the beams in areas, where horizontal forces are assumed to be carried in subsequent members (e.g. shear-walls).

Note according to 5.6.3 P(6):

The stiffness of diaphragms changes with the direction of the beams. If areas of different span-directions of the beams are touching over a subsequent bearing- and stiffening-member (e.g. a wall-element), the behaviour of the diaphragm cannot be estimated realistically.

5.7 SAFETY VERIFICATIONS AND LIMITATIONS

- P(1) The design strength values of the material shall be determined according to Eurocode 5 taking into account the k_{mod} -values for instantaneous loading.
- P(2) For ultimate limit state verifications of structures designed according to the concept of non-dissipative behaviour (see 5.2. P(2)) the partial safety factors for material properties γ_m for accidental load combinations from table 2.3.3.2 of Eurocode 5 shall apply.
- P(3) For ultimate limit state verifications of structures designed according to the concept of dissipative behaviour (see 5.2. P(2)) the partial safety factors for material properties γ_m for fundamental load combinations from table 2.3.3.2 of Eurocode 5 shall apply.

Note according to 5.7 P(1) and P(2):

To use the partial safety factors for the material properties γ_m for fundamental load combinations was used with respect to all other material chapters in Eurocode 8. Additionally the material has to fulfil the requirements of 5.4 P(4) so a general use of the partial safety factors for the material properties γ_m for accidental load combinations would be sufficient. For type A-structures the factor for γ_m for fundamental load combinations would simply be wrong according to the concept of non-dissipative behaviour.

- P(4) To allow the development of cyclic yielding in the dissipative zones, all structural members shall be designed with an overstrength such that their load-bearing resistance is higher than that of the connections. This applies especially for:

Note according to 5.7 P(4):

The main difference between the design of steel or concrete structures and timber structures is the fact, that the ductility is to be placed in the connections and not in the members. To ensure the development of the hysteretic mechanisms, which provide the justification of the load-reducing by q-values, the members have to be designed with an overstrength. The value of the overdimensioning (2%, 5%, 10% or 20% depends on the special application and counts on the knowledge and responsibility of the designer.

- a) Anchor-ties and any connections to massive subelements.
- b) Connection of horizontal diaphragms to the adjacent transmitting construction parts of the structure.

5.8 LIMITATION OF DAMAGE

- P(1) The provisions given in part 1.2 of Eurocode 8 apply.

5.9 CONTROL OF DESIGN AND CONSTRUCTION

- P(1) The provisions given in part 1.1 of Eurocode 8 and in Eurocode 5 apply.
- (2) In accordance to part 1.1 Clause 2.2.4.3 (2) of Eurocode 8 the following structural elements shall be identified on the design drawings and specification for special control during construction shall be provided:
- a) Anchor-ties and any connections to massive sub-elements
 - b) Diagonal tension steel trusses used for bracing
 - c) Connection of horizontal diaphragms to the construction parts above
 - d) Material and performance of the connection between sheathing panels and timber framing in horizontal and vertical diaphragms according to the regarded detailing parameters

DISCUSSION, ACKNOWLEDGEMENT AND CONCLUSIONS

Comments and further suggestions for the code text and its interpretation are welcome. In the hope of a fruitful discussion during this meeting the authors would like to thank all specialists, which participated in the meetings and correspondence to obtain a maximum of content and coordination in the redrafting work.

REFERENCES

The whole relating literature would surely blast the literature-list. On special requests the authors will try to give further literature-information.

- [1] **"Eurocode 8 - Buildings in seismic regions - Design"**
Part 1: General and Building
Commission of the European Communities
Different versions of several parts based on the version of May 1988
- [2] **"Eurocode 5 - Design of timber structures"**
Part 1: General rules and rules for buildings
Commission of the European Communities
Different versions of several parts based on the version of December 1991
- [3] **"Specific rules for timber structures"**
A. Ceccotti, H.J. Larsen
Background document for chapter 5 - part 1.3 of EC 8, April 1988
- [4] **Grundlagen der Bemessung von Holzbauwerken nach dem EC 5 Teil 1 - Vergleich mit DIN 1052**
H.J. Blaß, J. Ehlbeck, H. Werner
Verlag Ernst & Sohn Berlin, Betonkalender 1992
- [5] **"Holzbau: Theoretische und experimentelle Untersuchungen für die Anwendung des Eurocode 8"**
K. Becker, H. Zeitter
Research report at the Technical University of Darmstadt, August 1992

DISCUSSION, ACKNOWLEDGEMENT AND CONCLUSIONS

Comments and further suggestions for the code text and its interpretation are welcome. In the hope of a fruitful discussion during this meeting the authors would like to thank all specialists, which participated in the meetings and correspondence to obtain a maximum of content and coordination in the redrafting work.

REFERENCES

The whole relating literature would surely blast the literature-list. On special requests the authors will try to give further literature-information.

- [1] **"Eurocode 8 - Buildings in seismic regions - Design"**
Part 1: General and Building
Commission of the European Communities
Different versions of several parts based on the version of May 1988

- [2] **"Eurocode 5 - Design of timber structures"**
Part 1: General rules and rules for buildings
Commission of the European Communities
Different versions of several parts based on the version of December 1991

- [3] **"Specific rules for timber structures"**
A. Ceccotti, H.J. Larsen
Background document for chapter 5 - part 1.3 of EC 8, April 1988

- [4] **"Grundlagen der Bemessung von Holzbauwerken nach dem EC 5 Teil 1 - Vergleich mit DIN 1052"**
H.J. Blaß, J. Ehlbeck, H. Werner
Verlag Ernst & Sohn Berlin, Betonkalender 1992

- [5] **"Holzbau: Theoretische und experimentelle Untersuchungen für die Anwendung des Eurocode 8"**
K. Becker, H. Zeitter
Research report at the Technical University of Darmstadt, August 1992

INTERNATIONAL COUNCIL FOR BUILDING RESEARCH STUDIES AND DOCUMENTATION
WORKING COMMISSION W18 - TIMBER STRUCTURES

HURRICANE ANDREW
STRUCTURAL PERFORMANCE OF BUILDINGS IN SOUTH FLORIDA

by

M R O'Halloran
E L Keith
J D Rose
T P Cunningham
American Plywood Association, Tacoma, WA
USA

MEETING TWENTY - SIX

ATHENS, GEORGIA

USA

AUGUST 1993

HURRICANE ANDREW — STRUCTURAL PERFORMANCE OF BUILDINGS IN SOUTH FLORIDA

By Michael R. O'Halloran Ph.D., Edward L. Keith, P.E., John D. Rose
and Thomas P. Cunningham, Jr., Ph.D.¹

ABSTRACT

This report describes the structural performance of residential and low-rise commercial structures in South Florida, based on observations from on-site inspections conducted within one week after Hurricane Andrew struck the Miami region on August 24, 1992. All types of construction -- concrete, masonry, steel and wood -- were inspected by a 45-member task group including a team of three technical and field promotion staff members from the American Plywood Association. The report concentrates primarily on the observed performance of wood systems, but other types of construction also are covered. Observations and conclusions are presented dealing with roofing attachment; wood structural panel roof sheathing -- both plywood and oriented strand board (OSB) -- and its attachment to framing and gable-end roof systems in particular; walls and connections of components; attachment of metal roof deck panels to steel framing; connections between concrete and metal roof decks and concrete or masonry walls; and attachment of cladding for pre-engineered metal buildings.

This report also provides a review of work completed which recommended fastening schedules for oriented strand board and plywood roof sheathing. The recommended schedules were established to provide resistance to wind uplift pressure, with particular emphasis on high-wind exposures. The approach included laboratory testing, engineering and computer analysis.

¹Director, Senior Engineer, Senior Engineer, and Senior Scientist respectively, Technical Services Division, American Plywood Association, P.O. Box 11700, Tacoma, WA 98411 USA

HURRICANE ANDREW — STRUCTURAL PERFORMANCE OF BUILDINGS IN SOUTH FLORIDA

INTRODUCTION

During the early morning hours of August 24, 1992, Hurricane Andrew battered South Florida's Dade County, primarily in the region from Miami to Homestead and Florida City. Widespread damage occurred to most residential and many commercial structures in this region, which encompasses about 32 km (20 miles) north-south by 19.2 km (12 miles) east-west. To a lesser extent, damage to structures also extend northward to Broward County.

As the hurricane passed east-to-west across South Florida, its most destructive winds missed populated regions around Naples and Fort Meyers on Florida's west coast, where reports of damage were minimal.

However, the hurricane regained intensity in the Gulf of Mexico and struck the Louisiana coast west of New Orleans, outside of major population regions. Property damage, although reportedly substantial, was much less than in the more highly populated regions of South Florida.

Three members of American Plywood Association's (APA) technical and field promotion staff participated on a Damage Assessment Team coordinated and arranged by the Florida Concrete and Products Association (Orlando, Florida). The Damage Assessment Team was sanctioned by the State of Florida, Department of Community Affairs, and consisted of 45 structural engineers, scientists, building code officials, and technical representatives of construction industry trade associations and component and construction materials manufacturers. The team's investigative efforts were coordinated with the Board on Natural Disasters of the National Research Council, an agency of the National Academies of Sciences and Engineering (Washington, D.C.).

The Damage Assessment Team conducted ground level site observations of hurricane damage incurred by all types of construction -- concrete, masonry, steel and wood -- for residential and low-rise commercial buildings, over a five-day period within one week after the hurricane. Team members prepared individual summary reports of observations with photographs and descriptions. (All of the team reports were collected by the University of Florida, Department of Civil Engineering, for collation into a final, summary report.)

This report summarizes the observations of APA observers, and concentrates primarily on the performance of wood-framed buildings in South Florida, although performance of concrete, masonry and steel-framed buildings also is covered in more general terms. Also reviewed is the engineering work leading to improved fastening schedules.

Early reports of building damage from Hurricane Andrew indicate over 60,000 homes were damaged or destroyed in South Florida (late reports indicate that the total might be twice that amount), with damage estimates exceeding \$20-30 billion in Florida, and \$1 billion or more in Louisiana. Preliminary reports from South Florida indicated sustained hurricane winds as high as 62.6 m/s (140 mph), with gusts to over 71.5 m/s (160 mph), but further analysis by wind engineering experts (*Hurricane Andrew: August 24, 1992* by Ronald F. Zollo, Ph.D.) has revised these figures downward for inland regions to within 5% of the *South Florida Building Code's* design wind speed of 53.6 m/s (120 mph). By any standards, Hurricane Andrew likely will become the most destructive and costliest hurricane affecting the U.S. coastline.

WOOD CONSTRUCTION

By far, the majority of wood structural failures due to Hurricane Andrew can be attributed to improper connection details. An analysis of wind-damaged structures indicates that inadequate connection detailing falls into a number of general categories.

One of the major deficiencies contributing to much of the damage was the inadequate connection of wall units to adjacent wall units, roofs and floor structures. Top plates of walls occasionally were not lapped at corners, and wall sections were attached to adjoining walls with as few as three nails. Inadequate nailing was observed along the bottom plate-to-floor platform connection on many exterior walls.

By far the most common type of structural failure seen during the inspection was the loss of gable-end walls. This phenomena was almost always accompanied by the loss of from 1.2 to 3.7 m (4 to 12 feet) of either plywood or oriented strand board (OSB) roof sheathing immediately adjacent to the gable-end wall. Once the roof sheathing was blown off, the gable-end truss and adjacent trusses collapsed in domino fashion. Diagonal cross-bracing of end trusses was rarely observed in roofs that failed in this manner.

It was also noted that gable-end truss framing was infrequently toenailed to the top plate of the end wall below. Toenails, if used, often were spaced 1.2 to 1.8 m (4 to 6 feet) on center, and were inadequate to provide the necessary shear transfer to stiffen the building against lateral wind loads acting on the wall.

One of the most damaging failures in economic terms was not structural. This was the loss of gypsum wallboard ceilings. This form of damage, to one extent or another, affected many houses in the 624 km² (240-square mile) area. The rain accompanying and subsequent to Hurricane Andrew was driven in through gable-end vents, through the joints between roof sheathing panels after concrete or clay tile or shingle roofing was

blown off the roof, as well as directly into the attic space of failed roof systems. Rain saturated the insulation, as well as the ceiling. The loss of strength of the ceiling due to water saturation, as well as the increased weight of the wet insulation, caused widespread collapse of ceilings. In addition to causing extensive property damage to the house and furnishings, the loss of the ceilings also contributed to gable-end wall failures due to diminished lateral support of end roof trusses.

The practice of attaching gypsum wallboard ceiling over steel resilient channels or wood furring strips was also commonly observed in many instances. Due to this detail, the ceiling "diaphragm" was not mechanically attached to the roof framing or the walls at the perimeter of the rooms. Such detailing is especially detrimental to the performance of non-loadbearing gable-end walls as it does not provide lateral bracing to the end walls.

Much of the interior damage to structures was also caused by the loss of doors and windows under the wind pressure. Often the failed window or door frames were attached to the structural framework of the buildings with only a few fasteners. It was not uncommon to see failed sliding glass door frames fastened only by six small screws. In several cases, the rough framing opening was considerably larger than the sliding glass door. Consequently, the screws only penetrated the wall framing by 12.7 mm (1/2 inch) or so.

Non-loadbearing interior partition walls are highly susceptible to damage when wind forces reach the interior of the structure after the sudden failure of windows and doors. Such walls are normally only lightly attached to the structural frame at the top, bottom and ends of walls. This is especially true when light-gage steel framing is used in these applications. The heads of the fasteners attaching the light-gage steel top and bottom plates readily pulled through under applied loads, whereas non-loadbearing wood walls remained in place.

Also observed in some cases was an apparent lack of continuity in walls over window and door headers. This can be attributed to inadequate attachment of the wall top plate to window and door headers. Proper fastening could have, in many cases, prevented the damage observed.

In several residential developments, a non-structural rake-end roof overhang framing detail was commonly used on the gable ends where extensive gable-end roof failures occurred. A "ladder" frame about 305 mm (12 inches) wide was prefabricated using 38 x 89 mm (nominal 2 x 4) lumber. This frame was then placed on the rake end of the gable and attached to the end truss with minimal nailing. It was attached such that it cantilevered out from the roof at the gable end, thus providing the overhang. The sheathing was then applied to the roof with the sheathing edge-nail spacing [nominally 152 mm (6 in) o.c.] applied to the non-structural fascia at the end of the roof overhang. Very often the plywood or OSB roof sheathing was only occasionally nailed to the primary structural gable-end truss (the perimeter of the roof diaphragm). During the hurricane, when the roof overhang was exposed to the wind, the overhang lifted and "peeled" the roof sheathing off to the second or third truss. In cases where the sheathing was properly attached to the gable-end truss, the roof sheathing was not compromised.

In evaluating wind-damage structures it was observed that the builders in the South Florida area are relatively conscientious about using tiedown straps in roof-to-wall and wall-to-floor connections to resist uplift forces. In cases where tiedown straps were installed properly, there was almost no damage observed due to uplift in site-built wood frame construction. Tiedown strap inadequacies, when observed, were at the roof framing level. In some cases, the tiedowns were bent out of the way so as not to interfere with the roof truss placement, or only lightly nailed to roof framing, or ignored completely during attachment of the trusses. Often this error precipitated a total failure of the roof system and, in some cases, a complete loss of the structure below. It was also observed that these strap-type connections are ineffective in resisting forces normal to the wall, so that nominal code-required nailing of wall top and bottom plates to perimeter floor or roof gable-end framing must be provided.

MASONRY and WOOD CONSTRUCTION

Occasional failures of masonry buildings were observed throughout the affected area. This section will deal only with those buildings that combine masonry exterior walls with wood gable-end walls. There were, however, a number of masonry first-floor and wood second-floor structures observed.

Where failures occurred in buildings with masonry end walls and wood gable ends, failure almost always was accompanied by a collapsed gable-end wall and adjacent roof trusses. All of the collapsed gable ends observed can be attributed to improper attachment of the wood gable end to the masonry wall below, or loss of lateral bracing of the wall due to loss of the roof diaphragm.

As discussed previously, tiedown straps from gable-end walls to walls below have little or no ability to laterally brace the gable-end walls. In addition, the common practice of applying gypsum wallboard ceilings over wood furring or resilient channels provides no lateral bracing for the gable-end wall. The combination of the uncoupled ceiling diaphragm and the lack of adequate attachment between the block wall and gable-end wall often result in the gable-end wall pulling away from the building when subjected to wind forces normal to wall.

One connection detail that was seen in a number of heavily damaged multifamily dwellings concerned inadequate attachment of shed-roof trusses to the masonry fire wall separating units. While the bottoms of the trusses were placed in saddle-type connectors, the tops were inadequately anchored to the masonry wall. Lack of anchorage at the roof level prevented the transfer of lateral loads into the fire wall. The lack of structural connections between these two major elements severely restricted the structure's ability to resist the applied wind loads.

WOOD PANEL ROOF SHEATHING PERFORMANCE

Almost without exception plywood or oriented strand board (OSB) panel sheathing was used as the roof decking material for masonry, masonry/wood, and wood residential structures. There were no differences observed in the performance of plywood or OSB roof sheathing. Sheathing failures, where they did occur, were similar in all three building types.

The most prevalent type of roof sheathing failure occurred in the region of the gable-end walls. This failure type, discussed previously, was in all cases due to inadequate or improper fastening of the roof sheathing panel. The minimum attachment requirements are 6d nails for panels up to 12.7 mm (1/2 inch) and 8d nails for thicker panels, spaced at 152 mm (6 inches) on center along panel edges and at 305 mm (12 inches) on center over intermediate supports (South Florida Building Code, Section 2909.2). Typically nails spaced much further apart were observed in roof sheathing that had blown off. A more common observation was that erratic fastening patterns were used throughout the panels, ranging from 254 to 1220 mm (10 to 48 inches) on center.

When staples were used, the crown of the staples were often found to be perpendicular to the panel edge. This practice places one or the other of the staple legs too close to the edge of the panel or framing, thus reducing the capacity of the staple by at least one-half.

It is also important to note that the minimum fastening requirements may need reevaluation by local code jurisdictions for high wind regions¹. Note that staples do not necessarily have the same withdrawal and lateral capacity as do nails. Therefore, the fastening schedule for nails or staples must be determined by competent authority. Whatever the fastener type, however, the spacing should never be more than 152 mm (6 inches) at panel edges and 305 mm (12 inches) at intermediate supports.

It was not unusual to see a perfectly sound roof deck with a single 1.2 m x 2.4 m (4 ft x 8 ft) wood sheathing panel missing. When located, many of these panels were found to have been attached with as few as 8 - 10 fasteners, several times less than the minimum required by code. [When roof framing is spaced 610 mm (24 in.) o.c., 33 fasteners are required for a 1.2 m x 2.4 m (4 ft. x 8 ft.) panel using the minimum fastening schedule.] (See Figure 9.)

The recurring loss of roof sheathing at gable-end walls is consistent with currently accepted wind load theory. Current theory, as illustrated in the *Standard Building Code* in Section 1205, indicates that the applied wind loads are greater at these locations. It can be concluded that the required nail spacing at gable-ends should be more restrictive than other areas of the roof.

¹The American Plywood Association has published revised minimum fastening schedules for roof sheathing applications in high wind areas. These schedules are available in Data File No. T325 entitled "Roof Sheathing Fastening Schedules for Wind Uplift."

Sheathing Fastener Schedules for Wind Uplift

The emphasis in this study (*Cunningham, 1993*) was to provide the necessary background to design fastener schedules for wind uplift pressure. The primary focus on performance was drawn from the following considerations:

- Regions affected by high-wind events "experience" various magnitudes of wind velocities. Structures within the same region are exposed to different magnitudes of peak gusts and sustained velocities.
- Structures within affected regions "experience" various wind effects (pressures) depending upon such factors as site, geometry, orientation relative to wind direction, roof slope, etc.
- There exists a quantifiable probability that design wind speeds will be exceeded during the service life of the structure.
- Precise wind speeds and corresponding averaging times (periods) for Hurricane Andrew will not likely be established.
- Secondary damage caused by airborne roof sheathing may be significant.
- Loss of roof sheathing compromises the integrity of the affected structure.
- Considerable reserve uplift capacity can be detailed into roof sheathing fastening schedules at minimal additional expense.

Given these considerations, the approach was to demonstrate that adequately detailed fastening schedules will perform at levels well above those associated with high-wind loadings. A procedure that is keyed to performance (uplift resistance) was then developed to provide for design of fastening schedules.

Engineering Analysis

Engineering analysis established the fastener locations that carry critical proportions of forces from uplift pressure. Critical fasteners limit pressure capacities of fastening schedules. This knowledge allowed determination of the limits of fastening schedules as well as the most effective means of improving fastening schedules.

Engineering analysis, substantiated by tests, established that the performance of the minimum fastening schedule is sensitive to missing or ineffective fasteners. The absence of one fastener in the field of the minimum fastening schedule can have a significant detrimental impact on uplift resistance. This should be carefully considered in regions of this country that are subject to high-wind events.

Engineered Design

Design wind pressures, calculated on the basis of ASCE 7-88 provisions for components and cladding, provide an important perspective on the interaction of structural factors with wind. The procedure developed for design of fastening schedules was influenced by the brief duration associated with design wind uplift pressures.

Nail withdrawal testing demonstrated the significant difference between test capacities and conventional design capacities. For wind uplift design, nail withdrawal values were adjusted to a temporal basis more consistent with loading conditions.

Verification Testing

Verification tests demonstrated that the governing aspect of fastening schedule pressure capacities is fastener withdrawal from the framing. It is for this reason that, with the exception of the influence of sheathing thickness on depth of nail penetration, sheathing panel construction does not have a significant influence on pressure capacities.

Verification testing confirmed the results of engineering analyses. Significant verification test results include:

- Pressure capacities of the high-wind schedule provide adequate margins over uplift pressures anticipated from high-wind events. High-wind schedule capacities are at least double those of the minimum fastening schedule.
- Use of 8d Common nails significantly increased pressure capacities relative to use of 6d Common nails in comparable applications.
- Pressure capacities of the minimum schedule are impacted significantly by missing or ineffective critical fasteners.
- Moisture condition of the sheathing does not impact the pressure capacities of the high-wind schedule.

Fastener Recommendations

The research (Cunningham, 1993) resulted in modified fastening schedules consistent with the loads specified in ASCE 7-88. The increased fasteners improve the overall safety in high wind areas.

ROOF COVERING PERFORMANCE

Failure of roof covering material was observed on almost every structure in the Dade County area. All roofing types were included, with the possible exception of wood shakes. The effectiveness of the roofing materials can be categorized as follows: asphalt shingles, concrete flat tile roofing and concrete barrel tile roofing.

Asphalt shingle roofing failures were almost always related to "tear through" of shingles at fastener attachments. Stapled attachments seemed to be more prone to shingle tear through than nails, due to minimal contact area with the shingle. It was observed that shingle roofing fasteners consistently remained imbedded in plywood or OSB roof decks after shingles were blown off. Substantial evidence was observed that fastener withdrawal resistance is adequate for plywood or OSB roof sheathing of thicknesses of 11.1 mm (7/16 in.) or greater.

While flat concrete tiles appeared to have better resistance to blow off than barrel tiles, the failure mechanism for both was the same. Tiles of both types showed no adhesion of the cement mortar bedding to the tile back. (These tiles are generally installed by first laying down a small patch of cement mortar and then placing the tile onto the mortar. The mortar theoretically bonds the concrete tile to the roof deck.) There was little adhesion observed between the failed tiles and the cement mortar, although the mortar did stick well to the roof deck. Some concrete tile roofing that did survive was fully bedded in mortar as opposed to attached with an occasional patch of mortar as was the rule. The more satisfactory performance of flat concrete tile roofing is generally attributed to reduced exposure at the edges to wind uplift.

OTHER STRUCTURES

Steel roof decking systems were often used for roofing in low-rise commercial buildings. These roofing systems suffered much damage during the hurricane. While many of the metal roof systems observed were inadequately attached, even those that appeared to be attached "per code" failed. Failure modes observed were pull-through of the welds or fasteners attaching the metal roofing system to framing. There also appeared to be minimal attachment of the metal roofing systems to the supporting walls. This would, of course, minimize the effectiveness of the metal roofing to act as a diaphragm for the structure. Indeed, many of the failures of low-rise commercial buildings appeared to have been caused by loss of diaphragm action and the subsequent collapse of supporting walls.

On some commercial buildings, metal roofing panels were installed on sloped roof decks of plywood or oriented strand board (OSB) roof sheathing, with metal clip attachments and/or wood furring strips. Generally, it was observed that such roofing panels often were blown off the roof, indicating that the fastening system was inadequate to resist high winds. The metal clips and furring strips remained attached to the wood roof decks or framing, however.

Several examples of wall failures were observed in commercial buildings with pre-cast concrete T-beam panel roof decks and masonry walls. The number and strength of welded connections between the roof deck and non-loadbearing walls (parallel to the T-beam roof deck panels) was insufficient to withstand wind forces normal to the wall. This caused the wall to collapse inward, or outward if the interior of the structure was "pressurized" by wind forces after windows or doors failed.

Failure of one large commercial building (a rack storage warehouse) was observed where load-bearing reinforced masonry walls (in-fill panels between reinforced cast-in-place concrete frames) were connected to pre-cast concrete T-beam roof deck panels. A central portion of the windward wall of the structure collapsed, along with the supported roof deck, but the cause of failure was not determined.

In a few commercial buildings, failures of exterior masonry walls were observed where it was apparent that steel bar reinforcement to adjoining walls at the corners was not adequate. It was uncertain whether this was a building design or inspection deficiency.

Occasional failures of brick veneer exterior finish over masonry walls also were observed on several commercial buildings. The failures were attributed to inadequacy of structural tie or mortar bonding systems used to attach the brick veneer to the wall to resist hurricane wind forces.

Several examples of failed pre-engineered metal commercial buildings were observed. Generally, it appeared that the steel siding and its attachment to the steel framing were not capable of resisting the shear and uplift wind forces and impact forces from wind-blown debris or projectiles. When the building envelope was breached, the steel roofing or siding panels typically were blown away from the structural steel framing. The result was that the unbraced steel framing collapsed under the intense wind forces.

CONCLUSIONS

As can be seen from the observations discussed above, much of the structural damage done to the structures in South Florida was preventable through the proper design, specification and execution of connections between structural elements. It is hoped that, through publications such as this, knowledge of the importance of making proper connections can be conveyed to the building industry to eliminate the possibility of such preventable tragedies in the future. While it is difficult to imagine a natural disaster greater than Hurricane Andrew, it would be an even greater tragedy if we did not learn from the experience.

References

1. American Society of Civil Engineers, 1990. "Minimum Design Loads for Buildings and Other Structures" ASCE 7-88.
2. Cunningham, Thomas P., Jr., Ph.D., March 26, 1993. "Roof Sheathing Fastening Schedules for Wind Uplift" Report T92-28. American Plywood Association, Tacoma, WA.
3. Keith, Edward L., P.E. and John D. Rose. Sept, 1992. "Hurricane Andrew, Structural Performance of Buildings in Southern Florida (August 24, 1992). Report T92-21. American Plywood Association, Tacoma, WA.
4. "Manufactured Home Installations." 1987. NCSBCS Standard A225.1. National Conference of States on Building Codes and Standards, Inc.; Herndon, VA 22070.
5. Rose, John D. April 1993. "Hurricane Iniki, Structural Performance of Building on Kauai, Hawaii (September 11, 1992). Report T93-1, American Plywood Association, Tacoma, WA.
6. "Roof Sheathing Fastening Schedules for Wind Uplift, T325." 1993. American Plywood Association, P.O. Box 11700, Tacoma, WA 98411-0700.
7. "South Florida Building Code." 1988 with revisions. Board of County Commissioners; Metropolitan Dade County; Miami, FL 33128-1974.
8. "Standard Building Code." 1991 with revisions. Southern Building Code Congress International, Inc.; Birmingham, AL 35213-1206.
9. "Wood Particleboard." ANSI Standard A208.1. 1989. National Particleboard Association; Gaithersburg, MD 20879.
10. Zollo, Ronald F., Ph.D., P.E. (March 11, 1993) "Hurricane Andrew: August 24, 1992, Structural Performance of Building in Dade County, Florida."

INTERNATIONAL COUNCIL FOR BUILDING RESEARCH STUDIES AND DOCUMENTATION
WORKING COMMISSION W18 - TIMBER STRUCTURES

STRUCTURAL FIRE DESIGN ACCORDING TO EUROCODE 5, PART 1.2

by

J König
Swedish Institute for Wood Technology Research, Stockholm
Sweden

MEETING TWENTY - SIX

ATHENS, GEORGIA

USA

AUGUST 1993

STRUCTURAL FIRE DESIGN ACCORDING TO EUROCODE 5, PART 1.2

by J König, Swedish Institute for Wood Technology Research, Stockholm

SUMMARY

In June 1993 the final draft Eurocode 5, Part 1.2 - Structural Fire Design - was approved to be published and introduced as a European prestandard for provisional application in the EC and EFTA countries. In this paper an overview is given on the contents of Eurocode 5, Part 1.2, its background, requirements, methods and design philosophy.

BACKGROUND AND DRAFTING

Eurocode 5 - Design of Timber Structures - will include the following parts

Part 1.1 - General Rules
General Rules for Buildings
Part 1.2 - General Rules
Supplementary rules for structural fire design
Part 2.1 - Bridges

Part 1.1 has been approved by CEN TC 250/SC 5 in November 1992. For the time being editorial work and the translation into the other two CEN-languages French and German is going on. The publication of the document in the three languages English, French and German as a European prestandard will be done by CEN simultaneously and before the end of November 1993.

Part 1.2 has been approved by CEN TC 250/SC 5 in June 1993. The publication as a European prestandard will probably take place in spring 1994. It is expected that the document is introduced in 1994 in most EC and EFTA countries as a European prestandard for provisional application.

A first draft of the fire part of Eurocode 5 (EC 5) was published in April 1990. The drafting work was done by a group set up by the Commission of the EC. The result of the work was criticized, mainly for not being in line with EC 5, Part 1.1. When the work on Eurocodes was transferred to CEN, a new Project Team was set up with the goal to ensure compatibility with Part 1.1. The persons involved were G Hall (UK), H Hartl (A, convenor), M Kersken-Bradley (D), J Majamaa (SF), G Sagot (F) and J König (S), the latter also acting as technical secretary.

Part 1.2 of Eurocode 5 gives the supplements to Part 1.1 of Eurocode 5 which are necessary that structures also may comply with structural fire resistance requirements.

The fire parts of the Eurocodes deal with specific aspects of passive fire protection in terms of designing structures and parts thereof for adequate load bearing capacity and for limiting fire spread as relevant. The term "structural" in Structural Fire Design is used in a wider sense, since in the fire parts also purely separating parts of a building are considered,

since the resistance against fire loads of such parts of a building is essential.

Required functions and levels of performance are generally specified by the National authorities - mostly in terms of standard fire resistance ratings. In the case of timber structures, it is also the responsibility of the National authorities to give regulations in regarding where timber may be used. For example, in many countries the use of combustible material is limited with respect to the number of stories of the building. It is hoped that the development of Eurocodes will promote the introduction of performance based requirements in structural fire design in the National building laws and help to remove irrational obstacles for the use of timber. To this purpose new and more realistic methods may contribute, as e.g. the introduction of parametric fires which allow to account for a complete fire including the cooling period, and to consider active measures of fire fighting including the time which is needed for the fire-brigade to be in place. The principal procedure in European and other countries is based on results from standard fire resistance tests, and if ever such above mentioned influences are included, this is done implicitly, which makes it difficult to perform a rational design.

The project team had to face problems due to different conflicting interests:

- Different levels of development in different countries.
- Simplicity contra sophisticated rules
- Coordination with the fire parts of the other Eurocodes for other materials.

Eurocodes shall, as well as other national codes, reflect the generally acknowledged state-of-the-art. It is a general problem for code writers of international codes that there often exist different levels of development in different countries, and different opinions on what belongs to generally acknowledged state-of-the-art. Even in one country different designers would have different opinions on that. In the case of fire engineering the development during the last two decades has been in favour of more sophisticated calculation methods, especially in the Nordic countries, North America and New Zealand.

Considering the problem of simplicity contra sophisticated rules the project team choose to include options for different levels of complexity. Among the application rules the designer will in the first place find a simple method, which would lead to safe, but perhaps less economic structures. In the second place the designer will find more complicated methods, which would increase the amount of design work but would also in general lead to more economic constructions. In the third place the option is given for sophisticated methods, which require more information than is given in this Eurocode. Generally, as an alternative to calculation methods, it is possible to make use of design by testing.

Some of the fire parts of Eurocodes include design aids, as design tables and diagrams. The project team for EC 5, Part 1.2 was of the opinion that such design aids should be found in handbooks etc.

A problem to be solved by the project team was to chose values of material responses which are recognized by the designer. For example, the charring rate of timber is an essential parameter in structural fire design. In current fire design codes charring rates are used in the range between 0,6 and 1,1 mm/min. and the strength of timber is reduced to values between 50 and 100 % of strength at normal design. See the values in Table 1 which are partly taken from /1/ and reflect the situation in 1984.

An explanation of such variability of material properties can be that charring rates are notional, i.e. other effects are included as the increased charring rate at arrises and fissures

Table 1 Charring rates of softwood and relative bending strength in structural fire design in codes of various countries (1984)

Country	Charring rates		$f_{m,r}/f_m$
	Glued laminated timber	Solid timber	
Finland	0,6	0,8	0,75
Sweden	0,6	0,8	0,73 - 0,88
New Zealand	0,6	0,6	0,5
USSR	0,8	0,8	0,8
UK	0,65	0,65	0,68
Germany	0,8	1,1	1,0
France	0,65	0,65	0,83

(solid timber), and effects of strength reduction are partly or completely included. Moreover, to get a complete picture, in current codes also the actions and safety factors are different, which makes it difficult to compare different approaches. The goal of the project team was to give rules which lead to the same, in practice well approved safety level which has been accepted in most countries. It was chosen to make a clear distinction between material properties, analytical models and safety factors. The material properties should be defined such that they can be verified by standard test methods and the analytical models should not include hidden safety factors. Those should be given explicitly as partial safety factors only.

In current design codes no application rules for the calculation of the fire resistance of joints are given. Thus fire testing has been the only alternative. Eurocode 5, Part 1.2 is the first code to include application rules for joints exposed to standard fire.

CONTENTS OF EUROCODE 5, PART 1.2

In the following the contents is commented, see Appendix A. Chapters 1 and 2 are identical with the corresponding chapters in the fire parts for other materials, except those parts considering timber.

Chapter 1, Introduction

Scope. Part 1.2 applies to timber structures for the accidental situation of fire exposure. It identifies only differences or supplements to the design at normal temperature and gives rules for passive methods of fire protection. Functions to be fulfilled are premature collapse of the structure and the limitation of fire spread.

Definitions. Definitions in addition to those in Part 1.1 are given.

Units. Units in addition to those in Part 1.1 are given.

Symbols. Symbols were chosen following Part 1.1 when possible. In the ENV-stage a consistency with other fire parts could not be achieved in all cases.

References. Normative references are cited. These include European Standards (EN) and proposals for European Standards (prEN). No reference is made to standards to be written, e.g. a standard for the determination of charring rates.

Chapter 2, Basic Principles

Performance requirements. Performance requirements are defined for standard fire exposure in terms of mechanical resistance (load bearing function), integrity and insulation, expressed as R, E and I plus a figure representing the required time period in minutes, e.g. R60 or REI60.

Actions. Thermal and mechanical actions shall be taken from of Eurocode 1, Part 2.2, where (draft January 1993) thermal actions are given in terms of

- nominal temperature-time curves (a. Standard fire exposure according to ISO 834, b. External fire curve, c. Hydrocarbon curve)
- parametric fire exposure which is influenced by the fire load density and the magnitude of the fire compartment and openings

Design values of material properties. For strength verification design values of strength (and correspondingly of the modulus of elasticity) shall be determined from

$$f_{t,d} = k_{mod,f} k_f \frac{f_k}{\gamma_{m,f}} \quad (1)$$

For deformation verifications the stiffness values shall be taken as

$$E_f = k_{mod,f} \frac{E_{mean}}{\gamma_{m,f}} \quad (2)$$

where

f_k	Characteristic strength at normal temperature, defined as the population 5-percentile obtained from tests, see Part 1.1
E_{mean}	Mean value of modulus of elasticity at normal temperature as given in supporting material standards to Part 1.1
$k_{mod,f}$	Reduction factor taking into account the effect of the thermal effects (temperature and moisture content) of the fire on the strength and stiffness parameters. This factor $k_{mod,f}$ replaces k_{mod} used in Eurocode 5, Part 1.1
$k_f = 1,25$	for solid timber
$k_f = 1,15$	for glulam and wood based panels
$\gamma_{m,f} = 1,0$	Partial safety factor for material properties in fire design of timber structures

Design values of material properties for thermal analysis are determined by dividing the mean value of the material property by the partial coefficient for the material in fire design. Mean values were chosen because these have been used in the past and characteristic ones are known only in few cases.

In the past in most fire tests the specimens had mean properties rather than characteristic ones. For the time being it is not possible to determine the partial safety coefficient with respect to uncertainties in the case of fire and therefore it seems not be possible to obtain the same reliability in all structures regardless material. The partial safety factor of 1,0 was chosen in order to harmonize the fire part of Eurocode 5 with the fire parts of the other Eurocodes. The factor k_f was chosen in order to obtain a calibration to the safety level used in current national fire design codes and $k_f k_k$ corresponds approximately to a 20-percentile of the population. In order to allow for further adaption to the national level of safety, k_f and $\gamma_{m,f}$ are "boxed" values, i.e. during the ENV-period these values may be changed in the National Application Documents (NAD).

Basic design procedure. Where no specific rules for fire design of load bearing members are given in this Part 1.2, this implies that application rules should be used which are given in Part 1.1 for normal temperature design, with the exception that actions, partial safety coefficients, material and cross-sectional properties and parameters describing the structural system which are valid in normal temperature design, are replaced by the corresponding values which are valid in structural fire design. Effects on structural parameters, e.g. modified buckling lengths, shall be taken into account. Reference is made to three levels of complexity of design procedure.

Assessment methods. The structural system adopted for design in the fire situation shall reflect the performance of the structure in fire exposure. The structural analysis shall take into account the relevant failure mode in fire exposure and the temperature-dependent material properties and stiffnesses, and effects of thermal expansions and deformations.

As an alternative to an analysis of the entire structure, the structural analysis may be replaced by an **analysis of a part of the structure**. In this case support and boundary conditions may be assumed as time-independent during fire exposure. Interaction between members or assemblies in different parts of the structure should be taken into account in an approximate way.

The effect of actions $E_{f,d}$ in fire (for example internal forces and moments) related to the initial support and boundary conditions may, as a simplification of the rules in Eurocode 1, Part 2.2, be deduced from the global structural analysis for normal conditions of use as

$$E_{f,d} = 0,6 E_d \quad (3)$$

where E_d is the load effect at normal temperature. For some load combinations with large imposed loads this equation may give unsafe results.

For verifying standard fire resistance requirements analysis of single members is sufficient. In structural timber members the effects of thermal expansions need not be considered.

Chapter 3. Material

Charring depths. The main parameter for the designer is the charring depth. Charring shall be considered for all surfaces directly exposed to fire. Charring need not be considered for surfaces of members covered by fire protective claddings when the failure-time of the fire-protective panel exceeds the required fire resistance time by 5 minutes.

For standard fire exposure the charring depth is

$$d_{\text{char}} = \beta_0 t \quad (4)$$

where the factor β_0 is the charring rate under certain conditions. For the time being there exists no test standard for the determination of the charring rate. The following design values should be used for European softwoods and hardwoods with a minimum dimension of 35 mm, see Table 2.

Table 2 Charring rates β_0 for timber.

	β_0 mm/min.
a) Softwood	
Solid timber with characteristic density of $\geq 290 \text{ kg/m}^3$	0,8
Glued laminated timber with characteristic density of $\geq 290 \text{ kg/m}^3$	0,7
b) Solid or glued laminated hardwood with characteristic density of $\geq 450 \text{ kg/m}^3$ and oak	0,5
c) Solid or glued laminated hardwood with characteristic density of $\geq 290 \text{ kg/m}^3$	0,7

Charring rates for wood-based panels are given for a characteristic density of 600 kg/m^3 and a panel thickness of 20 mm. For other thicknesses and densities correction coefficients are given. The beneficial effect of closely packed multiple layers or layers in contact with the member may be considered.

Fire protective cladding. Failure times of claddings should be determined by testing, alternatively they may be calculated using the charring rates for wood-based panels. It is anticipated that certain conditions of fixing the panels to the member are fulfilled.

Adhesives. Adhesives of phenol-formaldehyde and aminoplastic type complying with Eurocode 5, Part 1.1 according to EN 301 satisfy the requirements that the integrity of the bond is maintained in the assigned fire resistance period.

Chapter 4, Structural fire design

Effective cross-section method. This is the simplest method of determining the load bearing capacity of a member. The charring depth is calculated as above and the residual cross-section is obtained without regarding roundings at arrises. Since the reduction of the strength and the modulus of elasticity is not considered in a direct way - i.e. $k_{mod,f} = 1,0$ in Equations (1) and (2) - this has to be compensated for by reducing the residual cross-section by $d_0 = 7$ mm along its periphery. The remaining cross section is called **effective cross section** and the total layer to be removed from the original cross section is the **effective charring depth**. See Figure 1. For shorter times than 20 minutes d_0 varies linearly between 0 and 7 mm.

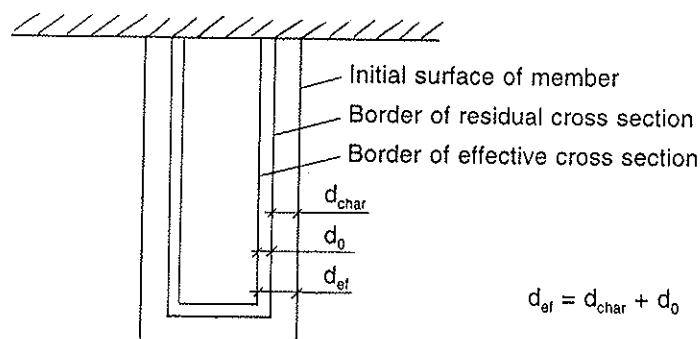


Figure 1 Definition of cross sections

Reduced strength and stiffness method. This method is described in Annex A of Part 1.2, see below.

General calculation method. Part 1.2 opens for general methods of determining the cross-sectional load bearing capacity and stiffness giving guidelines for which parameters should be included in the calculation:

- charring depths according to general charring models
- temperature profiles in the residual cross section
- moisture content profiles in the residual cross section
- strength and stiffness properties dependent on temperature and moisture content

The code does not give values for these parameters. They should be taken from handbooks or other relevant literature.

Special rules. In order to simplify, some additional rules are given. They reflect more current design practice rather than explicit research results:

- Compression perpendicular to grain may be disregarded.
- Shear may be disregarded in solid cross sections. For notched beams it should be verified that the residual cross section in the vicinity of the notch is at least 60 % of the cross section required for normal temperature design.

For beams and columns it should be considered that failure of bracings may change the buckling length. For a special case the boundary condition of columns may be more favourable than in design at normal temperature: A column in a fire compartment which is part of a continuous column may be considered as completely fixed at its ends, provided that the fire resistance of the enclosure of the compartment is not smaller than the fire resistance of the column.

For mechanically jointed components, slip moduli may be assumed as for the normal temperature design situation. For the design of mechanical fasteners. This rule is approximative and more information is needed.

For bracings a rule is given, saying that a bracing may be assumed not to fail if the remaining cross sectional area is 60 % of its area which is required with respect to normal temperature design.

Floors and walls.

The following requirements apply:

For separating constructions fire exposure from one side at a time shall be considered. For non-separating constructions fire exposure from both sides shall be considered.

In the design of floors and walls consisting of a timber frame and covered or topped with panels application rules are given in Annex C, see below.

Joints. The basis of the contents of this section is /2/, based on German fire test results, and test results from France.

The rules refer to joints with dowel-type fasteners under lateral load with symmetrical shape (joints with two side members only), exposed to standard fire.

A distinction is made between unprotected and protected joints.

Generally, wood-to-wood joints and steel-to-wood joints with steel plate middle members with **unprotected** nails, screws, bolts or dowels may be regarded to satisfy R 15 when observing the conditions of Eurocode 5, Part 1.1. Longer fire resistance times can be achieved by two measures:

1. by increasing the dimensions of members (thickness and edge and end distances of fasteners) by

$$a_f = \beta_0 (t_{f,req} - 15) \quad [\text{mm}] \quad (5)$$

where

β_0 Charring rate according to Table 2 in mm/min.

$t_{f,req}$ Required standard fire resistance in minutes.

2. by increasing the number of fasteners in the joint or by choosing stronger

fasteners, such that the ratio of loading in fire design and load bearing capacity at normal temperature is multiplied by the factor η_{30} . For example, for wood-to-wood joints, η_{30} should be equal to 0,80 for nails, 0,45 for bolts, 0,80 for non-projecting dowels and 0,45 for connectors (In Europe the term "connector" denotes ring or tooth plate connectors). These values should be used under certain conditions which are not given here. For fire resistances between 30 and 60 minutes, an extrapolation formula is given.

For unprotected side members of steel R30 is satisfied when the thickness of the steel plates is at least 6 mm and $\eta_{30} \leq 0,45$.

Joints are considered as **protected** if the fasteners are covered with protective plugs or wood or wood-based panels with a minimum thickness a_f .

Annex A, Reduced strength and stiffness method for standard fire exposure

This annex is normative. The method described is an alternative to the effective cross-section method and gives more precise and economic results.

The charring depth should be calculated according to one of two alternatives:

- When roundings at arrises are not considered, Equation (4) applies.
- Alternatively the charring depth is calculated as

$$d_{\text{char}} = \beta t \quad (6)$$

when roundings at arrises are considered in the calculation of the section modulus and the flexural stiffness. The charring rate β should be taken from Table 3.

Table 3: Design charring rates β

	β mm/min.
a) Softwoods	
Glued laminated timber with characteristic density of ≥ 290 kg/m ³	0,64
Solid timber with characteristic density of ≥ 290 kg/m ³	0,67
b) Solid or glued laminated hardwood with characteristic density of ≥ 350 kg/m	0,54

The shape of the char-line at arrises should be assumed as circular with a time-dependent radius according to Figure 2, but not greater than half of the smallest dimension of the residual cross section.

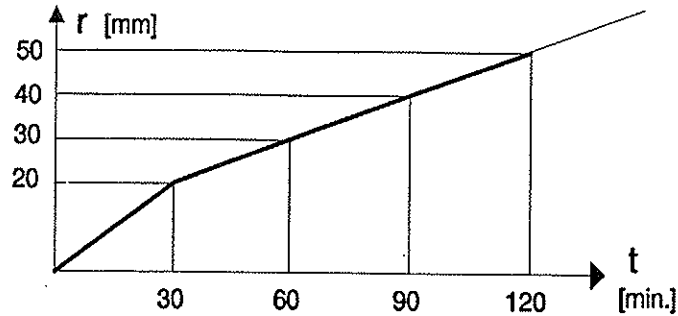


Figure 2 Time-dependent radius of the char-line at arrises

The residual cross-section is used for the calculation of the load bearing capacity. The reduction of strength and modulus of elasticity is considered by multiplication - see Equations (1) and (2) - by the reduction coefficient $k_{\text{mod},f}$ according to Figure 3

where

p Perimeter of the fire exposed residual cross section in m
 A_r Area of the residual cross section in m^2

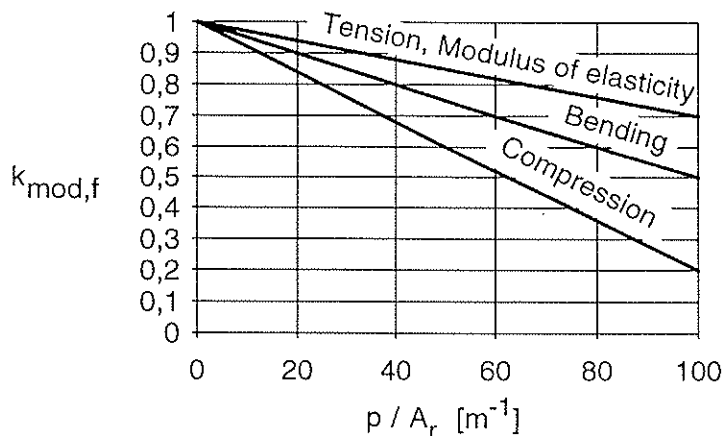


Figure 3 Modification factor for strength and stiffness properties

Since the temperature is different in different parts of the cross section, its influence on $k_{\text{mod},f}$ is implicitly included in the section factor p/A_r of the residual cross section and not given directly. During the drafting and commenting periods it became obvious that many users of the code would misinterpret data showing the relationship of strength and the effective temperature of the cross section. The concept of the section factor was adopted from the fire part of EC 3 (steel structures) and is calibrated to give right results.

Annex B, Supplementary rules for joints

This annex is normative. While in the main text of the code only simplified rules are given, this annex gives more complete formulae of which the values in the main text are deduced and additional rules which allow for more sophisticated design and more economic results.

Annex C. Walls and floors

This annex is normative. It contains application rules which fulfil the requirements of the main text. They apply to load bearing (R), separating (EI), load bearing and separating (REI) constructions. For the separating function the rules apply up to 60 minutes of standard fire resistance. Generally, the rules given in this annex are conservative and fire testing will give more economic results.

Panels dealt with in the code may

- perform as fire protection claddings of load bearing constructions, or
- be part of the load bearing construction, including panels used for diaphragm action and bracing and/or
- be used as sheet linings to provide for the separating function.

For separating constructions separation criteria are given. For load bearing constructions failure times of combustible and non-combustible panels are given as well as the influence of panel joints. Since the detailing of fixings of insulation material, panel connections and connections to adjoining floors and walls are essential, some examples are given. It was not possible to give a complete catalogue of solutions, since building practice varies too much in the different European countries.

Annex D. Parametric fire exposure

This annex is informative. It deals with parametric fires (also called natural fires) in fire compartments where the temperature time relationship is determined regarding the fire load density, the area of floors, walls and ceilings which enclose the fire compartment, and the total area of vertical openings. The rules for timber given in this annex are based on the work by Hadvig /3/ and Bolonius Olesen /4/.

Annex E. Thermal properties

This annex is informative and gives some information on the thermal conductivity and specific heat capacity of wood and charcoal.

REFERENCES

- /1/ Schaffer, E L, Structural Fire Design: Wood. Forest Products Laboratory, Research Paper FPL 450, Madison, 1984
- /2/ Kersken-Bradley, M, Klingsch, W & Witte, H, Vereinfachende Regeln für die Brandschutzbemessung von Holz und Holzverbindungen. Research Report Deutsche Gesellschaft für Holzforschung, Munich, June 1989
- /3/ Hadvig, S, Charring of wood in building fires, Technical University of Denmark, Lyngby 1981
- /4/ Bolonius Olesen, F & König, J, Tests on glued-laminated beams in bending exposed to natural fires. CIB/W18, Meeting Twenty-five in Åhus (1992), Paper 25-16-2

LIST OF CONTENTS

FOREWORD

1. INTRODUCTION

- 1.1 Scope
- 1.2 Definitions
- 1.3 Units
- 1.4 Symbols
- 1.5 Normative references

2. BASIC PRINCIPLES

- 2.1 Performance requirements
- 2.2 Actions
- 2.3 Design values of material properties
- 2.4 Basic design procedure
- 2.5 Assessment methods
 - 2.5.1 Global structural analysis
 - 2.5.2 Analysis of parts of structure
 - 2.5.3 Member analysis

3. MATERIALS

- 3.1 Charring depths
- 3.2 Fire protective cladding
- 3.3 Adhesives

4. STRUCTURAL FIRE DESIGN

- 4.1 Effective cross-section method
- 4.2 Reduced strength and stiffness method
- 4.3 General calculation method
- 4.4 Special rules
 - 4.5.1 General
 - 4.5.2 Beams
 - 4.5.3 Columns
 - 4.6.1 Mechanically jointed components
 - 4.6.2 Bracings
 - 4.6.3 Floors and walls
- 4.5 Joints
 - 4.5.1 General
 - 4.5.2 Unprotected joints with side members of wood
 - 4.5.3 Unprotected joints with external steel plates
 - 4.5.4 Protected joints

ANNEXES

- Annex A: (Normative)
Reduced strength and stiffness method for standard fire exposure
- Annex B: (Normative)
Supplementary rules for joints with unprotected fasteners
- B1 Joints with unprotected nails
 - B2 Joints with unprotected bolts
 - B3 Joints with unprotected dowels
 - B4 Dowels
 - B5 Joints with steel plates
- Annex C: (Normative)
Walls and floors
- C1 Scope
 - C2 Design procedure
 - C2.1 General
 - C2.2 Load bearing constructions
 - FC.3 Separating constructions
 - C3 Failure times
 - C3.1 Wood and wood-based panels
 - C3.2 Non-combustible linings and panels
 - C4 Minimum dimensions and detailing
 - C4.1 Minimum dimensions
 - C4.2 Detailing of panel connections
 - C4.3 Connections to adjoining floors and walls
- Annex D: (Informative)
Parametric Fire Exposure
- D1 Charring rates and charring depths
 - D2 Load bearing capacity of members in bending
- Annex E: (Informative)
Thermal properties